

**Genetic and Mechanistic Determinants of
Prostate Cancer Progression and Metastasis**

by

Sunny Y. Wong

B.A., Biology
Cornell University, 2000

SUBMITTED TO THE DEPARTMENT OF BIOLOGY IN PARTIAL
FULFILLMENT OF THE REQUIREMENTS FOR THE DEGREE OF

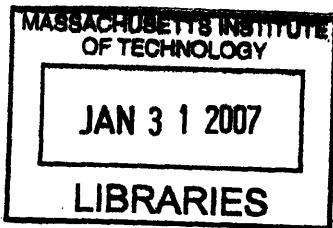
DOCTOR OF PHILOSOPHY IN BIOLOGY

AT THE

MASSACHUSETTS INSTITUTE OF TECHNOLOGY

FEBRUARY 2007

© 2007 Massachusetts Institute of Technology
All Rights Reserved



V.I ARCHIVES

Signature of Author:

[Handwritten signature]
Department of Biology
January 31, 2007

Certified By:

[Handwritten signature]
Richard O. Hynes
Professor of Biology

Accepted By:

[Handwritten signature]
Stephen P. Bell
Professor of Biology
Graduate Committee Chairperson

Genetic and Mechanistic Determinants of Prostate Cancer Progression and Metastasis

by

Sunny Y. Wong

Submitted to the Department of Biology on February 2007,
In Partial Fulfillment of the Requirements for the Degree
Of Doctor of Philosophy in Biology

ABSTRACT

In order to study a complex biological phenomenon such as tumor cell metastasis, one must focus on examining discrete aspects of the process which are amenable to experimentation. In this thesis, I made use of xenograft and spontaneous in vivo mouse models of prostate cancer to approach this problem from two perspectives. First, I sought to identify genes which were involved with metastasis. Second, I focused on the mechanistic elements involved with tumor cell intravasation into lymphatics. The results from this work have shown that loss of Protein 4.1B, a 4.1/ezrin/radixin/moesin (FERM) domain-containing cytoskeletal protein, is a frequent event in prostate cancer. The significance of this finding was confirmed by experimental ablation of 4.1B, which enhanced tumor progression and metastasis, at least in part, by protecting cells against apoptosis. This thesis has also shown that metastatic dissemination to lymph nodes is mediated primarily by peritumoral lymphatic vessels, which surround the tumor at the invasive margins. In contrast, inhibition of intratumoral lymphatics did not affect metastatic spread, indicating that these vessels were unnecessary for tumor cell dissemination. The genetic and mechanistic findings from this thesis were consistent across both model systems examined, and are also in concordance with observations made in human clinical prostate cancer. Thus, the results of this work have contributed small pieces of knowledge to our overall understanding of how tumors initiate, and frequently complete, the elaborate and often lethal process of spreading throughout the body.

Thesis Supervisor: Richard Hynes

Title: Professor of Biology

Table of Contents

Title Page	1
Abstract	2
Table of Contents	3
A Note About Publications	4
Chapter 1: Introduction	5
Chapter 2: Derivation and Analysis of Metastatic Variants of the Human Prostate Cancer Cell Line PC-3	27
Chapter 3: Protein 4.1B Suppresses Prostate Cancer Progression and Metastasis	56
Chapter 4: A Direct Test for the Role of SPARC in Spontaneous Prostate and Breast Cancer Progression	109
Chapter 5: Hematogenous Metastasis Is Associated With Lymphatic Dissemination in a Mouse Model of Prostate Cancer	130
Chapter 6: Lymphangiogenesis Is Unnecessary for Prostate Cancer Metastasis	143
Chapter 7: Discussion and Future Directions	181
Appendix A: Materials & Methods	191
Appendix B: Surgical Orthotopic Implantation	203
Appendix C: Preparation of RNA for Microarray Analysis	211
Appendix D: Staining Blood and Lymphatic Vessels	214
Appendix E: Microarray Results	216
Appendix F: Publications	224
Acknowledgements	251

A Note About Publications

Portions of this thesis were derived from the following papers that have been, or will soon be, published:

Wong, S.Y., Haack, H., Crowley, D., Barry, M., Bronson, R.T., and Hynes, R.O. "Tumor-secreted VEGF-C is necessary for prostate cancer lymphangiogenesis, but lymphangiogenesis is unnecessary for lymph node metastasis." 2005. 65(21): *Cancer Research*. pp. 9789-98.

Wong, S.Y. and Hynes, R.O. "Lymphatic or hematogenous dissemination: How does a metastatic tumor cell decide?" 2006. 5(8): *Cell Cycle*. pp. 812-817.

Wong, S.Y. and Hynes, R.O. "Tumor-lymphatic interactions in an activated stromal microenvironment." 2006. *Journal of Cellular Biochemistry*. (In Press)

Wong, S.Y., and Hynes, R.O. "Protein 4.1B suppresses prostate cancer progression and metastasis." (Submitted)

* * *

In all cases, these papers were written primarily by myself, with editing by Richard Hynes. The first three of these publications are included in Appendix F of this thesis.

CHAPTER 1. INTRODUCTION

Metastasis: Guiding Principles

The term “metastasis” derives from the Greek word *methistanai*, meaning “change of the state.” In the context of cancer, it is used to describe the process by which malignant cells from a primary tumor disseminate to other parts of the body. While it is estimated that metastasis is ultimately responsible for 90% of cancer-related deaths, the task of undergoing a “change of the state” is not an easy one, even for transformed cells. In order to metastasize, a tumor cell must possess or acquire the ability to surmount a variety of obstacles—challenges that include de-adhesion from the primary tumor, intravasation into blood or lymphatic vasculature, survival in circulation, extravasation, and growth at a secondary site. With so many barriers that need to be overcome, it is almost a wonder that tumors ever succeed at metastasis. This is likely accomplished, at least in part, through persistence: Each gram of primary tumor is believed to release up to 4×10^6 malignant cells into circulation daily, and even a single cell, if endowed with the appropriate capabilities, has the potential to be fatal [Butler and Gullino, 1975]. But what is it exactly that makes a cancer cell metastatic? As will become evident, the problem of understanding how a tumor embarks upon and completes its metastatic journey involves asking at least two fundamental questions: Where is the malignant cell going? And where did it come from?

A discussion about where tumor cells are going, or in other words, where they eventually metastasize to, invariably begins with the theories set forth by Stephen Paget. For it was Paget, an English surgeon at the turn of the twentieth century, who first popularized the “seed and soil” theory for metastasis in his 1889 paper, “The Distribution of Secondary Growths in Cancer of the Breast”¹ [Paget, 1889]. In his paper, he argued that the patterns of metastasis observed for tumors were non-random and could be explained by organ-specific factors that favored colonization by certain tumor cell types but not others. In other words, just as a seed cannot flourish unless sown into fertile soil, a metastatic tumor cell (“the seed”) cannot proliferate unless surrounded by an organ that provides a hospitable growth environment (“the soil”). In the case of breast cancer, that appropriate soil would be found in the lungs, bones, brain and liver—all common sites of metastasis for this tumor. For other cancer types, the right soil might exist within different organs. In this way, Paget was among the first to realize that the determinants of organ-specific metastasis rested not only on the tumor cell itself, but also, from a wider standpoint, on how it interacts with its surrounding microenvironment.

Paget’s views, to some extent, are contrasted by those proposed by James Ewing, an American pathologist who argued in 1929 that patterns of blood flow, rather than “seed and soil,” were the major factors that affected site-specific metastasis [Ewing, 1919]. As tumor cells in circulation are thought to arrest in the first or second capillary bed they encounter, how different organs are connected by blood

¹ Although Paget is widely credited for his “seed and soil” hypothesis, the idea likely originated from Fuchs, in his 1882 paper, “Das Sarkom des Uvealtractus.” In fact, Paget states in his paper that “the chief advocate of this theory of the relation between the embolus and the tissues which receive it is Fuchs.” (http://en.wikipedia.org/wiki/Stephen_Paget)

flow could potentially impact the eventual site of metastasis from a particular tumor. In fact, it is now believed that both Paget's and Ewing's hypotheses are likely true. A survey of eight different tumor types undertaken by Weiss et al., in 1992, revealed that venous blood flow patterns could account for the distribution of metastases observed in 68% of cases [Weiss, 1992]. In the roughly one-third of patients where Ewing's hypothesis did not apply, "seed and soil" was likely to be important. In any case, mechanical factors such as blood flow patterns almost certainly determine where tumor cells will end up. But whether these cells will eventually form metastases may depend on whether their microenvironment supports, or at least tolerates, the continued growth of these malignant cells.

As mentioned previously, any discussion about where tumors metastasize to, should be accompanied by an examination of where these cells first came from. This can entail several aspects, not only limited to where a metastatic cell physically started its journey, but also including the cell type from which it originated, and the patterns of genetic and epigenetic changes that differentiate it from normal. In regard to the location from which metastatic dissemination begins, it has already been mentioned that blood flow patterns at the site of origin are important. But Ewing's hypothesis might also be extended to include the lymphatic system, a common route of metastasis for many tumors. Indeed, the existence of this second system of fluid transport has been known since around 1650, when the lymphatic system was co-discovered by Thomas Bartholin and Olaus Rudbeck. And perhaps even more so than blood vessels, the patterns of lymphatic drainage determine where tumors will metastasize: Invasion invariably begins at the draining, or sentinel, lymph node, and spreads outwards based upon afferent and efferent lymphatic connections. If the sentinel lymph node is free of metastasis, the other 500-600 lymph nodes in the human body will almost certainly be un-invaded [Nathanson, 2003; Wittekind, 2000]. Given that the presence of lymph node metastases has important prognostic implications in the clinic, and that lymphatics provide an additional route by which tumors can enter venous circulation, attention will be focused on this important subject in the later chapters of this thesis.

We have already mentioned that Paget's original hypothesis emphasized the role of soil in the propagation of metastases at the final site of invasion. A corollary to this might surmise that the microenvironment, or stroma, that surrounds a primary tumor might also affect metastatic proclivity at the site of origin. This stroma comprises cellular components including fibroblasts, immune cells, endothelial cells and endothelial-associated cells. These different cell types could potentially communicate with each other, and/or with tumor cells, through a variety of signals, including cytokines, matrix molecules and other secreted factors. In fact, recent work has shown that the outcomes of these interactions can affect metastasis by enhancing the innate aggressiveness of the tumor cell, by inducing the local growth of blood and lymphatic vessels, and even perhaps by establishing a pre-metastatic niche at future sites of invasion [Gupta and Massague, 2006]. Therefore, the perception of metastasis as a solitary journey

undertaken by a single rogue cell can be regarded as overly simplistic and perhaps, these days, even antiquated.

By now we have discussed how factors extrinsic to the malignant cell might affect metastasis, and it is important to turn our attention to how intrinsic factors might also govern the process. In a sense, this also involves asking a metastatic cell where it came from—how it originally developed, whom it is immediately descended from, and how it became malignant. Genome-wide gene expression analyses have certainly revolutionized the way some of these questions are now viewed and studied, as will be discussed below, though some of the most thought-provoking principles about metastasis were originally conceived by Isaiah J. Fidler in the 1970s and 1980s. Work by Irving Zeidman in the 1950s had already shown that the number of experimental metastases formed in a mouse is a function of the number of cells introduced into the animal [Zeidman et al., 1950], but Fidler made efforts to quantitate this process temporally by injecting radiolabeled B16 melanoma cells [Fidler, 1970]. And, in fact, he found that metastasis is an exceedingly rare occurrence: less than 0.01% of these cells formed secondary growths in mice, and most cells were eliminated from the animal soon after they were introduced. He also observed that the metastatic phenotype was heritable, as cells derived from metastatic nodules following intravenous injection exhibited enhanced metastatic potential when subsequently re-introduced into mice [Fidler, 1973]. These observations led Fidler to propose that metastases were formed not by random cells that existed within the bulk of the primary tumor, but, instead, by rare cells that were somehow more adept than their peers at completing all the necessary steps of the process. By extension, this also suggested that primary tumors were heterogeneous, composed of cells that differed drastically in their ability to colonize other tissues.

Fidler proved these hypotheses using a modified version of the Luria-Debrück fluctuation test [Fidler and Kripke, 1977]. In the 1940s, Salvador Luria and Max Debrück had observed that mutations arose randomly in bacteria, and independently of selective pressure, rather than in response to it [Luria and Delbruck, 1943]. In the original fluctuation test, Luria and Debrück had shown that, within a population of bacteria, some members were resistant to phage infection, and that these had pre-existed prior to selection. This important concept has implications for evolution and, as Fidler demonstrated, for metastasis. Similar in approach to the Luria-Debrück fluctuation test, Fidler made single cell clones of his B16 melanoma cells and showed that these clones differed widely in metastatic ability when injected into mice [Fidler and Kripke, 1977]. This demonstrated that metastatic variants pre-existed within the original population of cells even prior to challenge. And what was responsible for this? As in the case of resistant bacteria and natural selection, the driving force was random variation. Indeed, subsequent work by Fidler later showed that highly metastatic tumor cells exhibited greater genetic instability than did poorly metastatic cells, and, overall, tumor cells are thought to be much more genetically unstable than normal

cells [Fidler, 2003]. These findings have laid the conceptual groundwork for some of the experiments described in the first few chapters of this thesis.

Also important has been the advent of microarray technology, which has transformed the way we study tumor biology. Gene expression analyses have aided not only in the discovery of genes responsible for tumor progression and metastasis, but have also enhanced our ability to make predictions concerning clinical outcome in ways that—some may argue—are improvements over traditional methods of histological evaluation and diagnosis. The ability to “fingerprint” tumors using array analysis has also allowed researchers to uncover many hidden connections. While recent gene expression studies have suggested that distant metastases resemble their primary tumors of origin [Ramaswamy et al., 2003; Sorlie et al., 2003; van't Veer et al., 2002], other studies have indicated that the expression of specific genes is altered in metastatic cells [Clark et al., 2000; Kang et al., 2003; Minn et al., 2005; Xu et al., 2006; Yang et al., 2004]. These two observations are not mutually exclusive. A model incorporating both these findings has speculated that cells derived from metastases and from their corresponding primary tumors share an overall gene expression pattern that confers the ability to complete some, but not all, of the steps required for metastasis [Hynes, 2003; Kang et al., 2003]. On top of this, the altered expression of a limited number of additional genes may render a sub-population of cells fully competent for metastasis, without changing its overall similarity to the primary tumor.

This model could help explain why a tumor's cell of origin and its accompanying differentiation program could affect its metastatic proclivity. For instance, it has long been known that epithelial tumors often metastasize to lymph nodes, whereas sarcomas rarely do; also, melanomas tend to be highly metastatic tumors [Friedl and Wolf, 2003; Gupta et al., 2005]. It is possible that, based on their developmental history and the accompanying signaling pathways and transcription factors that are activated/repressed, certain tumors may be more prone to metastasize than others. In other words, these tumors may sit at a knife's edge when it comes to metastasis, perhaps requiring few genetic or epigenetic changes to render them capable of completing the process. In the case of melanomas, these tumors are derived from melanocytes, which arose from migratory neural crest cells. It is therefore plausible that this history of migratory behavior might, upon transformation, subsequently reappear and drive the metastatic process.

The Path of the Metastatic Cell

The journey taken by a metastatic cell from a primary tumor to a secondary site is thought to be complex, involving the coordinated expression of dozens, if not hundreds, of genes. As will be discussed in the next chapter, many of the models developed to study metastasis over the past few decades have been suited for observing some, but not all, of the steps of this process. Consequently, the findings gleaned from these studies have been, in a way, fragmentary—some are relevant to the earlier stages of

metastasis, others to the later stages, and few studies have tracked the process from beginning to end. It is therefore useful, when examining the path of the metastatic cell, to divide this journey into two halves: those events that occur prior to entrance into circulation, and those that happen afterwards.

Early stages of metastasis: cell migration

In most cases, the appearance of a primary tumor precedes metastatic dissemination, although in certain instances, patients are diagnosed with distant metastases in the absence of a recognizable primary tumor² [Schmidt-Kittler et al., 2003]. In the more conventional situation, the metastatic process begins when cancer cells detach from the primary tumor and invade blood vessels or lymphatics. This may be a passive process where cells are simply sloughed off from the primary tumor or an active one involving directed migration [Condeelis and Segall, 2003; Wyckoff et al., 2004]. The way a tumor cell migrates, at least in part, may depend on the tissue from which it originates. Cells from connective tissue tumors such as fibrosarcomas and gliomas tend to migrate individually, for instance, whereas those from melanomas and carcinomas often migrate collectively [Friedl and Wolf, 2003]. In addition, highly differentiated epithelial tumors may initially display collective migration, only to de-differentiate and exhibit single cell invasion, a process termed epithelial-to-mesenchymal transition (EMT) [Thiery, 2002]. Indeed, genes that promote EMT—including Twist [Yang et al., 2004]; Slug and Snail transcription factors [Kurrey et al., 2005]; and components of the TGF- β signaling pathway [Oft et al., 2002; Siegel et al., 2003]—have all been reported to enhance the earliest stages of metastasis. E-cadherin, which is often lost during EMT, is thought to suppress cell migration and tumor progression [Perl et al., 1998].

The mechanisms by which cells migrate under normal physiological situations, such as during embryogenesis, wound healing and immune-cell trafficking, are likely also to be relevant during the earliest stages of metastasis. In large part, the surrounding extracellular matrix (ECM) and the integrity of cell-cell junctions likely affect how tumor cells accomplish this [Friedl and Wolf, 2003]. Mesenchymal, or elongated, single cell migration tends to occur in the presence of dense matrix networks. This sort of movement typically involves cell polarization and extension of a pseudopod at the leading edge, followed by contraction and movement of the trailing edge. A host of proteins, including cell surface receptors and cytoskeletal proteins, are almost certainly involved. In order to establish the proper traction and adhesive contacts needed to “pull” a cell forward, transmembrane proteins such as the heterodimeric family of integrins are necessary to negotiate interactions with ECM components like fibronectin, collagen and laminin [Webb and Horwitz, 2003]. This process is also aided by other cell surface receptors such as cadherin proteins, which primarily mediate homophilic interactions; the selectins, which bind proteins containing cell-surface carbohydrates; and certain members of the immunoglobulin-like superfamily of

² This cancer of unknown primary (CUP) scenario is reported to occur in up to 7% of patients who are initially found to possess systemic spread without a clearly discernible primary tumor.

proteins—the CAMs, or cell adhesion molecules—which exhibit both homo- or hetero-philic binding capabilities [Hynes and Lander, 1992].

The formation of adhesive contacts leads to clustering of these receptors, particularly of integrins, into focal complexes that incorporate actin-associated proteins such as α -actinin, talin, vinculin, paxilin and tensin . Integrin signaling can activate pro-migratory pathways by signaling through molecules such as focal adhesion kinase (FAK), which promotes cell movement through Src [Hood and Cheresch, 2002]. PI3-kinase is also often activated, and this leads to the synthesis of 3-phosphoinositides, which are bound by and cause re-localization of PH domain-containing proteins such as Akt to the plasma membrane [Comer and Parent, 2002; Funamoto et al., 2002]. At least one downstream consequence of this is activation of Rho family proteins such as Cdc42 and Rac1, which have long been observed to induce cellular protrusions such as filopodia and lamellipodia, respectively [Ridley et al., 2003]. Cdc42 has also been reported to activate proteins such as WASP, while Rac1 can activate WAVE (through a variety of adaptor proteins), and both of these can enhance the activity of Arp2/3, a critical protein which nucleates and catalyzes filamentous actin polymerization at the leading edge of the cell [Webb and Horwitz, 2003; Yamaguchi et al., 2005]. Not surprisingly, many of these cellular components have been implicated in metastasis, as have numerous other proteins which have been found to be involved with cell migration [Wang et al., 2005].

Interestingly, this cycle of cellular extension and retraction is not the only form of movement that can contribute to metastasis. Perhaps more relevant to tumors *in vivo* is a second form of migration where rounded cells are observed to “burrow,” or adopt an amoeboid morphology [Friedl and Wolf, 2003]. This is likely to be the favored mode of cellular movement under less adhesive conditions, as is often seen *in vivo* or in three-dimensional cultures, where focal contacts are lacking. Although the signaling pathways responsible for amoeboid migration have not been fully elucidated, it is known that the activity of cytoskeletal proteins such as RhoA and ezrin³ are required, while that of Rac1 is not [Sahai and Marshall, 2003]. In addition, amoeboid migration occurs independently of protease activity, in contrast to mesenchymal migration, which has been observed to rely on the activity of matrix metalloproteinases (MMPs). This is, perhaps, not surprising, given that the latter form of movement is thought to occur primarily within dense ECM networks that, unless proteolyzed, may impede cell migration.

Early stages of metastasis: stromal factors

Certainly, every tumor cell possesses the innate molecular machinery to make migratory behavior possible. But what are the stimuli and cues that actually elicit pro-invasive signaling pathways and gene expression programs from otherwise non-migratory cells? In some cases, malignant cells in a primary

³ Ezrin and other related ERM proteins are described in greater detail in Chapter 3.

tumor may be driven to metastasis in order to escape insults such as hypoxia, and, indeed, the presence of a hypoxic gene expression signature has been reported to correlate with increased metastatic behavior [Chi et al., 2006]. In most cases, however, directed migration—whether amoeboid or mesenchymal—tends to occur in response to attraction, either towards a gradient of cytokines (chemotaxis) or matrix molecules (haptotaxis) [Moore, 2001]. One recent illustration of this is a study performed by Wyckoff et al, who imaged rat mammary adenocarcinomas and reported that metastatic cells were more likely to polarize towards blood vessels than were non-metastatic cells [Wyckoff et al., 2004; Wyckoff et al., 2000]. This enhanced polarization was explained by increased expression of EGF receptor on the surface of aggressive cells, which made them chemotactic to EGF released by macrophages lining the blood vessels.

Based on this observation, a logical question might be: Why were there macrophages present in the tumor to begin with? Interestingly, further work showed that these immune cells themselves had been summoned by the tumors, which secreted the macrophage chemotactic factor CSF-1 [Wyckoff et al., 2004]. And so it would seem as if, at least in this experimental system, tumor-stromal communication occurring through a series of paracrine factors initiated the metastatic process.

While the nature of these sorts of interactions, for the most part, still remain to be characterized, it is now believed that the importance of tumor-stromal interloction is the rule, rather than the exception, in cancer. Within the tumor microenvironment, there are certainly many opportunities for this to take place, as immune cells and cancer-associated fibroblasts (CAFs) are frequently observed in close proximity to malignant cells. These CAFs have been reported to exhibit an “activated” phenotype characterized by expression of α -smooth muscle actin, as well as enhanced migration and abnormal secretion of cytokines and ECM [Cunha et al., 2003]. Importantly, transplantation/co-injection experiments have demonstrated that CAFs appear to be stably activated and can induce *de novo* tumorigenic growth in non-tumorigenic prostate epithelial cells [Olumi et al., 1999], or increased tumorigenicity in human MCF-7 breast cancer cells [Orimo et al., 2005]. In the latter case, CAFs in breast cancer were found to enhance angiogenesis and tumor growth by secreting the chemokine SDF-1/CXCL12 [Orimo et al., 2005]. This mobilized and recruited endothelial precursor cells which were derived from the bone marrow and expressed the receptor CXCR4.

Secretion of cytokines such as VEGF-A, VEGF-C, TGF- β , FGF, HGF, EGF, IGF and PDGF by stromal cells has also been reported [Cunha et al., 2003]. Not surprisingly, the presence of these cytokines can help drive several malignant processes, including the induction of tumor EMT (by TGF- β , EGF, HGF and/or IGF), and neovascularization [Christofori, 2006]. In particular, HGF ligand binding to c-Met receptor on tumor cells has long been known to induce scattering and an invasive phenotype [Christofori, 2006], while enhanced IGF signaling has been reported to promote metastasis in a mouse model of

pancreatic cancer [Lopez and Hanahan, 2002]. TGF- β also appears to be centrally important during cancer progression, although it can act as both a positive and a negative regulator of tumorigenesis. For instance, although TGF- β can suppress the growth of certain tumor cells, its upregulation in fibroblasts has been shown to induce mammary carcinomas [Kuperwasser et al., 2004]. Genetic deletion of TGF- β type II receptor specifically in fibroblasts was also associated with upregulated HGF, and induction of spontaneous prostate and forestomach carcinomas in mice [Bhowmick et al., 2004]. In addition, transgenic expression of constitutively active TGF- β type I receptor in mammary tumors has been reported to enhance metastasis [Siegel et al., 2003]. Thus, the effects of TGF- β as both a positive and negative regulator of tumorigenesis are likely cell-type and cell-context dependent.

A similar dual effect on tumor progression and metastasis has been observed in the case of MMPs, which are secreted by both tumor and stromal cells. MMPs act not only to degrade the surrounding ECM but also to activate latent cytokines as well as other MMPs. Furthermore, MMPs can release matrix-bound growth factors (e.g. VEGF-A and FGF) that can induce invasive behavior and vasculogenesis, though cryptic collagen IV fragments released by MMP-9 can also possess potent anti-angiogenic activity [Hamano et al., 2003]. Experimentally, spontaneous mouse mammary tumor formation was enhanced by fibroblasts that overexpressed MMP-1 and MMP-7, but was inhibited when fibroblasts had lost MMP-11 (reviewed in [Lynch and Matrisian, 2002]). Transgenic expression of MMP-3 in mammary tumors has also been reported to promote EMT through disruption of E-cadherin- β -catenin interactions [Sternlicht et al., 1999].

As illustrated previously in the case of macrophages, inflammatory cells of the innate immune system are now regarded as critical, if not indispensable, mediators of tumor progression [Coussens and Werb, 2002]. Immune cells are major sources of growth factors and cytokines that can induce tumor invasion and neovascularization. Tumor and/or stromal fibroblastic secretion of chemokines and other cytokines such as VEGF-A and CSF are key to recruiting specific leukocyte populations. Macrophages, in particular, are chemotactic to VEGF-A, M-CSF and monocyte chemotactic protein chemokines [Cursiefen et al., 2004]. In addition, neutrophils are also chemotactic to chemokines such as CXCL1/MIP-2 and are important for angiogenesis [Scapini et al., 2004]. Finally, natural killer cells have been found to aid progression of pre-neoplastic mammary lesions through secretion of MMPs [Bissell and Radisky, 2001].

Early stages of metastasis: intravasation and egress

In many cases, the net outcome of these varied interactions is an enhanced propensity on the part of malignant cells to invade into, or intravasate, blood or lymphatic vasculature. While the process of intravasation has been especially difficult to study, intravital microscopy has recently allowed real-time observation of tumor cells entering into blood or lymphatic circulation [Hoshida et al., 2006; Wyckoff et al.,

2000]. To some extent, the chicken chorioallantoic membrane (CAM) assay has also made possible the ability to quantitate this process indirectly, by detecting the number of tumor cells that migrate through blood and lymphatic vasculature from a source (the upper CAM) to a specific destination (the lower CAM). Studies using this model have shown, for instance, that intravasation of human breast, prostate and fibrosarcoma tumor cells into blood vessels requires the proteolytic activity of MMP-9 and urokinase plasminogen activator [Kim et al., 1998].

Successful completion of the intravasation stage of metastasis can also be assayed by detecting circulating tumor cells in the blood, both in animal models and in human patients. In fact, viable tumor cells have been isolated in the blood of patients bearing nearly all types of cancer, including the most common forms of carcinomas [Allard et al., 2004]. The presence of these circulating cells can be detected by RT-PCR, immunohistochemistry or by culturing these cells *in vitro*. Although the prognostic value of these detection methods has remained controversial, and mouse model studies have reported that circulating tumor cells are often apoptotic and less malignant than cells present at the primary site [Swartz et al., 1999], the entrance of tumors into the vasculature is, nonetheless, a necessary step for metastasis. Indeed, experimentally increasing the propensity by which tumors intravasate through vasculature—for instance, by elevating the expression of the EMT-inducing transcription factor Twist—has been reported to yield increased metastasis [Yang et al., 2004].

In the later chapters of this thesis and also in the appendix, we address additional issues concerning how tumor cells might be induced to enter blood and/or lymphatic circulation. Although lymphatic vessels are more permeable than blood vessels and are, therefore, believed to be more susceptible to intravasation by tumors, we will also explore potential molecular mechanisms that might influence this process⁴. Finally, the impact of the tumor microenvironment will be examined in greater detail within the latter parts of this thesis⁵.

Later stages of metastasis: arrest and survival in a new microenvironment

Once a tumor cell has successfully entered the throughways of the circulatory system, how does it know where to stop? As mentioned previously, size restriction is likely to be important, at least in most instances: While the diameter of capillaries ranges from 3-8 μm and permits the trafficking of red blood cells, which are approximately 7 μm in diameter and deformable, the size of most tumor cells is on the order of 20 μm [Chambers et al., 2002]. Thus, the mechanical aspects of Ewing's hypothesis likely come into play. However, in other cases, tumor cells have been reported to attach to the wider walls of pre- and post-capillary vessels [Al-Mehdi et al., 2000; Wong et al., 2002]. Size restriction, at least in these instances, seems unlikely to account for these observations.

⁴ Please see Appendix F: "Lymphatic or Hematogenous Dissemination: How Does a Metastatic Tumor Cell Decide?"

Certainly, the entrance and exit of cells from circulation are not unprecedented events. Immune cells are specialists at performing these feats, and heterotypic interactions mediated initially by selectin receptors, then subsequently by integrins and CAMs, allow exit, or extravasation, of leukocytes from circulation [Robinson et al., 1999]. At least the initial stages of the extravasation process, including the rolling of individual cells along a monolayer of endothelial cells, followed by arrest, can be modeled *in vitro* through use of a flow chamber. Such experimental systems have revealed, for instance, that carbohydrate-containing cell surface proteins are critical for the arrest of circulating prostate and breast cancer cells and, possibly, also for homotypic adhesive interactions that may facilitate the formation of tumor cell aggregates [Glinsky et al., 2003]. In addition, these and similar results have suggested that selectins play roles in tumor metastasis, and, indeed, several *in vivo* tumor studies have shown this to be the case. For instance, spontaneous pancreatic tumors overexpressing L-selectin were found to metastasize to lymph nodes, while tumors without L-selectin did not metastasize [Qian et al., 2001]. Mice lacking either P- and/or L-selectin were also resistant to metastasis by colon adenocarcinoma cells [Borsig et al., 2002], while carcinoma cells expressing elevated levels of E-selectin displayed enhanced metastasis [Krause and Turner, 1999]. Similarly, mis-expressing or inhibiting⁶ selectin ligands on tumor cells has been reported to affect their ability to disseminate [Borsig et al., 2002]. These selectin-ligand interactions likely enhance binding not just between tumor cells and the endothelium, but also between tumors and platelets/leukocytes. The consequences of this may be the formation of micro-emboli that help arrest tumor cells in the vasculature, or protect them against attack from the immune system [Borsig et al., 2002].

Numerous other tumor-endothelial interactions are likely important for extravasation. For instance, phage homing studies as well as gene expression analyses have identified molecular differences among vascular beds present in different organs, and the unique assortment of receptors/ligands on the surface of specific endothelial cells likely biases the types of interactions which occur [Croix et al., 2000; Ruoslahti, 2002]. For instance, trans-migration of tumor cells through bone marrow endothelial cells has been shown to require interactions between the receptor CD44 and its ligand hyaluronan; between integrin $\alpha 4\text{-}\beta 1$ (VLA-4) and V-CAM; and also between integrin $\alpha L\beta 2$ (LFA-1) and I-CAM [Simpson et al., 2001]. Tumor expression of the integrins $\alpha 3\beta 1$ and $\alpha 6\beta 4$ has also been implicated in binding laminin on the surface of lung endothelial cells [Guo and Giancotti, 2004; Wang et al., 2004], and recent studies have identified metadherin as an additional receptor for enhancing lung metastasis [Brown and Ruoslahti, 2004]. Finally, the cytoskeletal protein ezrin has been reported to be necessary for tumor cell extravasation in the lung [Khanna et al., 2004].

⁵ Please see Appendix F: "Tumor-Lymphatic Interactions in an Activated Stromal Microenvironment".

⁶ Through pre-treatment of cells with sialidase or glycoproteases, which cleave sialylated mucins

Although we have devoted some amount of attention to mechanisms by which tumor cells exit circulation, others have noted that extravasation may not be a necessary step for metastasis. As will be mentioned in Chapter 2, fluorescently-labeled fibrosarcoma and breast cancer cells have been observed to form intravascular metastatic colonies in the pre-capillary arterioles of the lung [Al-Mehdi et al., 2000; Wong et al., 2002]. Extravasation was rarely seen with these cells, which were wholly contained within vascular channels. These findings appear to contradict those of others, who have reported that as many as 80% of B16 melanoma cells extravasated into the lung parenchyma within three days after intravenous injection [Cameron et al., 2000; Luzzi et al., 1998].

Regardless of whether tumor cells have extravasated or not, one consistent observation from all these reports is that, in the majority of cases, these cells do not progress to form metastases. Of course, the difficulties associated with successful metastatic colonization have been known for some time, although it still remains unclear which step(s) of the process are rate-limiting. Given that primary tumors are capable of sending millions of cells into circulation daily, it is believed that the latter stages of metastatic dissemination are responsible for this inefficiency. Tumor cell survival within a new microenvironment likely presents a major challenge, and apoptosis may account for the rapid clearance of most malignant cells following arrest in the vasculature. Indeed, inhibiting apoptosis—through expression of anti-apoptotic genes such as Bcl2, Bcl-XL and XIAP in tumors—has been reported to enhance metastasis [Martin et al., 2004; Mehlen and Puisieux, 2006]. Downregulation of caspase-8 or upregulation of the receptor TrkB has also been found to increase metastasis by conferring tumor cell resistance to anoikis, a form of apoptosis that results when cells are detached from a substratum [Douma et al., 2004; Stupack et al., 2006]. In addition, some have observed that apoptosis may occur when malignant cells express integrins that are inappropriate for a novel microenvironment and are, therefore, likely to be unligated [Stupack et al., 2006]. Clearly, there are many mechanisms that can lead to cell death, and this is almost certainly a rate-limiting step for any metastatic cell.

Later stages of metastasis: flourishing in a novel microenvironment

Even after a tumor cell has reached its final destination and has managed to avoid undergoing apoptosis, it faces additional challenges, one of which is to initiate malignant growth at the secondary site. Paget's hypothesis is especially relevant at this stage, and tumors that resist apoptosis but are incapable of proliferating have been observed to lie dormant as solitary cells in experimental systems [Cameron et al., 2000]. In humans, bone marrow aspirates have revealed the presence of micrometastases in 20-40% of human carcinomas, and these may also represent viable tumor cells that have lodged in the bone without undergoing extensive proliferation [Pantel et al., 1999]. Whether such cells can ever form malignant growths is currently unclear, although in some instances, it has been suggested that primary tumors may

suppress the growth of distant metastases, a phenomenon mediated, at least in part, by the plasminogen fragment angiostatin [O'Reilly et al., 1994].

Even those cells that manage to proliferate in a novel microenvironment are confronted with numerous obstacles. Cameron et al., have observed, for instance, that while most injected B16 melanoma cells arrested in the lung and extravasated, only 1 in 40 cells initiated growth as micrometastases, and, even then, only 1 in 100 micrometastases progressed to form macrometastases, with the remainder being cleared from the lung [Cameron et al., 2000; Luzzi et al., 1998]. What is responsible for the inefficiency of the very last stage? Perhaps the inability to induce angiogenesis may be one reason, although this possibility remains to be validated.

The presence of cytokines at a secondary site which are favorable to the metastatic cell would certainly confer a growth and/or survival advantage, and, as we have already mentioned before, may be a major determinant of organ-specific metastasis. The ability to respond to these favorable signals, while ignoring potentially unfavorable ones [Xu et al., 2006], may be a property associated with a cell's gene expression program. This was recently demonstrated in studies where variants of the MDA-MB-231 human breast cancer cell line were isolated from either bone or lung metastases [Kang et al., 2003; Minn et al., 2005]. When re-introduced into mice, these cell line derivatives exhibited increased metastasis specifically to the organ from which they had been isolated. Microarray analyses revealed unique gene expression signatures that differentiated cells with different metastatic proclivities, and the causal role of specific genes in conferring organ-specific biases was confirmed by experimental overexpression or underexpression. For instance, cells which did not ordinarily metastasize to bone could be manipulated to do so by overexpressing the genes IL11, osteopontin, and either CXCR4 or CTGF [Kang et al., 2003]. Similarly, lung metastasis could be specifically enhanced by upregulating sets of other genes, including SPARC⁷, V-CAM1, IL13R- α 2, MMP1/2, among others, while downregulation of V-CAM1 or IL13R- α 2 was found to decrease lung metastasis [Minn et al., 2005]. Although the precise organ-specific signals that biased metastatic outcome were not as clear from these studies, at least in the case of the bone microenvironment, high levels of TGF- β may have necessitated the expression of specific genes to respond to this cytokine [Kang et al., 2003].

Finally, as chemokines are often used to direct immune cells to lymph nodes and other organs, it is not surprising that tumor cells have been found to make use of these signals to "home" to specific sites. While these cytokines may act over long distances, thus being more akin to hormones, and may affect some of the earliest steps of metastasis, such as directed cell migration, chemokines are likely also to promote cell proliferation at the secondary site [Homey et al., 2002]. This reinforces the notion that a certain logic may underlie the pattern of metastatic tropism exhibited by a particular tumor, and that this

⁷ We test the role of SPARC in prostate and breast cancer metastasis/tumorigenesis in Chapter 4.

pattern can be deciphered, at least in part, by analyzing the distribution of specific chemokine receptor-ligand pairs. The first and most notable demonstration of this was performed by Muller et al., who showed that CXCL12/SDF-1 was preferentially expressed in the lymph nodes, lung, liver and bone marrow[Muller et al., 2001]. These are all common sites of metastasis for breast cancers, which express the SDF-1 receptor CXCR4. Inhibiting the interaction between this receptor-ligand pair *in vivo* reduced the ability of MDA-MB-231 breast cancer cells to metastasize to both lung and lymph nodes. Furthermore, the chemokine CCL21 was also found to be highly expressed in lymph nodes, and its receptor, CCR7, is often present on the surface of breast cancer and melanoma cells. Indeed, work by others has shown that overexpressing CCR7 in B16 melanoma cells can augment lymph node metastasis[Wiley et al., 2001]. Finally, activated lymphatic endothelial cells may secrete increased levels of CCL1, which could possibly be a chemotactic signal for CCR8-expressing tumor cells[Alitalo et al., 2004].

Metastasis: Outstanding Questions

Some of the first genes believed to be involved with metastasis were identified years ago using laborious experimental approaches such as cDNA subtraction techniques and microcell-mediated chromosomal transfer. The finding that chromosomal DNA from non-metastatic cells could suppress the metastatic potential of aggressive cells has, long ago, suggested the existence of metastasis suppressor genes. Indeed, several candidates fitting this description have been cloned over the years, including nm23, KAI1 (CD82), KiSS-1, MKK4 (SEK1) and BRMS1 [Yoshida et al., 2000]. While numerous studies have since found that many of these genes are frequently lost in a variety of human metastatic tumors, their precise functions, for the most part, still remain to be determined [Maurer et al., 1999; Welch et al., 2000]. However, one very recent report has shown that KAI1 on the surface of tumor cells forms an intermolecular interaction with a protein known as DARC, a seven-pass transmembrane receptor expressed on the endothelium[Bandyopadhyay et al., 2006]. The outcome of this interaction, amazingly, was tumor cell senescence *in vitro*. Even more remarkably, further experiments revealed that upregulation of KAI1 on melanoma cells suppressed metastasis in wild-type, but not DARC-deficient, mice[Bandyopadhyay et al., 2006]. This is perhaps just one illustration of the complex types of cellular interactions that take place during metastasis, a process that will surely appear even more complex as the functions of additional metastasis-related genes become known in greater detail.

Whole genome expression analyses have certainly increased the pace by which potential metastasis- and tumorigenesis-related genes are identified, though further work will be needed in order to understand how networks of genes are co-regulated and how these might synergize during metastatic progression. This might be especially useful for differentiating between two classes of metastasis genes: those that initially pre-dispose a tumor to metastasis, and those that, perhaps, specifically function later in the

process. In other words, in the first case, expression of metastasis pre-disposition genes might be an indirect consequence of a tumor's developmental history and/or of cross-talk with certain signaling pathways commonly upregulated early on during tumorigenesis, such as the MAP kinase pathway [Gupta and Massague, 2006]. These are likely genes which are expressed both by the primary tumors and by distant metastases, and may confer growth advantages at both sites, an observation that was noted by Minn et al., for instance, who reported that genes involved with lung-specific metastasis could enhance primary tumor growth [Minn et al., 2005]. Predisposition to metastasis might also be an inherited characteristic, and at least one DNA mapping study has reported that *Sipa1*, a gene found within the metastasis efficiency modifier locus *Mtes1*, might encode a protein that functions as an enhancer of breast cancer metastasis [Park et al., 2005]. As was mentioned, the other class of metastasis genes—those that further enhance the aggressiveness of tumors already pre-disposed to spread—probably arises out of genomic instability and random mutation, and are likely to be uniquely expressed in metastases. Some of these include *RhoC*, *GPR56* and *Twist*, just to name a few which have been identified at this Institute [Clark et al., 2000; Xu et al., 2006; Yang et al., 2004], and this list will almost certainly continue to grow.

At the same time, many other lingering questions about metastasis will remain until better imaging technologies allow direct observation of this process at higher resolution. For instance, one important question concerns the phenomenon of EMT and whether this transition is relevant to metastasis. Although EMT is generally believed to be accompanied by increased cellular migration and/or invasion, a complete epithelial-to-mesenchymal transition is rarely observed in human clinical tumors, even those that metastasize [Christofori, 2006]. Related to this is another aspect of metastasis that has traditionally been difficult to observe: the process of intravasation from the primary tumor. Certainly, the mechanical aspects of intravasation, as well as the genes involved, need to be better defined, and this may someday help explain why certain tumors are capable of disseminating only through the lymphatic route, while others are endowed with the ability to intravasate into blood vessels. Indeed, we will focus further attention on this question below and in Chapters 5 and 6 of this thesis. In addition, improved imaging of the metastatic process may help address which of the numerous steps involved are rate-limiting. It might also help determine whether metastasis occurs early or late during tumorigenesis, a question some have attempted to answer using comparative genome hybridization techniques [Schmidt-Kittler et al., 2003].

Finally, the varied roles and interactions of the tumor microenvironment in determining metastatic outcome need to be better defined. For instance, the immune system can act both positively and negatively to affect tumor progression and metastasis; therefore, an important area of research involves determining how this balance might be tilted in one direction versus another [Coussens and Werb, 2002]. Also currently unclear is the importance of stem or progenitor cells during tumorigenesis and metastasis, and this will almost certainly become an area of extensive focus in the years to come.

Prostate Cancer Metastasis

This is a thesis about how prostate cancer metastasizes, although it is possible, and perhaps even likely, that some of our findings may be pertinent to other cancer types. The prostate is a non-essential organ; thus, among the approximately 230,000 men who are diagnosed with prostate cancer every year⁸, many choose to have the organ removed by prostatectomy. Nevertheless, nearly 30,000 patients die annually from prostate cancer, making this malignancy the second leading cause of cancer-related deaths in men. In nearly all cases, these deaths are a result of disseminated—and essentially incurable—metastatic disease.

And so this thesis seeks to apply some of the principles of Fidler and Paget and Ewing to address both the genetic and mechanistic determinants that affect prostate cancer progression and metastasis. The subsequent chapters are structured in the following manner:

- In **Chapter 2**, I will elaborate upon the animal models commonly used to study prostate cancer in the laboratory. I will also describe the systems we used for the majority of our experiments, including the process by which we derived prostate cancer cells that differed in metastatic potential. Finally, I will discuss the gene expression analyses performed on these tumors in our attempt to identify gene candidates that affect the metastatic process.
- In **Chapter 3**, I will provide an overview of the Protein 4.1 family of proteins, of which one member—Protein 4.1B, or DAL-1—was significantly downregulated in highly metastatic prostate tumors. This will be followed by a description of our experimental results which validate 4.1B as a suppressor of the metastasis in two different *in vivo* mouse models of prostate cancer.
- In **Chapter 4**, I will provide an overview about SPARC, another candidate metastasis suppressor which was identified in our screen. This will be followed by a discussion about our attempts to test the role of this protein in spontaneous mouse models of prostate and breast cancer.
- In **Chapter 5**, I will briefly describe the factors which might be involved during tumor cell intravasation. I will relate an observation we made in the course of our studies, which suggested that hematogenous dissemination of tumor cells was

⁸ Source: American Cancer Society, 2005.

dependent upon lymphatic spread. This observation was the impetus for experiments described in Chapter 6.

- In **Chapter 6**, I will review the process of lymphangiogenesis, both under normal and abnormal conditions. I will also describe our attempts to inhibit prostate cancer lymphangiogenesis, a set of experiments that evolved into a mechanistic study of how prostate tumors disseminate to lymph nodes. Finally, I will discuss the unexpected results that came out these experiments and their implications.
- In **Chapter 7**, I will summarize the work described in this thesis, the unanswered questions that came out of these studies, as well as potential avenues of future research that could be undertaken to answer them.

REFERENCES

- Al-Mehdi AB, Tozawa K, Fisher AB, Shientag L, Lee A, Muschel RJ (2000): Intravascular origin of metastasis from the proliferation of endothelium-attached tumor cells: a new model for metastasis. *Nature Medicine* 6:100-102.
- Alitalo K, Mohla S, Ruoslahti E (2004): Lymphangiogenesis and Cancer: Meeting Report. *Cancer Research* 64:9225-9229.
- Allard WJ, Matera J, Miller MC, Repollet M, Connelly MC, Rao C, Tibbe AG, Uhr JW, Terstappen LW (2004): Tumor cells circulate in the peripheral blood of all major carcinomas but not in healthy subjects or patients with nonmalignant diseases. *Clinical Cancer Research* 10:6897-6904.
- Bandyopadhyay S, Zhan R, Chaudhuri A, Watabe M, Pai SK, Hirota S, Hosobe S, Tsukada T, Miura K, Takano Y, Saito K, Pauza ME, Hayashi S, Wang Y, Mohinta S, Mashimo T, Iizumi M, Furuta E, Watabe K (2006): Interaction of KAI1 on tumor cells with DARC on vascular endothelium leads to metastasis suppression. *Nature Medicine* 12:933-938.
- Bhowmick NA, Chytil A, Plieth D, Gorska AE, Dumont N, Shappell S, Washington MK, Neilson EG, Moses HL (2004): TGF-beta signaling in fibroblasts modulates the oncogenic potential of adjacent epithelia. *Science* 303:848-851.
- Bissell MJ, Radisky D (2001): Putting tumours in context. *Nature Reviews Cancer* 1:46-54.
- Borsig L, Wong R, Hynes RO, Varki NM, Varki A (2002): Synergistic effects of L- and P-selectin in facilitating tumor metastasis can involve non-mucin ligands and implicate leukocytes as enhancers of metastasis. *PNAS* 99:2193-2198.
- Brown DM, Ruoslahti E (2004): Metadherin, a novel cell-surface protein in breast tumors that mediates lung metastasis. *Cancer Cell* 5:365-374.
- Butler TP, Gullino PM (1975): Quantitation of cell shedding into efferent blood of mammary adenocarcinoma. *Cancer Research* 35:512-516.
- Cameron MD, Schmidt EE, Kerkvliet N, Nadkarni KV, Morris VL, Groom AC, Chambers AF, MacDonald IC (2000): Temporal progression of metastasis in lung: cell survival, dormancy and location dependence of metastatic inefficiency. *Cancer Research* 60:2541-2546.
- Chambers AF, Groom AC, MacDonald IC (2002): Dissemination and growth of cancer cells in metastatic sites. *Nature Reviews Cancer* 2:563-572.
- Chi JT, Wang Z, Nuyten DS, Rodriguez EH, Schaner ME, Salim A, Wang Y, Kristensen GB, Helland A, Borresen-Dale AL, Giaccia A, Longaker MT, Hastie T, Yang GP, Vijver MJvd, Brown PO (2006): Gene expression programs in response to hypoxia: cell type specificity and prognostic significance in human cancers. *PLoS Med* 3:e47.
- Christofori G (2006): New signals from the invasive front. *Nature* 441:444-50.
- Clark EA, Golub TR, Lander ES, Hynes RO (2000): Genomic analysis of metastasis reveals an essential role for RhoC. *Nature* 406:532-535.
- Comer FI, Parent CA (2002): PI 3-Kinases and PTEN: How Opposites Chemoattract. *Cell* 109:541-544.
- Condeelis J, Segall J (2003): Intravital imaging of cell movement in tumours. *Nature Reviews Cancer* 3:921-930.
- Coussens LM, Werb Z (2002): Inflammation and Cancer. *Nature* 420:860-867.
- Croix BS, Rago C, Velculescu V, Traverso G, Romans KE, Montgomery E, Lal A, Riggins GJ, Lengauer C, Vogelstein B, Kinzler KW (2000): Genes expressed in human tumor endothelium. *Science* 289:1197-1202.
- Cunha GR, Hayward SW, Wang YZ, Ricke WA (2003): Role of the stromal microenvironment in carcinogenesis of the prostate. *International Journal of Cancer* 107:1-10.
- Cursiefen C, Chen L, Borges LP, Jackson D, Cao J, Radziejewski C, D'Amore PA, Dana MR, Wiegand SJ, Streilein JW (2004): VEGF-A stimulates lymphangiogenesis and hemangiogenesis in inflammatory neovascularization via macrophage recruitment. *J. Clin. Invest.* 113:1040-1050.
- Douma S, Laar Tv, Zevenhoven J, Meuwissen R, Garderen Ev, Peeper DS (2004): Suppression of anoikis and induction of metastasis by the neurotrophic receptor TrkB. *Nature* 430:1034-1040.

- Ewing J (1919): "Neoplastic diseases." Philadelphia: W.B. Saunders.
- Fidler IJ (1970): Metastasis: Quantitative analysis of distribution and fate of tumor embolilabeled with 125 I-5-iodo-2'-deoxyuridine. *J Natl Cancer Inst* 45:773-82.
- Fidler IJ (1973): Selection of successive tumour lines for metastasis. *Nat New Biol* 242:148-9.
- Fidler IJ (2003): The pathogenesis of cancer metastasis: the 'seed and soil' hypothesis revisited. *Nature Reviews Cancer* 3:453-458.
- Fidler IJ, Kripke ML (1977): Metastasis results from preexisting variant cells within a malignant tumor. *Science* 197:893-895.
- Friedl P, Wolf K (2003): Tumour-cell invasion and migration: diversity and escape mechanisms. *Nature Reviews Cancer* 3:362-374.
- Funamoto S, Meili R, Lee S, Parry L, Firtel R (2002): Spatial and temporal regulation of 3-phosphoinositides by PI 3-kinase and PTEN mediates chemotaxis. *Cell* 109:611-623.
- Glinsky VV, Glinsky GV, Glinsky OV, Huxley VH, Turk JR, Mossine VV, Deutscher SL, Pienta KJ, Quinn TP (2003): Intravascular metastatic cancer cell homotypic aggregation at the sites of primary attachment to the endothelium. *Cancer Research* 63:3805-3811.
- Guo W, Giancotti FG (2004): Integrin signalling during tumour progression. *Nat Rev Mol Cell Biol* 5:816-26.
- Gupta GP, Massague J (2006): Cancer metastasis: building a framework. *Cell* 127:679-695.
- Gupta PB, Kuperwasser C, Brunet JP, Ramaswamy S, Kuo WL, Gray JW, Naber SP, Weinberg RA (2005): The melanocyte differentiation program predisposes to metastasis after neoplastic transformation. *Nature Genetics* 37:1047-1054.
- Hamano Y, Zeisberg M, Sugimoto H, Lively JC, Maeshima Y, Yang C, Hynes RO, Werb Z, Sudhakar A, Kalluri R (2003): Physiological levels of tumstatin, a fragment of collagen IV alpha3 chain, are generated by MMP-9 proteolysis and suppress angiogenesis via alphaV beta3 integrin. *Cancer Cell* 3:589-601.
- Homey B, Muller A, Zlotnik A (2002): Chemokines: agents for the immunotherapy of cancer? *Nature Reviews Immunology* 3:175-184.
- Hood JD, Cheresh DA (2002): Role of integrins in cell invasion and migration. *Nature Reviews Cancer* 2:91-100.
- Hoshida T, Isaka N, Hagendoorn J, Tomaso Ed, Chen YL, Pytowski B, Fukumura D, Padera TP, Jain RK (2006): Imaging steps of lymphatic metastasis reveals that vascular endothelial growth factor-C increases metastasis by increasing delivery of cancer cells to lymph nodes: therapeutic implications. *Cancer Research* 66:8065-8075.
- Hynes RO (2003): Metastatic potential: genetic predisposition of the primary tumor or rare, metastatic variants-or both? *Cell* 113:821-823.
- Hynes RO, Lander AD (1992): Contact and adhesive specificities in the associations, migrations, and targeting of cells and axons. *Cell* 68:303-22.
- Kang Y, Siegel PM, Shu W, Drobnjak M, Kakonen SM, Cordon-Cardo C, Guise TA, Massague J (2003): A multigenic program mediating breast cancer metastasis to bone. *Cancer Cell* 6:537-49.
- Khanna C, Wan X, Bose S, Cassaday R, Olomu O, Mendoza A, Yeung C, Gorlick R, Hewitt SM, Helman LJ (2004): The membrane-cytoskeleton linker ezrin is necessary for osteosarcoma metastasis. *Nature Medicine* 10:182-186.
- Kim J, Yu W, Kovalski K, Ossowski L (1998): Requirement for specific proteases in cancer cell intravasation as revealed by a novel semiquantitative PCR-based assay. *Cell* 94:353-362.
- Krause T, Turner GA (1999): Are selectins involved in metastasis? *Clinical & Experimental Metastasis* 17:183-192.
- Kuperwasser C, Chavarria T, Wu M, Magrane G, Gray JW, Carey L, Richardson A, Weinberg RA (2004): Reconstruction of functionally normal and malignant human breast tissues in mice. *PNAS* 101:4966-4971.
- Kurrey NK, A K, Bapat SA (2005): Snail and Slug are major determinants of ovarian cancer invasiveness at the transcription level. *Gynecologic Oncology* 97:155-165.
- Lopez T, Hanahan D (2002): Elevated levels of IGF-1 receptor convey invasive and metastatic capability in a mouse model of pancreatic islet tumorigenesis. *Cancer Cell* 1:339-353.
- Luria SE, Delbruck M (1943): Mutations of bacteria from virus sensitivity to virus resistance. *Genetics* 28:491-511.

- Luzzi KJ, MacDonald IC, Schmidt EE, Kerkvliet N, Morris VL, Chambers AF, Groom AC (1998): Multistep nature of metastatic inefficiency. *American Journal of Pathology* 153:865-873.
- Lynch CC, Matrisian LM (2002): Matrix metalloproteinases in tumor-host cell communication. *Differentiation* 70:561-573.
- Martin SS, Ridgeway AG, Pinkas J, Lu Y, Reginato MJ, Koh EY, Michelman M, Daley GQ, Brugge JS, Leder P (2004): A cytoskeleton-based functional genetic screen identifies Bcl-xL as an enhancer of metastasis, but not primary tumor growth. *Oncogene* 26:4641-4645.
- Maurer CA, Graber HU, Friess H, Beyermann B, Willi D, Netzer P, Zimmermann A, Buchler MW (1999): Reduced expression of the metastasis suppressor gene KAI1 in advanced colon cancer and its metastases. *Surgery* 126:869-80.
- Mehlen P, Puisieux A (2006): Metastasis: a question of life or death. *Nat Rev Cancer* 6:449-58.
- Minn AJ, Gupta GP, Siegel PM, Bos PD, Shu W, Giri DD, Viale A, Olshen AB, Gerald WL, Massague J (2005): Genes that mediate breast cancer metastasis to lung. *Nature* 436:518-524.
- Moore MA (2001): The role of chemoattraction in cancer metastasis. *BioEssays* 23:674-676.
- Muller A, Homey B, Soto H, Ge N, Catron D, Buchanan ME, McClanahan T, Murphy E, Yuan W, Wagner SN, Barrera JL, Mohar A, Verastegui E, Zlotnik A (2001): Involvement of chemokine receptors in breast cancer metastasis. *Nature* 410:50-56.
- Nathanson SD (2003): Insights into the mechanisms of lymph node metastasis. *Cancer* 98:413-423.
- O'Reilly MS, Holmgren L, Shing Y, Chen C, Rosenthal RA, Moses M, Lane WS, Cao Y, Sage EH, Folkman J (1994): Angiostatin: a novel angiogenesis inhibitor that mediates the suppression of metastases by a Lewis lung carcinoma. *Cell* 79:315-28.
- Oft M, Akhurst RJ, Balmain A (2002): Metastasis is driven by sequential elevation of H-ras and Smad2 levels. *Nature Cell Biology* 4:487-494.
- Olumi AF, Grossfeld GD, Hayward SW, Carroll PR, Tlsty TD, Cunha GR (1999): Carcinoma-associated fibroblasts direct tumor progression of initiated human prostatic epithelium. *Cancer Research* 59:5002-5011.
- Orimo A, Gupta PB, Sgroi DC, Arenzana-Seisdedos F, Delaunay T, Naeem R, Carey VJ, Richardson AL, Weinberg RA (2005): Stromal fibroblasts present in invasive human breast carcinomas promote tumor growth and angiogenesis through elevated SDF-1/CXCL12 secretion. *Cell* 121:335-348.
- Paget S (1889): The distribution of secondary growths in cancer of the breast. *Lancet* 1:571-3.
- Pantel K, Cote RJ, Fodstad O (1999): Detection and clinical importance of micrometastatic disease. *Journal of the National Cancer Institute* 91:1113-1124.
- Park YG, Zhao X, Lesueur F, Lowy DR, Lancaster M, Pharoah P, Qian X, Hunter KW (2005): Sipa1 is a candidate for underlying the metastasis efficiency modifier locus Mtes1. *Nature Genetics* 37:1055-1062.
- Perl AK, Wilgenbus P, Dahl U, Semb H, Christofori G (1998): A causal role for E-cadherin in the transition from adenoma to carcinoma. *Nature* 392:190-193.
- Qian F, Hanahan D, Weissman IL (2001): L-selectin can facilitate metastasis to lymph nodes in a transgenic mouse model of carcinogenesis. *PNAS* 98:3976-3981.
- Ramaswamy S, Ross KN, Lander ES, Golub TR (2003): A molecular signature of metastasis in primary solid tumors. *Nature Genetics* 33:49-54.
- Ridley AJ, Schwartz MA, Burridge K, Firtel RA, Ginsberg MH, Borisy G, Parsons JT, Horwitz AR (2003): Cell migration: integrating signals from front to back. *Science* 302:1704-9.
- Robinson SD, Frenette PS, Rayburn H, Cumiskey M, Ullman-Cullere M, Wagner DD, Hynes RO (1999): Multiple, targeted deficiencies in selectins reveal a predominant role for P-selectin in leukocyte recruitment. *PNAS* 96:11452-7.
- Ruoslahti E (2002): Specialization of tumour vasculature. *Nature Reviews Cancer* 2:83-90.
- Sahai E, Marshall CJ (2003): Differing modes of tumour cell invasion have distinct requirements for Rho/ROCK signalling and extracellular proteolysis. *Nature Cell Biology* 5:711-718.
- Scapini P, Morini M, Tecchio C, Minghelli S, Carlo ED, Tanghetti E, Albini A, Lowell C, Berton G, Noonan DM, Cassatella MA (2004): CXCL1/macrophage inflammatory protein-2-induced angiogenesis in vivo is mediated by neutrophil-derived vascular endothelial growth factor-A. *The Journal of Immunology* 172:5034-5040.

- Schmidt-Kittler O, Ragg T, Daskalakis A, Granzow M, Ahr A, Blankenstein TJ, Kaufmann M, Diebold J, Arnholdt H, Muller P, Bischoff J, Harich D, Schlimok G, Riethmuller G, Eils R, Klein CA (2003): From latent disseminated cells to overt metastasis: genetic analysis of systemic breast cancer progression. *PNAS* 100:7737-7742.
- Siegel PM, Shu W, Cardiff RD, Muller WJ, Massague J (2003): Transforming growth factor beta signaling impairs Neu-induced mammary tumorigenesis while promoting pulmonary metastasis. *PNAS* 100:8430-8435.
- Simpson MA, Reiland J, Burger SR, Furcht LT, Spicer AP, Jr. TRO, McCarthy JB (2001): Hyaluronan synthase elevation in metastatic prostate carcinoma cells correlates with hyaluronan surface retention, a prerequisite for rapid adhesion to bone marrow endothelial cells. *JBC* 276:17949-17057.
- Sorlie T, Tibshirani R, Parker J, Hastie T, Marron JS, Nobel A, Deng S, Johnsen H, Pesich R, Geisler S, Demeter J, Perou CM, Lonning PE, Brown PO, Borresen-Dale AL, Botstein D (2003): Repeated observation of breast tumor subtypes in independent gene expression data sets. *PNAS* 100:8418-23.
- Sternlicht MD, Lochter A, Sympon CJ, Huey B, Rougier JP, Gray JW, Pinkel D, Bissell MJ, Werb Z (1999): The stromal proteinase MMP3/stromelysin-1 promotes mammary carcinogenesis. *Cell* 98:137-146.
- Stupack DG, Teitz T, Potter MD, Mikolon D, Houghton PJ, Kidd VJ, Lahti JM, Cheresch DA (2006): Potentiation of neuroblastoma metastasis by loss of caspase-8. *Nature* 439:95-9.
- Swartz MA, Kristensen CA, Melder RJ, Roberge S, Calautti E, Fukumura D, Jain RK (1999): Cells shed from tumours show reduced clonogenicity, resistance to apoptosis, and in vivo tumorigenicity. *British Journal of Cancer* 81:756-759.
- Thiery J (2002): Epithelial-mesenchymal transitions in tumor progression. *Nature Reviews Cancer* 2:442-454.
- van't Veer LJ, Dai H, Vijver MJvd, He YD, Hart AA, Mao M, Peterse HL, Kooy Kvd, Marton MJ, Kiteveen AT, Schreiber GJ, Kerkhoven RM, Roberts C, Linsley PS, Bernards R, Friend SH (2002): Gene expression profiling predicts clinical outcome of breast cancer. *Nature* 415:530-535.
- Wang H, Fu W, Im JH, Zhou Z, Santoro SA, Iyer V, DiPersio CM, Yu QC, Quaranta V, Al-Mehdi A, Muschel RJ (2004): Tumor cell alpha3beta1 integrin and vascular laminin-5 mediate pulmonary arrest and metastasis. *J Cell Biol* 164:935-41.
- Wang W, Goswami S, Sahai E, Wyckoff JB, Segall JE, Condeelis JS (2005): Tumor cells caught in the act of invading: their strategy for enhanced cell motility. *Trends in Cell Biology* 15:138-145.
- Webb DJ, Horwitz AF (2003): New dimensions in cell migration. *Nature Cell Biology* 5:690-692.
- Weiss L (1992): Comments on hematogenous metastatic patterns in humans as revealed by autopsy. *Clin Exp Metastasis* 10:191-9.
- Welch DR, Steeg PS, Rinker-Schaeffer CW (2000): Molecular biology of breast cancer metastasis. Genetic regulation of human breast carcinoma metastasis. *Breast Cancer Research* 2:408-16.
- Wiley HE, Gonzalez EB, Maki W, Wu M, Hwang ST (2001): Expression of CC chemokine receptor-7 and regional lymph node metastasis of B16 murine melanoma. *Journal of the National Cancer Institute* 93:1638-1643.
- Wittekind C (2000): Diagnosis and staging of lymph node metastasis. *Recent Results in Cancer Research: Lymphatic Metastasis and Sentinel Lymphonodectomy* 157:20-28.
- Wong CW, Song C, Grimes MM, Fu W, Dewhirst MW, Muschel RJ, Al-Mehdi A (2002): Intravascular location of breast cancer cells after spontaneous metastasis to the lung. *American Journal of Pathology* 161:749-753.
- Wyckoff J, Wang W, Lin EY, Wang Y, Pixley F, Stanley ER, Graf T, Pollard JW, Segall J, Condeelis J (2004): A paracrine loop between tumor cells and macrophages is required for tumor cell migration in mammary tumors. *Cancer Research* 64:7022-7029.
- Wyckoff JB, Jones JG, Condeelis JS, Segall JE (2000): A critical step in metastasis: in vivo analysis of intravasation at the primary tumor. *Cancer Research* 60:2504-2511.

- Xu L, Begum S, Hearn JD, Hynes RO (2006): GPR56, an atypical G protein-coupled receptor, binds tissue transglutaminase, TG2, and inhibits melanoma tumor growth and metastasis. *PNAS* 103:9023-9028.
- Yamaguchi H, Lorenz M, Kempiak S, Sarmiento C, Coniglio S, Symons M, Segall J, Eddy R, Miki H, Takenawa T, Condeelis J (2005): Molecular mechanisms of invadopodium formation: the role of the N-WASP-Arp2/3 complex pathway and cofilin. *JCB* 168:441-452.
- Yang J, Mani SA, Donaher JL, Ramaswamy S, Itzykson RA, Come C, Savagner P, Gitelman I, Richardson A, Weinberg RA (2004): Twist, a master regulator of morphogenesis, plays an essential role in tumor metastasis. *Cell* 117:927-939.
- Yoshida BA, Sokoloff MM, Welch DR, Rinker-Schaeffer CW (2000): Metastasis-suppressor genes: a review and perspective on an emerging field. *Journal of the National Cancer Institute* 92:1717-1730.
- Zeidman I, McCutcheon M, Coman DR (1950): Factors affecting the number of tumor metastases; experiments with a transplantable mouse tumor. *Cancer Research* 10:357-9.

CHAPTER 2.

DERIVATION AND ANALYSIS OF METASTATIC VARIANTS OF THE HUMAN PROSTATE CANCER CELL LINE PC-3

The work in this chapter was conceived by Sunny Wong, Herbert Haack and Richard Hynes. PC-3 cell lines were isolated from derivatives originally generated by Herbert Haack. Bioinformatics analysis was assisted by Steve Shen and Charlie Whittaker. The contents of this chapter were written by Sunny Wong, with editing by Richard Hynes.

INTRODUCTION

Mouse Models of Prostate Cancer

The major deterrent for studying metastasis stems from difficulties in observing and modeling the process in an experimentally tractable system. Without a doubt, the question of how tumors metastasize remains an amazingly challenging problem: the process is ephemeral, prone to stochasticity, difficult to observe directly, and immensely complex, both in terms of the complicated networks of genes involved, as well as the cellular interactions needed for metastasis to occur. While mouse models can approximate many of the steps of metastasis, even now, they provide a relatively low resolution view of what is actually taking place. Perhaps the best way to begin approaching this complex problem is to focus on specific genes or steps involved in the process. In this regard, the choice of a suitable model system to utilize is especially key.

Prostate cancer (CaP) is a disease of old age, and as such, mice do not ordinarily develop CaP, as they are more likely to succumb to other cancers or malignancies earlier in life[Shappell et al., 2004]. The sorts of experimental manipulations that do produce prostate cancer in mice generally fall into two categories: prostate cells (often transformed) can be introduced, or xenografted, from an outside source; or the animal itself can be genetically manipulated either through deletion or mis-expression of a gene (or genes) to develop prostate cancer spontaneously. Both types of manipulations have their advantages and disadvantages. While xenograft models provide the experimenter with systems that can readily be manipulated and are often less prone to variability, they are also, by their very nature, highly artificial methods for studying CaP. Spontaneous models, on the other hand, can offer more realistic views of prostate cancer, yet this realism comes at an experimental price: they are not easily manipulated, the tumors take longer to progress, and the variability inherent in these systems is often quite high. An ideal approach, therefore, might involve initially testing hypotheses using the first model, then validating findings in the second. Of course, the ultimate goal is to determine whether the findings that come out of these studies are relevant to the human situation and whether they bear even some degree of universal truth—a lofty standard, no doubt, but nonetheless, a critical one.

Xenograft Transplantation Models of Prostate Cancer

Xenograft models have traditionally involved injecting established cancer cell lines into immunodeficient mice. Three of the most frequently used human prostate adenocarcinoma cell lines were all derived in the late 1970s, and include PC-3 and DU-145 cells, which are both androgen-independent; and LNCaP cells, which are androgen-dependent[Horoszewicz et al., 1980; Kaighn et al., 1979; Mickey et al., 1977]. All three were derived from metastases that had arisen, respectively, in the lumbar vertebra, the brain and

in the left supraclavicular lymph node of human clinical patients. When injected subcutaneously underneath the skin, these cells have all been reported to form tumors, but in most cases, metastasis is rare or infrequent [Horoszewicz et al., 1980; Mickey et al., 1977; Stephenson et al., 1992]. Although intravenous injection of tumor cells into the bloodstream can often yield systemic metastases, such an approach is useful only for modeling the later stages of the process, subsequent to intravasation of cells into the bloodstream. In addition, while metastases in the lungs and liver often arise from intravenous injection of tumor cells, other physiologically relevant sites such as lymph nodes are rarely invaded.

A better model for tumor progression involves injecting cancer cells not underneath the skin, but rather, directly into the anatomical site most akin to the tissue of origin of these cells—in this case, into the mouse prostate. Such an approach, known as an *orthotopic* injection, has been reported to yield aggressive primary tumors for both PC-3 and LNCaP cells that frequently metastasize to the draining para-aortic/lumbar lymph nodes and, in the case of PC-3 cells, to lungs [Pettaway et al., 1996; Rembrink et al., 1997; Stephenson et al., 1992]. Although it remains unclear why prostate tumors metastasize more efficiently when introduced into the orthotopic, rather than subcutaneous, site, part of the explanation may have to do with prostate-specific stromal factors that evoke the invasive phenotype. Indeed, many recent studies have focused attention on the role of the tumor microenvironment in promoting cancer progression, as described in Chapter 1. In addition, experiments showing that stromal cells can promote tumorigenesis and metastasis when co-injected with malignant cells are in concordance with the hypothesis that the prostate microenvironment is a crucial regulator of tumor aggressiveness [Cunha et al., 2003].

However, even injecting tumor cells into the prostate presents certain problems and limitations. Because the cells are in fluid suspension when introduced as a single bolus injection, there is an absence of cell-cell contacts and supporting tissue architecture [Wang et al., 1999]. As a result, an element of artificiality is introduced. In addition, such an approach fails to reproduce the earliest step in metastasis—that is, the de-adhesion of invading cells away from the bulk of the primary tumor. Injecting tumor cells into the prostate, or any organ, for that matter, may also have other unforeseen consequences. In experiments where the dispersal of luciferase-expressing PC-3 cells was tracked following intramuscular injection, cells were found not long afterwards in numerous sites, including the femur, lungs and liver [Rubio et al., 2000]. This was likely not attributable to metastasis, at least as one normally envisions the process, but rather, to the leakage of cells away from the primary site of injection. Clearly, better systems are needed to model more precisely the many steps of the metastatic cascade.

To begin to address some of these concerns, An et al., in 1998 described a method for grafting solid PC-3-derived tumors into the prostate [An et al., 1998]. Termed “surgical orthotopic implantation” (SOI), this technique involves transplanting solid fragments of tumor material harvested from subcutaneous tumors

into the ventral or dorsal lobes of the prostate. The resulting primary tumors were reported to display an enhanced propensity to metastasize to the lymph nodes and lungs, in some cases even beyond the capacity previously observed for orthotopic injection[An et al., 1998; Hoffman, 1999]. When green fluorescent protein-labeled PC-3 cells were implanted by SOI, micrometastases were also observed in visceral organs such as the liver and kidneys, as well as in various parts of the mouse skeleton, including the skull, ribs, pelvis, femur and tibia[Yang et al., 1999]. The presence of skeletal metastases was an especially important observation, given that CaP frequently metastasizes to bone in human patients, but rarely does so in animal models, as will be discussed later. SOI has also been touted as a technique that circumvents problems previously seen when tumor cells are artificially dispersed following injection, and, in addition, provides a three-dimensional microenvironment where the metastatic potential of a tumor can be realized, and where all the relevant steps in this process can be recreated[Hoffman, 1999]. Therefore, SOI may provide the most accurate xenograft model of human prostate cancer in the mouse.

Spontaneous Mouse Models of Prostate Cancer

In spite of the many advantages offered by xenotransplant models, these are also, by their very nature, highly artificial systems. Spontaneous tumor models of CaP likely provide more realistic approximations of prostate cancer progression in the mouse, and, ideally, the genes most commonly deregulated in human CaP would also yield tumors when mis-expressed in mice. In human prostate cancer, abnormalities in chromosome region 8p12-8p22 are found in 80% of cases, while disruptions in region 10q are also associated with 50-80% of malignancies[Abate-Shen and Shen, 2000]. The homeobox transcription factor Nkx3.1 is important for prostate development and maps to the region on 8p, while the lipid phosphatase PTEN is found at 10q. Indeed, mice heterozygous for either Nkx3.1 or PTEN develop prostate intraepithelial neoplasia (PIN), although the lesions are relatively mild and non-invasive, and the time to onset is long—typically, > 12 months, with some variation depending on genetic background[Bhatia-Gaur et al., 1999; Kwabi-Addo et al., 2001]. PTEN^{+/-} mice that also lack the tumor suppressors p27, Nkx3.1 or Ink4a/Arf generally displayed enhanced progression of carcinogenesis, higher grade lesions and reduced survival, relative to mice mutant for any single one of these genes[Park et al., 2002]. However, progression to metastatic disease was not observed[Wang et al., 2003]. Subsequent studies involving Cre-mediated homozygous deletion of PTEN in the mouse prostate have reported the development of androgen-dependent adenocarcinomas by 9 weeks of age[Wang et al., 2003]. These tumors possessed upregulated Akt activity, and metastasized to the lymph nodes and lung by 12 weeks of age, but again, bone metastases were not seen.

Transgenic overexpression of oncogenes specifically in the prostate has also yielded prostate tumors. As upregulation of insulin growth factor (IGF) and of the Akt pathway are often observed in CaP, it is not surprising that overexpression of either IGF-1 or myristoylated Akt resulted in prostate

carcinogenesis[DiGiovanni et al., 2000; Majumder et al., 2003]. In the case of Akt transgenic mice, PIN was observed in the ventral prostates and was later shown to depend, at least in part, upon activation of S6 kinase, a component of the TOR pathway[Majumder et al., 2004]. These lesions, however, never progressed to invasive carcinomas even after 78 weeks of age[Majumder et al., 2003]. In the case of IGF-1 transgenic mice, PIN and focal areas of adenocarcinoma were seen in both the dorsal and ventral prostate lobes of mice at 6 months of age, and this was associated with upregulated activity of PI-3 kinase, an upstream activator of Akt[DiGiovanni et al., 2000]. However, as before, there was also no evidence of metastatic spread.

The TRAMP Prostate Cancer Model

Although there has been recent emphasis on developing tumor models that recapitulate, at least in part, the genetic abnormalities most often deregulated in human cancers [Dyke and Jacks, 2002], perhaps the most widely used spontaneous model of CaP involves transgenic overexpression of a gene that has never caused prostate cancer in any human individual. First described by Greenberg et al., in 1995, the Transgenic Adenocarcinoma of the Mouse Prostate (TRAMP) model relies upon the prostate-specific, rat probasin-promoter-driven expression of the Simian virus 40 (SV40) large T antigen[Greenberg et al., 1995]. SV40 inhibits the tumor suppressors pRb and p53¹, and transgenic expression of this gene in various organs, including the mouse mammary glands and pancreas, has reliably yielded tumors. In the TRAMP model, mice develop multi-focal prostate hyperplasia beginning at 10 weeks of age, and these foci progress to PIN and metastatic carcinomas after another 14-30 weeks [Gingrich et al., 1996]. The tumors themselves begin as androgen-dependent lesions but can manifest hormone-independent disease after androgen ablation therapy [Gingrich et al., 1997]. Although the precise time to onset varies significantly with genetic background, with pure C57BL/6 TRAMP mice displaying the slowest rate of spontaneous tumor progression and FVB/TRAMP mice exhibiting the fastest rate², metastases to the lymph nodes and lungs have been reported in older mice[Gingrich et al., 1997], and, at least in one case, extensive spinal metastases were observed[Gingrich et al., 1996].

The TRAMP model has also been useful for studying the modifying effects of other genes that, when mis-expressed on their own, either do not cause prostate cancer in the mouse, or lead to relatively mild tumorigenic phenotypes. For instance, mice heterozygous for PTEN, when also bearing the TRAMP transgene, displayed accelerated tumor progression relative to wild-type TRAMP mice[Kwabi-Addo et al., 2001]. Similarly, overexpression of the apoptosis inhibitor Bcl2 in TRAMP prostates enhanced the onset of carcinogenesis[Bruckheimer et al., 2000]. Hepsin, a transmembrane serine protease, is upregulated in 90% of prostate cancers, and, interestingly, probasin-promoter-driven overexpression of this gene in the

¹ Inhibition of these two tumor suppressors has been shown to be necessary but insufficient for transformation. Therefore, other as-yet unknown factors are likely affected by expression of SV40 large T antigen.

² <http://thegreenberglab.fhrc.org/protocols/TRAMPBreedingScheme.pdf>

prostate caused a weakening of the basement membranes that normally separate the epithelial and stromal layers[Dhanasekaran et al., 2001; Klezovitch et al., 2004]. Laminin and collagen staining appeared disorganized and fragmentary, but these mice did not develop prostate cancer. However, when hepsin overexpression was combined with a mouse model similar to TRAMP (LPB-Tag, which does not metastasize), doubly transgenic animals developed macrometastases to the lung and liver[Klezovitch et al., 2004]. Furthermore, at least 24% of 21 week old animals bore metastases to the bone.

Absence of Bone Metastasis in Mouse Models of Prostate Cancer

While each of these systems clearly has its own unique advantages and disadvantages, a common drawback of all these models, with perhaps the exception of Hepsin-Tag doubly transgenic mice, is the relative absence of bone metastases. Even in the case of the Hepsin experiments, the remarkable metastatic phenotypes observed were elicited only after significant overexpression of the transgene in the mouse prostate, which normally does not express any detectable levels of Hepsin[Klezovitch et al., 2004]. In other models, microscopic deposits of tumor cells in the bone were reported only after exhaustive approaches were taken to detect metastases or, otherwise, these were extremely rare events—certainly, a far cry from what is typically seen in the clinic, where 90% of human CaP patients with hematogenous spread have been reported to possess osseous invasion[Bubendorf et al., 2000]. The paucity of bone metastasis seen in the mouse models remains a major hurdle in the field. The hepsin experiments, and possibly others, have suggested that proper tumor-stromal interactions—both at the primary tumor and at the site of invasion—may not be taking place to encourage the formation of skeletal metastases in mice. This would be consistent with Paget's "seed and soil" hypothesis, as described in Chapter 1.

In contrast, others have speculated that anatomical differences in the plexus of veins that surround the prostate and urogenital systems (Batson's plexus) may account for the absence of bone metastases in rodents[Resnick, 1992; Shiraid and Ito, 1992]. In humans, well-developed anastomoses between the pelvic and vertebral vein systems may allow shunting of venous blood directly from the prostate to the spine, and, therefore, tumor cells could potentially reach the bone without having to enter systemic circulation. Indeed, radiolabelled tracers introduced into the human prostatic plexus of veins have been observed to reach the lower lumbar spine without having to pass through the inferior vena cava[Shiraid and Ito, 1992]. In rodents, the venous communications between the pelvic and vertebral systems are not as extensive. In addition, others have also hypothesized that high abdominal pressure in humans may re-direct the flow of blood towards the vertebral plexus, whereas rodents display relatively reduced abdominal pressure, owing to their non-erect posture[Shiraid and Ito, 1992]. Compellingly, several studies have shown that temporary occlusion of the inferior vena cava can re-direct the flow of abdominal blood and of intravenously-injected tumor cells towards the vertebral column[Harada et al., 1992; Nishijima et al., 1992; Shevrin et al., 1988]. Occluded animals frequently developed spinal lesions and, in

some cases, hind limb paralysis, while non-occluded control animals bore lung metastases, but in no cases was skeletal invasion observed. Bone tumors have also been reported when PC-3 or LNCaP cells were introduced by direct intra-tibial injection into the bone [Corey et al., 2002]. These results, therefore, seem to lend support to hypotheses first put forth by James Ewing, who proposed in the 1920s that patterns of blood flow, rather than “seed and soil,” were the major determinants of organ-specific metastasis. Likely, both his and Paget’s hypotheses are valid and are certainly not mutually exclusive, as distinct processes are likely to influence the patterns of metastasis at different temporal points of progression.

Experimental Approach

Metastasis is unquestionably a complicated process, and, given the available systems for studying prostate cancer progression in mice, we elected to begin our studies by focusing on the SOI xenograft approach. The major advantage of using SOI—that it models the earliest steps of metastasis—made this technique especially attractive, despite the fact that it is probably the most technically difficult of all the methods described thus far for introducing tumor cells into the mouse. Using SOI, we decided to carry out a screen to identify genes important for the metastatic process. This was similar to the screen described previously by Clark et al., where metastatic variants of a melanoma cell line were derived and analyzed by microarrays to identify potential metastasis genes³ [Clark et al., 2000]. We decided to focus our studies on derivatives of the cell line PC-3, mostly because these cells grow well in culture and when implanted *in vivo*. The rest of this chapter describes the derivation and initial characterization of these cell lines, as well the gene expression analyses that were performed on them. In subsequent chapters, we make use of these cells and the SOI technique to validate our gene candidates, as well as to study how prostate cancer spreads via the lymphatics and bloodstream. In all cases, we have turned to the TRAMP spontaneous tumor model to make additional observations in an attempt to test our findings from the SOI model. Whenever possible, we have also tried to view our results and their implications in light of what others have previously reported for human clinical prostate cancer. We believe that this combination of approaches is especially important, given the complexity and heterogeneity of this disease.

RESULTS

Establishment of an orthotopic xenograft mouse model of prostate cancer progression

As described earlier, tumor fragments derived from the human prostate adenocarcinoma cell line PC-3 can be introduced into immunodeficient mice using surgical orthotopic implantation (SOI) to generate a

³ For additional details, please refer to Chapter 1.

metastatic model of prostate cancer [An et al., 1998]. We began our studies by establishing this model in our laboratory and by adapting this technique to obtain reproducible results. It was also important that, by familiarizing ourselves with SOI, we could develop a set of expectations for this mouse model, both in terms of its advantages as well as its limitations. Finally, to study metastasis, it was necessary to develop methods for quantitating the spread of tumor cells. Some of these methods are described briefly below and in more detail in the Materials and Methods section (Appendix A).

We found that, typically, subcutaneous tumors from which fragments are derived for SOI required about 3 weeks of growth in CD-1 nude immunodeficient mice before transplantation (Figure 1A). Once implanted, mice began to appear moribund as a consequence of the primary tumor approximately 2 months afterwards and did not usually survive beyond 100 days post-surgery. Although we initially implanted tumors into both the mouse dorsal and ventral prostate lobes (Figure 1B), in later work, we implanted exclusively into the dorsal prostate for convenience and consistency of technique. Both approaches yielded palpable primary tumors that developed macroscopic lymph node metastases (Figures 1A and 2A). The para-aortic/lumbar lymph nodes were frequently invaded, as were the more distal renal lymph nodes. Injection of methylene blue into the prostate led to accumulation of the dye in the lumbar lymph nodes, indicating that these nodes directly drained the prostate (Figure 2B). In rare instances, metastases were also observed in the mediastinal lymph nodes and in the superficial inguinal lymph nodes, though these sites were not routinely examined.

The SOI technique also yielded tumors that formed lung micrometastases (Figure 3), though in no cases have we observed macrometastases in the lung, in other visceral organs, or in bone. By hematoxylin-and-eosin staining, the micrometastases in the lung were readily distinguishable from the rest of the lung parenchyma by their pleiomorphic nuclei, and were roughly classified according to the two-dimensional size of the metastatic cluster (Figure 3A). Metastatic deposits were observed both within the parenchyma and, in rare instances, within the lumens of blood vessels (Figure 3B). These metastatic cell clusters appeared not to have extravasated, a phenomenon first described by Al-Mehdi et al., for fibrosarcomas cells and, subsequently, by others for breast cancer [Al-Mehdi et al., 2000; Glinsky et al., 2003; Wong et al., 2002]. In at least one case, we observed a single row of tumor cells growing within a blood vessel, which was also noted by Al-Mehdi et al. Though these lung micrometastases were readily apparent, we further confirmed the prostatic origin of these cells by staining sections for the prostate-specific cell surface antigen STEAP (Figure 3B) [Hubert et al., 1999].

We found that we could recover viable tumor cells that had been circulating in hematogenous blood from animals implanted by SOI. This was accomplished by drawing whole blood from the right ventricles of tumor-bearing mice shortly after sacrifice, and cell number was quantitated by performing a colony formation assay on cultured blood (Figure 8A). We had also attempted other techniques to identify and

count rare tumor cells in circulation, including those based on flow-cytometry and human-specific quantitative Alu PCR, but both of these methods were difficult to carry out, had problems with high background, were plagued by poor and/or inconsistent detection of positive control test samples, and, importantly, did not differentiate between viable and non-viable tumor cells. Therefore, we used the colony formation assay to quantitate tumor cells in the blood, and initial control studies indicated that as few as ~5 tumor cells spiked into 100 ul of blood could be recovered, and that the plating efficiency of our different PC-3 cell lines was roughly equivalent (data not shown).

Finally, we found that we could recover, culture and expand tumor cells that had been previously implanted by SOI into mice. These were derived from the primary tumors, or from lymph node or lung metastases. Although, in most cases, these cells appeared morphologically similar to the starting PC-3 parental cell population, we confirmed the human origin of these cells by positive staining for a human-specific Class I MHC molecule (Figure 4A) and by negative staining for a mouse-specific MHC molecule marker (H-2K(b)/H-2D(b)) (Figure 4A). The human-specific antibody could also be used to identify individual tumor cells that had metastasized to lymph nodes (Figure 4B).

Overall, these preliminary studies were useful for establishing the SOI technique for prostate cancer in our laboratory, for determining how best to obtain reproducible results from this system, and for developing methods to quantitate the degree of metastatic spread both via the lymphatic and hematogenous routes. This is perhaps the greatest advantage of SOI for modeling how prostate cancer spreads—the multiple points of assay possible in a system that can also be readily manipulated to assess how perturbations in specific genes might affect different steps of the metastatic process. We make use of these assays, as well as others, in the following sections and chapters of this thesis to elucidate some of the genetic and mechanistic underpinnings of prostate cancer progression.

Derivation of the “core” PC-3 metastatic variant cell lines

Although numerous metastatic variants have been derived by us and others from PC-3 parental cells [Pettaway et al., 1996; Stephenson et al., 1992], the core cell lines used for the bulk of these studies included pMicro-1, pMicro2-#78 (also known as #78) and pMicro2-#82 (also known as #82) (Figure 5A). Derivation of these cells was initiated by Dr. Herbert Haack, a former postdoctoral researcher in the lab. PC-3 parental cells from American Type Culture Collection (ATCC) were injected subcutaneously into Balb/c nude immunodeficient mice on April 13, 2001. The subcutaneous tumors were harvested on June 1, 2001, and subsequently implanted by SOI into the ventral prostates of C57BL/6 nude immunodeficient mice. One of these mice (designated 6-1B or mouse 11V) developed a 300 mg tumor with lymph node macro-metastases when sacrificed on August 14, 2001, and single cells were dissociated from the lungs and put into culture. The cells that grew out of this culture were originally named 8-14A lung, and later,

pMicro-1, to indicate that they had been derived from micrometastases in the lung. pMicro-1 cells were then injected subcutaneously on November 1, 2001, into CD-1 nude immunodeficient mice, and tumor material was implanted into the dorsal or ventral prostates of CD-1 nude mice on December 13, 2001. From these implanted mice, mouse #78D (12-13D) was sacrificed on March 16, 2002, and mouse #82V (12-13H) was sacrificed on March 18, 2002. Each of these mice had developed bulky primary tumors with lymph node macro-metastases, and their lungs were placed into culture to isolate metastatic cells. The cells that grew out of the lungs of mouse #78D were named #78 cells; those that grew out to the lungs of mouse #82V were called #82 cells. Therefore, both #78 and #82 cells were derived from tumor cells present in the lung at the time of sacrifice, though no macroscopic lung metastases have yet to be observed from this orthotopic metastasis model.

Initial characterization of the “core” PC-3 metastatic variant cell lines

The core cell lines used in our studies—pMicro-1, #78 and #82—appeared morphologically indistinguishable *in vitro*. In all three cases, the cells attached slowly, but firmly, to tissue culture plates and did not spread well, often displaying phase enhancement at the cell borders under light microscopy. The three cell lines exhibited similar rates of growth compared to each other and to parental PC-3 cells under normal growth conditions *in vitro* (Figure 5B). When tested for migratory and invasive behavior towards serum, the cell lines also did not differ (data not shown). However, when injected as subcutaneous tumors into CD-1 nude immunodeficient mice, all three of the core cell lines formed significantly larger tumors than PC-3 parental cells that had either been injected into CD-1 or Balb/c immunodeficient mice (Figure 5C).

The overall gross genomic content of these cells was assessed by propidium iodide (PI) staining and flow cytometry. PC-3 parental cells, like most cancer cell lines, are aneuploid, and by PI staining, two major populations were identified that differed in overall genomic content by roughly a factor of two (Figure 6A, top graph, red peaks). Interestingly, the core selected cell lines possessed approximately identical genomic contents among themselves, but their ploidy levels fell between the two major populations identified within PC-3 parental cells. Comparisons made with other cell types indicated that, as expected, normal mouse lymphocyte cells displayed a low genomic content (Figure 6A, bottom graph, blue peaks), while an additional PC-3 “lymph node” line (pMacro), which was derived from a mediastinal lymph node macro-metastasis, possessed a high genomic content that exceeded even the ploidy of the highest PC-3 parental population (Figure 6A, bottom graph, green peaks). As a control for flow cytometry, when the PC-3 parental and #78 cells were pre-mixed prior to analysis, each of the peaks representing the two different cell lines could still be distinguished (Figure 6B). Furthermore, fifteen individual cell clones were isolated from the heterogeneous PC-3 parental cell population, and each of these was analyzed for genomic content. Not surprisingly, in most cases, the ploidy of these clones overlapped with one of the

two major peaks seen for the parental cells (data summarized in Figure 6C), though in some instances, a mixture of more than one clone may have yielded additional peaks.

Characterization of the core PC-3 metastatic variant cell lines by surgical orthotopic implantation

Solid tumor material derived from subcutaneous tumors from each of the three core cell lines was grafted into the dorsal prostates of CD-1 nude immunodeficient mice. After 2-3 months post-implantation, mice were sacrificed when they appeared moribund, and blood, lungs, tumors and lymph nodes were collected. Although the ages of the mice at the time of sacrifice differed slightly, the majority of lung metastases and the most severely invaded lymph nodes tended to be observed in mice that were analyzed 70-80 days after implantation (data not shown). In addition, a great majority of the para-aortic/lumbar lymph nodes recovered after SOI displayed either macroscopic or microscopic tumor metastases (see Chapter 6). Lymph nodes which were >30 mg in mass were designated as "macroscopic metastases" because they were found, in all cases, to contain significant levels of tumor invasion, as assessed by histology⁴ (see Chapter 6). In fact, those lymph nodes that exceeded >80 mg in mass were, in nearly all instances, completely replaced by tumor material. Therefore, the mass of the lymph nodes was a good measure of the degree by which tumors had metastasized via the lymphatic route, while the number of lung metastases could be used to measure the extent of hematogenous spread.

Quantitation of the masses of the draining para-aortic lumbar and renal lymph nodes revealed significant differences between the #78 and #82 cell lines. While orthotopic tumors derived from both cell lines yielded macroscopic para-aortic/lumbar lymph node metastases at about the same frequency (~70% of tumors), the average mass of the lumbar lymph nodes for #82 tumors was about two-fold greater than that of #78 tumors (176 mg. versus 90 mg., respectively; $p = 0.038$) (Figure 7A). When the masses of the more distal renal lymph nodes were assessed, there was a three-fold difference: Renal nodes from #82 tumors had an average mass of 150 mg, whereas those from #78 tumors had an average mass of 54 mg (Figure 7A). However, this difference approached, but did not exceed, statistical significance ($p = 0.064$) because of increased scatter in the data.

In terms of quantitating hematogenous dissemination, #82 tumors, on average, yielded approximately twelve-fold more lung metastases than did #78 tumors (on average, 71 micrometastases per animal versus 6 micrometastases, respectively; $p = 0.0071$) (Figure 7B). There were no statistically significant differences in terms of primary tumor size at the time of analysis ($p = 0.66$) (Figure 7B) or the number of viable circulating tumor cells recovered from the blood of these animals ($p = 0.67$) (Figure 8A). As a rough measure of the efficiency by which tumors formed micro-metastases in the lung, the total number

⁴ By comparison, uninvaded lymph nodes typically do not exceed 10 mg in dry mass.

of lung metastases for a given cell line was divided by the total number of circulating tumor cells in the blood (from only those animals which had both measurements taken). In this regard, #82 cells formed 6.1 lung micrometastases for every tumor cell recovered from the blood, whereas #78 cells formed only 0.44 lung metastases for every tumor cell recovered—or roughly, a fourteen-fold difference (Figure 8B). When the sizes of micrometastases in the lung were assessed, approximately 7% of those metastases derived from #82 tumors were greater than 20-cell clusters ($n = 78/1136$ total lung metastases observed), whereas 0% of metastases from #78 tumors exceeded that size ($n = 0/112$) (Figure 9A).

The data for the various assessments of metastasis are summarized in Figure 9B. Interestingly, the immediate precursor of both these cell lines, pMicro-1, displayed an intermediate metastatic phenotype between those of highly metastatic #82 cells and poorly metastatic #78 cells, but, in most cases, did not differ significantly from either cell line in any of the parameters used to assess metastasis. This would imply that pMicro-1 may have actually consisted of a metastatically heterogeneous population of cells, from which the #78 and #82 cell populations were subsequently isolated through *in vivo* passage. It is also reasonable to believe that additional passaging of #78 or #82 cells *in vivo* might yield cell lines that possess even more extreme metastatic characteristics.

Gene expression analysis of the core PC-3 metastatic variant cell lines

To identify genes that might be responsible for prostate cancer metastasis, we performed gene expression analysis on our selected set of core PC-3 metastatic variant cell lines. We elected to profile these cells, and not other variants of PC-3, for several reasons. First, the metastatic tendencies of the core set of pMicro-1, #78 and #82 cells were well-characterized in our orthotopic system, and had yielded significantly different invasive behaviors that could not merely be explained by differential growth of the primary tumor. In addition, many of the other cell lines, including the parental PC-3 cells and others, did not grow readily in mice, either as subcutaneous or orthotopic tumors. And importantly, our ploidy analysis revealed that the overall genomic content of the core metastatic variant cells most resembled one another, while exhibiting gross differences from those of other cells, such as PC-3 parentals. Although the gene expression effects manifested from chromosome-wide duplications and deletions are unclear, it is possible that hundreds, if not thousands, of genes irrelevant to the metastatic phenotype might be mis-expressed among cell lines that differed at such a drastic genomic level. Therefore, these were all justifications for our decision to focus on our three core cell lines.

We used RNA from three independent subcutaneous tumors derived from each cell line for gene expression profiling. Subcutaneous tumors, rather than cells grown *in vitro*, were previously used to profile melanoma cell lines that differed in metastatic potential, and may be less susceptible to random fluctuations in gene expression than cells grown in tissue culture (personal communication, Dr. E. A.

Clark). As expected, clustering analysis performed by dChip revealed that the gene expression profiles of independent replicate tumor samples were more closely related to one another than to tumors derived from other cell lines (Figure 10A). Among genes which were differentially expressed between highly metastatic #82 and poorly metastatic #78 cells, there was a notable enrichment for those whose protein products were classified by gene ontology to affect cell adhesion, matrix assembly and cytoskeletal regulation (Figures 10B-C; for complete list, please see Appendix E). Some of these genes upregulated in highly metastatic #82 cells included carcinoembryonic antigen-related cell adhesion molecule 5 (CAECAM5); thrombospondin-1; and cysteine-rich, angiogenic inducer 61 (CYR61). Genes downregulated in highly metastatic cells included connexin 43; bone morphogenetic protein 2 (BMP2); Rho GDI α ; and matrix metalloproteinase 1 (MMP1). Interesting, at least three members of the insulin growth factor (IGF) signaling pathway (IGF binding protein-3 and -6; and IGF 1 receptor) were also among the top genes upregulated in highly metastatic cells, as was the gene encoding interleukin 8, a pro-angiogenic factor previously found to be overexpressed in breast cancer cells that preferentially metastasized to bone[Kang et al., 2003].

However, we were particularly struck by two genes that came out of this analysis: erythrocyte membrane protein band 4.1-like 3 (also known as 4.1B, or DAL-1; ID# NM_012307); and secreted protein, acidic, cysteine-rich (also known as SPARC, osteonectin or BM-40; ID# NM_003118). Both these genes were severely downregulated in highly metastatic #82 cells relative to #78, were represented at the “top” of our list with multiple probe sets, and have previously been assigned cell biological functions that could affect the metastatic phenotype[Framson and Sage, 2004; Sun et al., 2002]. Coincidentally, 4.1B had recently been identified by a former M.I.T. post-doctoral researcher in our laboratory, Dr. Joseph McCarty, as a novel interactor of integrin β 8, and another former M.I.T. post-doctoral researcher in Dr. Tyler Jacks’s laboratory, Dr. Joseph Kissil, had generated 4.1B-deficient mice[McCarty et al., 2005; Yi et al., 2005]. Thus, not only was 4.1B the second most downregulated gene in our highly metastatic cells, but also there was biological justification for its possible role in metastasis, as well as reagents readily available to test that hypothesis. We took this fortuitous convergence of events as a good sign and proceeded to characterize the role of 4.1B in prostate cancer progression and metastasis, as described in Chapter 3. For many of the same reasons, we also examined whether SPARC, a matrix protein component, was involved, and the results of that work are described in Chapter 4.

DISCUSSION

The results from this chapter lay the foundation for subsequent studies in this thesis in three ways: we validated the SOI system as a reliable model for studying prostate cancer progression; we derived and characterized three metastatic variant cell lines that were used for the majority of our studies; and we performed gene expression analysis on these cells to identify candidates that might be causal for the

different metastatic phenotypes. Therefore, we now have the techniques and approaches needed to study metastasis; in the following chapters, we make use of these tools.

As expected, our experience with SOI has shown that this system is technically challenging and, in total, requires between 3-4 months before results can be obtained. In spite of this, we found it highly advantageous that SOI readily yields primary tumors in the prostate which often metastasize via the lymphatic and hematogenous routes. The fact that we could also isolate and quantitate viable, circulating tumor cells in the blood was another benefit; however, aside from lymph nodes, we have not yet detected any macrometastases from this system. It is unclear exactly why this is the case, but a likely explanation is that additional time is needed for these metastases to develop. Indeed, we have previously seen that intravenous injection of PC-3 cells can yield macroscopic lung and even bone metastases after 3 months (data not shown). Although animals implanted by SOI can often live up to 3 months, it is unclear when the primary orthotopic tumor actually begins to metastasize during this period. As will be discussed in Chapter 5, hematogenous dissemination of tumor cells was observed only after lymphatic spread; consequently, entrance of tumor cells into the blood might occur quite late. In any case, we found the SOI system to be a manageable model of CaP, and, because it recapitulates even the earliest steps of metastasis, this system has allowed us to obtain some interesting and pertinent results, as will be described in the subsequent chapters.

We derived the core cell lines used in our studies by repeated *in vivo* passaging using the SOI model. pMicro-1 cells were descendent from PC-3 parental cells, and, in turn, gave rise to #78 and #82 cells. *In vivo* characterization of these cells revealed that #82 cells were highly metastatic, that #78 cells were relatively poorly metastatic, and that pMicro-1 cells displayed an intermediate metastatic phenotype between these two. These results were slightly surprisingly, given that we had originally expected the metastatic potential of these cells to increase with each round of *in vivo* passage; in other words, we had initially expected #78 and #82 cells to be equally or more metastatic than their common predecessor, pMicro-1. We speculate that pMicro-1 may be a mixed population of highly and poorly metastatic cells, and, since we had derived both #78 and #82 by nondiscriminately culturing dissociated cells that were present in the lung, #82 cells may have consisted of actual pulmonary micro-metastases, whereas #78 cells may have been derived from cells that had merely been circulating in the blood within the lungs at the time of sacrifice. However, we had also realized that knowledge concerning the precise origins of these cells was not critical for completing the goals of our later studies. What was essential was that we had derived a set of related cell lines that differed significantly in metastatic potential, and that, as shown from the ploidy experiments, these cells did not vary so drastically at the genomic level that pinpointing the right gene(s) responsible for metastasis would be impossible.

We therefore proceeded to examine these three cell lines by gene expression analysis. We derived RNA, then eventually cDNA and cRNA, from three independent subcutaneous tumors for each of our three cell lines. Although we had originally carried out gene expression profiling on the pMicro-1 cell line, it later became unclear how this data could be useful for our studies, since the metastatic potential of pMicro-1 was neither relatively high nor low, and, in most cases, did not differ significantly between either #78 or #82 cells. The expression of metastasis-related genes might therefore be reflective of this intermediate phenotype in two ways: a gene (or genes) may also display an intermediate level of expression between that of #78 and #82; or, if a network of genes was responsible for metastasis, the expression of some of these genes might be identical to that of #78, while others might be identical to that of #82. If the latter explanation were true, the net phenotype would still be an intermediate metastatic potential for pMicro-1.

Because we could not distinguish between these possibilities, we focused primarily on genes whose expression levels differed significantly between the #78 and #82 cell lines. Our list of candidate genes was enriched for those which encoded proteins believed to be involved with cell cytoskeleton, matrix and adhesion. In particular, 4.1B/DAL-1 and SPARC were both severely downregulated in highly metastatic #82 cells relative to #78 cells, making them putative suppressors of metastasis. Although 4.1B/DAL-1 was originally identified as a potential tumor suppressor for lung adenocarcinomas and meningiomas[Tran et al., 1999], the effect of this cytoskeletal protein on tumor metastasis has not yet been reported. In contrast, the matrix component SPARC has been previously associated with a variety of cell biological processes, including tumorigenesis and metastasis, but these findings have also often been inconsistent or contradictory with results from other studies[Framson and Sage, 2004]. For these and other reasons previously described, we chose to examine further the effects of both 4.1B and SPARC on prostate cancer progression and metastasis. The results from this work will be described in the following two chapters.

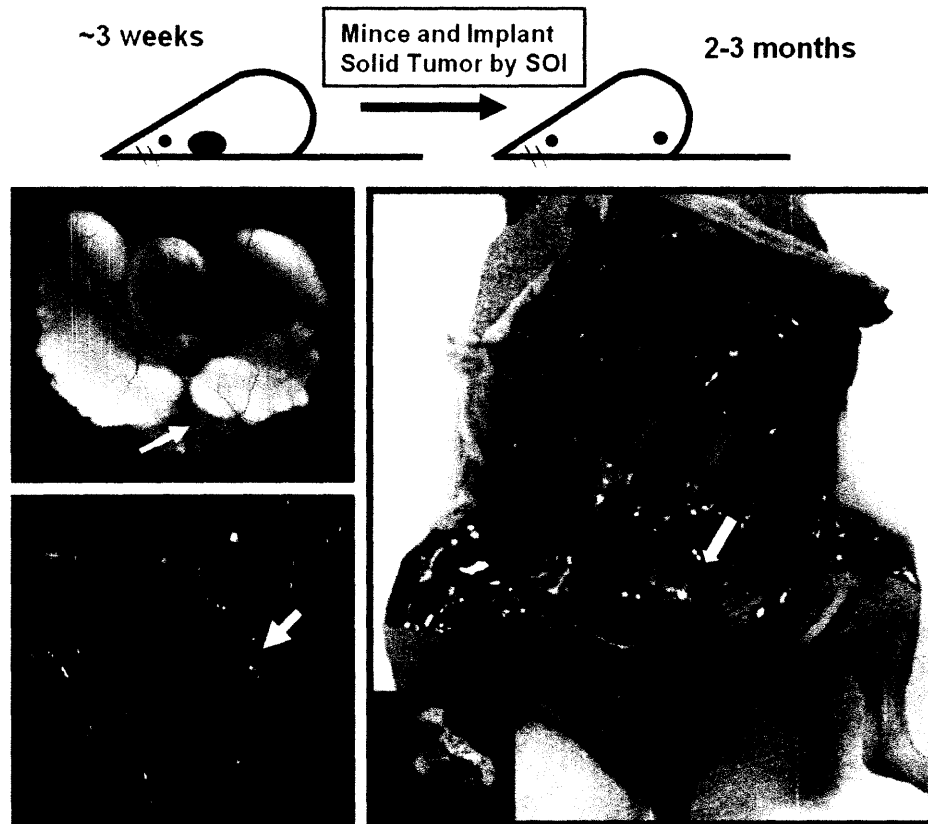
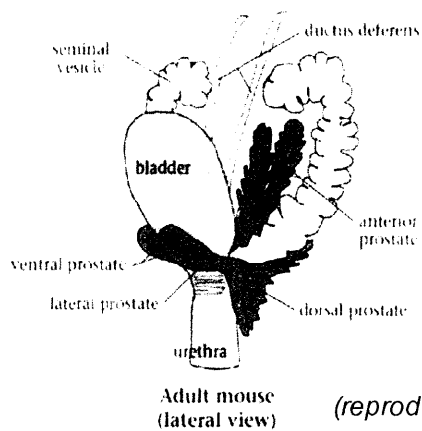
We were also intrigued by the observation that hematogenous dissemination of tumor cells following SOI correlated with lymphatic invasion, as will be discussed in Chapter 5. This suggested that tumor cells might be entering systemic circulation not by intravasating directly into venous capillaries but, rather, by utilizing a circuitous route involving the lymphatic system. Although we were not successful in either proving or disproving this hypothesis, we were able to gain some insights into how tumor cells entered lymphatic circulation, particularly by identifying the types of vessels that were either dispensable or indispensable for the process, as described in Chapter 6. As intravasation is one of the earliest steps in metastasis, these studies have validated the use of surgical orthotopic implantation as a model where even the most initial stages of tumor cell dissemination can be studied.

REFERENCES

- Abate-Shen C, Shen MM (2000): Molecular genetics of prostate cancer. *Genes & Development* 14:2410-2434.
- Al-Mehdi AB, Tozawa K, Fisher AB, Shientag L, Lee A, Muschel RJ (2000): Intravascular origin of metastasis from the proliferation of endothelium-attached tumor cells: a new model for metastasis. *Nature Medicine* 6:100-102.
- An Z, Wang X, Geller J, Moossa AR, Hoffman RM (1998): Surgical orthotopic implantation allows high lung and lymph node metastatic expression of human prostate carcinoma cell line PC-3 in nude mice. *The Prostate* 34:169-174.
- Bhatia-Gaur R, Donjacour AA, Sciavolino PJ, Kim M, Desai N, Young P, Norton CR, Gridley T, Cardiff RD, Cunha GR, Abate-Shen C, Shen MM (1999): Roles for Nkx3.1 in prostate development and cancer. *Genes and Development* 13:966-977.
- Bruckheimer EM, Brisbay S, Johnson DJ, Gingrich JR, Greenberg N, McDonnell TJ (2000): Bcl-2 accelerates multistep prostate carcinogenesis in vivo. *Oncogene* 19:5251-5258.
- Bubendorf L, Schopfer A, Wagner U, Sauter G, Moch H, Willi N, Gasser TC, Mihatsch MJ (2000): Metastatic patterns of prostate cancer: an autopsy study of 1,589 patients. *Human Pathology* 31:578-582.
- Clark EA, Golub TR, Lander ES, Hynes RO (2000): Genomic analysis of metastasis reveals an essential role for RhoC. *Nature* 406:532-535.
- Corey E, Quinn JE, Bladou F, Brown LG, Roudier MP, Brown JM, Buhler KR, Vessella RL (2002): Establishment and characterization of osseous prostate cancer models: intra-tibial injection of human prostate cancer cells. *Prostate* 52:20-33.
- Cunha GR, Hayward SW, Wang YZ, Ricke WA (2003): Role of the stromal microenvironment in carcinogenesis of the prostate. *International Journal of Cancer* 107:1-10.
- Dhanasekaran SM, Barrette TR, Ghosh D, Shah R, Varambally S, Kurachi K, Pienta KJ, Rubin MA, Chinnaiyan AM (2001): Delineation of prognostic biomarkers in prostate cancer. *Nature* 412:822-826.
- DiGiovanni J, Kiguchi K, Frijhoff A, Wilker E, Bol DK, Beltran L, Moats S, Ramirez A, Jorcano J, Conti C (2000): Deregulated expression of insulin-like growth factor 1 in prostate epithelium leads to neoplasia in transgenic mice. *PNAS* 97:3455-3460.
- Dyke TV, Jacks T (2002): Cancer modeling in the modern era: progress and challenges. *Cell* 108:135-144.
- Framson PE, Sage EH (2004): SPARC and tumor growth: where the seed meets the soil? *Journal of Cellular Biochemistry* 92:679-690.
- Gingrich JR, Barrios RJ, Kattan MW, Nahm HS, Finegold MJ, Greenberg NM (1997): Androgen-independent prostate cancer progression in the TRAMP model. *Cancer Research* 57:4687-4691.
- Gingrich JR, Barrios RJ, Morton RA, Boyce BF, DeMayo FJ, Finegold MJ, Angelopoulou R, Rosen JM, Greenberg NM (1996): Metastatic prostate cancer in a transgenic mouse. *Cancer Research* 56:4096-4102.
- Glinsky VV, Glinsky GV, Glinsky OV, Huxley VH, Turk JR, Mossine VV, Deutscher SL, Pienta KJ, Quinn TP (2003): Intravascular metastatic cancer cell homotypic aggregation at the sites of primary attachment to the endothelium. *Cancer Research* 63:3805-3811.
- Greenberg NM, DeMayo F, Finegold MJ, Medina D, Tilley WD, Aspinall JO, Cunha GR, Donjacour AA, Matusik RJ, Rosen JM (1995): Prostate cancer in a transgenic mouse. *PNAS* 92:3439-3443.
- Harada M, Shimizu A, Nakamura Y, Nemoto R (1992): Role of the vertebral venous system in metastatic spread of cancer cells to the bone. In Karr JP, Yamanaka H (eds): "Prostate Cancer and Bone Metastasis." New York: Plenum Press, pp 83-92.
- Hoffman RM (1999): Orthotopic metastatic mouse models for anticancer drug discovery and evaluation: a bridge to the clinic. *Investigational New Drugs* 17:343-359.
- Horoszewicz JS, Leong SS, Chu TM, Wajsman ZL, Friedman M, Papsidero L, Kim U, Chai LS, Kakati S, Arya SK, Sandberg AA (1980): The LNCaP cell line--a new model for studies on human prostatic carcinoma. *Prog Clin Biol Res* 37:115-132.

- Hubert RS, Vivanco I, Chen E, Rastegar S, Leong K, Mitchell SC, Madraswala R, Zhou Y, Kuo J, Raitano AB, Jakobovits A, Saffran DC, Afar DE (1999): STEAP: a prostate-specific cell-surface antigen highly expressed in human prostate tumors. *PNAS* 96:14523-14528.
- Kaighn ME, Narayan KS, Ohnuki Y, Lechner JF, Jones LW (1979): Establishment and characterization of a human prostatic carcinoma cell line (PC-3). *Investigative Urology* 17:16-23.
- Kang Y, Siegel PM, Shu W, Drobnjak M, Kakonen SM, Cordon-Cardo C, Guise TA, Massague J (2003): A multigenic program mediating breast cancer metastasis to bone. *Cancer Cell* 6:537-49.
- Klezovitch O, Chevillet J, Mirosevich J, Roberts RL, Matusik RJ, Vasioukhin V (2004): Hepsin promotes prostate cancer progression and metastasis. *Cancer Cell* 6:185-195.
- Kwabi-Addo B, Giri D, Schmidt K, Podsypanina K, Parsons R, Greenberg N, Ittmann M (2001): Haploinsufficiency of the Pten tumor suppressor gene promotes prostate cancer progression. *PNAS* 98:11563-11568.
- Majumder PK, Febbo PG, Bikoff R, Berger R, Xue Q, McMahon LM, Manola J, Brugarolas J, McDonnell TJ, Golub TR, Loda M, Lane HA, Sellers WR (2004): mTOR inhibition reverses Akt-dependent prostate intraepithelial neoplasia through regulation of apoptotic and HIF-1-dependent pathways. *Nature Medicine* 10:594-601.
- Majumder PK, Yeh JJ, George DJ, Febbo PG, Kum J, Xue Q, Bikoff R, Ma H, Kantoff PW, Golub TR, Loda M, Sellers WR (2003): Prostate intraepithelial neoplasia induced by prostate restricted Akt activation: the MPAKT model. *PNAS* 100:7841-7846.
- McCarty JH, Cook AA, Hynes RO (2005): An interaction between alpha(v)beta(8) integrin and Band 4.1B via a highly conserved region of the Band 4.1 C-terminal domain. *PNAS* 102:13479-13483.
- Mickey DD, Stone KR, Wunderli H, Mickey GH, Vollmer RT, Paulson DF (1977): Heterotransplantation of a human prostatic adenocarcinoma cell line in nude mice. *Cancer Research* 37:4049-4058.
- Nishijima Y, Uchida K, Koiso K, Nemoto R (1992): Clinical significance of the vertebral vein in prostate cancer metastasis. In Karr JP, Yamanaka H (eds): "Prostate Cancer and Bone Metastasis." New York: Plenum Press, pp 93-100.
- Park JH, Walls JE, Galvez JJ, Kim M, Abate-Shen C, Shen MM, Cardiff RD (2002): Prostatic intraepithelial neoplasia in genetically engineered mice. *American Journal of Pathology* 161:727-735.
- Pettaway CA, Pathak S, Greene G, Ramirez E, Wilson MR, Killion JJ, Fidler IJ (1996): Selection of highly metastatic variants of different human prostatic carcinomas using orthotopic implantation in nude mice. *Clinical Cancer Research* 2:1627-1636.
- Rembrink K, Romijn JC, Kwast THvd, Rubben H, Schroder FH (1997): Orthotopic implantation of human prostate cancer cell lines: a clinically relevant animal model for metastatic prostate cancer. *The Prostate* 31:168-174.
- Resnick MI (1992): Hemodynamics of prostate bone metastases. In Yamanaka JPKaH (ed): "Prostate Cancer and Bone Metastasis." New York: Plenum Press, pp 77-81.
- Rubio N, Villacampa MM, Hilali NE, Blanco J (2000): Metastatic burden in nude mice organs measured using prostate tumor PC-3 cells expressing the luciferase gene as a quantifiable tumor cell marker. *The Prostate* 44:133-143.
- Shappell SB, Thomas GV, Roberts RL, Herbert R, Ittmann MM, Rubin MA, Humphrey PA, Sundberg JP, Rozengurt N, Barrios R, Ward JM, Cardiff RD (2004): Prostate pathology of genetically engineered mice: definitions and classification. The consensus report from the Bar Harbor meeting of the mouse models of human cancer consortium prostate pathology committee. *Cancer Research* 64:2270-2305.
- Shevrin DH, Kukreja SC, Ghosh L, Lad TE (1988): Development of skeletal metastasis by human prostate cancer in athymic nude mice. *Clinical Experimental Metastasis* 6:401-409.
- Shiraid T, Ito N (1992): Animal prostate carcinoma models: limited potential for vertebral metastasis. In Yamanaka JPKaH (ed): "Prostate Cancer and Bone Metastasis." New York: Plenum Press, pp 151-158.

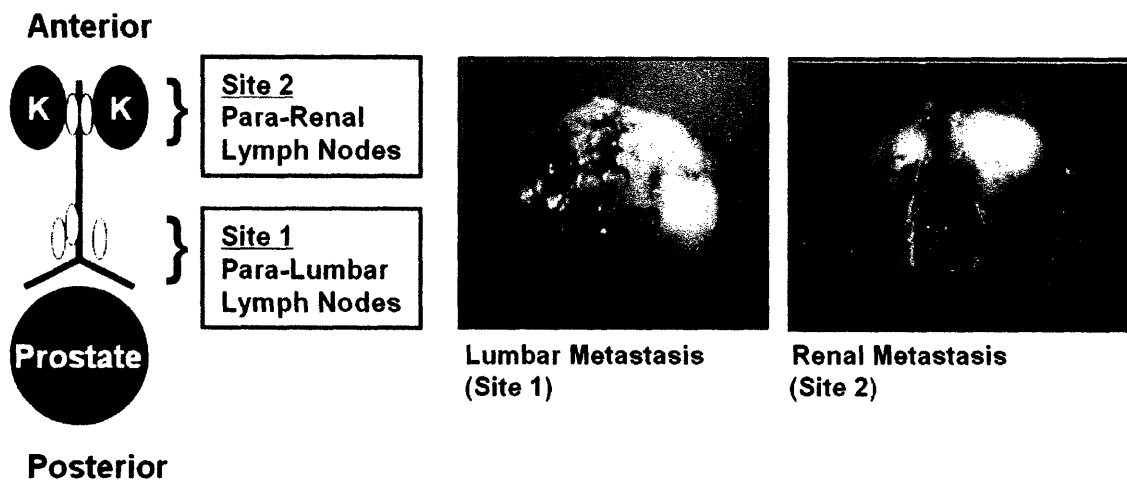
- Stephenson RA, Dinney CP, Gohji K, Ordonez NG, Killion JJ, Fidler IJ (1992): Metastatic model for human prostate cancer using orthotopic implantation in nude mice. *Journal of the NIH* 84:951-957.
- Sun CX, Robb VA, Gutmann DH (2002): Protein 4.1 tumor suppressors: getting a FERM grip on growth regulation. *Journal of Cell Science* 115:3991-4000.
- Tran YK, Bogler O, Gorse KM, Wieland I, Green MR, Newsham IF (1999): A novel member of the NF2/ERM/4.1 superfamily with growth suppressing properties in lung cancer. *Cancer Research* 59:35-43.
- Wang S, Gao J, Lei Q, Rozengurt N, Pritchard C, Jiao J, Thomas GV, Li G, Roy-Burman P, Nelson PS, Liu X, Wu H (2003): Prostate-specific deletion of the murine Pten tumor suppressor gene leads to metastatic prostate cancer. *Cancer Cell* 4:209-221.
- Wang X, An Z, Geller J, Hoffman RM (1999): High-malignancy orthotopic nude mouse model of human prostate cancer LNCaP. *The Prostate* 39:182-186.
- Wong CW, Song C, Grimes MM, Fu W, Dewhirst MW, Muschel RJ, Al-Mehdi A (2002): Intravascular location of breast cancer cells after spontaneous metastasis to the lung. *American Journal of Pathology* 161:749-753.
- Yang M, Jiang P, Sun FX, Hasegawa S, Baranov E, Chishima T, Shimada H, Moossa AR, Hoffman RM (1999): A fluorescent orthotopic bone metastasis model of human prostate cancer. *Cancer Research* 59:781-786.
- Yi C, McCarty JH, Troutman SA, M.S.Eckman, Bronson RT, Kissil JL (2005): Loss of the putative tumor suppressor Band 4.1B/Dal1 gene is dispensible for normal development and does not predispose to cancer. *Molecular and Cellular Biology* 25:10052-10059.

A**B**

Adult mouse (lateral view) (reproduced from Abate-Shen and Shen, 2000)

Figure 1. Surgical orthotopic implantation (SOI) can be used to model prostate cancer in mice. (A) A schematic of the SOI technique is shown (top), where solid tumor pieces derived from subcutaneous tumors are implanted into the prostate orthotopic site of CD-1 nude immunodeficient mice. The mouse dorsolateral prostate, unimplanted (top left photo, arrow, photo courtesy of Dr. A. Donjacour) or mock-implanted (bottom left photo, arrow) with a fluorescently-labeled tumor. After 2-3 months post-implantation, a mouse bearing a typical orthotopic tumor (white arrow) with para-aortic lumbar lymph node metastases (green arrows) is shown (right photo). (B) The mouse prostate consists of three pairs of lobes—ventral, lateral and dorsal—and is located beneath the bladder and seminal vesicles.

A



B

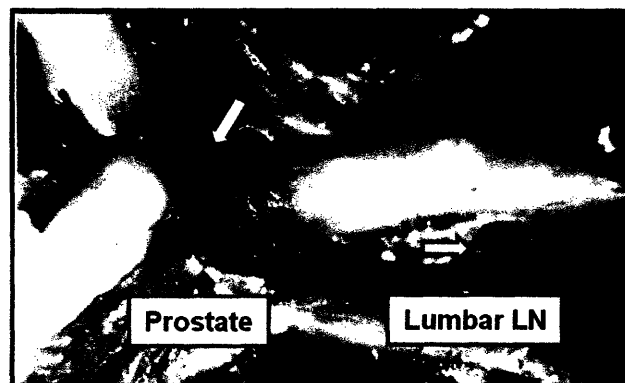
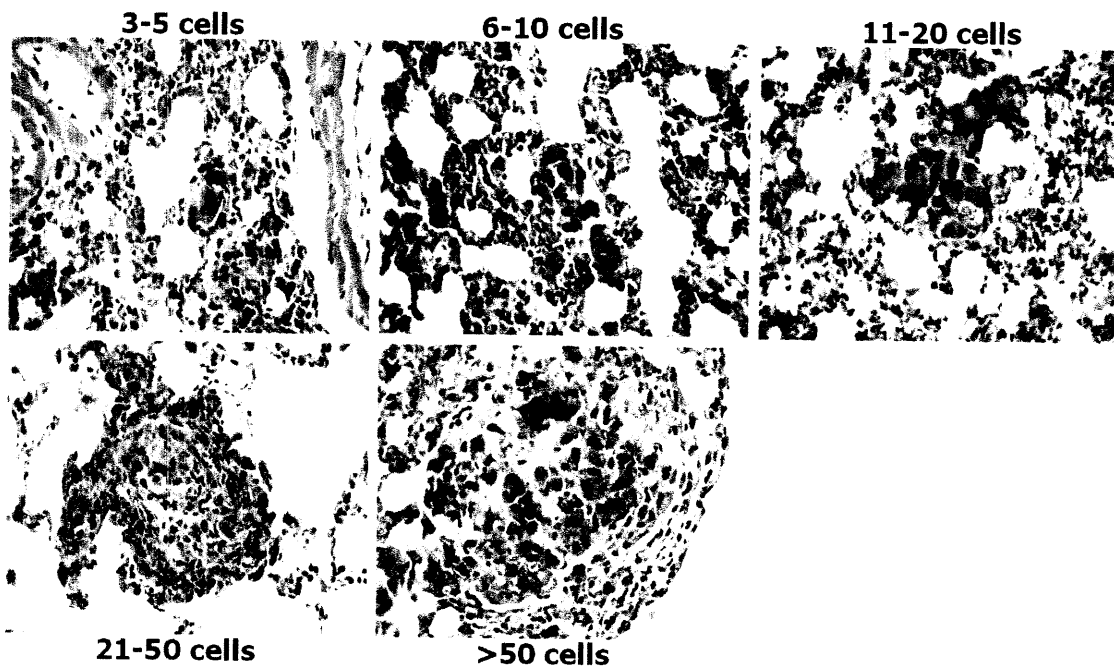


Figure 2. The para-aortic/lumbar lymph nodes drain the prostate and are frequent sites of metastasis. (A) An illustration is shown depicting the location of commonly invaded lymph nodes relative to the prostate (left). Typical lumbar and renal lymph node metastases are shown (right). **(B)** Dye tracking studies using Methylene Blue injected into the prostate indicate that the organ is directly drained by the lumbar lymph nodes. (K, kidney; LN, lymph node)

A



B

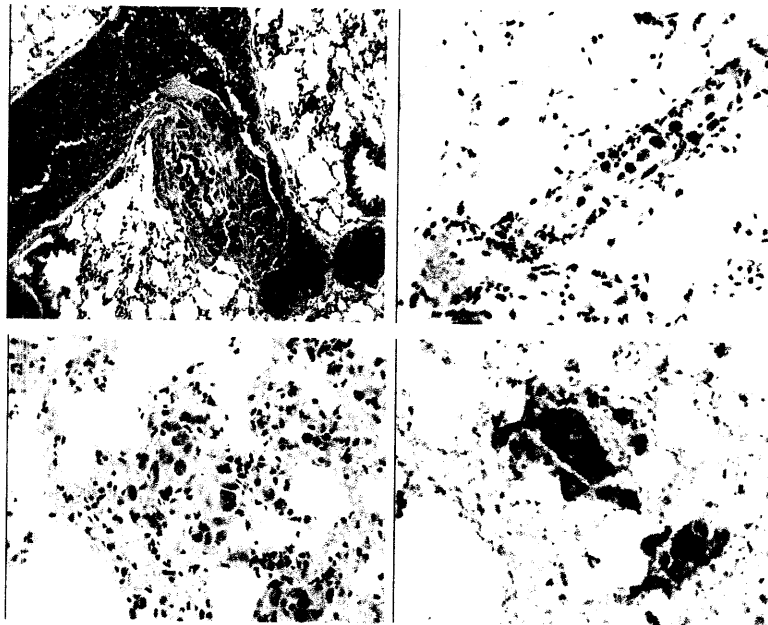
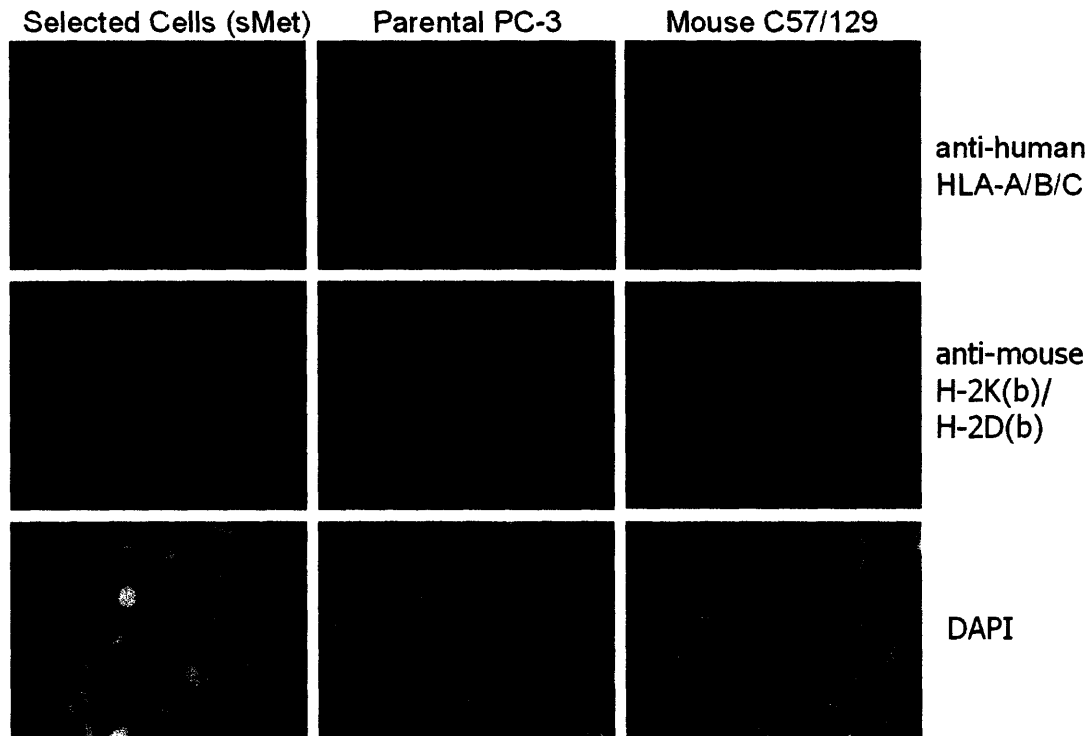


Figure 3. Orthotopic prostate tumors develop lung micro-metastases. (A) Micrometastases are visible by hematoxylin-and-eosin (H&E) staining and are characterized by enlarged nuclei relative to the surrounding lung parenchyma. Metastases consisting of at least 3 cells were counted and grouped by size into the classifications shown. (B) Lung micro-metastases were sometimes seen growing within blood vessel lumens without extravasating (top panels). Lung micro-metastases visible by H&E (bottom left) can be confirmed by immunohistochemical staining for the prostate-specific cell surface antigen STEAP (bottom right).

A



B

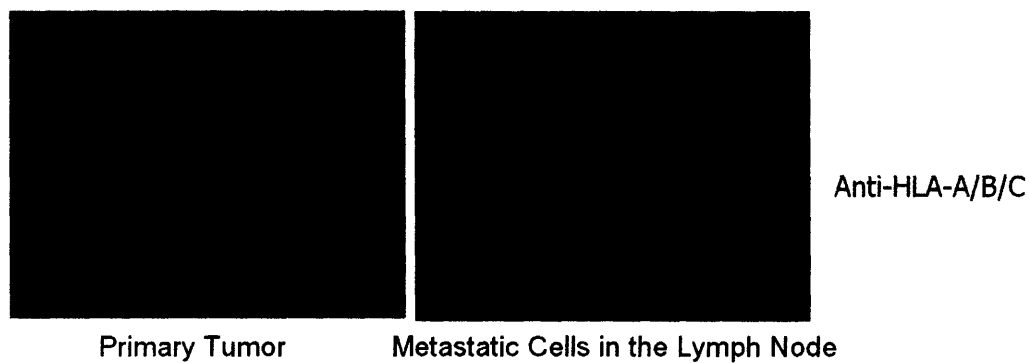
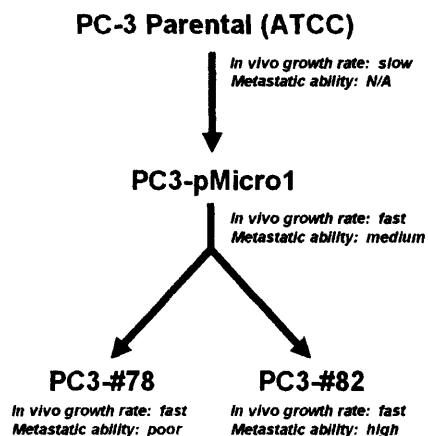


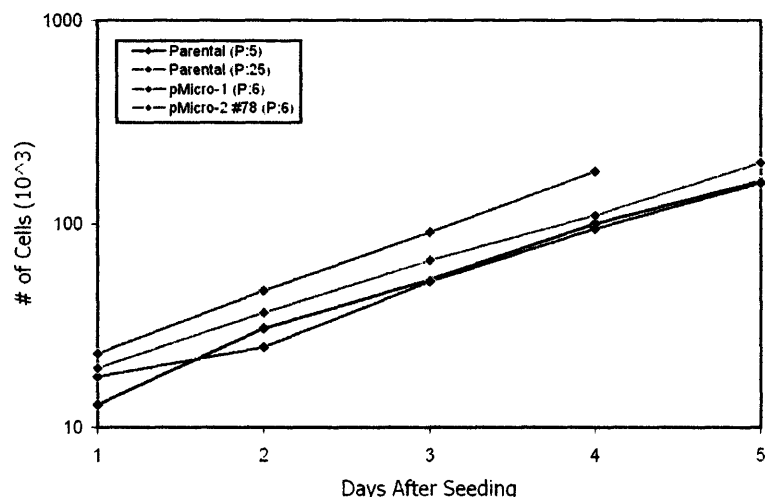
Figure 4. The human origin of PC-3 cells passaged *in vivo* can be confirmed by immunohistochemistry. (A) PC-3 parental cells, as well as an example of a PC-3 variant cell line passaged *in vivo* (sMet*), both stain positively with an antibody against a human-specific Class I MHC molecule (HLA-A/B/C) but not with an antibody against a mouse-specific MHC molecule (H-2K(b)/H-2D(b)). The opposite is true for mouse fibroblast cells. **(B)** The human-specific HLA-A/B/C antibody identifies both human cells in the orthotopic primary tumor (left), as well as isolated tumor cells that had metastasized to the draining lymph nodes (right) in frozen sections.

(*The sMet cell line was derived by H.H. from an axillary lymph node metastasis from a PC-3 subcutaneous tumor.)

A



B



C

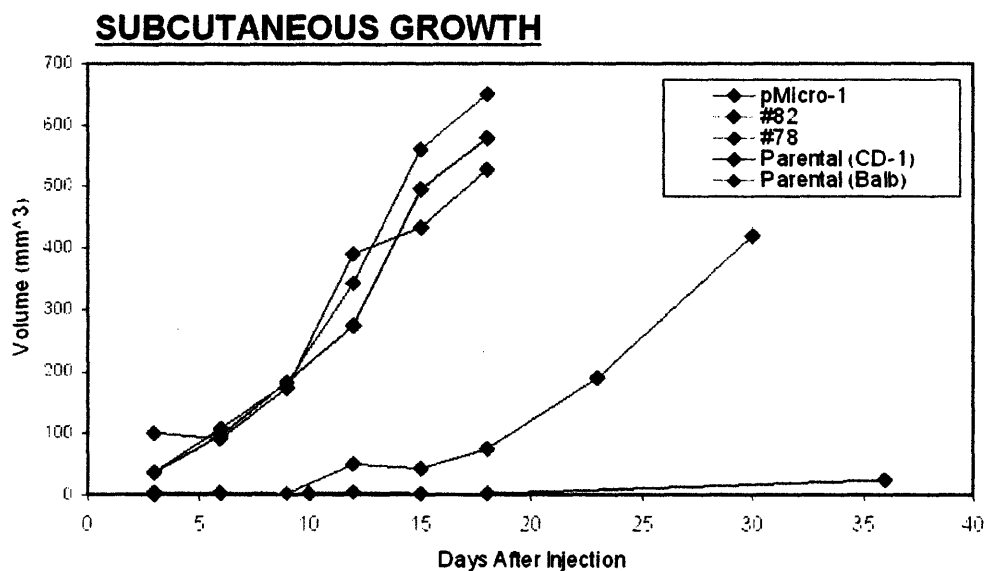


Figure 5. The “core” PC-3 variant cell lines were derived by *in vivo* passaging of tumor cells using surgical orthotopic implantation. (A) The PC-3 variant cell line pMicro-1 was derived from PC-3 parental cells, while #78 and #82 cells were both derived from pMicro-1. Additional details about cell line derivation are described in the Materials and Methods (Appendix A), and Results sections. (B) The cell lines displayed uniform growth rates *in vitro*. (C) When injected as subcutaneous tumors into CD-1 immunodeficient mice, the core PC-3 variant cells—pMicro-1, #78 and #82—displayed indistinguishable rates of growth. PC-3 parental cells exhibited markedly reduced rates of growth when injected into either CD-1 or Balb/c immunodeficient mice.

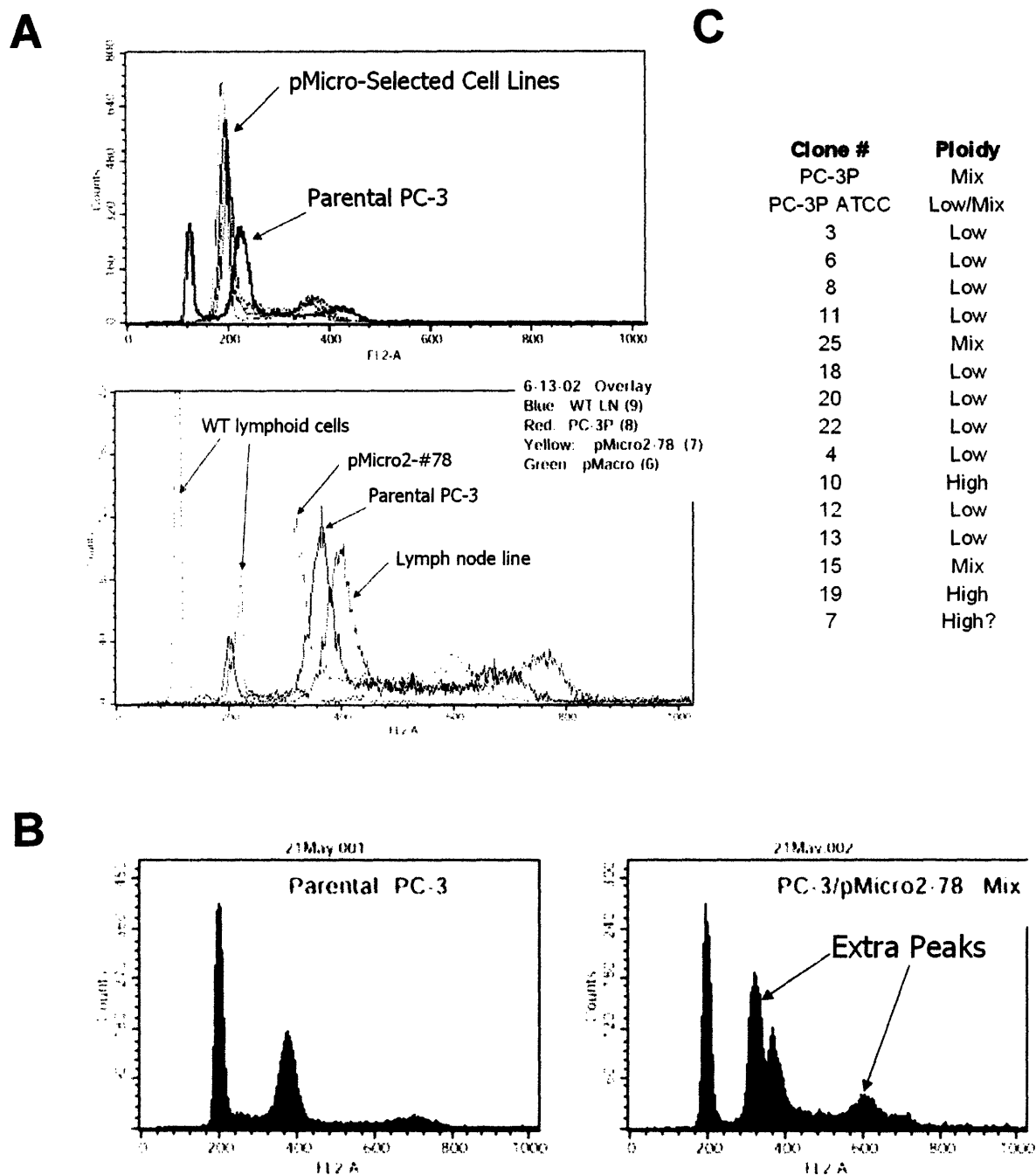


Figure 6. The genomic content of the “core” PC-3 variant cell lines resembled one another’s but was distinct from other cell lines or cell types. **(A)** Flow cytometry-based ploidy analysis revealed that the core PC-3 variant cell lines (“pMicro-selected”) possessed a similar genomic content, which was distinct from that of parental PC-3 cells (top left). An overlay of the ploidy results indicates the relative genomic content of various cell types (bottom left). **(B)** When PC-3 parental (PC-3P) cells and #78 cells were intentionally pre-mixed prior to analysis, peaks representing the two cell lines could be distinguished. **(C)** From the parental PC-3 cells, fifteen individual clones were analyzed for genomic content and classified as having high or low ploidy. In some cases, a mixture of both was detected.

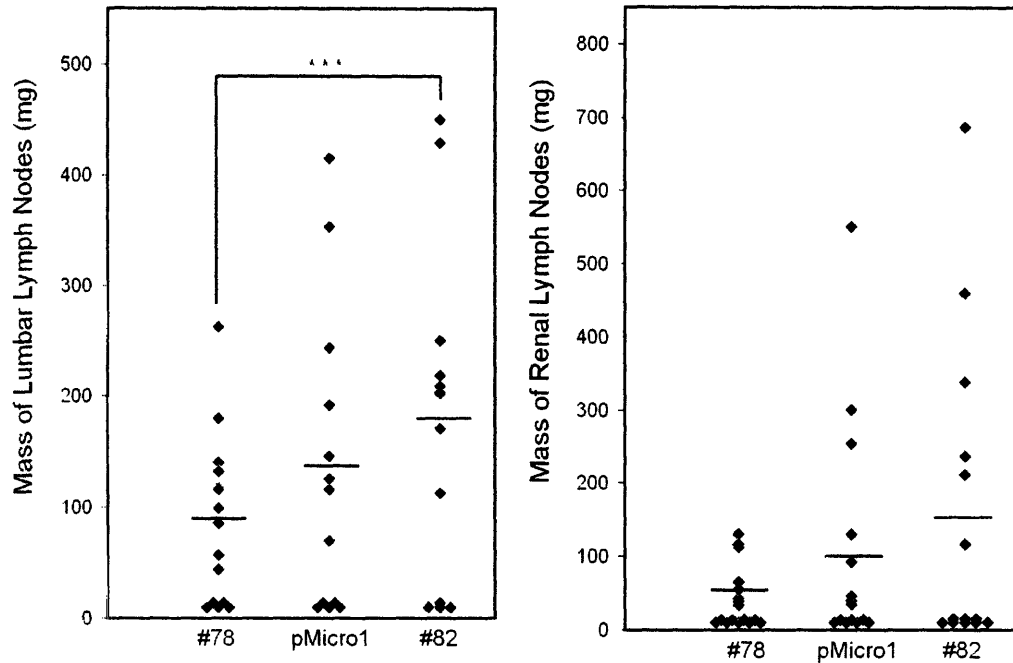
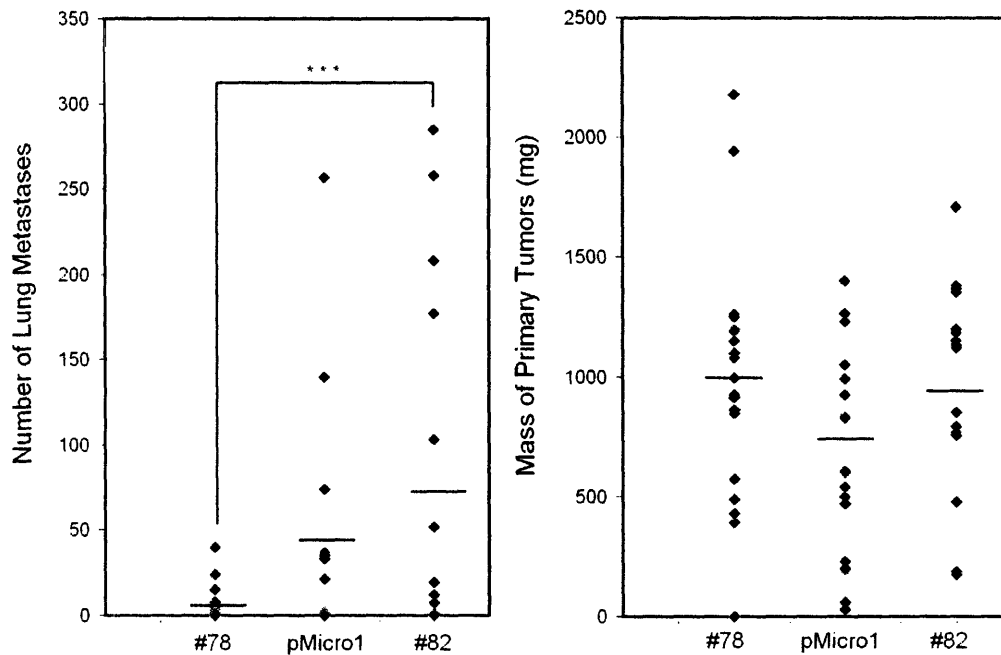
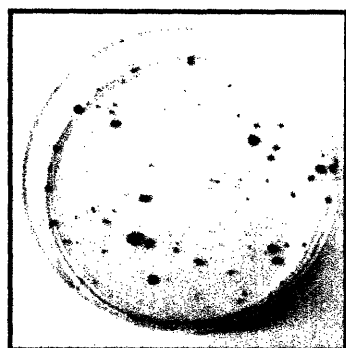
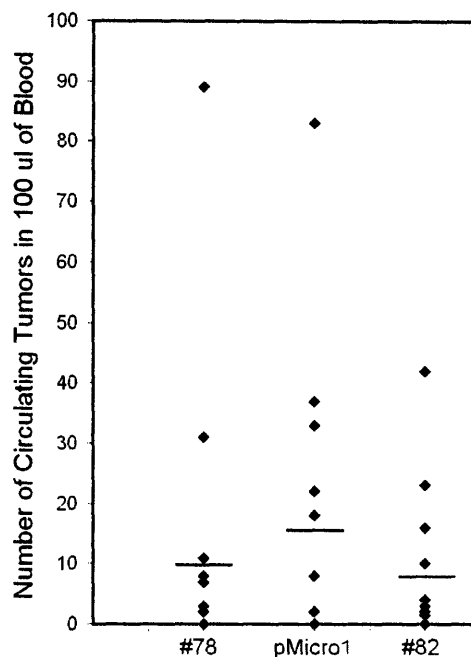
A**B**

Figure 7. The core PC-3 variant cell lines exhibited differing metastatic abilities after being implanted into the prostate. (A) The fixed masses of the para-aortic/lumbar (left) and renal lymph nodes (right) for mice bearing orthotopic prostate tumors are shown for the three core PC-3 variant cell lines: #78, pMicro-1 and #82. (B) The number of lung micrometastases (left) and the fresh masses of the orthotopic primary tumors (right) are shown for the three cell lines. (horizontal bars, mean; *, $p < 0.04$)**

A



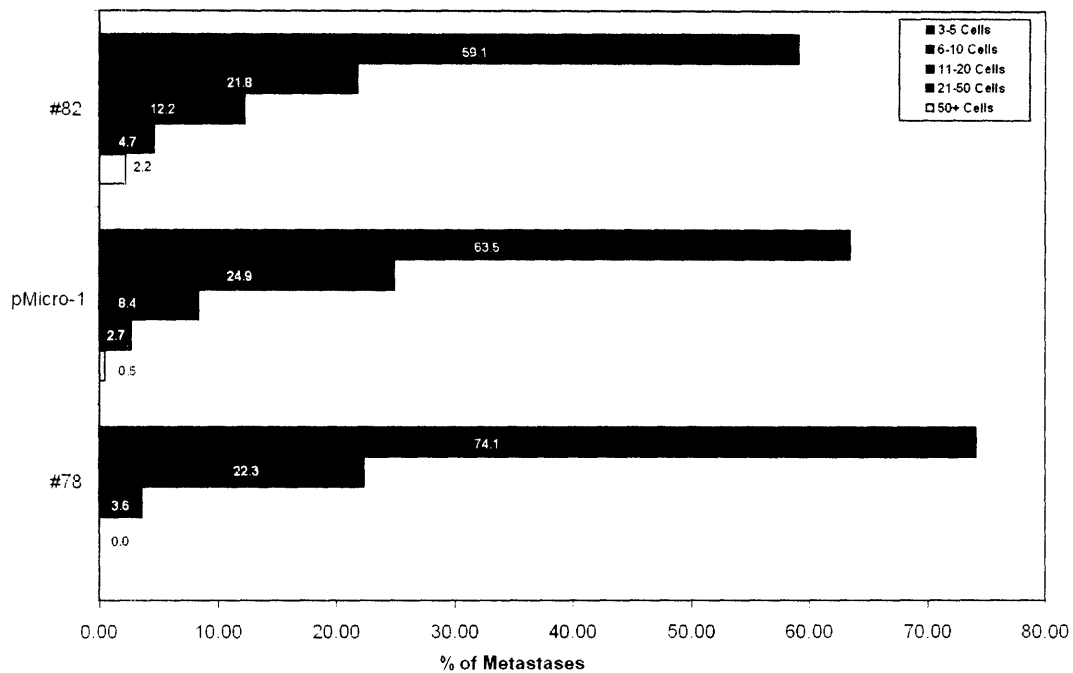
Circulating Tumor Cells



B

Cell Line	N	Total Lung Mets	Total Blood Colonies	Ratio	Fold
pMicro2-82	10	662	108	6.13	61
pMicro-1	7	304	203	1.50	15
pMacro	3	391	273	1.43	14
pMicro2-78	7	66	155	0.43	4
Parental	2	33	120	0.28	3
PC-3M	2	27	263	0.10	1
Total	31	1483	1022		

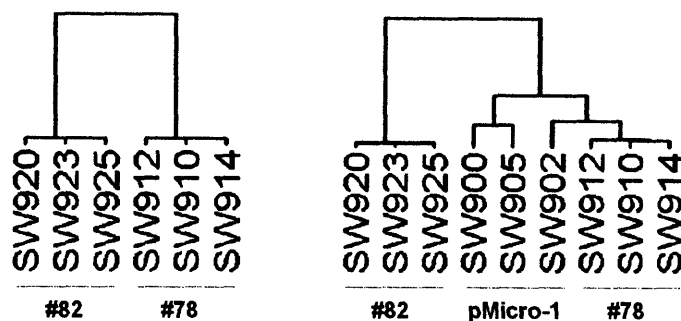
Figure 8. Circulating viable tumor cells in the blood can be detected and quantitated in order to assess lung metastatic efficiency. (A) A typical colony formation assay is used to quantitate tumor cells circulating in whole blood (left). The number of circulating tumor cells in the blood of animals bearing orthotopic tumors derived from the three core cell lines is shown (right). (horizontal bars, mean) (B) Shown is a table summarizing the number of mice from which both lung metastasis and circulating tumor cell data were collected ("N"), the total number of circulating tumor cells counted from these mice (in 100 ul of blood), the accompanying total number of lung metastases observed, and the efficiency of lung metastasis (expressed as the total number lung metastases divided by the total number of circulating tumor cells in the blood). The relative efficiency was obtained by normalizing all results to that of PC-3M, which was set to 1 ("Fold").

A**B**

	#78	pMicro-1	#82
Average lung metastases per mouse	1.0	7.2	11.8
Average lung mets > 5 cell clusters per mouse	1.0	10.4	19.0
Average size of primary tumor	1.0	0.7	0.9
Average size of lumbar lymph nodes	1.0	1.5	2.0
Average size of renal lymph nodes	1.0	1.9	2.8
Average number of blood colonies per mouse	1.0	1.5	0.7
Average lung metastases per blood colony	1.0	3.4	13.9

Figure 9. The core PC-3 variant cell lines exhibited differences in various parameters for metastasis following implantation into the prostate. (A) Depicted is the size distribution of lung metastasis clusters observed for the three core PC-3 variant cell lines. **(B)** Shown is a table summarizing various parameters of tumor growth and metastasis following orthotopic implantation of the three cell lines. All results were normalized relative to those of #78 cells, which were set to 1.

A



Source: Total RNA from age-matched subcutaneous tumors in CD-1/nude mice. Three per cell line
 Arrays: Affymetrix HU-133A
 Analysis: D-Chip unsupervised hierarchical clustering (filter for variation $0.5 < SD/Mean < 10$)

B

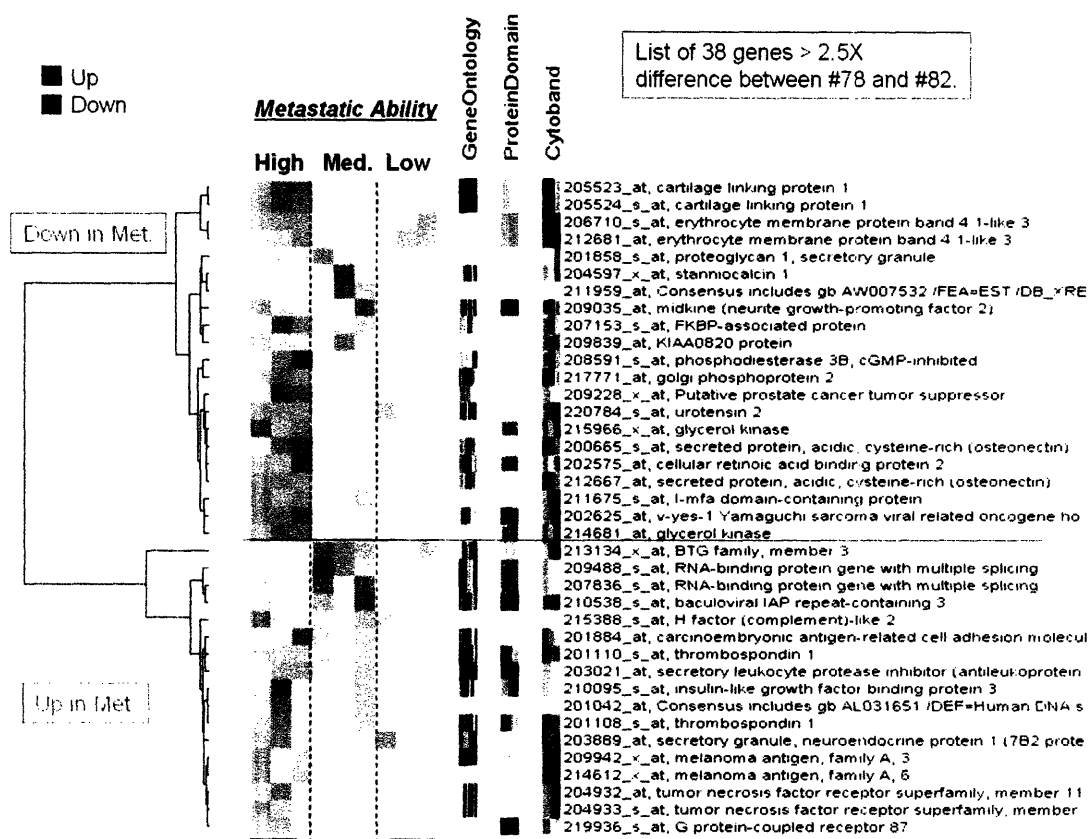


Figure 10. Candidate metastasis genes were identified by comparing the gene expressions of subcutaneous tumors derived from the three core PC-3 variant cell lines. (A) Unsupervised hierarchical clustering of the gene expression profiles of the three cell lines. (B) The 38 genes that differed by >2.5-fold expression between poorly metastatic #78 tumors and highly metastatic #82 tumors are shown, as analyzed by D-Chip (above the line, genes downregulated in highly metastatic cells; below the line, genes upregulated in highly metastatic cells).

C

Gene	Fold Change	
insulin-like growth factor binding protein 3	3.17	
G protein-coupled receptor 87	2.64	
protease inhibitor 3, skin-derived (SKALP)	2.47	
keratin 6B	2.37	
keratin 7	2.12	
G protein-coupled receptor 37 (endothelin receptor type B-like)	2.08	
insulin-like growth factor 1 receptor	2.06	
insulin-like growth factor binding protein 6	2.05	
interleukin 8	2.04	
interleukin 8	2.01	
endothelial PAS domain protein 1	1.91	
cysteine-rich, angiogenic inducer, 61	1.89	
G protein-coupled receptor, family C, group 5, member B	1.87	Up in Metastasis
gap junction protein, beta 3, 31kD (connexin 31)	1.86	
erythrocyte membrane protein band 7.2 (stomatin)	1.83	
mucin 5, subtypes A and C, tracheobronchial/gastric	1.81	
interleukin 7 receptor	1.78	
<hr/>		
gap junction protein, alpha 1, 43kD (connexin 43)	-1.82	
desmocollin 3	-1.82	
claudin 3	-1.84	
desmocollin 3	-1.84	
Rho GDP dissociation inhibitor (GDI) alpha	-1.86	Down in Metastasis
bone morphogenetic protein 2	-1.86	
phosphoinositide-3-kinase, regulatory subunit, polypeptide 3 (p55, gamma)	-1.87	
ornithine decarboxylase antizyme 2	-1.88	
matrix metalloproteinase 1 (interstitial collagenase)	-1.9	
Rho GDP dissociation inhibitor (GDI) alpha	-1.91	
myosin, light polypeptide 9, regulatory	-2.21	
fatty acid binding protein 4, adipocyte	-2.24	
LIM domain only 4	-2.3	
retinol binding protein 4, plasma	-2.3	
desmocollin 2	-2.39	
met proto-oncogene (hepatocyte growth factor receptor)	-2.42	
cellular retinoic acid binding protein 2	-2.53	
proteoglycan 1, secretory granule	-2.54	
Putative prostate cancer tumor suppressor	-2.59	
FKBP-associated protein	-2.81	

Figure 10. Candidate metastasis genes were identified by comparing the gene expressions of subcutaneous tumors derived from the three core PC-3 variant cell lines (cont). (C) Shown is a list of notable genes whose expression levels were also significantly changed, but to a lesser extent than those in (A) (above the line, genes upregulated in highly metastatic cells; below the line, genes downregulated in highly metastatic cells). For a complete list of differentially expressed genes, please see Appendix E.

CHAPTER 3.

PROTEIN 4.1B SUPPRESSES PROSTATE CANCER PROGRESSION AND METASTASIS

The work in this chapter was conceived by Sunny Wong and Richard Hynes. Antibodies and overexpression constructs for 4.1B and/or integrin $\beta 8$ were generated by and/or obtained from Joseph McCarty. 4.1B-deficient mice were generated by and obtained from Joseph Kissil. Bioinformatics analysis was assisted by Steve Shen. The contents of this chapter were written by Sunny Wong, with editing by Richard Hynes.

INTRODUCTION

The Protein 4.1 Superfamily of Proteins

Protein 4.1B is a member of the Protein 4.1 superfamily of proteins, which is characterized by the presence of a conserved N-terminal 4.1/ezrin/radixin/moesin (FERM) domain. These proteins serve to connect transmembrane glycoproteins such as CD44 to the actin cytoskeleton, and have been shown to affect numerous cellular processes, including polarization, migration and proliferation, among other functions[Bretscher et al., 2002]. Based on sequence homology, the Protein 4.1 superfamily of proteins can be further divided into five subgroups: Protein 4.1 molecules, ERM proteins, talin-related molecules, protein tyrosine phosphatase (PTPH) proteins, and novel band 4.1-like 4 (NBL4)(Figure 1A)[Sun et al., 2002]. Given their roles in numerous cellular processes, it is not surprising that several members of these subgroups have also been implicated in tumor progression. In particular, the ERM-like protein merlin (the product of the *NF2* gene) is a critical suppressor of meningiomas and schwannomas[Gutmann et al., 1997], while another ERM protein, ezrin, has recently been shown to enhance metastasis of bone and soft tissue sarcomas[Khanna et al., 2004; Yu et al., 2004a]. Roles for protein 4.1 subgroup members in tumorigenesis, however, are less clear, though 4.1B is believed to be a tumor suppressor that is commonly lost in a variety of cancers, as will be discussed later.

In total, the Protein 4.1 superfamily of proteins consists of greater than 40 members in mammals, and related proteins are also present in *Drosophila* and *C. elegans*, though the FERM domain is found only in multi-cellular organisms[Polesello and Payre, 2004]. Most of the mechanistic and structural studies that have been performed have focused on the ERM subgroup of proteins, which consists of three members: ezrin, radixin and moesin¹. Each of these proteins possesses a FERM domain, a central coiled-coil α -helical domain, and a C-terminal actin-binding domain (C-ERMAD)[Sun et al., 2002]. Since the FERM domains of ERM and Protein 4.1 proteins display high degrees of sequence homology, many of the properties exhibited by ERM FERM domains are predicted to be similar to those of Protein 4.1 FERM domains, though, in most cases, these predictions await experimental validation. However, it is important to note that, aside from their FERM domains, Protein 4.1 and ERM proteins are actually quite divergent[Sun et al., 2002]. Therefore, while these molecules may exhibit some common features due to their homologous FERM domains, such as localization and interaction partners, they are also likely to possess different functions within the cell.

¹ Merlin is related to the ERM proteins and is often also considered a member of this subgroup, although it lacks a C-terminal actin-binding domain. Merlin activity is also regulated differently than the ERM proteins, as will be discussed in the subsequent sections.

Functional Regulation of ERM/4.1 Proteins²

Crystallographic studies on the FERM domain of moesin have revealed a clover-leaf structure consisting of three subdomains: F1, F2 and F3 [Edwards and Keep, 2001]. While F1 is structurally similar to ubiquitin, F2 bears homology with acyl-CoA-binding proteins. At the sequence level, F3 exhibits homology with phosphotyrosine binding (PTB), pleckstrin homology (PH) and Enabled/VASP homology 1 (EVH1) domains. At least in the case of ERM proteins, these three subdomains appear critical for mediating both intra- and inter-molecular interactions. In the first scenario, the N-terminal FERM domain can fold upon itself and bind the C-terminal end of the same protein, thereby adopting a "closed" conformation that conceals binding sites for F-actin and other proteins including CD44, ICAM-1/2, ERM-binding phosphoprotein 50 (EBP50) and Rho-GDI (Figure 1B) [Bretscher et al., 2002]. In the second scenario, the FERM domain of any ERM protein is capable of interacting with the C-terminus of any other ERM protein, and this extended, "open" conformation thus exposes all the binding sites previously concealed. Conversion from the closed to open conformation can be induced by Rho kinase-mediated phosphorylation of a C-terminal threonine residue, or by binding of lipid phosphatidylinositol (4,5)-bisphosphate (PIP2) to the FERM domain [Yonemura et al., 2002]. In many cases, induction of the open conformation activates ERM proteins and re-localizes them from the cytoplasm to cortical actin protrusions at the plasma membrane.

As one might expect, overexpression of truncated ERM proteins can act as dominant active or dominant negative mutants. Introduction of the C-terminal half of ezrin or radixin into cells induces abnormally long membrane protrusions, presumably by locking endogenous ERM proteins into an extended, open conformation and exposing actin-binding sites [Henry et al., 1995]. Conversely, overexpression of the N-terminus of ezrin [Crepaldi et al., 1997] or introduction of antisense oligonucleotides targeted against ERM proteins can inhibit microvilli formation and reduce adhesion of cultured cells [Takeuchi et al., 1994].

As mentioned previously, the Rho pathway is critical for inducing the open (active) conformation of the ERM proteins and, interestingly, may act in a positive feedback loop. Lysophosphatidic acid (LPA) treatment of cells can activate Rho proteins, which leads to downstream induction of Rho kinase. Rho kinase, in turn, phosphorylates ERM proteins, which weakens the intramolecular interactions between the FERM and C-ERMAD domains [Matsui et al., 1998; Shaw et al., 1998]. This allows the protein to adopt an active conformation that exposes binding sites for Rho-GDI, an inhibitor of Rho-GTP [Takahashi et al., 1997]. The net effect is that active ERM proteins compete Rho-GDI away from their substrates, thus allowing prolonged activity of Rho-GTPases. As predicted from this model, overexpression of Rho-GTPases has been shown to activate ERM proteins and to cause their redistribution to the plasma membrane, while inhibition of Rho activity with C3-ADP-ribosyltransferase (C3) can block LPA-induced

² Merlin regulation differs in some respects and is discussed in more detail in the next section.

ERM protein activation[Yonemura et al., 2002]. In addition, expression of the radixin FERM domain is sufficient to activate Rho. Thus, ERM proteins act both upstream and downstream of Rho-GTPases[Matsui et al., 1998].

ERM self-folding can also be disrupted through binding of lipids such as PIP2 to their FERM domains. This Rho-independent mechanism of activation was hypothesized when *in vitro* studies suggested that PIP2 could activate recombinant ERM proteins[Anderson and Marchesi, 1985] and cause binding to purified CD44 in the absence of phosphorylation[Hirao et al., 1996]. In addition, unphosphorylated ERM proteins were observed to localize to the microvilli of A431 skin epithelial carcinoma cells following induction by EGF, even in the presence of the kinase inhibitor staurosporine[Yonemura et al., 2002]. A mutant form of ezrin containing an alanine substitution in place of threonine at the C-terminal phosphorylation site was also observed to localize to the plasma membrane after EGF induction. Indeed, titration of PIP2 by micro-injecting cells with the antibiotic neomycin—which binds polyphosphoinositides, particularly PIP2, with high affinity—re-localized ERMs from the plasma membrane to the cytoplasm and caused break-down of microvilli[Yonemura et al., 2002]. Finally, crystal-structure analysis of the radixin FERM domain in complex with inositol-(1,4,5)-triphosphate (IP3) has allowed direct observation of lipid binding[Hamada et al., 2000]. Thus, these studies have shown that both lipids and phosphorylation can activate ERM proteins by affecting their conformation.

Merlin: A Potent Tumor Suppressor

Merlin is perhaps the most well-studied member of the Protein 4.1 superfamily, although even now, there is a great deal that remains unknown about this important protein. Merlin is a tumor suppressor and the product of the *NF2* gene, which is named after the human disorder that arises—neurofibromatosis type 2—when merlin is absent or non-functional. Patients suffering from neurofibromatosis type 2 are predisposed to multiple tumors of the central nervous system, including schwannomas, meningiomas and ependymomas[Gutmann et al., 1997]. The disorder is dominantly inherited, loss of heterozygosity of *NF2* is frequent, and the tumor suppressive role of merlin is evident in that mice heterozygous for this protein develop metastatic osteosarcomas and lymphomas[McClatchey et al., 1998]. Like other ERM proteins, merlin possesses an N-terminal FERM domain that forms intramolecular interactions with its own C-terminal domain—this is the active, tumor suppressive form that localizes to adherens junctions in confluent fibroblasts[Lallemand et al., 2003; Sherman et al., 1997; Sun et al., 2002]. While loss of merlin does not appear to affect proliferation directly, mutant cells seem incapable of sensing normal contact growth inhibition and exhibit diffuse localization of adherens junction components like β -catenin[Lallemand et al., 2003]. In support of its role as a tumor suppressor, overexpression of merlin can induce cellular apoptosis[Lutchman and Rouleau, 1995; Sherman et al., 1997], while expression of various truncated forms of merlin (FERM domain only, or full length protein minus the FERM domain) can

act as dominant negatives against the endogenous protein. These dominant negatives, as expected, have been found to induce Schwann cell hyperplasia *in vivo* [Giovannini et al., 1999], and to confer anchorage-independent growth and insensitivity to contact inhibition in NIH-3T3 cells *in vitro* [Johnson et al., 2002].

As in the case of ERM proteins, merlin activity is conformation-dependent. Under conditions of high cell density, growth factor withdrawal and/or attachment to extracellular matrix, merlin is normally hypophosphorylated, folded up and inhibitory of cell growth [Lallemand et al., 2003; Morrison et al., 2001]. Although the exact mechanism by which merlin suppresses proliferation remains unclear, interaction with the receptor CD44 appears critical, and the hypophosphorylated, active form of merlin has also been shown to inhibit the Rac1 pathway [Kissil et al., 2003; Morrison et al., 2001]. Under growth permissive conditions, merlin is phosphorylated, possibly by Rho kinase or by p21-activated kinase (Pak-1), which opens up and inactivates the molecule [Kissil et al., 2002; Matsui et al., 1998]. In its extended conformation, merlin can interact with CD44 directly via its FERM domain or indirectly through head-to-tail associations with ERM proteins, particular ezrin [Morrison et al., 2001; Sun et al., 2002]. In addition, the open and inactive conformation of merlin exposes binding sites for actin and for other proteins, including β II spectrin and paxillin. Therefore, the sum of these interactions might provide not only a link between CD44 and the cytoskeleton to promote cell adhesion and polarity, but also a way to keep merlin in its inactive (and non-growth inhibiting) state.

Given the ample genetic evidence implicating merlin as a potent tumor suppressor, it is reasonable to expect that related proteins might also affect the cancer progression pathway. Indeed, ezrin has been reported to be necessary for Rho kinase/ROCK-mediated transformation of fibroblasts [Martin et al., 2002], and recent studies have shown that ezrin is also a critical and positive regulator of osteosarcoma and rhabdomyosarcoma metastasis [Khanna et al., 2004; Yu et al., 2004a]. Among the Protein 4.1 subgroup of proteins, relatively less is known about the normal functions of its members, which are characterized by an N-terminal FERM domain, a central spectrin-actin binding domain (SABD), and a C-terminal domain (CTD), as well as three unique domains (U1-U3). However, among this subgroup of proteins—which currently consists of 4.1R, 4.1G, 4.1N and 4.1B—and based on a growing number of studies, 4.1B has emerged as a leading tumor suppressor candidate in a variety of cell types.

Protein 4.1/DAL-1: A Putative Tumor Suppressor?

4.1B was first identified using differential display RT-PCR as a gene whose expression was reduced in human non-small cell lung carcinomas (NSCLC) [Tran et al., 1999]. The protein which was first cloned, unexpectedly, turned out to be a truncated version of 4.1B—this was originally named Deleted in Adenocarcinoma of the Lung-1, or DAL-1. Translation of DAL-1 initiates at Methionine 110, relative to

full-length 4.1B, and, consequently, this proteins lacks the 4.1B N-terminal U1 domain and the entire CTD[Gutmann et al., 2001]. DAL-1 also has internal deletions in portions of the U2 and U3 subdomains, and, interestingly, possesses a short stretch of unique amino acids in its FERM domain (Figure 1C-D). In a limited number of studies so far, no differences in function have been discerned between 4.1B and DAL-1; thus, the two are, at present, regarded interchangeably in the literature.

In terms of results obtained from human clinical studies, there is good reason to believe that 4.1B/DAL-1 could function as a tumor suppressor. The gene is located at chromosome position 18p11.3, a region that is lost in 38% of lung, brain and breast tumors[Tran et al., 1998]. 4.1B expression has also been reported to be downregulated in up to 70% of meningiomas and in up to 55% of breast cancers, while 18p is a frequent site of loss-of-heterozygosity in a variety of cancers[Charboneau et al., 2002; Gutmann et al., 2000; Gutmann et al., 2001; Kittiniyom et al., 2001]. 4.1B is also widely expressed, particularly in the brain, lungs and intestine, and has been observed to be downregulated in a spontaneous mouse model of colorectal cancer, as well as during the transition from adenoma to carcinoma in a spontaneous model of pancreatic cancer[Ohno et al., 2004; Terada et al., 2005]. Finally, 4.1B expression has been reported to be absent from several breast and lung cancer cell lines[Tran et al., 1999].

Protein 4.1B/DAL-1: *In vitro* Studies

Several studies have shown that experimental overexpression of 4.1B can suppress growth and, in some cases, induce apoptosis in human breast cancer, non-small cell lung cancer and meningioma cells[Charboneau et al., 2002; Jiang and Newsham, 2006; Robb et al., 2005]. Although the mechanism by which 4.1B induces apoptosis remains unclear, one report has recently observed that overexpression of 4.1B increases caspase-8 activity in MCF-7 cells, and that inhibitors of caspase-8 can block 4.1B-mediated apoptosis[Jiang and Newsham, 2006]. Others have reported that overexpression of 4.1B induces Rac1-dependent JNK signaling, which leads to growth suppression of meningioma cells[Gerber et al., 2006]. Truncation studies have also suggested that the U2 region of 4.1B contains the minimal growth suppressive domain when tethered to the membrane by FERM domain-mediated protein-protein interactions[Robb et al., 2005]. However, the growth inhibitory effects of 4.1B are not universal and may be cell-type-specific. For instance, overexpression of 4.1B inhibits the growth of some subclones of MCF-7 breast cancer cells, but not others, and 4.1B has been reported not to affect the growth of schwannomas[Charboneau et al., 2002; Gutmann et al., 2001].

Conceivably, expression or activity of known interactors of 4.1B—including CD44, the tumor suppressor TSCL1, other 4.1 proteins, merlin and potentially ERM proteins—could modulate its activity (Figure 1B) [Sun et al., 2002]. In most cases, binding likely occurs through the FERM domain, though recent work from our lab has also shown that the C-terminal domain of 4.1B can interact with another potential tumor

suppressor, integrin $\beta 8$ [McCarty et al., 2005a]. In most cases, the functional significance of these interactions is unknown. One exception is that 4.1B binding to the core domain of protein arginine N-methyltransferase 3 (PRMT3) has been reported to inhibit the ability of PRMT3 to methylate substrates *in vitro* [Singh et al., 2004]. Whether PRMT3 activity is important for 4.1B-mediated suppression of tumorigenesis remains unclear. Finally, it is worth noting that, in contrast to other members of the ERM and Protein 4.1 sub-families, 4.1B does not bind actin [Gutmann et al., 2001].

In terms of sub-cellular localization, 4.1B has been observed both in the cytoplasm and at the plasma membrane, either in a non-specific “honeycomb” pattern or enriched at points of cell-cell contact [Charboneau et al., 2002; Gutmann et al., 2001; Tran et al., 1999]. Localization of 4.1B, therefore, likely varies among different cell types, and may also be influenced by components of the surrounding extracellular matrix. For example, 4.1B was reported to co-localize with integrin $\beta 8$ only when the cells were plated on the $\beta 8$ ligand, LAP (the latency-associated peptide of TGF- β) [McCarty et al., 2005a]. In terms of cell adhesion and migration, one study has shown that overexpression of 4.1B in MCF-7 cells increased the strength, but not the rate, of cellular attachment to various matrix molecules [Charboneau et al., 2002]. In another study, overexpression of 4.1B somewhat inhibited cell motility (down ~20%) in schwannoma cells [Gutmann et al., 2001]. Clearly, further characterization of this protein in different cellular contexts is needed to validate and extend these observations.

Protein 4.1B/DAL-1: *In vivo* Studies

Knock-out mice lacking 4.1B have been generated by Yi, et al., and mutant animals are healthy and viable, without any detectable predisposition to spontaneous tumor formation above background levels [Yi et al., 2005]. In addition, 4.1B^{-/-} mouse embryonic fibroblasts were also reported to exhibit no differences in proliferation compared with wild-type fibroblasts. Thus far, the only phenotype observed in null animals has been a relatively minor one: Mammary glands from 4.1B^{-/-} female mice displayed a 60% increase in Ki67-positive epithelial cells during pregnancy, but not during the lactating or involution stages [Kuns et al., 2005]. In some rare instances, we have observed 4.1B^{-/-} mice experiencing seizures (J.L.K. and S.Y.W.) and premature death, which may, in some ways, resemble what has been reported in mice bearing a conditional deletion of integrin αv in neurons [McCarty et al., 2005b]. Unfortunately, this phenotype is not fully penetrant in 4.1B-deficient animals. Consequently, the absence of any readily apparent and reproducible phenotypes in these mice has precluded efforts to assign a physiological or cellular function to this protein. While this may be due to genetic redundancy and/or compensation by other Protein 4.1 subgroup members, another possibility is that loss of 4.1B may yield very subtle phenotypes, discernible only under specific assay conditions. For instance, absence of 4.1B may not affect tumor initiation or predisposition in mice, but can it affect the later stages of cancer progression to metastasis?

As described in the previous chapter, using a screen to identify genes that might be responsible for prostate cancer metastasis, we found that 4.1B was significantly downregulated in highly metastatic tumor cells. As was also mentioned, loss of 4.1B has been associated with a variety of human clinical tumors, and several studies have shown that overexpression of 4.1B suppresses growth *in vitro*. None of these studies, however, examined the effects of 4.1B on tumorigenesis *in vivo*. In the following section, I describe our work validating the role of 4.1B in prostate cancer progression and metastasis. Notably, I use both a spontaneous model and a xenotransplant orthotopic model of prostate cancer to validate that, indeed, 4.1B can act as a suppressor of tumor progression *in vivo*. Finally, I show that 4.1B is also frequently downregulated in human clinical prostate cancer.

RESULTS

Downregulation of Protein 4.1B increases the metastatic propensity of human prostate adenocarcinoma cells in a xenotransplant orthotopic model of prostate cancer

As described in the previous chapter, in a screen for genes that might be responsible for prostate cancer metastasis, we found that Protein 4.1B expression was downregulated in highly metastatic PC3-#82 cells, relative to poorly metastatic PC3-#78 cells (Figure 2A). This was originally observed by gene expression analysis of RNA from subcutaneous tumors, using the software program D-Chip. As 4.1B was the second most downregulated gene in #82 cells, and the purported functions of the Protein 4.1 subgroup of proteins appear relevant to processes such as migration and proliferation—steps which are certainly involved with metastasis—we decided to examine this gene further. We began by confirming the microarray results by performing quantitative real-time PCR on both subcutaneous tumors and on cells cultured *in vitro*. We found that in either case, as with our gene expression analysis, 4.1B RNA was severely reduced in highly metastatic #82 cells, relative to poorly metastatic #78 and medium metastatic pMicro-1 cells (Figure 2B). This result was subsequently confirmed at the protein level by Western blot against 4.1B in total soluble lysates from tissue culture cells, which detected doublet bands around 125 kDa (Figure 2C). In this case, we found that 4.1B was abundant in #78 cells and in PC-3 parental cells, which were purchased from ATCC and had not been passaged *in vivo*. In addition, 4.1B appeared to be expressed at an intermediate level in pMicro-1 cells and was almost completely lost both in #82 cells and in highly metastatic PC-3M cells obtained from Dr. I.J. Fidler (Figures 2C-D). Thus, our results for 4.1B at the RNA and protein levels coincided and, together, showed that 4.1B was selectively lost in aggressive prostate cancer cells.

The fact that 4.1B expression was inversely associated with metastatic potential suggested that this protein might act as a potential suppressor of prostate cancer progression and metastasis. We first approached this hypothesis by determining whether experimental ablation of 4.1B expression was

sufficient to enhance the metastatic ability of poorly metastatic cells. To downregulate 4.1B, we generated #78 cell lines expressing stable siRNAs targeted against this gene and found that cells expressing any of four different siRNAs (DL1-DL4) exhibited significant reductions in 4.1B protein and RNA levels *in vitro* (Figure 3A). This inhibition was also maintained after these cells had been injected as subcutaneous tumors. For the rest of our studies, we decided to focus on the two cell lines displaying the most severe ablation of 4.1B (#78-DL1 and #78-DL2) and used as controls #78 cells expressing an empty vector (pSIRISP) or an siRNA against GFP (siGFP). We found no significant differences in proliferation among the cell lines *in vitro*, either in the presence or absence of serum (Figure 3B), and subcutaneous tumors derived from these cells also grew at similar rates (Figure 3C). This is in concordance with our findings that #78 and #82 cells did not differ in proliferation, despite expressing varying levels of 4.1B.

We next xenotransplanted #78 tumors expressing siRNAs against 4.1B or control plasmids into the dorsolateral lobes of the prostate using surgical orthotopic implantation (SOI). Approximately 2-3 months after implantation, mice were analyzed when they appeared moribund, and, at the time of dissection, the average masses of the orthotopic primary tumors in the prostate did not differ among the cell lines (Figure 4A). However, the average masses of the draining para-aortic/lumbar lymph nodes were significantly larger in mice implanted with 78-DL1 and -DL2 tumors, relative to those implanted with control tumors (Figure 4B, $p = 0.039$). In many cases, histological examination revealed that lymph nodes from mice implanted with 78-DL1 and -DL2 tumors were completely infiltrated with tumor cells ($n = 46$ nodes examined), whereas nodes from animals implanted with control tumors more frequently exhibited only partial, if any, invasion (Figure 4C, $n = 42$ nodes examined, $p < 0.0001$).

Partial invasion of lymph nodes by control tumors commonly involved subcapsular infiltration of malignant cells, without deeper penetration into the interior of the node. This was also often a site where many tumor cells appeared apoptotic, as assessed by TUNEL staining (Figure 4D, top, arrows). In contrast, TUNEL staining was rare in nodal regions which were completely replaced by tumor cells (Figure 4D, bottom), as was often the case with DL1- and DL2-expressing tumors, though central areas of necrosis were sometimes stained in exceptionally large nodal metastases (not shown). Mice implanted with siRNA-expressing tumors also possessed more lung metastases than those implanted with control tumors, though these differences did not reach statistical significance due to the small number of animals that had exhibited systemic spread (Figure 4E). Overall, these results indicate that 4.1B suppresses prostate cancer metastasis, and that downregulation of 4.1B is sufficient to increase the metastatic potential of poorly metastatic #78 cells.

Protein 4.1B interacts with integrin $\beta 8$

To try and elucidate how high levels of 4.1B might be suppressing metastasis in PC-#78 cells, we attempted to confirm known binding partners of this protein, in an effort to place it within the context of potential signaling pathways. Notable 4.1B-interacting proteins have been reported to include CD44, merlin, calmodulin, TSLC1, PRMT3, 14-3-3 proteins, β -II spectrin, microtubules, as well as other ERM and 4.1 proteins. In nearly all cases, however, rather than being 4.1B-specific interactors, these binding partners likely interact with all members of the 4.1 subgroup of proteins via either their FERM or SABD domains. Recently, studies by Dr. Joseph McCarty in our lab identified the 4.1B C-terminal domain as a novel interactor of integrin $\beta 8$ in a yeast two-hybrid screen. Follow-up work showed that, in fact, $\beta 8$ interacted with all 4.1 subgroup proteins through their CTDs. As $\beta 8$ has been shown to suppress the growth of tumor cells through activation of TGF- β [Mu et al., 2002], we sought to confirm the 4.1B- $\beta 8$ interaction in PC-3 cells, as well as to test whether this interaction affected cell growth and/or survival.

We began by determining whether PC-3 cells expressed integrin $\beta 8$ and its heterodimeric binding partner, αv . Neither integrin subunits were detectable by Western blot on soluble whole cell lysates (data not shown), so we attempted to immunoprecipitate either the αv or $\beta 8$ subunits, and to determine whether their respective binding partners ($\beta 8$ or αv , respectively) were enriched by co-immunoprecipitation (co-IP). We found that immunoprecipitation of $\beta 8$ could co-IP endogenous αv integrin from PC-3 cells, as assessed by Western blot (Figure 5A). This was also true in mouse TRAMP prostate cancer cells (data not shown). In the reverse experiment, immunoprecipitation of αv integrin did not co-IP $\beta 8$, although this may have been due to technical reasons (data not shown). A summary of the antibodies most useful for detecting mouse or human $\alpha v\beta 8$ in different applications is shown in Figure 5B.

Upon confirming that PC-3 cells expressed $\alpha v\beta 8$, we next determined whether 4.1B could interact with integrin $\beta 8$. Initial studies focused on #78 cells, as they were known to express $\alpha v\beta 8$ as well as high levels of 4.1B; however, in no cases were we successful at co-IP experiments involving endogenous proteins (data not shown). Therefore, we co-expressed both 4.1B and integrin $\beta 8$ fused with the epitope tags myc and V5, respectively, to their C-termini. Following co-transfection of cells, immunoprecipitation of integrin $\beta 8$ using an antibody against V5, followed by Western blot detection of the myc tag yielded a single band of the expected size for the 4.1B-myc fusion protein (Figure 5C). This experiment lends support to the possibility that 4.1B and integrin $\beta 8$ can interact in prostate tumor cells. Although endogenous co-IP of these proteins was unsuccessful, this was not surprising, given that protein-protein interactions *in vivo* are often weak in nature, thereby easily disruptable by detergent solubilization of protein lysates. Therefore, it is possible that endogenous 4.1B and integrin $\beta 8$ can interact in our cells, but this interaction may occur at a level that is below our current limits of detection.

Once we were able to confirm the 4.1B- β 8 interaction, we were interested in determining whether overexpression of either of these genes could impact cell growth and/or morphology. Early attempts to overexpress 4.1B stably in PC-3 cells were unsuccessful, and, therefore, both myc-tagged 4.1B and V5-tagged integrin β 8 were cloned into separate doxycycline-inducible vectors, which were delivered into #82 cells by viral infection. Induction of 4.1B and β 8 expression upon addition of doxycycline was confirmed by Western blot (Figure 6A). Subsequently, the growth of induced versus non-induced cells was assayed in the presence or absence of serum. In either situation, we found no significant differences in growth between non-induced cells and cells induced to express 4.1B (Figure 6B-C and data not shown). Induction of β 8 expression did result in an apparent 20% reduction in cell number, but given that these cells had been induced and grown for 6-7 days prior to quantitation, the differences appeared quite subtle (Figure 6B and data not shown). However, these findings were complicated by the observation that inducible gene expression for either 4.1B or β 8 was apparent in only about one-third of cells, as assessed by immunofluorescence staining (Figure 6D).

Protein 4.1B suppresses tumor progression in a spontaneous model of prostate cancer

As discussed previously, xenotransplant models offer convenient approaches for studying tumorigenesis *in vivo*; however, these approaches only recapitulate some of the steps of cancer progression and are, by their nature, relatively artificial systems. We were therefore interested in confirming and extending our observations—that 4.1B suppresses metastasis following SOI xenotransplantation—in a spontaneous model of prostate cancer. For this, we utilized the transgenic adenocarcinoma of the mouse prostate (TRAMP) tumorigenesis model, where transgenic overexpression of SV40 large T antigen in the prostate causes spontaneous prostate cancer development in the mouse. Whereas normal prostate ductal structures consist of a single layer of cytokeratin 8-positive luminal cells surrounded by occasional cytokeratin 5-positive basal cells (Figure 7A), tumor development in TRAMP mice involves expansion of the luminal cell compartment, loss of differentiation and cell polarization, and finally, invasion through the basement membranes and metastasis (Figure 7B) [Abate-Shen and Shen, 2000]. This progression is believed to be gradual, occurring in a step-wise fashion, and has been described by a grading system, as will be described shortly.

To determine if 4.1B could modulate TRAMP tumor progression, we first obtained 4.1B knock-out mice and confirmed the absence of the protein by performing Western blot on brain and prostate lysates from 4.1B^{+/+} or 4.1B^{-/-} animals (Figure 8A). We then crossed these animals into a TRAMP background and analyzed the mice after 26 weeks of age. We found that 11/19 (58%) of 4.1B^{-/-};TRAMP^{+/+} mice developed a variety of palpable carcinomas in the prostate, compared to 2/26 (7.7%) of 4.1B^{+/+};TRAMP^{+/+} mice ($p = 0.0002$, Figures 8B and 8D). As was seen in our xenotransplant model, 4.1B-deficient TRAMP

tumorigenic prostates also displayed an increased propensity to metastasize to para-aortic/lumbar lymph nodes, relative to 4.1B-heterozygous TRAMP prostates. The presence of metastatic tumor cells in the nodes was confirmed by staining lymph node sections with antibodies against the epithelial marker cytokeratin 8 (Figure 8C). The overall results from these experiments are summarized in Figure 8D.

We next micro-dissected and sectioned the tumorigenic TRAMP prostates from all mice. Histopathologic grading of these sections, using the system described by Hurwitz et al. [Hurwitz et al., 2001], was blindly performed by a pathologist from our lab, Dr. Marc Barry. Sections were scored on a scale of 1-6, with '1' being normal prostate and '6' representing poorly differentiated adenocarcinoma, with intermediate grades denoting precursor lesions of varying severity (Figure 9A). Since tumorigenic prostates often exhibited heterogeneity even within the same section, two grades were assigned for each prostate lobe of each animal: a highest grade and a predominant grade. For instance, in the section shown in Figure 9B, a highest grade of 6 was awarded for the focal areas of undifferentiated adenocarcinoma observed, while a predominant grade of 4 was also assigned. We found that, regardless of genotype, nearly all mice developed tumors. However, using either grading approach on either the ventral or dorsolateral lobes of the prostate, we invariably found that 4.1B^{-/-};TRAMP^{+/-} mice developed the highest, least differentiated, and most aggressive grades of prostate cancer at a significantly increased frequency relative to heterozygous TRAMP mice (Figures 9C, p = 0.003). These results indicate that loss of 4.1B is sufficient to enhance the progression of spontaneous prostate cancer to metastatic disease.

To understand how absence of 4.1B promotes tumor progression, we stained sections for proliferation and apoptotic markers (Ki67 and TUNEL, respectively). Because cancer progression in the TRAMP model is believed to proceed in a step-wise fashion, beginning at Grade 1 and increasing with severity over time, we reasoned that if proliferative or apoptotic differences were manifested in the lower-graded prostatic lesions, that would affect the rate of progression to Grade 6 adenocarcinoma. Therefore, we began by staining 26-week old, Grade 4-matched prostate sections with Ki67 antibody and by TUNEL (Figure 10A). We found no differences between 4.1B^{-/-} or 4.1B^{+/-} TRAMP prostates for either proliferation or apoptosis, and we also found no differences when we stained 26-week old, Grade 5-matched sections (Figure 10B). However, especially for the 4.1B^{-/-} prostates, these samples were biased in that many tumors had already progressed to Grade 6 and could not be used for this analysis; in other words, what was actually analyzed was the remaining prostates that had not progressed to the higher grades. To perform a more unbiased study, we removed and sectioned prostates from a younger cohort of 22-week old TRAMP mice for both genotypes. At this age, prostates from both 4.1B^{-/-} and 4.1B^{+/-} mice had mostly progressed to Grades 3-4 severity, but had not yet reached Grade 6 (Figure 10C). Although there was again no statistically significant difference in proliferation (p = 0.15), we found that 4.1B^{-/-};TRAMP prostates displayed about 50% fewer apoptotic cells, compared to heterozygous TRAMP mice (Figures 10D-E, p < 0.001). These results suggest that absence of 4.1B, at the very least, protects prostatic

precursor lesions from undergoing cell death at 22 weeks, which may facilitate enhanced progression to higher and more invasive tumorigenic grades by 26 weeks.

Characterization of 4.1B in murine TRAMP prostate cancer cells

TRAMP prostate cancer cell lines were derived by Foster, et al. (1997), and were isolated from a single spontaneous TRAMP prostate primary tumor. Three cell lines were established, TRAMP-C1, -C2 and -C3; and while TRAMP-C1 and -C2 cells were reported to form colonies in soft agar and subcutaneous tumors when injected into syngeneic animals, TRAMP-C3 cells displayed longer doubling times *in vitro*, did not form colonies in soft agar and were non-malignant in animals (Figure 11A). We obtained TRAMP-C1 and -C3 cells from American Type Culture Collection (ATCC) and began by confirming that TRAMP-C1, but not TRAMP-C3, cells formed soft agar colonies (Figure 11B). In concordance with our xenotransplant and spontaneous tumor results, we also found that 4.1B protein levels were specifically reduced in malignant TRAMP-C1 cells, relative to non-malignant TRAMP-C3 cells (Figure 11C), while levels of the related proteins, 4.1G and 4.1N, were unchanged. We next performed immunofluorescence staining for 4.1B on both cell lines, and observed that while non-aggressive TRAMP-C3 cells generally exhibited uniformly high levels of this protein, aggressive TRAMP-C1 cells displayed remarkable heterogeneity (Figure 11D). While most cells had lost expression of 4.1B, a significant minority still retained expression and “co-existed” in a mixed population.

We next sought to determine whether ablation of 4.1B expression could increase the aggressiveness of TRAMP-C3 cells—in essence, making them more akin to TRAMP-C1 cells. Stable expression of any of three siRNAs targeted against mouse 4.1B effectively ablated expression of the protein (Figure 12A), and this was confirmed by immunofluorescence (Figure 12B). The two cell lines with the most significant reductions in 4.1B protein levels (C3-mDL1 and -mDL4) were tested for their ability to form colonies in soft agar; however, regardless of whether the TRAMP-C3 cells expressed high or low levels of 4.1B, as before, no colonies were seen (data not shown). These cells also exhibited no growth differences in the presence or absence of serum and/or testosterone (data not shown). Therefore, ablation of 4.1B expression did not appear to be sufficient for inducing the malignant phenotype from non-malignant cells, at least not in the assays we attempted.

In light of these results, we decided to ask a less ambitious question: If loss of 4.1B could not induce a malignant phenotype *de novo* in TRAMP-C3 cells, could loss of 4.1B enhance the aggressiveness of already-malignant TRAMP-C1 cells? Because a subpopulation of TRAMP-C1 cells was found by immunofluorescence to express high levels of 4.1B, we decided to clone and expand members of this subpopulation. We began by isolating 30 single cell clones derived from the heterogeneous bulk population and by testing each of these clones by immunofluorescence for 4.1B expression (Figure 13A).

In most cases, these cloned TRAMP-C1 subpopulations expressed uniformly high, low or intermediate levels of 4.1B, as expected, though in some rare instances, heterogeneous expression was observed—these subpopulations may have been derived from more than one clone, or they might be genetically unstable. For 8 independent clones (four expressing high levels of 4.1B, four expressing low levels, as determined by immunofluorescence), we further validated these observations by Western blot (Figure 13B). Interestingly, even among cells that expressed uniformly high/intermediate levels of 4.1B, localization of the protein varied significantly, ranging from diffuse localization in the cytoplasm (Clone 1), to membrane enrichment at sites of cell-cell contact (Clone 29) (Figure 13C). In non-malignant TRAMP-C3 cells, 4.1B localization was also found in circular, actin-rich structures (Figure 13D). siRNA-mediated ablation 4.1B appeared to have no apparent effect on these structures, which superficially resembled podosomes, although this inference awaits further validation.

To determine if varying levels of endogenous 4.1B affected soft agar colony formation, we subjected 29 of our 30 clones to this assay. We found that the ability of these cells to initiate anchorage-independent growth varied drastically, even though these clones were derived from an aggressive, albeit heterogeneous, starting population. The results, which are shown in Figure 14A and are sorted by soft agar colony size, ranged from cells that had not proliferated (-), to those that had undergone only a couple of rounds of cell division (+/-), to those that had formed larger colonies (+ and ++) after two weeks. Unfortunately, no correlation was evident between the level of endogenous 4.1B expression and soft agar colony size. We did notice, however, that among those cells that had formed colonies, two general types of morphologies could be distinguished: The colonies either took on a reflective appearance with a smooth outer border (“smooth”), or they appeared dense and possessed an uneven outer edge (“jagged”) (Figure 14B). When we compared colony morphology with 4.1B expression, we found that 6/9 clones that had formed smooth colonies expressed high levels of 4.1B, whereas 7/10 clones that had formed jagged colonies expressed low levels of the protein (Figure 14B). This suggested to us that, perhaps to some degree, high levels of 4.1B might be associated with a smooth colony morphology, and, conversely, absence of 4.1B might be associated with a jagged morphology.

We tested this hypothesis by ablating 4.1B using stable siRNAs in five TRAMP-C1 cell clones which had exhibited both high levels of 4.1B protein and a smooth, soft agar colony morphology (Clones 8, 9, 14, 17 and 27). Although we succeeded in downregulating this gene in all five independent clones (Figure 14C), we did not observe any differences in either the size or morphology of the colonies formed in soft agar, relative to that of control-infected cells (data not shown). The sum of these results suggests that although 4.1B is downregulated in highly aggressive TRAMP-C1 cells, loss of this protein is neither sufficient to convert non-aggressive cells into aggressive cells, nor is it capable of augmenting the aggressiveness of already-malignant cells. Our results, however, do not rule out the possibility that other assays might

identify phenotypic differences directly affected by 4.1B expression. This, as well as other interpretations of our results, will be elaborated upon in the Discussion section.

Expression of Protein 4.1B is often downregulated in human clinical prostate tumors

We have just shown that loss of 4.1B can enhance tumor progression and metastasis in two independent mouse models of prostate cancer; however, an important question still remains: Does loss of this gene actually occur in human clinical patients? Although it is not possible to test whether 4.1B has a direct causal effect in tumor suppression in human samples, nonetheless, it would be reassuring and in concordance with our experimental findings if loss of 4.1B were a frequently observed event during human prostate cancer progression. That would at least imply that 4.1B might function as a potential negative modulator of tumorigenesis in humans.

As mentioned previously, several studies have reported downregulation of 4.1B in various tumor types relative to their corresponding normal tissues, but none have implicated this protein, thus far, in prostate cancer. We therefore began by examining the Oncomine gene expression database for studies where 4.1B expression was significantly changed. We were pleased to discover that among a total of five independent data-sets comparing prostate cancer versus normal/benign tissue, four showed significant downregulation of 4.1B in the tumors (in all cases, $p \leq 0.001$) (Figures 15A-B). These data-sets were originally collected by Welsh et al. (2001)[Welsh et al., 2001], Singh et al. (2002)[Singh et al., 2002], Yu et al. (2004)[Yu et al., 2004b], and LaPointe et al. (2004)[Lapointe et al., 2004]. In particular, in the study by LaPointe et al. (2004), 4.1B expression was significantly downregulated in prostate tumor samples relative to normal prostate tissues (Figure 15B, $p < 0.001$), and further downregulated in lymph node metastases compared to prostate tumors ($p < 0.001$).

Recent studies have shown that the genes encoding the Ets family transcription factors ERG and ETV1 are frequently translocated in as many as 80% of human prostate cancers. In the majority of cases, these genes were fused to the coding sequence of TMPRSS2, causing androgen-regulated overexpression of the chimeric proteins in tumors. Interestingly, Oncomine analysis revealed that prostate tumors with ERG overexpression exhibited significantly lower levels of 4.1B expression, relative to tumors that did not overexpress Ets family transcription factors (Figure 16, $p = 0.0001$; data originally from LaPointe et al. (2004)). Although, again, this is not proof that one protein inversely regulates the expression of the other, it suggests that there might exist a link between 4.1B and ERG. Overall, we have found that four out of a total of five independent human clinical prostate cancer data-sets exhibited very significant downregulation of 4.1B expression in tumors. This would appear to be in concordance with our findings from two *in vivo* mouse tumor models that loss of the tumor suppressor 4.1B is a relevant and important event during progression of human prostate cancer.

DISCUSSION

Although Protein 4.1B was originally identified as a protein whose expression was reduced in human non-small cell lung carcinomas[Tran et al., 1999], subsequent studies have shown that downregulation occurs across many different tumor cell types, including colorectal, breast and renal clear cell carcinomas. 4.1B protein has also been reported to be lost in up to 70% of sporadic meningiomas and in 55% of ductal carcinomas *in situ*, and has been observed to be downregulated during tumorigenesis in spontaneous mouse models of pancreatic and intestinal cancer[Gutmann et al., 2000; Kittiniyom et al., 2001; Ohno et al., 2004; Terada et al., 2005]. While *in vitro* experiments have suggested that 4.1B might act as a tumor suppressor, these results have awaited experimental validation *in vivo*.

We have shown here that Protein 4.1B acts as a negative modulator of the aggressive tumor phenotype in two different *in vivo* models of prostate cancer. In a screen for genes involved with metastasis, we found that 4.1B expression was significantly reduced in highly metastatic human prostate adenocarcinoma cells, and that downregulation of 4.1B in poorly metastatic cells was sufficient to increase their metastatic potential in our xenotransplant orthotopic model. Furthermore, we showed that prostates from 4.1B^{-/-} TRAMP mice displayed increased progression to invasive, undifferentiated adenocarcinomas, relative to those from 4.1B^{+/-} TRAMP mice, in a spontaneous tumor model of prostate cancer. In both systems, tumorigenic cells lacking 4.1B appeared to exhibit reduced apoptosis, which may have accounted for enhanced invasion. 4.1B expression was also downregulated in tumors relative to normal tissues in four independent studies of human clinical prostate cancer, and was also significantly reduced in prostate samples displaying high ERG expression. These results suggest that downregulation of 4.1B is a frequent event in human prostate cancer that may contribute to a malignant tumor phenotype.

Our *in vivo* findings are in concordance with studies that have suggested that overexpression of 4.1B can induce apoptosis *in vitro* for some tumor cell types[Charboneau et al., 2002; Gutmann et al., 2001; Jiang and Newsham, 2006; Robb et al., 2005; Tran et al., 1999]. However, we have yet to observe any apparent *in vitro* consequences associated with manipulating 4.1B levels in either PC-3 or TRAMP cells. In experiments where 4.1B was overexpressed, the growth suppression phenotype has been reported to be cell-type-specific. High 4.1B, for instance, inhibited growth of meningiomas but not schwannomas[Gutmann et al., 2001], and suppressed proliferation of some MCF-7 breast cancer cell clones but not others[Charboneau et al., 2002]. Our own negative results from overexpression of 4.1B may have been complicated by the fact that only a minority of cells were induced by doxycycline to express 4.1B. Yet, at the same time, the lack of any observable differences in growth also agreed with our findings that siRNA-mediated ablation of 4.1B did not affect cell proliferation; that our original #78 and #82 cells did not grow differently; that both 4.1B^{-/-} and 4.1B^{+/-} mice initiated TRAMP tumors similarly and

did not display significant differences in proliferation; and that mouse embryonic fibroblasts deficient in 4.1B have not been observed to exhibit any growth phenotypes *in vitro* [Yi et al., 2005].

In light of these results, we believe that 4.1B likely exerts its apoptotic and/or proliferative effects in a cell type- and/or context-specific manner. It is possible that 4.1B sensitizes prostate cells to apoptosis under specific conditions, and, in future work, it will be critical to determine how to challenge these cells appropriately *in vitro*, such that the 4.1B-associated phenotypes are manifested. Along these lines, we explored the possibility that the interaction between 4.1B and a potential tumor suppressor, integrin $\beta 8$, might be important for regulating cell proliferation and apoptosis. While we were able to confirm this interaction in our PC-3 cells, we have not yet been able to attribute any biological significance to this observation. As with 4.1B, overexpression of integrin $\beta 8$ in our cells did not affect proliferation, and no effects were seen when cells were grown on plates coated with $\alpha \nu \beta 8$ ligands, including vitronectin and LAP (data not shown). Because $\alpha \nu \beta 8$ has been reported to contribute to protease-mediated processing and activation of TGF- β [Cambier et al., 2005; Mu et al., 2002], we examined whether varying levels of 4.1B in PC-3 cells could affect the activity of $\beta 8$ and, thus, the ratio of activated to non-activated TGF- β secreted into the medium. Our preliminary results were inconclusive, as the amount of TGF- β found in cell-conditioned media was quite low and consisted almost entirely of non-activated TGF- β (data not shown). Clearly, it will be important to examine further the significance of the 4.1B interaction with $\beta 8$, as well as its interactions with other known binding partners, including CD44 and merlin.

In addition, it will also be interesting to determine whether varying the levels of 4.1B has any effects on the TRAMP tumor cell lines and, if so, how these effects are mediated. Although we found that aggressive TRAMP-C1 cells showed downregulation of 4.1B relative to poorly aggressive TRAMP-C3 cells, we were unable to attach any functional significance relating 4.1B expression with cell phenotype. We found that loss of 4.1B was insufficient for converting non-malignant TRAMP-C3 cells into malignant cells, and also insufficient for increasing the malignancy of already-malignant TRAMP-C1 cells. Again, it is very possible that we may not have sufficiently challenged the cells in a manner that would elicit phenotypes that hinged on 4.1B expression. For example, while cells suspended in soft agar did not display any apparent differences in morphology or growth, perhaps growing cells in a more realistic three-dimensional environment (e.g. collagen gels or Matrigel) might have yielded a noticeable phenotype. As TRAMP-C1 cells have been observed to form tumors when injected into syngeneic (C57Bl/6) hosts [Foster et al., 1997], we have also attempted to inject subclones derived from TRAMP-C1 cells expressing either high or low levels of 4.1B. Unfortunately, preliminary results were complicated by the fact that tumor formation was inconsistent for all cell clones tested and occurred only after a long latency period (> 2 months, data not shown). Therefore, it may be imperative to develop more reproducible assays to test these cells.

Another avenue of future research will be to determine in more detail how loss of 4.1B protects tumor cells from apoptosis *in vivo*. Based on the distribution of tumor grades found at 26 weeks for TRAMP prostates from 4.1B^{-/-} and 4.1B^{+/-} mice (Figure 9C), it appears, at least from a preliminary analysis, that heterozygous prostate tumors tended to accumulate at Grade 4, whereas knock-out prostate tumors proceeded more efficiently to the higher Grades 5 and 6. The finding that there was reduced apoptosis in Grade 4-matched 22-week old prostates is in concordance with the hypothesis that the Grade 4-to-Grade 5 transition during tumor progression might be a rate-limiting step in heterozygous mice. However, since we did not examine apoptosis in lower-graded sections, we cannot rule out the possibility that 4.1B might also be acting earlier in tumorigenesis. This is an issue that can easily be resolved through analysis of additional TRAMP mice.

Similarly, in our xenotransplant orthotopic model of prostate cancer, additional mice may need to be examined, and possibly at earlier time-points, to determine how the presence or absence of 4.1B affects the most initial stages of tumor colonization in the lymph node. In this study, we have observed that #78 tumors with high 4.1B expression did not metastasize efficiently to the draining lymph nodes and, thus, exhibited incomplete—and, in many cases, subcapsular—invasion of the nodes. In contrast, tumors with low 4.1B expression (#78-DL1 and -DL2) yielded lymph nodes which often consisted almost entirely of tumor material. The differences in the degree of lymph node infiltration made it difficult to make direct (and accurate) comparisons of apoptosis frequency between cell lines, although there did appear to be increased cell death in nodes that possessed subcapsular invasion. This observation, however, does not distinguish between cause and effect for apoptosis and subcapsular invasion. In other words, cells which are apoptosis-prone might be restricted to grow merely as subcapsular metastases (apoptosis “causes” partial invasion); on the other hand, as the subcapsular spaces are where afferent lymphatics connect with lymph nodes and are usually the initial sites of tumor colonization, this might also be a site where, and/or a period when, increased apoptosis is normally seen (partial invasion “causes” apoptosis). Therefore, it remains unclear in our SOI model whether loss of 4.1B enhances the arrival of tumor cells to the node, and/or whether it augments the ability of malignant cells to colonize the node once they have arrived. As mentioned previously, examining mice at earlier timepoints may resolve this issue by allowing more direct comparisons to be made between cell lines of differing metastatic ability.

In conclusion, our findings from this chapter have validated the role of 4.1B as a negative modulator of prostate cancer progression *in vivo*. The additional observation that 4.1B is significantly downregulated in four out of five studies of human clinical prostate cancer is consistent with the idea that loss of 4.1B is an important and physiologically relevant event during progression of this disease. It will be critical in future work to understand, at a molecular level, the mechanism by which 4.1B suppresses tumorigenesis, and also to confirm the human clinical gene expression results at the protein level. As translocation of Ets family transcription factors has emerged as a common phenomenon in clinical prostate cancer [Tomlins et

al., 2005], it will also be interesting to determine whether 4.1B expression is directly regulated by Ets family members such as ERG, which can both induce or suppress gene transcription in a context-dependent manner[Hsu et al., 2004; Sementchenko and Watson, 2000].

REFERENCES

- Abate-Shen C, Shen MM (2000): Molecular genetics of prostate cancer. *Genes & Development* 14:2410-2434.
- Anderson RA, Marchesi VT (1985): Regulation of the association of membrane skeletal protein 4.1 with glycophorin by a polyphosphoinositide. *Nature* 318:295-8.
- Bretscher A, Edwards K, Fehon RG (2002): ERM proteins and merlin: integrators at the cell cortex. *Nature Reviews Molecular Cell Biology* 3:586-599.
- Cambier S, Gline S, Mu D, Collins R, Araya J, Dolganov G, Einheber S, Boudreau N, Nishimura SL (2005): Integrin alpha(v)beta(8)-mediated activation of transforming growth factor-beta by perivascular astrocytes. *American Journal of Pathology* 166:1883-1894.
- Charboneau AL, Singh V, Yu T, Newsham IF (2002): Suppression of growth and increased cellular attachment after expression of DAL-1 in MCF-7 breast cancer cells. *International Journal of Cancer* 100:181-188.
- Crepaldi T, Gautreau A, Comoglio PM, Louvard D, Arpin M (1997): Ezrin is an effector of hepatocyte growth factor-mediated migration and morphogenesis in epithelial cells. *J Cell Biol* 138:423-434.
- Edwards SD, Keep NH (2001): The 2.7 Å crystal structure of the activated FERM domain of moesin: an analysis of structural changes on activation. *Biochemistry* 40:7061-7068.
- Foster BA, Gingrich JR, Kwon ED, Madias C, Greenberg NM (1997): Characterization of prostatic epithelial cell lines derived from transgenic adenocarcinoma of the mouse prostate (TRAMP) model. *Cancer Research* 57:3325-3330.
- Gerber MA, Bahr SM, Gutmann DH (2006): Protein 4.1B/differentially expressed in adenocarcinoma of the lung-1 functions as a growth suppressor in meningioma cells by activating Rac1-dependent c-Jun-NH2-kinase signaling. *Cancer Research* 66:5295-5303.
- Giovannini M, Robanus-Maandag E, Niwa-Kawakita M, Valk Mvd, Woodruff JM, Goutebroze L, Merel P, Berns A, Thomas G (1999): Schwann cell hyperplasia and tumors in transgenic mice expressing a naturally occurring mutant NF2 protein. *Genes and Development* 13:978-986.
- Gutmann DH, Donahoe J, Perry A, Lemke N, Gorse K, Kittiniyom K, Rempel SA, Gutierrez JA, Newsham IF (2000): Loss of DAL-1, a protein 4.1-related tumor suppressor, is an important early event in the pathogenesis of meningiomas. *Hum Mol Genet* 9:1495-1500.
- Gutmann DH, Giordano MJ, Fishback AS, Guha A (1997): Loss of merlin expression in sporadic meningiomas, ependymomas and schwannomas. *Neurology* 49:267-270.
- Gutmann DH, Hirbe AC, Huang ZY, Haipek CA (2001): The protein 4.1 tumor suppressor, DAL-1, impairs cell motility, but regulates proliferation in a cell-type-specific fashion. *Neurobiology of Disease* 8:266-278.
- Hamada K, Shimizu T, Matsui T, Tsukita S, Hakoshima T (2000): Structural basis of the membrane-targeting and unmasking mechanisms of the radixin FERM domain. *EMBO J* 19:4449-4462.
- Henry MD, Agosti CG, F FS (1995): Molecular dissection of radixin: distinct and interdependent functions of the amino- and carboxy-terminal domains. *J Cell Biol* 129:1007-1022.
- Hirao M, Sato N, Kondo T, Yonemura S, Monden M, Sasaki T, Takai Y, Tsukita S, Tsukita S (1996): Regulation mechanism of ERM (ezrin/radixin/moesin) protein/plasma membrane association: possible involvement of phosphatidylinositol turnover and Rho-dependent signaling pathway. *J Cell Biol* 135:37-51.
- Hsu T, Trojanowska M, Watson DK (2004): Ets proteins in biological control and cancer. *Journal of Cellular Biochemistry* 91:896-903.
- Hurwitz AA, Foster BA, Allison JP, Greenberg NM, Kwon ED (2001): The TRAMP mouse as a model for prostate cancer: "Current Protocols in Immunology." John Wiley & Sons, Inc., pp 20.5.1-20.5.23.
- Jiang W, Newsham IF (2006): The tumor suppressor DAL-1/4.1B and protein methylation cooperate in inducing apoptosis in MCF-7 breast cancer cells. *Molecular Cancer* 5:1-8.
- Johnson KC, Kissil JL, Fry JL, Jacks T (2002): Cellular transformation by a FERM domain mutant of the Nf2 tumor suppressor gene. *Oncogene* 21:5990-5997.

- Khanna C, Wan X, Bose S, Cassaday R, Olomu O, Mendoza A, Yeung C, Gorlick R, Hewitt SM, Helman LJ (2004): The membrane-cytoskeleton linker ezrin is necessary for osteosarcoma metastasis. *Nature Medicine* 10:182-186.
- Kissil JL, Johnson KC, Eckman MS, Jacks T (2002): Merlin phosphorylation by p21-activated kinase 2 and effects of phosphorylation on merlin localization. *JBC* 277:10394-10399.
- Kissil JL, Wilker EW, Johnson KC, Eckman MS, Yaffe MB, Jacks T (2003): Merlin, the product of the Nf2 tumor suppressor gene, is an inhibitor of the p21-activated kinase, Pak1. *Molecular Cell* 12:841-849.
- Kittiniyom K, Gorse KM, Dalbague F, Lichy JH, Taubenberger JK, Newsham IF (2001): Allelic loss on chromosome band 18p11.3 occurs early and reveals heterogeneity in breast cancer progression. *Breast Cancer Research* 3:192-198.
- Kuns R, Kissil JL, Newsham IR, Jacks T, Gutmann DH, Sherman LS (2005): Protein 4.1B expression is induced in mammary epithelial cells during pregnancy and regulates their proliferation. *Oncogene*:1-14.
- Lallemant D, Curto M, Saotome I, Giovannini M, McClatchey AI (2003): NF2 deficiency promotes tumorigenesis and metastasis by destabilizing adherens junctions. *Genes & Development* 17:1090-1100.
- Lapointe J, Li C, Higgins JP, Rijn Mvd, Bair E, Montgomery K, Ferrari M, Egevad L, Rayford W, Bergerheim U, Ekman P, DeMarzo AM, Tibshirani R, Botstein D, Brown PO, Brooks JD, Pollack JR (2004): Gene expression profiling identifies clinically relevant subtypes of prostate cancer. *PNAS* 101:811-816.
- Lutchman M, Rouleau GA (1995): The neurofibromatosis type 2 gene product, schwannomin, suppresses growth of NIH 3T3 cells. *Cancer Research* 55:2270-2274.
- Martin TA, Harrison G, Mansel RE, Jiang WG (2002): The role of the CD44/ezrin complex in cancer metastasis. *Critical reviews in oncology/hematology* 46:165-186.
- Matsui T, Maeda M, Doi Y, Yonemura S, Amano M, Kaibuchi K, Tsukita S, Tsukita S (1998): Rho-kinase phosphorylates COOH-terminal threonines of Ezrin/Radixin/Moesin (ERM) proteins and regulates their head-to-tail association. *JCB* 140:647-657.
- McCarty JH, Cook AA, Hynes RO (2005a): An interaction between alpha(v)beta(8) integrin and Band 4.1B via a highly conserved region of the Band 4.1 C-terminal domain. *PNAS* 102:13479-13483.
- McCarty JH, Lacy-Hulbert A, Charest A, Bronson RT, Crowley D, Housman D, Savill J, Roes J, Hynes RO (2005b): Selective ablation of alphav integrins in the central nervous system leads to cerebral hemorrhage, seizures, axonal degeneration and premature death. *Development* 132:165-176.
- McClatchey AI, Saotome I, Mercer K, Crowley D, Gusella JF, Bronson RT, Jacks T (1998): Mice heterozygous for a mutation at the Nf2 tumor suppressor locus develop a range of highly metastatic tumors. *Genes & Development* 12:1121-1133.
- Morrison H, Sherman LS, Legg J, Banine F, Isacke C, Haipek CA, Gutmann DH, Ponta H, Herrlich P (2001): The NF2 tumor suppressor gene product, merlin, mediates contact inhibition of growth through interactions with CD44. *Genes and Development* 15:968-980.
- Mu D, Cambier S, Fjellbirkeland L, Baron JL, Munger JS, Kawakatsu H, Sheppard D, Broaddus VC, Nishimura SL (2002): The integrin alpha(v)-beta(3) mediates epithelial homeostasis through MT1-MMP-dependent activation of TGF-beta1. *JCB* 157:493-507.
- Ohno N, Terada N, Murata S, Yamakawa H, Newsham IF, Katoh R, Ohara O, Ohno S (2004): Immunolocalization of protein 4.1B/DAL-1 during neoplastic transformation of mouse and human intestinal epithelium. *Histochem Cell Biol* 122:579-586.
- Polesello C, Payre F (2004): Small is beautiful: what flies tell us about ERM protein function in development. *Trends in Cell Biology* 14:294-302.
- Robb VA, Gerber MA, Hart-Mahon EK, Gutmann DH (2005): Membrane localization of the U2 domain of protein 4.1B is necessary and sufficient for meningioma growth suppression. *Oncogene* 24:1946-1957.
- Sementchenko VI, Watson DK (2000): Ets target genes: past, present and future. *Oncogene* 19:6533-6548.

- Shaw RJ, Henry M, Solomon F, Jacks T (1998): RhoA-dependent phosphorylation and relocalization of ERM proteins into apical membrane/actin protrusions in fibroblasts. *Mol Biol Cell* 9:403-419.
- Sherman L, Xu HM, Geist RT, Saporito-Irwin S, Howells N, Ponta H, Herrlich P, Gutmann DH (1997): Interdomain binding mediates tumor growth suppression by the NF2 gene product. *Oncogene* 15:2505-2509.
- Singh D, Febbo PG, Ross K, Jackson DG, Manola J, Ladd C, Tamayo P, Renshaw AA, D'Amico AV, Richie JP, Lander ES, Loda M, Kantoff PW, Golub TR, Sellers WR (2002): Gene expression correlates of clinical prostate cancer behavior. *Cancer Cell* 1:203-209.
- Singh V, Miranda TB, Jiang W, Frankel A, Roemer ME, Robb VA, Gutmann DH, Herschman HR, Clarke S, Newsham IF (2004): DAL-1/4.1B tumor suppressor interacts with protein arginine N-methyltransferase 3 (PRMT3) and inhibits its ability to methylate substrates in vitro and in vivo. *Oncogene* 23:7761-7771.
- Sun CX, Robb VA, Gutmann DH (2002): Protein 4.1 tumor suppressors: getting a FERM grip on growth regulation. *Journal of Cell Science* 115:3991-4000.
- Takahashi K, Sasaki T, Mammoto A, Takaishi K, Kameyama T, Tsukita S, Takai Y (1997): Direct interaction of the Rho GDP dissociation inhibitor with ezrin/radixin/moesin initiates the activation of the Rho small G protein. *JBC* 272:23371-23375.
- Takeuchi K, Sato N, Kasahara H, Funayama N, Nagafuchi A, Yonemura S, Tsukita S, Tsukita S (1994): Perturbation of cell adhesion and microvilli formation by antisense oligonucleotides to ERM family members. *J Cell Biol* 125:1371-1384.
- Terada N, Ohno N, Yamakawa H, Ohara O, Ohno S (2005): Topographical significance of membrane skeletal component protein 4.1B in mammalian organs. *Anatomical Science International* 80:61-70.
- Tomlins SA, Rhodes DR, Perner S, Dhanasekaran SM, Mehra R, Sun XW, Varambally S, Cao X, Tchinda J, Kuefer R, Lee C, Montie JE, Shah RB, Pienta KJ, Rubin MA, Chinnaiyan AM (2005): Recurrent fusion of TMPRSS2 and ETS transcription factor genes in prostate cancer. *Science* 310:644-648.
- Tran Y, Benbatoul K, Gorse K, Rempel S, Futreal A, Green M, Newsham I (1998): Novel regions of allelic deletion on chromosome 18p in tumors of the lung, brain and breast. *Oncogene* 17:3499-3505.
- Tran YK, Bogler O, Gorse KM, Wieland I, Green MR, Newsham IF (1999): A novel member of the NF2/ERM/4.1 superfamily with growth suppressing properties in lung cancer. *Cancer Research* 59:35-43.
- Welsh JB, Sapinoso LM, Su AI, Kern SG, Wang-Rodriguez J, Moskaluk CA, H.F Frierson J, Hampton GM (2001): Analysis of gene expression identifies candidate markers and pharmacological targets in prostate cancer. *Cancer Research* 61:5974-5978.
- Yi C, McCarty JH, Troutman SA, M.S.Eckman, Bronson RT, Kissil JL (2005): Loss of the putative tumor suppressor Band 4.1B/Dal1 gene is dispensible for normal development and does not predispose to cancer. *Molecular and Cellular Biology* 25:10052-10059.
- Yonemura S, Matsui T, Tsukita S, Tsukita S (2002): Rho-dependent and -independent activation mechanisms of ezrin/radixin/moesin proteins: an essential role for polyphosphoinositides in vivo. *Journal of Cell Science* 115:2569-2580.
- Yu Y, Khan J, Khanna C, Helman L, Meltzer PS, Merlino G (2004a): Expression profiling identifies the cytoskeletal organizer ezrin and the developmental homeoprotein Six-1 as key metastatic regulators. *Nature Medicine* 10:175-181.
- Yu YP, Landsittel D, Jing L, Nelson J, Ren B, Liu L, McDonald C, Thomas R, Dhir R, Finkelstein S, Michalopoulos G, Becich M, Luo JH (2004b): Gene expression alterations in prostate cancer predicting tumor aggression and preceding development of malignancy. *Journal of Clinical Oncology* 22:2790-2799.

A

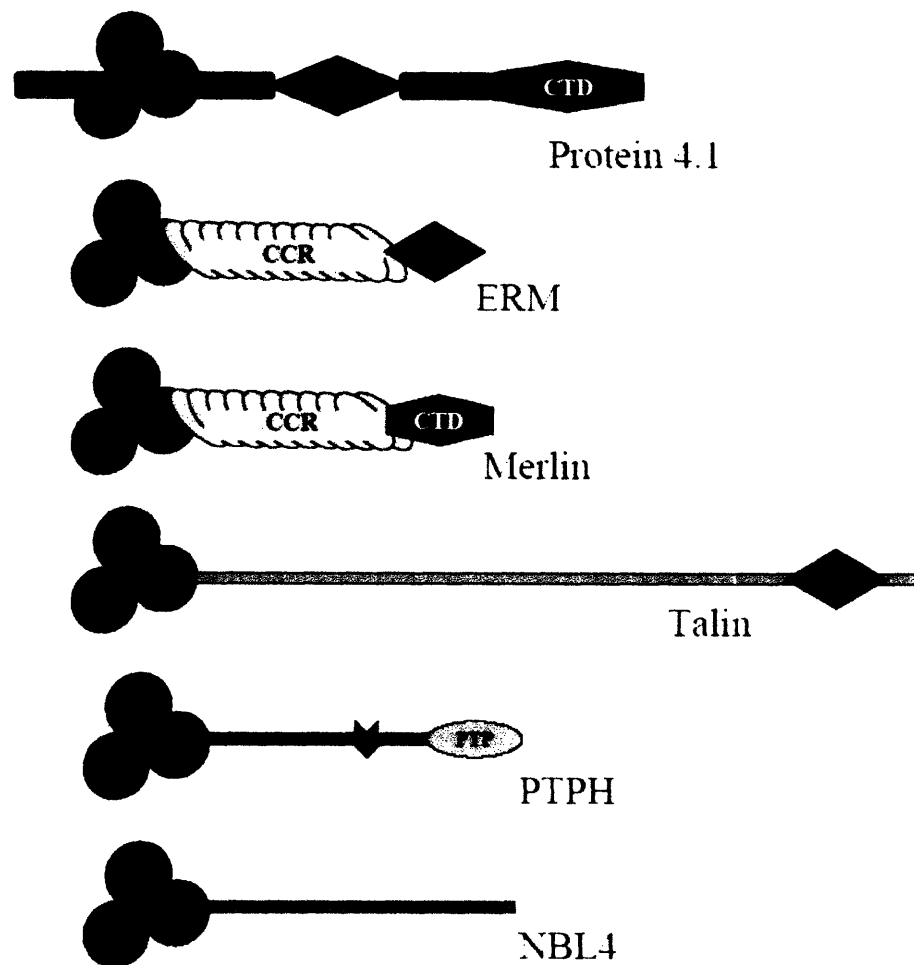


Figure 1. The Protein 4.1 superfamily can be divided into five subgroups and is characterized by a conserved FERM Domain. (A) These subgroups include protein 4.1 proteins, ERM proteins (to which Merlin is related), talin-related molecules, protein tyrosine phosphatase (PTPH) proteins and novel band 4.1-like 4 (NBL4) (reproduced from Sun et al., 2002). (FERM, 4.1/ezrin/radixin/moesin domain; CCR, coiled coil region; ABD, actin binding domain; CTD, C-terminal domain; PTP, protein tyrosine phosphatase domain)

B

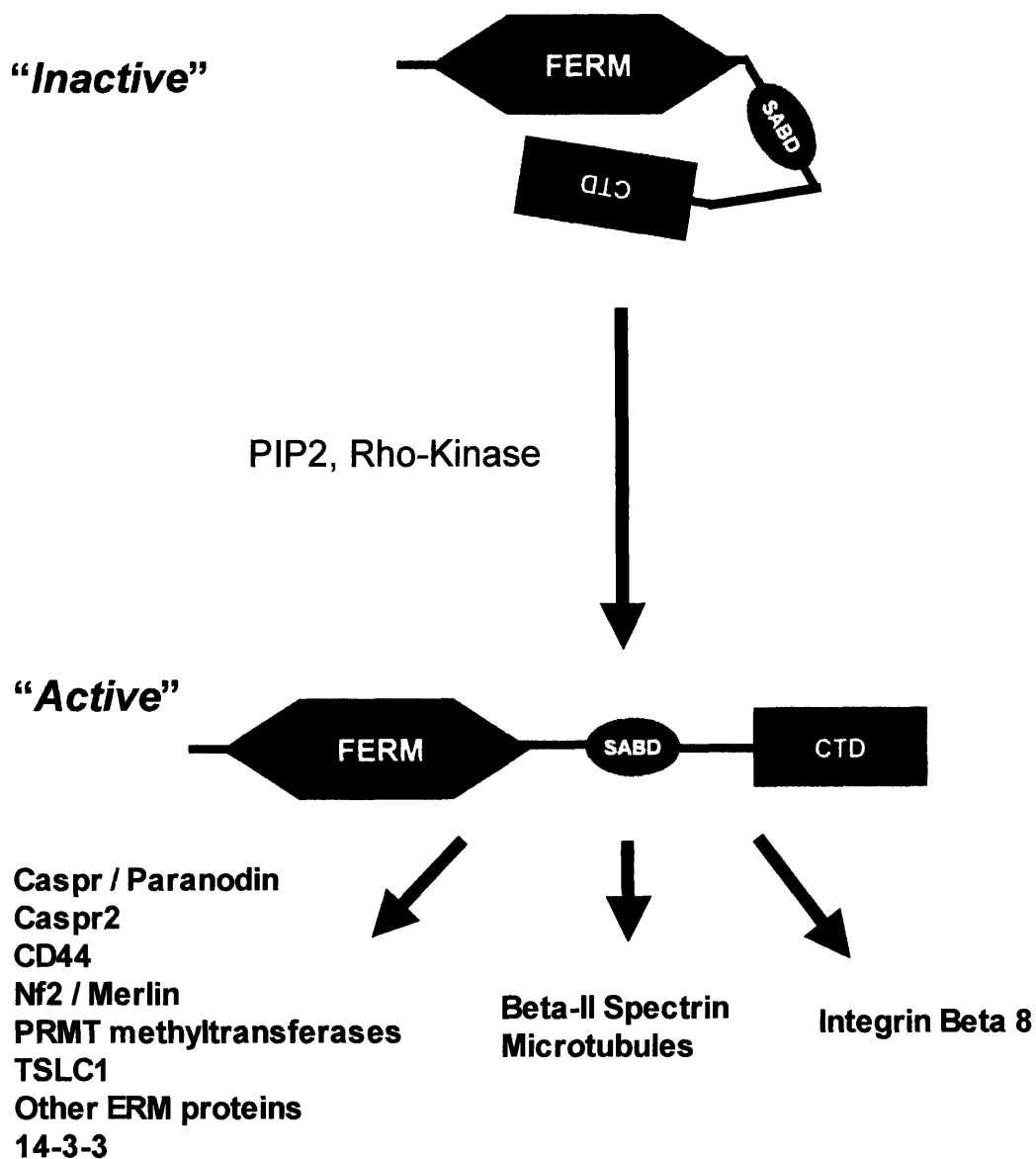


Figure 1. The Protein 4.1 superfamily can be divided into five subgroups and is characterized by a conserved FERM Domain. (B) Regulation of 4.1 subgroup proteins may resemble that of ERM proteins, which normally adopt a “closed,” inactive conformation. Phosphorylation by Rho kinase or binding of PIP2 “activates” and unfolds these proteins, exposing interaction sites for other proteins. Listed above are known binding partners of Protein 4.1B.

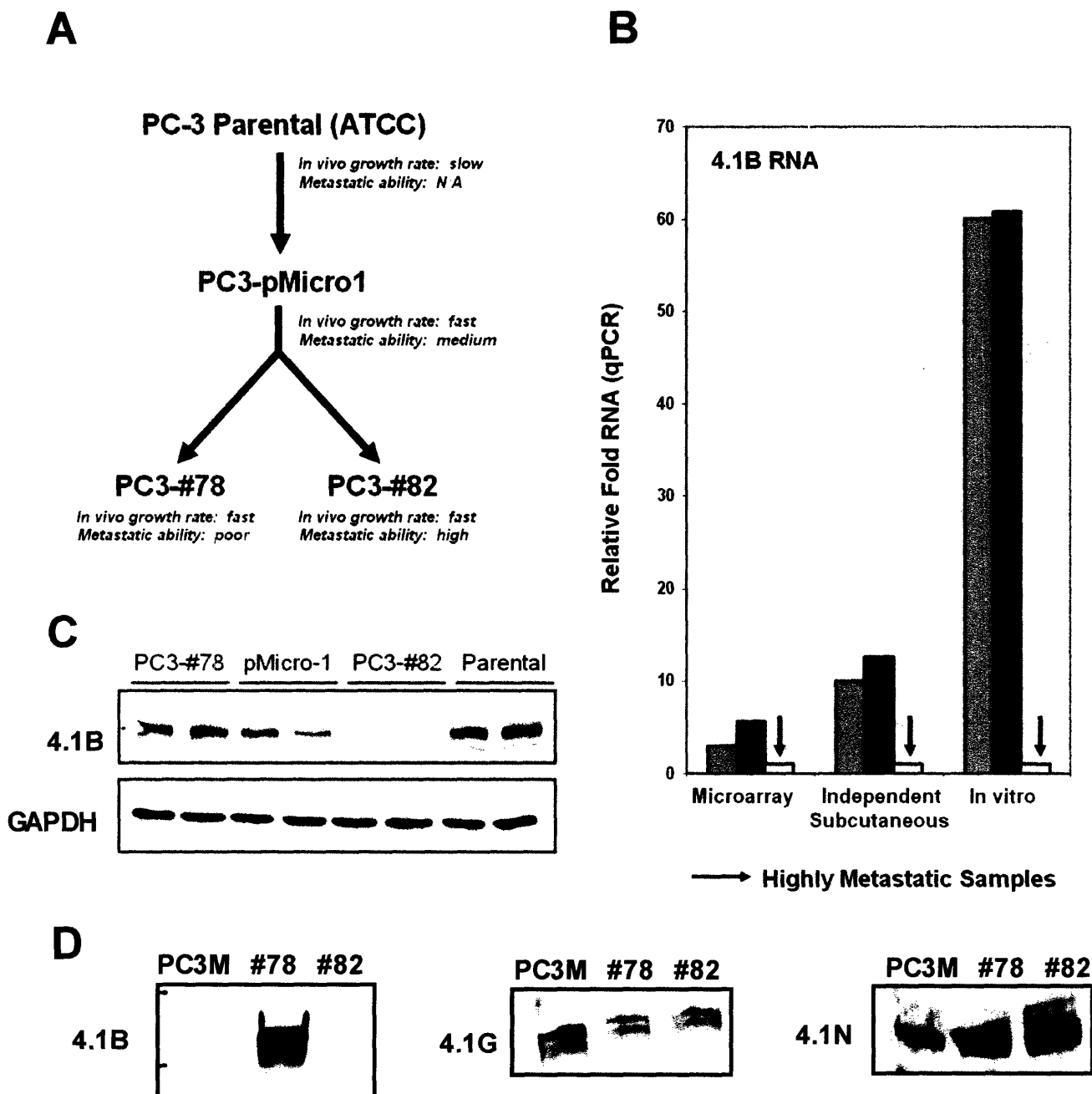
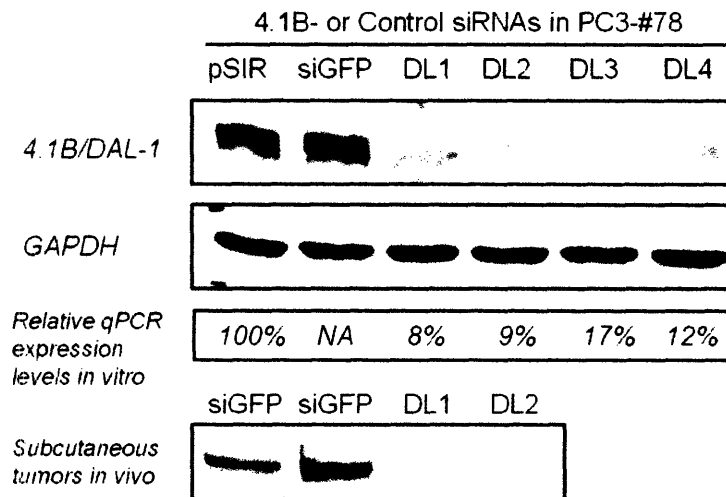


Figure 2. Derivation of metastatic variant prostate cancer cell lines and identification of 4.1B as a protein that is downregulated in highly metastatic cells. (A) Highly metastatic #82 cells and poorly metastatic #78 cells were isolated after repeated *in vivo* passaging of human PC-3 cells using surgical orthotopic implantation. (B) Quantitative RT-PCR results from RNA derived from subcutaneous tumors (middle bars, "independent subcutaneous") and from tissue culture cells (right bars, "in vitro") confirmed microarray results (left bars, "microarray") showing that 4.1B expression is downregulated in #82 cells (arrows, beige bars), relative to #78 cells (blue bars) and pMicro-1 cells (purple bars). All results shown are denoted as fold change, normalized to #82 cells. (C) Western blotting for 4.1B confirms its absence in #82 cells (top), with GAPDH as a loading control (bottom). (D) Western blotting for Protein 4.1 subgroup proteins shows specific loss of 4.1B in #82 and PC-3M cells. 4.1G and 4.1N levels were mostly unchanged. (Parental, PC-3 cells originally purchased from ATCC)

A



B

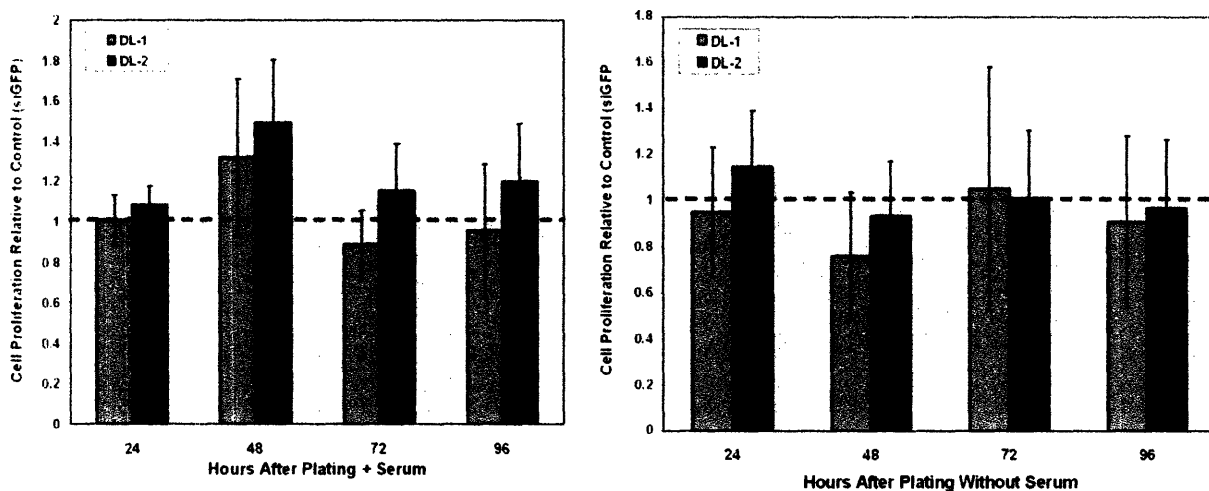


Figure 3. Stable downregulation of 4.1B expression in poorly metastatic #78 does not affect tumor growth *in vitro* or *in vivo*. (A) #78 cells expressing any of four different siRNAs against 4.1B (DL1-4) exhibited stable downregulation of 4.1B expression *in vitro*, relative to cells expressing vector only (pSIR) or an siRNA against GFP (siGFP), as assessed by Western blot (top two rows). siRNA-mediated inhibition of 4.1B expression was maintained in subcutaneous tumors (bottom row). (B) Proliferation of #78 cells expressing DL1 (blue bars) or DL2 siRNAs (purple bars) was unchanged relative to that of #78 cells expressing siGFP control (hatched line). Cell numbers were assessed every 24 hours after plating for 4 days, in the presence (left graph) or absence (right graph) of serum.

C

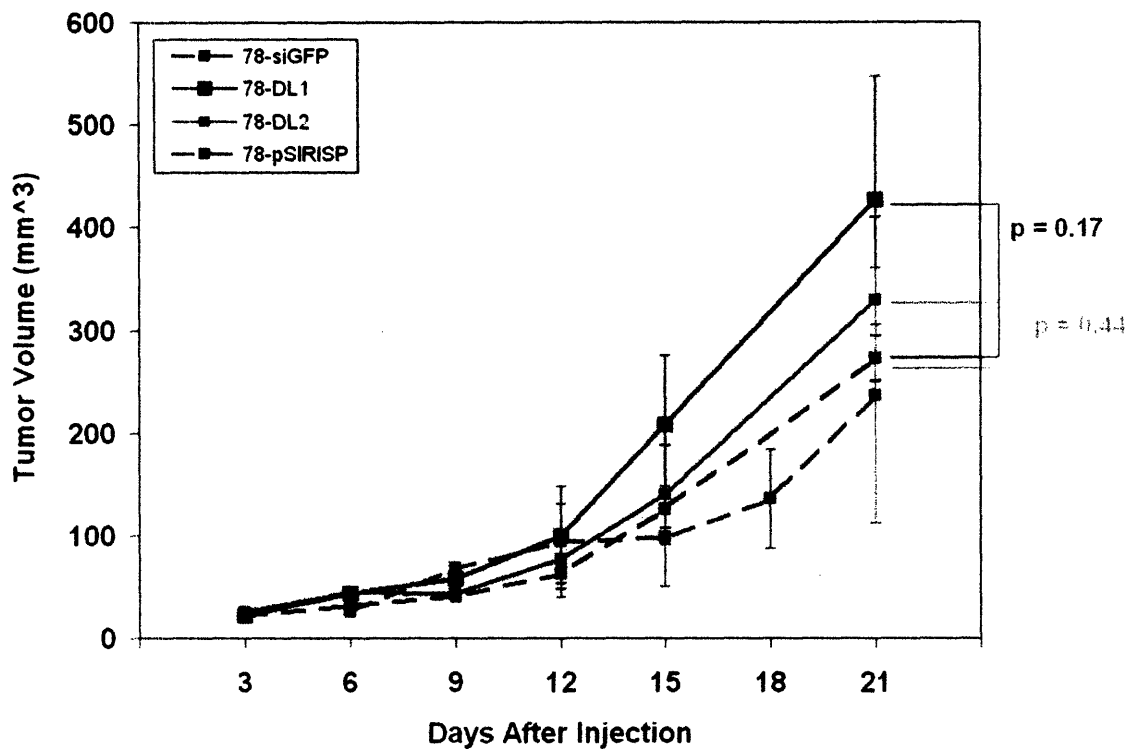


Figure 3. Stable downregulation of 4.1B expression in poorly metastatic #78 does not affect tumor growth *in vitro* or *in vivo* (cont.). (C) Growth of these cells as subcutaneous tumors was also not significantly changed.

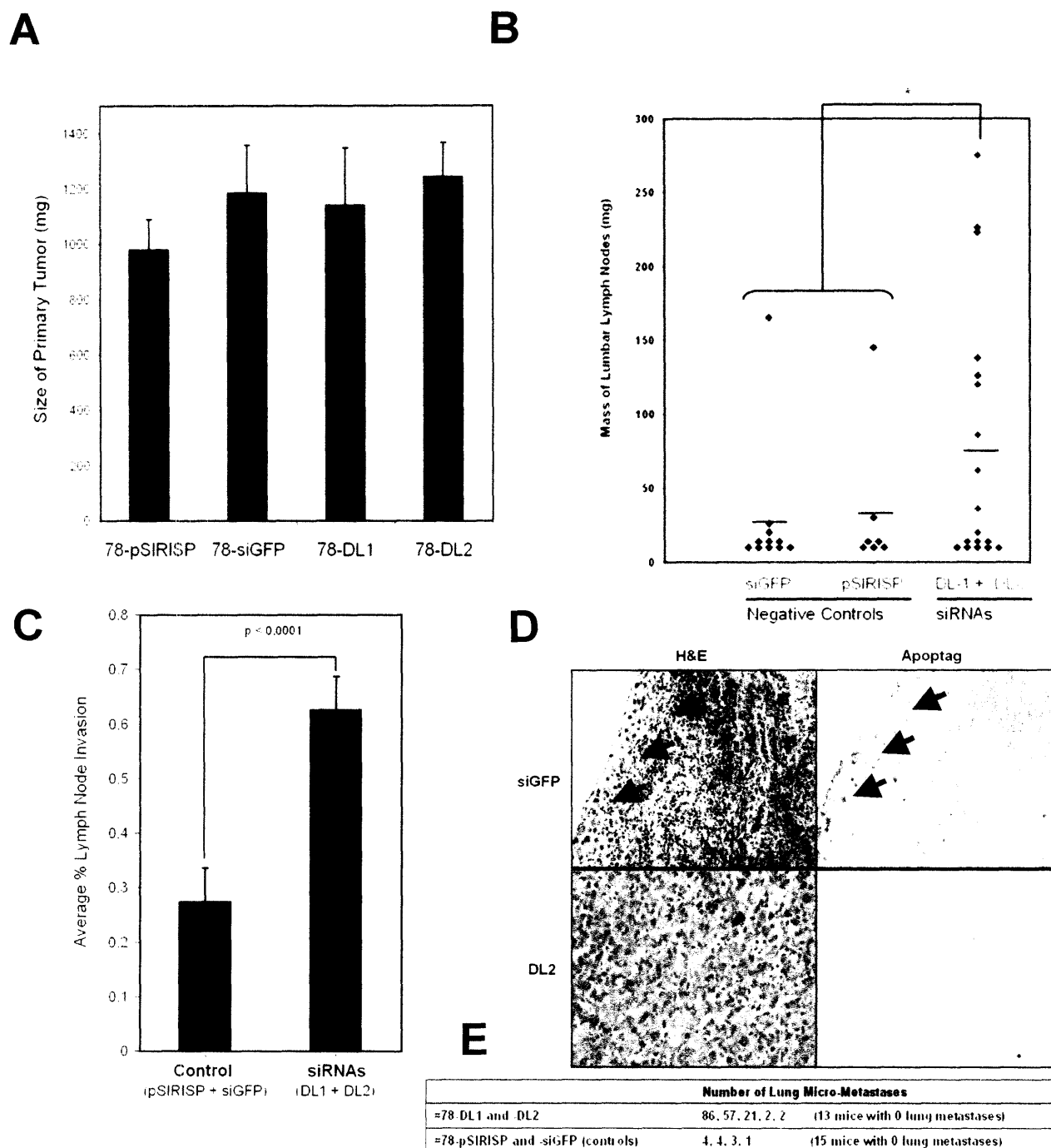
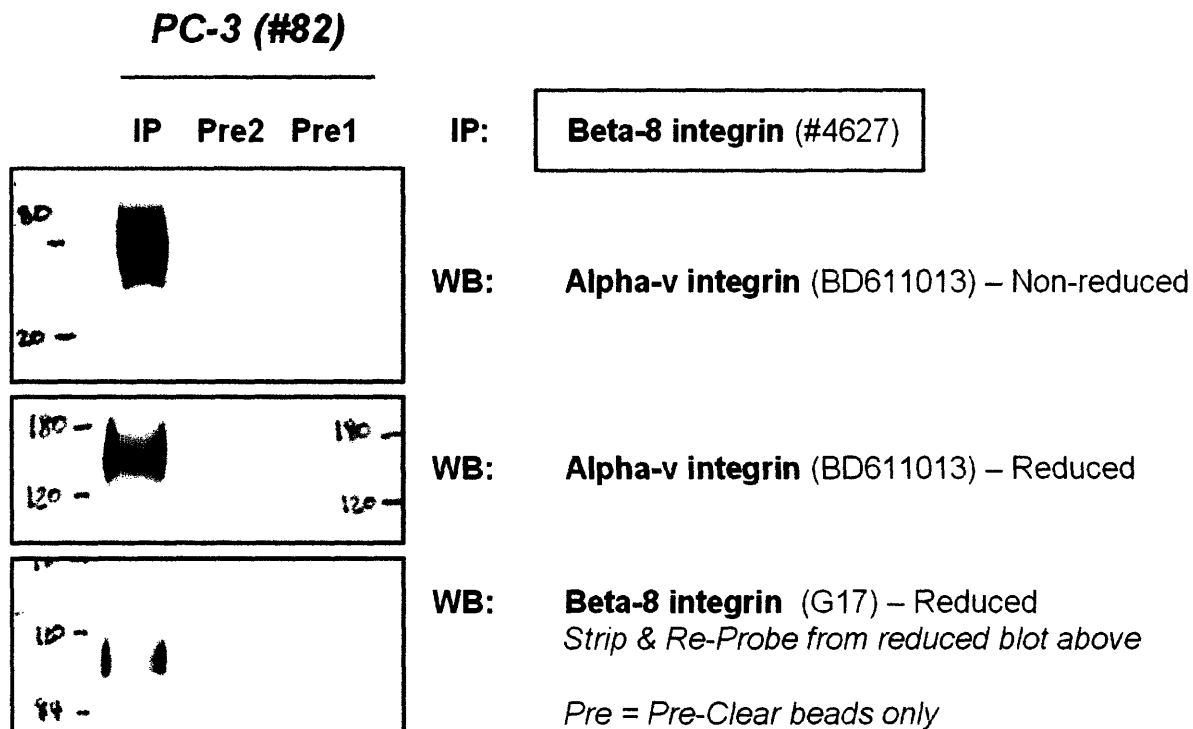


Figure 4. Downregulation of 4.1B increases the metastatic potential of poorly metastatic #78 cells. (A) The average mass of the orthotopic prostate primary tumors did not differ among cell lines. (B) The average mass of lymph nodes from mice bearing DL1- and DL2-expressing tumors was significantly larger than that of mice bearing control tumors. (C) The average percent area of the para-aortic lymph nodes infiltrated by tumor cells was significantly increased in mice bearing orthotopic tumors expressing DL1 or DL2 siRNAs, relative to those with controls. (D) Lymph nodes from mice bearing control #78 tumors (top row) commonly possessed areas of subcapsular tumor invasion, where apoptotic cells were frequently observed (arrows), while nodes from mice bearing DL1- and DL2-expressing #78 orthotopic tumors were often completely infiltrated by tumor cells, with few apoptotic cells present (bottom row). (E) The number of lung micrometastases arising from the different orthotopic tumors is shown.

A



B

Antibody Applications

Immunoprecipitation

Human Alpha(v) → AB1930
 Mouse Alpha(v) → AB1930

Human Beta(8) → #4627
 Mouse Beta(8) → #4627

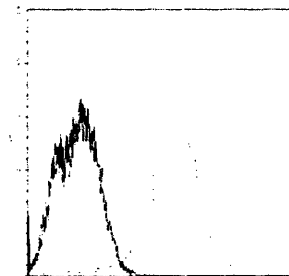
Western Blot

Human Alpha(v) → BD611013
 Mouse Alpha(v) → BD611013

Human Beta(8) → G17
 Mouse Beta(8) → H-160

Flow Cytometry

Human Alpha(v) → ???
 Mouse Alpha(v) → CBL1346B



TRAMP-C3
 Anti-Integrin Alpha(v)
 (CBL1346B-Biot)

Figure 5. Protein 4.1B interacts with integrin $\beta 8$ in PC-3 cells. (A)

Immunoprecipitation of endogenous integrin $\beta 8$ also pulled down endogenous integrin αv , its α subunit interactor, in PC-3 cells. (B) Shown is a list of antibodies that have been successfully used to detect $\alpha v \beta 8$ in mouse or human cells, organized by application. The graph depicts flow cytometric analysis of mouse TRAMP-C3 cells stained with anti- αv (blue) antibody or with control antibodies/unstained (red and green).

C

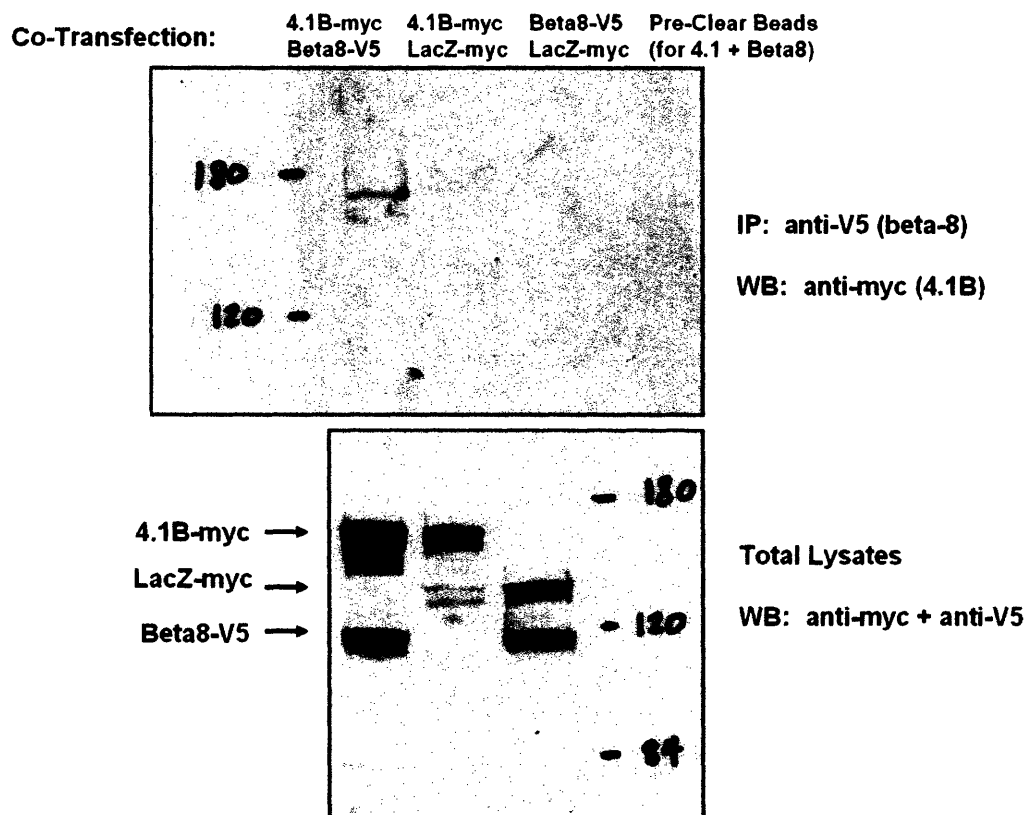


Figure 5. Protein 4.1B interacts with integrin $\beta 8$ in PC-3 cells (cont). (C) Co-transfected myc-tagged Protein 4.1B and V5-tagged integrin $\beta 8$ were overexpressed in PC-3 cells (bottom), and were shown to interact by co-immunoprecipitation with anti-V5 antibody, followed by Western blot against myc-tag (bottom). (IP, immunoprecipitation; WB, Western blot; Pre, pre-cleared beads)

A

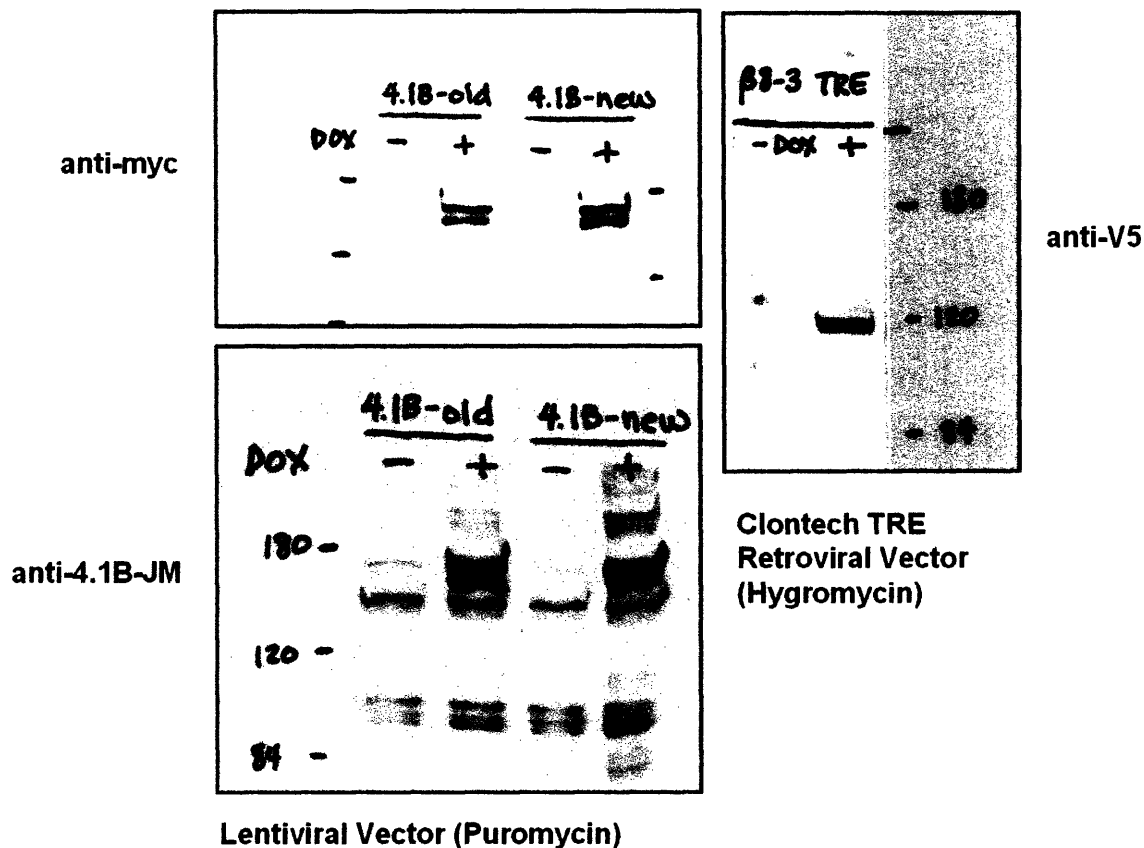


Figure 6. Inducible overexpression of either myc-tagged 4.1B or V5-tagged integrin β 8 does not affect proliferation in PC-3 cells. Both coding sequences were cloned downstream of a Tet responsive element (TRE) that is rendered transcriptionally active in the presence of doxycycline (DOX). (A) Inducible overexpression of 4.1B was observed by Western blot upon addition of doxycycline in two independently infected #82 cell lines ("old" and "new"), and as assessed by antibodies against the myc epitope tag (top left) or against 4.1B (bottom left). Similarly, V5-tagged $\beta 8$ was inducibly overexpressed upon addition of doxycycline, as assessed by detection of the V5 epitope tag (right).

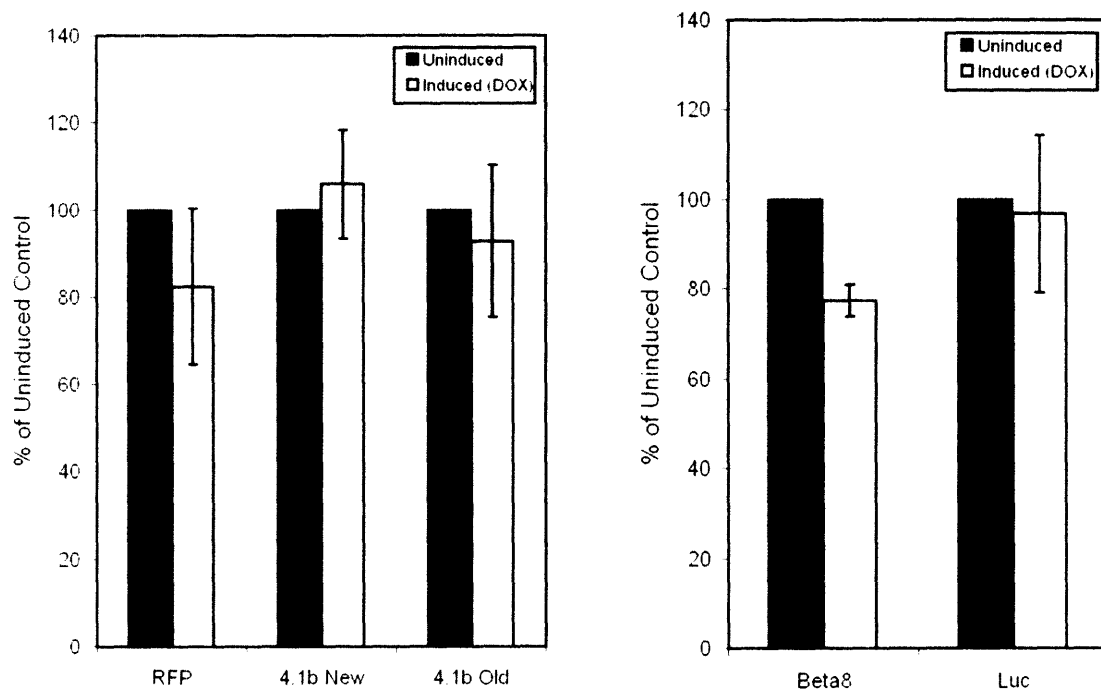
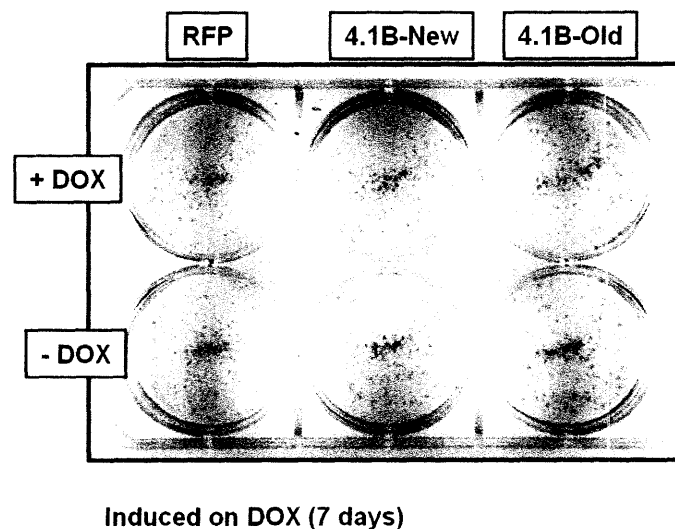
B**C**

Figure 6. Inducible overexpression of either myc-tagged 4.1B or V5-tagged integrin β 8 does not affect proliferation in PC-3 cells. (cont.). (B) Cells induced (white bars) or not induced (black bars) to overexpress 4.1B, RFP or luciferase did not exhibit significant differences in cell number, 6-7 days after addition of doxycycline, as assessed by manual cell counting and normalized to the non-induced control. Inducible overexpression of β 8 showed a slight (~20%) reduction in cell number. **(C)** Cell counting results were confirmed visually by staining plated cells with crystal violet following 6-7 days +/- doxycycline.

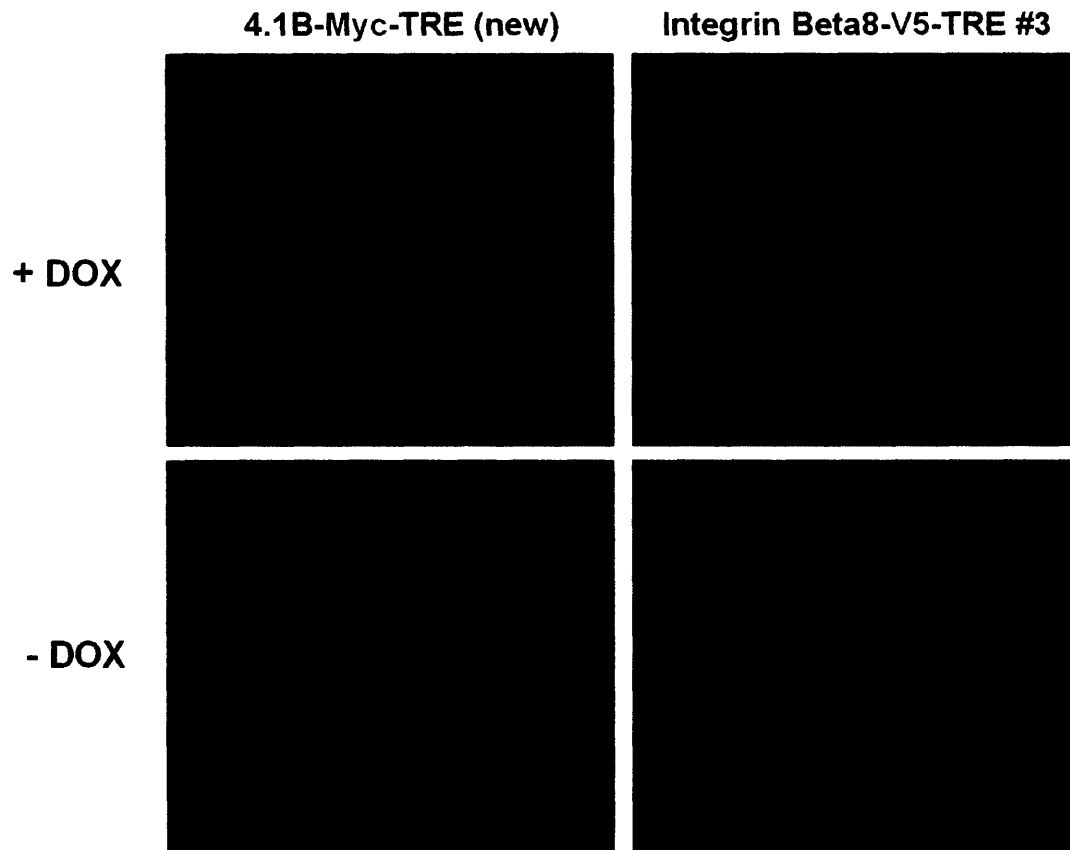
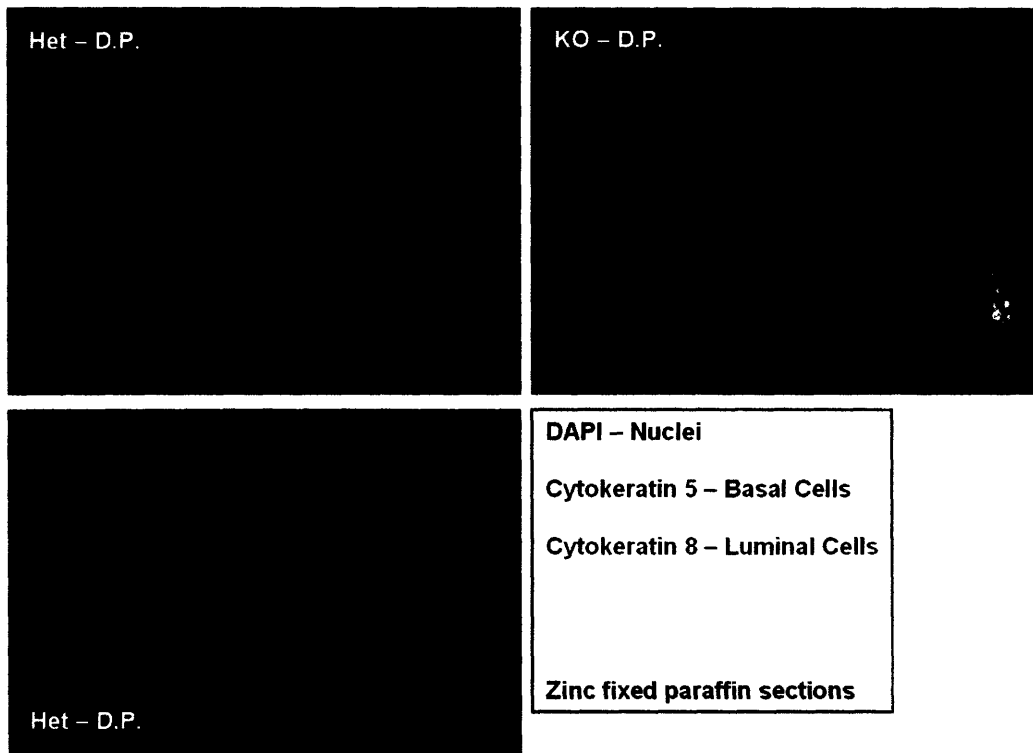
D

Figure 6. Inducible overexpression of either myc-tagged 4.1B or V5-tagged integrin β 8 does not affect proliferation in PC-3 cells. (cont). (D) Immunofluorescence staining for myc- or V5-epitope tags revealed that only about one-third of induced cells displayed visually detectable overexpression of either 4.1B (left) or integrin β 8 (right).

A



B

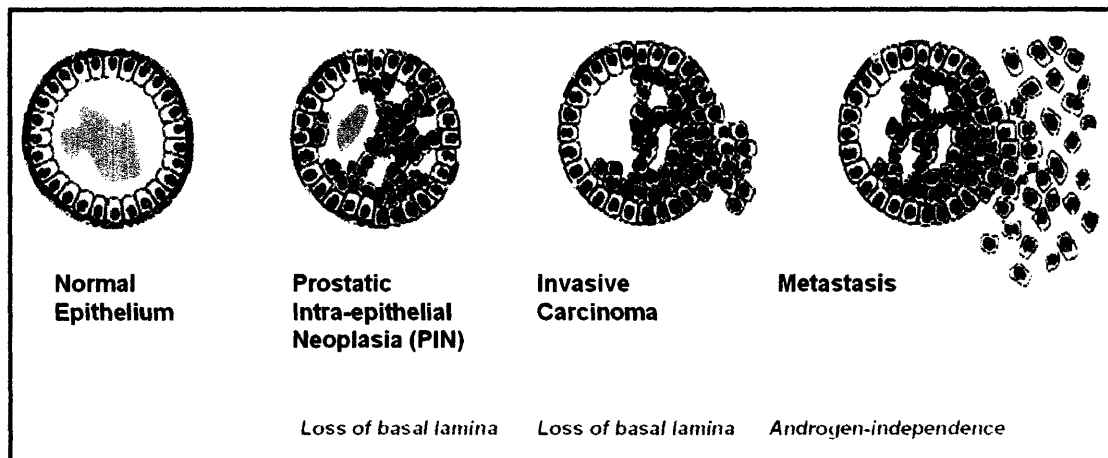


Figure 7. The transgenic adenocarcinoma of the mouse prostate (TRAMP) tumor model allows study of spontaneous prostate cancer development and progression. (A) TRAMP-negative 4.1B^{-/-} (KO) or 4.1B^{+/-} (Het) dorsolateral prostates (D.P.) were stained with antibodies against the basal cell marker cytokeratin 5 (green) or the luminal cell marker cytokeratin 8 (red), imaged at low (top rows) or high magnification (bottom row). **(B)** TRAMP prostate tumors initiate spontaneously and likely involve overgrowth of luminal cells, followed by loss of attachment to the basement membrane, and invasion. (Figure reproduced from Abate-Shen and Shen, 2000.)

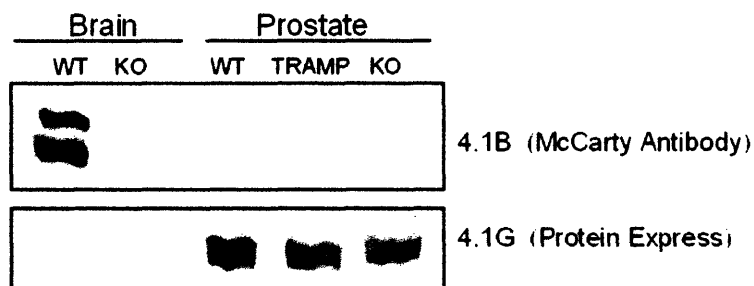
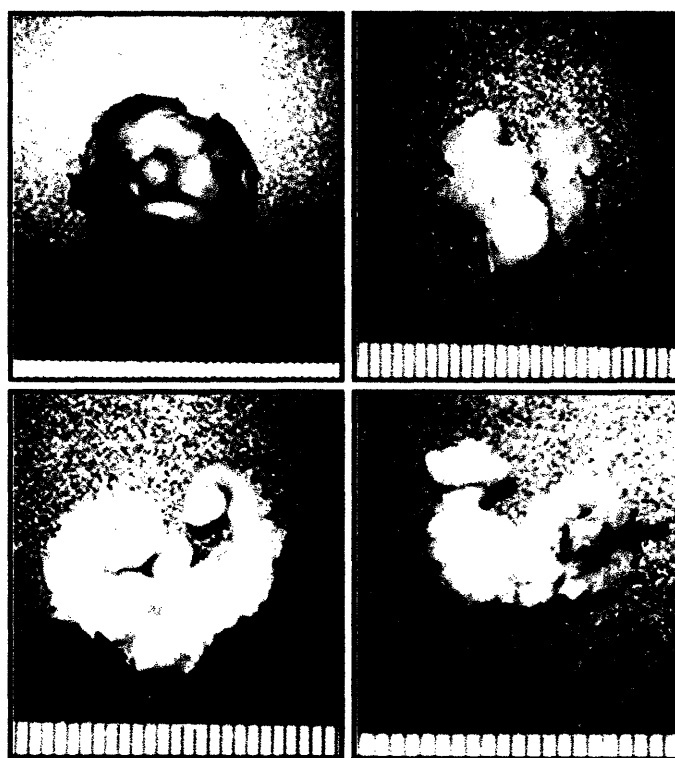
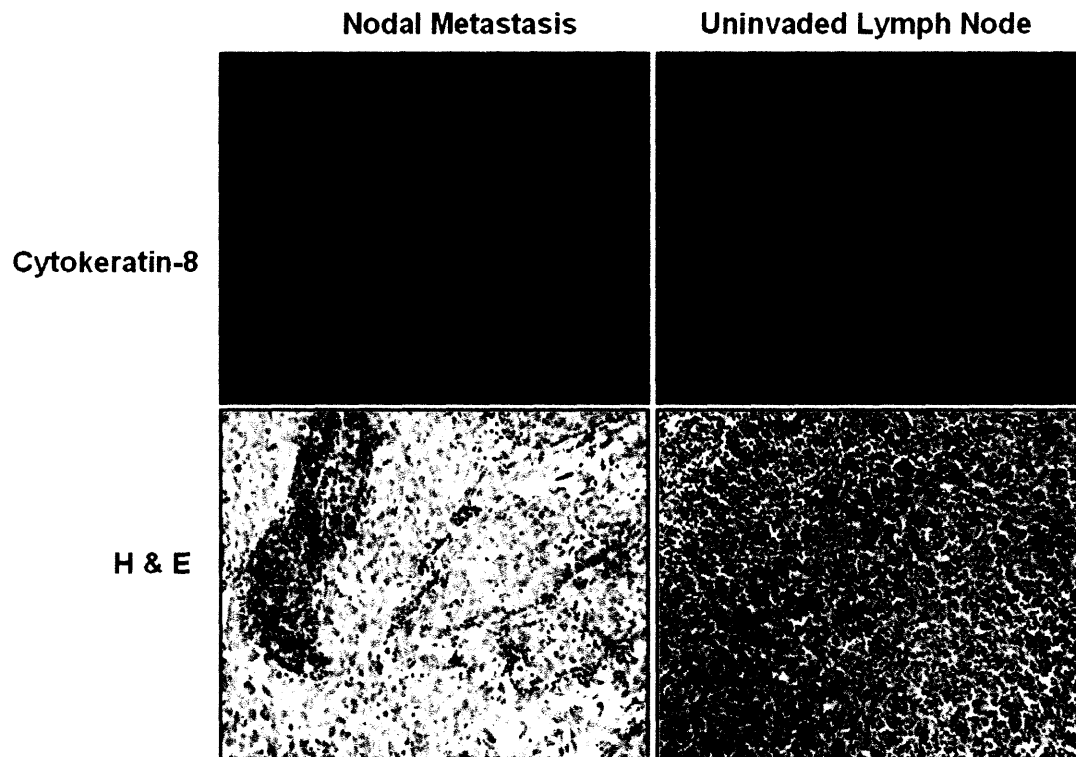
A**B**

Figure 8. 4.1B^{-/-} mice develop aggressive adenocarcinomas in the TRAMP spontaneous tumor model of prostate cancer. (A) Western blotting for 4.1B (top) or 4.1G (bottom) in brain or prostate tissues shows that 4.1B is specifically lost in knock-out animals. **(B)** 4.1B^{-/-};TRAMP^{+/-} mice more commonly developed a variety of palpable, high-grade carcinomas in the prostate (arrows), including (starting from upper left and proceeding clockwise) compound, multi-lobed carcinomas; ventral-lobed carcinomas; anterior-lobed carcinomas; and dorsal-lobed carcinomas.

C

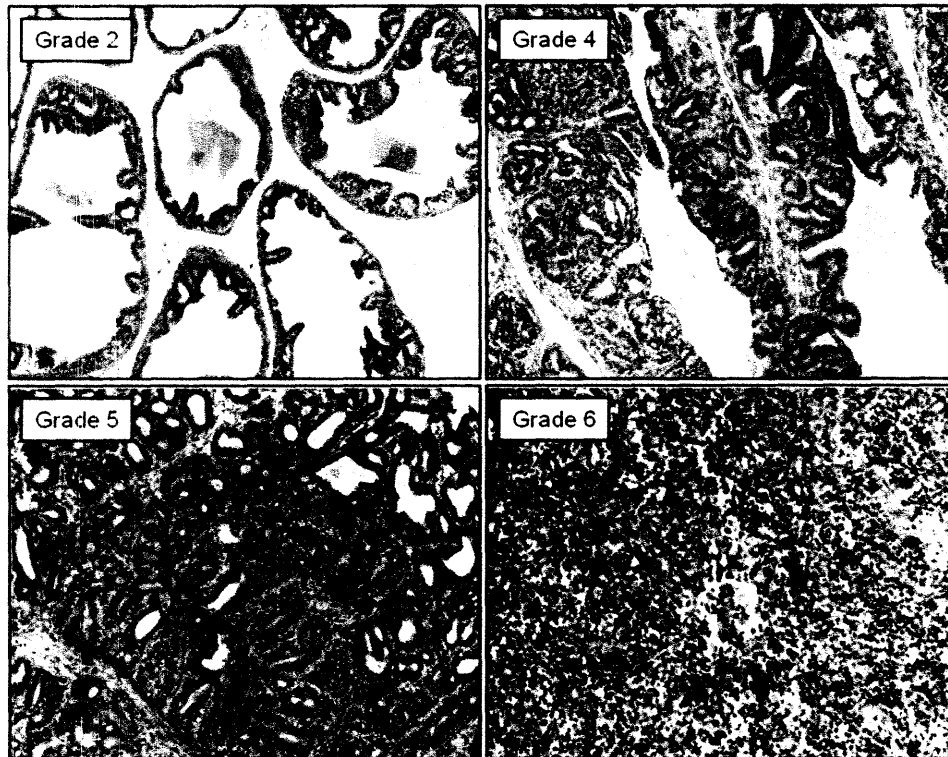


D

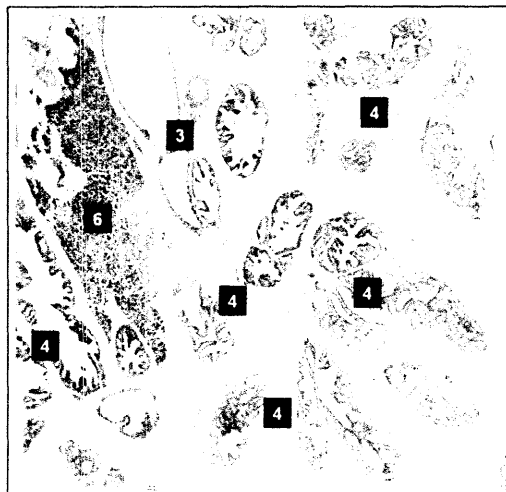
	4.1B +/- ; TRAMP +/-	4.1B -/- ; TRAMP +/-	p-value
Incidence of Grade 6 Carcinoma	4/26 (15.4%)	11/19 (58%)	0.003
Incidence of Palpable Grade 6 Carcinoma	2/26 (7.7%)	11/19 (58%)	0.0002
Incidence of Lymph Node Metastasis	2/26 (7.7%)	6/19 (32%)	0.04

Figure 8. 4.1B^{-/-} mice develop aggressive adenocarcinomas in the TRAMP spontaneous tumor model of prostate cancer (cont.). (C) These tumors frequently invaded the draining para-aortic/lumbar lymph nodes, as observed directly by hematoxylin-and-eosin staining (bottom) or by staining for the epithelial marker cytokeratin 8 (top). The results of these tumor studies and their statistical significance are summarized in (D).

A



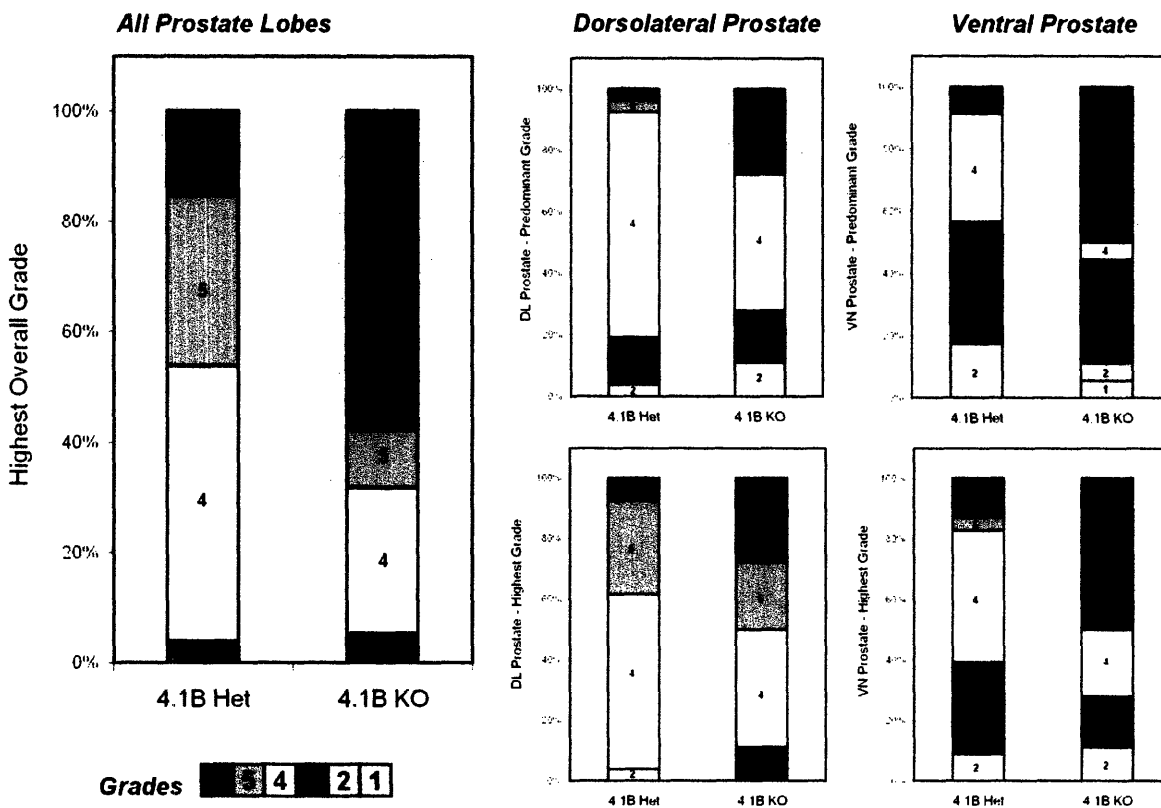
B



Section S830: 4.1B-Het/TRAMP+ Ventral Prostate
 Predominant Grade 4
 Highest Grade 6

Figure 9. 4.1B-deficient animals develop higher grade and less differentiated prostate adenocarcinomas. (A) Histopathologic grades (minimum, 1; maximum, 6) were assigned to TRAMP prostates according to the system described by Hurwitz et al (2001). Higher graded section exhibited increased luminal cell expansion, loss of normal tissue architecture, and reduced differentiation. **(B)** TRAMP prostates were assigned two grades per section per lobe: a highest grade and a predominant grade. An H&E-stained prostate section is shown with highest focal areas of grade 6 and with a predominant grade of 4.

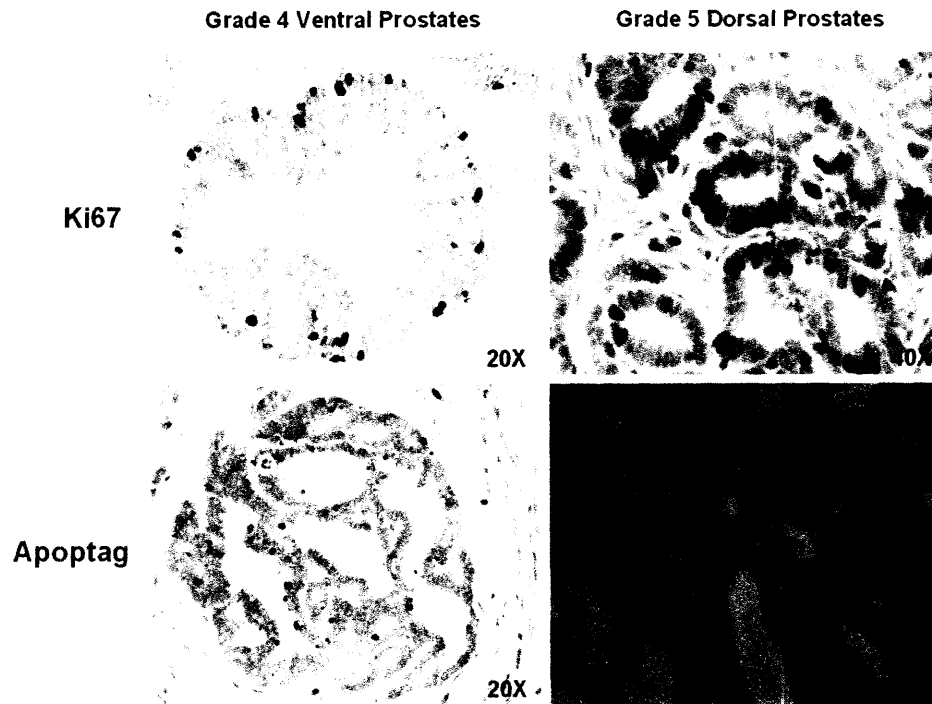
C



	Prostate Lobes	P-Value
Predominant Grade of 6	Dorsal Only	0.02
Predominant Grade of 6	Ventral Only	0.003
Highest Grade of 6	Dorsal Only	0.07
Highest Grade of 6	Ventral Only	0.01
Highest Overall Grade of 6	All Lobes	0.003

Figure 9. 4.1B-deficient animals develop higher grade and less differentiated prostate adenocarcinomas (cont.). (C) The ventral (VN) and dorsolateral (DL) lobes of 26-week old 4.1B^{-/-};TRAMP and 4.1B^{+/-};TRAMP prostates were separately evaluated with both scoring systems. In either case, 4.1B^{-/-} mice developed the highest grade carcinomas (Grade 6, red bars) more frequently than did 4.1B^{+/-} mice (right graphs). The same result was also true if each entire prostate was assigned a single highest grade, based on the highest grade assigned to any one constituent lobe (left graph). Significance values for these analyses are shown.

A



B

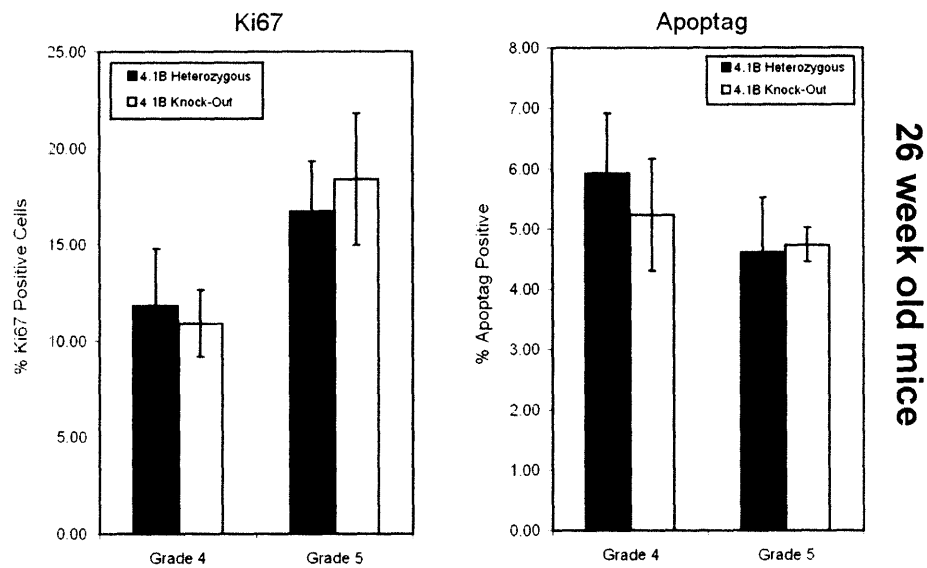


Figure 10. 4.1B^{-/-};TRAMP^{+/-} prostates exhibited reduced apoptosis relative to those of 4.1B heterozygous mice. (A) Typical grade 4 ventral (left) and grade 5 dorsal (right) prostate sections are shown following staining with the proliferation marker Ki67 (top) or by TUNEL, using the Apoptag detection kit (bottom). **(B)** Quantitation of staining results for Ki67 and TUNEL (apoptag) is shown for 26-week-old mice.

C

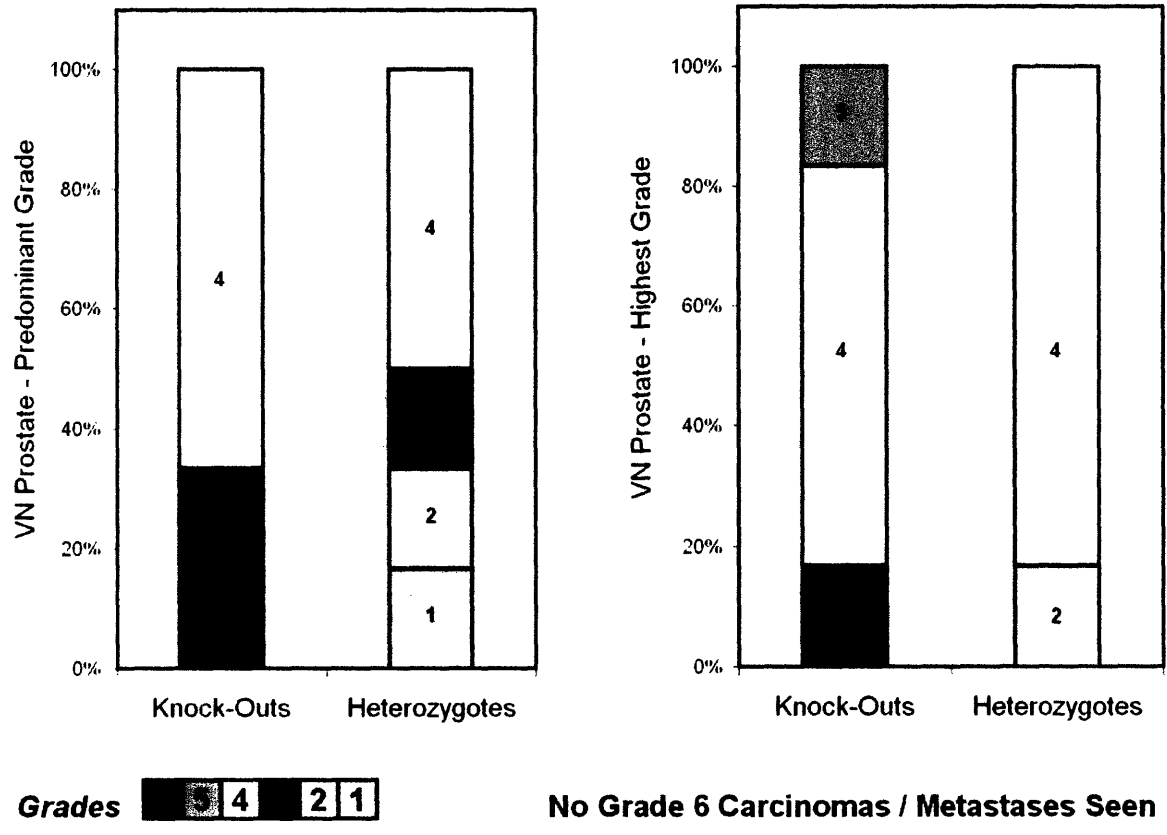


Figure 10. 4.1B^{-/-};TRAMP^{+/-} prostates exhibited reduced apoptosis relative to those of 4.1B heterozygous mice (cont.). (C) Prostate sections from a cohort of 22-week-old TRAMP mice were also graded.

D



E

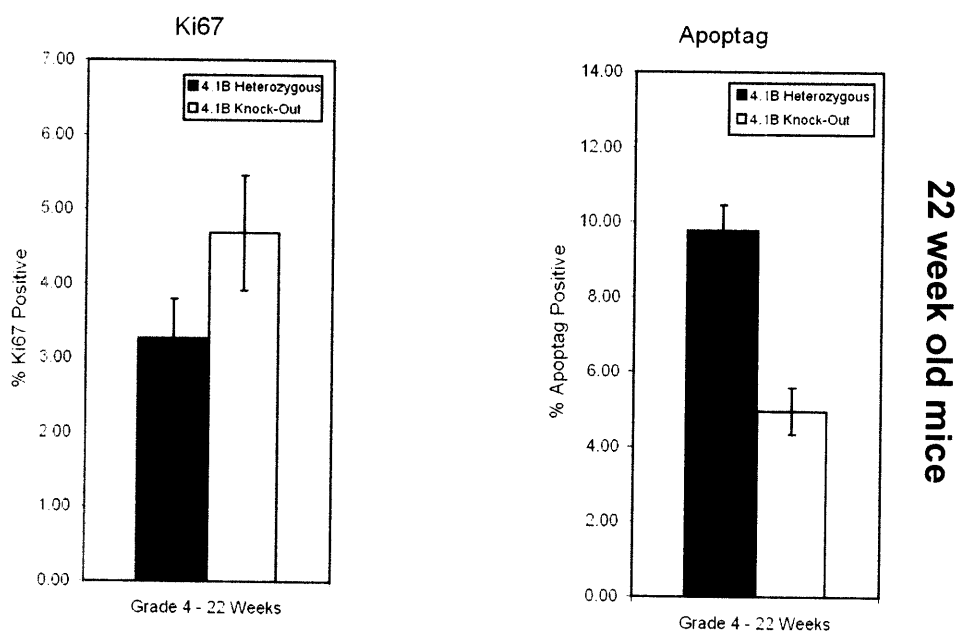
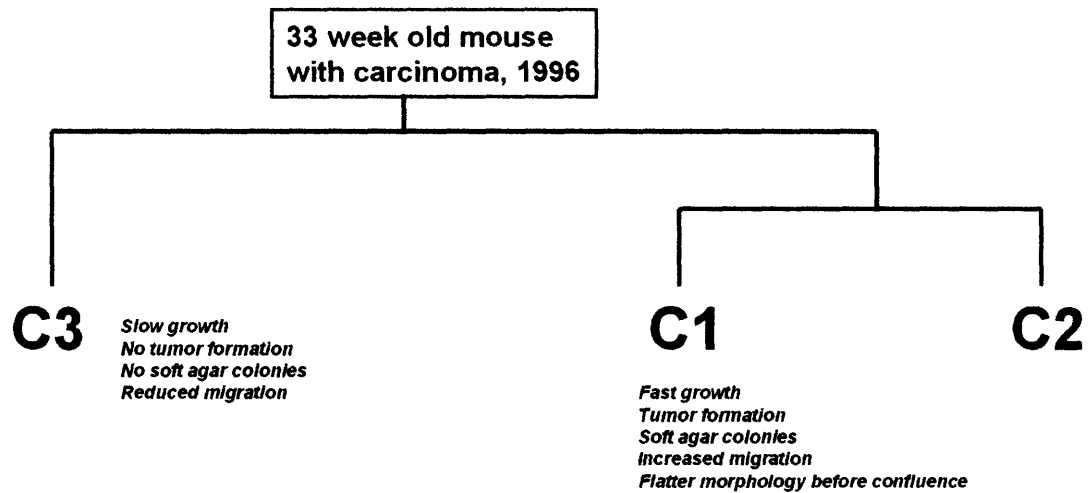


Figure 10. 4.1B^{-/-};TRAMP^{+/-} prostates exhibited reduced apoptosis relative to those of 4.1B heterozygous mice (cont). (D) 22-week-old grade 4 ventral prostate sections from 4.1B^{-/-};TRAMP^{+/-} prostates showed reduced staining by TUNEL (left), compared to prostates from 4.1B heterozygous TRAMP mice (right). (E) Quantitation of these results is shown.

A



B

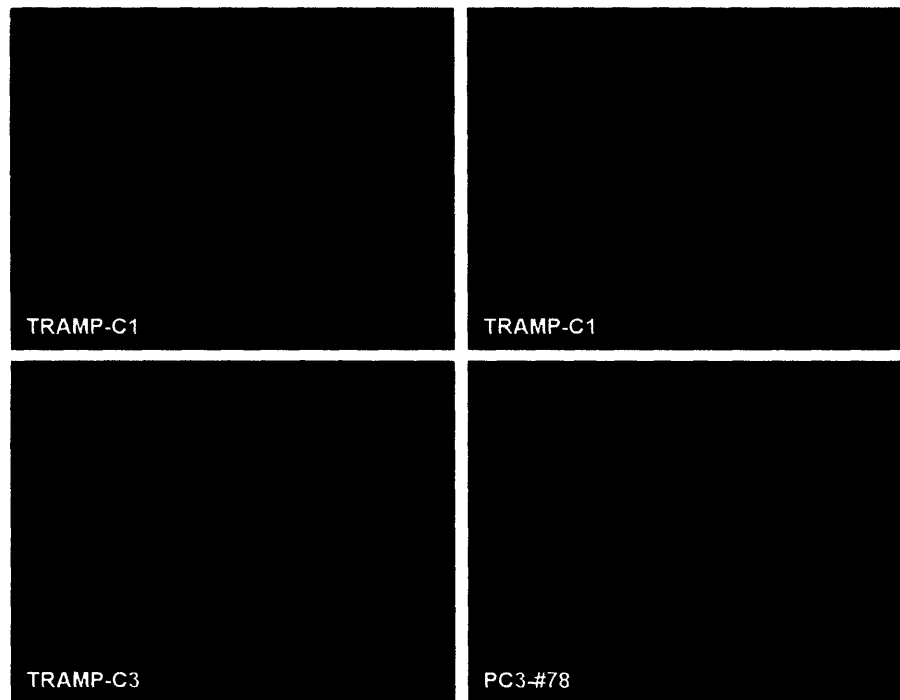
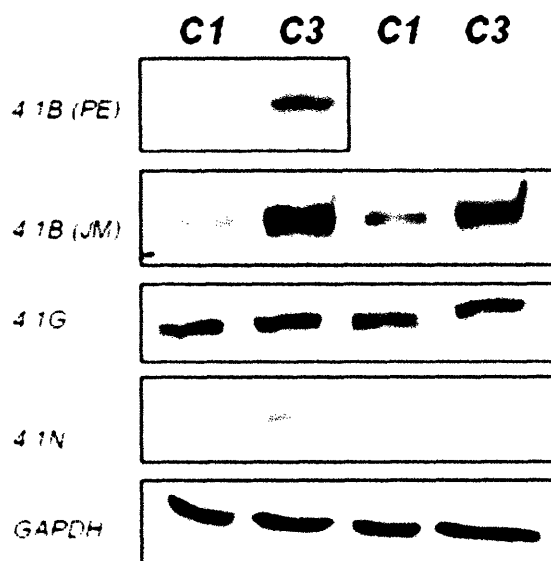


Figure 11. Protein 4.1B levels are reduced in aggressive TRAMP tumor cell lines. (A) The malignant TRAMP-C1 and non-malignant TRAMP-C3 mouse prostate cell lines were derived by Foster et al. (1997), from a single TRAMP primary tumor. (B) Aggressive TRAMP-C1 cells formed colonies in soft agar, but TRAMP-C3 cells remained as single cells. PC3-#78 cells also formed colonies.

C



D

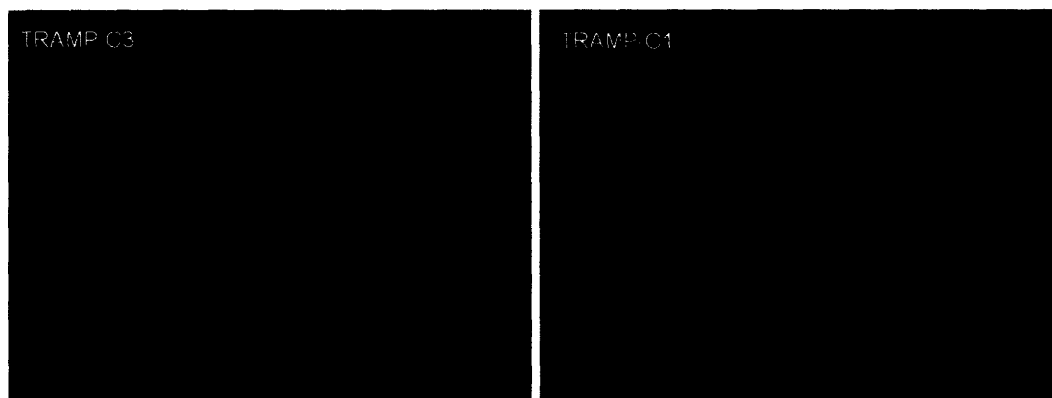
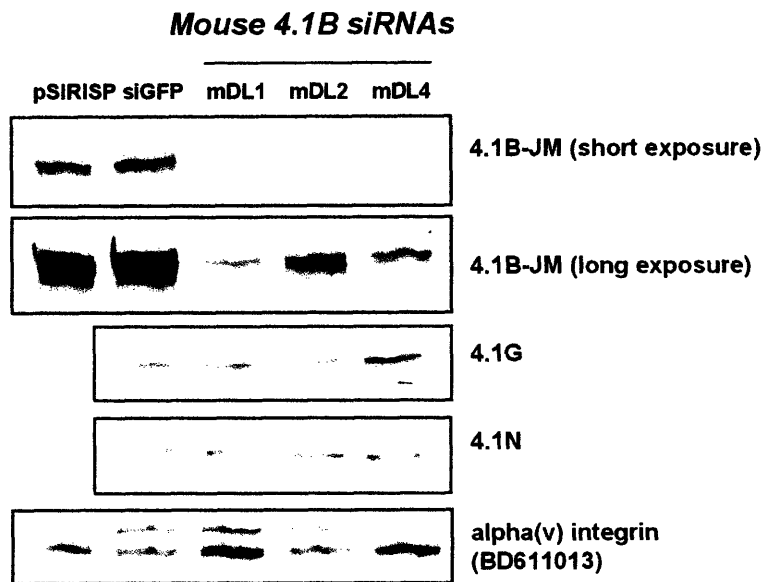


Figure 11. Protein 4.1B levels are reduced in aggressive TRAMP tumor cell lines (cont). (C) 4.1B protein levels were specifically reduced in malignant TRAMP-C1 cells (C1), relative to non-malignant TRAMP-C3 cells (C3), as assessed by two different antibodies against 4.1B (4.1B PE and 4.1B JM). (D) Immunofluorescence staining of TRAMP cells using the 4.1B-PE antibody revealed that 4.1B was non-uniformly downregulated in aggressive TRAMP-C1 cells.

A



B

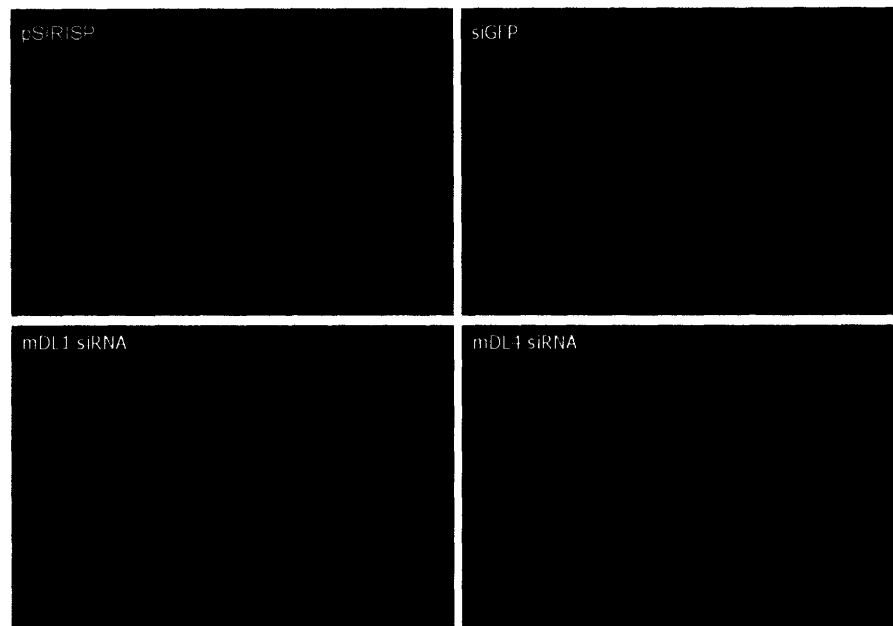


Figure 12. Stable siRNAs can downregulate murine 4.1B in non-malignant TRAMP-C3 cells. (A) Western blotting shows that 4.1B was specifically downregulated in cells expressing any of three different siRNAs targeted against mouse 4.1B, relative to that of control cells expressing the vector only (pSIRISP) or an siRNA against GFP (siGFP). (B) Immunofluorescence staining revealed that cells expressing mDL1 or mDL4 siRNAs exhibited reduced 4.1B protein relative to that of cells expressing control vectors.

A

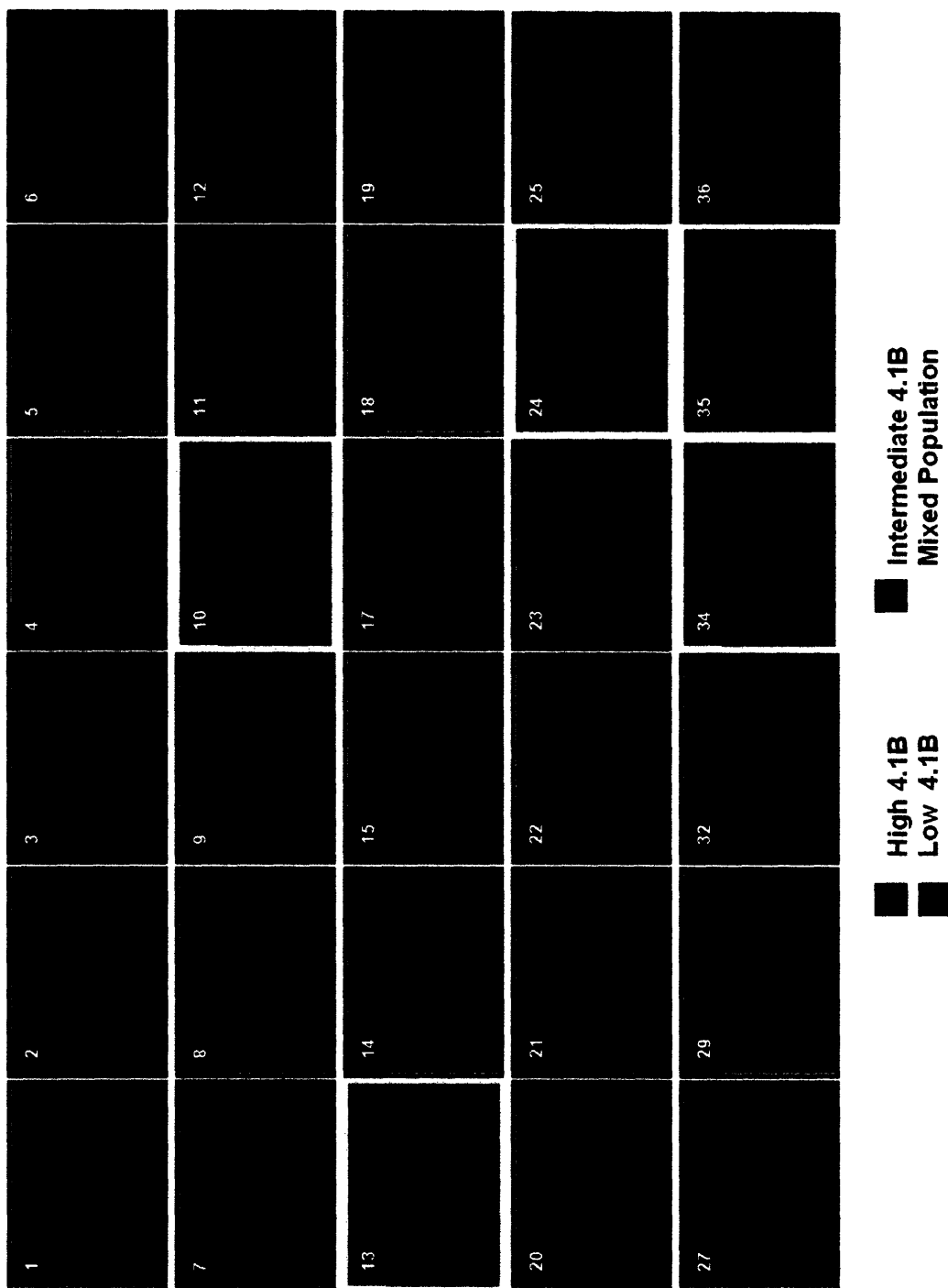
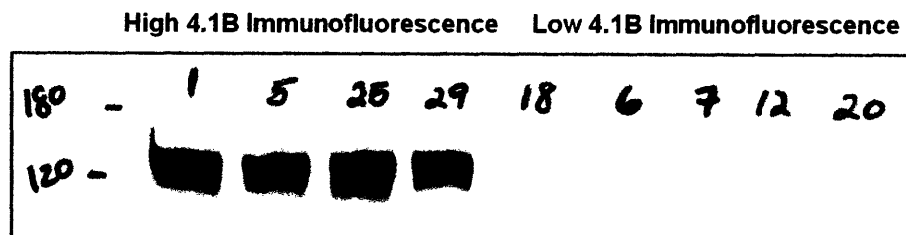


Figure 13. TRAMP-C1 cells expressing uniformly high or low 4.1B protein can be cloned from the original heterogeneous population. (A) Thirty clones derived from malignant TRAMP-C1 cells were analyzed for 4.1B expression by immunofluorescence using the 4.1B-PE antibody. Most clones exhibited uniformly high, low or intermediate levels of expression (red, green or purple boxes, respectively). In a few instances, heterogeneous expression was still observed (gray boxes).

B



C

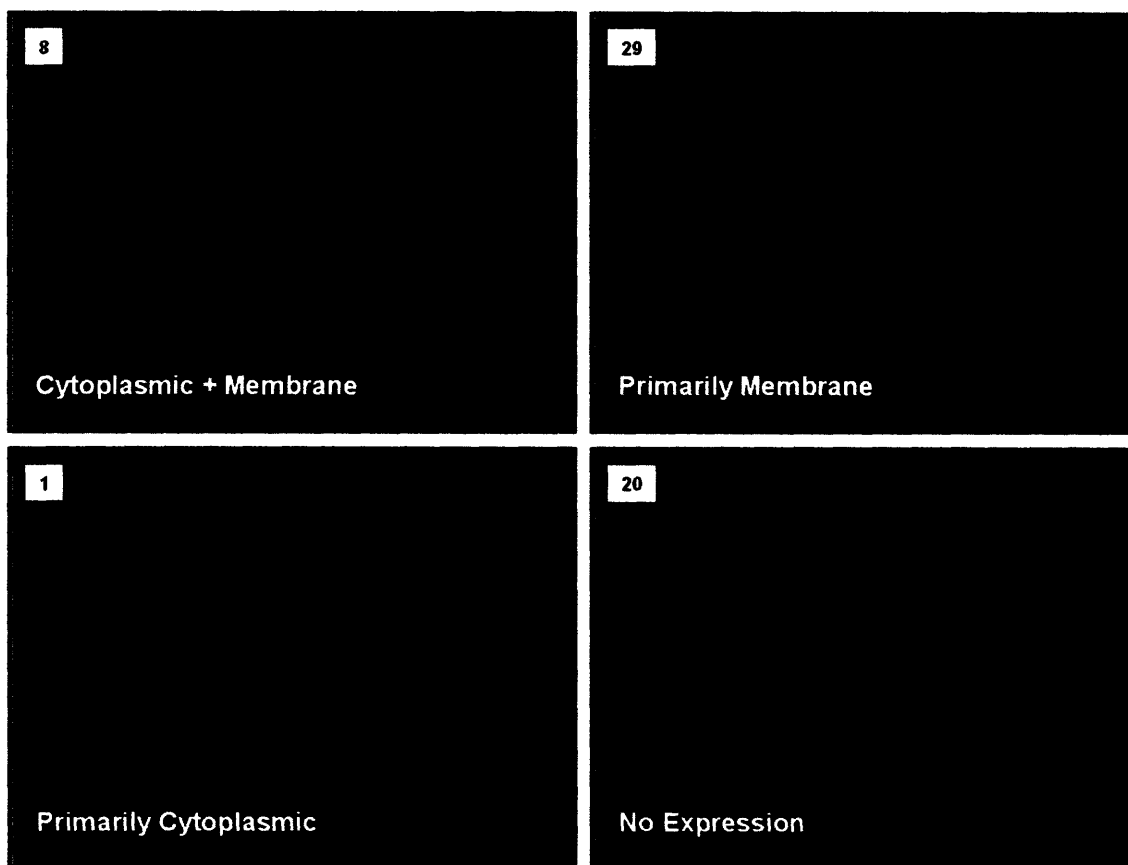


Figure 13. TRAMP-C1 cells expressing uniformly high or low 4.1B protein can be cloned from the original heterogeneous population (*cont.*). (B) In eight different clones, immunofluorescence staining intensity for 4.1B was confirmed by Western blot. (C) The cloned cell lines exhibited differences in 4.1B localization, ranging from both cytoplasmic and membrane localization (Clone 8), to membrane-only localization (Clone 29), cytoplasmic-only localization (Clone 1), and no expression (Clone 20).

D

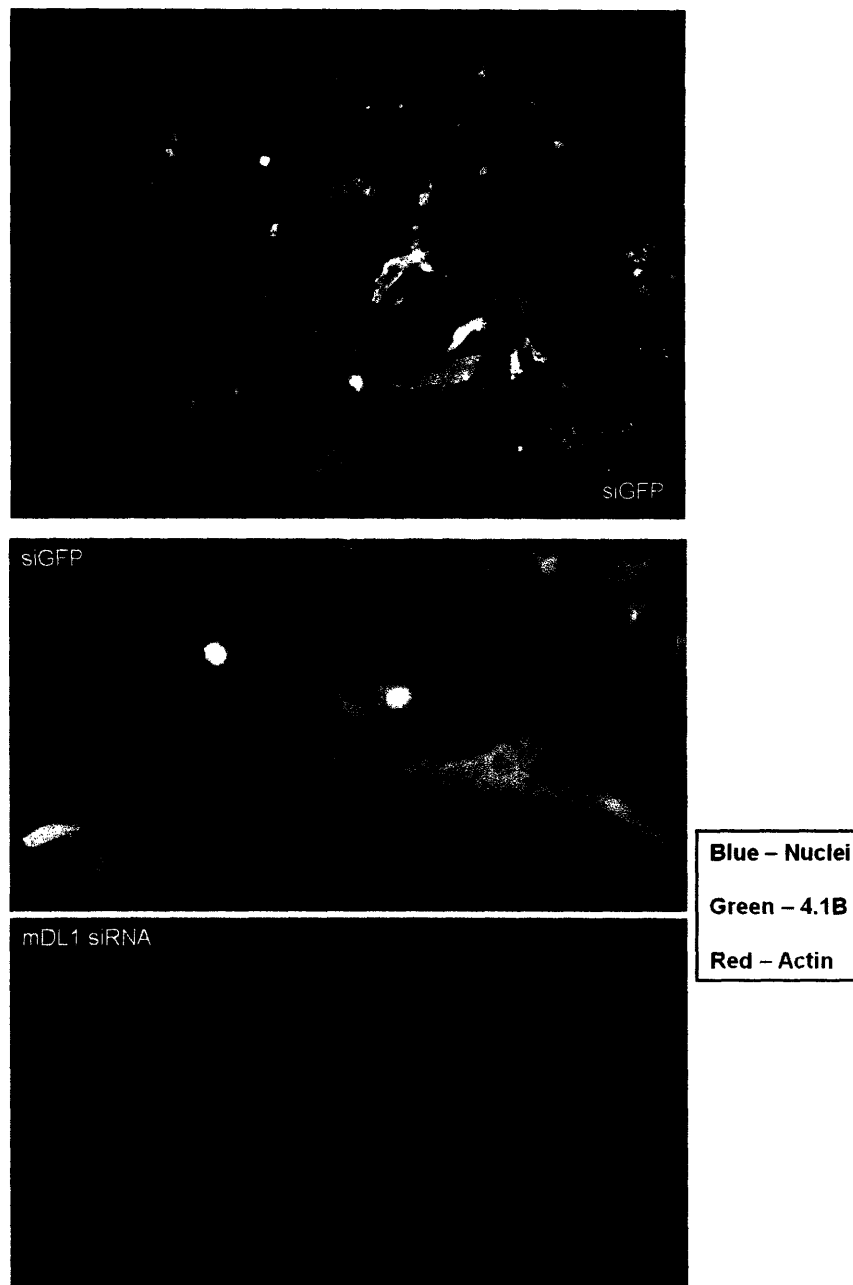


Figure 13. TRAMP-C1 cells expressing uniformly high or low 4.1B protein can be cloned from the original heterogeneous population (cont). (D) Co-staining for 4.1B and actin revealed that 4.1B protein was often co-localized with circular actin-rich structures in TRAMP-C3 cells (top two photographs). siRNA expression of mDL1 ablated 4.1B protein but did not affect these actin-rich structures (bottom photograph).

A

sorted
↓

Soft Agar Size			
3	-	-	
6	-	-	
5	(+)	-	
23	(+)	-	
25	(+)	-	
29	(+)	-	
32	(+)	-	
4	(weak +)	-	
7	-	(+/-)	Jagged
19	-	(+/-)	Jagged
36	(+)	(+/-)	Jagged
34	mix	(+/-)	Jagged
21	-	(+/-)	Smooth
27	(+)	(+/-)	Smooth
24	mix	(+/-)	Smooth
13	mix - mostly (+)	(+/-)	Smooth
12	-	(+)	Jagged
8	(+)	(+)	Smooth
14	(+)	(+)	Smooth
17	(+)	(+)	Smooth
9	(++)	(+)	Smooth
18	-	(+)	Smooth
22	(weak +)	(+)	Smooth / Jagged
2	-	(++)	Jagged
11	-	(++)	Jagged
20	-	(++)	Jagged
1	(++)	(++)	Jagged
35	mix - mostly (-)	(++)	Jagged
10	mix - mostly (+)	(++)	Smooth / Jagged

Figure 14. TRAMP-C1 cell clones exhibit differences in colony size and morphology when suspended in soft agar. (A) Cell clones were grouped according to the size of the colonies formed when plated in soft agar (purple column), which ranged from single cells (-) to small colonies (+/-) and larger (+ and ++).

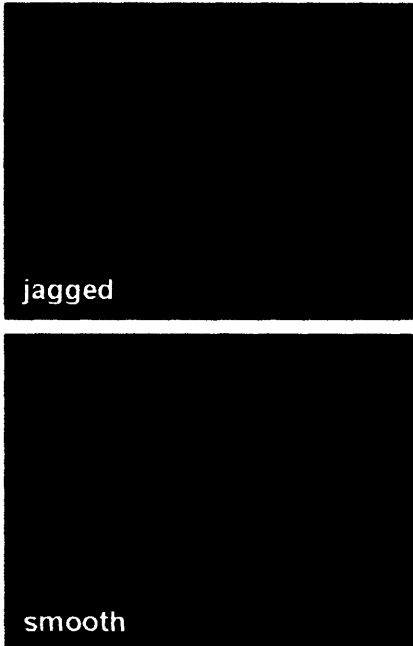
B

sorted
↓

			S.A. Morphology
2	-	(++)	Jagged
7	-	(+/-)	Jagged
11	-	(++)	Jagged
12	-	(+)	Jagged
19	-	(+/-)	Jagged
20	-	(++)	Jagged
36	(+)	(+/-)	Jagged
1	(++)	(++)	Jagged
34	mix	(+/-)	Jagged
35	mix - mostly (-)	(++)	Jagged
21	-	(+/-)	Smooth
8	(+)	(+)	Smooth
14	(+)	(+)	Smooth
17	(+)	(+)	Smooth
27	(+)	(+/-)	Smooth
9	(++)	(+)	Smooth
18	-	(+)	Smooth
24	mix	(+/-)	Smooth
13	mix - mostly (+)	(+/-)	Smooth
22	(weak +)	(+)	Smooth / Jagged
10	mix - mostly (+)	(++)	Smooth / Jagged
3	-	-	-
6	-	-	-
5	(+)	-	-
23	(+)	-	-
25	(+)	-	-
29	(+)	-	-
32	(+)	-	-
4	(weak +)	-	-

7/10 jagged colonies were mostly 4.1B (-)

6/9 smooth colonies were mostly 4.1B (+)



C

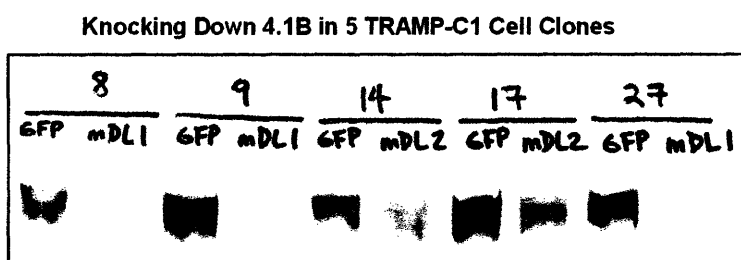


Figure 14. TRAMP-C1 cell clones exhibit differences in colony size and morphology when suspended in soft agar (cont.). (B) Cell clones were grouped according to colony morphology in soft agar (purple column), which varied between clones that had formed colonies with either a smooth or uneven (“jagged”) outer edge. (C) 4.1B protein expression was ablated with stable siRNAs (mDL1 or mDL2) in five independent clones expressing high levels of 4.1B and exhibiting a smooth soft agar colony morphology. Downregulation of 4.1B did not alter colony size or morphology in these cells.

A

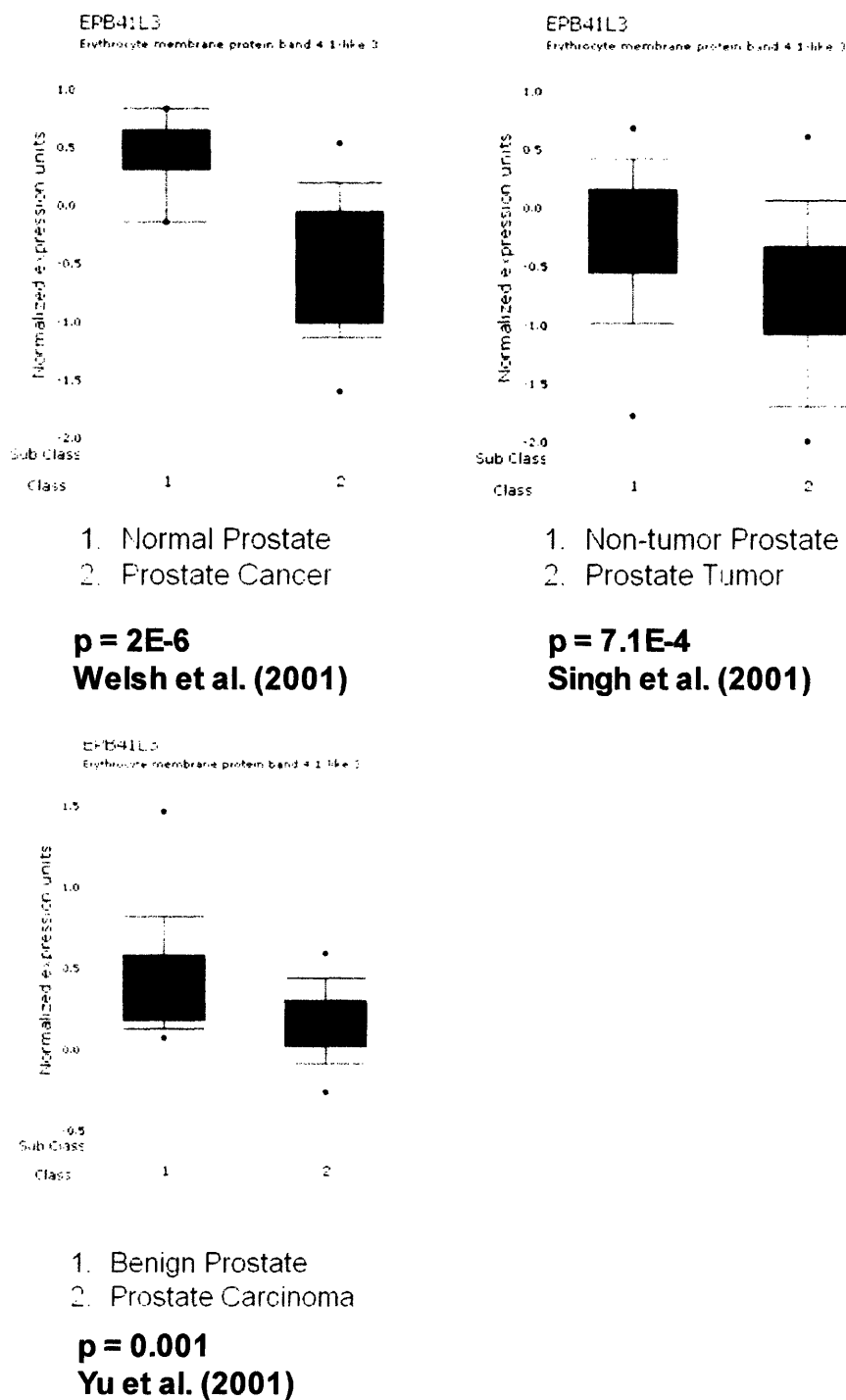


Figure 15. 4.1B expression is reduced in human clinical prostate cancer relative to normal prostate tissue. (A) 4.1B is significantly downregulated in prostate tumors relative to normal/benign prostate tissues in data-sets obtained from Welsh et al. (2001); Singh et al. (2002); and Yu et al. (2004), as analyzed by Oncomine. In all graphs, blue bars represent non-tumorigenic/benign prostate tissue, while red bars represent prostate cancer.

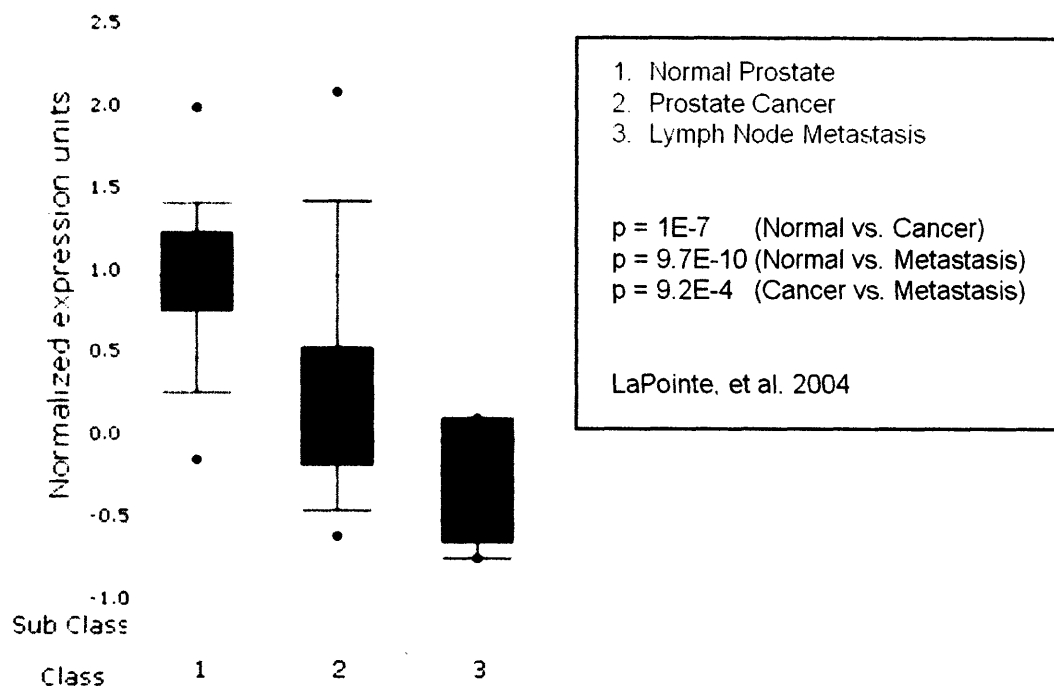
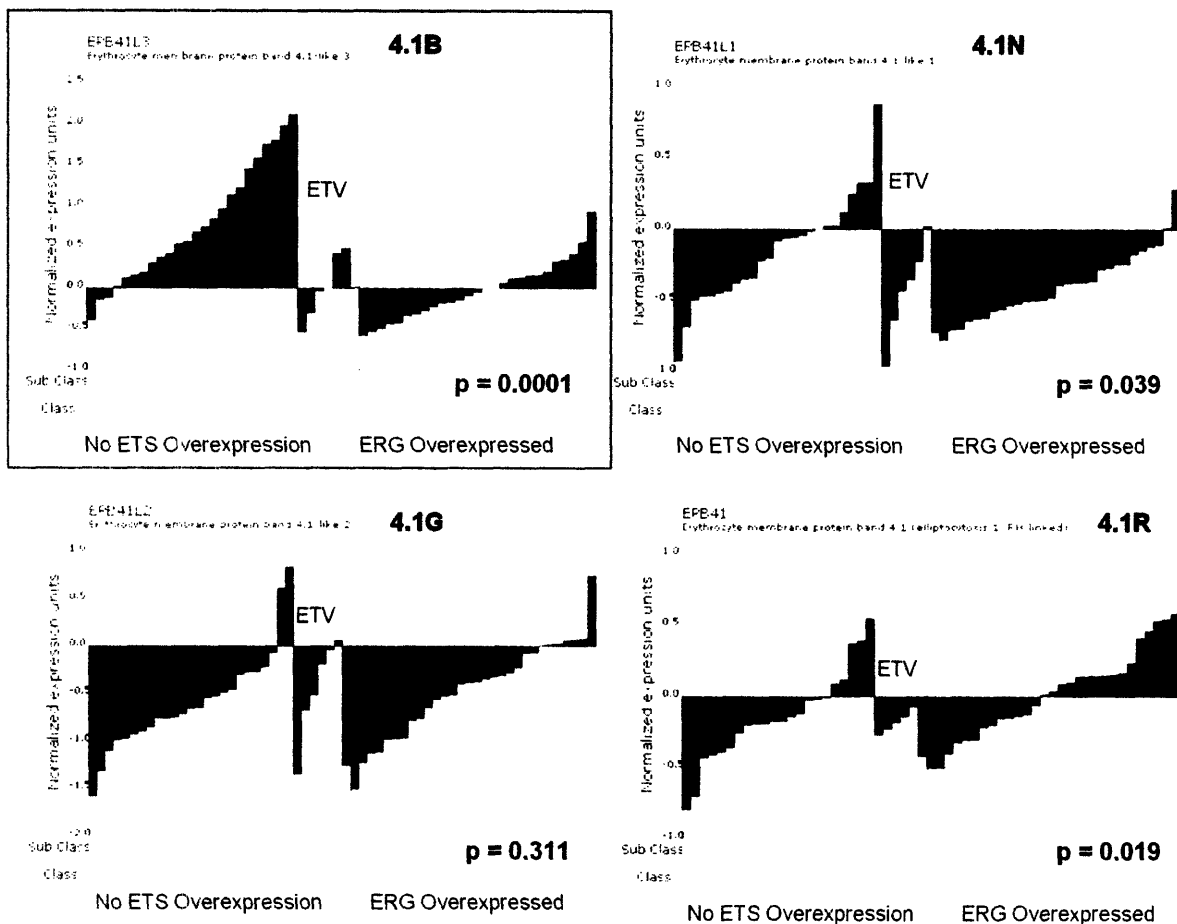
B

Figure 15. 4.1B expression is reduced in human clinical prostate cancer relative to normal prostate tissue (cont). (B) 4.1B expression is significantly downregulated during human clinical prostate cancer progression, from normal prostate tissue, to prostate cancer and finally to prostate cancer metastases (raw data originally from LaPointe et al. (2004) and analyzed by OncoPrint).



Y axis: Normalized expression level of the 4.1 gene in question

Each bar: Expression data from individual patients, ranked from lowest to highest, and separated into two categories: samples that showed no ETS overexpression, and those where ERG was overexpressed.

Figure 16. 4.1B expression is inversely associated with expression of the ETS family transcription factor ERG in human clinical prostate cancer. Oncomine analysis of data collected by LaPointe et al., (2004) revealed that, among patients bearing tumors with ERG overexpression (red bars), 4.1B levels are significantly reduced (upper left graph, $p = 0.0001$), compared to those of patients bearing tumors without overexpression of ETS family transcription factors (blue bars). To a lesser extent, 4.1N levels are also inversely associated with ERG overexpression (upper right graph), while expression of 4.1R is positively associated with ERG (lower right graph). Each bar represents gene expression results from a single human patient, and, within each group ("no ETS overexpression" or "ERG overexpression), patients were ranked from lowest to highest expression for a particular gene (e.g. 4.1B or 4.1N).

CHAPTER 4.

A DIRECT TEST FOR THE ROLE OF SPARC IN SPONTANEOUS PROSTATE AND BREAST CANCER PROGRESSION

The work in this chapter was conceived by Sunny Wong and Richard Hynes. SPARC-deficient mice were obtained from E. Helene Sage. The contents of this chapter were written by Sunny Wong, with editing by Richard Hynes.

INTRODUCTION

SPARC: A Multi-Functional Conundrum

Secreted protein, acidic and rich in cysteine (SPARC, also known as osteonectin or BM-40) is an extensively studied, albeit enigmatic, protein. SPARC is abundant, estimated to account for about 15% of the non-collagenous extracellular matrix in bone, and widely expressed during development, tissue remodeling and tumorigenesis[Framson and Sage, 2004; Koblinksi et al., 2005]. But while the cell biological and signaling functions ascribed to SPARC are many, this protein also seems to be necessary for none of these processes, as the phenotypes manifested in SPARC null mice are relatively minor, as will be discussed later. Perhaps fitting with its seemingly contradictory “all and none” role, studies examining the effects of SPARC on tumor progression have produced compelling, although often contradictory, results: SPARC is upregulated in tumorigenesis; SPARC is downregulated in tumorigenesis. While compensation may account for the lack of major phenotypes seen in knock-out mice, and the varied effects manifested by SPARC may be cell type- and context-dependent, a greater understanding of the mechanism of action of this protein will surely be needed before clarity is brought to the confounding results observed thus far.

In fact, the gene ontology generally agreed upon for SPARC seems almost contrarian in itself: It is a de-adhesive protein component of the extracellular matrix (ECM), belonging to a class of molecules known as matricellular proteins[Murphy-Ullrich, 2001]. This class of proteins also consists of the thrombospondins and tenascins, which together promote what has been termed an “intermediate” state of cell adhesion. Such a cell state has been postulated to be ideal for a variety of processes involving cell movement. One can imagine that a cell which is too-firmly attached to its surrounding matrix—via mature, integrin-containing focal contacts linked to stress fibers in the cytoskeleton—would hardly be inclined to migrate[Friedl and Wolf, 2003]. At the same time, complete loss of cell adhesion would deprive cells of the traction needed for movement and might even lead to cell death. An intermediate adhesive state, therefore, might be useful. Indeed, SPARC has been shown to induce cytoskeletal rearrangements and to disassemble focal adhesions for a variety of cell types *in vitro*, including tumor cell lines, fibroblasts, endothelial cells and smooth muscle cells[Brekken and Sage, 2001]. A specific receptor for SPARC has not been isolated; instead, SPARC has been postulated to function as a modulator of other known ligand-receptor interactions[Murphy-Ullrich, 2001]. At the same time, while SPARC is a component of the ECM and binds matrix molecules such as collagen and laminin, it is not believed to contribute directly to the structural integrity of these networks[Brekken et al., 2003].

Cellular Effects of SPARC

The three major domains present in SPARC are modular and have each been attributed to specific cell biological effects [Bradshaw and Sage, 2001]. Most of the studies examining the bioactivity of these individual domains were performed using isolated peptides added to cells *in vitro*, though there is likely to be some relevance for these studies *in vivo*, as matrix metalloproteinases (MMPs) have been reported to cleave and release fragments of SPARC, with consequent effects on various processes, from cell proliferation to angiogenesis [Framson and Sage, 2004; Sage et al., 2003]. At the N-terminus of the protein (amino acids 1-50) is a low-affinity calcium-binding domain that has been reported to inhibit cell spreading and attachment to matrix [Brekken and Sage, 2001]. A follistatin-like domain is present in the central portion of SPARC (amino acids 51-130) and may function as a pro-angiogenic molecule. Importantly, the C-terminal extracellular calcium-binding (E-C) module (amino acids 131-280) consists of two calcium-binding loops, or EF-hands, that, by themselves, functionally mirror the cell biological effects observed with full-length SPARC [Framson and Sage, 2004]. These include inhibition of cell proliferation; rearrangement of the cytoskeleton and disassembly of focal adhesions; and binding to growth factors such as VEGF and PDGF, as well as to ECM components.

Given the effects of SPARC on cell morphology, it is not surprising that this protein has also been found to affect gene expression in responding cells, often in ways that lead to upregulation of proteins that ultimately weaken the integrity of the pericellular matrix environment. In various cell types, physiological levels of SPARC have been reported to induce the expression of MMPs, including collagenase, gelatinase and stromelysin, as well as plasminogen activator inhibitor-1 [Gilles et al., 1998; Lane et al., 1992]. At the same time, expression of matrix components, including fibronectin, is decreased [Lane et al., 1992]. In this way, SPARC may indirectly attenuate cell-cell and cell-matrix interactions. However, the gene expression effects of SPARC likely reach beyond those that merely affect matrix integrity. The potentiation of TGF- β signaling is one proposed mechanism by which SPARC has been found to induce anti-proliferative effects on cells [Francki et al., 1999]. This SPARC-TGF- β connection might occur through an autocrine loop, as SPARC has been shown to induce TGF- β in mesangial cells, while TGF- β can induce SPARC expression in fibroblasts, keratinocytes, smooth muscle cells and endothelial cells [Francki et al., 1999; Schiemann et al., 2003]. In Mv1Mu epithelial cells, SPARC-mediated inhibition of growth could be prevented by expressing a dominant negative form of Smad3, a necessary downstream signaling component of the TGF- β pathway. SPARC has also been hypothesized to activate TGF- β post-translationally, as TGF- β is initially synthesized as a latent propeptide [Schiemann et al., 2003].

In concordance with its proposed role as a pro-migratory factor for cells, SPARC has been isolated from bone extracts as the major chemoattractant for prostate (PC-3 and DU-145) and breast cancer cells

(MDA-MB-231)[Jacob et al., 1999]. SPARC induced migration and invasion of these cells possibly by eliciting upregulated MMP-2 expression, and this may, at least in part, underlie the phenomenon of organ-specific metastasis—in this case, the propensity of prostate and breast tumors to metastasize to bone. Further work by De et al., has shown that PC-3 cells and another prostate cancer cell line, LNCaP, both responded to SPARC in Transwell migration assays[De et al., 2003]. In addition, SPARC was found to induce VEGF expression in the LNCaP cells, and all the cell biological effects seen with SPARC were inhibitable with blocking antibodies against either integrins $\alpha v\text{-}\beta 3/\text{-}\beta 5$, or VEGFR-2 (Flk1). Thus, there seem to be several interesting, although somewhat disparate, strands of data from these studies: VEGF, acting through Flk1, can activate αv integrins[Byzova et al., 2000]. Activated $\alpha v\text{-}\beta 3$ or $\text{-}\beta 5$ may then engage SPARC, leading to enhanced cell migration¹[De et al., 2003]. Finally, binding of SPARC may upregulate VEGF, thereby possibly completing an autocrine loop.

SPARC As a Mediator of Angiogenesis

The connection between SPARC and VEGF is of particular interest, given that SPARC, after cleavage by plasmin or by MMPs, can act as a pro-angiogenic factor[Framson and Sage, 2004]. Crucial to all this is a (K)GHK sequence-containing peptide that is released upon proteolysis and which has been demonstrated to promote endothelial cell proliferation both *in vitro* and *in vivo*[Lane et al., 1994; Sage et al., 2003]. In addition to inducing VEGF expression, SPARC has also been reported to downregulate expression of thrombospondin, a potent inhibitor of angiogenesis[Lane et al., 1992]. In spite of all this, however, a preponderance of evidence has suggested that, in most instances, SPARC is actually an inhibitor of angiogenesis. *In vitro*, SPARC inhibits the proliferation of endothelial cells[Kupprion et al., 1998]. It is also known to bind to and modulate the activity of several angiogenic factors, including VEGF, PDGF, FGF-2, TGF- β and IGF-1[Framson and Sage, 2004]. For instance, VEGF- and FGF-2-induced angiogenesis is inhibited by direct binding of these cytokines to SPARC, which prevents them from activating their cognate receptors on the surface of endothelial cells[Kupprion et al., 1998]. In addition, polyvinyl sponges implanted subcutaneously into SPARC-null mice have been observed to possess increased vascular and fibroblastic invasion, relative to those implanted into wild-type mice[Bradshaw et al., 2001]. SPARC-null dermal fibroblasts in this study were also found to secrete significantly higher levels of VEGF. It is difficult to reconcile many of these findings, except to say that the effects observed with SPARC—either as an angiogenic or anti-angiogenic factor—are likely influenced by the cell type(s) under study, as well as by factors such as the protease profile of the local microenvironment.

¹ Direct binding of $\alpha v\beta 3/\alpha v\beta 5$ to SPARC has not been conclusively proven, and indirect evidence has suggested that G protein-coupled receptors may also bind to SPARC.

SPARC As a Mediator of Matrix Integrity and Tumorigenesis

While it is widely believed that SPARC affects the integrity of cellular matrices, particularly those comprised of collagen fibrils, it is still very unclear how it contributes to the ECM and how a compromised matrix might affect tumor progression. What is clear is that loss of SPARC impairs collagen fibril assembly both *in vitro* and *in vivo*, and that SPARC knock-out mice possess about 50% less collagen in their skin[Brekken and Sage, 2001]. The reduction in collagen content has been hypothesized to underlie many of the non-lethal phenotypes manifested in SPARC-null mice, including reduced tensile strength in the dermis, cataracts, a kinked tail, severe bone loss in older mice, and abnormal expansion of subdermal adipocytes[Bradshaw et al., 2003; Framson and Sage, 2004]. SPARC knock-out mice also display accelerated wound closure, which may be indicative of a more contractible ECM with reduced collagen/hydroxyproline content[Bradshaw et al., 2002].

In nearly all cases, SPARC-mediated regulation of matrix integrity has been postulated to mediate its effects on tumor growth, although whether SPARC aids or hampers cancer progression is still a matter of debate and may be tumor-type-specific. In subcutaneous cancer models, Lewis lung carcinoma cells and EL4 T-cell lymphoma cells formed larger tumors in SPARC-null mice, relative to wild-type mice[Brekken et al., 2003]. A similar result was also obtained when PAN02 pancreatic adenocarcinoma cells were injected[Puolakkainen et al., 2004]. Although a slight difference in apoptosis was seen in the case of PAN02 cells, and no differences in tumor cell proliferation or angiogenesis were observed, these studies all noted that there was a significant decrease in tumor encapsulation within SPARC-null animals. In these mice, Masson's trichrome staining revealed that the abundance of collagen fibrils surrounding the tumors was sparse, and that the fibrils appeared smaller in diameter, relative to those in wild-type mice. Thus, SPARC may normally function as a tumor suppressor with a novel mechanism: It may act as a physical restraint against tumor cell expansion by maintaining a dense collagen network.

However, even this simple explanation—where SPARC and the ECM both negatively affect tumor progression—has become more complicated with the finding that, contrary to the results discussed just previously, MMTV-driven Her-2/neu breast cancer cells² formed smaller tumors when injected into SPARC knock-out mice, relative to wild-type[Sangaletti et al., 2003]. This study was notable in that adoptive transfer experiments revealed that leukocyte-secreted SPARC was the major determining factor for tumor growth. If SPARC⁺ leukocytes were transplanted into knock-out mice, tumor growth was increased; conversely, when SPARC⁻ leukocytes were transferred into wild-type mice, tumor growth was inhibited. Therefore, in this case, it would seem as if SPARC enhanced breast cancer progression. But what is the underlying mechanism for this effect? Interestingly, Sangaletti et al., went on to show in this study that leukocytes deficient in SPARC infiltrated deep into the tumor parenchyma, whereas those

² These Her-2/neu breast cancer cells were wild-type for SPARC.

which were wild-type for SPARC localized mainly to the periphery. This would imply that immune cell infiltration into the tumor inhibited growth, a conclusion that was supported by the fact that immune suppression of SPARC knock-out mice increased tumor size. Therefore, this study suggests that leukocyte-secreted SPARC may somehow act as a deterrent for immune cell entry into the tumor, and that the immune system suppresses tumor growth. Differences in macrophage infiltration into tumors have also been observed in SPARC knock-out mice, relative to wild-type, but the experimental evidence for this, as well as its implications on tumor growth, have been inconsistent and difficult to reconcile[Brekken et al., 2003; Puolakkainen et al., 2004]. In any case, SPARC is likely to regulate the ECM in ways that affect immune cell trafficking to the tumor. How SPARC ultimately affects tumor growth likely also impinges upon how the immune system influences tumorigenesis[Coussens and Werb, 2002].

SPARC As a Mediator of Tumor Metastasis

Finally, the role of SPARC as a modulator of ECM integrity and cell migration would seemingly make it an ideal candidate for affecting the final stage of tumor progression to metastasis. Given the often-contradictory observations already seen with SPARC, it is not surprising that its effects on metastasis are also confusing. In prostate cancer, SPARC expression was highest in cell lines that metastasized to bone, leading Thomas et al., to propose that tumor cells which efficiently form bone metastases often display “osteomimetic” characteristics—in other words, they become similar to those cells that normally reside and thrive in the bone[Thomas et al., 2000]. This may, in part, explain why certain tumors display organ-specific metastatic preferences. Downregulation of SPARC expression using anti-sense RNA in melanoma cells also inhibited their invasive capabilities *in vitro*, as well as their tumorigenicity and metastasis *in vivo*, in concordance with the hypothesis that SPARC promotes metastasis[Ledda et al., 1997]. However, overexpression of SPARC in breast cancer MDA-MB-231 cells specifically inhibited cell invasion, but not migration, proliferation or apoptosis[Koblinski et al., 2005]. When SPARC-overexpressing cells were injected into mice, a slight, but significant, reduction in platelet binding to the tumor cells was noted, and, though not validated directly, this might be responsible for the reduction seen in metastasis. In addition, in human clinical ovarian carcinomas, SPARC expression was downregulated in invasive tumors, and *in vitro*, SPARC induced apoptosis in the ovarian tumor cell lines[Yiu et al., 2001].

These experimental data, coupled with the fact that SPARC expression has often been found to be both significantly upregulated and downregulated in different human clinical tumors (Figure 1C), imply that SPARC regulation is important for tumorigenesis. However, the exact nature of its effects on tumorigenesis remains controversial. Our interest in SPARC grew out of our finding that its expression was severely downregulated in our highly metastatic PC-3 #82 variant cell line, relative to our poorly metastatic PC-3 #78 cells. If these differences were functionally important, that would indicate that SPARC acts as a metastasis suppressor in our orthotopic model of prostate cancer. To begin to

approach this question, we elected to study spontaneous prostate and breast cancer progression in mice that either possessed or were deficient in SPARC. Although the role of SPARC in tumorigenesis and metastasis has been examined in numerous studies using cell culture and xenograft experiments, to date, none have utilized spontaneous tumor mouse models. Therefore, we felt this was a novel and more realistic approach for testing the effects of SPARC on cancer progression, relative to what has already been described in the literature. I will describe the results for these experiments in the next section.

RESULTS

SPARC mRNA and protein are downregulated in highly metastatic #82 prostate cancer cells

In addition to 4.1B/DAL-1, gene expression analysis on metastatic variants of the prostate adenocarcinoma cell line PC-3 revealed that highly metastatic #82 cells displayed significantly downregulated expression of SPARC/osteonectin, relative to poorly metastatic #78 cells and medium metastatic pMicro-1 cells (Figure 1A). To further confirm this result, quantitative real-time PCR was performed on additional subcutaneous tumors and also on tissue culture cells. In all cases, SPARC expression was highest in #78 cells, slightly reduced in pMicro-1 cells, and severely downregulated in #82 cells (results summarized in Figure 1A). Gene expression data were also validated at the protein level by Western blot for SPARC in subcutaneous tumors (Figure 1B, arrows). Together, these results suggest that SPARC may be acting to suppress metastasis in our prostate cancer orthotopic model, and that, therefore, loss of SPARC expression/protein may enhance tumor progression and invasion.

SPARC expression is significantly altered in a variety of tumor types

SPARC expression levels were also examined in different human clinical gene expression studies to determine if there were data to support our hypothesis that SPARC may function as a tumor/metastasis suppressor. An initial comparison of tumor versus normal samples from the Oncomine database revealed that SPARC expression levels were frequently altered in a variety of cancers (Figure 1C). For example, SPARC was significantly upregulated in liver, colon and B-cell tumors relative to their respective normal tissues of origin, and downregulated in three studies of prostate cancer, relative to normal prostate. These seemingly contradictory results appear to parallel those obtained in experimental studies where SPARC has been reported to act both as a tumor-suppressor and -promoter in different mouse tumor models [Brekken et al., 2003; Puolakkainen et al., 2004; Sangaletti et al., 2003].

SPARC expression levels were extracted from additional published cancer data-sets for analysis. In a study by Dhanasekaran et al., microarray profiling of human clinical prostate material yielded gene expression signatures that could distinguish among samples derived from normal prostate tissue, benign

prostate hyperplasia (BPH), localized prostate cancer, and prostate cancer metastases [Dhanasekaran et al., 2001]. Interestingly, our analysis of data from this study revealed that SPARC mRNA was reduced in samples derived from hormone-refractory prostate cancer metastases, compared to those from normal prostate, BPH, and localized prostate cancer (Figure 2A). Since this study also recorded a significant reduction of SPARC in tumors relative to normal prostate tissue, this might indicate that SPARC downregulation could be important for progression of human prostate cancer, starting from the point of tumor initiation, to the formation of distant metastases in a variety of organs, including lymph nodes, lung and bone (Figure 2A).

In studies by van't Veer et al., a gene expression signature consisting of 70 features was found to distinguish between patients bearing node-negative breast cancers that were either likely ("Poor Prognosis") or unlikely ("Good Prognosis") to metastasize within 5 years from the time of diagnosis [van't Veer et al., 2002]. Patients with poor prognosis tended to bear tumors which were estrogen receptor (ER)-negative and which displayed increased lymphocyte infiltration; patients with BRCA1 germline mutations also bore tumors that were classified by gene expression to belong to the poor prognosis group. However, prognosis was not correlated with tumor grade or degree of angiogenesis. Although this optimized 70 gene expression signature did not include SPARC, subsequent analysis by Smid et al. (2003) [Smid et al., 2003], and by us revealed that reduced SPARC expression was associated with patients who had developed metastases within 5 years of diagnosis (Figure 2B). Furthermore, the level of SPARC expression, by itself, was capable of distinguishing between two groups of patients who differed, to some extent, in their susceptibility to metastatic disease (Figure 2C). As illustrated by the Kaplan Meier plot, 67% of patients with tumors that expressed high levels of SPARC remained free of metastasis within 5 years of diagnosis, whereas only 40% of patients with tumors that expressed low levels of SPARC remained metastasis-free during the same time-frame. Furthermore, tumors with the BRCA1 mutation, which also tended to be ER-negative [van't Veer et al., 2002], were found to exhibit lower SPARC expression relative to tumors without the mutation (Figure 3A). These data would therefore seem to be in concordance with our hypothesis that SPARC suppresses tumor aggressiveness.

Perhaps even more interestingly, analysis of data obtained by Dr. Lei Xu in our lab revealed that SPARC expression was specifically reduced in highly metastatic sub-clones (MA and MC series) derived from a bulk, mixed population of parental A375 melanoma cells (Figure 3B) [Xu et al., 2006]. The MA and MC cells exhibited increased lung metastasis when injected intravenously into immunocompromised mice; therefore, it is conceivable that downregulation of SPARC may be responsible, at least in part, for the aggressive phenotype of these cells. This apparent association of SPARC expression with many of the specific clinical parameters discussed previously, including tumor initiation, growth and metastasis, was subsequently tested, as described below, in different mouse models of cancer.

The role of SPARC in spontaneous prostate cancer formation and progression in TRAMP mice

SPARC heterozygous and knock-out mice bearing a single copy of the TRAMP transgene were evaluated for tumor formation, using similar procedures as those described previously for 4.1B in Chapter 3. At 26 weeks of age, there was no difference in the percentage of mice that had developed palpable grade 6 carcinomas for the heterozygous (6/19, 32%) and knock-out (4/13, 31%) mice (Figure 4A). Mice that had not formed palpable carcinomas, nevertheless, possessed enlarged prostate glands that likely contained non-invasive precursor lesions, as was the case with the 4.1B-TRAMP studies. Of those mice that had developed grade 6 carcinomas, there was no difference in the percentage of animals that had also developed palpable para-aortic/lumbar lymph node metastases (5/6 for SPARC^{+/-}; and 3/4 for SPARC^{-/-}) (Figure 4A). Furthermore, the masses of the urogenital systems did not differ significantly between genotype (mean = 4,059 mg for SPARC^{+/-} and 3,727 mg for SPARC^{-/-}, $p = 0.74$) (Figure 4B). Lastly, the urogenital mass of mice lacking the TRAMP transgene was also not significantly affected by genotype (mean = 554 mg for SPARC^{+/-} and 516 mg for SPARC^{-/-}, $p = 0.44$) (Figure 4B). Therefore, these results suggest that the presence or absence of SPARC does not influence prostate cancer progression in the TRAMP tumor model.

The role of SPARC in spontaneous mammary carcinoma formation and progression in PyMT mice

SPARC heterozygous and knock-out mice bearing a single copy of the MMTV transgene were evaluated for tumor initiation, rate of growth and metastasis. Beginning at 10 weeks of age, mice were inspected twice weekly for palpable tumors within any of the 10 mammary glands. These were clearly visible as small masses underneath the skin, and, over time, 100% of mice developed multiple malignant growths within the majority of their mammary glands. The earliest age at which a tumor was detected was recorded and used as a rough estimate of tumor initiation. Using this metric, we found no significant difference in the time to tumor initiation between SPARC^{+/-} or SPARC^{-/-} mice, whose tumors were first observed at an average age of 15.3 weeks and 15.6 weeks, respectively (Figure 5A). As a rough measure of the rate of tumor growth, mice were sacrificed four weeks after the initial observation of tumors, and the total mass of all malignant growths that had occurred during that time was also recorded. In this regard, there was also no significant difference between genotypes, as SPARC^{+/-} mice bore tumors of an average mass of 5.3 grams, while SPARC^{-/-} mice bore tumors of an average mass of 4.2 grams ($p = 0.2$) (Figure 5B). There was also no difference when only tumors at specific sites (e.g. upper right quadrant, lower left quadrant, etc.) were compared (data not shown). Macroscopic examination of the lungs at the time of sacrifice revealed no significant differences in the number of metastases present (Figure 5B). On average, SPARC^{+/-} mice possessed 9.6 lung metastases, while SPARC^{-/-} mice possessed 23.3 lung metastases ($p = 0.17$), though the results for the SPARC null mice were partially skewed by a single animal (out of eight total), which bore >100 lung metastases. In addition, there was

no correlation between the number of lung metastases observed and either the age of the animal or the total primary tumor burden (Figure 6). Therefore, and similar to the results seen with prostate cancer, these data suggest that the presence or absence of SPARC does not influence breast cancer progression in the MMTV tumor model.

DISCUSSION

As was observed from the Oncomine analysis, as well as from data gleaned from cancer bioinformatics studies originally performed by Dhanasekaran et al.; van't Veer et al.; and Xu et al.; among others, expression of SPARC/osteonectin is frequently altered during tumor progression [Dhanasekaran et al., 2001; van't Veer et al., 2002; Xu et al., 2006]. Our own studies have shown that SPARC expression is significantly downregulated in highly metastatic prostate cancer cells, implying that SPARC may normally act to suppress metastasis, and that genetic or epigenetic loss of expression of this gene may allow the highly metastatic phenotype to manifest itself. Because alterations in SPARC have been linked to a variety of cell morphological phenotypes, and because SPARC is a component of the ECM, we felt that this was a protein that was well-positioned to have significant effects on tumor progression and metastasis. We therefore decided to examine the role of SPARC in the context of spontaneous prostate and breast cancer development in mice.

Contrary to published tumor studies, thus far, we have found no evidence that SPARC is important during either prostate or breast cancer progression. However, these findings do not preclude the possibility that future, more detailed and/or sophisticated analyses may identify an important function for SPARC in tumorigenesis, particularly in other mouse cancer models. At the very least, it is evident from this initial study that SPARC plays little, if any, role in two SV40-driven mouse models of tumorigenesis. In TRAMP mice, the presence or absence of SPARC yielded no differences in urogenital-prostate mass or in the frequency of high grade prostate cancer formation. There was also no difference in the percentage of mice that developed local lymph node metastases. As observed previously, metastases were present only in mice that had developed histologic Grade 6, and often palpable, prostate tumors. In MMTV mice, the presence or absence of SPARC yielded no differences in time to mammary tumor initiation, rate of tumor growth or the number of lung metastasis. There was also no correlation between the extent of metastasis and primary tumor size or the age of the animal.

Given the results previously published identifying SPARC as a causal regulator of tumor progression, both positively and negatively [Brekken et al., 2003; Puolakkainen et al., 2004; Sangaletti et al., 2003], it is difficult to explain precisely why SPARC appeared to have no apparent effect in our tumor models. There are, however, several possibilities that could account for these discrepant results. Perhaps most importantly, the use of spontaneous mouse tumor models in our studies differed dramatically from the

experimental approaches of others, who examined the role of SPARC often in tissue culture and in xenograft models of tumorigenesis. As spontaneous tumor models reproduce every step along the cancer progression pathway, they are generally regarded as more realistic *in vivo* systems for studying cancer, although they are also significantly less amenable to experimental manipulation. Thus, SPARC may act both positively and negatively at several points along this cancer progression pathway, and the differential effects may, in some way, cancel out, or at least obfuscate our ability to assign a specific role for SPARC in tumorigenesis. This is a realistic possibility, considering that SPARC has been observed to act as a tumor inducer, a tumor suppressor, a pro-angiogenic factor, an anti-angiogenic factor, a metastasis inducer, as well as a metastasis suppressor[Framson and Sage, 2004]. A possible explanation for these often-contrasting findings may be that the effects of SPARC are heavily biased by the tumor microenvironment. Various proteolytic enzymes and MMPs are known to process SPARC post-translationally[Sage et al., 2003], and the various fragments that are consequently generated, as well as the stromal context in which they are present, and the tumor cell types that ultimately respond to them—these are all determinants of the bioactivity of SPARC.

Another important difference in our experimental approach is that we had compared tumor progression in animals that were either completely heterozygous or completely null for SPARC. This is in contrast with other published reports utilizing SPARC-deficient mice, which compared fully null animals with fully wild-type ones[Brekken et al., 2003; Puolakkainen et al., 2004; Sangaletti et al., 2003]. In addition, in studies where pancreatic carcinoma, T-cell lymphoma and mammary carcinoma cells were injected into these mice, the tumor cells themselves expressed SPARC. In some cases, this could be useful for discriminating between tumor-derived and stromally-derived SPARC[Sangaletti et al., 2003]. Two important questions, therefore, come to mind when we consider why our results might have differed from those of others: Firstly, does a two-fold reduction in SPARC (wild-type versus heterozygous) affect tumorigenesis? And secondly, is the source of SPARC (tumor- and/or stromal-derived) important? Neither of these questions can be fully answered with certainty, but given that SPARC null mice exhibit few significant phenotypic defects, it is not as likely that SPARC is haploinsufficient during tumorigenesis. Nonetheless, if SPARC heterozygous mice did, in fact, display some enhancement in tumor formation relative to wild-type animals³, the background for our analysis would have been increased, making it more difficult to observe statistically significant differences in tumor formation.

Similarly, the importance of tumor- versus stromally-derived SPARC remains unclear, though one study has suggested that leukocyte SPARC—and not tumor-derived SPARC—is all-important for affecting breast cancer formation[Sangaletti et al., 2003]. As ours was a preliminary study on the role of SPARC in spontaneous tumor progression, we have not yet analyzed the tumors to determine whether SPARC affected leukocyte localization within the cancer, and this remains to be examined in future studies. In

addition, it will also be interesting to determine whether the extracellular matrix within, or encapsulated around, the tumor was affected by SPARC, as has been previously noted by others [Brekken et al., 2003; Puolakkainen et al., 2004]. Effects on tumor angiogenesis could also potentially be evaluated. Interestingly, in studies by Puolakkainen, et al., pancreatic tumors injected into SPARC-deficient mice were reported to possess fewer pericyte-associated blood vessels [Puolakkainen et al., 2004]. As the blood vessels in that study were identified using the pan-endothelial marker MECA32, it is tempting to speculate that these vessels could very well have actually been lymphatic capillaries, which are not normally surrounded by pericytes. Could SPARC be important for lymphatics? Given that this molecule affects endothelial cells *in vitro* and is a component of the ECM, it would not be surprising if SPARC were, indeed, found to be a regulator of tumor lymphangiogenesis. Future immunohistochemical studies using the marker LYVE-1 to identify lymphatics in tumors and in surrounding normal tissue of SPARC wild-type and deficient mice could help determine whether this is the case.

In conclusion, we found no overall difference in spontaneous prostate or breast cancer progression in SPARC knock-out mice, relative to heterozygous animals. Therefore, this raises the possibility that, at least in some cases, altered levels of SPARC may be associated with, but not be causative for, tumorigenesis. In future studies, it will be important to determine how the tumor microenvironment influences the activity of SPARC. This may someday provide an explanation for the contrasting effects that have been reported for this multi-functional protein.

³ No SPARC wild-type mice were generated from our cross for experimental mice, and the few wild-type mice we did analyze arose from unrelated matings.

REFERENCES

- Bradshaw AD, Graves DC, Motamed K, Sage EH (2003): SPARC-null mice exhibit increased adiposity without significant differences in overall body weight. *PNAS* 100:6045-6050.
- Bradshaw AD, Reed MJ, Carbon JG, Pinney E, Brekken RA, Sage EH (2001): Increased fibrovascular invasion of subcutaneous polyvinyl alcohol sponges in SPARC-null mice. *Wound Repair and Regeneration* 9:522-530.
- Bradshaw AD, Reed MJ, Sage EH (2002): SPARC-null mice exhibit accelerated cutaneous wound closure. *The Journal of Histochemistry & Cytochemistry* 50:1-10.
- Bradshaw AD, Sage EH (2001): SPARC, a matricellular protein that functions in cellular differentiation and tissue response to injury. *Journal of Clinical Investigation* 107:1049-1054.
- Brekken RA, Puolakkainen P, Graves DC, Workman G, Lubkin SR, Sage EH (2003): Enhanced growth of tumors in SPARC null mice is associated with changes in the ECM. *The Journal of Clinical Investigation* 111:487-495.
- Brekken RA, Sage EH (2001): SPARC, a matricellular protein: at the crossroads of cell-matrix communication. *Matrix Biology* 19:816-827.
- Byzova TV, Goldman CK, Pampori N, Thomas KA, Bett A, Shattil SJ, Plow EF (2000): A mechanism for modulation of cellular responses to VEGF: activation of integrins. *Molecular Cell* 6:851-860.
- Coussens LM, Werb Z (2002): Inflammation and Cancer. *Nature* 420:860-867.
- De S, Chen J, Narizhneva NV, Heston W, Brainard J, Sage EH, Byzova TV (2003): Molecular pathway for cancer metastasis to bone. *JBC* 278:39044-39050.
- Dhanasekaran SM, Barrette TR, Ghosh D, Shah R, Varambally S, Kurachi K, Pienta KJ, Rubin MA, Chinnaiyan AM (2001): Delineation of prognostic biomarkers in prostate cancer. *Nature* 412:822-826.
- Framson PE, Sage EH (2004): SPARC and tumor growth: where the seed meets the soil? *Journal of Cellular Biochemistry* 92:679-690.
- Francki A, Bradshaw AD, Bassuk JA, Howe CC, Couser WG, Sage EH (1999): SPARC regulates the expression of collagen type I and transforming growth factor-beta1 in mesangial cells. *JBC* 274:32145-32152.
- Friedl P, Wolf K (2003): Tumour-cell invasion and migration: diversity and escape mechanisms. *Nature Reviews Cancer* 3:362-374.
- Gilles C, Bassuk JA, Pulyaeva H, Sage EH, Foidart JM, Thompson EW (1998): SPARC/osteonectin induces matrix metalloproteinase 2 activation in human breast cancer cell lines. *Cancer Research* 58:5529-5536.
- Jacob K, Webber M, Benayahu D, Kleinman HK (1999): Osteonectin promotes prostate cancer cell migration and invasion: a possible mechanism for metastasis to bone. *Cancer Research* 59:4453-4457.
- Koblinski JE, Kaplan-Singer BR, VanOsdol SJ, Wu M, Engbring JA, Wang S, Goldsmith CM, Piper JT, Vostal JG, Harms JF, Welch DR, Kleinman HK (2005): Endogenous osteonectin/SPARC/BM-40 expression inhibits MDA-MB-231 breast cancer cell metastasis. *Cancer Research* 65:7370-7377.
- Kupprion C, Motamed K, Sage EH (1998): SPARC (BM-40, osteonectin) inhibits the mitogenic effect of vascular endothelial growth factor on microvascular endothelial cells. *JBC* 273:29635-29640.
- Lane TF, Iruela-Arispe ML, Johnson RS, Sage EH (1994): SPARC is a source of copper-binding peptides that stimulate angiogenesis. *Journal of Cellular Biology* 125:929-943.
- Lane TF, Iruela-Arispe ML, Sage EH (1992): Regulation of gene expression by SPARC during angiogenesis in vitro. Changes in fibronectin, thrombospondin-1, and plasminogen activator inhibitor-1. *JBC* 267:16736-16745.
- Ledda MF, Adris S, Bravo AI, Kairiyama C, Bover L, Chernajovsky Y, Mordoh J, Podhajcer OL (1997): Suppression of SPARC expression by antisense RNA abrogates the tumorigenicity of human melanoma cells. *Nature Medicine* 3:171-176.
- Murphy-Ullrich JE (2001): The de-adhesive activity of matricellular proteins: is intermediate cell adhesion an adaptive state? *The Journal of Clinical Investigation* 107:785-790.

- Puolakkainen PA, Brekken RA, Muneer S, Sage EH (2004): Enhanced growth of pancreatic tumors in SPARC-null mice is associated with decreased deposition of extracellular matrix and reduced tumor cell apoptosis. *Molecular Cancer Research* 2:215-224.
- Sage EH, Reed M, Funk SE, Truong T, Steadele M, Puolakkainen P, Maurice DH, Bassuk JA (2003): Cleavage of the matricellular protein SPARC by matrix metalloproteinase 3 produces polypeptides that influence angiogenesis. *JBC* 278:37849-37857.
- Sangaletti S, Stoppacciaro A, Guiducci C, Torrisi MR, Colombo MP (2003): Leukocytes, rather than tumor-produced SPARC, determines stroma and collagen type IV deposition in mammary carcinoma. *J. Exp. Med.* 198:1475-1485.
- Schiemann BJ, Neil JR, Schiemann WP (2003): SPARC inhibits epithelial cell proliferation in part through stimulation of the transforming growth factor-beta-signaling system. *Molecular Biology of the Cell* 14:3977-3988.
- Smid M, Dorssers LC, Jenster G (2003): Venn Mapping: clustering of heterologous microarray data based on the number of co-occurring differentially expressed genes. *Bioinformatics* 19:2065-2071.
- Thomas R, True LD, Bassuk JA, Lange PH, Vessella RL (2000): Differential expression of osteonectin/SPARC during human prostate cancer progression. *Clinical Cancer Research* 6:1140-1149.
- van't Veer LJ, Dai H, Vijver MJvd, He YD, Hart AA, Mao M, Peterse HL, Kooy Kvd, Marton MJ, Kiteveen AT, Schreiber GJ, Kerkhoven RM, Roberts C, Linsley PS, Bernards R, Friend SH (2002): Gene expression profiling predicts clinical outcome of breast cancer. *Nature* 415:530-535.
- Xu L, Begum S, Hearn JD, Hynes RO (2006): GPR56, an atypical G protein-coupled receptor, binds tissue transglutaminase, TG2, and inhibits melanoma tumor growth and metastasis. *PNAS* 103:9023-9028.
- Yiu GK, Chan WY, Ng SW, Chan PS, Cheung KK, Berkowitz RS, Mok SC (2001): SPARC (secreted protein acidic and rich in cysteine) induces apoptosis in ovarian cancer cells. *American Journal of Pathology* 159:609-622.

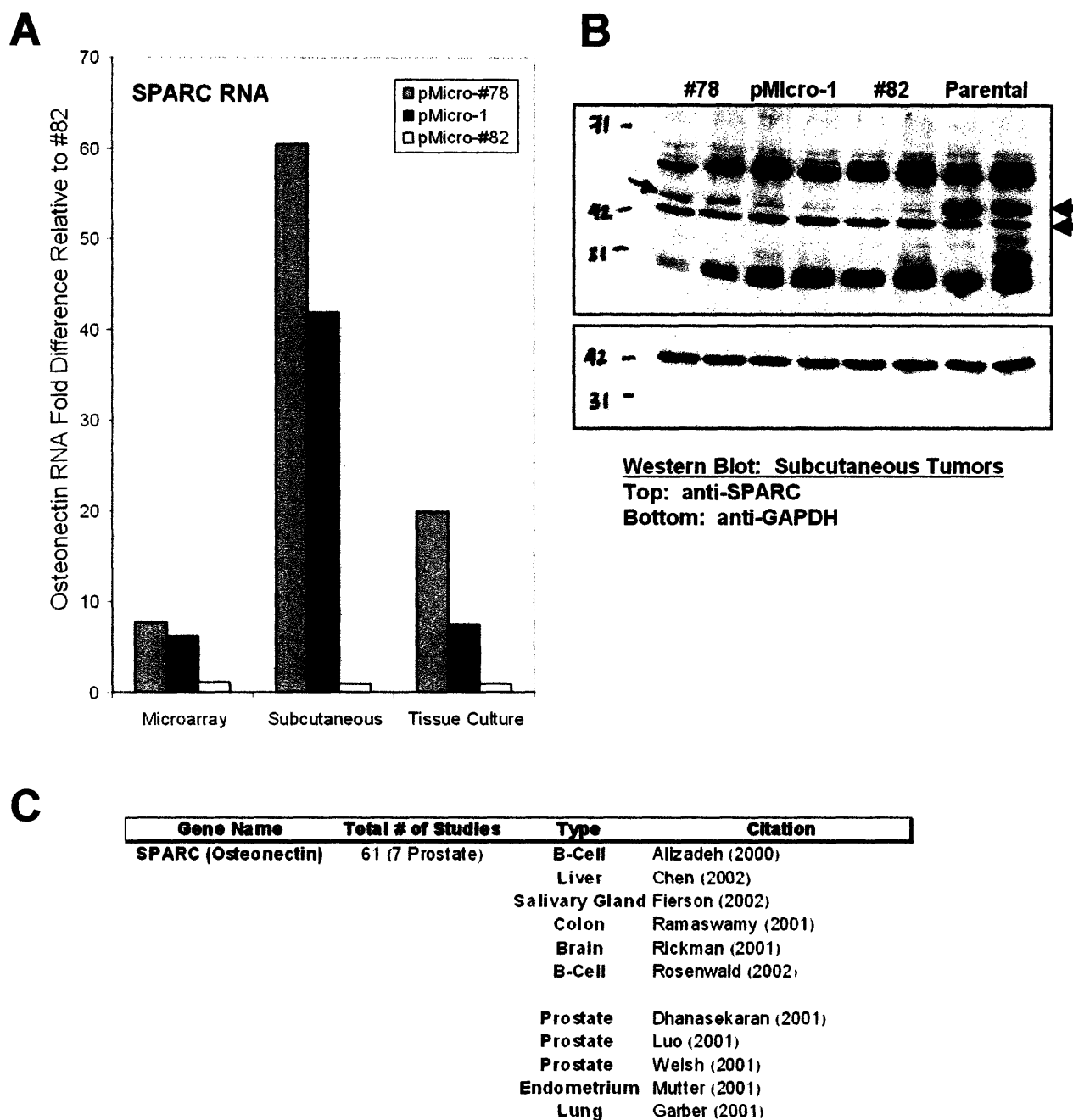


Figure 1. SPARC/Osteonectin expression is frequently downregulated in metastatic prostate cancer. (A) Expression of SPARC in metastatic variants of PC-3 was compared using gene expression analysis on subcutaneous tumors ("Microarray"), and quantitative RT-PCR on subcutaneous tumors ("Subcutaneous") and on tissue culture cells ("Tissue Culture"). All expression values were normalized relative to that of the highly metastatic variant, pMicro-#82 (beige bars), whose mRNA levels were set to one. (blue bars, #78 samples; purple bars, pMicro-1 samples) (B) Western blot for SPARC protein (arrows) confirmed the RNA results. The other bands present may be non-specific background bands. (C) SPARC expression was significantly upregulated (red) or downregulated (green) in different tumors, relative to normal tissue, according to Oncomine.

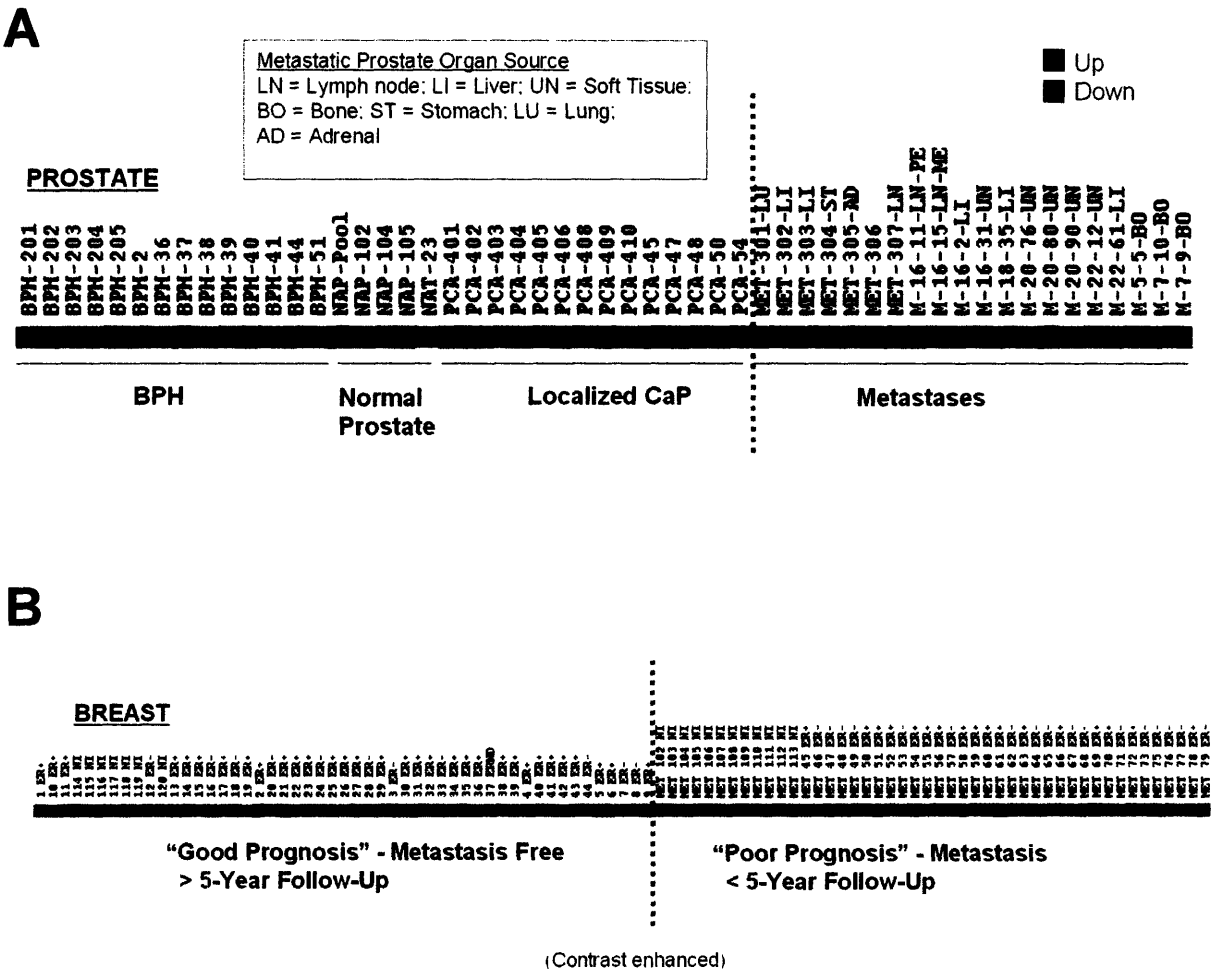


Figure 2. SPARC/Osteonectin expression is downregulated in metastatic prostate and breast cancer. (A) SPARC expression was compared between human clinical prostate cancer metastases, localized prostate cancer, benign prostate hyperplasia (BPH) and normal prostate tissue, using data obtained by Dhanasekaran et al. (2001). Each column represents a single tumor sample whose SPARC gene expression level was normalized relative to the mean intensity of all samples (red, relative up-regulation; green, relative down-regulation). (B) SPARC expression was compared between human clinical breast tumors from patients that had exhibited either “good” or “poor” prognosis, using data obtained by van’t Veer et al. (2002), and later processed by Smid et al. (2003).

C

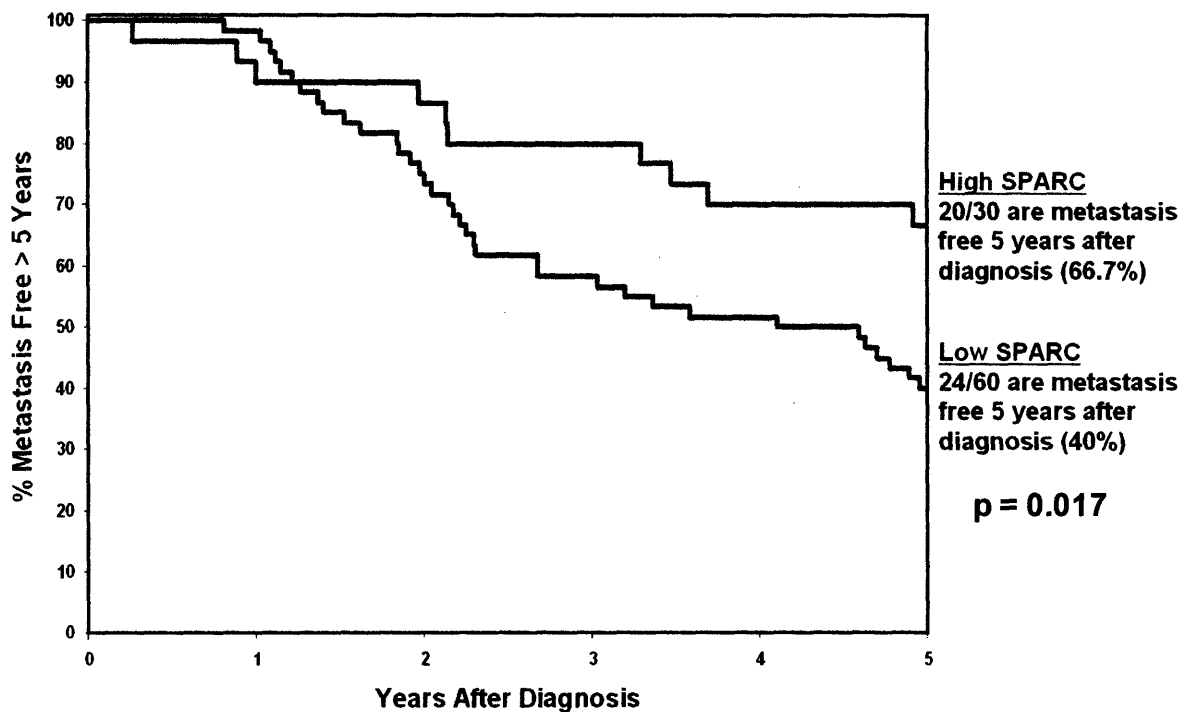
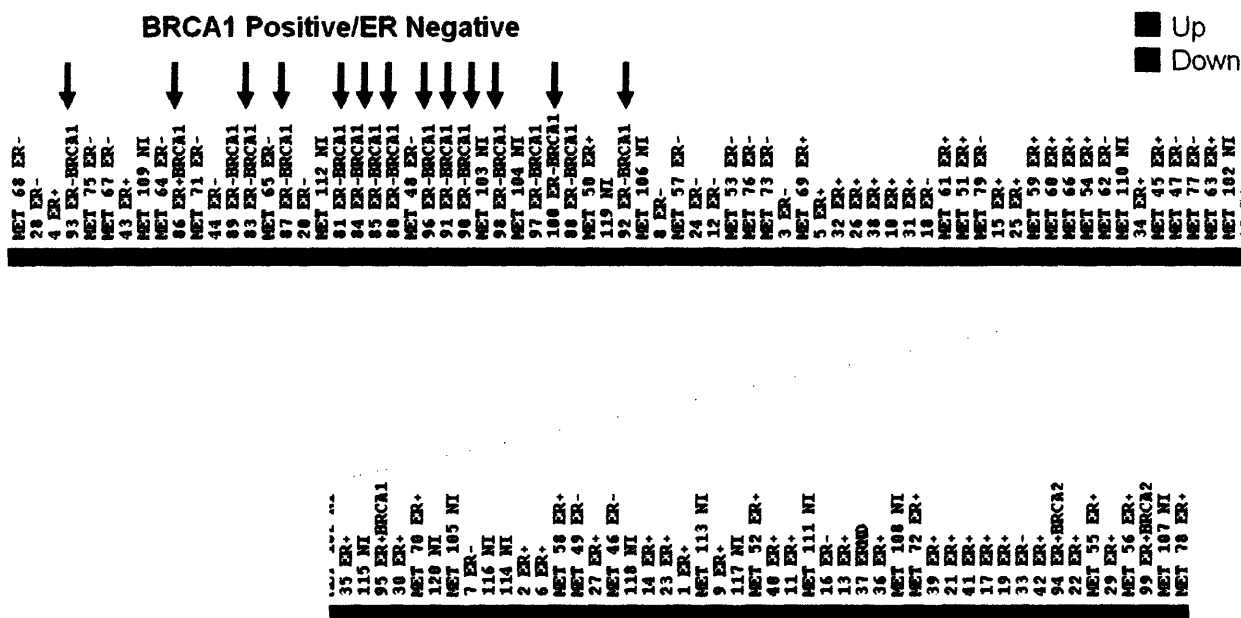


Figure 2. SPARC/Osteonectin expression is downregulated in metastatic prostate and breast cancer (cont). (C) Human clinical patients bearing mammary tumors were divided into two groups based on relative SPARC expression levels, and the percentage of patients remaining metastasis-free was plotted for up to 5 years after the initial time of diagnosis ($p = 0.017$ by Chi-square test, at the 5 year time-point).

A



B

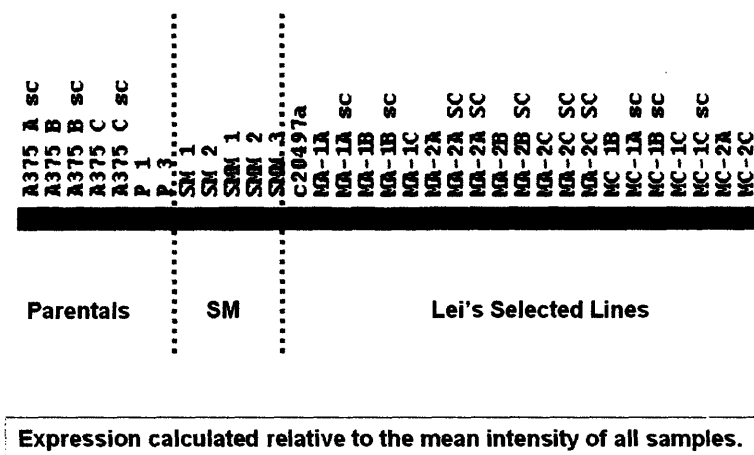


Figure 3. SPARC/Osteonectin expression is downregulated in BRCA1 positive/Estrogen Receptor negative breast cancer and in highly metastatic melanoma cells. (A) SPARC expression was compared among human clinical breast cancer patients with various clinical parameters, using data obtained by van't Veer et al. (2002). Each column represents a single tumor sample whose SPARC gene expression level was normalized relative to the mean intensity of all samples. Arrows depict patients bearing mammary tumors found to be both BRCA1-positive and ER-negative. **(B)** SPARC expression was compared among metastatic variants of the melanoma cell line A375. (red, relative upregulation; green, relative downregulation)

A

	Genotype	Macroscopic Carcinomas
HET	SPARC +/-; TRAMP	6/19 (32%)
KO	SPARC -/-; TRAMP	4/13 (31%)

	Genotype	Macroscopic Lymph Node Metastases
HET	SPARC +/-; TRAMP	5/6 (83%)
KO	SPARC -/-; TRAMP	3/4 (75%)

B

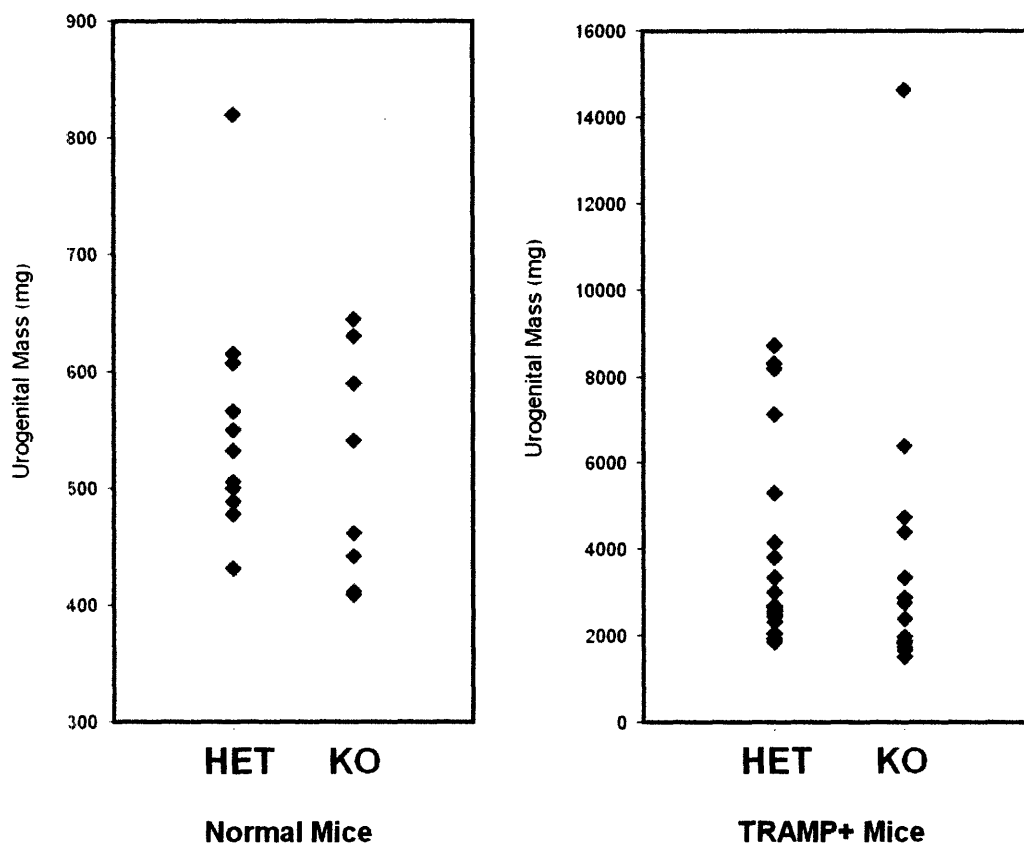


Figure 4. SPARC/Osteonectin does not affect spontaneous prostate cancer tumorigenesis or metastasis in TRAMP mice. (A) The incidence of palpable macroscopic prostate carcinomas (top) and lymph node metastases (bottom) was compared between SPARC knock-out (KO) and heterozygous (Het) animals at 26 weeks of age. **(B)** Urogenital mass of TRAMP-negative (left) and TRAMP-positive (right) mice was assessed for SPARC knock-out and heterozygous animals at 26 weeks of age.

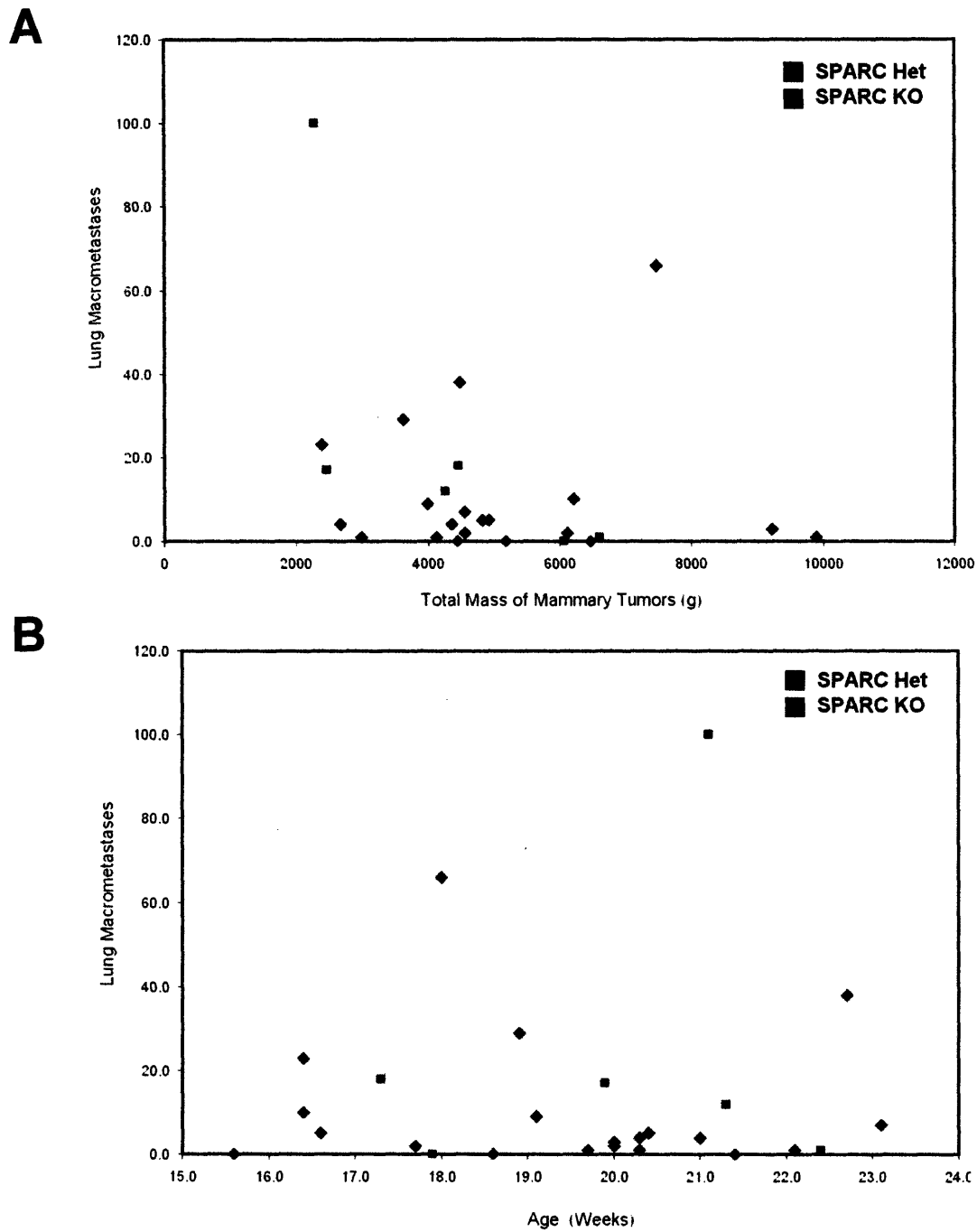


Figure 6. No apparent correlation is seen in lung metastasis plotted against total tumor burden (A) or age (B), for either SPARC knock-out or heterozygous mice.

CHAPTER 5.

HEMATOGENOUS METASTASIS IS ASSOCIATED WITH LYMPHATIC DISSEMINATION IN A MOUSE MODEL OF PROSTATE CANCER

The work in this chapter was conceived by Sunny Wong and Richard Hynes. The contents of this chapter were written by Sunny Wong, with editing by Richard Hynes.

INTRODUCTION

Blood vessel or lymphatic dissemination?

The formation of distant metastases is the deadliest phase of cancer progression. Although numerous studies, including our own, have identified genes that affect metastasis after tumors have reached secondary sites, our knowledge about how cancer cells initially gain access to systemic circulation is limited. Part of the complexity arises from the fact that, once a migratory cancer cell has detached from the primary tumor, it may intravasate into either a blood or lymphatic vessel. Either route of dissemination can lead to venous circulation, as lymphatics drain into the blood, most commonly through the left lymphatic duct (thoracic duct) or the right lymphatic duct, and then subsequently into the subclavian veins. Therefore, it is imperative that we understand the physiological and molecular mechanisms that affect what might be the first decision an invasive cell needs to make: whether it will metastasize via blood vessels or lymphatics.

To a large extent, this decision likely rests on physical restrictions imposed on invasive tumors, although active mechanisms for attracting malignant cells to specific types of vasculature have also recently been postulated (see below). Lymphatics have long been regarded as the “default” pathway for tumor cell dissemination, and this is likely due to the fact that lymphatic capillaries lack the tight interendothelial junctions typically seen in blood vessels, as well as the surrounding layers of pericytes/smooth muscle cells and basement membranes[Alitalo and Carmeliet, 2002]. This inevitably renders lymphatics “porous” relative to blood vessels, thus making them more susceptible to invasion by tumors. In addition, the survival of malignant cells might benefit from the passive, low-shear fluid flow characteristic of lymphatics. However, the increased hemodynamic flow rate, as is observed within blood vessels, might also help to dislodge individual malignant cells from the primary tumor[Byers et al., 1995].

Accessibility of blood and lymphatic vasculature might be another factor that influences the pathway taken for metastasis. Induction of angiogenesis, the growth of blood vessels, has been shown to be necessary for tumors growing beyond 0.4 mm in diameter[Ferrara, 2002; Gimbrone et al., 1972]. On the other hand, lymphatic vessels appear to be dispensable for primary tumor growth in several experimental mouse models[Chen et al., 2005; He et al., 2002; Karpanen et al., 2001; Krishnan et al., 2003; Lin et al., 2005; Shimizu et al., 2004]. Because blood and lymphatic vessels share a common embryonic origin, and respond to many similar growth factors—VEGF-A, VEGF-C, VEGF-D, FGF2, PDGF-B, HGF and others[Alitalo et al., 2005]—tumors might be expected to induce lymphangiogenesis concomitant with angiogenesis. But for reasons unclear, this is often not the case. While proliferating intratumoral lymphatics have been detected in human melanomas[Dadras et al., 2003], as well as in head and neck squamous cell carcinomas[Maula et al., 2003], evidence for lymphangiogenesis in other cancers has

been less well documented. In the absence of intratumoral lymphatics, therefore, only tumor cells at the invasive margins would be expected to have access to the surrounding lymphatic vasculature. In contrast, most cancer cells should have ready access to blood vessels, which are present throughout the tumor.

As mentioned previously, active recruitment of tumor cells towards either blood vessels or lymphatics may occur through paracrine interactions, for instance involving an EGF-EGFR axis. Studies by Wyckoff et al., for instance, have shown that metastatic rat mammary adenocarcinoma cells expressing high levels of EGFR often polarize towards blood vessels, which are lined by macrophages that secrete EGF [Wyckoff et al., 2004]. Macrophages are often also found in proximity to lymphatic vessels [Schoppmann et al., 2002; Skobe et al., 2001], and in recent studies, macrophages have even been observed to transdifferentiate into lymphatics [Kerjaschki, 2005; Maruyama et al., 2005]. In addition, lymphatic stromal cells have been reported to be a source of EGF and IGF-I [LeBedis et al., 2002]. Lymph node secretion of chemokines such as SCL/CCL21 and CCL1 might also attract tumor cells that express the receptors CCR7 and CCR8, respectively [Homey et al., 2002]. Overexpression of CCR7 in B16 melanoma cells has been shown to increase lymph node metastasis [Wiley et al., 2001], while others have reported that breast cancer cells or melanomas expressing CXCR4 may actively home to lymph nodes containing CXCL12/SDF-1 ligand [Muller et al., 2001].

How do tumor cells reach systemic circulation?

Related to the topic of how malignant cells exit from the primary tumor is another issue that possesses far-reaching implications: How do tumor cells actually reach systemic circulation? Resolving this question is especially important, considering the large number of cancer cells that are thought to be released into the blood—estimated in one study to be up to $\sim 4 \times 10^6$ cells per gram of primary tumor daily [Butler and Gullino, 1975]. The obvious and simple answer is that tumor cells enter into blood circulation through blood vessels; yet, as we have discussed previously, the lymphatic system might provide a more circuitous, though perhaps less treacherous, route for tumor cell dissemination.

The exact answer, or even a generalized answer, for how tumor cells enter hematogenous circulation has yet to be determined. A major obstacle arises from difficulties in observing and tracking the movements of individual tumor cells *in vivo*, although recent intravital imaging studies have provided views of tumor cell intravasation into vasculature [Hoshida et al., 2006; Wyckoff et al., 2000]. In addition, there has been little evidence to prove that tumor cells in lymph nodes can actually reach blood circulation. Even if this phenomenon does occur, it is unclear how frequently tumor cells choose one pathway over the other. At the very least, if cancer cells must rely on lymphatics to enter into the blood, a positive correlation between lymphatic and hematogenous spread should be seen in human tumors. In fact, this is exactly

the case for a variety of cancers observed in the clinic. For instance, Bubendorf et al. reported that 84% of patients with node-positive prostate cancer bore evidence of hematogenous dissemination, as opposed to 16% of patients without local lymph node spread[Bubendorf et al., 2000]. In breast cancer, lymph node metastasis has been linked with poor prognosis and distant metastasis[Cianfrocca and Goldstein, 2004], and similar observations have also been noted in pancreatic cancer[Yoshida et al., 2004], ovarian cancer[Dvoretzky et al., 1988], and head and neck cancer[Leemans et al., 1993], among others. It should come as no surprise, therefore, that lymph node status is often used as a diagnostic tool to predict the extent to which a primary tumor has already spread throughout the body.

While it is tempting to speculate that these associations arise from the fact that hematogenous metastasis is dependent upon lymphatic spread, of course, this hypothesis needs to be proven in an experimental setting. We initially became interested in answering some of the questions raised in this section, after observing an apparent association between lymphatic and systemic metastasis in our surgical orthotopic mouse model of prostate cancer. In the following Results and Discussion sections, I will describe our findings related to this, as well as an experimental approach for determining how tumor cells might enter blood circulation. This approach, as well as the results that came out of it, will be discussed in detail in the following chapter.

RESULTS

Hematogenous Dissemination Is Associated With Lymphatic Metastasis in an Orthotopic Model of Prostate Cancer

As described in Chapter 2, we utilized surgical orthotopic implantation (SOI) as a method for introducing human prostate PC-3 cells into immunodeficient mice. An advantage of this model, as was also previously mentioned, was that the primary tumors developed both lymphatic and systemic metastases, 2-3 months post-surgery (Figure 1). Importantly, we were able to develop techniques to quantitate the degree of tumor spread to the lymph nodes and to the lung, as well as to count the number of viable circulating cancer cells in the blood of tumor-bearing mice.

With these three assays for measuring tumor cell presence in the lymph nodes, blood and lungs, we began noticing certain trends that have, for the most part, held true after analysis of >196 mice successfully implanted by SOI with our PC-3 cell line derivatives. Interestingly, we observed a strong correlation between lymphatic and hematogenous dissemination in our mouse orthotopic xenograft model of prostate cancer (Figure 2). As expected, the lymph nodes directly draining the prostate, the para-aortic/sub-lumbar lymph nodes, were invaded first by the tumors, followed by the more distant sub-renal lymph nodes. Mice that bore tumors which had not formed macroscopic metastases in the lumbar lymph

nodes (~ 50% of mice) were unlikely to possess renal lymph node macro-metastases. Not surprisingly, the appearance of lung micrometastases was well-correlated with the detection of viable circulating tumor cells in the blood (Figure 2A). Unexpectedly, however, significant numbers of circulating tumor cells (Figure 2B) and lung metastases (Figure 2C) were observed only in mice that possessed both renal and lumbar lymph node macro-metastases, regardless of primary tumor size.

This apparent correlation between lymphatic and hematogenous spread can be interpreted in at least three ways (Figure 3). It is possible that PC-3 tumor cells may be unable to intravasate directly into blood vessels; thus they must first establish satellite lymph node metastases in order to disperse metastatic cells via the thoracic duct into the blood. Another possibility is that the primary tumors may be completely non-invasive until somehow triggered to metastasize via both lymphatics and blood vessels simultaneously. A third explanation is that distinct sub-populations of tumor cells may be capable only of metastasizing via either the lymphatic or blood vessel routes, but not both, and that dissemination also occurs at about the same time. Any of these possibilities would potentially yield an apparent correlation between lymphatic and hematogenous spread. In the last two scenarios, tumor cells which have reached lymph nodes may or may not disseminate further into venous circulation.

It is interesting to note that, in our system, subcutaneous tumors rarely metastasize, in spite of the fact that—at least in the case of PC-3 cells—highly angiogenic and lymphangiogenic tumors are formed (Figure 4). Although there are numerous reasons why tumors might metastasize from an orthotopic site but not from an ectopic site, a simple explanation is as follows: Although we have observed microscopic subcapsular lymph node invasion from subcutaneous tumors, these nodes were not invaded to the degree that would favor widespread systemic tumor cell dispersal. This hypothesis would be in agreement with our orthotopic results and would argue that hematogenous dissemination is dependent upon substantial lymphatic spread. A prediction from this model would therefore be that, if given enough time, subcutaneous tumors should also be expected to develop systemic metastases—but only after forming macrometastases in the draining, axillary lymph nodes.

DISCUSSION

We have observed that hematogenous dissemination of tumor cells is associated with lymphatic metastasis in an orthotopic model of prostate cancer. We have also proposed three explanations that might explain our findings. In the first possibility, hematogenous dissemination might be dependent upon lymphatic spread; an alternative explanation is that primary tumors might be induced by an unknown mechanism to metastasize via both the lymphatic and hematogenous routes simultaneously; and, finally, a third possibility is that distinct sub-populations of tumor cells may be adept at disseminating via either vascular routes, but not both, and that this dissemination occurs at roughly the same time. In support of

the first possibility, Sleeman et al., have noted that the physiology of lymph nodes may actually favor formation of local metastases that could serve as “bridgeheads” for further dissemination [Sleeman, 2000]. Similarly, others have proposed that lymph nodes might act as initial “selection” sites where tumor cells with partial metastatic competence could seed and expand, while selecting for increasingly malignant variants that could later spread to more distant sites [Krishnan et al., 2003]. However, it remains to be seen whether tumor cells can efficiently enter blood circulation via lymphatics.

If entrance into systemic circulation were dependent on lymphatics, experimental inhibition of lymph node metastasis should also inhibit hematogenous spread. But, while some have indeed reported such results [Chen et al., 2005; Krishnan et al., 2003; Lin et al., 2005], others found that inhibiting lymph node metastasis had no effect on lung metastasis [He et al., 2002; He et al., 2004; He et al., 2005]. These findings are likely attributable to differences in the cell lines utilized and whether the cells were implanted orthotopically or ectopically. In another study, resection of MT-100-TC mammary carcinomas along with draining lymph nodes prevented metastatic recurrence, but removal of the primary tumors alone did not [Ward and Weiss, 1989]. This would suggest that MT-100-TC cells reached systemic circulation via lymphatics, a progression the authors termed “metachronous seeding.”

In contrast, the presence of hematogenous metastases in the absence of lymphatic spread would clearly indicate direct dispersal of tumor cells into blood vessels. This is a likely scenario for human patients harboring bone marrow micrometastases in the absence of other detectable signs of spread, which has been reported to occur in 20-40% of carcinomas [Pantel and Brakenhoff, 2004]. Interestingly, comparative genomic hybridization (CGH) analyses have suggested that malignant cells may disseminate through the blood very early in breast cancer [Schardt et al., 2005; Schmidt-Kittler et al., 2003]. These cells were also found to be distinct from lymph node metastases by CGH, thus arguing against metachronous seeding.

Although different tumor types may vary in regard to the mechanisms by which they spread throughout the body, it is clear that in many human clinical studies, as well as animal models including our own, an apparent association is observed for hematogenous and lymphatic dissemination. Given the three possible explanations that might account for these results (Figure 3), in the next Chapter, I will describe our attempts to use our orthotopic model of prostate cancer to distinguish between these possibilities. Our approach was to try and selectively inhibit lymphatic metastasis in our system. If hematogenous spread were dependent upon metastasis to lymph nodes, both pathways should be simultaneously inhibited. On the other hand, if hematogenous metastasis and lymphatic spread occurred independently, it is expected that bloodborne dissemination of tumor cells should be unaffected by inhibition of lymph node metastasis.

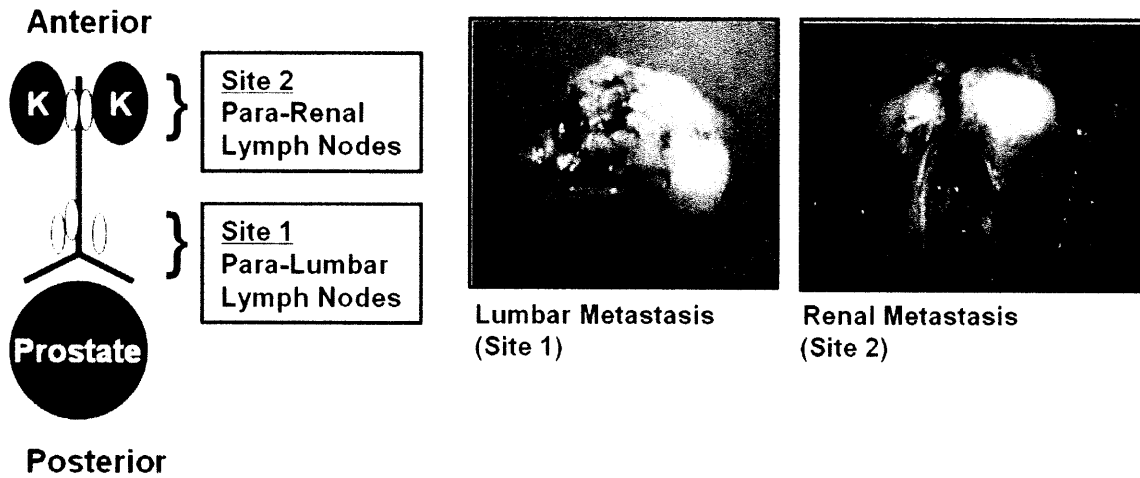
REFERENCES

- Alitalo K, Carmeliet P (2002): Molecular mechanisms of lymphangiogenesis in health and disease. *Cancer Cell* 1:219-227.
- Alitalo K, Tammela T, Petrova TV (2005): Lymphangiogenesis in development and human disease. *Nature* 438:946-953.
- Bubendorf L, Schopfer A, Wagner U, Sauter G, Moch H, Willi N, Gasser TC, Mihatsch MJ (2000): Metastatic patterns of prostate cancer: an autopsy study of 1,589 patients. *Human Pathology* 31:578-582.
- Butler TP, Gullino PM (1975): Quantitation of cell shedding into efferent blood of mammary adenocarcinoma. *Cancer Research* 35:512-516.
- Byers SW, Sommers CL, Hoxter B, Mercurio AM, Tozeren A (1995): Role of E-cadherin in the response of tumor cell aggregates to lymphatic, venous and arterial flow: measurement of cell-cell adhesion strength. *Journal of Cell Science* 108:2053-2064.
- Chen Z, Varney ML, Backora MW, Cowan K, Solheim JC, Talmadge JE, Singh RK (2005): Down-regulation of vascular endothelial cell growth factor-C expression using small interfering RNA vectors in mammary tumors inhibits tumor lymphangiogenesis and spontaneous metastasis and enhances survival. *Cancer Research* 65:9004-9011.
- Cianfrocca M, Goldstein LJ (2004): Prognostic and predictive factors in early-stage breast cancer. *The Oncologist* 9:606-616.
- Dadras SS, Paul T, Bertoincini J, Brown LF, Muzikansky A, Jackson DG, Ellwanger U, Garbe C, Mihm MC, Detmar M (2003): Tumor lymphangiogenesis: a novel prognostic indicator for cutaneous melanoma metastasis and survival. *American Journal of Pathology* 162:1951-1960.
- Dvoretzky PM, Richards KA, Angel C, Rabinowitz L, Stoler MH, Beecham JB, Bonfiglio TA (1988): Distribution of disease at autopsy in 100 women with ovarian cancer. *Human Pathology* 19:57-63.
- Ferrara N (2002): VEGF and the quest for tumor angiogenesis factors. *Nature Reviews Cancer* 2:795-803.
- Gimbrone MA, Leapman SB, Cotran RS, Folkman J (1972): Tumor dormancy in vivo by prevention of neovascularization. *Journal of Experimental Medicine* 136:261-276.
- He Y, Kozaki K, Karpanen T, Koshikawa K, Yla-Herttuala S, Takahashi T, Alitalo K (2002): Suppression of tumor lymphangiogenesis and lymph node metastasis by blocking vascular endothelial growth factor receptor-3 signaling. *Journal of the National Cancer Institute* 94:819-825.
- He Y, Rajantie I, Ilmonen M, Makinen T, Karkkainen MJ, Haiko P, Salven P, Alitalo K (2004): Preexisting lymphatic endothelium but not endothelial progenitor cells are essential for tumor lymphangiogenesis and lymphatic metastasis. *Cancer Research* 64:3737-3740.
- He Y, Rajantie I, Pajusola K, Jeltsch M, Holopainen T, Yla-Herttuala S, Harding T, Jooss K, Takahashi T, Alitalo K (2005): Vascular endothelial cell growth factor receptor 3-mediated activation of lymphatic endothelium is crucial for tumor cell entry and spread via lymphatic vessels. *Cancer Research* 65:4739-4746.
- Homey B, Muller A, Zlotnik A (2002): Chemokines: agents for the immunotherapy of cancer? *Nature Reviews Immunology* 3:175-184.
- Hoshida T, Isaka N, Hagendoorn J, Tomaso Ed, Chen YL, Pytowski B, Fukumura D, Padera TP, Jain RK (2006): Imaging steps of lymphatic metastasis reveals that vascular endothelial growth factor-C increases metastasis by increasing delivery of cancer cells to lymph nodes: therapeutic implications. *Cancer Research* 66:8065-8075.
- Karpanen T, Egeblad M, Karkkainen MJ, Kubo H, Yla-Herttuala S, Jaattela M, Alitalo K (2001): Vascular endothelial growth factor C promotes tumor lymphangiogenesis and intralymphatic tumor growth. *Cancer Research* 61:1786-1790.
- Kerjaschki D (2005): The crucial role of macrophages in lymphangiogenesis. *The Journal of Clinical Investigation* 115:2316-2319.
- Krishnan J, Kirkin V, Steffen A, Hegen M, Weih D, Tomarev S, Wilting J, Sleeman JP (2003): Differential in vivo and in vitro expression of vascular endothelial growth factor (VEGF)-C and

- VEGF-D in tumors and its relationship to lymphatic metastasis in immunocompetent rats. *Cancer Research* 63:713-722.
- LeBedis C, Chen K, Fallavollita L, Boutros T, Brodt P (2002): Peripheral lymph node stromal cells can promote growth and tumorigenicity of breast carcinoma cells through the release of IGF-I and EGF. *International Journal of Cancer* 100:2-8.
- Leemans CR, Tiwari R, Nauta JJ, Waal Ivd, Snow GB (1993): Regional lymph node involvement and its significance in the development of distant metastases in head and neck carcinoma. *Cancer* 71:452-456.
- Lin J, Lalani AS, Harding TC, Gonzalez M, Wu WW, Luan B, Tu GH, Koprivnikar K, VanRoey MJ, He Y, Alitalo K, Jooss K (2005): Inhibition of lymphogenous metastasis using adeno-associated virus-mediated gene transfer of a soluble VEGFR-3 decoy receptor. *Cancer Research* 65:6901-6909.
- Maruyama K, Ii M, Cursiefen C, Jackson DG, Keino H, Tomita M, Rooijen NV, Takenaka H, D'Amore PA, Stein-Streilen J, Losordo DW, Streilein JW (2005): Inflammation-induced lymphangiogenesis in the cornea arises from CD11b-positive macrophages. *The Journal of Clinical Investigation* 115:2363-2372.
- Maula S, Luukka M, Grenman R, Jackson D, Jalkanen S, Ristamaki R (2003): Intratumoral lymphatics are essential for the metastatic spread and prognosis in squamous cell carcinomas of the head and neck region. *Cancer Research* 63:1920-1926.
- Muller A, Homey B, Soto H, Ge N, Catron D, Buchanan ME, McClanahan T, Murphy E, Yuan W, Wagner SN, Barrera JL, Mohar A, Verastegui E, Zlotnik A (2001): Involvement of chemokine receptors in breast cancer metastasis. *Nature* 410:50-56.
- Pantel K, Brakenhoff RH (2004): Dissecting the metastatic cascade. *Nature Reviews Cancer* 4:448-456.
- Schardt JA, Meyer M, Hartmann CH, Schubert F, Schmidt-Kittler O, Fuhrmann C, Polzer B, Petronio M, Eils R, Klein CA (2005): Genomic analysis of single cytokeratin-positive cells from bone marrow reveals early mutational events in breast cancer. *Cancer Cell* 8:227-239.
- Schmidt-Kittler O, Ragg T, Daskalakis A, Granzow M, Ahr A, Blankenstein TJ, Kaufmann M, Diebold J, Arnholdt H, Muller P, Bischoff J, Harich D, Schlimok G, Riethmuller G, Eils R, Klein CA (2003): From latent disseminated cells to overt metastasis: genetic analysis of systemic breast cancer progression. *PNAS* 100:7737-7742.
- Schoppmann SF, Birner P, Stockl J, Kalt R, Ullrich R, Caucig C, Kriehuber E, Nagy K, Alitalo K, Kerjaschki D (2002): Tumor-associated macrophages express lymphatic endothelial growth factors and are related to peritumoral lymphangiogenesis. *American Journal of Pathology* 161:947-956.
- Shimizu K, Kubo H, Yamaguchi K, Kawashima K, Ueda Y, Matsuo K, Awane K, Shimahara Y, Takabayashi A, Yamaoka Y, Satoh S (2004): Suppression of VEGFR-3 signaling inhibits lymph node metastasis in gastric cancer. *Cancer Science* 95:328-333.
- Skobe M, Hamberg LM, Hawighorst T, Schirner M, Wolf GL, Alitalo K, Detmar M (2001): Concurrent induction of lymphangiogenesis, angiogenesis, and macrophage recruitment by vascular endothelial growth factor-C in melanoma. *American Journal of Pathology* 159:893-903.
- Sleman J (2000): The Lymph Node As a Bridgehead In the Metastatic Dissemination of Tumors. *Recent Results in Cancer Research* 157:55-81.
- Ward PM, Weiss L (1989): Metachronous seeding of lymph node metastases in rats bearing the MT-100-TC mammary carcinoma: the effect of elective lymph node dissection. *Breast Cancer Research and Treatment* 14:315-320.
- Wiley HE, Gonzalez EB, Maki W, Wu M, Hwang ST (2001): Expression of CC chemokine receptor-7 and regional lymph node metastasis of B16 murine melanoma. *Journal of the National Cancer Institute* 93:1638-1643.
- Wyckoff J, Wang W, Lin EY, Wang Y, Pixley F, Stanley ER, Graf T, Pollard JW, Segall J, Condeelis J (2004): A paracrine loop between tumor cells and macrophages is required for tumor cell migration in mammary tumors. *Cancer Research* 64:7022-7029.
- Wyckoff JB, Jones JG, Condeelis JS, Segall JE (2000): A critical step in metastasis: in vivo analysis of intravasation at the primary tumor. *Cancer Research* 60:2504-2511.

Yoshida T, Matsumoto T, Sasaki A, Shibata K, Aramaki M, Kitano S (2004): Outcome of paraaortic node-positive pancreatic head and bile duct adenocarcinoma. *The American Journal of Surgery* 187:736-740.

A



B

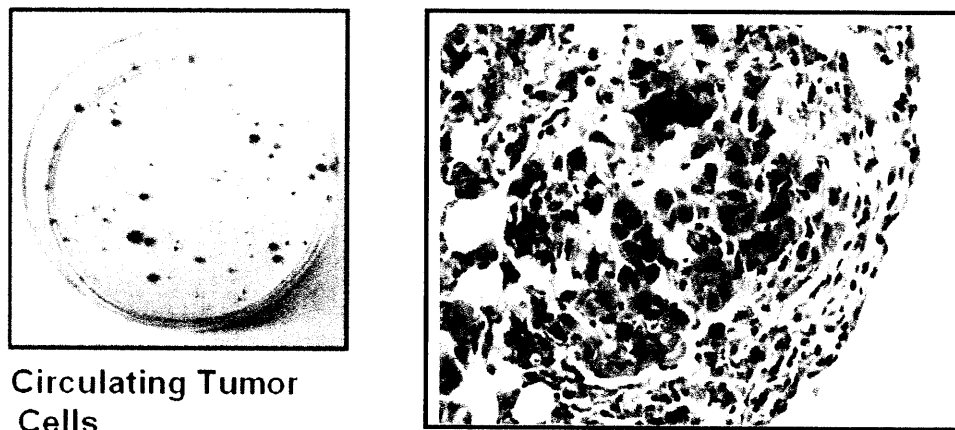


Figure 1. Hematogenous and lymphatic metastasis can be assayed and quantitated in a surgical orthotopic implantation mouse model of prostate cancer. (A) A schematic depicting the lymph nodes which primarily drain the urogenital system is shown (left). Para-aortic/lumbar and renal lymph nodes bearing macrometastatic tumor deposits are often seen after surgical orthotopic implantation (right). **(B)** A colony formation assay can be used to quantitate the number of viable circulating tumor cells in the blood (left), while micrometastases can be observed and counted in lung sections (right). (Reproduced from Chapter 2)

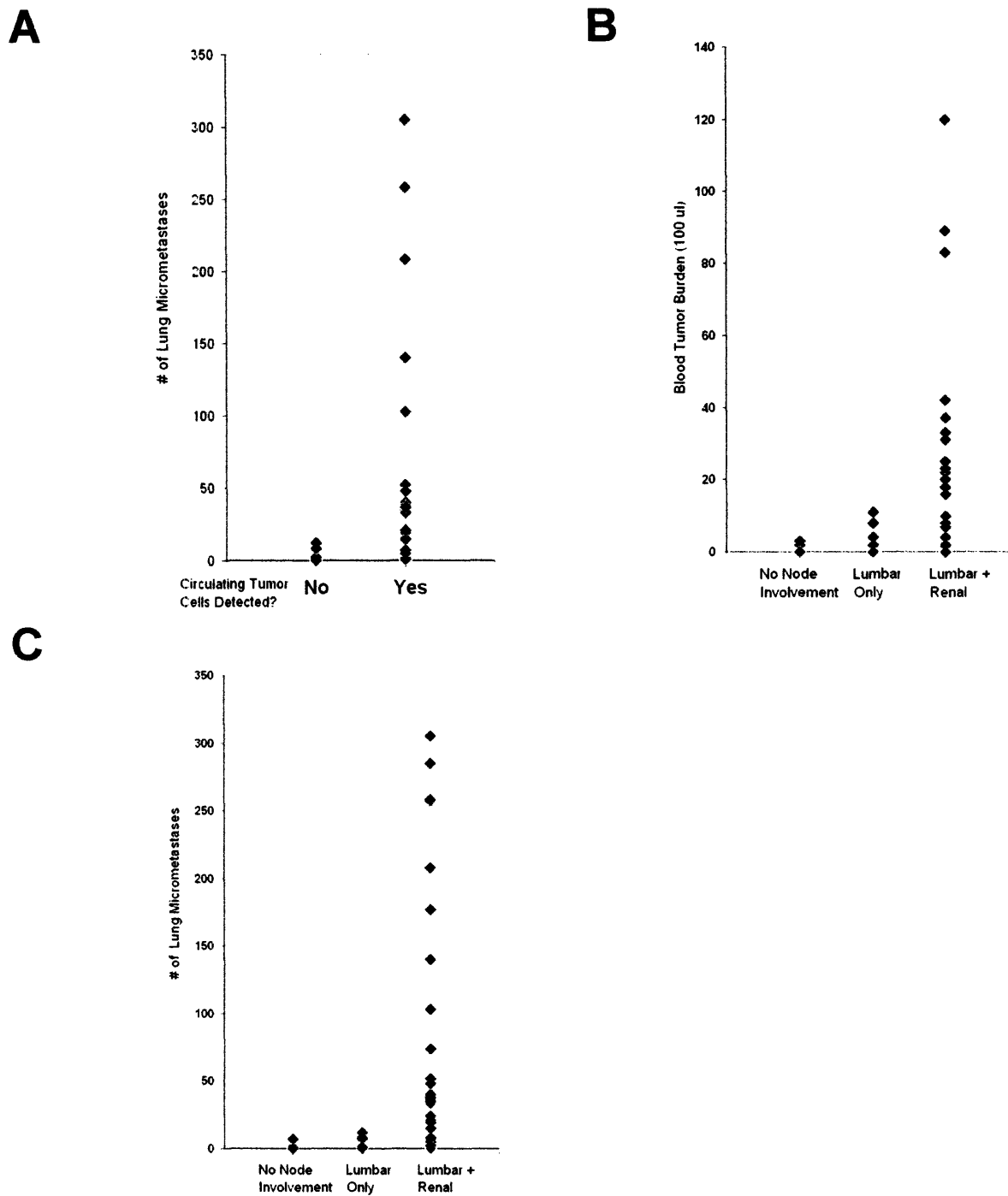


Figure 2. Associations between hematogenous and lymphatic metastasis after surgical orthotopic implantation. (A) The presence of lung metastases was correlated with the presence of circulating tumor cells in the blood. **(B)** Significant numbers of circulating tumor cells in the blood were detected only in mice that bore macrometastases in both the lumbar and renal lymph nodes. **(C)** Similarly, most lung metastases were seen in mice with both lymph node sites invaded.

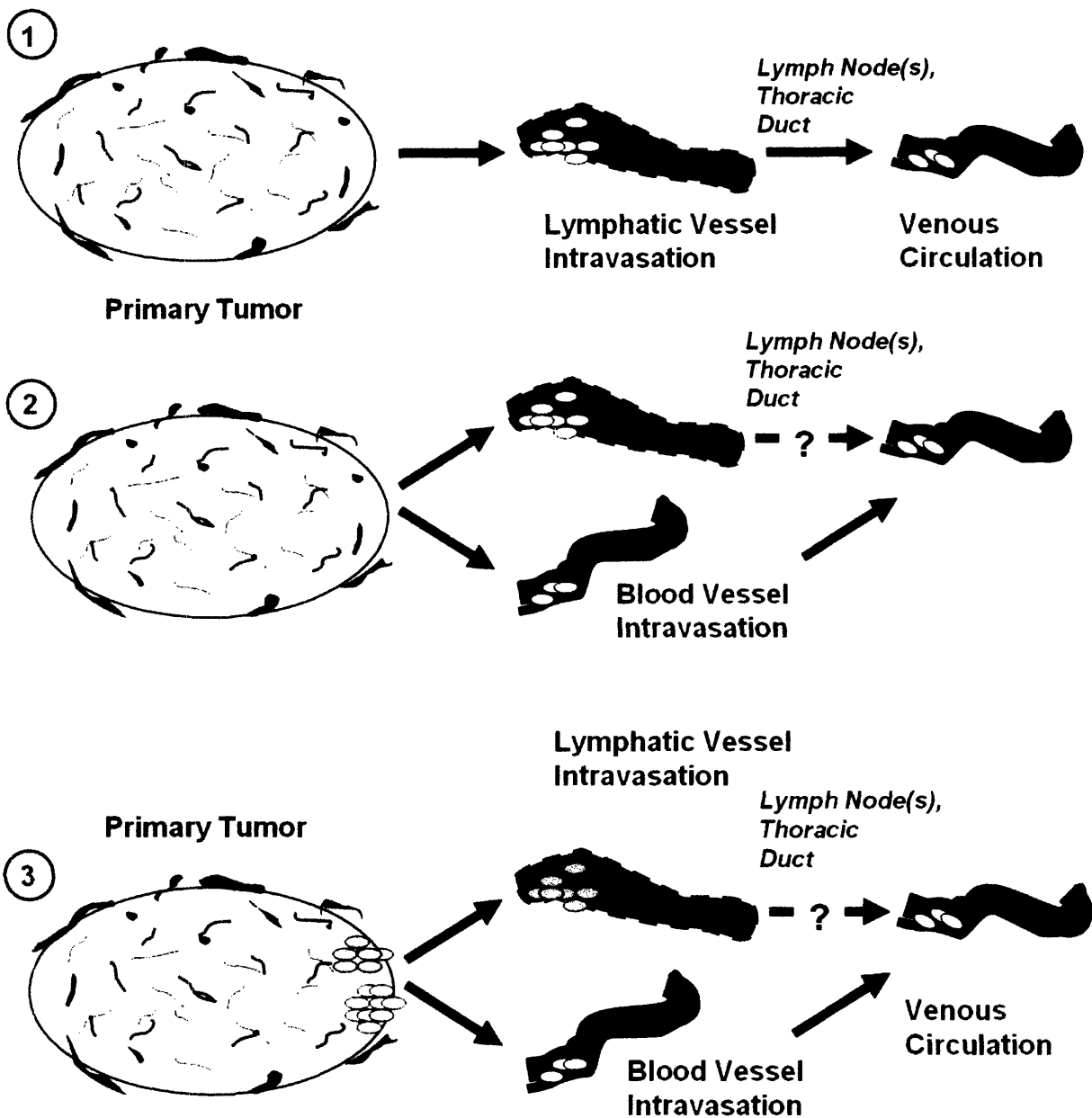


Figure 3. Three possible explanations to explain why, in a mouse model of prostate cancer, hematogenous spread is observed only in the presence of significant lymphatic spread. (1) The tumors might be incapable of intravasating directly into blood vessels, so metastatic cells enter venous circulation indirectly via lymphatics (“metachronous seeding”). Or, the tumor is completely non-metastatic until mobilized to metastasize via both lymphatic and hematogenous routes at the same time (2). Similar to (2), it is also possible that distinct subpopulations of tumor cells may be capable of only metastasizing via either lymphatic or blood vessel routes, but not both (3). In the last two scenarios, tumor cells which disseminate through the lymphatic system may or may not eventually reach blood circulation.

PC-3 Subcutaneous Tumors

Type	Label	Tumor Size (mg)	Age (d)	Blood
pMicro2-78	6-8D	188	19	0
pMicro2-78	6-8E	250	19	0
pMicro2-78	6-8F	85	19	0
pMicro2-78	6-14A	1150	25	0
pMicro2-78	6-25D	956	36	0
pMicro2-78	6-25E	250	36	0
pMicro2-82	6-8G	420	19	0
pMicro2-82	6-8H	150	19	0
pMicro2-82	6-8I	240	19	0
pMicro2-82	6-25A	250	36	0
pMicro2-82	6-25B	610	36	0
pMicro2-82	6-25C	466	36	0
pMicro-1	6-8A	250	19	0
pMicro-1	6-8B	500	19	0
pMicro-1	6-8C	140	19	0
pMicro-1	6-14B	1590	25	0
pMicro-1	6-25F	1330	36	0
pMicro-1	6-25G	600	36	0

A375 Subcutaneous Tumors

Type	Volume	Age	Blood Colonies
10-22A (vector)	2187 mm ³	49	0
10-22B (vector)	2618 mm ³	49	1
10-22C (vector)	557 mm ³	49	0
10-22D (C14)	2033 mm ³	49	0
10-22E (C14)	612 mm ³	49	0

Figure 4. Circulating tumor cells in the blood are not detected from subcutaneous tumors. Eighteen mice bearing subcutaneous tumors derived from the core PC-3 cell line derivatives were found, in all cases, not to possess any tumor cells circulating in the blood (top graph). This is also mostly true for mice bearing subcutaneous tumors derived from A375 melanoma cells (bottom graph).

CHAPTER 6.

LYMPHANGIOGENESIS IS UNNECESSARY FOR PROSTATE CANCER METASTASIS

The work in this chapter was conceived by Sunny Wong and Richard Hynes. LYVE-1 antibody was obtained from Erkki Ruoslahti. The Flt4-Ig expression plasmid was obtained from Kari Alitalo. The contents of this chapter were written by Sunny Wong, with editing by Richard Hynes.

INTRODUCTION

Lymphangiogenesis: Background

The study of how lymphatic vessels proliferate, a process known as lymphangiogenesis, is a relatively young field when compared to the study of angiogenesis, the roughly analogous process involving the growth of blood vessels. At least partly, this has been due to the absence of reliable markers for identifying lymphatics, a technical hurdle which has not been overcome until the past decade. But another explanation likely stems from the fact that the importance of angiogenesis is immediately obvious: blood vessels are essential for the development and maintenance of virtually every organ in the body¹, and studies by Folkman et al., have long focused attention on targeting angiogenesis as a means of inhibiting tumor progression[Kerbel and Folkman, 2002]. This is not to suggest that lymphangiogenesis is unimportant; the growth of lymphatic vessels is, in fact, necessary for many physiological processes, including trafficking of immune cells, re-absorption of macromolecules extravasated from blood vessels, and regulation of interstitial fluid pressure. But is lymphangiogenesis critical for cancer progression and metastasis?

Lymphatic vessels are found in almost every organ in the body, with the exception of the central nervous system, bone marrow and avascular tissues[Alitalo et al., 2005]. Unlike blood vessels, lymphatic capillaries begin as blind-ended tubes in connective tissues and consist of a single layer of overlapping endothelial cells which lack tight interendothelial junctions and pericytes, and, at most, are ensheathed by an incomplete basement membrane[Baldwin et al., 2002]. Individual lymphatic endothelial cells are anchored to interstitial collagen by reticular fibers (Figure 1A), and, under conditions of elevated tissue pressure, these reticular fibers stretch, drawing apart the attached cells and permitting the influx of fluid and macromolecules. Lymph fluid which is absorbed through lymphatic capillaries eventually collects into the larger lymphatic collecting vessels, which themselves later converge to form the even larger right and left (thoracic) lymph ducts (Figure 1A). Fluid flow is passive and occurs uni-directionally down pressure gradients acting against the exterior of the vessels, while back-flow is prevented by a system of semilunar valves². Along the way, lymphatic fluid is filtered through at least one lymph node, where a portion re-enters blood circulation through lymphatico-venous anastomoses; however, the majority of fluid reaches venous circulation via the thoracic duct[Sleeman, 2000].

In humans, lymphatic endothelial cells first appear in 6-7-week-old embryos, while in mice, these cells originate at embryonic day 10.5, after the formation of the cardiovascular system[Alitalo et al., 2005]. In both cases, it is now widely believed that lymphatic vessels arise from the budding of embryonic veins, an

¹ Cartilage, epidermis and the cornea are all avascular tissues, and appear to be exceptions to this rule.

² In large lymphatics, lymphatic fluid is actively pumped against a pressure gradient.

observation that was first noted in the early 1900s by the renowned anatomist Florence R. Sabin³. These buds sprout from veins located in the jugular, retroperitoneal and perimesonephric areas, and initially migrate to form primary lymph sacs, from which a primary lymphatic plexus eventually develops[Jussila and Alitalo, 2002].

Differentiation of endothelial cells along the lymphatic lineage requires the function of the transcription factor Prox1, a master regulator of the lymphatic phenotype[Petrova et al., 2002]. While mouse embryos deficient for this gene initiate rudimentary lymphatic buds, these fail to undergo proper lineage commitment[Wigle et al., 2002]. An important function of Prox1 is to upregulate expression of the major lymphatic receptor, VEGF receptor-3 (VEGFR-3 or Flt4)[Petrova et al., 2002; Wigle et al., 2002], although, early on, VEGFR-3 is expressed throughout the embryonic cardiovascular network and only later is its expression restricted to lymphatics[Baldwin et al., 2002]. Mouse knock-out studies have also identified a host of other factors that, when absent, lead to lymphatic developmental defects. Among these, Ephrin B2, Foxc2 and neuropilin-2 have all been implicated in lymphatic remodeling[Alitalo et al., 2005], while the transmembrane glycoprotein podoplanin has been found to be necessary for proper lymphatic development[Schacht et al., 2003]. In addition, the intracellular proteins Syk and SLP76 appear to regulate the divergence of blood and lymphatic vasculature, and mice deficient for either of these molecules exhibit abnormal communication between the two vessel types[Abtahian et al., 2003], a phenotype that resembles a human condition known as congenital arteriovenous malformation[Jain and Padera, 2003]. The hyaluronan receptor LYVE-1 has also been found to be an early marker of lymphatic commitment, but knock-out studies have shown that this receptor is unnecessary for proper lymphatic development[Gale et al., 2006]. Nonetheless, LYVE-1, along with several other proteins, including podoplanin and, to some extent, VEGFR-3, have all been useful as markers for identifying lymphatic vessels.

Perhaps the best characterized signaling pathway for lymphangiogenesis is mediated by VEGFR-3 binding to either vascular endothelial growth factor-C or -D (VEGF-C and -D) (Figure 1B). Although the normal physiological role of VEGF-D still remains relatively unclear, VEGF-C has been found to be critically important, beginning from the earliest stages of lymphatic development. Mice completely deficient for VEGF-C do not exhibit sprouting of lymphatic buds from the cardinal vein, while heterozygous mice develop lymphadema[Karkkainen et al., 2004]. This is a condition characterized by excessive fluid accumulation and swelling as a consequence of defective lymphatic function, and, in humans, hereditary lymphadema has been linked to missense mutations in VEGFR-3[Makinen et al., 2001]. The downstream components of this signaling pathway still remain to be characterized in detail, although it is known that signaling through VEGFR-3, a receptor tyrosine kinase, leads to activation of PKC and PI3K[Karkkainen et al., 2002], while inhibition of receptor signaling downregulates the activity of

³ Sabin also bears the distinction of being the first woman elected into the National Academy of Sciences, in 1925.

the MAP kinase pathway[Makinen et al., 2001]. Not surprisingly, given the central role of VEGFR-3 in lymphatic development, *in vitro* experiments have shown that the activity of this receptor can regulate the growth, survival, migration and morphology of lymphatic endothelial cells[Stacker et al., 2002].

Experimental Studies of Tumor Lymphangiogenesis

In some cases, xenografted tumors have been found to induce lymphangiogenesis, both within the tumor itself (intratumoral lymphatics) and/or at the periphery (peritumoral lymphatics). Indeed, overexpression studies using cancer mouse models have been instrumental in identifying and validating factors that can induce lymphangiogenesis and, oftentimes, enhance lymph node metastasis. The first demonstration of this involved tumor overexpression of VEGF-C and VEGF-D, both of which increased lymphatic metastasis[Skobe et al., 2001; Stacker et al., 2001]. As mentioned previously, the predominant receptor for these cytokines is VEGFR-3, although proteolytic processing of VEGF-C/D by plasmin or by proprotein convertases can allow efficient binding to VEGF receptor-2 (VEGFR-2 or Flk1), which is expressed on the surface of both blood vessels and lymphatics [McColl et al., 2003; Siegfried et al., 2003]. Subsequent studies have also identified additional lymphangiogenesis-promoting factors, including VEGF-A, FGF2, PDGF-B, HGF and others (reviewed in [Alitalo et al., 2005]). Because lymphatics and blood vessels share a common embryonic origin, it is not surprising that these factors have previously been found to possess angiogenic activity.

Transgenic Rip-Tag mice overexpressing VEGF-C in the pancreas have been reported to display *de novo* generation of lymphatics near β -cell islets and increased metastasis to the regional mesenteric lymph nodes[Mandriota et al., 2001]. Similarly, loss of the cell adhesion molecule N-CAM was associated with upregulated VEGF-C in pancreatic tumors, again yielding increased lymph node metastasis[Crnic et al., 2004]. The opposite result—reduced lymphangiogenesis—was commonly found when Flt4-mediated signaling was blocked. This has been accomplished by injecting antibodies against VEGF-D into tumor-bearing mice[Stacker et al., 2001], by adenoviral delivery of a truncated soluble receptor for Flt4[He et al., 2002], or by expressing in tumor cells RNAi against VEGF-C[Chen et al., 2005; Wong et al., 2005]. In many cases, lymphatic spread was also concomitantly inhibited.

Aside from increasing the abundance of lymphatic vessels in proximity to the tumor, activation of local lymphatic vessels has also been proposed as a way to enhance tumor cell intravasation and lymph node metastasis. He et al., recently noted that peritumoral lymphatics proximal to subcutaneous LNM35 lung tumors often displayed an “activated” phenotype—that is, increased vessel sprouting, dilation and permeability[He et al., 2005]. A similar observation was also made by Hoshida et al., who reported that tumor overexpression of VEGF-C induced hyperplasia of peritumoral lymphatics in the ear, accompanied by increased lymphatic flow rate and metastasis[Hoshida et al., 2006]. Others have speculated that

activated lymphatics might upregulate secretion of chemokines that could attract tumor cells[Alitalo et al., 2004]. This activated phenotype can apparently be reversed by adenoviral delivery of soluble Flt4[He et al., 2005], an effect that is reminiscent of tumor blood vessel normalization, which is seen upon interference with VEGF-A- or Flk1-mediated signaling[Tong et al., 2004].

In addition to affecting lymphatics in their immediate vicinity, tumors have been reported to pre-condition future sites of metastasis in the lymph node. As observed by Hirakawa et al., carcinogen-induced squamous cell carcinomas in transgenic mice overexpressing VEGF-A in the skin displayed increased angiogenesis and lymphangiogenesis, as well as enhanced lymphatic and systemic metastasis[Hirakawa et al., 2005]. Surprisingly, increased lymphangiogenesis was also seen within draining lymph nodes prior to, and after, metastatic colonization. This suggests that tumors might somehow prepare the lymph node for metastasis. Although the exact mechanism underlying this phenomenon remains unclear, lymph-node lymphangiogenesis could perhaps be mediated directly by binding of VEGF-A to Flk1 on the surface of lymphatic endothelial cells. Or, VEGF-A might increase the permeability of local blood vessels, and the consequent extravasation of fluid might serve as a lymphangiogenic signal. Interestingly, lymphangiogenesis within lymph node metastases was also proposed as a possible way for tumors to disseminate further throughout the lymphatic system and, subsequently, to systemic sites. At present, however, the exact implications and generalities of these novel findings remain to be seen.

Stromal Induction of Lymphangiogenesis

The stromal fibroblasts and immune cells that surround tumors can also exert direct effects on lymphatics by secreting growth factors, remodeling the ECM, and maybe even by incorporating into nascent lymphatic vessels. Stromal contributions to neovascularization are well-documented and perhaps best illustrated in transgenic mice made to express GFP under control of the human VEGF-A promoter[Fukumura et al., 1998]. When these mice were crossed with the PyMT spontaneous mammary tumor model, the fibroblasts surrounding the neoplasm, but not the tumor cells themselves, were GFP-positive, suggesting that the main source of VEGF-A was stromally derived. Although it is tempting to speculate that many principles applying to tumor angiogenesis also apply to lymphangiogenesis—and many have indeed been shown to be relevant for both processes—it is important to note that angiogenic tumors do not necessarily induce lymphangiogenesis. Furthermore, lymphangiogenesis has not often been seen in human clinical tumors, even in those that metastasize to lymph nodes. The reasons for this are presently unclear.

In addition to VEGF-A, fibroblasts have been known to secrete many potential lymphangiogenic factors, including VEGF-C, FGF, HGF, IGF and PDGF[Cunha et al., 2003]. *In vitro* stimulation of normal human skin fibroblasts with TGF- β and EGF induced secretion of both VEGF-C and VEGF-D [Trompezinski et

al., 2004]. Cancer-associated fibroblasts (CAFs) in breast cancer were also found to enhance angiogenesis and tumor growth by secreting the chemokine SDF-1/CXCL12 [Orimo et al., 2005]. This mobilized and recruited endothelial precursor cells which were derived from the bone marrow and expressed the receptor CXCR4. SDF-1 has also recently been found to be important for retaining pro-angiogenic bone marrow-derived circulating cells that associated near blood vessels [Grunewald et al., 2006]. Whether these phenomena occur in other tumors, and whether similar mechanisms are important for inducing lymphangiogenesis, is still highly controversial.

Since stromal fibroblasts secrete abundant matrix proteins, their influence on the composition and ordering of the ECM microenvironment likely serves as another signal for blood vessels and lymphatics. During angiogenesis, endothelial cell matrix receptors such as integrins are upregulated and serve several important capacities such as enhancing VEGF-mediated signaling through direct association with Flk1 [Soldi et al., 1999]. In the case of lymphatics, cell proliferation *in vitro* seems dependent on the matrix molecule fibronectin, which may be supplied *in vivo* by tumor cells, fibroblasts and/or endothelial cells [Zhang et al., 2005]. Lymphatic endothelial cell binding to fibronectin leads to direct association between the integrin $\beta 1$ subunit and Flt4, which may enhance VEGF-C/D signaling pathways [Wang et al., 2001]. The integrin heterodimer $\alpha 9\beta 1$ has also been implicated in the development of lymphatics and may act to bind ECM components like fibronectin and/or, as recently reported, VEGF-C and -D [Mlahakis et al., 2005]. Lastly, fibroblast-mediated contraction of the ECM, particularly of collagen networks, is increased when those cells are activated, and likely contributes to high tumor interstitial fluid pressure (IFP) [Heldin et al., 2004]. While high IFP is thought to signal the growth of new lymphatics, tumor cells may also cause the collapse of intratumoral lymphatic vessels [Padera et al., 2002].

Importantly, the role of immune cells in mediating angiogenesis and lymphangiogenesis has recently received great attention, leading to some valuable insights. Once recruited to tumors, leukocytes release an abundant cache of cytokines and MMPs that can directly affect lymphatics. In support of this idea, the degree of inflammation in two studies of human cervical cancer positively correlated with both lymphatic vessel density and the number of VEGF-C-expressing peritumoral cells [Schoppmann et al., 2002; Schoppmann et al., 2001]. Many of these cells were CD68+ macrophages that also expressed VEGF-C/VEGF-D and Flt4. Increased inflammatory response, however, was negatively correlated with lymph node metastasis [Schoppmann et al., 2001]. These findings illustrate the complexities that shape the metastatic tendencies of a tumor—how, for instance, the stromal inflammatory reaction might wield a double-edged sword, acting both as a way to promote lymphangiogenesis and as an anti-tumor response.

But what exactly is the mechanism for inflammation-induced lymphangiogenesis? Novel findings have been obtained from experiments utilizing traditional xenograft models, as well as *de novo* lymphangiogenesis models involving either the murine cornea or Matrigel plugs implanted into mice.

Many of these studies have confirmed the important role of macrophages, which have been found to secrete many potential lymphatic growth factors, including VEGF-C, VEGF-D, VEGF-A and FGF[Cursiefen et al., 2004; Jin et al., 2006]. Expression of these factors seems to be induced in these cells by chemotactic factors such as M-CSF[Eubanks et al., 2003] and possibly by an autocrine loop in a subpopulation that expresses Flt4[Eubanks et al., 2003; Schoppmann et al., 2002]. In addition, macrophage secretion of proteinases such as MMP-9 could remodel the ECM, thereby releasing additional cytokines while providing a hospitable environment for lymphatic proliferation[Carmeliet and Collen, 1998].

In the cornea, which is normally avascular, inflammation can induce local formation of blood and lymphatic vessels. Interestingly, CD11b+/LYVE-1+ macrophages have been reported to integrate into inflammation-induced lymphatics *in vivo* and could also form lymphatic-like tubes when cultured *in vitro*[Maruyama et al., 2005]. These findings were recently supported by studies in human renal transplants that had exhibited immune rejection, chronic inflammation and lymphatic proliferation[Kerjaschki et al., 2006]. Circulating lymphatic progenitors derived either from a minor CD133⁺VEGFR-3⁺CD34⁺ subpopulation or from a major CD14⁺VEGFR-3⁺CD31⁺VEGFR-2⁻ monocyte population incorporated into lymphatics. However, this was contrasted by findings in the same study where circulating progenitor cells did not incorporate into lymphatics associated with two cases of human carcinomas, an observation that had been similarly noted in tumor xenograft models utilizing B16 melanoma or Lewis lung carcinoma cells[He et al., 2004b]. Therefore, at present, these data seem to suggest that proliferation of pre-existing lymphatics accounts for tumor lymphangiogenesis, though increased inflammation might coax macrophages to transdifferentiate into lymphatics. Obviously, the generality of these recent findings, while exciting, remains to be further validated in different systems.

Other as-yet-unknown factors affecting lymphatic growth will almost certainly be elucidated in future studies. For instance, CXC-ERL+ chemokines can induce angiogenesis by binding the receptors CXCR2/CXCR1 on blood endothelial cells—do chemokines have any direct or indirect effects on lymphatics, which express SDF-1 and specifically express the atypical, and perhaps non-signaling, chemokine receptor D6[Nibbs et al., 2001]? It is also known that blood vessels are molecularly heterogeneous, exhibiting tissue- and tumor-specific patterns of gene expression[Croix et al., 2000]. Most notably, sprouting angiogenic vessels upregulate the integrins $\alpha\text{v}\beta\text{3}$ and $\alpha\text{v}\beta\text{5}$, thereby possibly implicating specific matrix molecules such as vitronectin in angiogenesis[Carmeliet and Collen, 1998]. Since peritumoral lymphatics often appear physiologically distinct from normal lymphatics, these nascent lymphatics will almost certainly possess an altered gene expression program, and consequently, a unique reliance on different growth factors and matrix molecules.

Lymphatic Function in Prostate Cancer and Other Tumors: Clinical and Experimental Studies

As discussed earlier, human clinical tumors arising from various cell types often metastasize to lymph nodes, and prostate cancer (CaP) is no exception. Indeed, analysis of metastasis patterns for CaP[Bubendorf et al., 2000; Flocks et al., 1959], as well as lymphatic mapping studies using tracking dyes in breast cancer and melanoma[Giuliano et al., 1994; Morton et al., 1992], have shown that the pattern of tumor-to-lymph-node dissemination is non-random. Tumors first invade draining (sentinel) lymph nodes before seeding more distant nodes[Nathanson, 2003]. If the sentinel node is free of metastasis, other lymph nodes will also likely be uninvaded[Wittekind, 2000]. Therefore, lymphatic vessels within or in proximity to tumors mediate dissemination to draining lymph nodes, which may then allow further seeding to more distant sites.

In the case of CaP, metastasis to regional nodes is correlated with poor clinical prognosis and often guides the therapeutic course of action[Flocks et al., 1959; Smith et al., 1982]. Typically, pelvic lymphadenectomy is performed prior to radical prostatectomy to assess lymph node status. In patients with lymph-node-positive CaP, 75% will possess bone metastases within 5 years regardless of treatment[Smith et al., 1982]. Although lymphatic vessels can be detected in CaP[Trojan et al., 2004; Tsurusaki et al., 1999; Zeng et al., 2004], the role of intratumoral lymphatics in mediating lymph node metastasis has been controversial. While numerous clinical studies have correlated lymphatic vessel density (LVD) with lymph node metastasis in various cancers, nearly as many have failed to detect such associations (for a summary of clinical data, see[Jain and Padera, 2002]). In CaP, increased LVD has been correlated both with lymph node metastasis[Tsurusaki et al., 1999; Zeng et al., 2004] and with higher Gleason Score[Trojan et al., 2004; Zeng et al., 2004], an indicator of more aggressive tumors. Consequently, it is unclear whether tumoral lymphatics actually facilitate lymph node metastasis, or are simply markers of tumors prone to disseminate regardless of LVD.

Importantly, experimental studies have shown that intratumoral lymphatics are often compressed, physiologically abnormal and non-functional for fluid drainage[Padera et al., 2002; Padera et al., 2004]. This apparent absence of functional intratumoral lymphatics would imply that tumor cells intravasated into these vessels would encounter blockages and dead ends that actually impede metastasis. The fact that many tumors metastasize to local lymph nodes despite absence of lymphangiogenesis or functional intratumoral lymphatics, has led some to propose that it is the peripheral, peritumoral lymphatics at the invasive margins that are the predominant routes of egress from the primary tumor[Jain and Fenton, 2002; Pepper and Skobe, 2003; Sleeman, 2000]. This view is supported by clinical data showing that the abundance of peritumoral, but not intratumoral, lymphatics correlated with metastasis in breast and prostate cancer; and that lymphangiogenesis does not occur in many tumors that nevertheless metastasize to lymph nodes, including those of the breast, prostate and pancreas [Sipos et al., 2005;

Trojan et al., 2004; Vleugel et al., 2004; Wong and Hynes, 2006]. In contrast, several clinical studies have correlated intratumoral lymphatic vessel density (LVD) with metastasis (reviewed by [Achen et al., 2005; Stacker et al., 2002]). Consequently, the importance of tumor lymphangiogenesis in regard to metastasis is debatable, and may depend on the organ and/or experimental model in question.

Experimental Goals and Approach

Our interest in tumor lymphangiogenesis, as described in the previous chapter, grew out of our observation that hematogenous metastasis was associated with lymphatic spread in our orthotopic mouse model of prostate cancer. We were therefore interested to determine whether these two events were inter-dependent. We decided to test this possibility by attempting to inhibit lymphatic metastasis and then determining the consequent effects on systemic spread. If bloodborne dissemination was also found to be inhibited, that would suggest that a tumor's ability to develop lymphatic metastases was epistatic to its ability to form systemic metastases. As will become evident in the next section, we were unable to properly test our hypotheses in this system because we were, ultimately, unsuccessful at inhibiting lymph node metastasis. However, based on our results, we were able to gain some insights into the mechanisms by which tumors metastasize to draining lymph nodes. Perhaps most importantly, we were able to distinguish whether intratumoral and/or peritumoral lymphatics were important for metastatic dissemination of prostate cancer. I will discuss these and other results, as well as their implications, in the next two sections.

RESULTS

Stable siRNAs Specifically Reduce VEGF-C or VEGF-A Expression and Protein Secretion.

Our original goal was to inhibit lymphatic metastasis by disrupting tumor lymphangiogenesis in our surgical orthotopic implantation (SOI) mouse model of prostate cancer. As SOI is a two-step approach that involves grafting of solid subcutaneous tumor fragments into the mouse prostate, we were able to assess the efficacy of various lymphatic-inhibitory approaches on both subcutaneous and orthotopic tumors. We began by confirming that subcutaneous tumors formed by a highly metastatic subline of PC-3 prostate cancer cells (designated PC3-#82) possessed abundant intratumoral lymphatic vessels. Lymphatic vessels were identified by immunohistochemical staining for the lymphatic markers LYVE-1 and VEGFR-3/Flt4, and by absence of staining for the blood vessel marker CD34 (Figure 2). Because blood vessels in some tumors have been reported to express VEGFR-3/Flt4 [Valtola et al., 1999], we used LYVE-1 to identify lymphatics and CD34 to identify blood vessels for the rest of our studies.

We next determined that PC3-#82 cells expressed and secreted the lymphangiogenesis-promoting factors VEGF-C and VEGF-A (Figure 3A-B), but not VEGF-D (data not shown). To examine the importance of tumor-secreted VEGF-C in promoting lymphangiogenesis, we stably expressed siRNAs against VEGF-C in PC3-#82 cells. We also generated siRNAs against VEGF-A, which has previously been reported to stimulate lymphatic growth [Cao et al., 2004; Nagy et al., 2002]. C13 and C14 siRNAs knocked down VEGF-C mRNA 81% and 88%, respectively, relative to vector control (Figure 3A). A2 and A3 siRNAs reduced VEGF-A mRNA 67% and 74%, respectively (Figure 3A). Quantitative PCR showed that VEGF-C siRNAs had little effect on VEGF-A expression, and vice-versa. C14-MM and A3-MM mismatch (MM) controls exhibited little siRNA efficacy. Relative RNA message levels for VEGF-C/A were reflected in their relative protein abundance in conditioned media, as assayed by ELISA (Figure 3B). Cells expressing C14 siRNA accumulated virtually no VEGF-C in conditioned medium after 72 hours, while cells expressing C13 showed modest accumulation (Figure 3C). VEGF-A protein secretion was not significantly reduced by either C13 or C14 siRNAs, but was slightly increased in cells expressing the C14-MM control (Figure 3B).

As an additional approach for ablating lymphatics, we expressed the soluble VEGFR-3/Flt4-human Fc-Ig fusion protein (Flt4-Ig) in PC3-#82 cells, as described previously [He et al., 2002; Karpanen et al., 2001]. This secreted chimeric protein should act as a competitive inhibitor for endogenous VEGFR-3 expressed on the surface of lymphatic endothelial cells, and is expected to bind both VEGF-C and VEGF-D. Indeed, secretion of Flt4-Ig was confirmed by immunoprecipitating the Fc region of this protein from the conditioned media of PC3-#82-Flt4-Ig cells, followed by Western blot against VEGFR-3 (Figure 3D).

Tumor-Secreted VEGF-C Is Necessary for Lymphangiogenesis

PC3-#82 cells expressing siRNAs against VEGF-C or VEGF-A, or control siRNAs were injected subcutaneously into CD-1 immunodeficient mice. We did not see consistent tumor growth effects correlated with VEGF-C or VEGF-A inhibition (data not shown). Tumors were removed approximately 3.5 weeks post-injection, sectioned and stained for LYVE-1 and CD34. PC3-#82 cells expressing C14 siRNA showed a >99% reduction in lymphatic vessel density (LVD) (Figure 4A-c and 4B) relative to controls (Figure 4A-a-b and 4B). Tumors expressing C13, a less effective siRNA against VEGF-C, yielded an 83% reduction in LVD relative to controls (Figure 4B). Interestingly, both siRNAs against VEGF-A (A2, A3) yielded nearly a 50% reduction in LVD versus controls (Figure 4A-d and 4B; combined p value = 0.052). As both VEGF-A siRNAs were only partially effective in reducing VEGF-A gene expression, it is possible that more potent VEGF-A siRNAs would have yielded a greater reduction in lymphatics. LVD quantitation of siRNA- or siRNA control-expressing tumors is shown in Figure 4B. In agreement with results by others [He et al., 2002; Krishnan et al., 2003], expression of soluble Flt4-Ig (Figure 4A-f) yielded complete inhibition of lymphangiogenesis versus Ig-Neg control (Figure 4A-e and 4B). In all

cases, blood vessel density was not consistently affected (Figure 4B, images not shown), though C14-MM control tumors had somewhat increased angiogenesis. Also, staining appeared slightly lighter in some tumors expressing siRNA. Taken together, these results indicate that tumor-secreted VEGF-C is necessary for intratumoral lymphangiogenesis. To a lesser extent, tumor-secreted VEGF-A may also be important. The lack of reduction in blood vessels, especially by A2 and A3, may reflect the limited mRNA knock-down, and/or suggest that other angiogenic factors are sufficient for inducing tumor angiogenesis.

Ablation of Prostate Intratumoral Lymphatics Does Not Inhibit Lymph Node Metastasis

PC-3 cells have been reported to metastasize infrequently from subcutaneous tumors [Glinskii et al., 2003]. In contrast, prostate tumor cells introduced orthotopically metastasize in patterns similar to human CaP, including invasion of lymph nodes, lung and bone [An et al., 1998; Chang et al., 1999]. To model the early stages of metastasis, where malignant cells must detach from the primary tumor before intravasating into vasculature, we used surgical orthotopic implantation to graft a single piece of solid tumor into the dorsolateral prostate lobes of CD-1 mice⁴. As expected, the tumors introduced by SOI developed initially from a single focus in the interluminal spaces of the prostate (Figure 8A-a). Between 2-3 months after implant, ~50% of mice developed lymph node macrometastases, and the orthotopic primary tumors possessed abundant blood and lymphatic vessels (data not shown; similar to Figure 2).

To determine the metastatic effects of ablating lymphatic vessels in orthotopic prostate tumors, we used SOI to transplant PC3-#82 tumors expressing either VEGF-C siRNA (C14), Flt4-Ig, or controls. LVD was reduced ~50% in both C14- and Flt4-Ig-expressing tumors (Figure 4C). Although statistically significant ($p = 0.012$ for C14 vs. control; $p = 0.0046$ for Flt4-Ig vs. control), this reduction was far less severe than was seen in subcutaneous tumors. Expression of either C14 siRNA or Flt4-Ig in orthotopic tumors did not affect the incidence of macroscopic lymph node metastasis (Figure 4D), the average mass of macroscopically invaded lymph nodes (Figure 4D, $p = 0.92$), or the average size of the primary tumors (data not shown). For lymph nodes without obvious macrometastases, histological analysis identified micrometastases in virtually all samples analyzed, regardless of cell line (Figure 6E).

To understand why inhibition of lymphangiogenesis was less effective in orthotopic versus subcutaneous tumors, we measured by ELISA human VEGF-C protein levels in subcutaneous and orthotopic tumors expressing C14 or siRNA control. The concentration of human VEGF-C protein in C14 orthotopic tumors was increased relative to C14 subcutaneous tumors and was positively correlated with LVD in both C14 and control tumors (Figure 5A-B). Reduced siRNA-mediated inhibition of VEGF-C secretion over the duration of the experiment possibly accounted for less severe inhibition of tumor lymphangiogenesis. In

⁴ Please refer to Chapter 2, "Xenograft Transplantation Models of Prostate Cancer," for more details on SOI.

the case of Flt4-Ig-expressing tumors, Western blot for VEGFR3/Flt4 indicated that, in some orthotopic tumors, expression of the fusion protein was also severely reduced (Figure 5C).

To further ablate orthotopic intratumoral lymphatics, we generated a derivative of PC3-#82 cells that combined expression of VEGF-C siRNA and Flt4-Ig (Flt-C14), in addition to a cell line expressing both empty-vector controls (Ig-pSIRISP). Specific knock-down of VEGF-C mRNA and secretion of Flt4-Ig, this time from within the same cell line, were confirmed (Figure 6A). As expected, Flt-C14 subcutaneous tumors possessed no lymphatic vessels, whereas Ig-pSIRISP control tumors had abundant LYVE-1 staining (Figure 6B). When implanted orthotopically, Flt-C14 tumors (n = 11) exhibited a 92% reduction in LVD versus controls (n = 8, p <0.001) (Figure 6C). A single Flt-C14 tumor possessed moderate LVD, and without this outlier, inhibition of LVD increases to 98% versus control. Interestingly, blood vessel density was also reduced ~35% in Flt-C14 tumors versus Ig-pSIRISP control (Figure 6C).

Despite >92% reduction in intratumoral lymphatics, the incidence of microscopic and macroscopic lymph node invasion, and the mass of macroscopically invaded lymph nodes were again largely unaffected in Flt-C14 tumors versus Ig-pSIRISP control (Figure 6D, p = 0.15), or versus other controls used in this study (Figures 4C and 6D, p = 0.80 for Flt-C14 versus pSIRISP). As before, nearly all local lymph nodes evaluated harbored micro- or macrometastatic tumor invasion (Figure 6E). Also, we found no significant correlation between LVD and lymph node metastasis in individual orthotopic tumors whose lymphatics were ablated (Figure 7). Our data argue that intratumoral lymphangiogenesis is unnecessary for prostate cancer metastasis to lymph nodes.

Abundance of Pre-Existing Marginal Lymphatics Is Unaffected in Flt-C14 Orthotopic Tumors

At least two possible explanations could account for how orthotopic prostate tumors metastasized efficiently to lymph nodes despite >98% inhibition of intratumoral lymphangiogenesis in 10/11 Flt-C14 tumors. Formally, it is possible that a minority of lymphatic vessels (<2% of total) is sufficient for metastasis. A likelier explanation is that marginal lymphatic vessels at the tumor-stromal margin—and not intratumoral lymphatics—are responsible for mediating lymph node metastasis.

Because orthotopic tumors were analyzed 2-3 months after implantation, the tumors tended to be large (~1 gram) and almost completely devoid of stromal tissue. To examine tumor interaction with pre-existing marginal lymphatics, we transplanted Flt-C14 or control tumors by SOI and analyzed them 2-3 weeks after implantation. In most cases, tumors were not palpable and were found by sectioning through the dorsolateral prostate (Figure 8A-a). As expected, primary tumors consistently arose from a single focus.

We stained microscopic Flt-C14 or control orthotopic tumors with LYVE-1 and found that both were in contact with lymphatics located at the tumor-stromal margin (Figure 8A, *b-d*, and data not shown for control tumors). In Flt-C14 tumors, all stages of lymphatic invasion were observed, including tumor growth up against individual lymphatic vessels without compression (Figure 8A-*b*); intravasation of tumor cells into lymphatics (Figure 8A-*c*); and crushing of vessels (Figure 8A-*d*). Typically, these marginal lymphatics delineated the exact region of contact between the expanding tumor periphery and the surrounding prostatic stroma. Quantitation of marginal lymphatics revealed little difference between Flt-C14 and control orthotopic tumors (Figure 8B, $p = 0.55$). However, intratumoral lymphatics were present in control tumors but completely absent in Flt-C14 tumors (Figure 8B). These results indicate that a combination of VEGF-C siRNA and Flt4-Ig fusion protein selectively inhibited intratumoral lymphangiogenesis without affecting marginal, possibly pre-existing, lymphatics and suggest that these vessels at the periphery are sufficient for mediating lymph node metastasis.

Spontaneous TRAMP Tumors Do Not Induce Lymphangiogenesis

To extend our observations, we examined the lymphatics in spontaneous TRAMP (Transgenic Adenocarcinoma of the Mouse Prostate) tumors. As described previously, TRAMP transgenic mice express the SV40 large T antigen driven by the prostate-specific rat probasin promoter [Greenberg et al., 1995], and prostate sections are graded on a scale of 1-6, based on parameters including cell differentiation and invasion through basement membrane [Gingrich et al., 1999; Hurwitz et al., 2001]⁵. Importantly, by 28 weeks, 100% of TRAMP mice have been reported to harbor lymph node and/or lung metastases [Gingrich et al., 1996]. Local and distal dissemination is predominantly observed only in mice bearing primary tumors of grade 4 or higher [Hurwitz et al., 2001].

We examined the prostatic lymphatics in eight normal C57BL/6 mice, and fourteen TRAMP mice at different ages and/or tumor stages. The lymphatics in normal prostates were located in the interluminal spaces outside individual ductal structures (Figure 9A), and their abundance and location did not differ in mice between 15-35 weeks of age (data not shown). In TRAMP prostates, PIN develops from the initial expansion of luminal cells within ductal structures. As with wild type, lymphatics in TRAMP prostates were consistently located outside of ductal structures and did not infiltrate into tumorigenic areas (Figure 9A). Tumorigenic prostates graded from 1-4 did not exhibit significant differences in LVD versus normal prostates (Figure 9B). In the most severe cases of prostate cancer (grades 5 and 6), the tumorigenic regions had overtaken the surrounding stroma, and lymphatic density in the prostate was reduced seven-fold versus either areas of normal prostate or low grade PIN (Fig. 9A-B, $p < 0.001$). Since, as mentioned previously, metastasis to lymph nodes is predominantly seen only in high grade TRAMP tumors [Hurwitz

⁵ Please refer to Chapter 2, "The TRAMP Prostate Cancer Model," for more general information on TRAMP; please refer to Chapter 3 results, "Protein 4.1B suppresses tumor progression in a spontaneous model of prostate cancer," for information about grading TRAMP prostate sections.

et al., 2001], it is likely that these spontaneous tumors also utilized pre-existing lymphatics located at the tumor-stromal border prior to vessel compression and destruction. These results support our findings in the xenograft SOI model that intratumoral lymphangiogenesis is not required for lymph node metastasis.

Expression of VEGF-C and VEGF-A Are Not Sufficient for Induction of Tumor Lymphangiogenesis

In the course of our studies, we also tested whether A375 melanoma cells expressed lymphangiogenic growth factors and induced lymphangiogenesis as subcutaneous tumors. As assessed by ELISA, we could detect VEGF-C secretion by these cells, though at lower levels than PC-3 cells (Figure 10A); however, we could not detect any VEGF-A from medium conditioned by these cells (Figure 10A). In addition, we found that highly metastatic variant A375 cell lines also did not express VEGF-A (data not shown), and, out of eleven subcutaneous tumors derived from A375 cells, none of these possessed intratumoral lymphatic vessels (Figure 10B). As human VEGF-A isoform 165 has been shown to induce angiogenesis and lymphangiogenesis[Cao et al., 2004; Nagy et al., 2002], we tested whether overexpression of this VEGF splice variant could induce lymphatic growth in A375 tumors. Although we succeeded in generating cells that stably overexpressed VEGF-A and secreted the protein into conditioned medium (Figure 10A), these cells, again, did not induce lymphangiogenesis when injected as subcutaneous tumors (data not shown). However, our negative results were complicated by the observation that VEGF-A-overexpressing A375 cells exhibited downregulated secretion of VEGF-C (Figure 10A), for unknown reasons, relative to control cells. Interestingly, we did detect LYVE-1 staining within individual lung metastases following intravenous injection of A375 cells (Figure 10C). Although some of the vessels stained may have been lymphatics, in many cases, these were often also stained with CD34 and possessed red blood cells in their lumens. Therefore, it would seem as if LYVE-1 staining is non-specific in the lung. As one final note, we detected intratumoral lymphatics in subcutaneous tumors derived from Lewis lung carcinoma cells but not from B16 melanoma cells, and, in a preliminary study, average LVD in these tumors was unchanged, regardless of whether the cells had been injected into wild-type mice or mice deficient for all three selectins transmembrane receptors (E-, L- and P-selectins)(data not shown).

DISCUSSION

Lymph node status has traditionally been used as a prognostic indicator of prostate cancer aggressiveness, dissemination to distant sites and likelihood of recurrence after therapy[Bubendorf et al., 2000; Flocks et al., 1959; Smith et al., 1982; Zincke et al., 1982]. Although recent clinical studies have examined the abundance of lymphatics and/or lymphatic growth factors in CaP, the results have been difficult to interpret. In most cases, VEGFR-3/Flt4 was upregulated in advanced or node-positive CaP[Kaushal et al., 2005; Li et al., 2004; Tsurusaki et al., 1999; Zeng et al., 2004]. One study found

augmented tyrosine phosphorylation of VEGFR-3/Flt4 in advanced versus early stage (node-negative) CaP [Kaushal et al., 2005], while another found upregulation of a truncated form of VEGFR3/Flt-4, but not full-length receptor [Stearns et al., 2004]. Furthermore, VEGF-C was upregulated in some cases of metastatic CaP [Tsurusaki et al., 1999; Zeng et al., 2004] but not others [Kaushal et al., 2005; Stearns et al., 2004]. VEGF-D was also increased in node-positive versus node-negative CaP in some studies [Kaushal et al., 2005; Stearns et al., 2004] but unchanged in another [Zeng et al., 2004].

Part of the complexity in analyzing these data arises from the difficulty of distinguishing whether VEGFR-3/Flt4 was upregulated in tumor-associated lymphatics or in the tumor cells themselves [Kaushal et al., 2005; Li et al., 2004; Stearns et al., 2004]. Indeed, *in vitro* studies have shown that CaP cell lines can express the related receptors VEGFR-1/Flt1 [Chevalier et al., 2002; Ferrer et al., 1999] and VEGFR-2/Flk1 [Chevalier et al., 2002; De et al., 2003; Ferrer et al., 1999]. Furthermore, staining for VEGFR-3/Flt4 in one study of CaP exclusively highlighted tumor and epithelial cells, but not endothelial vessels [Kaushal et al., 2005].

In studies where VEGFR-3/Flt4 staining identified lymphatics associated with CaP, the localization of these vessels was either reported to be peritumoral [Tsurusaki et al., 1999], or both peri- and intratumoral [Zeng et al., 2004]. However, VEGFR-3/Flt4 has also been found to be expressed in some tumor blood vessels [Valtola et al., 1999]. One clinical study of prostate cancer reported lymphatics primarily in the tumor periphery and in non-tumorigenic stromal regions [Trojan et al., 2004]. Because lymphatics were significantly reduced in tumors, the authors speculated that CaP progression causes lymphatic destruction. LYVE-1-positive vessels were also correlated with increased Gleason score [Trojan et al., 2004], but a detailed study comparing node-positive- with node-negative-CaP using LYVE-1 has not been performed.

Upregulated VEGFR-3/Flt4, VEGF-C and VEGF-D have also been correlated with other parameters of CaP progression, including Gleason score [Li et al., 2004; Tsurusaki et al., 1999; Zeng et al., 2004] and PSA level [Li et al., 2004; Tsurusaki et al., 1999]. Consequently, it is difficult to distinguish whether increased lymphatics actually facilitate nodal metastasis or are simply markers of more aggressive primary tumors. Similarly, in experimental mouse models, whether lymphangiogenesis is required for lymph node metastasis may depend on the innate aggressiveness of the tumor in question. It is possible, that for tumors already adept at colonizing distant sites, pre-existing lymphatics may be sufficient for lymph node metastasis, whereas less aggressive cancers may require additional vessels to disperse more cells and increase the probability of metastasis. This may explain why overexpression of insulin-like growth factor receptor I in pancreatic islet tumors by Hanahan's group yielded aggressive tumors that metastasized to lymph nodes without significant lymphangiogenesis (as reported by Alitalo, et al. [Alitalo et al., 2004]).

Functional studies using assays for microlymphangiography and interstitial fluid pressure have suggested that intratumoral lymphatics may be nonfunctional [Leu et al., 2000; Padera et al., 2002]. Tumor compression of intratumoral lymphatic vessels may be responsible for absence of function, though tumor-induced lymphatics may inherently be physiologically abnormal [Isaka et al., 2004; Padera et al., 2004]. Although this apparent absence of function has been interpreted to suggest that intratumoral lymphatics are unimportant for metastasis, that hypothesis needs further testing.

In contrast with our results, work by others has shown that inhibiting tumor lymphatics with soluble VEGFR-3/Flt4-Ig fusion protein can reduce metastasis to lymph nodes both in xenograft models [He et al., 2002; He et al., 2005; Krishnan et al., 2003; Lin et al., 2005; Papoutsis et al., 2000], and in Rip-Tag spontaneous tumors [Crnic et al., 2004]. In most studies, both peritumoral and intratumoral lymphatics were inhibited, though some have suggested that Flt4-Ig may have no effect on pre-existing lymphatics [He et al., 2004a; He et al., 2005; Lin et al., 2005; Papoutsis et al., 2000], or may inhibit peripheral, but not intratumoral, lymphatics [Crnic et al., 2004]. The varying effectiveness of Flt4-Ig may reflect how and when the inhibitor was administered; its concentration; diffusion to surrounding tissues; abundance of pre-existing lymphatics; and local concentration of VEGF-C/D ligands. Given that the tumors in our SOI model arose from a single solid focus (Figure 8A-a), it is possible that diffusion of Flt4-Ig was reduced, when compared to models where tumor cells were injected in suspension. Indeed, several papers have reported that high-level, systemic expression of Flt4-Ig fusion protein can suppress metastasis [Crnic et al., 2004; He et al., 2005; Lin et al., 2005] and a similar result was also recently achieved by injection of an antibody against VEGFR-3 [Hoshida et al., 2006]. However, recent work by Pytowski et al. has suggested that VEGF-C-mediated VEGFR-3 signaling may be unnecessary for maintenance of pre-existing lymphatics in the mouse tail [Pytowski et al., 2005].

We began these studies with the goal of trying to determine whether tumor cell entrance into blood circulation was dependent on lymphatic dissemination. That question still remains unresolved, as we were unable to inhibit lymph node metastasis in our system. Instead, we have shown that intratumoral lymphangiogenesis can be inhibited in prostate cancer (Flt-C14) without significantly affecting lymph node metastasis (Figure 11). In early-stage Flt-C14 tumors, we found that despite absence of intratumoral lymphangiogenesis, the abundance of peritumoral lymphatics was not statistically different from controls, and in all cases, tumor-intravasated lymphatic vessels were observed. These data suggest that intratumoral lymphangiogenesis is unnecessary for lymph node metastasis in CaP, and that marginal, possibly pre-existing, lymphatics are sufficient. He et al. reported that tumor-secreted VEGF-C can promote dilation and sprouting/hyperplasia in pre-existing lymphatics and that this can be inhibited by high levels of systemic Flt4-Ig, although the tumor cells still co-opted the pre-existing lymphatics and lymph node metastases still occurred, albeit at reduced levels [He et al., 2005]. Those results could be

reconciled with ours if the high levels of Flt4-Ig partially inhibited the intravasation of tumor cells into pre-existing lymphatics. Another possibility is that, in our system, lymphatic hyperplasia may not be dependent upon VEGFR3/Flt4-mediated signaling.

We have also obtained corroborative results using the TRAMP spontaneous model of prostate cancer. In TRAMP, metastasis to lymph nodes is primarily observed only in tumors of grade 4 or higher [Hurwitz et al., 2001]. In TRAMP prostates, we found that lymphatics were typically located outside the luminal acinar regions where PIN and adenocarcinoma develop. Peritumoral, but not intratumoral lymphatics, were seen, and as the tumors invaded through the basement membrane into surrounding stromal regions (grades 5-6), significantly fewer lymphatics were observed, suggesting destruction of pre-existing lymphatics and absence of lymphangiogenesis. This is similar to human clinical CaP[Trojan et al., 2004], and also indicates that pre-existing peritumoral lymphatics are sufficient for lymph node metastasis.

In summary, we have shown that in prostate cancer, lymph node metastasis relies on peritumoral, and not intratumoral, lymphatics, suggesting that the peritumoral lymphatics that pre-exist before tumor development may be sufficient for disseminating tumor cells to local and more distal lymph nodes (Figure 11). Our results also suggest that inhibiting lymphangiogenesis may be easier than ablating pre-existing lymphatics. As targeting lymphatic vasculature has recently been proposed as an anti-metastatic approach for limiting spread of primary tumors[Achen et al., 2005], this study demonstrates that the need to target the surrounding marginal lymphatics is especially imperative.

REFERENCES

- Abtahian F, Guerriero A, Sebzda E, Lu M, Zhou R, Mocsai A, Myers EE, Huang B, Jackson DG, Ferrari VA, Tybulewicz V, Lowell CA, Lepore JJ, Koretzky GA, Kahn ML (2003): Regulation of blood and lymphatic vascular separation by signaling proteins SLP-76 and Syk. *Science* 299:247-251.
- Achen MG, McColl BK, Stacker SA (2005): Focus on lymphangiogenesis in tumor metastasis. *Cancer Cell* 7:121-127.
- Alitalo K, Mohla S, Ruoslahti E (2004): Lymphangiogenesis and Cancer: Meeting Report. *Cancer Research* 64:9225-9229.
- Alitalo K, Tammela T, Petrova TV (2005): Lymphangiogenesis in development and human disease. *Nature* 438:946-953.
- An Z, Wang X, Geller J, Moossa AR, Hoffman RM (1998): Surgical orthotopic implantation allows high lung and lymph node metastatic expression of human prostate carcinoma cell line PC-3 in nude mice. *The Prostate* 34:169-174.
- Baldwin ME, Stacker SA, Achen MG (2002): Molecular control of lymphangiogenesis. *BioEssays* 24:1030-1040.
- Bubendorf L, Schopfer A, Wagner U, Sauter G, Moch H, Willi N, Gasser TC, Mihatsch MJ (2000): Metastatic patterns of prostate cancer: an autopsy study of 1,589 patients. *Human Pathology* 31:578-582.
- Cao R, Eriksson A, Kubo H, Alitalo K, Cao Y, Thyberg J (2004): Comparative evaluation of FGF-2-, VEGF-A-, and VEGF-C-induced angiogenesis, lymphangiogenesis, vascular fenestrations, and permeability. *Circulation Research* Pre-print.
- Carmeliet P, Collen D (1998): Vascular development and disorders: molecular analysis and pathogenic insights. *Kidney International* 53:1519-1549.
- Chang XH, Fu YW, Na WL, Wang J, Sun H, Cai L (1999): Improved metastatic animal model of human prostate carcinoma using surgical orthotopic implantation (SOI). *Anticancer Research* 19:4199-4202.
- Chen Z, Varney ML, Backora MW, Cowan K, Solheim JC, Talmadge JE, Singh RK (2005): Down-regulation of vascular endothelial cell growth factor-C expression using small interfering RNA vectors in mammary tumors inhibits tumor lymphangiogenesis and spontaneous metastasis and enhances survival. *Cancer Research* 65:9004-9011.
- Chevalier S, Defoy I, Lacoste J, Hamel L, Guy L, Begin LR, Aprikian AG (2002): Vascular endothelial growth factor and signaling in the prostate: more than angiogenesis. *Molecular and Cellular Endocrinology* 189:169-179.
- Crnici I, Strittmatter K, Cavallaro U, Kopfstein L, Jussila L, Alitalo K, Christofori G (2004): Loss of neural cell adhesion molecule induces tumor metastasis by up-regulating lymphangiogenesis. *Cancer Research* 64:8630-8638.
- Croix BS, Rago C, Velculescu V, Traverso G, Romans KE, Montgomery E, Lal A, Riggins GJ, Lengauer C, Vogelstein B, Kinzler KW (2000): Genes expressed in human tumor endothelium. *Science* 289:1197-1202.
- Cunha GR, Hayward SW, Wang YZ, Riche WA (2003): Role of the stromal microenvironment in carcinogenesis of the prostate. *International Journal of Cancer* 107:1-10.
- Cursiefen C, Chen L, Borges LP, Jackson D, Cao J, Radziejewski C, D'Amore PA, Dana MR, Wiegand SJ, Streilein JW (2004): VEGF-A stimulates lymphangiogenesis and hemangiogenesis in inflammatory neovascularization via macrophage recruitment. *J. Clin. Invest.* 113:1040-1050.
- De S, Chen J, Narizhneva NV, Heston W, Brainard J, Sage EH, Byzova TV (2003): Molecular pathway for cancer metastasis to bone. *JBC* 278:39044-39050.
- Eubanks TD, Galloway M, Montague CM, Waldman WJ, Marsh CB (2003): M-CSF induces vascular endothelial growth factor production and angiogenic activity from human monocytes. *The Journal of Immunology* 171:2637-2643.
- Ferrer FA, Miller LJ, Lindquist R, Kowalczyk P, Laudone VP, Albertsen PC, Kreutzer DL (1999): Expression of vascular endothelial growth factor receptors in human prostate cancer. *Urology* 54:567-572.

- Flocks RH, Culp D, Porto R (1959): Lymphatic spread from prostatic cancer. *The Journal of Urology* 81:194-196.
- Fukumura D, Xavier R, Sugiura T, Chen Y, Park EC, Lu N, Selig M, Nielsen G, Taksir T, Jain RK, Seed B (1998): Tumor induction of VEGF promoter activity in stromal cells. *Cell* 94:715-725.
- Gale NW, Prevo R, Fematt JE, Ferguson DJ, Dominguez MG, Yancopoulos GD, Thurston G, Jackson DG (2006): Normal lymphatic development and function in mice deficient for the lymphatic hyaluronan receptor LYVE-1. *Mol Cell Biol* Epub ahead of print.
- Gingrich JR, Barrios RJ, Foster BA, Greenberg NM (1999): Pathologic progression of autochthonous prostate cancer in the TRAMP model. *Prostate Cancer and Prostatic Diseases* 2:70-75.
- Gingrich JR, Barrios RJ, Morton RA, Boyce BF, DeMayo FJ, Finegold MJ, Angelopoulou R, Rosen JM, Greenberg NM (1996): Metastatic prostate cancer in a transgenic mouse. *Cancer Research* 56:4096-4102.
- Giuliano AE, Kirgan DM, Guenther JM, Morton DL (1994): Lymphatic mapping and sentinel lymphadenectomy for breast cancer. *Annals of Surgery* 220:391-401.
- Glinskii AB, Smith BA, Jiang P, Li X, Yang M, Hoffman RM, Glinsky GV (2003): Viable circulating metastatic cells produced in orthotopic but not ectopic prostate cancer models. *Cancer Research* 63:4239-4243.
- Greenberg NM, DeMayo F, Finegold MJ, Medina D, Tilley WD, Aspinall JO, Cunha GR, Donjacour AA, Matusik RJ, Rosen JM (1995): Prostate cancer in a transgenic mouse. *PNAS* 92:3439-3443.
- Grunewald M, Avraham I, Dor Y, Bachar-Lustig E, Itin A, Yung S, Chimenti S, Landsman L, Abramovitch R, Keshet E (2006): VEGF-induced adult neovascularization: recruitment, retention, and role of accessory cells. *Cell* 124:175-189.
- He Y, Karpanen T, Alitalo K (2004a): Role of lymphangiogenic factors in tumor metastasis. *Biochimica et Biophysica Acta* 1654:3-12.
- He Y, Kozaki K, Karpanen T, Koshikawa K, Yla-Herttuala S, Takahashi T, Alitalo K (2002): Suppression of tumor lymphangiogenesis and lymph node metastasis by blocking vascular endothelial growth factor receptor-3 signaling. *Journal of the National Cancer Institute* 94:819-825.
- He Y, Rajantie I, Ilmonen M, Makinen T, Karkkainen MJ, Haiko P, Salven P, Alitalo K (2004b): Preexisting lymphatic endothelium but not endothelial progenitor cells are essential for tumor lymphangiogenesis and lymphatic metastasis. *Cancer Research* 64:3737-3740.
- He Y, Rajantie I, Pajusola K, Jeltsch M, Holopainen T, Yla-Herttuala S, Harding T, Jooss K, Takahashi T, Alitalo K (2005): Vascular endothelial cell growth factor receptor 3-mediated activation of lymphatic endothelium is crucial for tumor cell entry and spread via lymphatic vessels. *Cancer Research* 65:4739-4746.
- Heldin CH, Rubin K, Pietras K, Ostman A (2004): High interstitial fluid pressure - an obstacle in cancer therapy. *Nature Reviews Cancer* 4:806-813.
- Hirakawa S, Kodama S, Kunstfeld R, Kajiya K, Brown LF, Detmar M (2005): VEGF-A induces tumor and sentinel lymph node lymphangiogenesis and promotes lymphatic metastasis. *The Journal of Experimental Medicine* 201:1089-1099.
- Hoshida T, Isaka N, Hagendoorn J, Tomaso Ed, Chen YL, Pytowski B, Fukumura D, Padera TP, Jain RK (2006): Imaging steps of lymphatic metastasis reveals that vascular endothelial growth factor-C increases metastasis by increasing delivery of cancer cells to lymph nodes: therapeutic implications. *Cancer Research* 66:8065-8075.
- Hurwitz AA, Foster BA, Allison JP, Greenberg NM, Kwon ED (2001): The TRAMP mouse as a model for prostate cancer: "Current Protocols in Immunology." John Wiley & Sons, Inc., pp 20.5.1-20.5.23.
- Isaka N, Padera TP, Hagendoorn J, Fukumura D, Jain RK (2004): Peritumor lymphatics induced by vascular endothelial growth factor-C exhibit abnormal function. *Cancer Research* 64:4400-4404.
- Jain RK, Fenton BT (2002): Intratumoral lymphatic vessels: a case of mistaken identity or malfunction? *Journal of the National Cancer Institute* 94:417-421.
- Jain RK, Padera TP (2002): Prevention and treatment of lymphatic metastasis by antilymphangiogenic therapy. *Journal of the National Cancer Institute* 94:785-787.

- Jain RK, Padera TP (2003): Lymphatics make the break. *Nature* 299:209-210.
- Jin H, Su J, Garmy-Susini B, Kleeman J, Varner J (2006): Integrin alpha4-beta1 promotes monocyte trafficking and angiogenesis in tumors. *Cancer Research* 66:2146-2152.
- Jussila L, Alitalo K (2002): Vascular Growth Factors and Lymphangiogenesis. *Physiological Reviews* 82:673-700.
- Karkkainen MJ, Haiko P, Sainio K, Partanen J, Taipale J, Petrova TV, Jeltsch M, Jackson DG, Talikka M, Rauvala H, Betsholtz C, Alitalo K (2004): Vascular endothelial growth factor C is required for sprouting of the first lymphatic vessels from embryonic veins. *Nature Immunology* 5:74-80.
- Karkkainen MJ, Makinen T, Alitalo K (2002): Lymphatic endothelium: a new frontier of metastasis research. *Nature Cell Biology* 4:E2-E5.
- Karpanen T, Egeblad M, Karkkainen MJ, Kubo H, Yla-Herttuala S, Jaattela M, Alitalo K (2001): Vascular endothelial growth factor C promotes tumor lymphangiogenesis and intralymphatic tumor growth. *Cancer Research* 61:1786-1790.
- Kaushal V, Mukunyadzi P, Dennis RA, Siegel ER, Johnson DE, Kohli M (2005): Stage-specific characterization of the vascular endothelial growth factor axis in prostate cancer: expression of lymphangiogenic markers is associated with advanced-stage disease. *Clinical Cancer Research* 11:584-593.
- Kerbel R, Folkman J (2002): Clinical translation of angiogenesis inhibitors. *Nature Reviews Cancer* 2:727-739.
- Kerjaschki D, Huttary N, Raab I, Regele H, Bojarski-Nagy K, Bartel G, Krober SM, Greinix H, Rosenmaier A, Karlhofer F, Wick N, Mazal PR (2006): Lymphatic endothelial progenitor cells contribute to de novo lymphangiogenesis in human renal transplants. *Nature Medicine* 12:230-234.
- Krishnan J, Kirkin V, Steffen A, Hegen M, Weih D, Tomarev S, Wilting J, Sleeman JP (2003): Differential in vivo and in vitro expression of vascular endothelial growth factor (VEGF)-C and VEGF-D in tumors and its relationship to lymphatic metastasis in immunocompetent rats. *Cancer Research* 63:713-722.
- Leu AJ, Berk DA, Lymboussaki A, Alitalo K, Jain R (2000): Absence of functional lymphatics within a murine sarcoma: a molecular and functional evaluation. *Cancer Research* 60:4324-4327.
- Li R, Younes M, Wheeler TM, Scardino P, Ohori M, Frolov A, Ayala G (2004): Expression of the vascular endothelial growth factor receptor-3 (VEGFR-3) in human prostate. *Prostate* 58:193-199.
- Lin J, Lalani AS, Harding TC, Gonzalez M, Wu WW, Luan B, Tu GH, Koprivnikar K, VanRoey MJ, He Y, Alitalo K, Jooss K (2005): Inhibition of lymphogenous metastasis using adeno-associated virus-mediated gene transfer of a soluble VEGFR-3 decoy receptor. *Cancer Research* 65:6901-6909.
- Makinen T, Jussila L, Veikkola T, Karpanen T, Kettunen MI, Pulkkanen KJ, Kauppinen R, Jackson DG, Kubo H, Nishikawa S, S.Yla-Herttuala, Alitalo K (2001): Inhibition of lymphangiogenesis with resulting lymphedema in transgenic mice expressing soluble VEGF receptor-3. *Nature Medicine* 7:199-205.
- Mandriota SJ, Jussila L, Jeltsch M, Compagni A, Baetens D, Prevo R, Banerji S, Huarte J, Montesano R, Jackson DG, Orci L, Alitalo K, Christofori G, Pepper MS (2001): Vascular endothelial growth factor-C-mediated lymphangiogenesis promotes tumour metastasis. *The EMBO Journal* 20:672-682.
- Maruyama K, Ii M, Cursiefen C, Jackson DG, Keino H, Tomita M, Rooijen NV, Takenaka H, D'Amore PA, Stein-Streilen J, Losordo DW, Streilein JW (2005): Inflammation-induced lymphangiogenesis in the cornea arises from CD11b-positive macrophages. *The Journal of Clinical Investigation* 115:2363-2372.
- McCull BK, Baldwin ME, Roufail S, Freeman C, Moritz RL, Simpson RJ, Alitalo K, Stacker SA, Achen MG (2003): Plasmin activates the lymphangiogenic growth factors VEGF-C and VEGF-D. *J. Exp. Med.* 198:863-868.
- Morton DL, Wen D, Wong JH, Economou JS, Cagle LA, Storm FK, Foshag LJ, Cochran AJ (1992): Technical details of intraoperative lymphatic mapping for early stage melanoma. *Archives of Surgery* 127:392-399.

- Nagy JA, Vasile E, Feng D, Sundberg C, Brown LF, Detmar MJ, Lawitts JA, Benjamin L, Tan X, Manseau EJ, Dvorak AM, Dvorak HF (2002): Vascular permeability factor/vascular endothelial growth factor induces lymphangiogenesis as well as angiogenesis. *Journal of Experimental Medicine* 196:1497-1506.
- Nathanson SD (2003): Insights into the mechanisms of lymph node metastasis. *Cancer* 98:413-423.
- Nibbs RJ, Kriehuber E, Ponath PD, Parent D, Qin S, Campbell JD, Henderson A, Kerjaschki D, Maurer D, Graham GJ, Rot A (2001): The beta-chemokine receptor D6 is expressed by lymphatic endothelium and a subset of vascular tumors. *American Journal of Pathology* 158:867-877.
- Orimo A, Gupta PB, Sgroi DC, Arenzana-Seisdedos F, Delaunay T, Naeem R, Carey VJ, Richardson AL, Weinberg RA (2005): Stromal fibroblasts present in invasive human breast carcinomas promote tumor growth and angiogenesis through elevated SDF-1/CXCL12 secretion. *Cell* 121:335-348.
- Padera TP, Kadambi A, Tomaso Ed, Carreira CM, Brown EB, Boucher Y, Choi NC, Mathisen D, Wain J, Mark EJ, Munn LL, Jain RK (2002): Lymphatic metastasis in the absence of functional intratumor lymphatics. *Science* 296:1883-1886.
- Padera TP, Stoll BR, Tooredman JB, Capen D, Tomaso Ed, Jain RK (2004): Pathology: cancer cells compress intratumour vessels. *Nature* 427:695.
- Papoutsis M, Siemeister G, Weindel K, Tomarev SI, Kurz H, Schachtele C, Martiny-Baron G, Christ B, Marme D, Wilting J (2000): Active interaction of human A375 melanoma cells with the lymphatics in vivo. *Histochemical Cell Biology* 114:373-385.
- Pepper MS, Skobe M (2003): Lymphatic endothelium: morphological, molecular and functional properties. *JCB* 163:209-213.
- Petrova TV, Makinen T, Makela TP, Saarela J, Virtanen I, Ferrell RE, Finegold DN, Kerjaschki D, Yla-Herttuala S, Alitalo K (2002): Lymphatic endothelial reprogramming of vascular endothelial cells by the Prox-1 homeobox transcription factor. *The EMBO Journal* 21:4593-4599.
- Pytowski B, Goldman J, Persaud K, Wu Y, Witte L, Hicklin DJ, Skobe M, Boardman KC, Swartz MA (2005): Complete and specific inhibition of adult lymphatic regeneration by a novel VEGFR-3 neutralizing antibody. *Journal of the National Cancer Institute* 97:14-21.
- Schacht V, Ramirez MI, Hong YK, Hirakawa S, Feng D, Harvey N, Williams M, Dvorak AM, Dvorak HF, Oliver G, Detmar M (2003): T1alpha/podoplanin deficiency disrupts normal lymphatic vasculature formation and causes lymphedema. *EMBO J* 22:3546-3556.
- Schoppmann SF, Birner P, Stockl J, Kalt R, Ullrich R, Caucig C, Kriehuber E, Nagy K, Alitalo K, Kerjaschki D (2002): Tumor-associated macrophages express lymphatic endothelial growth factors and are related to peritumoral lymphangiogenesis. *American Journal of Pathology* 161:947-956.
- Schoppmann SF, Schindl M, Breiteneder-Geleff S, Soleiman A, Breiteneker G, Karner B, Birner P (2001): Inflammatory stromal reaction correlates with lymphatic microvessel density in early-stage cervical cancer. *Anticancer Research* 21:3419-3424.
- Siegfried G, Basak A, Cromlish JA, Benjannet S, Marcinkiewicz J, Chretien M, Seidah NG, Khatib AM (2003): The secretory proprotein convertases furin, PC5, and PC7 activate VEGF-C to induce tumorigenesis. *J. Clin. Invest.* 111:1723-1732.
- Sipos B, Kojima M, Tiemann K, Klapper W, Kruse ML, Kalthoff H, Schniewind B, Tepel J, Weich H, Kerjaschki D, Kloppel G (2005): Lymphatic spread of ductal pancreatic adenocarcinoma is independent of lymphangiogenesis. *Journal of Pathology* 207:301-312.
- Skobe M, Hawighorst T, Jackson DG, Prevo R, Janes L, Velasco P, Riccardi L, Alitalo K, Claffey K, Detmar M (2001): Induction of tumor lymphangiogenesis by VEGF-C promotes breast cancer metastasis. *Nature Medicine* 7:192-198.
- Sleeman J (2000): The Lymph Node As a Bridgehead In the Metastatic Dissemination of Tumors. *Recent Results in Cancer Research* 157:55-81.
- Smith JA, Seaman JP, Gleidman JB, Middleton RG (1982): Pelvic lymph node metastasis from prostatic cancer: influence of tumor grade and stage in 452 consecutive patients. *The Journal of Urology* 130:290-292.

- Soldi R, Mitola S, Strasly M, Defilippi P, Tarone G, Bussolino F (1999): Role of alphavbeta3 integrin in the activation of vascular endothelial growth factor receptor-2. *EMBO J* 18:882-892.
- Stacker SA, Achen MG, Jussila L, Baldwin ME, Alitalo K (2002): Lymphangiogenesis and cancer metastasis. *Nature Reviews Cancer* 2:573-583.
- Stacker SA, Caesar C, Baldwin ME, Thornton GE, Williams RA, Prevo R, Jackson DG, Nishikawa S, Kubo H, Achen MG (2001): VEGF-D promotes the metastatic spread of tumor cells via the lymphatics. *Nature Medicine* 7:186-191.
- Stearns ME, Wang M, Hu Y, Kim G, Garcia FU (2004): Expression of a flt-4 (VEGFR3) splicing variant in primary human prostate tumors. VEGF D and flt-4t (Delta773-1081) overexpression is diagnostic for sentinel lymph node metastasis. *Laboratory Investigation* 84:785-795.
- Tong RT, Boucher Y, Kozin SV, Winkler F, Hicklin DJ, Jain RK (2004): Vascular normalization by vascular endothelial growth factor receptor 2 blockade induces a pressure gradient across the vasculature and improves drug penetration in tumors. *Cancer Research* 64:3731-3736.
- Trojan L, Michel MS, Rensch F, Jackson DG, Alken P, Grobholz R (2004): Lymph and blood vessel architecture in benign and malignant prostatic tissue: lack of lymphangiogenesis in prostate carcinoma assessed with novel lymphatic marker lymphatic vessel endothelial hyaluronan receptor (LYVE-1). *The Journal of Urology* 172:103-107.
- Trompezinski S, Berthier-Vergnes O, Denis A, Schmitt D, Viac J (2004): Comparative expression of vascular endothelial growth factor family members, VEGF-B, -C and -D, by normal human keratinocytes and fibroblasts. *Experimental Dermatology* 13:98-105.
- Tsurusaki T, Kanda S, Sakai H, Kanetake H, Saito Y, Alitalo K, Koji T (1999): Vascular endothelial growth factor-C expression in human prostatic carcinoma and its relationship to lymph node metastasis. *British Journal of Cancer* 80:309-313.
- Valtola R, Salven P, Heikkila P, Taipale J, Joensuu H, Rehn M, Pihlajaniemi T, Weich H, deWaal R, Alitalo K (1999): VEGFR-3 and its ligand VEGF-C are associated with angiogenesis in breast cancer. *American Journal of Pathology* 154:1381-1390.
- Vlahakis NE, Young BA, Atakilil A, Sheppard D (2005): The lymphangiogenic vascular endothelial growth factors VEGF-C and -D are ligands for the integrin alpha9beta1. *JBC* 280:4544-4552.
- Vleugel MM, Bos R, Groep Pvd, Greijer AE, Shvarts A, Stel HV, Wall Evd, Diest Pjv (2004): Lack of lymphangiogenesis during breast carcinogenesis. *Journal of Clinical Pathology* 57:746-751.
- Wang JF, Zhang XF, Groopman JE (2001): Stimulation of beta 1 integrin induces tyrosine phosphorylation of vascular endothelial growth factor receptor-3 and modulates cell migration. *JBC* 276:41950-41957.
- Wigle JT, Harvey N, Detmar M, Lagutina I, Grosveld G, Gunn MD, Jackson DG, Oliver G (2002): An essential role for Prox1 in the induction of the lymphatic endothelial cell phenotype. *EMBO J* 21:1505-1513.
- Wittekind C (2000): Diagnosis and staging of lymph node metastasis. *Recent Results in Cancer Research: Lymphatic Metastasis and Sentinel Lymphonodectomy* 157:20-28.
- Wong SY, Haack H, Crowley D, Barry M, Bronson RT, Hynes RO (2005): Tumor-secreted vascular endothelial growth factor-C is necessary for prostate cancer lymphangiogenesis, but lymphangiogenesis is unnecessary for lymph node metastasis. *Cancer Research* 65:9789-9798.
- Wong SY, Hynes RO (2006): Lymphatic or hematogenous dissemination: how does a metastatic tumor cell decide? *Cell Cycle* 5:812-817.
- Zeng Y, Opeskin K, Baldwin ME, Horvath LG, Achen MG, Stacker SA, Sutherland RL, Williams ED (2004): Expression of vascular endothelial growth factor receptor-3 by lymphatic endothelial cells is associated with lymph node metastasis in prostate cancer. *Clinical Cancer Research* 10:5137-5144.
- Zhang X, Groopman JE, Wang JF (2005): Extracellular matrix regulates endothelial functions through interaction of VEGFR-3 and integrin alpha5beta1. *J. Cell Physiol.* 202:205-14.
- Zincke H, Farrow GM, Myers RP, Benson RC, Furlow WL, Utz DC (1982): Relationship between grade and stage of adenocarcinoma of the prostate and regional pelvic lymph node metastases. *The Journal of Urology* 128:498-501.

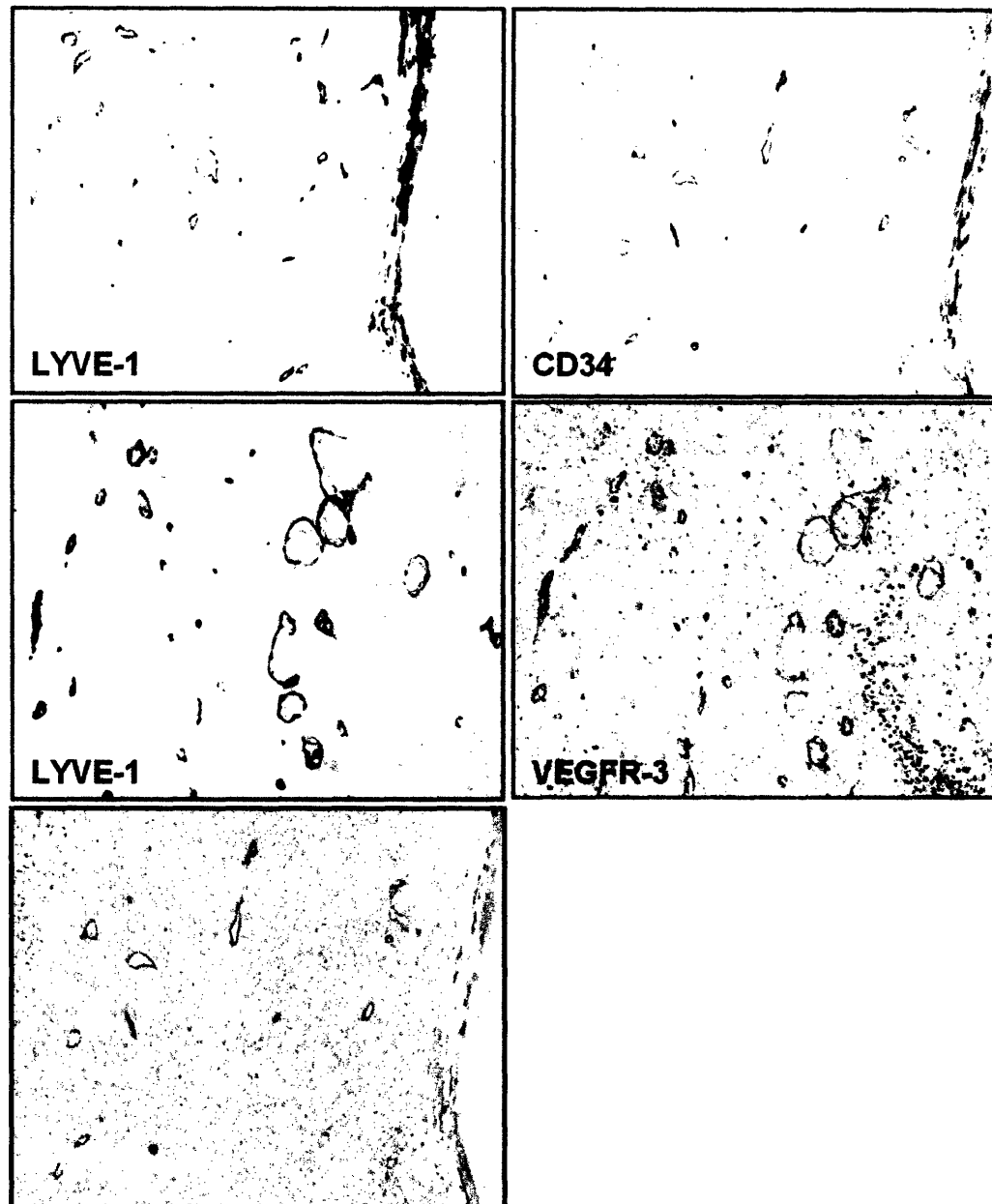
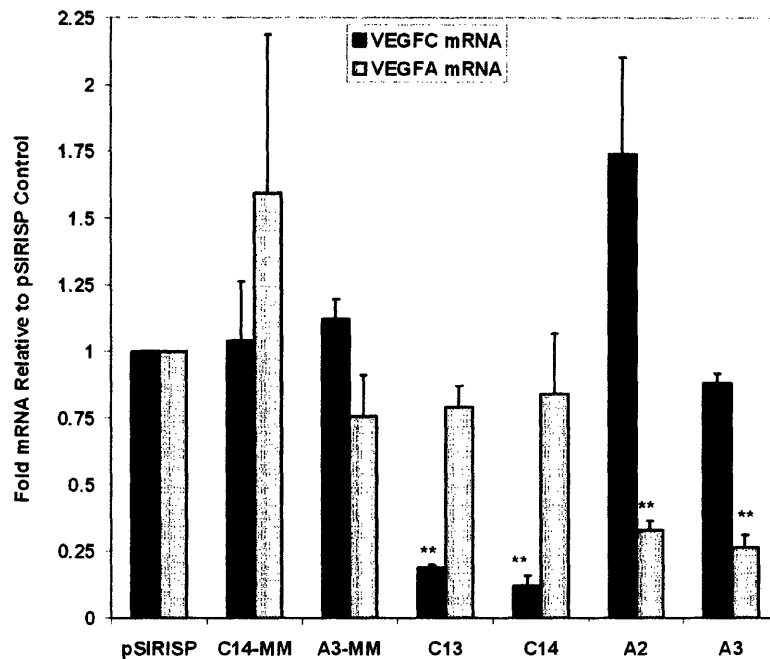


Figure 2. PC3-#82 cells form subcutaneous tumors with intratumoral lymphatic and blood vessels. Serial tumor sections probed with antibodies against LYVE-1 or CD34 show specific, non-overlapping staining for lymphatics or blood vessels, respectively (top panels). This is also evident when the two sections are merged, with lymphatics colored white and blood vessels black (bottom panel). Serial sections probed with LYVE-1 and anti-mouse VEGFR-3/Fit4 show coincident staining (middle panels).

A



B

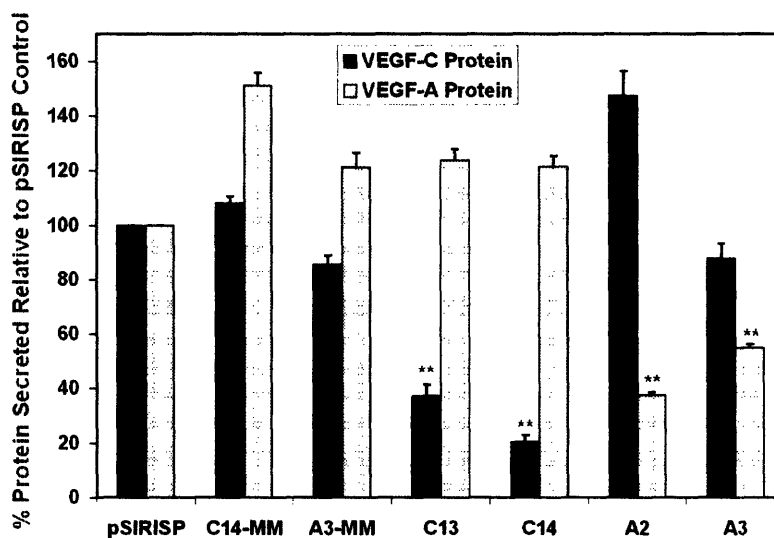
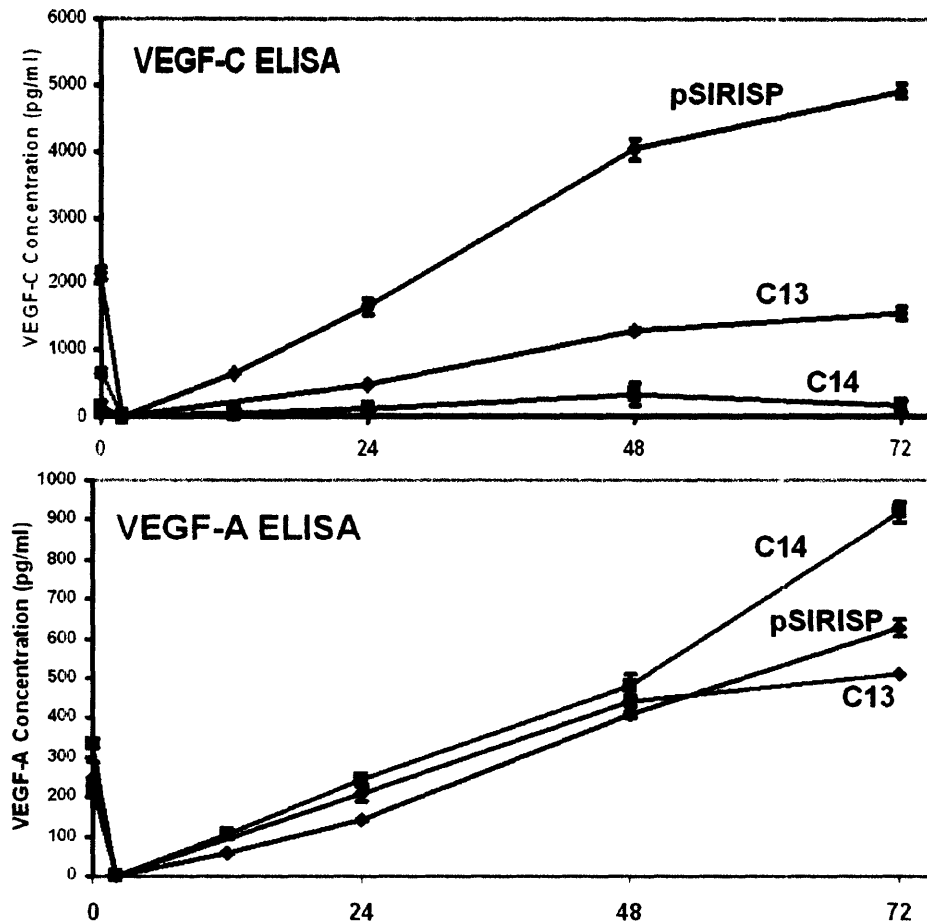


Figure 3. PC3-#82 cell expression and secretion of VEGF-C or VEGF-A can be reduced by siRNA. (A) Relative mRNA levels for VEGF-C (black) or VEGF-A (gray) were measured by quantitative PCR, and normalized to pSIRISP vector control. C13 and C14 cells express siRNAs against VEGF-C. A2 and A3 cells express siRNAs against VEGF-A. C14-MM and A3-MM (MM = "mismatch") are siRNA specificity controls. **(B)** siRNAs specifically reduced accumulation of either VEGF-C or VEGF-A protein in conditioned media, as assessed by ELISA.

C



D

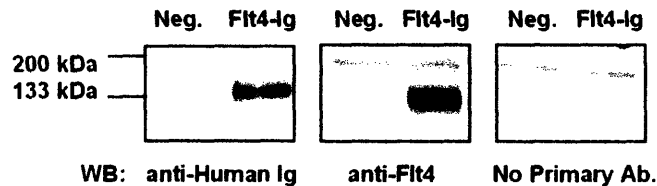
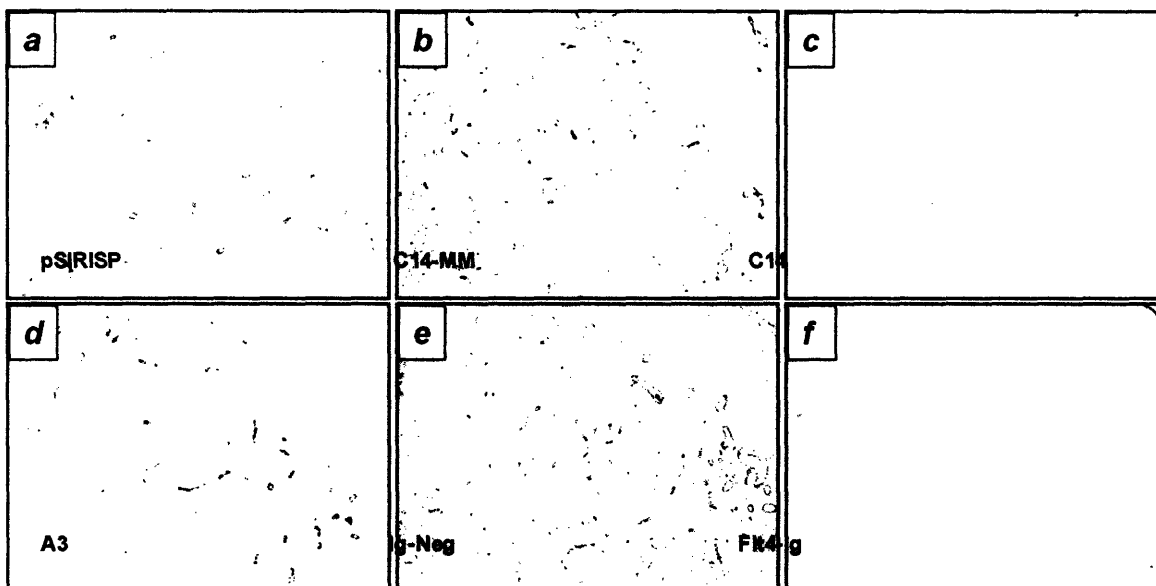


Figure 3. PC3-#82 cell expression and secretion of VEGF-C or VEGF-A can be reduced by siRNA (cont). (C) Accumulation of VEGF-C protein (top graph), but not VEGF-A protein (bottom graph), in conditioned media is severely inhibited in PC3-#82 cells expressing C14 siRNA (red), and less so for C13 siRNA (green), compared to control (blue). Minimal accumulation of VEGF-C was seen in C14-expressing cells even 72 hours after media change. (D) Secretion of soluble VEGFR-3/Flt4-Ig fusion protein in PC3-#82 cells was confirmed by immunoprecipitating fusion protein from conditioned medium and by Western blot. (** $p < 0.001$)

A



B

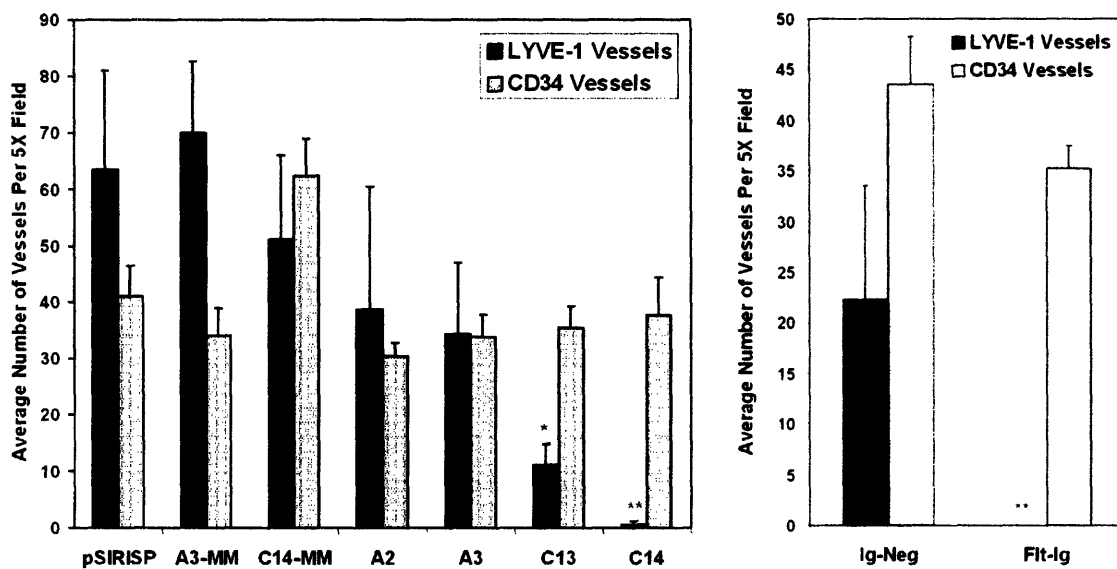
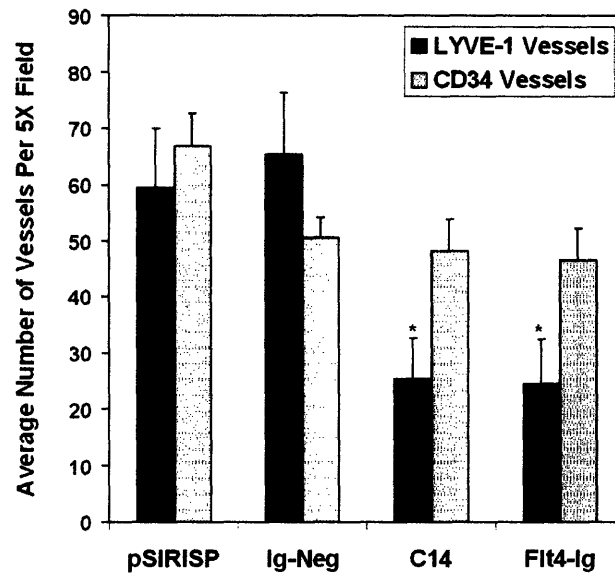


Figure 4. Tumor-secreted VEGF-C is necessary for tumor lymphangiogenesis. (A) Subcutaneous tumors were stained with LYVE-1: (a) pSIRISP control; (b) C14-MM control; (c) C14 siRNA; (d) A3 siRNA; (e) Ig-Neg control; (f) Flt4-Ig. **(B)** Staining results for blood vessels (gray bars) and lymphatics (dark bars) were quantitated for siRNA-expressing subcutaneous tumors (left graph) and for tumors expressing soluble receptor or control (right graph) (* $p = 0.01$; ** $p < 0.001$).

C



D

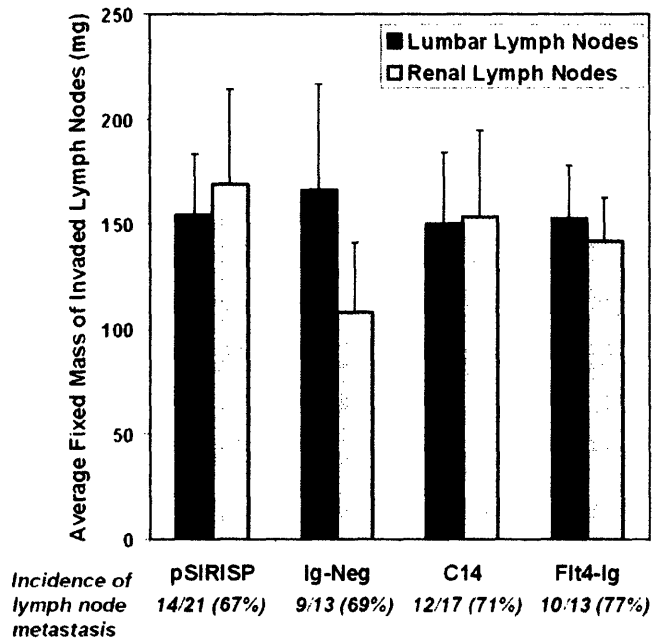
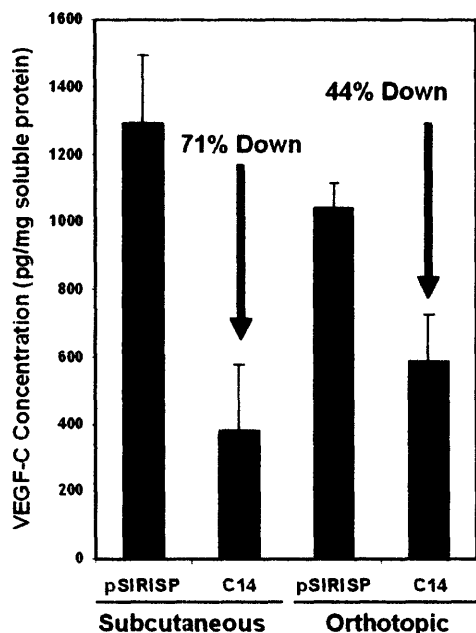
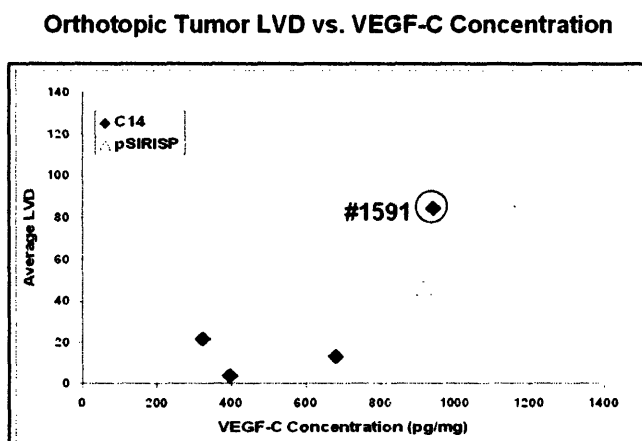


Figure 4. Tumor-secreted VEGF-C is necessary for tumor lymphangiogenesis (cont.). (C) Quantitation of lymphatic (black) and blood vessels (gray) from orthotopic tumors is shown (* $p < 0.02$). (D) Metastasis to the draining (lumbar) and more distant (renal) lymph nodes was unaffected after the tumors were implanted by SOI (for lumbar lymph node mass, $p = 0.92$ for C14 vs. pSIRISP; $p = 0.81$ for Flt4-Ig vs. Ig-Neg; and similarly not significant for renal lymph nodes).

A

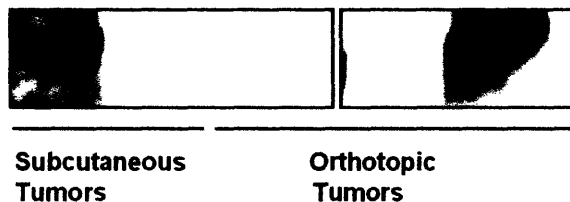


B



C

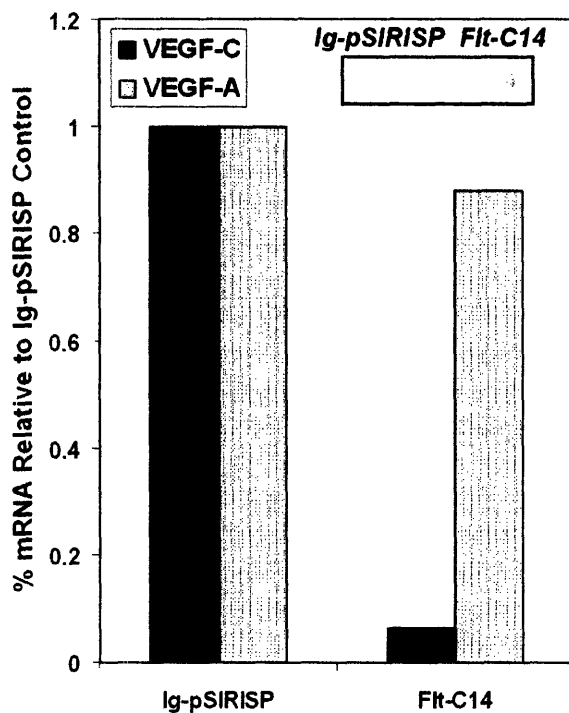
Tumor #	2045	2053	2120	2360*	2410
Type	Flt4-Ig	Ig-Neg	Ig-Neg	Flt4-Ig	Flt4-Ig
High LVD?	No	Yes	Yes	Yes	No



Western Blot: Anti-Human VEGFR-3
 (*example of tumor that lost expression of Flt4-Ig)

Figure 5. Durability of siRNA or Flt4-Ig expression in orthotopic tumors. (A) Subcutaneous tumors expressing C14 siRNA had a 71% reduction in VEGF-C protein compared with control, but only a 44% reduction in orthotopic tumors, as assessed by ELISA. Absolute VEGF-C concentration was increased in C14 orthotopic versus C14 subcutaneous tumors, but not in control orthotopic versus control subcutaneous tumors. (B) Tumor LVD is plotted against human VEGF-C concentration of orthotopic primary tumors, revealing a general positive correlation. Samples expressing C14 siRNA are represented by black diamonds, and control samples are represented by white triangles. Note that a single C14 tumor (#1591) lost siRNA inhibition against VEGF-C and possessed high LVD. (C) Subcutaneous and orthotopic tumors were assayed for Flt4-Ig fusion protein by Western blot against VEGFR-3/Flt4. Flt4-Ig was expressed at high levels in subcutaneous tumors, but severely reduced or absent in one of two orthotopic tumors tested, #2360. Ig-Neg are control tumors.

A



B

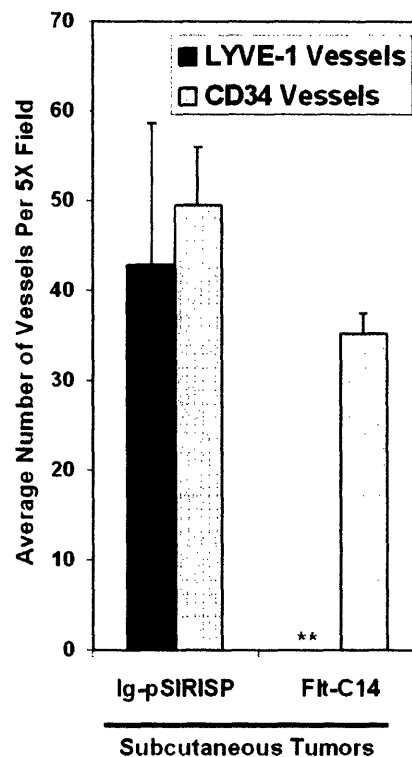
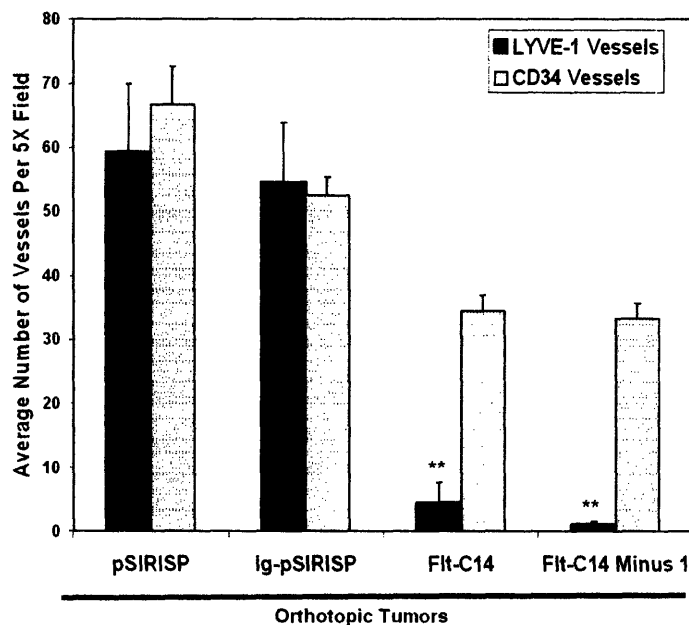


Figure 6. Combined expression of VEGF-C siRNA and Fit4-Ig in PC3-#82 cells effectively reduces orthotopic tumor LVD without markedly affecting lymph node metastasis. (A) Combined Fit-C14-expressing cells were validated for VEGF-C mRNA knock-down and secretion of fusion protein (inset). (B) Lymphatic and blood vessel densities were quantitated from Fit-C14 and control Ig-pSIRISP subcutaneous tumors. ($p < 0.001$)**

C



D

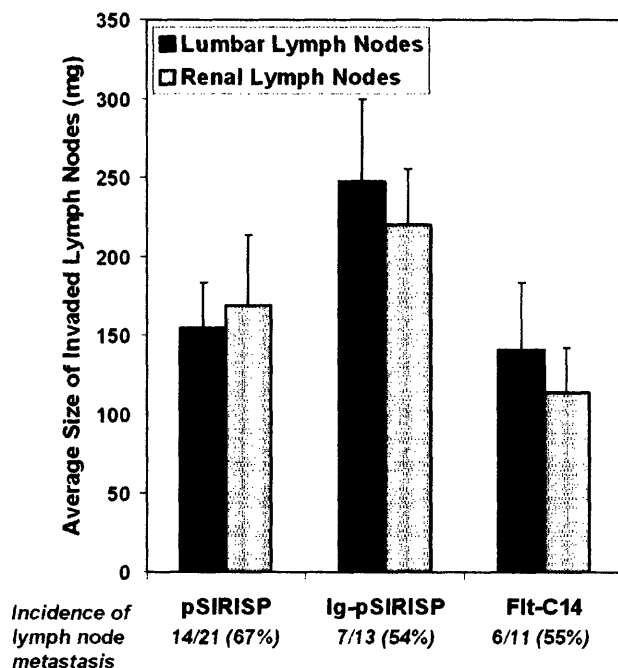


Figure 6. Combined expression of VEGF-C siRNA and Flt4-Ig in PC3-#82 cells effectively reduces orthotopic tumor LVD without markedly affecting lymph node metastasis (cont.). (C) Lymphatic and blood vessels in orthotopic primary tumors were quantitated. Combination of Flt4-Ig with C14 siRNA inhibited average LVD 100% in subcutaneous tumors and >92% in orthotopic tumors (n = 11). In 10/11 Flt-C14 orthotopic tumors, average LVD was reduced >98% ("minus 1"), compared with Ig-pSIRISP control (n = 8). For reference, vessel density for pSIRISP vector control from Fig. 4C is shown. (D) Metastasis to draining and more distant lymph nodes was not significantly affected in Flt-C14 tumors compared with Ig-pSIRISP control (p = 0.15 for lumbar lymph nodes) or pSIRISP control (p = 0.80; data reproduced from Fig. 4D).

E

Tumor Cell Line	A	B	C	D
	Incidence of Mice With Lumbar Lymph Node Mass > 30 mg	Incidence of Mice With Lumbar Lymph Node Mass < 30 mg	Incidence of Lumbar Lymph Nodes With Mass < 30 mg, Found to Possess Micrometastases	Overall Incidence of Lumbar Lymph Node Micro- or Macrometastases
Flt-C14	6/11 (55%)	5/11 (45%)	3/3 (100%)	9/9 (100%)
Ig-pSIRISP	7/13 (54%)	6/13 (46%)	3/3 (100%)	10/10 (100%)
Flt4-Ig	10/13 (77%)	3/13 (23%)	1/1 (100%)	11/11 (100%)
Ig-Neg	9/13 (69%)	4/13 (31%)	2/2 (100%)	11/11 (100%)
C14	12/17 (71%)	5/17 (29%)	1/2 (50%)	13/14 (93%)
pSIRISP	14/21 (67%)	7/21 (33%)	3/3 (100%)	17/17 (100%)

A set of 2-3 lumbar lymph nodes was removed, fixed and weighed. (The collective mass of lumbar lymph nodes from non-tumor-bearing mice typically does not typically exceed 10 mg.) Lymph node sets weighing >30 mg were scored as positive for macrometastasis (Column A). Ten "borderline-positive" lumbar lymph node sets (mass 30-80 mg) were examined by histology (one H&E section per lymph node). 8/10 consisted of at least one node with >80% tumor invasion; the remaining two samples consisted of at least one node with >50% invasion. Since the majority of lymph node macrometastases greatly exceeded 100 mg in mass, it is likely that the majority of the node mass (>90%) consisted of metastasized tumor cells. The incidence of macrometastasis was unchanged in the case of manipulated cell lines vs. controls (Columns A, B). A representative sample of lymph nodes < 30 mg in mass was further evaluated by histology (Column C). A single H&E section per lymph node was examined for micro-metastatic invasion. Overall, 13/14 lymph node sets were found to possess tumor cells. Column D shows that essentially all mice bore lymph node metastases (macro or micro), regardless of cell line.

Figure 6. Combined expression of VEGF-C siRNA and Flt4-Ig in PC3-#82 cells effectively reduces orthotopic tumor LVD without markedly affecting lymph node metastasis (cont.). (E) The incidence of macroscopic (> 30 mg) and microscopic lumbar lymph node metastasis is shown for the cell lines used in this study. In 71/72 animals examined, metastasis to local lymph nodes was observed.

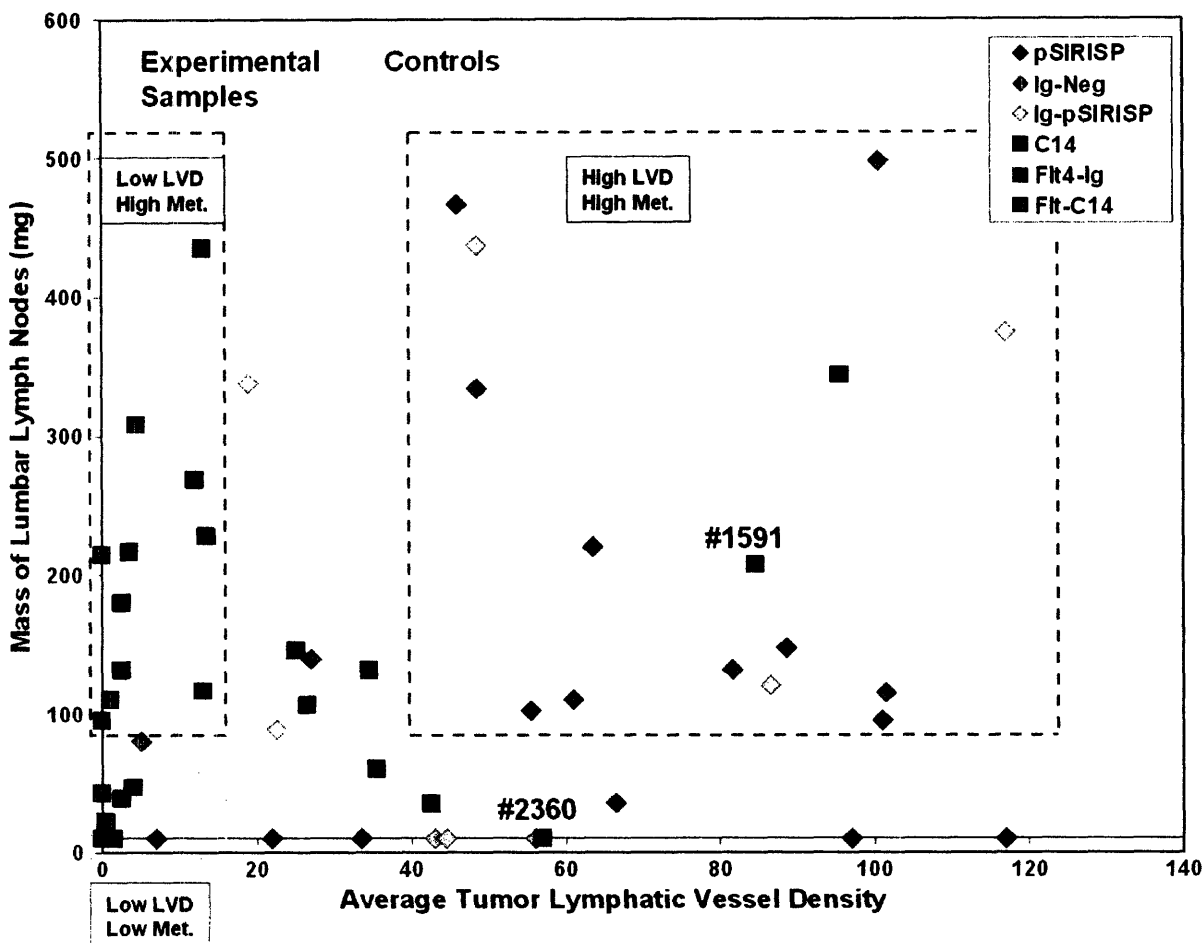
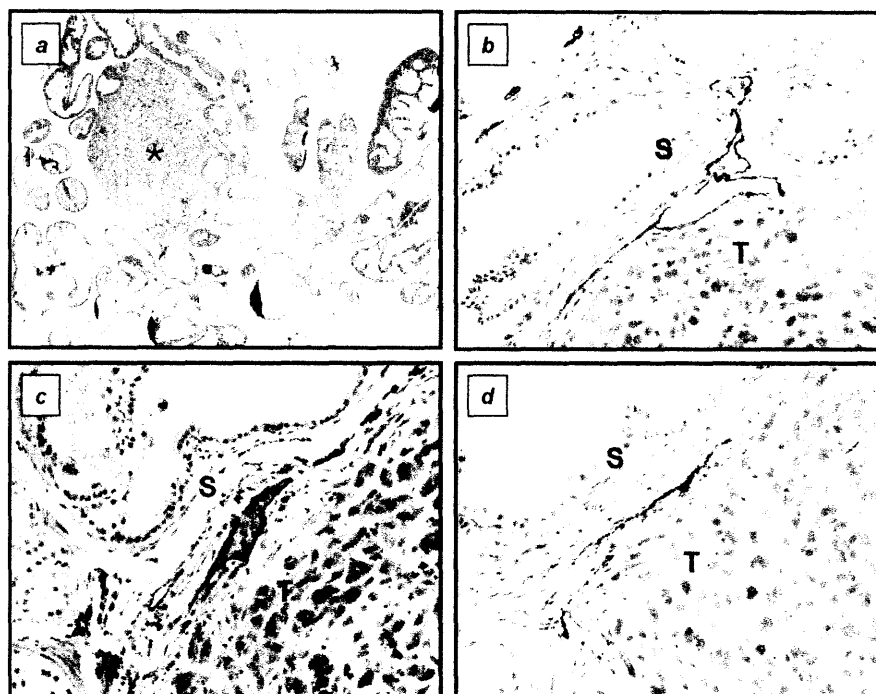


Figure 7. Metastasis is not correlated with LVD in individual orthotopic tumors. Each point represents data from a single tumor/mouse. Different control tumors are shaded red, while experimental tumors are shaded green (refer to labels for cell line identification). The upper right box identifies tumors with heavy lymph node metastatic burdens (> 100 mg mass, or ~10X the typical mass of uninvaded lymph nodes) and high LVD. Note that tumors in this zone consist predominantly of control samples (red shaded). The lower left box identifies tumors with low lymph node metastatic burdens and low LVD. Note that tumors in this zone predominantly consist of samples where LVD was experimentally reduced (green shaded). The upper left box identifies tumors with heavy lymph node metastatic burdens despite low LVD. Note that all samples in this zone are experimentally manipulated (green shaded). Tumor #1591 (C14) was subsequently found to have lost siRNA inhibition of VEGF-C (Fig. 5B), while tumor #2360 showed reduced Flt4-Ig protein levels (Fig. 5C).

A



B

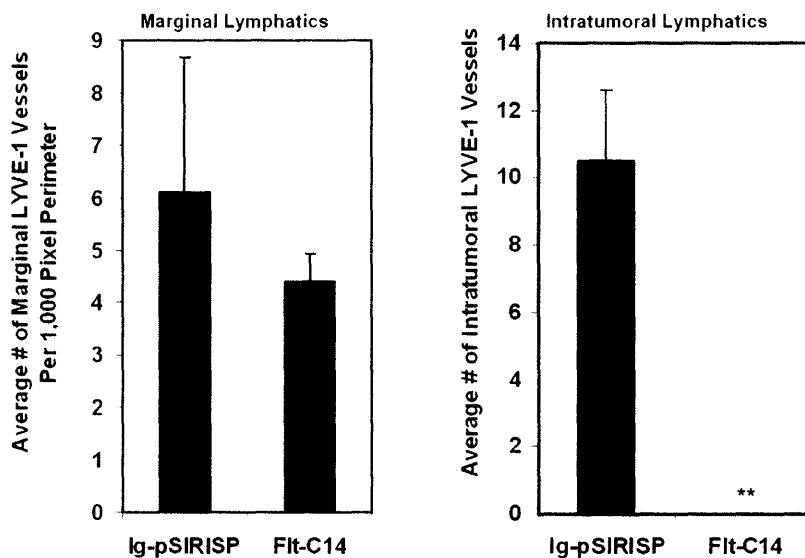
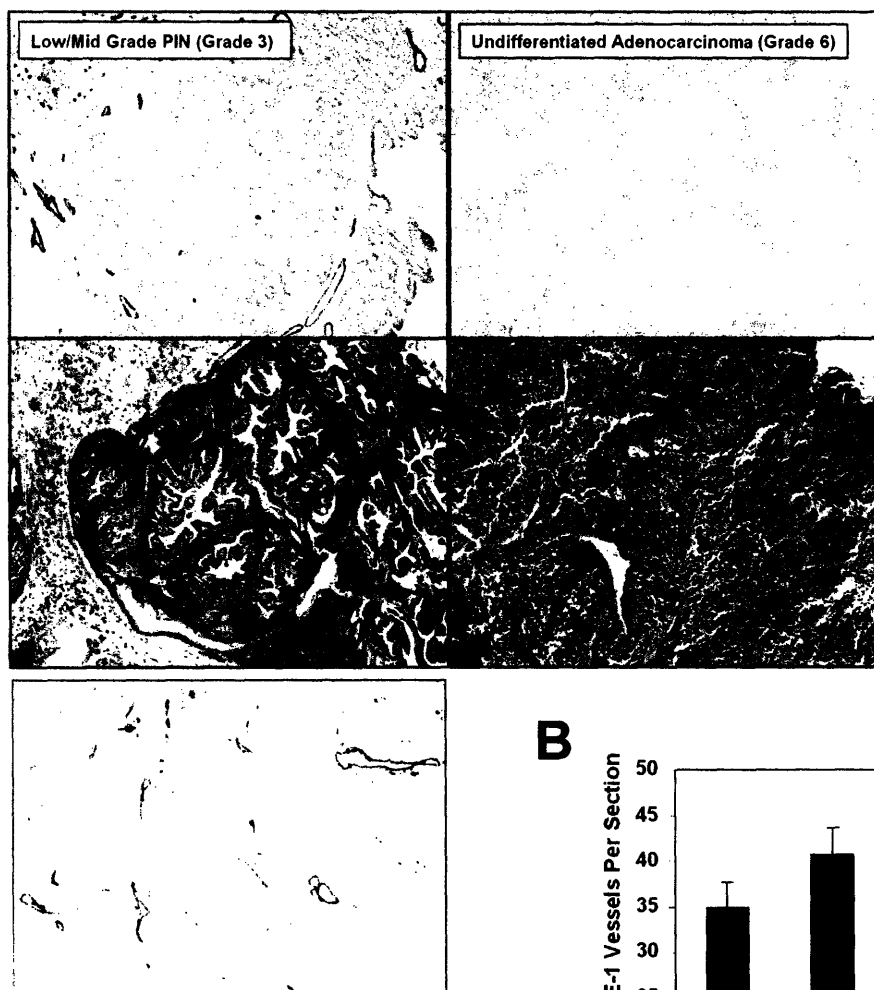


Figure 8. Peritumoral lymphatics are found at the tumor-stromal interface of Flt-C14 orthotopic tumors. (A) H&E staining of the prostate 2-3 weeks after SOI reveals a single focal microscopic tumor (star) surrounded by prostatic ductal acinar structures (a). All stages of lymphatic invasion were seen in Flt-C14 orthotopic tumors stained with LYVE-1, including tumor growth against lymphatic vessels (b), intravasated vessels containing tumor cells (c), and compression of vessels (d). Note that, in all cases, peritumoral lymphatics delineated the tumor-stromal junction ("T," tumor region; "S," stromal region). **(B)** Quantitation of peritumoral lymphatics in Flt-C14 and control orthotopic tumors is shown on the left, and quantitation of intratumoral lymphatics is shown on the right. Flt-C14 tumors possessed peritumoral, but not intratumoral lymphatics. (** $p < 0.001$)

A



B

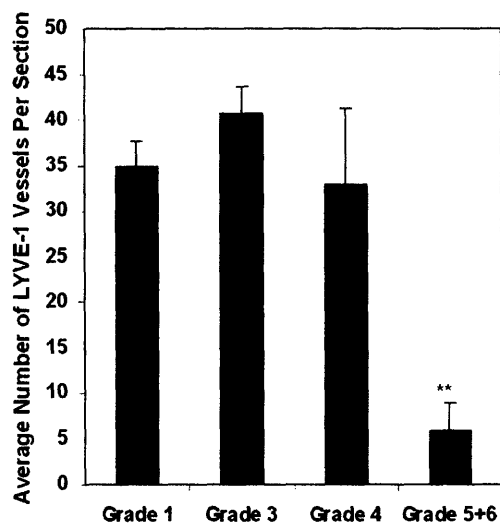


Figure 9. TRAMP spontaneous prostate tumors do not induce lymphangiogenesis.

(A) Regions of grade 3 prostate intraepithelial neoplasia (left), or grade 6 undifferentiated adenocarcinoma (right) from TRAMP prostates were stained with LYVE-1 (top panels) or H&E (middle panels). Normal prostate was also stained with LYVE-1 (bottom panel). Lymphatics were located in the stroma and excluded from tumorigenic regions. Lymphatics were mostly absent in regions of undifferentiated adenocarcinoma. (B) Quantitation of total lymphatics in normal and TRAMP prostate sections. Grade 5-6 TRAMP prostates possess significantly fewer lymphatic vessels than lower grade or normal (grade 1) prostates ($p < 0.001$).

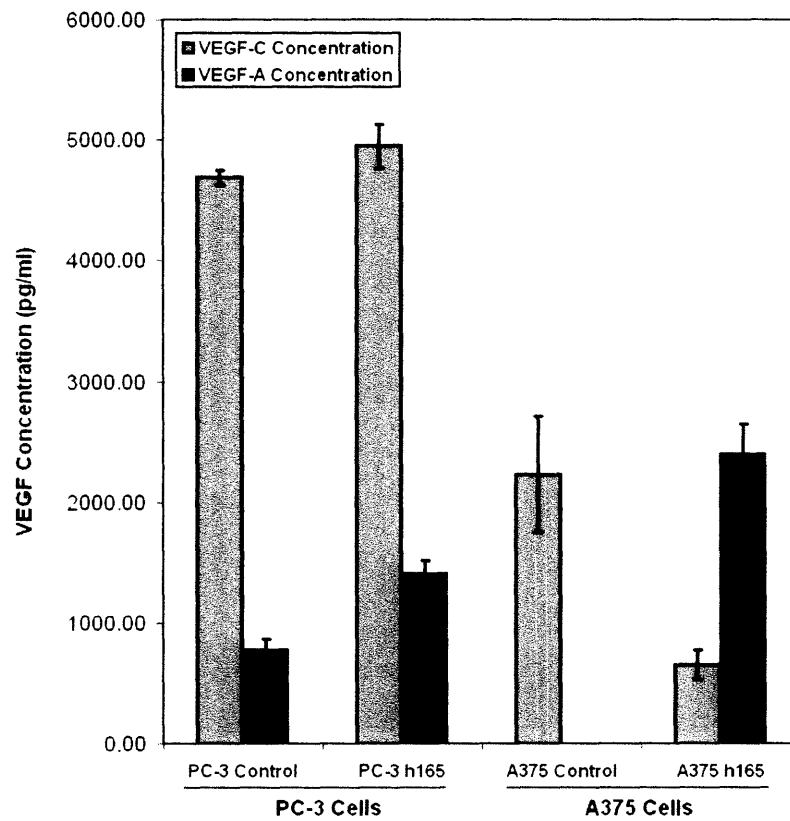
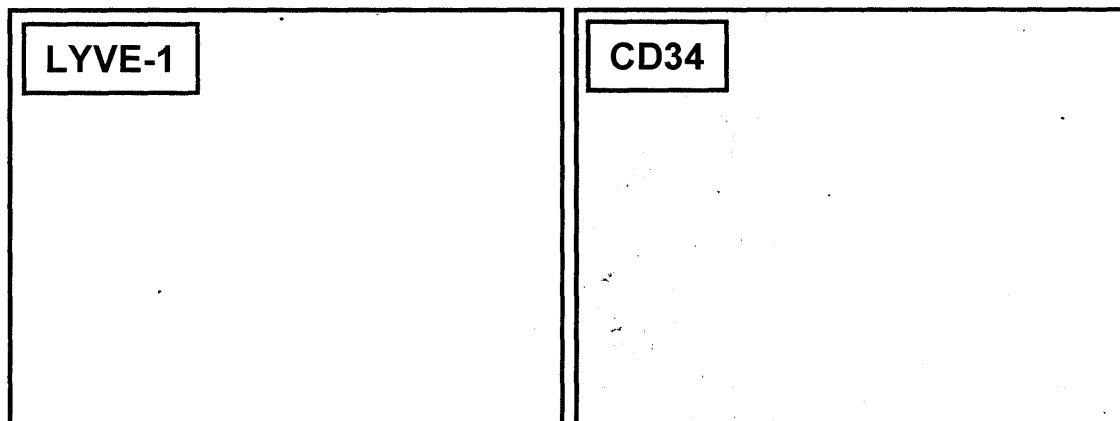
A**B**

Figure 10. A375 melanoma tumors do not induce lymphangiogenesis. (A) A375 control cells secreted VEGF-C (blue bars), but not VEGF-A (purple bars), into conditioned medium, as assessed by ELISA. Secretion of human VEGF-A could be detected in A375-h165 cells overexpressing human VEGF-A 165. **(B)** A375 subcutaneous tumors were angiogenic (right) but not lymphangiogenic (left), regardless of VEGF secretion.

C

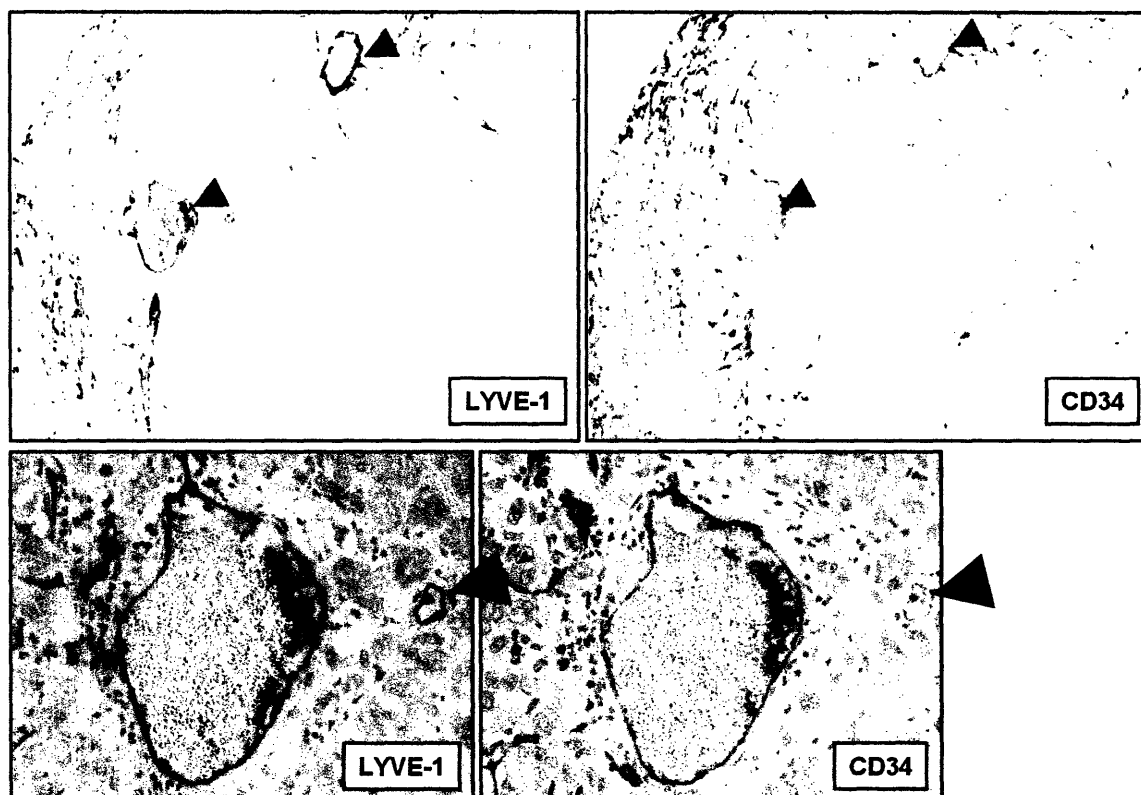
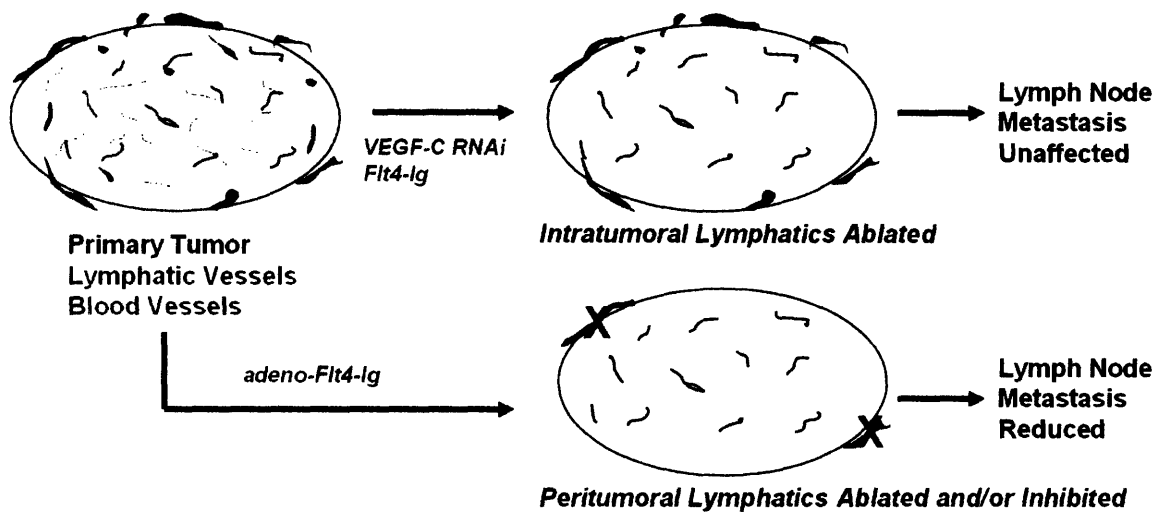


Figure 10. A375 melanoma tumors do not induce lymphangiogenesis (cont.). (C) A375 lung metastases exhibited LYVE-1 staining that was often coincident with CD34 staining (top row). Red blood cells could be seen, indicating these were blood vessels (bottom row). In some cases, LYVE-1 staining appeared specific and did not overlap with CD34 staining (bottom row, arrows).



Reproduced from Wong and Hynes, 2006. *Cell Cycle*.

Figure 11. Inhibition of peritumoral lymphatics is likely critical for blocking lymph node metastasis. Various inhibitory approaches can inhibit intratumoral and, in some cases, peritumoral lymphatics. High *in vivo* expression of Flt4-Ig by adenovirus-mediated gene transfer (adeno-Flt4-Ig) is likely more effective at inhibiting peritumoral lymphatics than tumor expression and secretion of the chimeric protein in our orthotopic system.

CHAPTER 7.

DISCUSSION AND FUTURE DIRECTIONS

Summary of Results

The complexity of a biological process such as metastasis necessitates that, with our current technology, discrete steps or aspects of the problem are analyzed. We decided to focus our studies on prostate cancer because this is a malignancy that frequently metastasizes, and, indeed, it is the metastases—rather than the primary tumor—that make this a lethal disease. Among the many questions about how tumor cells accomplish this process, we decided to focus on three of them in this thesis:

1. What are the genes involved with metastasis?
2. How do tumor cells enter blood circulation?
3. How do tumor cells enter lymphatic circulation?

As these are all questions that seek to address events that occur *in vivo*, we approached these problems by using two different mouse models of prostate cancer. In all cases, we began our studies by xenografting human adenocarcinoma PC-3 cells into the prostate orthotopic site. The major advantage of xenotransplant mouse models of cancer is that the input cells can readily be manipulated to over- or under-express genes of interest. However, these approaches do not recapitulate all the steps of tumorigenesis; the techniques by which tumor cells are introduced are often highly artificial; and tumor progression is usually observed in immunodeficient mice. Thus, whenever possible, we extended our observations using the TRAMP spontaneous model of prostate cancer. We also attempted to view our experimental findings from these two models in the larger context of human clinical prostate cancer: Are the results we obtained in mice relevant to the human situation? And if so, what are the implications?

We began our studies by deriving from the original PC-3 cell population a set of core cell lines that differed in metastatic potential. The PC3-pMicro-1 cell population was first isolated, from which two key cell lines were subsequently derived: PC3-#78 and PC3-#82. Repeated implantation of #78 tumors using surgical orthotopic implantation (SOI) revealed that these cells were poorly metastatic to lymph nodes and lung in the orthotopic system; #82 cells, on the other hand, displayed significantly increased metastatic potential. With knowledge about the *in vivo* properties of these cells, we performed gene expression analysis in an attempt to identify genes which were responsible for the differing metastatic phenotypes. This approach yielded a list of gene candidates that differed between poorly metastatic #78 cells and highly metastatic #82 cells, and we were pleased to find that many of these genes encoded proteins with known or putative functions related to cell adhesion, migration and invasion. Ultimately, we decided to pursue further two genes which were both severely downregulated in highly metastatic cells—Protein 4.1B and SPARC—on the hypothesis that these were potential suppressors of the metastatic phenotype.

Protein 4.1B is a member of the Protein 4.1 superfamily of proteins, and is believed to function as a cytoskeletal linker that connects transmembrane proteins with the actin cytoskeleton [Sun et al., 2002]. 4.1B possesses an N-terminal FERM interaction domain and is related to ERM proteins, although the precise physiological functions of this poorly-characterized molecule are currently unknown. *In vitro* overexpression experiments, in some cases, have suggested that 4.1B can function as a tumor suppressor, and, more importantly, expression of this protein is lost in a variety of human tumors [Charboneau et al., 2002; Jiang and Newsham, 2006; Robb et al., 2005; Sun et al., 2002; Tran et al., 1999]. However, mice deficient in 4.1B are viable and phenotypically normal, without any enhanced predisposition to tumor formation [Yi et al., 2005].

We began examining the role of this protein in prostate cancer metastasis by downregulating 4.1B expression in poorly metastatic #78 cells, which expressed high levels of the protein. When implanted by SOI, #78 cells expressing siRNAs against 4.1B exhibited significantly increased metastasis to lymph nodes relative to controls, whereas the size of the orthotopic primary tumors did not differ. Lymph nodes from mice bearing siRNA-expressing tumors tended to be fully infiltrated with tumor cells, with low rates of apoptosis, while nodes from mice bearing control tumors frequently exhibited incomplete, microscopic subcapsular invasion where tumor cell death was quite apparent. These experiments thus suggest that downregulation of 4.1B may have protected tumor cells against apoptosis, which consequently increased their overall metastatic potential.

In light of these xenotransplant results, we decided to test whether 4.1B was important during spontaneous prostate cancer progression. Mice lacking this gene were generated by and obtained from Dr. Joseph Kissil, and these animals were crossed with TRAMP mice, which expressed SV40 large T antigen in the prostate. We observed that 4.1B^{-/-}; TRAMP^{+/-} mice, on average, developed higher grade, less differentiated and more aggressive primary prostate tumors than did 4.1B^{+/-}; TRAMP^{+/-} littermates or cousins. In addition, tumors from knock-out mice more frequently metastasized to the draining lymph nodes than did those from heterozygous mice. Again, we found significant differences in apoptosis: At 22 weeks of age, 4.1B-deficient, Grade 4 prostatic lesions displayed significantly reduced apoptosis compared to that of their heterozygous, age- and grade-matched counterparts. We believe that loss of 4.1B therefore conferred tumors with an increased ability to resist apoptosis, and this ultimately enhanced their propensity to progress to a metastatic state. As 4.1B expression is significantly downregulated in prostate cancer relative to normal tissue in four out of five studies of human clinical prostate cancer, this again supports our finding that loss of this protein is important during disease progression.

As mentioned previously, we also examined whether SPARC, an extracellular matrix component, was important during tumor progression and metastasis. Much *in vitro* and *in vivo* work has been done on this protein, although these studies have, often-times, yielded contradictory results implicating SPARC as

both a tumor/metastasis suppressor and enhancer [Framson and Sage, 2004]. However, we were interested to find that SPARC levels frequently changed during tumor progression and metastasis, not just in our own studies, but also in breast and prostate human clinical data. SPARC expression was also downregulated in highly metastatic A375 melanoma cells relative to poorly metastatic cells, similar to our results using PC-3 cell line derivatives. Given that the role of SPARC in tumorigenesis has already been examined *in vitro* and in several *in vivo* xenograft cancer studies [Brekken et al., 2003; Koblinski et al., 2005; Puolakkainen et al., 2004; Yiu et al., 2001], we elected to test its function directly in spontaneous tumor mouse models of prostate and mammary cancer. For this, we utilized SPARC-deficient mice, which were obtained from Dr. E. Helene Sage and mated with either TRAMP animals, or with MMTV mice expressing SV40 in the mammary glands. Surprisingly, we observed no statistically significant differences in tumor formation or progression in either systems, when comparing SPARC^{-/-} mice with SPARC^{+/-} littermates and cousins. These results, if also true in humans, would indicate that while levels of SPARC are frequently altered during tumorigenesis, this is a change which is associated with, rather than causal for, the tumorigenesis and/or metastasis phenotypes observed.

Over the course of our studies, we also made an interesting observation regarding the patterns of lymphatic and hematogenous spread that were manifested in the SOI prostate cancer model. We noted that lung micro-metastases and circulating tumor cells in the blood were detected, in almost all cases, only in those mice that bore macro-metastases in both the para-aortic/lumbar and para-renal lymph nodes. Mice that had not displayed macroscopic invasion at both sets of nodes rarely exhibited hematogenous dissemination of tumor cells. As hematogenous spread has been observed to be associated with lymphatic metastasis in human clinical prostate cancer and other tumor types [Bubendorf et al., 2000; Cianfrocca and Goldstein, 2004], this finding could bear important implications for how we regard some of the earliest steps of the process. At least three explanations could account for these apparent associations. One possibility is that tumor cells rely on lymphatics to enter systemic circulation. A second possibility is that tumors metastasize through both the lymphatic and hematogenous routes simultaneously but independently of one another. A third possibility, related to the second, is that lymphatic and hematogenous metastasis are independently mediated by distinct sub-populations of tumor cells.

We tried to differentiate between these three possibilities by attempting specifically to inhibit lymph node metastasis. If hematogenous dissemination were dependent on lymphatic spread, both routes of metastasis should be, consequently, inhibited; however, if bloodborne metastasis occurred concomitantly with, but independently of, lymphatic spread, stopping one route of dissemination should have no effects on the other. Our approach to inhibiting lymph node metastasis was based on previous findings by others that VEGF-C is an important lymphangiogenic cytokine, and that blocking the activation of its receptor, VEGFR-3/Flt4, could reduce tumor metastasis to lymph nodes [Alitalo et al., 2005; He et al., 2002].

Indeed, we were successful at inhibiting lymphangiogenesis by either ablating tumor expression of VEGF-C, or by expressing a competitive soluble inhibitor of its receptor. What was surprising, though, was that inhibiting tumor lymphangiogenesis had no statistically significant effects on lymph node metastasis in our orthotopic prostate cancer model. Micro- and macro-metastases to the lymph nodes were observed in nearly all cases, regardless of whether there was an abundance or dearth of intratumoral lymphatic vessels. Therefore, we concluded that lymphangiogenesis was unnecessary for tumor-to-lymph node metastasis.

In the absence of lymphangiogenesis, then, how did tumor cells reach the lymph nodes? Work by others had previously shown that intratumoral lymphatics were non-functional [Padera et al., 2002; Padera et al., 2004], suggesting that the peritumoral lymphatics at the tumor periphery were the main routes of egress for metastasis. We explored this possibility by examining orthotopic tumors at an earlier stage, before the onset of metastasis, when individual microscopic tumor foci were still surrounded by prostatic stromal tissue at the primary site. We observed that while we were successful at inhibiting intratumoral lymphatics, the abundance of peritumoral lymphatics was unchanged between our experimental and control tumors. These results suggest that peritumoral lymphatics that likely pre-existed in the prostate prior to tumor implantation—and not induced, intratumoral lymphatics—mediated the dissemination of metastatic cells.

We next turned again to the TRAMP spontaneous model of prostate cancer to try and validate our xenograft results. We observed that TRAMP prostate primary tumors, which frequently metastasize to lymph nodes, possessed few intratumoral lymphatics and likely did not induce lymphangiogenesis. Indeed, lymphatics were present specifically outside the luminal areas where tumors arose and did not infiltrate into malignant regions. These findings, in concordance with our previous results and with recent reports by others who noted that lymphangiogenesis does not occur in human clinical prostate, breast and pancreatic cancer [Sipos et al., 2005; Trojan et al., 2004; Vleugel et al., 2004], suggest that only peritumoral lymphatics are necessary for lymph node metastasis.

Thus, this thesis has answered, at least in part, two specific, though inter-related, questions regarding how prostate cancer spreads throughout the body. We identified Protein 4.1B as a gene that potentially suppresses prostate cancer progression and metastasis. We also determined that tumors likely utilize peritumoral lymphatics to disseminate to draining lymph nodes. A third question which was posed earlier in this chapter—that is, how tumor cells enter blood circulation—could not be answered because we were ultimately unable to inhibit lymphatic metastasis. Therefore, we were unable to test the hypotheses we formulated to explain the apparent association observed between hematogenous and lymphatic dissemination. How these hypotheses might be tested in future work is discussed below.

Future Work

In many ways, the work described in this thesis remains ongoing. Although we have shown that loss of 4.1B was associated with reduced apoptosis and increased tumor aggressiveness *in vivo*, a major unresolved question remains regarding the mechanism by which this protein functions in the cell. The development of an *in vitro* assay to assess 4.1B function will surely be a critical step forward, and this has become the major focus of our current studies. We have subjected tumor cells expressing high or low levels of 4.1B to various apoptotic stimuli, including serum starvation, staurosporine, and cycloheximide/TNF- α treatment, but in no cases have we seen significant differences in response. These cells also appear to undergo anoikis at similar rates. As 4.1B overexpression experiments have been reported to induce caspase-8-mediated cell death [Jiang and Newsham, 2006], and loss of this caspase has also recently been shown to be important for metastasis and for avoidance of unligated integrin-mediated cell death [Stupack et al., 2006], we are planning to focus more of our studies on this pathway. For instance, we are planning to assay cellular responses to FasL and TRAIL, two ligands which induce caspase-8-mediated apoptosis. In addition, it might be informative to examine the morphology and apoptosis rates of our cells when grown in three-dimensional cultures that might better recapitulate *in vivo* conditions.

We are also trying to approach this problem from a biochemical angle. As mentioned previously in this thesis, in order to determine the function of 4.1B, it will be important to link this protein with a signaling pathway. Efforts towards this end have already revealed that 4.1B interacts with integrin $\beta 8$ in prostate cancer, although the biological significance of this interaction remains unclear. Current work is focused on determining whether the presence or absence of 4.1B has effects on the abundance and/or the activation status of the ERM proteins. Indeed, 4.1B has been reported to interact with all members of this family, including merlin; however, the outcomes of these interactions are unknown [Sun et al., 2002]. We are planning experiments to determine, firstly, if these interactions can be confirmed in prostate cancer, and secondly, to assess whether these interactions might be meaningful. For instance, one experiment will involve stimulating our cells with a cytokine such as EGF and then determining whether phosphorylation levels of the ERM proteins are affected by the presence or absence 4.1B. This can readily be accomplished using antibodies that specifically detect the phosphorylated versions of these proteins. We are also interested in determining whether 4.1B has effects on the Rho pathway. It is interesting to note that both integrin $\beta 8$ and ERM proteins have been reported to bind Rho-GDI- α [Bretscher et al., 2002; Lakhe-Reddy et al., 2006], and it is therefore possible that 4.1B might regulate Rho activity through this protein. Finally, 4.1B has been reported to interact with CD44, a hyaluronan receptor that has been widely implicated in tumorigenesis, and the functional significance of this interaction will need to be explored further [Robb et al., 2005].

There are also some lingering questions regarding the *in vivo* role of 4.1B during tumor progression and metastasis, and some of these questions might be answered through analysis of additional animals. In our TRAMP spontaneous tumor studies, we observed that loss of 4.1B protected Grade 4 precursor prostatic lesions from apoptosis at 22 weeks of age, and this may have contributed to enhanced progression to malignancy. A more thorough study still remains to be performed comparing prostatic lesions of other grades to determine if 4.1B might also be acting during some of the earlier or later stages of tumor progression. Similarly, apoptosis studies should be performed on lymph node metastases from 4.1B-heterozygous and knock-out TRAMP mice.

As we have noted that 4.1B is significantly downregulated in prostate tumors relative to normal tissues, in four studies of human clinical prostate cancer, it will be important in future work to confirm these findings at the protein level. In collaboration with Dr. Marc Barry, working in Dr. Mark Rubin's laboratory at Harvard, we began a preliminary immunohistochemical study by probing for 4.1B protein in human prostate tissue arrays. In most cases, we observed strong staining of malignant luminal areas of the prostate; however, there was no correlation between intensity of staining and tumor severity, based on a limited number of samples observed. It is likely that background staining may have obscured our results, as our 4.1B antibodies are known to detect non-specific human proteins by Western blot. In fact, we have found that our 4.1B antibodies are useful for immunofluorescence only when probing mouse cells such as TRAMP, but not human cells like PC-3. Therefore, in order to determine whether 4.1B protein levels are downregulated in human prostate cancer, it will either be necessary to generate a cleaner antibody, or to obtain total protein lysates for Western blot analysis.

In the case of our lymphatic studies, as mentioned above, we were unsuccessful at blocking lymph node metastasis, and, therefore, we were unable to test our models regarding how tumor cells enter blood circulation. Although it may be informative to examine why our experimental approaches failed to inhibit peritumoral lymphatics, perhaps a more interesting and important problem is to determine whether there are alternative approaches that can be taken to test our original hypotheses. One possibility we have considered is to remove the draining para-aortic lymph nodes from mice prior to surgical implant of tumors. The reasoning is that, if the formation of macrometastases at this site were important for systemic dissemination of tumor cells, the physical removal of these nodes might prevent metastasis to distant organs such as the lung. While it is unclear how tumor cells might behave in the presence of lymphatics but in the absence of lymph nodes, our ability to inhibit lymphatic spread could be assessed by examining the para-renal lymph nodes, which are more distant from the prostate and also appear to be necessary for systemic spread. Certain controls would also be needed to ensure that removal of the draining lymph nodes did not significantly affect the immune system, particularly the composition and abundance of immune cells within the primary tumor. In addition, it would also be necessary to confirm that the lymphatics present in the prostate are unaffected by lymph node removal.

Perhaps a more complicated experiment might entail mixing tumor cells that expressed a series of readily detectable and distinguishable markers, such as fluorescent tags or genomic bar-codes. It would then be possible to perform relationship studies among tumor cells isolated from the primary tumor, lymph nodes, blood and lung. For instance, if hematogenous spread were dependent on lymphatics, the systemic metastases should resemble tumor cells in the lymph nodes more closely than those in the primary tumor. If the opposite were true—that hematogenous spread occurred directly from the primary tumor and independently of lymphatic metastasis—then the systemic and lymphatic metastases would not be expected to resemble one another¹. Obviously, the exact approach and controls needed for experiments such as these would require careful thought and planning.

Concluding Remarks

The results from this thesis have contributed small pieces of knowledge to our overall understanding of the problem of cancer metastasis. We have examined the genetic basis of this complex process and have experimentally implicated one gene as a negative regulator of metastasis. We have also studied the mechanistic aspects of tumor cell dissemination, and determined how some of the earliest steps of the process are completed. In both instances, there is supporting human clinical data to validate our results in prostate cancer and, perhaps, in other tumor types as well. This is, in many ways, generally reassuring, that results obtained in the mouse also appear to be applicable in humans. Whether this is truly the case remains to be seen, as future work in the field of cancer metastasis will certainly allow us one day to understand, in far greater detail, the genetic and mechanistic basis of this elaborate and important disease process.

¹ This would be the expected result if metastasis, in least in this experimental system, were a rare and perfectly stochastic occurrence.

REFERENCES

- Alitalo K, Tammela T, Petrova TV (2005): Lymphangiogenesis in development and human disease. *Nature* 438:946-953.
- Brekken RA, Puolakkainen P, Graves DC, Workman G, Lubkin SR, Sage EH (2003): Enhanced growth of tumors in SPARC null mice is associated with changes in the ECM. *The Journal of Clinical Investigation* 111:487-495.
- Bretscher A, Edwards K, Fehon RG (2002): ERM proteins and merlin: integrators at the cell cortex. *Nature Reviews Molecular Cell Biology* 3:586-599.
- Bubendorf L, Schopfer A, Wagner U, Sauter G, Moch H, Willi N, Gasser TC, Mihatsch MJ (2000): Metastatic patterns of prostate cancer: an autopsy study of 1,589 patients. *Human Pathology* 31:578-582.
- Charboneau AL, Singh V, Yu T, Newsham IF (2002): Suppression of growth and increased cellular attachment after expression of DAL-1 in MCF-7 breast cancer cells. *International Journal of Cancer* 100:181-188.
- Cianfrocca M, Goldstein LJ (2004): Prognostic and predictive factors in early-stage breast cancer. *The Oncologist* 9:606-616.
- Framson PE, Sage EH (2004): SPARC and tumor growth: where the seed meets the soil? *Journal of Cellular Biochemistry* 92:679-690.
- He Y, Kozaki K, Karpanen T, Koshikawa K, Yla-Herttuala S, Takahashi T, Alitalo K (2002): Suppression of tumor lymphangiogenesis and lymph node metastasis by blocking vascular endothelial growth factor receptor-3 signaling. *Journal of the National Cancer Institute* 94:819-825.
- Jiang W, Newsham IF (2006): The tumor suppressor DAL-1/4.1B and protein methylation cooperate in inducing apoptosis in MCF-7 breast cancer cells. *Molecular Cancer* 5:1-8.
- Koblinski JE, Kaplan-Singer BR, VanOsdol SJ, Wu M, Engbring JA, Wang S, Goldsmith CM, Piper JT, Vostal JG, Harms JF, Welch DR, Kleinman HK (2005): Endogenous osteonectin/SPARC/BM-40 expression inhibits MDA-MB-231 breast cancer cell metastasis. *Cancer Research* 65:7370-7377.
- Lakhe-Reddy S, Khan S, Konieczkowski M, Jarad G, Wu KL, Reichardt LF, Takai Y, Bruggeman LA, Wang B, Sedor JR, Schelling JR (2006): Beta8 integrin binds Rho GDP dissociation inhibitor-1 and activates Rac1 to inhibit mesangial cell myofibroblast differentiation. *JBC* 281:19688-99.
- Padera TP, Kadambi A, Tomaso Ed, Carreira CM, Brown EB, Boucher Y, Choi NC, Mathisen D, Wain J, Mark EJ, Munn LL, Jain RK (2002): Lymphatic metastasis in the absence of functional intratumor lymphatics. *Science* 296:1883-1886.
- Padera TP, Stoll BR, Tooredman JB, Capen D, Tomaso Ed, Jain RK (2004): Pathology: cancer cells compress intratumour vessels. *Nature* 427:695.
- Puolakkainen PA, Brekken RA, Muneer S, Sage EH (2004): Enhanced growth of pancreatic tumors in SPARC-null mice is associated with decreased deposition of extracellular matrix and reduced tumor cell apoptosis. *Molecular Cancer Research* 2:215-224.
- Robb VA, Gerber MA, Hart-Mahon EK, Gutmann DH (2005): Membrane localization of the U2 domain of protein 4.1B is necessary and sufficient for meningioma growth suppression. *Oncogene* 24:1946-1957.
- Sipos B, Kojima M, Tiemann K, Klapper W, Kruse ML, Kalthoff H, Schniewind B, Tepel J, Weich H, Kerjaschki D, Kloppel G (2005): Lymphatic spread of ductal pancreatic adenocarcinoma is independent of lymphangiogenesis. *Journal of Pathology* 207:301-312.
- Stupack DG, Teitz T, Potter MD, Mikolon D, Houghton PJ, Kidd VJ, Lahti JM, Cheresch DA (2006): Potentiation of neuroblastoma metastasis by loss of caspase-8. *Nature* 439:95-9.
- Sun CX, Robb VA, Gutmann DH (2002): Protein 4.1 tumor suppressors: getting a FERM grip on growth regulation. *Journal of Cell Science* 115:3991-4000.
- Tran YK, Bogler O, Gorse KM, Wieland I, Green MR, Newsham IF (1999): A novel member of the NF2/ERM/4.1 superfamily with growth suppressing properties in lung cancer. *Cancer Research* 59:35-43.

- Trojan L, Michel MS, Rensch F, Jackson DG, Alken P, Grobholz R (2004): Lymph and blood vessel architecture in benign and malignant prostatic tissue: lack of lymphangiogenesis in prostate carcinoma assessed with novel lymphatic marker lymphatic vessel endothelial hyaluronan receptor (LYVE-1). *The Journal of Urology* 172:103-107.
- Vleugel MM, Bos R, Groep Pvd, Greijer AE, Shvarts A, Stel HV, Wall Evd, Diest PJv (2004): Lack of lymphangiogenesis during breast carcinogenesis. *Journal of Clinical Pathology* 57:746-751.
- Yi C, McCarty JH, Troutman SA, M.S.Eckman, Bronson RT, Kissil JL (2005): Loss of the putative tumor suppressor Band 4.1B/Dal1 gene is dispensible for normal development and does not predispose to cancer. *Molecular and Cellular Biology* 25:10052-10059.
- Yiu GK, Chan WY, Ng SW, Chan PS, Cheung KK, Berkowitz RS, Mok SC (2001): SPARC (secreted protein acidic and rich in cysteine) induces apoptosis in ovarian cancer cells. *American Journal of Pathology* 159:609-622.

APPENDICES

A. MATERIALS & METHODS

B. SURGICAL ORTHOTOPIC IMPLANTATION

C. PREPARATION OF RNA FOR MICROARRAY ANALYSIS

D. STAINING BLOOD AND LYMPHATIC VESSELS

E. MICROARRAY RESULTS

F. PUBLICATIONS

APPENDIX A. MATERIALS & METHODS

CELL LINES

PC-3 cells were obtained from American Type Culture Collection (ATCC, Manassas, VA) and cultured in F-12K medium (Kaign's modification, Gibco-Invitrogen, Frederick, MD) containing 10% fetal bovine serum (FBS), glutamine and antibiotics. Cells were passaged approximately every 5 days and released with 0.25% trypsin (Gibco-Invitrogen). Cell freezing was accomplished by re-suspending cells in 90% complete medium, 5% FBS and 5% dimethyl sulfoxide (DMSO) Hybri-Max (Sigma-Aldrich; St. Louis, MO). Derivation of PC-3 metastatic variants is described below, and all cells were cultured in complete PC-3 medium. PC-3M cells were obtained from the lab of Dr. Isaiah J. Fidler (M. D. Anderson Cancer Center, Houston, TX). TRAMP-C1 and -C3 cells were obtained from ATCC and cultured in Dulbecco's modified Eagle's medium with high glucose containing 5% FBS, 5% fetal Nu-serum IV (Becton Dickinson, San Diego, CA), 5 ug/ml insulin and 10 nM dihydrotestosterone. These cells were frozen in 95% complete medium containing 5% DMSO. Phoenix cells (ATCC) were cultured in Modified Eagle Medium (DME) supplemented with HEPES, 10% FCS, glutamine and antibiotics. These were frozen in 50% complete medium, 40% fetal calf serum (FCS) and 10% DMSO. Single cell clones of PC-3 and TRAMP-C1 were isolated by plating cells at a concentration of 0.3 cells per well in 24-well tissue culture plates.

MOUSE TUMOR MODELS

Subcutaneous Injections and Growth Curves

PC-3 cell lines were grown to near-confluence in T-175 cell culture flasks, removed by trypsin and collected in 50 ml conical tubes. The cells were pelleted by centrifugation and washed once with normal growth medium, followed by two washes with chilled PBS buffer. Subsequently, cell numbers were quantitated by hemocytometer, and the final pellet was re-suspended in chilled PBS at a concentration of 4×10^7 cells/ml and moved into a 5 ml polystyrene round-bottom tube (Becton Dickinson). Four- to five-week-old CD-1 nude immunodeficient mice (Charles River Laboratories, Wilmington, MA) were anesthetized by avertin/tribromethanol (Sigma) intraperitoneal injection and lain on their side within a fume hood. The cell suspension was mixed in the tube and drawn up into the barrel of a 1 ml syringe, which was subsequently capped with a 16-gauge needle (Becton Dickinson). The area of injection—underneath the skin adjacent to the armpit of the left front paw—was cleaned with alcohol prep pads (Dynarex Corporation, Orangeburg, NY), after which the needle was inserted and 50 ul of cell suspension (2×10^6 cells) were injected. Formation of a "bleb," or bump, at the site of injection was indicative of a successful injection. For growth curves, the tumors were measured by calipers every three days for approximately three weeks following injection. The two-dimensional length and height of the tumor were recorded, and tumor volume was estimated by the equation: $\text{volume} = 0.5 \times d^2 \times D$, where "d" was equivalent to the shorter of the two measurements, and "D" was equivalent to the longer of the two measurements [Bartolazzi et al., 1995].

Surgical Orthotopic Implantation (SOI)

Subcutaneous tumors were removed for analysis and/or used as donor material for surgical orthotopic implantation (SOI) approximately 3.5 weeks after injection, as described previously [An et al., 1998; Chang et al., 1999]. Briefly, a peripheral portion of the tumor was removed and sliced into $\sim 1 \text{ mm}^3$ cubes under a dissecting microscope. CD-1 mice were anesthetized, and the abdominal regions exposed with an incision along the lower midline. A single tumor fragment was embedded into the right dorsolateral capsule and secured with 9-0 micro-sutures (Ethicon; Somerville, NJ). The peritoneum and overlying skin were each closed with one set of 5-0 sutures (United States Surgical; Norwalk, CT). The entire protocol was performed in sterile conditions inside a fume hood, in accordance with animal care guidelines. For detailed instructions regarding SOI, please refer to Appendix B.

Preservation of Organs and Analysis (for SOI)

Mice with orthotopic tumors were analyzed when moribund, as judged by bladder/abdominal distension and/or severe weight loss (typically 2-3 months after implantation). Tumors were removed from the mouse, cleaned and weighed on a balance. Portions of the tumor were then flash frozen in liquid nitrogen; fixed overnight in 3.7% formalin buffered in PBS; and/or fixed for 48 hours in Zinc Fixative IHC

solution (Becton Dickinson), depending on the experiment. Following fixation in formalin or zinc, tumors were transferred into 70% ethanol for storage. In most cases, visceral organs were fixed overnight in 3.7% formalin, following inflation of the lungs by injecting 1-2 ml of formalin through the mouse trachea. Bone material was separated from the visceral organs, cleaned and fixed for three weeks in Bouin's solution (Sigma), before being transferred into 70% ethanol. Lymph nodes were removed, fixed in formalin overnight and weighed after fixation. A lymph node set was considered macroscopically invaded if its total mass exceeded 30 mg (by histology, typically >80% of the node is tumor material at this size). Lymph node sets smaller than 30 mg could not be reliably weighed, and were given a mass of 10 mg and sectioned. Two sections at different levels were obtained for each node, percent invasion was scored blindly by a pathologist (Dr. Roderick T. Bronson, R.T.B.), and the higher of the two scores was recorded for each lymph node. To quantitate lung metastases, the five lobes of the lung were removed after fixation and randomly minced into ~20 pieces. These were then paraffin-embedded, sectioned for histology at three different levels, and stained by hematoxylin-eosin (H&E). The lung sections at each of the three levels were examined under microscopy. Tumor cells in the lung were clearly evident, often as small, dysplastic cell clusters bearing grossly expanded nuclei relative to the lung stroma. A single lung metastasis was defined as a cluster of at least 3 tumor cells, and the approximate size of each cluster was recorded: 3-5 cells; 6-10 cells; 11-20 cells; 21-50 cells; or greater than 50 cells. The number of lung metastases in each mouse was expressed as the sum total of micrometastases observed in the three sections.

Derivation of Cell Lines (for SOI)

At the time of sacrifice, mice were sprayed down with 70% ethanol. Sterile dissection scissors and forceps were used to remove the lobes of the lung. The tissue was placed over a 70 μ m nylon cell strainer (Becton Dickinson), and, together, these were placed in a 60 mm tissue culture plate containing complete PC-3 media. Cell straining was accomplished by working the back (blunt) end of a pair of sterile forceps against the tissue into the nylon mesh. This was done repeatedly until the lung material was mostly dissociated. The entire procedure was performed in a sterile fume hood, and cells were grown under normal tissue culture conditions.

Quantitation of Circulating Blood Tumor Cells (for SOI)

Immediately after sacrifice, the tumor-bearing mouse was placed ventral-side up in a fume hood and cleaned with alcohol wipes. Approximately 0.5-1.0 ml of blood was withdrawn by cardiac puncture from the right ventricle of the heart, using a 1 ml syringe capped with a 16-gauge needle, inserted at a 30 degree angle into the right lower portion of the rib cage. The blood was immediately transferred into a Vacutainer (Becton Dickinson) blood collection tube and mixed. From this, 100 μ l of blood was removed and divided between two 10 cm^2 plates containing 10 ml of normal PC-3 cell culture medium. These cultures were then incubated, undisturbed, for seven days. Afterwards, the plates were gently washed twice with PBS containing calcium/magnesium to remove the unattached red blood cells and debris. The remaining cells were fixed on the plate with 3.7% formalin and stained with 0.1% crystal violet solution for 20 minutes. The dye was subsequently removed, and the plates were washed three times with PBS. Individual tumor colonies appeared as macroscopic spots on the plate, and each colony was confirmed by visual inspection under a light microscope. The number of confirmed cell colonies was added for the two plates and expressed as the number of tumor cells circulating in 100 μ l of mouse blood at the time of sacrifice.

Immunohistochemistry – Blood Vessels and Lymphatics

For immunohistochemistry, 2-3 mm thick portions were removed near the periphery of the anterior-facing end of the tumor. For wild-type and TRAMP prostates, the dorsolateral lobes were dissected. In most cases, the tissue was fixed in zinc (Becton Dickinson) for 48 hours. For short-term orthotopic analysis, prostate tissue was fixed in 3.7% formalin overnight. Primary antibodies for immunohistochemistry included rabbit anti-LYVE-1 (Ruoslahti lab; 1:450)[Laakkonen et al., 2002], goat anti-mouse VEGFR-3 (Clone AF743, R&D Systems, Minneapolis, MN; 1:25) and rat anti-CD34 (Clone RAM34; Becton Dickinson-Pharmingen; 1:25). Sections were de-waxed, microwaved in Retrieval buffer (Becton Dickinson), and stained using standard protocols. Biotin-conjugated secondary antibodies included swine anti-rabbit Ig (Dako, Glostrup, Denmark) and rabbit anti-rat Ig (Vector Labs; Burlingame, CA), both diluted 1:250. Staining was amplified with Vectastain ABC kit (Vector Labs), developed with Vector VIP

peroxidase substrate and counter-stained with methyl-green. Lymphatic and blood vessels were quantitated by counting the number of LYVE-1- or CD34-positive vessels, respectively, in two random, low-power fields (2.25 mm X 1.7 mm) per tumor. About 30-100% of the tumor area is covered with this approach, and the LVD from a minimum of seven independent tumors was typically quantitated for each cell line. In TRAMP and normal prostates, a single low-power field was used for lymphatic quantitation, typically covering 70-100% of the sample. TRAMP tumor grading was based on a system described by Hurwitz et al [Hurwitz et al., 2001]. Two pathologists (Dr. Marc Barry (M.B.) and R.T.B.) independently graded H&E TRAMP sections, and then together arrived at an agreed-upon grade. For short-term SOI analysis, the length of the tumor periphery at 105X final magnification was quantitated in pixel units by OpenLab software (Improvision Inc.; Lexington, MA), and the number of lymphatics at the periphery was normalized to a 1,000 pixel perimeter. We defined "intratumoral" lymphatics as LYVE-1-positive vessels completely surrounded by tumor cells, and "marginal" or "peritumoral" lymphatics as vessels in contact with both tumor cells and stroma. For detailed instructions for staining vasculature, please refer to Appendix D.

TRAMP Mice

Prostate cancer-prone transgenic adenocarcinoma of the mouse prostate (TRAMP) mice expressing SV40 large T antigen in the prostate were generated by Dr. Norman Greenberg (Fred Hutchinson Cancer Research Center, Seattle, WA) [Greenberg et al., 1995] and obtained from Dr. Ailin Bai, from Dr. Jianzhu Chen's lab. The mice were maintained in a pure C57BL/6 background. 4.1B^{-/-} mice were generated by and obtained from Dr. Joseph Kissil (formerly at MIT, currently at the Wistar Institute, Philadelphia, PA) [Yi et al., 2005], and were back-crossed into a C57BL/6 background for 2-3 generations. SPARC^{-/-} mice were obtained from Dr. E. Helene Sage (Hope Heart Institute, Seattle, WA) [Norose et al., 2000] and were of a mixed background. Primer sequences for genotyping were as follows:

TRAMP:	TR-For	5'-CCGGTCGACCGGAAGCTTCCACAAGTGCATTTA-3'
	TR-Rev	5'-CTCCTTTCAAGACCTAGAAGGTCCA-3'
Casein:	Cas-For	5'-GATGTGCTCCAGGCTAAAGTT-3'
	Cas-Rev	5'-AGAAACGGAATGTTGTGGAGT-3'
4.1B:	G2	5'-CGCCACCGTCTGAGCAGC-3'
	G4	5'-GCACGTTTGGTAGCAGTTCCC-3'
	PURO-1300	5'-GCACGACCCCATGCATCG-3'
SPARC:	S-For	5'-TCTTTCTTGCAACCCTCTCC-3'
	S-Rev	5'-ATTCTCCCATTTCACCTGG-3'
Neomycin:	Neo-For	5'-CTTGGGTGGAGAGGCTATTC-3'
	Neo-Rev	5'-AGGTGAGATGACAGGAGATC-3'

For detection of the TRAMP transgene, the TR-For, TR-Rev, Cas-For and Cas-Rev primers was combined equally, and genomic DNA from mouse ears was amplified with the PCR cycles enumerated below. The casein positive control should yield an amplification product of 500 bps., while the TRAMP transgene should yield a product of 600 bps.

TRAMP/Cas	Step 1.	94 degrees Celsius, 10 min.
	Step 2.	94 degrees Celsius, 1 min.
	Step 3.	60 degrees Celsius, 2 min.
	Step 4.	72 degrees Celsius, 3 min.
	Step 5.	<i>Repeat steps 2-4, 30 cycles</i>
	Step 6.	72 degrees Celsius, 5 min.

For detection of 4.1B, a combination of the G2 + G4 primers should yield an amplification product of 300 bps. for wild-type, but no amplification product for the knock-out allele. A combination of the G2 and PURO-1300 primers should yield an amplification product of 700 bps. for the knock-out allele, and no

amplification product for wild-type. In most cases, based on our mating scheme (which generated either 4.1B heterozygous or knock-out mice), we multiplexed the G2, G4, TR-For, TR-Rev, Cas-For and Cas-Rev primers in a single reaction using TRAMP amplification cycles. Heterozygous mice yielded an amplification product of 300 bps.; knock-out mice yielded no amplification product.

4.1B	Step 1.	94 degrees Celsius, 10 min.
	Step 2.	92 degrees Celsius, 2 min.
	Step 3.	54 degrees Celsius, 1 min.
	Step 4.	72 degrees Celsius, 45 sec.
	Step 5.	<i>Repeat steps 2-4, 30 cycles for G2/G4; 34 cycles for G2/Puro</i>
	Step 6.	72 degrees Celsius, 10 min. <i>(The TRAMP/Cas amplification cycles can also be used)</i>

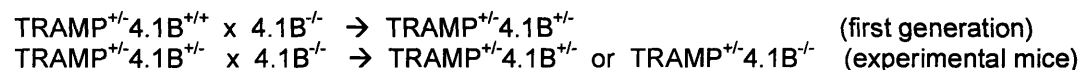
For detection of SPARC, a combination of the S-For, S-Rev, Neo-For and Neo-Rev primers were used. After amplification with the cycles enumerated below, SPARC wild-type DNA should yield a product of 121 bps; heterozygous DNA, 121 and 280 bps; and knock-out DNA, 280 bps. In practice, wild-type DNA also often yielded a weak amplification product of size 280 bps, as shown below:

	SP ^{+/+}	SP ^{+/-}	SP ^{-/-}
280 bps	—	—	—
121 bps	—	—	—

The amplification cycles are enumerated below:

SPARC	Step 1.	94 degrees Celsius, 10 min.
	Step 2.	94 degrees Celsius, 20 sec.
	Step 3.	64 degrees Celsius, 30 sec.
	Step 4.	72 degrees Celsius, 35 sec.
	Step 5.	<i>Repeat steps 2-4, 4 cycles</i>
	Step 6.	94 degrees Celsius, 20 sec.
	Step 7.	62 degrees Celsius, 30 sec.
	Step 8.	72 degrees Celsius, 35 sec.
	Step 9.	<i>Repeat steps 6-8, 4 cycles</i>
	Step 10.	94 degrees Celsius, 20 sec.
	Step 11.	58 degrees Celsius, 30 sec.
	Step 12.	72 degrees Celsius, 35 sec.
	Step 13.	<i>Repeat steps 10-12, 29 cycles</i>
	Step 14.	72 degrees Celsius, 2 min.

The following mating scheme was used to generate male experimental 4.1B/TRAMP mice:



SPARC-TRAMP mice were generated in a similar manner. Mice were analyzed in their 26th week of age, or earlier if they appeared moribund. The urogenital system (bladder, seminal vesicles and all lobes of the prostate) was dissected in bulk and weighed. The para-aortic/lumbar lymph nodes and all visceral organs were also removed, and all organs were preserved in either formalin or zinc fixative. Individual ventral or dorsal lobes of the prostate were later isolated under a dissecting microscope, sectioned for histology and stained by H&E. All prostate sections were graded on a scale of 1-6, according to the system described by Hurwitz et al, and were evaluated by R.T.B. and M.B.[Hurwitz et al., 2001]. All grading was performed blindly, using coded sections. In all cases, palpable tumors were found by histology to consist of undifferentiated Grade 6 carcinomas. In two cases, non-palpable microscopic foci of Grade 6 carcinoma were detected upon sectioning. For each section, a highest grade was assigned based on the area of greatest pathological severity in each section. A predominant grade was assigned based on the most common grade seen in each section.

MMTV Mice

Mammary carcinoma-prone polyoma middle T (PyMT or MMTV) mice expressing SV40 large T antigen in the mammary glands were obtained from Dr. Lei Xu. The mice were obtained in an FVB background and genotyped using MMTV primer sets with the aid of ReddyMix PCR Master Mix (AbGene, Rochester, NY). Primer sequences and PCR conditions are described below:

MMTV:	IMR0384	5'-GGAAGCAAGTACTTCACAAGGG-3'
	IMR0385	5'-GGAAAGTCACTAGGAGCAGGG-3'
	Step 1.	94 degrees Celsius, 4 min.
	Step 2.	94 degrees Celsius, 30 sec.
	Step 3.	62 degrees Celsius, 30 sec.
	Step 4.	72 degrees, Celsius, 30 sec.
	Step 5.	<i>Repeat steps 2-4, 31 cycles</i>
	Step 6.	72 degrees, Celsius, 5 min.

The presence of the MMTV transgene results in an amplification product of 550 bps. MMTV mice deficient or heterozygous for SPARC were generated in the following mating scheme:



Beginning in their 10th week of age, mice were visually inspected twice a week for macroscopic tumors in any of their ten mammary glands. Mice were sacrificed and analyzed four weeks after the date when the first macroscopic tumor was detected. Each of the mammary glands was removed and weighed, then fixed in formalin. The lungs were inflated and preserved in formalin, and macroscopic lung metastases were counted under a dissecting microscope.

Proliferation, Apoptosis, Cytokeratins and STEAP

Zinc-fixed prostate lobes from TRAMP mice, and formalin-fixed lymph nodes from mice implanted by SOI were stained with Ki67 antibody (Sigma) for proliferation and/or by TUNEL for apoptosis (ApopTag Plus apoptosis detection kit, Chemicon, Temecula, CA). Grade-, age- and lobe-matched TRAMP sections were quantitated by counting the number of positively stained cells, as well as the total number of cells, from two different fields per section imaged at 20X magnification, except for Grade 5 sections, which were imaged at 40X magnification. Grade 4 sections were all derived from the ventral lobes of the prostate, while Grade 5 sections were all derived from dorsolateral lobes. All staining, image capturing with OpenLab 5.0.0 software (Improvision), and quantitation were blindly performed, using 4-5 independent prostate samples per genotype. For cytokeratin staining, zinc-fixed prostate or formalin-fixed lymph node sections were stained with rat anti-cytokeratin 8 antibody (clone TROMA-1, 1:250, which detects luminal cells), originally developed by Brulet et al. (Developmental Studies Hybridoma Bank, Iowa City, IA)[Brulet et al., 1980]; and/or with rabbit anti-cytokeratin 5 antibody (1:5,000, detects basal cells) (Covance, Princeton, NJ). Rabbit anti-STEAP antibody (Zymed Laboratories, San Francisco, CA) was used at a dilution of 1:100.

MOLECULAR BIOLOGY**Overexpression Plasmids**

The human 4.1B coding sequence was originally inserted into pcDNA3.1/myc-His vector (Stratagene, Cedar Creek, TX) by Dr. Joseph McCarty (J.M., formerly at MIT, currently at M. D. Anderson Cancer Center), using the 5'-BamHI and 3'-XhoI restriction sites, as an in-frame fusion with the myc-His6 tag coding sequences at the 3' end. The human integrin β 8 coding sequence was inserted into pcDNA3.1/V5-His vector (Stratagene) by J.M., using the 5'-BamHI and 3'-XhoI restriction sites, as an in-frame fusion with the V5-His6 tag coding sequences at the 3' end. The Flt4-Ig expression plasmid (originally "VEGFR-3-Ig/pEBS7") was obtained from Dr. K. Alitalo (University of Helsinki, Helsinki, Finland)[He et al., 2002; Karpanen et al., 2001]. Ig-Neg control plasmid was made by removing the Flt4

coding sequence and re-annealing the empty vector. A plasmid expressing human VEGF-A (isoform 165, cDNA cloned between EcoRV and BamHI restriction sites), and containing LacZ and Hygromycin resistance marker ("H165Z") was obtained from Dr. P. D'Amore (Harvard Medical School, Boston, MA). In addition, an ecotropic receptor-expressing plasmid was obtained from Dr. H. Lodish, MIT. All transient and stable transfections were performed on adherent cells using Effectene reagent (Qiagen, Valencia, CA), according to manufacturer's protocols. In the case of Flt4-Ig/Ig-Neg, transfected cells were selected with 100-200 ug/ml Hygromycin for ~3 weeks for stable expression. For the ecotropic receptor, transfected cells were selected with 800 ug/ml of G418/neomycin for ~2-3 weeks.

Tet-Inducible Plasmids

For Tet-induction studies, a retroviral vector expressing trans-activator protein (MSCV-rtTA I-02G, obtained from Dr. Patrick Stern (P.S.)) was first transfected with Effectene reagent into Phoenix cells, from which retroviral supernatant was obtained and used to infect PC-#82 cells expressing ecotropic receptor. This vector has no selectable marker; instead, infected cells were sorted for GFP expression. The genes to be inducibly overexpressed were cloned into either the retroviral vector pRevTRE (Clontech, Mountain View, CA), which contains a hygromycin-resistance marker; or into the lentiviral vector "Tet-ON" (adapted by P.S. from pRevTRE), which contains a puromycin-resistance marker. The entire 4.1B-myc-His coding sequence was inserted into Tet-ON using the 5'-XmaI and 3'-EcoRI restriction sites to generate 4.1B-Tet-ON, while the entire β 8-V5-His coding sequence was inserted into pRevTRE using the 5'-BamHI and 3'-HpaI restriction sites to generate β 8-TRE. As controls, pRevTRE containing the luciferase coding sequence was obtained (Luc-TRE, Clontech) and Tet-ON containing the red fluorescence protein coding sequence was obtained from P.S. (RFP-Tet-ON). pRevTRE retrovirus generation involved transfection of the viral plasmid into Phoenix cells, as described previously. Tet-ON lentivirus generation utilized 293 cells from P.S. and involved co-transfection of the following lentiviral components (all obtained from P.S.) in the following ratios:

3 gag/pol : 2 VSVg-env : 1 RSV-rev : 6 Tet-On plasmid (2 ug total DNA)

Co-transfections were performed using Effectene reagent, and media were replaced after overnight incubation at 37 degrees Celsius. Lentivirus-containing supernatant was obtained after another 24-48 hours incubation at 37 degrees Celsius, and used for infection of PC-#82 cells expressing trans-activator protein. Cells infected with Tet-ON vectors were selected with 2.5 ug/ml puromycin for ~1-2 weeks, while those infected with pRevTRE vectors were selected with 400 ug/ml Hygromycin for ~3 weeks.

siRNA Plasmids and Sequences

All siRNAs were inserted into the retroviral vector pSIRISP (W.C. Hahn, Dana Farber Cancer Institute, Boston, MA)[Masutomi et al., 2003]. The siRNA plasmids were transfected with Effectene into Phoenix cells (ATCC), and the secreted virus was subsequently used for stable infection of PC3-#82 cells expressing ecotropic receptor. After infection, cells were selected on puromycin for stable siRNA expression. All siRNAs were synthesized as long oligonucleotides in the following hairpin configuration: forward oligo: 5'-CCGGT-(19 bp. sense)-TTCAAGAGA-(19 bp. anti-sense)-TTTTTG-3'; reverse oligonucleotide: 5'-AATTCAAAAA-(19 bp. sense)-TCTCTTGAA-(19 bp. anti-sense)-A-3'. The oligonucleotides were annealed and then inserted into the retroviral vector pSIRISP, digested with AgeI and EcoRI. The 19 base-pair siRNA sequences or controls used in this study were as follows:

Against human Protein 4.1B (only 19 bp. core sense sequences shown):

DL1: 5'-GCAATTAGAAGACGATAAA-3'
 DL2: 5'-CGAGCTGCCAAGCGTTTAT-3'
 DL3: 5'-TCTCGATGGATCAGAATAT-3'
 DL4: 5'-GCTCGAATATCAGCAATTA-3'

Against mouse Protein 4.1B (only 19 bp. core sense sequences shown)

mDL1: 5'-CCAGTGGTCTGTTGATATA-3'
 mDL2: 5'-CCAAAGTAGTAGTCCATAA-3'

mDL4: 5'-CGTGACCGGCTTCGAATAA-3'

Against human VEGF-C (only 19 bp. core sense sequences shown)

C13: 5'-ACTGGATGTTTACAGACAA-3'

C14: 5'-GTTTCATTCCATTATTAGAC-3'

C14-MM: 5'-GTTTCATTCCACCATTAGAC-3'

Against human VEGF-A (only 19 bp. core sense sequences shown)

A2: 5'-GTGAATGCAGACCAAAGAA-3'

A3: 5'-GGAGTACCCTGATGAGATC-3'

A3-MM: 5'-GGAGTACCCACATGAGATC-3'

Against GFP (negative control, only 19 bp. core sense sequences shown)

GFP: 5'-CAAGCTGACCCTGAAGTTC-3'

Real-time PCR / RNA Quantitation

Total RNA was extracted using RNeasy (Qiagen). RNA was digested with DNase (Ambion; Austin, TX), then re-cleaned with RNeasy. 1 ug of total RNA was reverse-transcribed into cDNA using TaqMan Reverse Transcription Reagent (Applied Biosystems; Branchburg, NJ). cDNAs were analyzed by quantitative PCR using SYBR Green PCR amplification kit (Applied Biosystems), measured in a Biorad iCycler (Hercules, CA). Target-gene message levels were normalized to GAPDH levels, and then to the control sample. The following primer pairs were used for real-time PCR:

Human 4.1B:	Forward	5'-GCACAGATCTGGAGCCAGGC-3'
	Reverse	5'-CTGGTCATGGTCAATGTCTGCA-3'
Human SPARC:	Forward	5'-GAGAGCGCGCTCTGCCTGCCG-3'
	Reverse	5'-CACCACCTCTGTCTCATCAGGC-3'
Human VEGF-C:	Forward	5'-GCCAATCACACTTCCTGCCGA-3'
	Reverse	5'-GTTGCTGCCTGACACTGTGG-3'
Human VEGF-A:	Forward	5'-CACTGAGGAGTCCAACATCAC-3'
	Reverse	5'-TTCTTGCTTTGCTCTATCTTTCTTG-3'
Human GADH:	Forward	5'-GGAAGGTGAAGGTCGGAGTC-3'
	Reverse	5'-CTGGAAGATGGTGTGATGGGATTC-3'

Extraction of Tumor RNA and Preparation of Biotinylated cRNA for Microarray Hybridization

Detailed instructions for preparing biotinylated cRNA for hybridization to Affymetrix U133A arrays can be found below in the "Bioinformatics" section and in Appendix C.

CELL BIOLOGY (IN VITRO)

Growth Curves

Growth curve experiments were performed in either of two ways. For doxycycline induction studies, 1,000 cells were plated on Day 0 in 6-well tissue culture plates. On Day 1, and every other day subsequently, medium +/- 3 ug/ml doxycycline (Clontech) was added. Manual cell counts by hemocytometer were performed 6-7 days after induction. Proliferation was also assessed using the CellTiter 96 proliferation reagent (Promega, Madison, WI) in 96 well plates, where 500 cells were plated on Day 0 and incubated in the presence or absence of serum or other medium components. Substrate formation as a function of cell density was assessed after 3 hours incubation at 37 degrees Celsius, with a VersaMax microplate reader (Molecular Devices, Sunnyvale, CA) at a wavelength of 490 nm. In some

cases, cell growth was confirmed by staining plates with crystal violet, similar to the method for detecting blood tumor colonies described previously.

Ploidy Experiments

Tissue culture cells were released with trypsin, washed with PBS and counted. 500,000 cells were pelleted and re-suspended in 1 ml of 70% ethanol, then incubated overnight at 4 degrees Celsius. The next day, the cells were pelleted and re-suspended in 1ml of fresh propidium iodide staining solution (10 mg/ml propidium iodide (Sigma) and 100 units/ml RNase A (New England Biolabs, Ipswich, MA) mixed in water), then incubated for 30 minutes at room temperature. Cells were then washed twice with PBS and analyzed by FACScan (Becton Dickinson).

Soft Agar Assay

In a 24-well plate, wells were coated with 500 ul of media containing 0.8% agar, and this was allowed to solidify at room temperature. Tissue culture cells were released with trypsin, and equalized to a concentration of 20,000 cells/ml. This suspension was mixed 1:1 with media containing 0.8% agar (final concentration = 0.4% agar), and 500 ul of this mix were plated over the denser base and allowed to solidify. Cell colonies were observed under a light microscope over a two-week period.

Immunofluorescence

For detection of 4.1B protein in TRAMP cells, cells were grown in 8-well Lab-Tek Permanox slides (Nalg Nunc International, Rochester, NY), fixed in 3.7% formalin, permeabilized with 0.3% Triton/PBS and probed with rabbit anti-4.1B-PE (1:1,500, 30 minutes at room temperature) (Protein Express, Chiba, Japan). Subsequently, the cells were probed with Alexa Fluor 488-conjugated goat anti-rabbit antibody (1:100, 30 minutes) (Molecular Probes-Invitrogen, Carlsbad, CA). For detection of the V5 and myc epitope tags, cells were prepared similarly to above and stained with mouse anti-V5 (1:1,000) or anti-myc (1:200) (Invitrogen), then detected with Alex Fluor 594-conjugated goat anti-mouse antibody (1:200) (Molecular Probes-Invitrogen). A rabbit antibody against the MHC Class I antigen HLA-A,B,C (Becton Dickinson) was used at a dilution of 1:100 to stain all human cells, while a monoclonal antibody against the MHC Class I antigen H-2Kb/H-2Db (Becton Dickinson) was used at a dilution of 1:100 to stain all mouse cells.

Inducible Overexpression

Normal growth medium containing 3 ug/ml of doxycycline was added to cells and replaced every 48 hours. Induced gene/protein expression was assayed, > 72 hours after induction.

BIOCHEMISTRY

Immunoblotting

Soluble Flt4-Ig was detected by immunoprecipitating conditioned media with Protein A beads (Invitrogen). The beads were spun, washed and boiled in Laemmli SDS buffer containing 5% β -mercaptoethanol (Sigma). The protein was run on 8% SDS gel and detected with goat anti-human VEGFR-3 antibody (Clone AF349; 1:100 diluted; R&D Systems) or rabbit anti-human antibody conjugated to horse-radish peroxidase (Dako; 1:1000 diluted). Tumor Flt4-Ig was detected in tumors by homogenizing in CellLytic-MT lysis buffer (Sigma), and running supernatant on SDS-PAGE. Antibodies against 4.1 Proteins used for Western blot included rabbit anti-4.1B (JM)[McCarty et al., 2005]; and rabbit anti-4.1B (PE), anti-4.1G and anti-4.1N (all diluted 1:500, Protein Express). Total soluble protein was extracted from tissue culture cells, or from homogenized frozen tumors or fresh tissue lysates, in NP-40 lysis buffer (50 mM Tris 7.4, 150 mM NaCl, 1% NP-40, 5 mM EDTA) containing protease inhibitor cocktail (Roche, Mannheim, Germany), then reduced in Laemmli buffer containing 5% β -mercaptoethanol, and separated by 8% SDS-PAGE. For SPARC, the monoclonal antibody ON1-1 (Zymed Laboratories) was utilized. Detection of epitope tags was accomplished with monoclonal antibodies against V5 or Myc (1:500, Invitrogen). The monoclonal GAPDH antibody was obtained from Chemicon. For total soluble protein quantitation, the Micro BCA Protein Assay kit (Pierce, Rockford, IL) was used.

VEGF-C and VEGF-A Protein Quantitation

5 X 10⁵ PC3-#82 cells were plated into 10 cm² plates and grown for 72 hours. Media were replaced, conditioned for the times specified, collected and spun to remove debris. Frozen subcutaneous and orthotopic tumors were thawed and homogenized in 1 ml cold CellLytic-MT lysis buffer per gram tumor material. Lysis buffer contained protease inhibitors (Roche). After homogenization, the lysate was chilled for > 30 minutes, then spun to remove debris. Total soluble protein was quantitated by BCA protein assay to normalize ELISA results. The supernatant was diluted 1:4 or 1:10 in PC-3 medium for ELISA. 200 ul of diluted tumor supernatant or undiluted conditioned media were analyzed by human VEGF-A Quantikine ELISA (R&D Systems); 100 ul of the same were analyzed by human VEGF-C ELISA (IBL, Tokyo, Japan).

Co-Immunoprecipitation (Co-IP) of Integrin β 8 and 4.1B

PC-3 #82-Eco cells were grown to ~60% confluence in a 10 cm² cell culture plate. The cells were then transiently co-transfected by Effectene reagent with two of the following plasmids (2 ug of DNA each, 4 ug total): 4.1B-myc-pcDNA3.1, integrin β 8-V5-pcDNA3.1, lacZ-myc-pcDNA3.1, 4.1B-CTD-myc-pTag3B and/or 4.1B-FERM-myc-pcDNA3.1. Transfections were performed according to manufacturer's directions, with the following modifications: DNA and EC transfection buffer were combined in a final volume of 400 ul, and 32 ul of Enhancer reagent and 100 ul of Effectene reagent were subsequently added to this mixture. Cells were cultured overnight at 37 degrees Celsius, after which the medium was replaced, and allowed to incubate for an additional 48 hours. Total cell lysates were extracted with 700 ul of NP-40 lysis buffer containing protease inhibitors. The lysates were cleared by centrifugation, and the supernatant was further pre-cleared by incubating with two rounds of unconjugated, equilibrated Protein-G agarose beads (Invitrogen) for one hour each at 4 degrees Celsius. Meanwhile, monoclonal antibodies against the V5-epitope tag were conjugated to equilibrated Protein-G agarose beads, using 2 ug of antibody per co-IP reaction. The antibody-conjugated beads were then added to the twice-pre-cleared protein supernatant and allowed to incubate overnight at 4 degrees, under steady rotation in a 1.5 ml Eppendorf tube (Eppendorf, Westbury, NY). The next day, the beads were pelleted by centrifugation and washed four times with PBS. After the final wash, the beads were resuspended in 30 ul of hot 2X Laemmli buffer containing 5% β -mercaptoethanol and boiled for 5 minutes. The sample was then electrophoresed in 8% or 13% SDS-PAGE gels; transferred to Protran BA85 nitrocellulose membrane (Whatman Inc, Florham Park, NJ); and probed using an anti-myc monoclonal antibody, diluted 1:500, and subsequently, with a horseradish peroxidase-conjugated anti-mouse secondary antibody, diluted 1:2,000.

BIOINFORMATICS

Microarrays and Bioinformatics

For a detailed description of the preparation of cRNA from tumor material, please refer to Addendix C. Briefly, total RNA was extracted from flash-frozen subcutaneous tumors (of approximate mass 130-250 mg) using the RNeasy Midi isolation kit (Qiagen). DNA contamination in the preparation was then removed by DNase digestion (Ambion), and the RNA sample was re-cleaned using the RNeasy Mini kit (Qiagen). Between 1-3 ug of total RNA was electrophoresed to check for sample integrity, as assessed by the relative intensity levels of the 26S and 16S RNA bands. Total RNA was reverse-transcribed using Superscript II reverse transcriptase (Invitrogen), primed with a poly-dT-24 primer, according to Affymetrix protocols. Second-strand synthesis was performed with DNA polymerase I (Invitrogen), also according to Affymetrix protocols. The resulting cDNA was purified using Qiagen's PCR purification kit. In vitro transcription was then performed using the ENZO BioArray RNA transcript labeling kit (Enzo Life Sciences, Farmingdale, NY), following standard protocols, which produced biotin-labeled cRNA. This cRNA was subsequently purified using the RNeasy mini kit, and the yield and quality were assessed. Finally, the cRNA was fragmented and submitted to the Biopolymers core facility for hybridization to U133A chips (Affymetrix, Santa Clara, CA). Hybridization intensity levels were assessed with the aid of a GeneArray 2500 scanner (Affymetrix). Data analysis was performed using D-Chip software (Harvard Medical School, Boston, MA) and, with the help of Dr. Steve Shen, using Gene Pattern 2.0.2 (The Broad Institute, Cambridge, MA). Oncomine analyses were performed on August 2006, using Oncomine 3.0 at www.oncomine.org (University of Michigan, Ann Arbor, MI).

Additional Gene Expression Data-Sets

In most cases, gene expression data from prostate cancer datasets were obtained from the OncoPrint website. In the case of the van't Veer et al. breast cancer study [Veer et al., 2002], gene expression results were obtained from Dr. Marcel Smid (Josephine Nefkens Institute, Rotterdam, The Netherlands) who had processed the data using the program Venn Mapper [Smid et al., 2003]. Additional human clinical patient data from that study were downloaded from the Rosetta Inpharmatics website: <http://www.rii.com/publications/2002/vantveer.html>. In the case of the Dhanasekaran et al. prostate cancer study [Dhanasekaran et al., 2001], gene expression data were downloaded from the Supplementary Info section at the *Nature* website: www.nature.com. The A375 melanoma gene expression data-set was obtained from Dr. Lei Xu from our lab. In some cases, visualization of gene expression from these data-sets was performed using Tree View 1.60 software (University of California Berkeley, Berkeley, CA).

Statistics

In most cases, statistics were performed using an unpaired Student's t-test (<http://www.physics.csbsju.edu/stats/Index.html>), except in the case of TRAMP tumor incidence data, which were assessed by Chi-Square (<http://www.psych.ku.edu/preacher/chisq/chisq.htm>). Box plots were generated after data entry online at: <http://www.physics.csbsju.edu/stats/Index.html>. All error bars shown, +/- SE.

REFERENCES

- An Z, Wang X, Geller J, Moossa AR, Hoffman RM (1998): Surgical orthotopic implantation allows high lung and lymph node metastatic expression of human prostate carcinoma cell line PC-3 in nude mice. *The Prostate* 34:169-174.
- Bartolazzi A, Jackson D, Bennett K, Aruffo A, Dickinson R, Shields J, Whittle N, Stamenkovic I (1995): Regulation of growth and dissemination of a human lymphoma by CD44 splice variants. *Journal of Cell Science* 108:1723-1733.
- Brulet P, Babinet C, Kemler R, Jacob F (1980): Monoclonal antibodies against trophectoderm-specific markers during mouse blastocyst formation. *PNAS* 77:4113-4117.
- Chang XH, Fu YW, Na WL, Wang J, Sun H, Cai L (1999): Improved metastatic animal model of human prostate carcinoma using surgical orthotopic implantation (SOI). *Anticancer Research* 19:4199-4202.
- Dhanasekaran SM, Barrette TR, Ghosh D, Shah R, Varambally S, Kurachi K, Pienta KJ, Rubin MA, Chinnaiyan AM (2001): Delineation of prognostic biomarkers in prostate cancer. *Nature* 412:822-826.
- Greenberg NM, DeMayo F, Finegold MJ, Medina D, Tilley WD, Aspinall JO, Cunha GR, Donjacour AA, Matusik RJ, Rosen JM (1995): Prostate cancer in a transgenic mouse. *PNAS* 92:3439-3443.
- He Y, Kozaki K, Karpanen T, Koshikawa K, Yla-Herttuala S, Takahashi T, Alitalo K (2002): Suppression of tumor lymphangiogenesis and lymph node metastasis by blocking vascular endothelial growth factor receptor-3 signaling. *Journal of the National Cancer Institute* 94:819-825.
- Hurwitz AA, Foster BA, Allison JP, Greenberg NM, Kwon ED (2001): The TRAMP mouse as a model for prostate cancer: "Current Protocols in Immunology." John Wiley & Sons, Inc., pp 20.5.1-20.5.23.
- Karpanen T, Egeblad M, Karkkainen MJ, Kubo H, Yla-Herttuala S, Jaattela M, Alitalo K (2001): Vascular endothelial growth factor C promotes tumor lymphangiogenesis and intralymphatic tumor growth. *Cancer Research* 61:1786-1790.
- Laakkonen P, Porkka K, Hoffman JA, Ruoslahti E (2002): A tumor-homing peptide with a targeting specificity related to lymphatic vessels. *Nature Medicine* 8:751-755.
- Masutomi K, Yu EY, Khurts S, Ben-Porath I, Currier JL, Metz GB, Brooks MW, Kaneko S, Murakami S, DeCaprio JA, Weinberg RA, Stewart SA, Hahn WC (2003): Telomerase maintains telomere structure in normal human cells. *Cell* 114:241-253.
- McCarty JH, Cook AA, Hynes RO (2005): An interaction between alpha(v)beta(8) integrin and Band 4.1B via a highly conserved region of the Band 4.1 C-terminal domain. *PNAS* 102:13479-13483.
- Norose K, Lo WK, Clark JI, Sage EH, Howe CC (2000): Lenses of SPARC-null mice exhibit an abnormal cell surface-basement membrane interface. *Exp Eye Res* 71:295-307.
- Smid M, Dorssers LC, Jenster G (2003): Venn Mapping: clustering of heterologous microarray data based on the number of co-occurring differentially expressed genes. *Bioinformatics* 19:2065-2071.
- Veer LJvt, Dai H, Vijver MJvd, He YD, Hart AA, Mao M, Peterse HL, Kooy Kvd, Marton MJ, Kitteveen AT, Schreiber GJ, Kerkhoven RM, Roberts C, Linsley PS, Bernards R, Friend SH (2002): Gene expression profiling predicts clinical outcome of breast cancer. *Nature* 415:530-535.
- Yi C, McCarty JH, Troutman SA, M.S.Eckman, Bronson RT, Kissil JL (2005): Loss of the putative tumor suppressor Band 4.1B/Dal1 gene is dispensible for normal development and does not predispose to cancer. *Molecular and Cellular Biology* 25:10052-10059.

APPENDIX B. SURGICAL ORTHOTOPIC IMPLANTATION (SOI)

December 1, 2006

All surgical tools are autoclaved or baked overnight prior to surgery, and all manipulations are performed under sterile conditions in a laminar flow hood. Preferably, keep a set of tools for surgery use only. The following materials are needed to prepare the tumor fragments for implantation (in most cases, these materials can be obtained from Samuel Perkins, Inc. (Quincy, MA)):

Dissecting microscope and light source
 3 pairs of Dumont jeweler's forceps (#5)
 1 pair of dissection scissors (RS-5910; Roboz, Germany)
 1 pair of standard forceps
 Bard-Parker disposable scalpels (#11) (Becton Dickinson)

F-12K medium (Kaign's modification, Gibco-Invitrogen)
 L-Glutamine (200 mM stock, Gibco-Invitrogen)
 HEPES buffer (1 M stock, Gibco-Invitrogen)
 Phosphate-buffered saline

2 buckets of ice
 4 60 mm² tissue culture plates
 1 Bunsen burner and lighter
 70% ethanol

Prior to the procedure, prepare the media as follows: combine 37.5 ml of F-12K medium, 0.5 ml of glutamine and 12 ml of HEPES. Fill three 60 mm² plates with PBS and one plate with media. Chill on ice. For all subsequent manipulations, sterilize dissecting tools by flaming. Following sacrifice of a subcutaneous tumor-bearing mouse, lay the animal tumor-side up and spray with ethanol to sterilize the dissection site. Pinch the skin above the center of the tumor using a pair of standard forceps and begin cutting away the skin underneath with a pair of dissection scissors. In most cases, the skin should separate easily from the rest of the tumor. Cut away the muscular tissue between the tumor and the rib cage, extract the tumor and deposit in one of the plates of PBS. All subsequent manipulations are visualized under a dissecting microscope set at low magnification. Clean the tumor of stray adipose, muscle and skin tissue using fine jeweler's forceps. Move the cleaned tumor into a second plate of PBS. In most cases, the tumor should be oval-shaped at this point. As shown in Figure A, make a cross-section cut through the tumor approximately 3-4 mm from one end. Afterwards, make a second cross-section cut 1 mm from the newly formed edge. What should result is a flat circular wedge, 1 mm thick. Confirm that the tissue appears healthy and free of discoloration, and move this wedge into the third plate of PBS. From this wedge, peel away the outer, fibrous capsular layer surrounding the periphery of the tumor using the jeweler's forceps. Next, grip the tumor with the forceps and use the scalpel to cut cubes of solid tumor material with dimensions of about 1 mm³. These cubes should then be moved into the final plate containing the media prepared above.

For surgical orthotopic implantation of these pieces, the following tools are needed:

1 stainless steel instrument tray
 3 pairs of Dumont jeweler's forceps (#5)
 2 pairs of dissection scissors (RS-5910; Roboz, Germany)
 2 pairs standard forceps
 1 pair of skin retractors (SC02; Roboz, Germany)
 1 pair Iris forceps (Half curved)
 1 Castroviejo needle holder (RS-6403; Roboz, Germany)

9-0 Ethilon black monofilament nylon sutures with a BV130-4 Tapered needle (#2813G, Ethicon)

5-0 Sofsilk braided silk sutures with a C-1 cutting needle
 (#S-1173, United States Surgical, Norwalk, Connecticut)

Dissecting microscope and light source
 Lab diapers
 Alcohol prep pads (Dynarex, Orangeburg, NY)
 PVA surgical spears (Allegiance Healthcare Corp., McGaw Park, IL).
 500 ml 70% ethanol
 Heating pad

1 ml syringes capped with 26-3/8 gauge needles (Becton Dickinson)
 Avertin/tribomethanol (Sigma)
 30 ug/ml Buphreneprine (MIT Division of Comparative Medicine)

Set up the surgical area. Place the instrument tray containing the surgical tools in the hood, as well as the microscope and light source. Place the heating pad on the microscope stage, and overlay with a lab diaper. Anesthetize the mouse (30-35 days of age) by intraperitoneal injection of avertin/tribomethanol¹. Wipe down the abdomen with alcohol pads and lay the animal on its back with its head facing towards you. Pinch and lift the outer skin, as shown in Figure B, with a pair of standard forceps and make a midline incision using dissection scissors until reaching the top of the Cowper's glands. Now pinch and lift the peritoneum layer in a similar manner and make a midline incision through this layer, exposing the visceral organs. Insert skin retractors underneath the peritoneum on both sides of the midline incision. Use surgical spears to gently lift out the urogenital system (Figure C). The dorsal prostate (DP) is a clear, glandular, triangular piece of tissue located just beneath the point where the seminal vesicles meet. The DP is deeply buried but should be lifted to face upwards during the dissection, and kept in place the entire time using surgical spears held in one hand.

Make a single 9-0 suture near the right edge of the right lobe of the DP (Figure D(a)). Next, use the jeweler's forceps to make a small pocket in the tissue (yellow oval), adjacent to the site of the suture (Figure D(b)). This is accomplished by working the tip of the forcep back and forth against the tissue until a small gap forms. Next, use the forceps to insert the tumor fragment into the pocket (Figure D(c)), burying it inside the prostate tissue (Figure D(d)). Take hold of the free end of the needle attached to the 9-0 suture, and make a second suture on the other side of the implant (Figure D(e)). Ideally, the suture should cross over the middle of the pocket containing the implant. Finally, take hold of both free ends of the suture and draw the two ends together (Figure D(f)). The tissue to each side of the implant should come together (arrows). Secure with a knot, as depicted in Figure D(g) and D(h). A side view of this procedure, before and after the implant is secured, is shown in Figure D(i) (beige - prostate; gray - tumor; red - suture; arrow-head - needle).

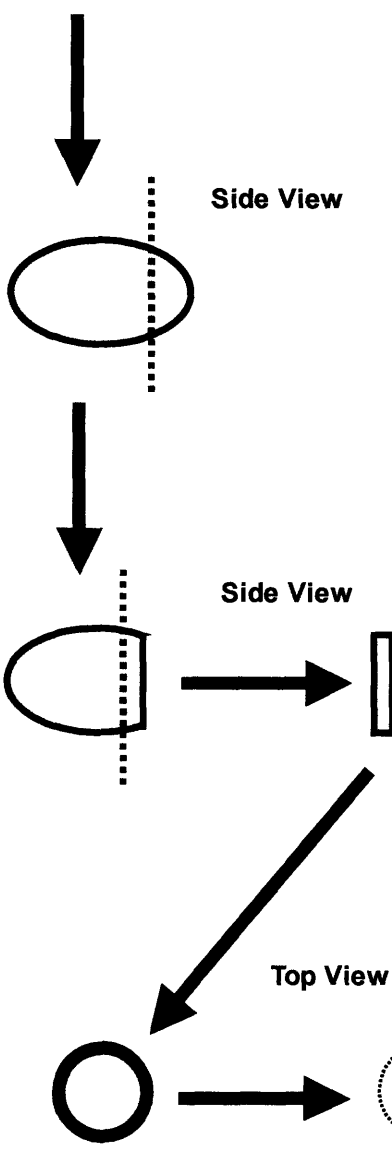
After implanting the tumor, use surgical spears to push the visceral organs back into the abdomen. Close the inner peritoneum layer using a row of 5-0 sutures. Drip buphreneprine along the wound site, and subsequently, close the overlying skin layer using a second row of 5-0 sutures. Wipe down the surgical site with alcohol pads and return the mouse to its cage. Sterilize all tools by soaking in ethanol in between mice. Check the health of implanted animals 24 and 48 hours post-surgery and, if needed, apply additional buphreneprine.

¹ It is critically important that a minimal volume of avertin/tribomethanol is used, and that the preparation is made fresh and filtered prior to use. Older stocks of anesthesia often precipitate, and, following surgery, mice seem especially susceptible to intestinal dysfunction as a consequence of using old or excessive avertin.

Figure A



CD-1 nude mouse 3-4 weeks after injection of a subcutaneous tumor.



Remove the subcutaneous tumor from the mouse and clean. Make a cross-section cut through the tumor, ~3 mm from the end.

Make a second cut ~1 mm from the new edge

Strip away the capsular layer surrounding the tumor and mince into ~1 mm cubes. Maintain in media prior to implantation.

Figure B

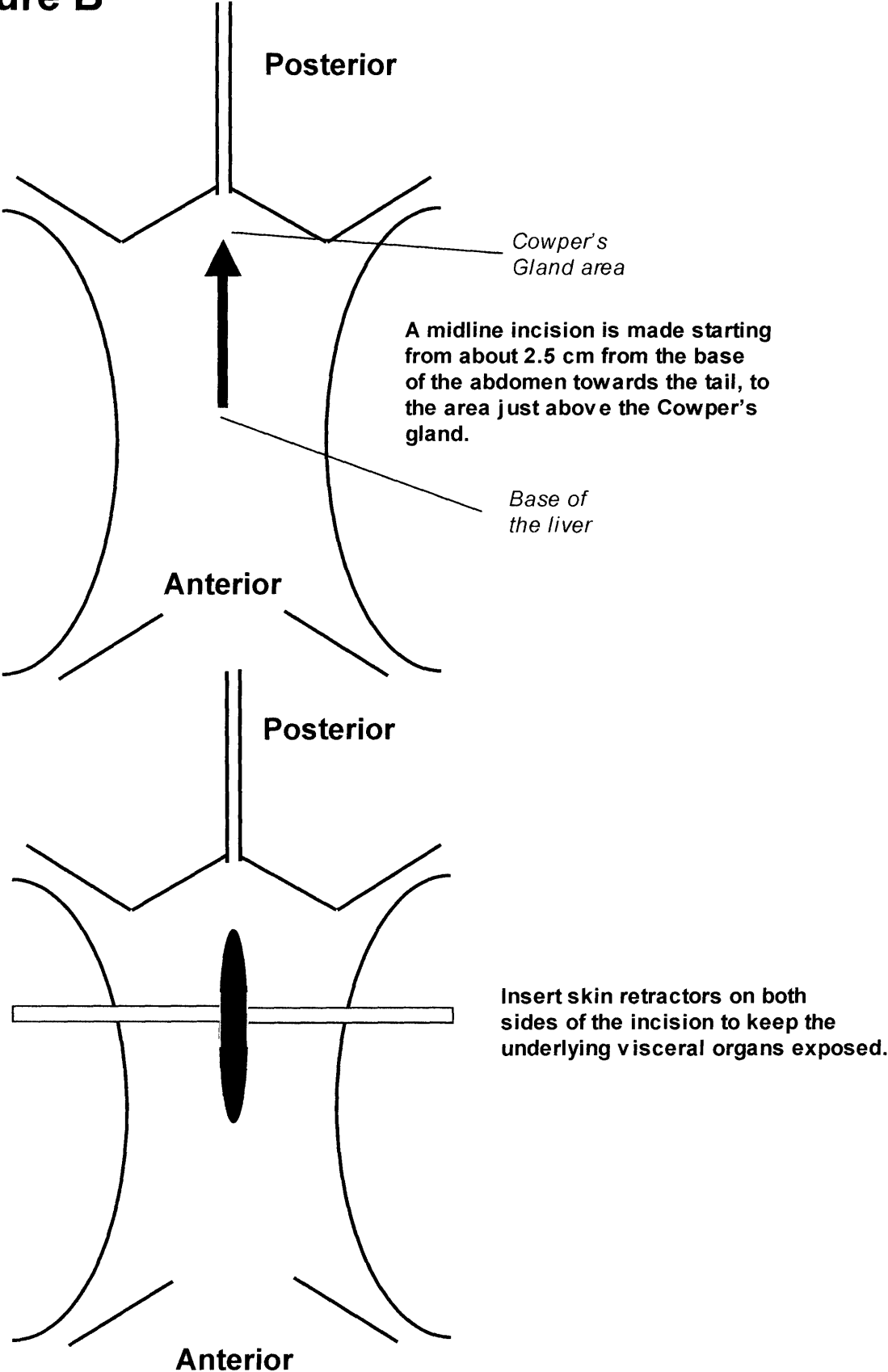
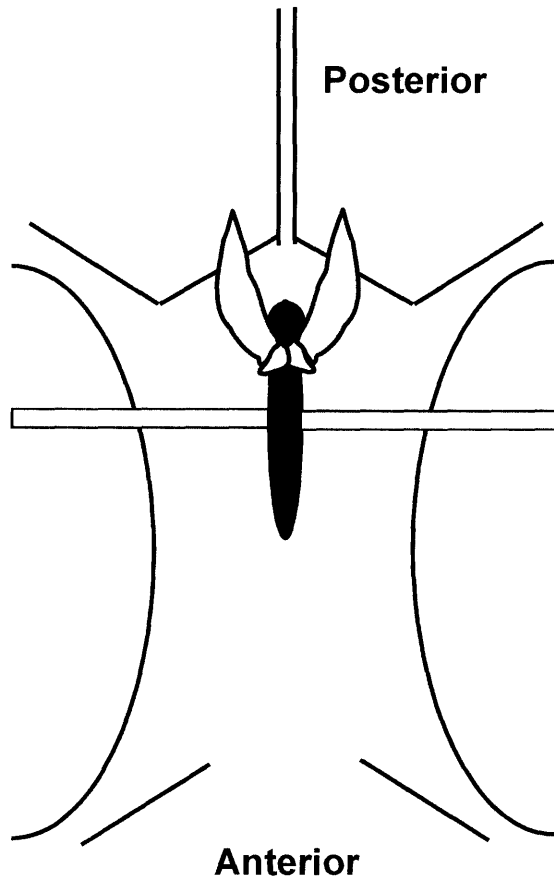


Figure C



Gently lift out the urogenital system with the dorsal prostate facing upwards (gray).



Arrow: dorsal prostate glands

Figure D

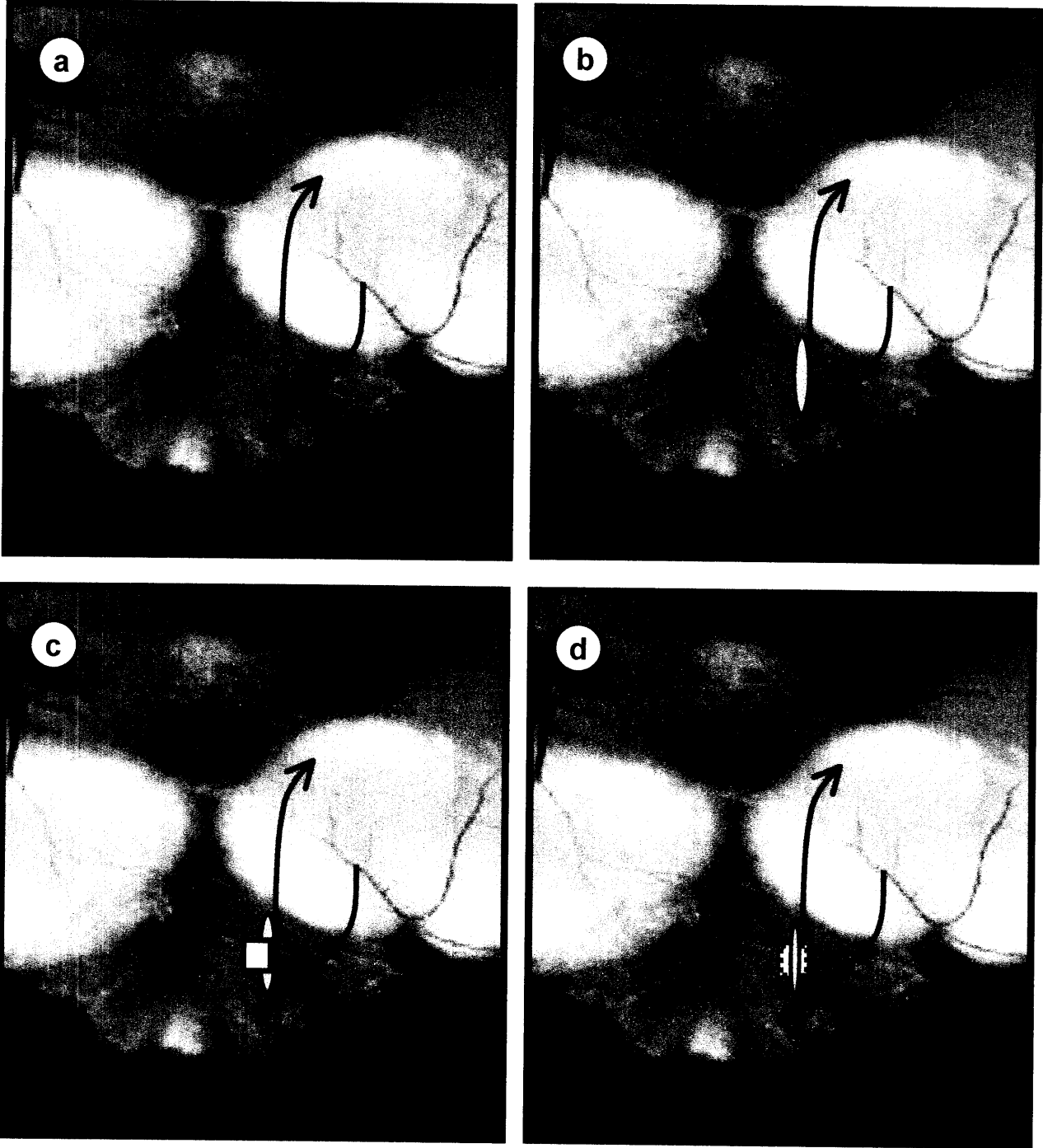


Figure D (cont.)

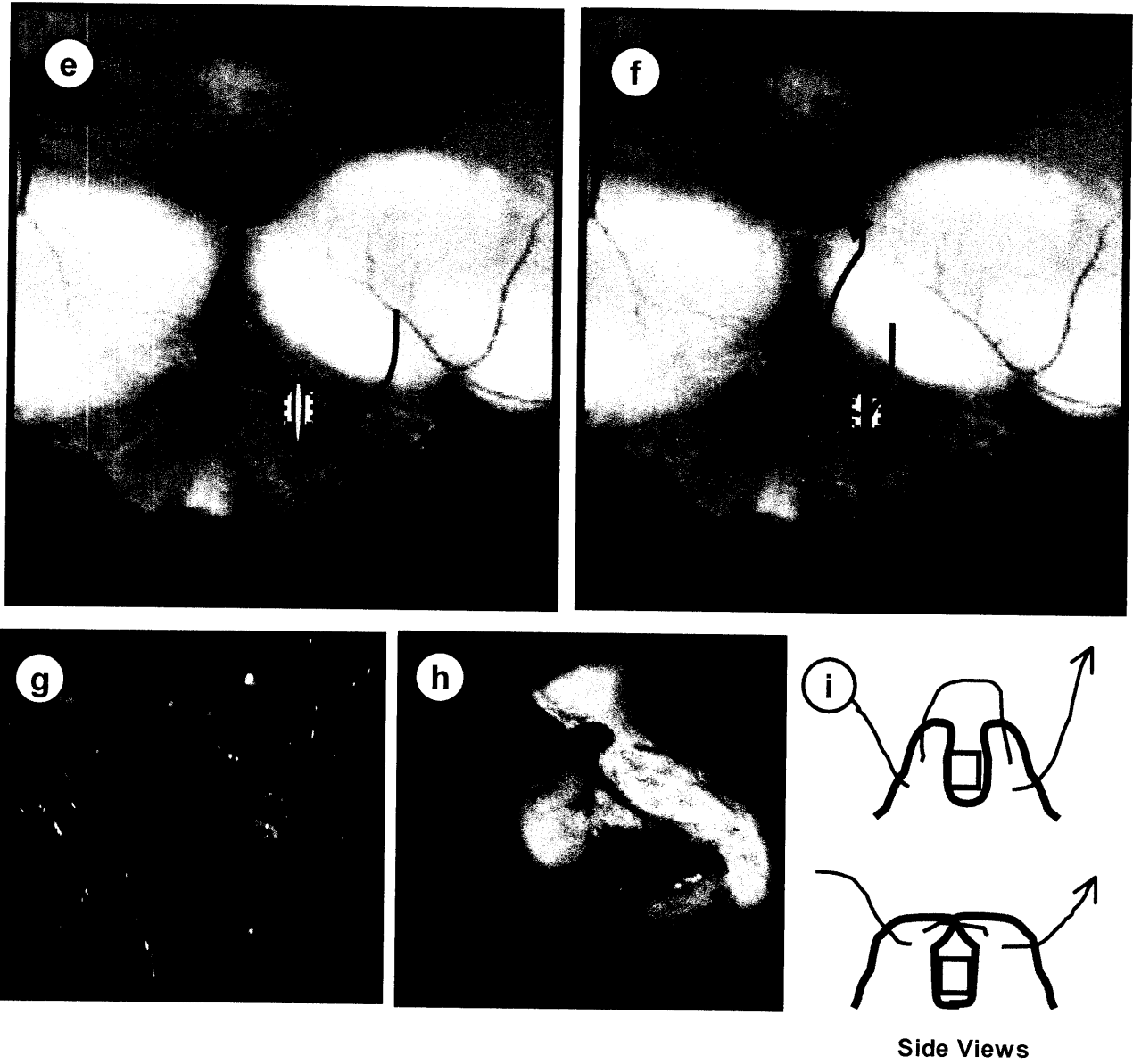
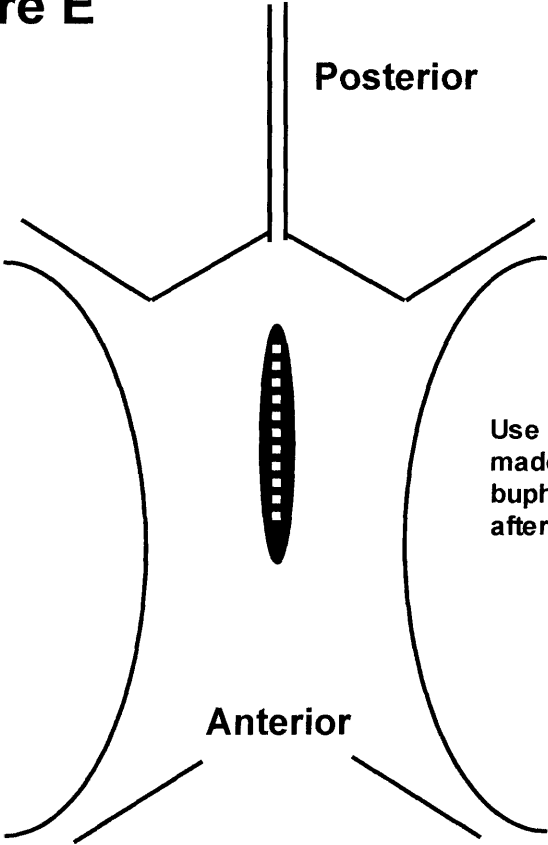
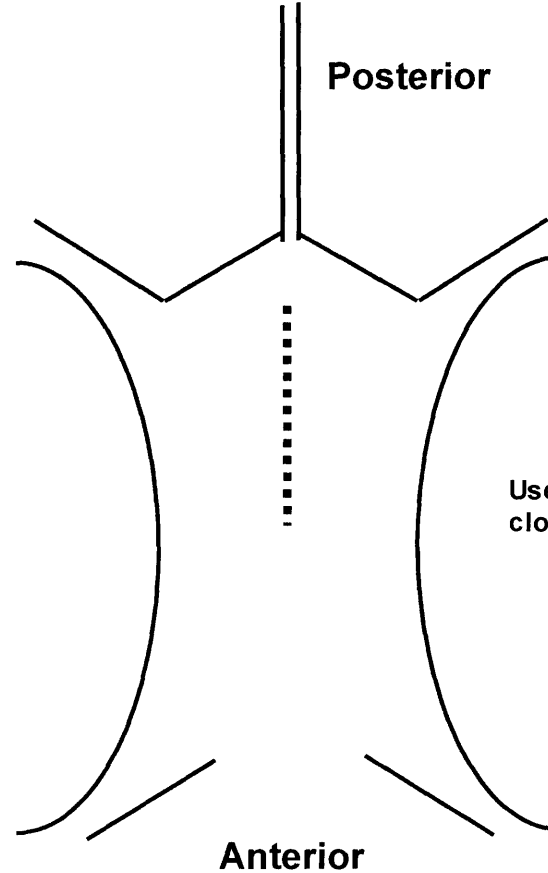


Figure E



Use 5-0 sutures to close the incision made into the peritoneum. Drip buphreneprine into the wound area after closure.



Use a second set of 5-0 sutures to close the skin above the peritoneum.

APPENDIX C. Preparation of Biotinylated cRNA from Prostate Tumors for Array Analysis

October 1, 2003

I. Preparation for RNA Extraction (Room Temp)

1. Wash the glass homogenizer and plunger 3X with de-ionized water
2. Wash the glass homogenizer and plunger 2X with distilled water (carboy)
3. Soak glass homogenizer and plunger >5" in 1-2 ml of RLT buffer with 10 ul β -ME/1 mL buffer
4. Lean the homogenizer sideways so that buffer/ME also contacts the bulb at the top

II. Thawing Flash Frozen Tumor Tissue and RNA Extraction (Room Temp)

Ideally, extract RNA from tumors of mass 130-250 mg, using the following volumes of RLT to homogenize:

75-130 mg tissue	2.5 mL RLT/ β -ME
130-250 mg tissue	4.5 mL RLT/ β -ME
250-375 mg tissue	6.5 mL RLT/ β -ME

RNA Extraction is done with Qiagen's RNeasy Midi isolation kit

1. Remove tumor from -135 freezer and keep on ice – do NOT allow to thaw completely
2. Tap Eppendorf to drop tumor into the RLT buffer already in the glass homogenizer ASAP
3. Push in pestle 15X, rotating the plunger halfway with each push
4. Check for large tumor pieces that might later clog the column
5. Pour the lysate into a 15 mL Falcon tube
6. Shear genomic DNA in the lysate with a 20 g. syringe, 10X
7. Centrifuge the lysate at 4000 g. for 10"
8. Transfer lysate to a new 15 mL Falcon tube, keeping 1 mL of pellet at the bottom of the tube
(e.g. if 4.5 mL RLT/ β -ME was used above, transfer 3.5 mL RLT/ β -ME)
9. Add 1 volume of 70% EtOH-DEPC to the lysate and mix thoroughly.
10. Complete the standard Qiagen RNeasy Midi instructions, spinning at 4000 g for each step.
- 11A. For 75-130 mg tissue: Elute the sample with 125 ul DEPC-water, pass it through 2X
- 11B. For 130-250 mg tissue: Elute the sample with 250 ul DEPC-water, pass it through 2X
12. Dilute 3 ul sample into 200 ul water and take an initial OD₂₆₀ (260/280 ratio will be bad)
(e.g. for 250 mg tissue sample, got OD₂₆₀ = 0.26 at this dilution)

III. DNase Digestion

- 1A. For 130-250 mg tissue (elution volume = 250 ul), combine:

RNA: ~200 ul actual volume
DNase buffer: 25 ul
Ambion DNase: 25 ul
<u>Water</u>
Final volume = 250 ul

- 1B: For 75-130 mg tissue (elution volume = 125 ul), combine:

RNA: ~100 ul actual volume
DNase buffer: 15 ul
Ambion DNase: 15 ul
<u>Water</u>
Final volume = 150 ul

2. Incubate for 2 hours at 37 degrees

IV. Cleaning Total RNA

- 1A. For 130-250 mg tissue (250 ul), split sample into 2, clean individually w/ Qiagen RNeasy Mini
- 2A. Elute the first tube using 30 ul DEPC-water, two passes
Take this liquid and elute the second, again with two passes (final volume = 30 ul)
- 1B. For 75-130 mg tissue (150 ul), clean with Qiagen's RNeasy Mini
- 2B. Elute using 20 ul DEPC-water, two passes
3. Dilute the sample 1:200 in water for quantitation, or 10 mM Tris-Cl pH 7.5 to determine purity
(e.g. for 250 mg starting tissue, got concentration of > 3 ug/ul, 260/280 = 2.0)
(minimum concentration for reverse transcription = 1.77 ug/ul)
4. Run 1-3 ug of total RNA on a gel to check integrity

V. Reverse Transcription of Total RNA – First Strand Synthesis

1. For reverse transcription, it is preferred to use 16 ug total RNA + 2 ul Superscript II RT (later)
2. Combine the following for primer hybridization:

16 ug RNA + DEPC Water: 9 ul
50 pmol/ul T7-(dT)₂₄ primer: 2 ul

3. Follow the Affymetrix protocols. Perform all incubations in PCR machines.

VI. Reverse Transcription of Total RNA – Second Strand Synthesis

1. Follow Affymetrix protocols. Incubation is performed at 16 degrees in the PCR machine
2. The final volume of the reaction = 162 ul

VII. cDNA Clean-Up

1. Clean up the RT reaction with Qiagen's PCR purification kit
2. Elute with 2 volumes of DEPC-water, 25 ul each (total = 50 ul)
3. Check the cDNA integrity by running 4 ul on a gel. A smear should be present.
It is critical to check for cDNA before proceeding to labelling reaction.

VIII. In vitro Transcription of Biotin-Labelled cRNA

1. From an elution volume of 50 ul from above, use 44% (22 ul) for IVT
2. Use the ENZO labelling kit, following Affymetrix protocols.
3. Incubate at 37 degrees for 4.5 hours, tapping the tube every 45 minutes, 5 secs each.

IX. cRNA Clean-Up

1. Clean the entire IVT sample (40 uL) with Qiagen's RNeasy Mini kit
2. Pass the initial sample through the column 2X
3. Elute the sample w/ 30 ul DEPC-water, using 2 passes (total 30 ul)
4. Dilute 1:100 and take spec
(e.g. for 250 mg tissue sample, got concentration of ~2 ug/ul)
(minimum conc. for sample fragmentation is 0.6 ug/ul after adjustment – see below)
5. Calculate the adjusted cRNA yield:

Adjusted cRNA yield = (Amount cRNA measured after IVT) – (Total starting RNA)(% for IVT)

Example: Adjusted yield = (IX #5 above) – (16 ug)(44%)
(Does adjusted concentration exceed 0.6 ug/ul?)

X. Fragmentation

15 ug cRNA is sufficient for 1 test chip and 1 real chip.

1. Fragment with the following protocol, keeping final cRNA concentration at 0.5 ug/ul:

15 ug cRNA + DEPC-water: 24 ul
5X Frag buffer: 6 ul

2. Incubate at 94 degrees for 35 minutes. Place on ice afterwards.
3. Submit for hybridization upstairs in Biopolymers facility.

APPENDIX D. STAINING BLOOD AND LYMPHATIC VESSELS IN ZINC-FIXED TUMOR SECTIONS

Sunny Wong (syw5@mit.edu) / May 22, 2003 / revised December 1, 2006

Anti-Mouse Antibodies

Rat anti-CD31 (PECAM)	Pan-endothelial; Pharmingen stock: 15.625 ug/ml
Rat anti-CD34 (RAM34)	Blood vessel-specific; Pharmingen stock: 0.5 mg/ml
Goat anti-VEGFR3 (Flt4)	Expressed in lymphatics and in some tumor blood vessels; R&D (AF743)
Rabbit anti-LYVE-1	Expressed in lymphatics and on some macrophages; Ruoslahti Lab
Rat anti-CD11b (Mac1- α)	Expressed on macrophage and some stromal cells; Pharmingen
Rat anti-F4/80	Expressed on mouse macrophages; Serotec

Secondary Antibodies

Rabbit anti-Rat (Vector Laboratories)
 Pig anti-Rabbit (DAKO-Cytomation)
 Rabbit anti-Goat

Dilutions and Treatments

CD31:	Dilute stock 1:3. No specific treatments necessary after de-waxing. Antigen retrieval inhibits staining of antibody
CD34:	Dilute stock 1:25. Antigen retrieval necessary only.
VEGFR3:	Dilute stock 1:25. Antigen retrieval necessary only.
LYVE-1:	Dilute stock 1:500. Antigen retrieval necessary only.
CD11b:	Dilute stock 1:25. Antigen retrieval necessary only.
F4/80:	Dilute stock 1:10. Antigen retrieval AND detergent treatment necessary.

Antigen Retrieval: Prepare Retrieval A pH 6.0 (BD) as described. Heat sections in Coplin Jar containing Retrieval A in microwave at full power until boiling begins (~1 min). Reduce power to lowest level so that section simmers for an additional 9 min.

Detergent Treatment: Prepare 0.2% Triton X-100/PBS. Incubate at room temp, 10 min.

Trypsin Treatment: Prepare 0.2% trypsin/PBS. Incubate at room temp, 10-15 min.

Zinc Fixation: Immerse samples (no greater than 3 mm thick) in formalin-free IHC zinc-fixative (BD). Incubate at room temperature for ~48 hours.

Basic Protocol

- 1) De-wax slides in H₂O.
- 2) If necessary, perform antigen retrieval, 10" in microwave. Cool 15" and wash 2X 10" in PBS.
- 3) Treat with 3% fresh H₂O₂/PBS, 10". Wash 2X with 0.2% PBST, 1X with PBS.
- 4) If necessary, treat with trypsin or detergent.
- 5) Wash 2X with PBS, 10" each.
- 6) Block with 20% serum, 2% fish oil in PBS at 37 degrees, 30 min.
- 7) Add primary antibody diluted in 4% serum/PBS. Spin down antibody before use. Incubate o/n at room temperature.
- 8) Wash 2X with PBST, 10 min each, and 1X with PBS.
- 9) Add secondary antibody conjugated to biotin (1:200-1:250) diluted in 4% antibody-specific serum/4% mouse serum/PBS. Spin down antibody before use. Incubate 45" at room temperature. Go to step #10.
- 10) Prepare Vector ABC complex 30 minutes prior to usage. Add 1 drop solution A and 1 drop solution B to 2.5 ml of PBS. Vortex.
- 11) Wash off antibody 2X with PBST and 1X with PBS, 5-10 minutes each.
- 12) Add ABC complex and incubate 30" at room temperature.

- 13) Wash off ABC 3X with PBS, 5 minutes each.
- 14) Prepare VIP substrate following manufacturer's protocols immediately prior to usage. To 1.67 ml PBS, add single drops from bottles 1-4, vortexing between each drop.
- 15) Add VIP to sections and incubate for color development.

For VEGFR3, develop < 5 minutes

For LYVE-1, develop 7 minutes

For CD34, develop 45 minutes

- 16) Stop the reaction by washing with H₂O.
- 17) Counterstain sections with Methyl Green, treat with xylenes and mount.

Up In:	Features	Descriptions	Score	Feature P	Feature P c	Feature P FDR(BH)	Q Value	FWER	Fold Change	
PC3-78	220784_s_at	UTS2	5.1643	0.168317	0.1137632	0.2148486	0.654556	0.59655	0.89	14.3743928
PC3-78	209839_at	DNM3	3.6162	0.168317	0.1137632	0.2148486	0.654556	0.59655	1	7.019521346
PC3-78	200665_s_at	SPARC	16.322	0.168317	0.1137632	0.2148486	0.654556	0.59655	0	4.975622193
PC3-78	205523_at	HAPLN1	8.1191	0.168317	0.1137632	0.2148486	0.654556	0.59655	0.41	3.576273213
PC3-78	212667_at	SPARC	4.8488	0.168317	0.1137632	0.2148486	0.654556	0.59655	0.89	3.14958413
PC3-78	208116_s_at	MAN1A1	1.4517	0.168317	0.1137632	0.2148486	0.654556	0.59655	1	3.005262602
PC3-78	209035_at	MDK	1.778	0.168317	0.1137632	0.2148486	0.654556	0.59655	1	2.901220789
PC3-78	211675_s_at	MPFIC	5.2915	0.168317	0.1137632	0.2148486	0.654556	0.59655	0.89	2.894841435
PC3-78	204818_at	HSD17B2	9.6754	0.168317	0.1137632	0.2148486	0.654556	0.59655	0.145	2.78993694
PC3-78	201667_at	GJA1	3.1996	0.168317	0.1137632	0.2148486	0.654556	0.59655	1	2.769417986
PC3-78	204749_at	NAP1L3	1.7738	0.168317	0.1137632	0.2148486	0.654556	0.59655	1	2.751849435
PC3-78	204751_x_at	DSC2	2.75	0.168317	0.1137632	0.2148486	0.654556	0.59655	1	2.705844334
PC3-78	211776_s_at	EPB41L3	2.5414	0.168317	0.1137632	0.2148486	0.654556	0.59655	1	2.628950507
PC3-78	213273_at	ODZ4	2.4929	0.168317	0.1137632	0.2148486	0.654556	0.59655	1	2.477097985
PC3-78	217771_at	GOLPH2	2.6035	0.168317	0.1137632	0.2148486	0.654556	0.59655	1	2.453879353
PC3-78	206224_at	CST1	0.9388	0.168317	0.1137632	0.2148486	0.654556	0.59655	1	2.443805056
PC3-78	206710_s_at	EPB41L3	3.1969	0.168317	0.1137632	0.2148486	0.654556	0.59655	1	2.417085756
PC3-78	212681_at	EPB41L3	4.4666	0.168317	0.1137632	0.2148486	0.654556	0.59655	1	2.39869006
PC3-78	219327_s_at	GPRC5C	6.8678	0.168317	0.1137632	0.2148486	0.654556	0.59655	0.745	2.341216218
PC3-78	211549_s_at	HPGD	2.2273	0.168317	0.1137632	0.2148486	0.654556	0.59655	1	2.322029774
PC3-78	221618_s_at	TAF9L	1.0294	0.168317	0.1137632	0.2148486	0.654556	0.59655	1	2.312163627
PC3-78	211959_at	IGFBP5	2.2227	0.168317	0.1137632	0.2148486	0.654556	0.59655	1	2.261722464
PC3-78	204597_x_at	STC1	2.645	0.168317	0.1137632	0.2148486	0.654556	0.59655	1	2.257505637
PC3-78	207276_at	CDR1	0.2336	0.168317	0.1137632	0.2148486	0.654556	0.59655	1	2.239631474
PC3-78	201362_at	IVNS1ABP	2.0252	0.168317	0.1137632	0.2148486	0.654556	0.59655	1	2.213315964
PC3-78	203980_at	FABP4	2.6097	0.168317	0.1137632	0.2148486	0.654556	0.59655	1	2.20271242
PC3-78	217787_s_at	GALNT2	1.4545	0.168317	0.1137632	0.2148486	0.654556	0.59655	1	2.189504934
PC3-78	205524_s_at	HAPLN1	8.7701	0.168317	0.1137632	0.2148486	0.654556	0.59655	0.265	2.18521569
PC3-78	217028_at	CXCR4	1.4871	0.168317	0.1137632	0.2148486	0.654556	0.59655	1	2.185152878
PC3-78	202272_s_at	FBXO28	3.2684	0.168317	0.1137632	0.2148486	0.654556	0.59655	1	2.158452953
PC3-78	206214_at	PLA2G7	0.7626	0.168317	0.1137632	0.2148486	0.654556	0.59655	1	2.120698385
PC3-78	213423_x_at	TUSC3	2.2272	0.168317	0.1137632	0.2148486	0.654556	0.59655	1	2.088766124
PC3-78	207387_s_at	GK	2.5415	0.168317	0.1137632	0.2148486	0.654556	0.59655	1	2.084715936
PC3-78	209205_s_at	LMO4	2.8209	0.168317	0.1137632	0.2148486	0.654556	0.59655	1	2.078286093
PC3-78	202626_s_at	LYN	4.9796	0.168317	0.1137632	0.2148486	0.654556	0.59655	0.89	2.067309256
PC3-78	211599_x_at	MET	2.1288	0.168317	0.1137632	0.2148486	0.654556	0.59655	1	2.052376041
PC3-78	201363_s_at	IVNS1ABP	2.825	0.168317	0.1137632	0.2148486	0.654556	0.59655	1	2.035030506
PC3-78	215977_x_at	GK	4.7305	0.168317	0.1137632	0.2148486	0.654556	0.59655	0.89	2.028555021
PC3-78	201858_s_at	PRG1	3.4071	0.168317	0.1137632	0.2148486	0.654556	0.59655	1	2.024262954
PC3-78	212385_at	TCF4	1.8438	0.168317	0.1137632	0.2148486	0.654556	0.59655	1	2.01366347
PC3-78	203180_at	ALDH1A3	4.4041	0.168317	0.1137632	0.2148486	0.654556	0.59655	1	2.004540462
PC3-78	221805_at	NEFL	3.1664	0.168317	0.1137632	0.2148486	0.654556	0.59655	1	1.992443735
PC3-78	203914_x_at	HPGD	2.0852	0.168317	0.1137632	0.2148486	0.654556	0.59655	1	1.984662871
PC3-78	206424_at	CYP26A1	1.927	0.168317	0.1137632	0.2148486	0.654556	0.59655	1	1.982335275
PC3-78	218000_s_at	PHLDA1	1.2494	0.168317	0.1137632	0.2148486	0.654556	0.59655	1	1.98100496
PC3-78	200796_s_at	MCL1	1.2741	0.168317	0.1137632	0.2148486	0.654556	0.59655	1	1.976668998
PC3-78	212382_at	TCF4	1.372	0.168317	0.1137632	0.2148486	0.654556	0.59655	1	1.976621705
PC3-78	221731_x_at	CSPG2	4.3009	0.168317	0.1137632	0.2148486	0.654556	0.59655	1	1.976038223
PC3-78	211161_s_at	COL3A1	1.5722	0.168317	0.1137632	0.2148486	0.654556	0.59655	1	1.974729428
PC3-78	206033_s_at	DSC3	1.9475	0.168317	0.1137632	0.2148486	0.654556	0.59655	1	1.954469774
PC3-78	209228_x_at	TUSC3	1.9532	0.168317	0.1137632	0.2148486	0.654556	0.59655	1	1.949666278
PC3-78	217167_x_at	GK	3.7414	0.168317	0.1137632	0.2148486	0.654556	0.59655	1	1.948338481
PC3-78	209844_at	HOXB13	1.2416	0.168317	0.1137632	0.2148486	0.654556	0.59655	1	1.944701558
PC3-78	205500_at	C5	3.3149	0.168317	0.1137632	0.2148486	0.654556	0.59655	1	1.931438547
PC3-78	219140_s_at	RBP4	1.9428	0.168317	0.1137632	0.2148486	0.654556	0.59655	1	1.928382524
PC3-78	214975_s_at	MTMR1	1.6525	0.168317	0.1137632	0.2148486	0.654556	0.59655	1	1.928033193
PC3-78	213807_x_at	MET	2.0787	0.168317	0.1137632	0.2148486	0.654556	0.59655	1	1.927315788
PC3-78	204404_at	SLC12A2	2.5833	0.168317	0.1137632	0.2148486	0.654556	0.59655	1	1.920968582
PC3-78	204475_at	MMP1	3.4233	0.168317	0.1137632	0.2148486	0.654556	0.59655	1	1.919141737
PC3-78	211548_s_at	HPGD	1.9605	0.168317	0.1137632	0.2148486	0.654556	0.59655	1	1.916797635
PC3-78	213865_at	DCBLD2	1.6116	0.168317	0.1137632	0.2148486	0.654556	0.59655	1	1.916558853
PC3-78	203913_s_at	HPGD	1.5239	0.168317	0.1137632	0.2148486	0.654556	0.59655	1	1.908739374
PC3-78	201852_x_at	COL3A1	1.7526	0.168317	0.1137632	0.2148486	0.654556	0.59655	1	1.900378258
PC3-78	218352_at	RCBTB1	1.0544	0.168317	0.1137632	0.2148486	0.654556	0.59655	1	1.900336863
PC3-78	206042_x_at	SNRPN /// SNL	2.5218	0.168317	0.1137632	0.2148486	0.654556	0.59655	1	1.900059613
PC3-78	212098_at	LOC151162	3.7945	0.168317	0.1137632	0.2148486	0.654556	0.59655	1	1.891282684
PC3-78	206245_s_at	IVNS1ABP	8.2354	0.168317	0.1137632	0.2148486	0.654556	0.59655	0.41	1.885812547
PC3-78	211559_s_at	CCNG2	2.4519	0.168317	0.1137632	0.2148486	0.654556	0.59655	1	1.875664841

PC3-78	215073_s_at	NR2F2	1.8626	0.168317	0.1137632	0.2148486	0.654556	0.59655	1	1.871597205
PC3-78	214804_at	FSHPRH1	0.6987	0.29703	0.2302494	0.3550604	0.772047	0.68489	1	1.861140573
PC3-78	220462_at	TAIP-2	0.9258	0.29703	0.2302494	0.3550604	0.772047	0.68489	1	1.860351329
PC3-78	206429_at	F2RL1	1.5376	0.168317	0.1137632	0.2148486	0.654556	0.59655	1	1.856812056
PC3-78	203953_s_at	CLDN3	1.076	0.168317	0.1137632	0.2148486	0.654556	0.59655	1	1.850837399
PC3-78	204540_at	EEF1A2	0.8681	0.168317	0.1137632	0.2148486	0.654556	0.59655	1	1.84680378
PC3-78	218748_s_at	SEC10L1	0.8883	0.168317	0.1137632	0.2148486	0.654556	0.59655	1	1.844995962
PC3-78	214336_s_at	COPA	2.2847	0.168317	0.1137632	0.2148486	0.654556	0.59655	1	1.827883215
PC3-78	218976_at	DNAJC12	3.0921	0.168317	0.1137632	0.2148486	0.654556	0.59655	1	1.825766782
PC3-78	221679_s_at	ABHD6	1.6032	0.168317	0.1137632	0.2148486	0.654556	0.59655	1	1.824699431
PC3-78	210754_s_at	LYN	8.9637	0.168317	0.1137632	0.2148486	0.654556	0.59655	0.265	1.816434232
PC3-78	215966_x_at	GK	3.4683	0.168317	0.1137632	0.2148486	0.654556	0.59655	1	1.814475492
PC3-78	219304_s_at	PDGFD	3.3502	0.168317	0.1137632	0.2148486	0.654556	0.59655	1	1.810175595
PC3-78	214433_s_at	SELENBP1	1.9285	0.168317	0.1137632	0.2148486	0.654556	0.59655	1	1.800543338
PC3-78	221583_s_at	KCNMA1	2.8018	0.168317	0.1137632	0.2148486	0.654556	0.59655	1	1.79823305
PC3-78	211874_s_at	MYST4	1.311	0.168317	0.1137632	0.2148486	0.654556	0.59655	1	1.795956095
PC3-78	202342_s_at	TRIM2	1.6975	0.168317	0.1137632	0.2148486	0.654556	0.59655	1	1.794772967
PC3-78	206032_at	DSC3	1.8075	0.168317	0.1137632	0.2148486	0.654556	0.59655	1	1.79232534
PC3-78	209505_at	NR2F1	1.932	0.168317	0.1137632	0.2148486	0.654556	0.59655	1	1.78050169
PC3-78	219399_at	LIN7C	1.8172	0.168317	0.1137632	0.2148486	0.654556	0.59655	1	1.779117405
PC3-78	220342_x_at	C1orf22	3.615	0.168317	0.1137632	0.2148486	0.654556	0.59655	1	1.779012036
PC3-78	204716_at	CCDC6	2.0627	0.168317	0.1137632	0.2148486	0.654556	0.59655	1	1.777807265
PC3-78	203256_at	CDH3	4.647	0.168317	0.1137632	0.2148486	0.654556	0.59655	0.89	1.775113581
PC3-78	201490_s_at	PPIF	1.5612	0.168317	0.1137632	0.2148486	0.654556	0.59655	1	1.769963475
PC3-78	205924_at	RAB3B	1.241	0.168317	0.1137632	0.2148486	0.654556	0.59655	1	1.7623599
PC3-78	214496_x_at	MYST4	2.1464	0.168317	0.1137632	0.2148486	0.654556	0.59655	1	1.760833152
PC3-78	201340_s_at	ENC1	0.3832	0.168317	0.1137632	0.2148486	0.654556	0.59655	1	1.758642048
PC3-78	204620_s_at	CSPG2	3.955	0.168317	0.1137632	0.2148486	0.654556	0.59655	1	1.755510656
PC3-78	204750_s_at	DSC2	0.8123	0.168317	0.1137632	0.2148486	0.654556	0.59655	1	1.750829641
PC3-78	213606_s_at	ARHGDI1A	0.7967	0.257426	0.1935828	0.3127404	0.772047	0.68489	1	1.746497292
PC3-78	212452_x_at	MYST4	1.8867	0.168317	0.1137632	0.2148486	0.654556	0.59655	1	1.743185511
PC3-78	204298_s_at	LOX	1.4435	0.168317	0.1137632	0.2148486	0.654556	0.59655	1	1.735338019
PC3-78	213816_s_at	MET	2.4128	0.168317	0.1137632	0.2148486	0.654556	0.59655	1	1.734753282
PC3-78	201211_s_at	DDX3X	1.5097	0.168317	0.1137632	0.2148486	0.654556	0.59655	1	1.727076423
PC3-78	206667_s_at	SCAMP1	1.0975	0.168317	0.1137632	0.2148486	0.654556	0.59655	1	1.726112128
PC3-78	211823_s_at	PXN	1.4101	0.168317	0.1137632	0.2148486	0.654556	0.59655	1	1.721942581
PC3-78	204623_at	TFF3	1.2845	0.217822	0.1575902	0.2697481	0.743866	0.65684	1	1.719118126
PC3-78	220253_s_at	LRP12	2.5453	0.168317	0.1137632	0.2148486	0.654556	0.59655	1	1.716551437
PC3-78	207379_at	EDIL3	1.128	0.168317	0.1137632	0.2148486	0.654556	0.59655	1	1.712490058
PC3-78	201971_s_at	ATP6V1A	1.2019	0.168317	0.1137632	0.2148486	0.654556	0.59655	1	1.711980507
PC3-78	221974_at	SNRPN	1.6011	0.168317	0.1137632	0.2148486	0.654556	0.59655	1	1.706415695
PC3-78	212614_at	ARID5B	2.3178	0.168317	0.1137632	0.2148486	0.654556	0.59655	1	1.70360351
PC3-78	216316_x_at	---	4.6047	0.168317	0.1137632	0.2148486	0.654556	0.59655	0.89	1.699380295
PC3-78	218782_s_at	ATAD2	0.6684	0.168317	0.1137632	0.2148486	0.654556	0.59655	1	1.698556625
PC3-78	210317_s_at	YWHAE	1.5155	0.168317	0.1137632	0.2148486	0.654556	0.59655	1	1.696446654
PC3-78	205680_at	MMP10	6.3947	0.168317	0.1137632	0.2148486	0.654556	0.59655	0.89	1.693121844
PC3-78	221489_s_at	SPRY4	2.2581	0.168317	0.1137632	0.2148486	0.654556	0.59655	1	1.692122455
PC3-78	202743_at	PIK3R3	3.2382	0.168317	0.1137632	0.2148486	0.654556	0.59655	1	1.691984146
PC3-78	201859_at	PRG1	1.2607	0.168317	0.1137632	0.2148486	0.654556	0.59655	1	1.691717058
PC3-78	204040_at	RNF144	4.0295	0.168317	0.1137632	0.2148486	0.654556	0.59655	1	1.690614553
PC3-78	214895_s_at	ADAM10	2.3238	0.168317	0.1137632	0.2148486	0.654556	0.59655	1	1.689129388
PC3-78	220892_s_at	PSAT1	4.2221	0.168317	0.1137632	0.2148486	0.654556	0.59655	1	1.688066072
PC3-78	212107_s_at	DHX9	1.4433	0.168317	0.1137632	0.2148486	0.654556	0.59655	1	1.685914556
PC3-78	213447_at	IPW	1.6577	0.168317	0.1137632	0.2148486	0.654556	0.59655	1	1.6843781
PC3-78	203716_s_at	DPP4	2.4804	0.168317	0.1137632	0.2148486	0.654556	0.59655	1	1.683317445
PC3-78	213325_at	PVRL3	1.6817	0.168317	0.1137632	0.2148486	0.654556	0.59655	1	1.68265002
PC3-78	220738_s_at	RPS6KA6	3.1751	0.168317	0.1137632	0.2148486	0.654556	0.59655	1	1.681399516
PC3-78	218888_s_at	NETO2	2.6897	0.168317	0.1137632	0.2148486	0.654556	0.59655	1	1.678388565
PC3-78	201058_s_at	MYL9	1.8485	0.168317	0.1137632	0.2148486	0.654556	0.59655	1	1.6775925
PC3-78	208664_s_at	TTC3	1.4401	0.168317	0.1137632	0.2148486	0.654556	0.59655	1	1.671207293
PC3-78	211812_s_at	B3GALT3	1.3645	0.168317	0.1137632	0.2148486	0.654556	0.59655	1	1.670393111
PC3-78	201116_s_at	CPE	4.0419	0.168317	0.1137632	0.2148486	0.654556	0.59655	1	1.667842824
PC3-78	202271_at	FBXO28	2.6614	0.168317	0.1137632	0.2148486	0.654556	0.59655	1	1.663095804
PC3-78	207153_s_at	GLMN	1.7415	0.168317	0.1137632	0.2148486	0.654556	0.59655	1	1.661433088
PC3-78	209754_s_at	TMPO	0.7148	0.168317	0.1137632	0.2148486	0.654556	0.59655	1	1.659277977
PC3-78	215076_s_at	COL3A1	1.3584	0.168317	0.1137632	0.2148486	0.654556	0.59655	1	1.659277157
PC3-78	214078_at	PAK3	1.8544	0.168317	0.1137632	0.2148486	0.654556	0.59655	1	1.65872223
PC3-78	206345_s_at	PON1	4.345	0.168317	0.1137632	0.2148486	0.654556	0.59655	1	1.657842106
PC3-78	215446_s_at	LOX	1.4789	0.168317	0.1137632	0.2148486	0.654556	0.59655	1	1.657045058

PC3-78	206172_at	IL13RA2	2.252	0.168317	0.1137632	0.2148486	0.654556	0.59655	1	1.656745843
PC3-78	200598_s_at	TRA1	2.3218	0.168317	0.1137632	0.2148486	0.654556	0.59655	1	1.656627974
PC3-78	208853_s_at	CANX	2.3383	0.168317	0.1137632	0.2148486	0.654556	0.59655	1	1.656527683
PC3-78	209424_s_at	AMACR	1.289	0.168317	0.1137632	0.2148486	0.654556	0.59655	1	1.654573456
PC3-78	221760_at	MAN1A1	1.44	0.168317	0.1137632	0.2148486	0.654556	0.59655	1	1.653004169
PC3-78	202007_at	NID1	1.5343	0.168317	0.1137632	0.2148486	0.654556	0.59655	1	1.65238692
PC3-78	214581_x_at	TNFRSF21	2.2042	0.168317	0.1137632	0.2148486	0.654556	0.59655	1	1.65080993
PC3-78	203176_s_at	TFAM	1.1069	0.168317	0.1137632	0.2148486	0.654556	0.59655	1	1.650165574
PC3-78	203429_s_at	C1orf9	2.2341	0.168317	0.1137632	0.2148486	0.654556	0.59655	1	1.649927251
PC3-78	202625_at	LYN	2.8399	0.168317	0.1137632	0.2148486	0.654556	0.59655	1	1.647251702
PC3-78	212092_at	PEG10	1.4274	0.168317	0.1137632	0.2148486	0.654556	0.59655	1	1.64585352
PC3-78	202438_x_at	IDS	1.1605	0.168317	0.1137632	0.2148486	0.654556	0.59655	1	1.642611386
PC3-78	206631_at	PTGER2	0.8423	0.168317	0.1137632	0.2148486	0.654556	0.59655	1	1.639559891
PC3-78	210286_s_at	SLC4A7	1.7141	0.168317	0.1137632	0.2148486	0.654556	0.59655	1	1.638465142
PC3-78	219793_at	SNX16	3.4837	0.168317	0.1137632	0.2148486	0.654556	0.59655	1	1.636573063
PC3-78	207172_s_at	CDH11	0.7666	0.168317	0.1137632	0.2148486	0.654556	0.59655	1	1.630903682
PC3-78	204995_at	CDK5R1	1.5046	0.168317	0.1137632	0.2148486	0.654556	0.59655	1	1.62575046
PC3-78	219869_s_at	SLC39A8	3.614	0.168317	0.1137632	0.2148486	0.654556	0.59655	1	1.623987902
PC3-78	204426_at	TMED2	1.5685	0.168317	0.1137632	0.2148486	0.654556	0.59655	1	1.623890807
PC3-78	204128_s_at	RFC3	0.875	0.168317	0.1137632	0.2148486	0.654556	0.59655	1	1.62336878
PC3-78	201043_s_at	ANP32A	1.8591	0.168317	0.1137632	0.2148486	0.654556	0.59655	1	1.621293537
PC3-78	203799_at	CD302	0.9085	0.168317	0.1137632	0.2148486	0.654556	0.59655	1	1.617587146
PC3-78	206917_at	GNA13	2.2916	0.168317	0.1137632	0.2148486	0.654556	0.59655	1	1.616736329
PC3-78	221428_s_at	TBL1XR1	1.7921	0.168317	0.1137632	0.2148486	0.654556	0.59655	1	1.615330234
PC3-78	205808_at	ASPH	2.385	0.168317	0.1137632	0.2148486	0.654556	0.59655	1	1.615290165
PC3-78	202134_s_at	WWTR1	1.4343	0.168317	0.1137632	0.2148486	0.654556	0.59655	1	1.615186405
PC3-78	219201_s_at	TWSG1	1.5203	0.168317	0.1137632	0.2148486	0.654556	0.59655	1	1.613409998
PC3-78	201196_s_at	AMD1	1.9514	0.168317	0.1137632	0.2148486	0.654556	0.59655	1	1.61323666
PC3-78	202765_s_at	FBN1	3.3504	0.168317	0.1137632	0.2148486	0.654556	0.59655	1	1.613147851
PC3-78	215581_s_at	MCM3AP	1.704	0.168317	0.1137632	0.2148486	0.654556	0.59655	1	1.613072261
PC3-78	218349_s_at	ZWILCH	0.9197	0.168317	0.1137632	0.2148486	0.654556	0.59655	1	1.612117614
PC3-78	209468_at	LRP5	1.0246	0.267327	0.2026906	0.3233796	0.772047	0.68489	1	1.608468641
PC3-78	218113_at	TMEM2	1.0563	0.168317	0.1137632	0.2148486	0.654556	0.59655	1	1.607344499
PC3-78	209506_s_at	NR2F1	1.4948	0.168317	0.1137632	0.2148486	0.654556	0.59655	1	1.607146833
PC3-78	202886_s_at	PPP2R1B	2.3535	0.168317	0.1137632	0.2148486	0.654556	0.59655	1	1.603199438
PC3-78	208062_s_at	NRG2	0.9107	0.168317	0.1137632	0.2148486	0.654556	0.59655	1	1.6028091
PC3-78	209863_s_at	TP73L	1.7593	0.168317	0.1137632	0.2148486	0.654556	0.59655	1	1.596936592
PC3-78	203058_s_at	PAPSS2	0.514	0.168317	0.1137632	0.2148486	0.654556	0.59655	1	1.595449738
PC3-78	201868_s_at	TBL1X	1.1064	0.168317	0.1137632	0.2148486	0.654556	0.59655	1	1.593689245
PC3-78	211478_s_at	DPP4	3.2405	0.168317	0.1137632	0.2148486	0.654556	0.59655	1	1.593415011
PC3-78	211814_s_at	CCNE2	0.7087	0.168317	0.1137632	0.2148486	0.654556	0.59655	1	1.589774697
PC3-78	204715_at	PANX1	2.3298	0.168317	0.1137632	0.2148486	0.654556	0.59655	1	1.588320671
PC3-78	204352_at	TRAF5	1.8192	0.168317	0.1137632	0.2148486	0.654556	0.59655	1	1.587443763
PC3-78	207029_at	KITLG	1.8749	0.168317	0.1137632	0.2148486	0.654556	0.59655	1	1.58717109
PC3-78	207992_s_at	AMPD3	2.3883	0.168317	0.1137632	0.2148486	0.654556	0.59655	1	1.586587932
PC3-78	201341_at	ENC1	1.8784	0.168317	0.1137632	0.2148486	0.654556	0.59655	1	1.584660076
PC3-78	209895_at	PTPN11	1.2917	0.168317	0.1137632	0.2148486	0.654556	0.59655	1	1.584066703
PC3-78	221638_s_at	STX16	0.9862	0.168317	0.1137632	0.2148486	0.654556	0.59655	1	1.581590228
PC3-78	208930_s_at	ILF3	0.6667	0.168317	0.1137632	0.2148486	0.654556	0.59655	1	1.57923856
PC3-78	221487_s_at	ENSA	2.3464	0.168317	0.1137632	0.2148486	0.654556	0.59655	1	1.579022129
PC3-78	203214_x_at	CDC2	1.6047	0.168317	0.1137632	0.2148486	0.654556	0.59655	1	1.578097025
PC3-78	213256_at	-	2.1439	0.168317	0.1137632	0.2148486	0.654556	0.59655	1	1.57555942
PC3-78	212446_s_at	LASS6	1.109	0.168317	0.1137632	0.2148486	0.654556	0.59655	1	1.575403197
PC3-78	209006_s_at	C1orf63	2.9918	0.168317	0.1137632	0.2148486	0.654556	0.59655	1	1.575090832
PC3-78	203570_at	LOXL1	2.1248	0.168317	0.1137632	0.2148486	0.654556	0.59655	1	1.574439531
PC3-78	87100_at	ABHD2	1.8369	0.168317	0.1137632	0.2148486	0.654556	0.59655	1	1.574410272
PC3-78	208459_s_at	XPO7	1.7465	0.168317	0.1137632	0.2148486	0.654556	0.59655	1	1.572466518
PC3-78	214684_at	MEF2A	1.657	0.168317	0.1137632	0.2148486	0.654556	0.59655	1	1.570213064
PC3-78	212607_at	AKT3	0.8857	0.168317	0.1137632	0.2148486	0.654556	0.59655	1	1.567233614
PC3-78	209456_s_at	FBXW11	1.0784	0.168317	0.1137632	0.2148486	0.654556	0.59655	1	1.566081065
PC3-78	202132_at	WWTR1	1.1069	0.168317	0.1137632	0.2148486	0.654556	0.59655	1	1.566022518
PC3-78	207431_s_at	DEGS1	1.2573	0.168317	0.1137632	0.2148486	0.654556	0.59655	1	1.56352788
PC3-78	210559_s_at	CDC2	1.17	0.316832	0.2488067	0.3759975	0.772047	0.68489	1	1.562262159
PC3-78	200841_s_at	EPRS	1.1749	0.168317	0.1137632	0.2148486	0.654556	0.59655	1	1.560582536
PC3-78	202651_at	LPGAT1	0.9353	0.168317	0.1137632	0.2148486	0.654556	0.59655	1	1.559651568
PC3-78	210544_s_at	ALDH3A2	4.9168	0.168317	0.1137632	0.2148486	0.654556	0.59655	0.89	1.558953967
PC3-78	201073_s_at	SMARCC1	0.7932	0.168317	0.1137632	0.2148486	0.654556	0.59655	1	1.556628458
PC3-78	202008_s_at	NID1	1.6926	0.168317	0.1137632	0.2148486	0.654556	0.59655	1	1.554375946
PC3-78	207781_s_at	ZNF6	1.2351	0.168317	0.1137632	0.2148486	0.654556	0.59655	1	1.553849766

PC3-78	205732_s_at	NCOA2	1.6382	0.168317	0.1137632	0.2148486	0.654556	0.59655	1	1.553717994
PC3-78	208663_s_at	TTC3	0.8902	0.168317	0.1137632	0.2148486	0.654556	0.59655	1	1.552348878
PC3-78	204427_s_at	TMED2	1.6021	0.168317	0.1137632	0.2148486	0.654556	0.59655	1	1.551988871
PC3-78	214930_at	SLITRK5	1.6455	0.168317	0.1137632	0.2148486	0.654556	0.59655	1	1.551957275
PC3-78	201646_at	SCARB2	0.7791	0.168317	0.1137632	0.2148486	0.654556	0.59655	1	1.548506017
PC3-78	208653_s_at	CD164	1.2671	0.168317	0.1137632	0.2148486	0.654556	0.59655	1	1.545748247
PC3-78	213156_at	---	0.976	0.29703	0.2302494	0.3550604	0.772047	0.68489	1	1.545345015
PC3-78	212387_at	TCF4	1.5402	0.168317	0.1137632	0.2148486	0.654556	0.59655	1	1.54305473
PC3-78	207291_at	PRRG4	2.0528	0.168317	0.1137632	0.2148486	0.654556	0.59655	1	1.542843882
PC3-78	217997_at	PHLDA1	1.9557	0.168317	0.1137632	0.2148486	0.654556	0.59655	1	1.539234176
PC3-78	204454_at	LDOC1	2.3339	0.168317	0.1137632	0.2148486	0.654556	0.59655	1	1.539090767
PC3-78	211273_s_at	TBX1	0.186	0.475248	0.4017935	0.5389654	0.845043	0.74969	1	1.537682281
PC3-78	205920_at	SLC6A6	3.5347	0.168317	0.1137632	0.2148486	0.654556	0.59655	1	1.537312514
PC3-78	206483_at	LRRC6	1.8198	0.168317	0.1137632	0.2148486	0.654556	0.59655	1	1.535006779
PC3-78	209120_at	NR2F2	1.6172	0.168317	0.1137632	0.2148486	0.654556	0.59655	1	1.534452303
PC3-78	213158_at	---	0.9596	0.39604	0.3243521	0.4584289	0.814185	0.71485	1	1.531383515
PC3-78	218006_s_at	ZNF22	1.2136	0.168317	0.1137632	0.2148486	0.654556	0.59655	1	1.528305939
PC3-78	210904_s_at	IL13RA1	2.1454	0.168317	0.1137632	0.2148486	0.654556	0.59655	1	1.527640408
PC3-78	201476_s_at	RRM1	1.4518	0.168317	0.1137632	0.2148486	0.654556	0.59655	1	1.527369605
PC3-78	203357_s_at	CAPN7	1.4021	0.168317	0.1137632	0.2148486	0.654556	0.59655	1	1.527011649
PC3-78	213891_s_at	TCF4	1.5115	0.168317	0.1137632	0.2148486	0.654556	0.59655	1	1.526701519
PC3-78	209426_s_at	AMACR	2.146	0.168317	0.1137632	0.2148486	0.654556	0.59655	1	1.526328958
PC3-78	210457_x_at	HMGGA1	0.9423	0.29703	0.2302494	0.3550604	0.772047	0.68489	1	1.526016635
PC3-78	200890_s_at	SSR1	1.0481	0.168317	0.1137632	0.2148486	0.654556	0.59655	1	1.52444572
PC3-78	208955_at	DUT	0.9858	0.168317	0.1137632	0.2148486	0.654556	0.59655	1	1.524106711
PC3-78	205071_x_at	XRCC4	1.3823	0.168317	0.1137632	0.2148486	0.654556	0.59655	1	1.52345566
PC3-78	201291_s_at	TOP2A	0.462	0.445545	0.3725421	0.5089743	0.841576	0.74674	1	1.522940375
PC3-78	203428_s_at	ASF1A	1.6015	0.168317	0.1137632	0.2148486	0.654556	0.59655	1	1.522857655
PC3-78	203032_s_at	FH	1.236	0.316832	0.2488067	0.3759975	0.772047	0.68489	1	1.522131755
PC3-78	91816_f_at	RKHD1	2.165	0.168317	0.1137632	0.2148486	0.654556	0.59655	1	1.522034985
PC3-78	212220_at	PSME4	1.1101	0.316832	0.2488067	0.3759975	0.772047	0.68489	1	1.521419714
PC3-78	202514_at	DLG1	0.9693	0.316832	0.2488067	0.3759975	0.772047	0.68489	1	1.521332562
PC3-78	211080_s_at	NEK2	1.4199	0.168317	0.1137632	0.2148486	0.654556	0.59655	1	1.520578093
PC3-78	203294_s_at	LMAN1	1.6261	0.168317	0.1137632	0.2148486	0.654556	0.59655	1	1.518051818
PC3-78	211019_s_at	LSS	0.8827	0.168317	0.1137632	0.2148486	0.654556	0.59655	1	1.517768864
PC3-78	209817_at	PPP3CB	2.732	0.168317	0.1137632	0.2148486	0.654556	0.59655	1	1.517016691
PC3-78	217788_s_at	GALNT2	1.9706	0.168317	0.1137632	0.2148486	0.654556	0.59655	1	1.516902983
PC3-78	220334_at	RGS17	2.191	0.168317	0.1137632	0.2148486	0.654556	0.59655	1	1.516119818
PC3-78	201879_at	ARIH1	2.763	0.168317	0.1137632	0.2148486	0.654556	0.59655	1	1.515387246
PC3-78	207469_s_at	PIR	2.2565	0.168317	0.1137632	0.2148486	0.654556	0.59655	1	1.515155238
PC3-78	218005_at	ZNF22	1.9121	0.168317	0.1137632	0.2148486	0.654556	0.59655	1	1.513178292
PC3-78	205364_at	ACOX2	1.639	0.168317	0.1137632	0.2148486	0.654556	0.59655	1	1.511588177
PC3-78	203196_at	ABCC4	1.0813	0.168317	0.1137632	0.2148486	0.654556	0.59655	1	1.510458274
PC3-78	222146_s_at	TCF4	1.4844	0.168317	0.1137632	0.2148486	0.654556	0.59655	1	1.509943824
PC3-78	217999_s_at	---	0.7608	0.316832	0.2488067	0.3759975	0.772047	0.68489	1	1.509014915
PC3-78	212651_at	RHOBTB1	1.6694	0.168317	0.1137632	0.2148486	0.654556	0.59655	1	1.508185508
PC3-78	205923_at	RELN	1.7901	0.168317	0.1137632	0.2148486	0.654556	0.59655	1	1.508074818
PC3-78	222019_at	HKE2	4.2358	0.168317	0.1137632	0.2148486	0.654556	0.59655	1	1.508042512
PC3-78	212453_at	KIAA1279	3.2783	0.168317	0.1137632	0.2148486	0.654556	0.59655	1	1.507887197
PC3-78	201654_s_at	HSPG2	0.5052	0.168317	0.1137632	0.2148486	0.654556	0.59655	1	1.507880104
PC3-78	219961_s_at	C20orf19	1.2427	0.168317	0.1137632	0.2148486	0.654556	0.59655	1	1.507448803
PC3-78	210148_at	HIPK3	2.1113	0.168317	0.1137632	0.2148486	0.654556	0.59655	1	1.507058569
PC3-78	203753_at	TCF4	1.1917	0.29703	0.2302494	0.3550604	0.772047	0.68489	1	1.506288759
PC3-78	215842_s_at	ATP11A	1.4252	0.168317	0.1137632	0.2148486	0.654556	0.59655	1	1.505319148
PC3-78	200917_s_at	SRPR	0.9409	0.168317	0.1137632	0.2148486	0.654556	0.59655	1	1.503176621
PC3-78	206748_s_at	SPAG9	1.0937	0.168317	0.1137632	0.2148486	0.654556	0.59655	1	1.502045906
PC3-78	208767_s_at	LAPTM4B	1.8364	0.168317	0.1137632	0.2148486	0.654556	0.59655	1	1.501584899
PC3-78	212105_s_at	DHX9	1.9587	0.168317	0.1137632	0.2148486	0.654556	0.59655	1	1.501384772
PC3-78	201663_s_at	SMC4L1	0.8751	0.168317	0.1137632	0.2148486	0.654556	0.59655	1	1.501221297
PC3-78	201580_s_at	TXNDC13	2.0537	0.168317	0.1137632	0.2148486	0.654556	0.59655	1	1.500652824
PC3-78	209121_x_at	NR2F2	1.4697	0.168317	0.1137632	0.2148486	0.654556	0.59655	1	1.50031084
PC3-78	212218_s_at	FASN	0.7186	0.267327	0.2026906	0.3233796	0.772047	0.68489	1	1.499293441
PC3-78	210116_at	SH2D1A	2.5578	0.168317	0.1137632	0.2148486	0.654556	0.59655	1	1.498423895
PC3-78	203394_s_at	HES1	0.7563	0.168317	0.1137632	0.2148486	0.654556	0.59655	1	1.498194139
PC3-78	203803_at	PCYOX1	1.0251	0.29703	0.2302494	0.3550604	0.772047	0.68489	1	1.49768387
PC3-78	218589_at	P2RY5	1.8161	0.168317	0.1137632	0.2148486	0.654556	0.59655	1	1.497581694
PC3-78	220643_s_at	FAIM	1.3855	0.168317	0.1137632	0.2148486	0.654556	0.59655	1	1.496376777
PC3-78	214908_s_at	TRRAP	1.4506	0.168317	0.1137632	0.2148486	0.654556	0.59655	1	1.495605328
PC3-78	208839_s_at	CAND1	0.7202	0.168317	0.1137632	0.2148486	0.654556	0.59655	1	1.495163002

PC3-78	217370_x_at	FUS	0.9639	0.168317	0.1137632	0.2148486	0.654556	0.59655	1	1.495036538
PC3-78	220014_at	LOC51334	1.0592	0.168317	0.1137632	0.2148486	0.654556	0.59655	1	1.494728957
PC3-82	204932_at	TNFRSF11B	-4.1977	0.009901	0	0.0147936	0.113315	0.19791	1	5.261552164
PC3-82	201110_s_at	THBS1	-5.4867	0.009901	0	0.0147936	0.113315	0.19791	0.89	4.831408115
PC3-82	214612_x_at	MAGEA6	-3.497	0.009901	0	0.0147936	0.113315	0.19791	1	4.407316704
PC3-82	204933_s_at	TNFRSF11B	-4.492	0.009901	0	0.0147936	0.113315	0.19791	1	4.309530831
PC3-82	209942_x_at	MAGEA3	-7.7611	0.009901	0	0.0147936	0.113315	0.19791	0.41	4.233286822
PC3-82	201109_s_at	THBS1	-2.7305	0.009901	0	0.0147936	0.113315	0.19791	1	4.196244383
PC3-82	201884_at	CEACAM5	-2.8697	0.009901	0	0.0147936	0.113315	0.19791	1	4.163698675
PC3-82	203021_at	SLPI	-4.3713	0.009901	0	0.0147936	0.113315	0.19791	1	3.539616523
PC3-82	211657_at	CEACAM6	-1.4178	0.009901	0	0.0147936	0.113315	0.19791	1	3.260180324
PC3-82	201042_at	TGM2	-2.3711	0.009901	0	0.0147936	0.113315	0.19791	1	3.142785598
PC3-82	203757_s_at	CEACAM6	-1.773	0.009901	0	0.0147936	0.113315	0.19791	1	2.970001386
PC3-82	210095_s_at	IGFBP3	-2.4807	0.009901	0	0.0147936	0.113315	0.19791	1	2.900522273
PC3-82	201108_s_at	THBS1	-4.2542	0.009901	0	0.0147936	0.113315	0.19791	1	2.89938604
PC3-82	209487_at	RBPMS	-3.0084	0.009901	0	0.0147936	0.113315	0.19791	1	2.873170687
PC3-82	211573_x_at	TGM2	-0.9845	0.009901	0	0.0147936	0.113315	0.19791	1	2.853109972
PC3-82	209488_s_at	RBPMS	-7.7124	0.009901	0	0.0147936	0.113315	0.19791	0.545	2.829891835
PC3-82	204455_at	DST	-2.934	0.009901	0	0.0147936	0.113315	0.19791	1	2.805763282
PC3-82	201242_s_at	ATP1B1	-4.8635	0.009901	0	0.0147936	0.113315	0.19791	0.89	2.712985019
PC3-82	219936_s_at	GPR87	-7.4629	0.009901	0	0.0147936	0.113315	0.19791	0.545	2.711751637
PC3-82	203691_at	PI3	-5.3318	0.009901	0	0.0147936	0.113315	0.19791	0.89	2.680088074
PC3-82	214292_at	ITGB4	-1.5998	0.009901	0	0.0147936	0.113315	0.19791	1	2.604842701
PC3-82	204351_at	S100P	-0.6978	0.009901	0	0.0147936	0.113315	0.19791	1	2.593216084
PC3-82	205992_s_at	IL15	-1.0286	0.009901	0	0.0147936	0.113315	0.19791	1	2.553093039
PC3-82	203889_at	SGNE1	-2.4597	0.009901	0	0.0147936	0.113315	0.19791	1	2.516567263
PC3-82	203918_at	PCDH1	-1.9273	0.009901	0	0.0147936	0.113315	0.19791	1	2.487016398
PC3-82	41469_at	PI3	-3.9739	0.009901	0	0.0147936	0.113315	0.19791	1	2.478560074
PC3-82	209016_s_at	KRT7	-2.8159	0.009901	0	0.0147936	0.113315	0.19791	1	2.439616212
PC3-82	205376_at	INPP4B	-2.6869	0.009901	0	0.0147936	0.113315	0.19791	1	2.394823668
PC3-82	218723_s_at	RGC32	-0.6472	0.009901	0	0.0147936	0.113315	0.19791	1	2.384602104
PC3-82	201243_s_at	ATP1B1	-2.5264	0.009901	0	0.0147936	0.113315	0.19791	1	2.304572792
PC3-82	214476_at	TFF2	-2.6409	0.009901	0	0.0147936	0.113315	0.19791	1	2.260509744
PC3-82	205016_at	TGFA	-1.7361	0.009901	0	0.0147936	0.113315	0.19791	1	2.235132275
PC3-82	218804_at	TMEM16A	-2.6256	0.009901	0	0.0147936	0.113315	0.19791	1	2.232202342
PC3-82	202859_x_at	IL8	-2.4158	0.009901	0	0.0147936	0.113315	0.19791	1	2.227670292
PC3-82	206025_s_at	TNFAIP6	-1.545	0.009901	0	0.0147936	0.113315	0.19791	1	2.174025472
PC3-82	202672_s_at	ATF3	-0.9031	0.009901	0	0.0147936	0.113315	0.19791	1	2.140088878
PC3-82	209631_s_at	GPR37	-11.003	0.009901	0	0.0147936	0.113315	0.19791	0.145	2.137312471
PC3-82	211003_x_at	TGM2	-1.6288	0.009901	0	0.0147936	0.113315	0.19791	1	2.111381407
PC3-82	202411_at	IFI27	-0.9692	0.009901	0	0.0147936	0.113315	0.19791	1	2.076565547
PC3-82	203851_at	IGFBP6	-2.3217	0.009901	0	0.0147936	0.113315	0.19791	1	2.065813514
PC3-82	205552_s_at	OAS1	-1.1705	0.009901	0	0.0147936	0.113315	0.19791	1	2.062107176
PC3-82	201473_at	JUNB	-1.5469	0.009901	0	0.0147936	0.113315	0.19791	1	2.051192084
PC3-82	210827_s_at	ELF3	-1.4138	0.009901	0	0.0147936	0.113315	0.19791	1	2.032826702
PC3-82	204990_s_at	ITGB4	-3.9353	0.009901	0	0.0147936	0.113315	0.19791	1	1.997688199
PC3-82	207574_s_at	GADD45B	-2.0077	0.009901	0	0.0147936	0.113315	0.19791	1	1.964067208
PC3-82	207850_at	CXCL3	-2.1982	0.009901	0	0.0147936	0.113315	0.19791	1	1.960282348
PC3-82	200878_at	EPAS1	-4.2236	0.009901	0	0.0147936	0.113315	0.19791	1	1.95114435
PC3-82	220468_at	ARF7	-2.4171	0.009901	0	0.0147936	0.113315	0.19791	1	1.95086702
PC3-82	219209_at	IFIH1	-1.8359	0.009901	0	0.0147936	0.113315	0.19791	1	1.946175795
PC3-82	204748_at	PTGS2	-1.7386	0.009901	0	0.0147936	0.113315	0.19791	1	1.922670646
PC3-82	214385_s_at	MUC5AC	-1.6848	0.009901	0	0.0147936	0.113315	0.19791	1	1.913011062
PC3-82	202869_at	OAS1	-1.1822	0.009901	0	0.0147936	0.113315	0.19791	1	1.911311112
PC3-82	213418_at	HSPA6	-0.1752	0.009901	0	0.0147936	0.113315	0.19791	1	1.911245129
PC3-82	209183_s_at	C10orf10	-1.0122	0.089109	0.0477178	0.1229598	0.654556	0.59655	1	1.90879553
PC3-82	208937_s_at	ID1	-1.7101	0.009901	0	0.0147936	0.113315	0.19791	1	1.903939696
PC3-82	217546_at	MT1M	-2.9978	0.009901	0	0.0147936	0.113315	0.19791	1	1.900745102
PC3-82	206026_s_at	TNFAIP6	-1.8251	0.009901	0	0.0147936	0.113315	0.19791	1	1.893361102
PC3-82	203789_s_at	SEMA3C	-0.6938	0.009901	0	0.0147936	0.113315	0.19791	1	1.890395019
PC3-82	202149_at	NEDD9	-3.4852	0.009901	0	0.0147936	0.113315	0.19791	1	1.884959272
PC3-82	213134_x_at	BTG3	-3.4059	0.009901	0	0.0147936	0.113315	0.19791	1	1.876810143
PC3-82	213711_at	KRTHB1	-2.6485	0.009901	0	0.0147936	0.113315	0.19791	1	1.8748312
PC3-82	204682_at	LTBP2	-3.5913	0.009901	0	0.0147936	0.113315	0.19791	1	1.870217023
PC3-82	208078_s_at	SNF1LK	-1.1452	0.009901	0	0.0147936	0.113315	0.19791	1	1.867663119
PC3-82	205869_at	PRSS1	-1.2771	0.009901	0	0.0147936	0.113315	0.19791	1	1.854357593
PC3-82	211564_s_at	PDLIM4	-2.0663	0.009901	0	0.0147936	0.113315	0.19791	1	1.854221876
PC3-82	211506_s_at	IL8	-1.5132	0.009901	0	0.0147936	0.113315	0.19791	1	1.851528519

PC3-82	205366_s_at	HOXB6	-4.859	0.009901	0	0.0147936	0.113315	0.19791	0.89	1.850382427
PC3-82	209160_at	AKR1C3	-1.5109	0.009901	0	0.0147936	0.113315	0.19791	1	1.843714511
PC3-82	222108_at	AMIGO2	-4.6016	0.009901	0	0.0147936	0.113315	0.19791	0.89	1.83797613
PC3-82	219371_s_at	KLF2	-1.2703	0.158416	0.1051867	0.2036806	0.654556	0.59655	1	1.819544114
PC3-82	203632_s_at	GPRC5B	-9.6873	0.009901	0	0.0147936	0.113315	0.19791	0.145	1.818833229
PC3-82	206508_at	TNFSF7	-4.9798	0.009901	0	0.0147936	0.113315	0.19791	0.89	1.808769363
PC3-82	213258_at	TFPI	-0.6435	0.009901	0	0.0147936	0.113315	0.19791	1	1.798947994
PC3-82	221009_s_at	ANGPTL4	-0.6032	0.009901	0	0.0147936	0.113315	0.19791	1	1.790994464
PC3-82	212099_at	RHOB	-1.3629	0.009901	0	0.0147936	0.113315	0.19791	1	1.770553594
PC3-82	201289_at	CYR61	-2.9714	0.009901	0	0.0147936	0.113315	0.19791	1	1.755235577
PC3-82	210999_s_at	GRB10	-1.7471	0.009901	0	0.0147936	0.113315	0.19791	1	1.754550234
PC3-82	218543_s_at	PARP12	-1.412	0.009901	0	0.0147936	0.113315	0.19791	1	1.752992513
PC3-82	201061_s_at	STOM	-2.2993	0.009901	0	0.0147936	0.113315	0.19791	1	1.749881682
PC3-82	204512_at	HIVEP1	-1.6047	0.009901	0	0.0147936	0.113315	0.19791	1	1.744202213
PC3-82	215243_s_at	GJB3	-3.1653	0.009901	0	0.0147936	0.113315	0.19791	1	1.738502334
PC3-82	205807_s_at	TUFT1	-3.3936	0.009901	0	0.0147936	0.113315	0.19791	1	1.728400969
PC3-82	209774_x_at	CXCL2	-2.3825	0.009901	0	0.0147936	0.113315	0.19791	1	1.727453976
PC3-82	219352_at	HERC6	-1.4488	0.009901	0	0.0147936	0.113315	0.19791	1	1.725394645
PC3-82	203153_at	IFIT1	-1.702	0.009901	0	0.0147936	0.113315	0.19791	1	1.722735357
PC3-82	206114_at	EPHA4	-3.0531	0.009901	0	0.0147936	0.113315	0.19791	1	1.721844205
PC3-82	214974_x_at	CXCL5	-0.5937	0.009901	0	0.0147936	0.113315	0.19791	1	1.721260612
PC3-82	201502_s_at	NFKBIA	-2.4875	0.009901	0	0.0147936	0.113315	0.19791	1	1.71835573
PC3-82	204989_s_at	ITGB4	-1.2814	0.009901	0	0.0147936	0.113315	0.19791	1	1.717823281
PC3-82	212242_at	TUBA1	-3.156	0.009901	0	0.0147936	0.113315	0.19791	1	1.71690428
PC3-82	205490_x_at	GJB3	-2.6502	0.009901	0	0.0147936	0.113315	0.19791	1	1.71614472
PC3-82	205009_at	TFF1	-2.1042	0.009901	0	0.0147936	0.113315	0.19791	1	1.705570815
PC3-82	212268_at	SERPINB1	-1.1464	0.009901	0	0.0147936	0.113315	0.19791	1	1.702156497
PC3-82	203726_s_at	LAMA3	-1.8461	0.009901	0	0.0147936	0.113315	0.19791	1	1.698279027
PC3-82	212647_at	RRAS	-2.5527	0.009901	0	0.0147936	0.113315	0.19791	1	1.697643694
PC3-82	211006_s_at	KCNB1	-3.6497	0.009901	0	0.0147936	0.113315	0.19791	1	1.69501591
PC3-82	219010_at	C1orf106	-3.6581	0.009901	0	0.0147936	0.113315	0.19791	1	1.69379636
PC3-82	202086_at	MX1	-0.9811	0.158416	0.1051867	0.2036806	0.654556	0.59655	1	1.693175829
PC3-82	209270_at	LAMB3	-1.7127	0.009901	0	0.0147936	0.113315	0.19791	1	1.691713168
PC3-82	213572_s_at	SERPINB1	-0.8857	0.009901	0	0.0147936	0.113315	0.19791	1	1.690300382
PC3-82	210665_at	TFPI	-1.2713	0.009901	0	0.0147936	0.113315	0.19791	1	1.689862079
PC3-82	209949_at	NCF2	-2.3185	0.009901	0	0.0147936	0.113315	0.19791	1	1.680796101
PC3-82	205780_at	BIK	-1.8876	0.009901	0	0.0147936	0.113315	0.19791	1	1.680383454
PC3-82	212530_at	NEK7	-0.9195	0.009901	0	0.0147936	0.113315	0.19791	1	1.677658992
PC3-82	201540_at	FHL1	-0.7354	0.009901	0	0.0147936	0.113315	0.19791	1	1.677314797
PC3-82	219529_at	CLIC3	-1.4255	0.009901	0	0.0147936	0.113315	0.19791	1	1.676805624
PC3-82	204337_at	RG54	-2.0788	0.009901	0	0.0147936	0.113315	0.19791	1	1.676249917
PC3-82	202052_s_at	RAI14	-1.8535	0.009901	0	0.0147936	0.113315	0.19791	1	1.674871953
PC3-82	210689_at	CLDN14	-2.7382	0.009901	0	0.0147936	0.113315	0.19791	1	1.674066352
PC3-82	203438_at	STC2	-0.5796	0.009901	0	0.0147936	0.113315	0.19791	1	1.67143366
PC3-82	202863_at	SP100	-1.6145	0.009901	0	0.0147936	0.113315	0.19791	1	1.67137622
PC3-82	205798_at	IL7R	-2.8162	0.009901	0	0.0147936	0.113315	0.19791	1	1.669780507
PC3-82	210002_at	GATA6	-2.1431	0.009901	0	0.0147936	0.113315	0.19791	1	1.668120788
PC3-82	218573_at	MAGEH1	-2.8453	0.009901	0	0.0147936	0.113315	0.19791	1	1.666554227
PC3-82	213793_s_at	HOMER1	-2.4371	0.009901	0	0.0147936	0.113315	0.19791	1	1.666097644
PC3-82	207836_s_at	RBPMS	-2.4429	0.009901	0	0.0147936	0.113315	0.19791	1	1.664938464
PC3-82	212923_s_at	C6orf145	-2.0895	0.009901	0	0.0147936	0.113315	0.19791	1	1.663808237
PC3-82	210664_s_at	TFPI	-1.6055	0.009901	0	0.0147936	0.113315	0.19791	1	1.654580799
PC3-82	217572_at	---	-1.0611	0.009901	0	0.0147936	0.113315	0.19791	1	1.654510836
PC3-82	205463_s_at	PDGFA	-3.3303	0.009901	0	0.0147936	0.113315	0.19791	1	1.649643329
PC3-82	214303_x_at	MUC5AC	-1.1773	0.009901	0	0.0147936	0.113315	0.19791	1	1.649369961
PC3-82	202864_s_at	SP100	-1.5082	0.009901	0	0.0147936	0.113315	0.19791	1	1.648698874
PC3-82	202150_s_at	NEDD9	-1.8527	0.009901	0	0.0147936	0.113315	0.19791	1	1.648171358
PC3-82	201012_at	ANXA1	-1.576	0.009901	0	0.0147936	0.113315	0.19791	1	1.647561318
PC3-82	212143_s_at	IGFBP3	-1.7884	0.009901	0	0.0147936	0.113315	0.19791	1	1.644993559
PC3-82	209304_x_at	GADD45B	-1.3841	0.009901	0	0.0147936	0.113315	0.19791	1	1.642731474
PC3-82	206884_s_at	SCEL	-6.7554	0.009901	0	0.0147936	0.113315	0.19791	0.745	1.635582291
PC3-82	209761_s_at	SP110	-1.6133	0.009901	0	0.0147936	0.113315	0.19791	1	1.635477686
PC3-82	214175_x_at	PDLIM4	-2.5342	0.009901	0	0.0147936	0.113315	0.19791	1	1.632209509
PC3-82	205856_at	SLC14A1	-1.2843	0.009901	0	0.0147936	0.113315	0.19791	1	1.629023804
PC3-82	215617_at	---	-0.5151	0.009901	0	0.0147936	0.113315	0.19791	1	1.628866275
PC3-82	202409_at	LOC492304	-1.2903	0.009901	0	0.0147936	0.113315	0.19791	1	1.625352309
PC3-82	202504_at	TRIM29	-3.0079	0.009901	0	0.0147936	0.113315	0.19791	1	1.619549293
PC3-82	209762_x_at	SP110	-1.9885	0.009901	0	0.0147936	0.113315	0.19791	1	1.617509509
PC3-82	218611_at	IER5	-1.443	0.009901	0	0.0147936	0.113315	0.19791	1	1.613354089

PC3-82	203824_at	TSPAN8	-2.3822	0.009901	0	0.0147936	0.113315	0.19791	1	1.611770218
PC3-82	207517_at	LAMC2	-2.1025	0.009901	0	0.0147936	0.113315	0.19791	1	1.611443001
PC3-82	212256_at	GALNT10	-2.7903	0.009901	0	0.0147936	0.113315	0.19791	1	1.609638013
PC3-82	208012_x_at	SP110	-1.9761	0.009901	0	0.0147936	0.113315	0.19791	1	1.608860958
PC3-82	216060_s_at	DAAM1	-1.1838	0.009901	0	0.0147936	0.113315	0.19791	1	1.605334575
PC3-82	215206_at	EXT1	-0.9203	0.009901	0	0.0147936	0.113315	0.19791	1	1.604850616
PC3-82	206277_at	P2RY2	-3.0564	0.009901	0	0.0147936	0.113315	0.19791	1	1.60416036
PC3-82	213001_at	ANGPTL2	-2.5011	0.009901	0	0.0147936	0.113315	0.19791	1	1.60290644
PC3-82	220180_at	SE57-1	-2.0144	0.009901	0	0.0147936	0.113315	0.19791	1	1.602253147
PC3-82	205548_s_at	BTG3	-2.2756	0.009901	0	0.0147936	0.113315	0.19791	1	1.600089089
PC3-82	209493_at	PDZK3	-0.9119	0.009901	0	0.0147936	0.113315	0.19791	1	1.594394157
PC3-82	220104_at	ZC3HAV1	-0.9118	0.009901	0	0.0147936	0.113315	0.19791	1	1.590647022
PC3-82	202458_at	PRSS23	-2.1909	0.009901	0	0.0147936	0.113315	0.19791	1	1.590549428
PC3-82	205173_x_at	CD58	-0.6022	0.009901	0	0.0147936	0.113315	0.19791	1	1.58080049
PC3-82	204612_at	PKIA	-2.3202	0.009901	0	0.0147936	0.113315	0.19791	1	1.578759272
PC3-82	204338_s_at	RGS4	-2.2911	0.009901	0	0.0147936	0.113315	0.19791	1	1.578482608
PC3-82	221884_at	EVI1	-1.3923	0.009901	0	0.0147936	0.113315	0.19791	1	1.578174402
PC3-82	201641_at	BST2	-0.8124	0.158416	0.1051867	0.2036806	0.654556	0.59655	1	1.577828795
PC3-82	204151_x_at	AKR1C1	-1.6504	0.009901	0	0.0147936	0.113315	0.19791	1	1.577581805
PC3-82	200904_at	HLA-E	-0.9498	0.009901	0	0.0147936	0.113315	0.19791	1	1.574261028
PC3-82	202267_at	LAMC2	-1.8057	0.009901	0	0.0147936	0.113315	0.19791	1	1.57343645
PC3-82	202481_at	DHR83	-1.05	0.009901	0	0.0147936	0.113315	0.19791	1	1.571988156
PC3-82	209969_s_at	STAT1	-0.7681	0.376238	0.3052793	0.4380074	0.809472	0.70959	1	1.57096365
PC3-82	202410_x_at	IGF2	-0.3327	0.009901	0	0.0147936	0.113315	0.19791	1	1.567222451
PC3-82	213004_at	ANGPTL2	-2.3953	0.009901	0	0.0147936	0.113315	0.19791	1	1.563848817
PC3-82	213089_at	LOC153561	-1.9258	0.009901	0	0.0147936	0.113315	0.19791	1	1.560811029
PC3-82	203592_s_at	FSTL3	-1.4473	0.009901	0	0.0147936	0.113315	0.19791	1	1.559133248
PC3-82	213644_at	MGC33887	-0.6071	0.009901	0	0.0147936	0.113315	0.19791	1	1.5567953
PC3-82	201506_at	TGFBI	-3.2381	0.009901	0	0.0147936	0.113315	0.19791	1	1.554635662
PC3-82	203939_at	NT5E	-1.3086	0.009901	0	0.0147936	0.113315	0.19791	1	1.55458718
PC3-82	204326_x_at	MT1X	-1.4526	0.009901	0	0.0147936	0.113315	0.19791	1	1.550475269
PC3-82	218456_at	C1QDC1	-3.1403	0.009901	0	0.0147936	0.113315	0.19791	1	1.548549581
PC3-82	209409_at	GRB10	-2.621	0.009901	0	0.0147936	0.113315	0.19791	1	1.544106919
PC3-82	200696_s_at	GSN	-1.5853	0.009901	0	0.0147936	0.113315	0.19791	1	1.543961016
PC3-82	215248_at	GRB10	-1.3539	0.009901	0	0.0147936	0.113315	0.19791	1	1.543177739
PC3-82	219165_at	PDLIM2	-2.7221	0.009901	0	0.0147936	0.113315	0.19791	1	1.540358694
PC3-82	201250_s_at	SLC2A1	-0.8316	0.009901	0	0.0147936	0.113315	0.19791	1	1.539143619
PC3-82	218986_s_at	FLJ20035	-1.5991	0.009901	0	0.0147936	0.113315	0.19791	1	1.53747311
PC3-82	211905_s_at	ITGB4	-0.4268	0.009901	0	0.0147936	0.113315	0.19791	1	1.536227258
PC3-82	221765_at	UGCG	-1.4488	0.009901	0	0.0147936	0.113315	0.19791	1	1.535322558
PC3-82	212444_at	GPCR5A	-2.5073	0.009901	0	0.0147936	0.113315	0.19791	1	1.53527282
PC3-82	205659_at	HDAC9	-1.0563	0.009901	0	0.0147936	0.113315	0.19791	1	1.534789977
PC3-82	216442_x_at	FN1	-2.225	0.009901	0	0.0147936	0.113315	0.19791	1	1.533721545
PC3-82	205660_at	OASL	-1.7796	0.009901	0	0.0147936	0.113315	0.19791	1	1.532941133
PC3-82	210764_s_at	CYR61	-1.3965	0.009901	0	0.0147936	0.113315	0.19791	1	1.53243383
PC3-82	202071_at	SDC4	-1.1506	0.158416	0.1051867	0.2036806	0.654556	0.59655	1	1.531429332
PC3-82	212488_at	COL5A1	-0.5875	0.009901	0	0.0147936	0.113315	0.19791	1	1.527337776
PC3-82	209800_at	KRT16	-1.4388	0.009901	0	0.0147936	0.113315	0.19791	1	1.526383915
PC3-82	202177_at	GAS6	-2.3575	0.009901	0	0.0147936	0.113315	0.19791	1	1.526274175
PC3-82	215717_s_at	FBN2	-0.5072	0.237624	0.1754954	0.2913356	0.770626	0.68347	1	1.523549453
PC3-82	204345_at	COL16A1	-0.8745	0.009901	0	0.0147936	0.113315	0.19791	1	1.523182755
PC3-82	217764_s_at	RAB31	-2.0261	0.009901	0	0.0147936	0.113315	0.19791	1	1.523052057
PC3-82	204114_at	NID2	-0.9521	0.009901	0	0.0147936	0.113315	0.19791	1	1.522445732
PC3-82	201841_s_at	HSPB1	-0.5312	0.138614	0.0882631	0.1811164	0.654556	0.59655	1	1.522182827
PC3-82	214453_s_at	IFI44	-1.0579	0.158416	0.1051867	0.2036806	0.654556	0.59655	1	1.519056152
PC3-82	219691_at	SAMD9	-1.0819	0.09901	0.0555734	0.134841	0.654556	0.59655	1	1.517564229
PC3-82	204439_at	IFI44L	-1.2557	0.158416	0.1051867	0.2036806	0.654556	0.59655	1	1.514477111
PC3-82	217683_at	HBE1	-0.5688	0.009901	0	0.0147936	0.113315	0.19791	1	1.514142517
PC3-82	204148_s_at	ZP3 /// POMZP	-2.6643	0.009901	0	0.0147936	0.113315	0.19791	1	1.51337432
PC3-82	213526_s_at	PSENFEN /// F2	-0.7208	0.009901	0	0.0147936	0.113315	0.19791	1	1.513311602
PC3-82	216594_x_at	AKR1C1	-1.8227	0.009901	0	0.0147936	0.113315	0.19791	1	1.513099524
PC3-82	202796_at	SYNPO	-1.9355	0.009901	0	0.0147936	0.113315	0.19791	1	1.512643554
PC3-82	210511_s_at	INHBA	-2.0763	0.009901	0	0.0147936	0.113315	0.19791	1	1.511347257
PC3-82	211653_x_at	AKR1C2	-2.4678	0.009901	0	0.0147936	0.113315	0.19791	1	1.511110678
PC3-82	203108_at	GPRC5A	-1.1125	0.009901	0	0.0147936	0.113315	0.19791	1	1.510251648
PC3-82	201482_at	QSCN6	-0.8971	0.158416	0.1051867	0.2036806	0.654556	0.59655	1	1.509984372
PC3-82	205402_x_at	PRSS2	-0.5254	0.009901	0	0.0147936	0.113315	0.19791	1	1.509878394
PC3-82	201466_s_at	JUN	-1.0354	0.009901	0	0.0147936	0.113315	0.19791	1	1.506635015
PC3-82	221911_at	ETV1	-0.9633	0.079208	0.0400305	0.1109139	0.654556	0.59655	1	1.506498603

PC3-82	204675_at	SRD5A1	-2.2267	0.009901	0	0.0147936	0.113315	0.19791	1	1.505271434
PC3-82	217591_at	SKIL	-1.512	0.009901	0	0.0147936	0.113315	0.19791	1	1.503326439
PC3-82	206027_at	S100A3	-5.1148	0.009901	0	0.0147936	0.113315	0.19791	0.89	1.498578549
PC3-82	210740_s_at	ITPK1	-2.8412	0.009901	0	0.0147936	0.113315	0.19791	1	1.498179993
PC3-82	213930_at	---	-2.261	0.009901	0	0.0147936	0.113315	0.19791	1	1.498100296
PC3-82	218677_at	S100A14	-0.9996	0.009901	0	0.0147936	0.113315	0.19791	1	1.498037515
PC3-82	215495_s_at	SAMD4	-1.5774	0.009901	0	0.0147936	0.113315	0.19791	1	1.497517067
PC3-82	214321_at	NOV	-1.2855	0.009901	0	0.0147936	0.113315	0.19791	1	1.496948607
PC3-82	212096_s_at	MTUS1	-5.5705	0.009901	0	0.0147936	0.113315	0.19791	0.89	1.496818331
PC3-82	211719_x_at	FN1	-1.4436	0.009901	0	0.0147936	0.113315	0.19791	1	1.496013118
PC3-82	204646_at	DPYD	-0.4358	0.009901	0	0.0147936	0.113315	0.19791	1	1.495408843

Tumor-Secreted Vascular Endothelial Growth Factor-C Is Necessary for Prostate Cancer Lymphangiogenesis, but Lymphangiogenesis Is Unnecessary for Lymph Node Metastasis

Sunny Y. Wong,^{1,2} Herbert Haack,¹ Denise Crowley,¹ Marc Barry,¹ Roderick T. Bronson,³ and Richard O. Hynes^{1,2}

¹Howard Hughes Medical Institute, Center for Cancer Research; ²Department of Biology, Massachusetts Institute of Technology, Cambridge; and ³Department of Biomedical Sciences, Tufts University School of Veterinary Medicine, North Grafton, Massachusetts

Abstract

Dissemination to draining lymph nodes is a frequent first step in prostate cancer metastasis. Although tumors metastasize to lymph nodes via the lymphatics, the importance of lymphangiogenesis in mediating the process remains controversial. Here, we inhibit intratumoral lymphangiogenesis in s.c. and surgical orthotopic implantation mouse models of human prostate cancer using several strategies. Stable expression of small interfering RNAs (siRNA) targeted against human vascular endothelial growth factor-C (VEGF-C) in PC-3 cells reduced intratumoral lymphatics by 99% in s.c. tumors, indicating that tumor-secreted VEGF-C is necessary for lymphangiogenesis. Expression of siRNAs against human VEGF-A somewhat reduced tumor lymphangiogenesis. Secretion of a soluble VEGF receptor-3/Flt4 fusion protein by PC-3 cells reduced intratumoral lymphatics by 100% in s.c. tumors. Combination of soluble Flt4 and VEGF-C siRNA yielded >92% reduction of intratumoral lymphatics in orthotopic prostate tumors. However, metastasis to lymph nodes was not significantly affected regardless of intratumoral lymphatic vessel density. The abundance of marginal lymphatics at the tumor-stromal interface was unchanged in orthotopic tumors whose intratumoral lymphatics were inhibited, suggesting that these marginal vessels could be sufficient for lymph node metastasis. Hematogenous metastasis (blood tumor burden, lung metastasis) correlated with degree of lymph node invasion. We also analyzed the lymphatics in spontaneous transgenic adenocarcinomas of the mouse prostate which metastasize to lymph nodes. Progression from well-differentiated prostate intraepithelial neoplasia to metastatic, undifferentiated adenocarcinoma was accompanied by loss of lymphatics. These results suggest that tumor-secreted VEGF-C and, to a lesser extent, VEGF-A, are important for inducing prostate cancer intratumoral lymphangiogenesis but are unnecessary for lymph node metastasis. (Cancer Res 2005; 65(21): 9789-98)

Introduction

In prostate cancer, metastasis to regional lymph nodes is a frequent early event that is correlated with poor clinical prognosis

(1, 2). Typically, pelvic lymphadenectomy is done prior to radical prostatectomy to assess lymph node status. In patients with lymph node-positive prostate cancer, 75% will possess bone metastases within 5 years regardless of treatment (2).

Analysis of metastasis patterns in human prostate cancer (1, 3) as well as lymphatic mapping studies using tracking dyes in breast and melanoma (4, 5) have shown that the pattern of tumor-to-lymph node dissemination is nonrandom. Tumors first invade draining (sentinel) lymph nodes before seeding more distant nodes (6). If the sentinel node is free of metastasis, other lymph nodes will also likely be uninvaded (7). Therefore, lymphatic vessels within or in proximity to tumors mediate dissemination to draining lymph nodes, which may then allow further seeding to more distant sites.

Although lymphatic vessels can be detected in prostate cancer (8–10), the role of intratumoral lymphatics in mediating lymph node metastasis has been controversial. While numerous clinical studies have correlated lymphatic vessel density (LVD) with lymph node metastasis in various cancers, nearly as many have failed to detect such associations (for a summary of clinical data, see ref. 11). In prostate cancer, increased LVD has been correlated both with lymph node metastasis (9, 10) and with higher Gleason score (8, 9), an indicator of more aggressive tumors. Consequently, it is unclear whether tumoral lymphatics actually facilitate lymph node metastasis, or are simply markers of tumors prone to disseminate regardless of LVD.

Tumor lymphangiogenesis is thought to rely on preexisting lymphatics (12). The major lymphangiogenic cytokines are vascular endothelial growth factors-C and -D (VEGF-C and VEGF-D), although platelet-derived growth factor-BB has also recently been implicated (13). VEGF-C and VEGF-D primarily bind VEGF receptor-3 (VEGFR-3, or Flt4) on the surface of lymphatic endothelial cells (14). Levels of VEGF-C/D have generally correlated with lymph node metastasis in human patients (13), and experimental overexpression of VEGF-C (15–17), VEGF-D (18), and platelet-derived growth factor-BB (19) in cell lines has resulted in increased tumor LVD and lymph node metastasis in tumor implantation models. Similar results were also obtained when VEGF-C was overexpressed in spontaneous Rip-Tag tumors (20). Whether the effects are due to increased lymphatic permeability or activation and/or increased abundance of intratumoral and/or peritumoral lymphatics remains unclear (13, 21).

Other studies have suggested that intratumoral lymphatics may be nonfunctional (17, 22, 23), or display abnormal function at the periphery (24), implying that lymphangiogenesis plays little role in facilitating primary tumor dissemination. In contrast, others have shown that interfering with ligand binding to VEGFR-3/Flt4 using a soluble receptor can inhibit tumor lymphangiogenesis and reduce lymph node metastasis (25–29). In most cases, both peritumoral

Note: Supplementary data for this article are available at Cancer Research Online (<http://cancerres.aacrjournals.org/>).

H. Haack is presently at Cell Signaling Technology, 166B Cummings Center, Beverly, MA 01915.

Requests for reprints: Richard O. Hynes, E17-227, Massachusetts Institute of Technology, Cambridge, MA 02139. Phone: 617-253-6422; Fax: 617-253-8357; E-mail: rohynes@mit.edu.

©2005 American Association for Cancer Research.

doi:10.1158/0008-5472.CAN-05-0901

and intratumoral lymphatic vessels were affected, although some have speculated that the soluble receptor may have little or no effect on preexisting lymphatics (28, 30). Consequently, the requirement for tumor lymphangiogenesis, and the relative roles of intratumoral and peritumoral—preexisting or induced—lymphatics in mediating lymph node metastasis have remained controversial (13).

To address these questions, we investigated the contributions of intratumoral, tumor-induced lymphatics and peritumoral lymphatics in facilitating lymph node metastasis by inhibiting lymphangiogenesis in a surgical orthotopic implantation (SOI) model of human prostate cancer. Our results show that, although intratumoral lymphangiogenesis can be selectively ablated, this has no effect on lymph node metastasis. We also found that spontaneous transgenic adenocarcinoma of the mouse prostate (TRAMP) tumors do not induce lymphangiogenesis but nevertheless metastasize to lymph nodes. These results argue that peritumoral lymphatic vessels, perhaps preexisting at the tumor margins—and not intratumoral lymphatics induced by lymphangiogenesis—are critical for mediating lymph node dissemination.

Materials and Methods

Cell culture and mice. A subline of the human prostate adenocarcinoma cell line PC-3 (American Type Culture Collection, Manassas, VA) was derived in our laboratory and used in these studies (designated PC3-#82). Cells were cultured in F-12K medium (Kaign's modification; Life Technologies-Invitrogen, Frederick, MD) containing 10% fetal bovine serum, glutamine, and antibiotics. Small interfering RNA (siRNA) experiments used PC3-#82 cells expressing ecotropic receptor (plasmid provided by H. Lodish, Biology, Massachusetts Institute of Technology, Cambridge, MA). Immunodeficient CD-1 nude mice, 30 to 35 days old (Charles River Laboratories, Wilmington, MA), were used for xenograft experiments. TRAMP mice (The Jackson Laboratory, Bar Harbor, ME; ref. 31) in a C57BL/6 background were obtained from A. Bai, Biology, Massachusetts Institute of Technology, Cambridge, MA.

Plasmids. PC3-#82 cells were transfected with Flt4-Ig expression plasmid (originally "VEGFR-3-Ig/pEBS7", K. Alitalo, Biomedicum, University of Helsinki, Helsinki, Finland; refs. 25, 32) using Effectene reagent (Qiagen, Valencia, CA) and selected with hygromycin (100–200 $\mu\text{g}/\text{mL}$) for stable expression. Ig-Neg control plasmid was made by removing the Flt4 coding sequence. All siRNAs were inserted into the retroviral vector pSIRISP (W.C. Hahn, Dana Farber Cancer Institute, Boston, MA; ref. 33). The siRNA plasmids were transfected with Effectene into Phoenix cells (American Type Culture Collection), and the secreted virus was subsequently used for stable infection of PC3-#82 cells expressing ecotropic receptor. After infection, cells were selected on puromycin (2.5 $\mu\text{g}/\text{mL}$) for stable siRNA expression. Please refer to Supplementary Materials for siRNA sequences.

Xenografts. s.c. tumors were obtained by injecting 2×10^6 cells into CD-1 nude mice anesthetized with avertin/tribromethanol. Tumors were removed for analysis and/or used as donor material for SOI ~3.5 weeks after injection, as described previously (34, 35). Briefly, a peripheral portion of the tumor was removed and sliced into ~1 mm³ cubes under a dissecting microscope. CD-1 mice were anesthetized, and the abdominal regions exposed with an incision along the lower midline. A single tumor fragment was embedded into the right dorsolateral capsule and secured with 9-0 microsutures (Ethicon, Somerville, NJ). The peritoneum and overlying skin were each closed with one set of 5-0 sutures (United States Surgical, Norwalk, CT). The entire protocol was done in sterile conditions inside a fume hood, in accordance with animal care guidelines. Mice were analyzed when moribund, as judged by bladder/abdominal distension and/or severe weight loss (typically 2–3 months after implantation). Primary tumors were flash-frozen or fixed for immunohistochemistry. Lymph nodes were removed, fixed, weighed, and sectioned. A lymph node set was considered macroscopically invaded if its total mass exceeded 30 mg (by histology, typically >80% of the node is tumor material at this size; see Supplementary Table S1).

Vascular endothelial growth factor-C and -A RNA quantitation. Total RNA was extracted using RNeasy (Qiagen). RNA was digested with DNase (Ambion, Austin, TX), then re-cleaned with RNeasy. One microgram of total RNA was reverse-transcribed into cDNA using TaqMan reverse transcription reagent (Applied Biosystems, Branchburg, NJ). cDNAs were analyzed by quantitative PCR using SYBR Green PCR amplification kit (Applied Biosystems), measured in a Bio-Rad iCycler (Bio-Rad, Richmond, CA). Target gene message levels were normalized to glyceraldehyde-3-phosphate dehydrogenase levels, and then to the control sample. See Supplementary Materials for real-time PCR primer sequences.

Vascular endothelial growth factor-C and -A protein quantitation. PC3-#82 cells (5×10^5) were plated into 10 cm² plates and grown for 72 hours. Medium was replaced, conditioned for the times specified, collected, and spun to remove debris. Frozen s.c. and orthotopic tumors were thawed and homogenized in 1 mL cold CellLytic-MT mammalian cell lysis buffer (Sigma-Aldrich, St. Louis, MO) per gram of tumor material. Lysis buffer contained protease inhibitors (Roche, Mannheim, Germany). After homogenization, the lysate was chilled for >30 minutes, then spun to remove debris. Total soluble protein was quantitated by bicinchoninic acid protein assay (Pierce, Rockford, IL) to normalize ELISA results. The supernatant was diluted 1:4 or 1:10 in PC-3 medium for ELISA. Diluted tumor supernatant (200 μL) or undiluted conditioned medium was analyzed by human VEGF-A Quantikine ELISA (R&D Systems, Minneapolis, MN); 100 μL of the same were analyzed by human VEGF-C ELISA (IBL, Tokyo, Japan).

Immunoblotting. Soluble Flt4-Ig was detected by immunoprecipitating conditioned medium with Protein A beads (Invitrogen, Carlsbad, CA). The beads were spun, washed, and boiled in Laemmli SDS buffer containing 5% β -mercaptoethanol. The protein was run on 8% SDS gel and detected with goat anti-human VEGFR-3 antibody (clone AF349; 1:100 diluted; R&D Systems) or rabbit anti-human antibody conjugated to horseradish peroxidase (1:1,000 diluted; DAKO, Glostrup, Denmark). Tumor Flt4-Ig was detected in tumors by homogenizing in CellLytic-MT lysis buffer, as above, and running supernatant on SDS-PAGE.

Histology and immunohistochemistry. For immunohistochemistry, 2- to 3-mm-thick portions were removed near the periphery of the anterior-facing end of the tumor. For wild-type and TRAMP prostates, the dorsolateral lobes were dissected. In most cases, the tissue was fixed in zinc (Becton Dickinson, San Diego, CA) for 48 hours. For short-term orthotopic analysis, prostate tissue was fixed in 3.7% formaldehyde overnight. Primary antibodies for immunohistochemistry included rabbit anti-LYVE-1 (Ruoslahti lab; 1:450; ref. 36), goat anti-mouse VEGFR-3 (clone AF743, R&D Systems; 1:25) and rat anti-CD34 (clone RAM34, BD Pharmingen, San Diego, CA; 1:25). Sections were dewaxed, microwaved in BD Retrieval buffer, and stained using standard protocols. Biotin-conjugated secondary antibodies included swine anti-rabbit immunoglobulin (DAKO) and rabbit anti-rat immunoglobulin (Vector Labs, Burlingame, CA), both diluted 1:250. Staining was amplified with Vectastain ABC kit (Vector Labs), developed with Vector VIP peroxidase substrate and counterstained with methyl green. Lymphatic and blood vessels were quantitated by counting the number of LYVE-1 or CD34-positive vessels, respectively, in two random, low-power fields (2.25 \times 1.7 mm) per tumor. About 30% to 100% of the tumor area is covered with this approach, and the LVD from a minimum of seven independent tumors was typically quantitated for each cell line. In TRAMP and normal prostates, a single low-power field was used for lymphatic quantitation, typically covering 70% to 100% of the sample. TRAMP tumor grading was based on a system described by Hurwitz et al. (37). Two pathologists (M. Barry and R. Bronson) independently graded H&E TRAMP sections, and then together arrived at an agreed upon grade. For short-term SOI analysis, the length of the tumor periphery at $\times 105$ final magnification was quantitated in pixel units by OpenLab software (Improvision Inc., Lexington, MA), and the number of lymphatics at the periphery was normalized to a 1,000-pixel perimeter. We defined "intratumoral" lymphatics as LYVE-1-positive vessels completely surrounded by tumor cells, and "marginal" or "peritumoral" lymphatics as vessels in contact with both tumor cells and stroma.

Statistics. All statistical comparisons were calculated with the unpaired Student's *t* test. All error bars show \pm SE.

Results

Stable small interfering RNAs specifically reduce vascular endothelial growth factor-C or -A expression and protein secretion. s.c. tumors formed by a subline of PC-3 prostate cancer cells (designated PC3-#82) possessed abundant intratumoral lymphatic vessels, as confirmed by immunohistochemical staining for the lymphatic markers LYVE-1 and VEGFR-3/Flt4, and absence of staining for the blood vessel marker CD34 (Fig. 1). Because blood vessels in some tumors have been reported to express VEGFR-3/Flt4 (38), we used LYVE-1 and CD34 for the rest of these studies.

PC3-#82 cells expressed and secreted VEGF-C (Fig. 2A and B), but not VEGF-D (data not shown). To examine the importance of tumor-secreted VEGF-C in promoting lymphangiogenesis, we stably expressed siRNAs against VEGF-C in PC3-#82 cells. We also generated siRNAs against VEGF-A, a potent inducer of angiogenesis previously reported to stimulate lymphatic growth in the mouse ear (39). C13 and C14 siRNAs knocked down VEGF-C mRNA by 81% and 88%, respectively, relative to vector control (Fig. 2A). A2 and A3 siRNAs reduced VEGF-A mRNA by 67% and 74%, respectively (Fig. 2A). Quantitative PCR showed that VEGF-C siRNAs had little effect on VEGF-A expression, and vice versa. C14-MM and A3-MM mismatch (MM) controls showed little siRNA efficacy. Relative RNA message levels for VEGF-C/A were reflected in their relative protein abundance in conditioned medium, as assayed by ELISA (Fig. 2B). Cells expressing C14 siRNA accumulated virtually no VEGF-C in conditioned medium after 72 hours, whereas cells expressing C13 showed modest accumulation (Supplementary Fig. S1). VEGF-A secretion was not significantly reduced by either C13 or C14 siRNAs, but was slightly increased in C14-MM control.

As an additional approach for ablating lymphatics, we expressed the soluble VEGFR-3/Flt4-human Fc-Ig fusion protein (Flt4-Ig) in PC3-#82 cells, as described previously (25, 32). Protein secretion was confirmed by immunoprecipitation from conditioned medium and Western blot against VEGFR-3 (Fig. 2C).

Tumor-secreted vascular endothelial growth factor-C is necessary for lymphangiogenesis. PC3-#82 cells expressing siRNAs against VEGF-C or VEGF-A, or control siRNAs were injected s.c. into CD-1 immunodeficient mice. We did not see consistent tumor growth effects correlated with VEGF-C or VEGF-A inhibition. Tumors were removed \sim 3.5 weeks postinjection, sectioned and stained for LYVE-1 and CD34. PC3-#82 cells expressing C14 siRNA showed a $>99\%$ reduction in LVD (Fig. 3A, c) relative to controls (Fig. 3A, a and b). Tumors expressing C13, a less effective siRNA against VEGF-C, yielded an 83% reduction in LVD relative to controls (Fig. 3B). Interestingly, both siRNAs against VEGF-A (A2, A3) yielded a nearly 50% reduction in LVD versus controls (Fig. 3A, d for A3 and data not shown for A2; combined $P = 0.052$). As both VEGF-A siRNAs were only partially effective in reducing VEGF-A gene expression, it is possible that more potent VEGF-A siRNAs would have yielded greater reduction in LVD. LVD quantitation of siRNA- or siRNA control-expressing tumors is shown in Fig. 3B. In agreement with results by others (25, 26), expression of soluble Flt4-Ig (Fig. 3A, f) yielded complete inhibition of lymphangiogenesis versus Ig-Neg control (Fig. 3A, e and C). In all cases, blood vessel density was not consistently affected (Fig. 3B and C; images not shown), although C14-MM control tumors had somewhat increased angiogenesis. Staining also appeared slightly lighter in some tumors expressing siRNA. Taken together, these results indicate that tumor-secreted VEGF-C is necessary for intratumoral lymphangiogenesis. To a lesser extent, tumor-secreted VEGF-A may also be important. The lack of reduction in blood vessels, especially by A2 and A3, might

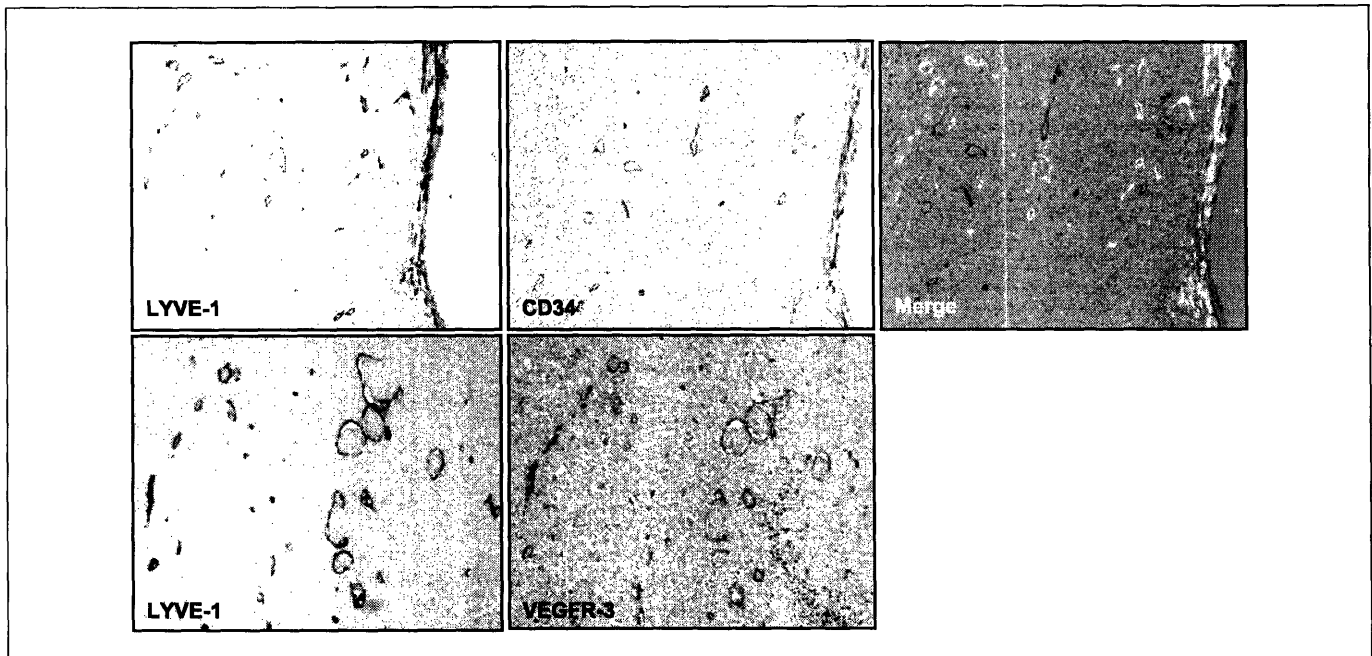


Figure 1. PC3-#82 cells form s.c. tumors with intratumoral lymphatic and blood vessels. Serial tumor sections probed with antibodies against LYVE-1 or CD34 show specific, nonoverlapping staining for lymphatics or blood vessels, respectively (top). In the merged image, lymphatics are colored white, and blood vessels black. Serial sections probed with LYVE-1 and anti-mouse VEGFR-3/Flt4 show coincident staining (bottom).

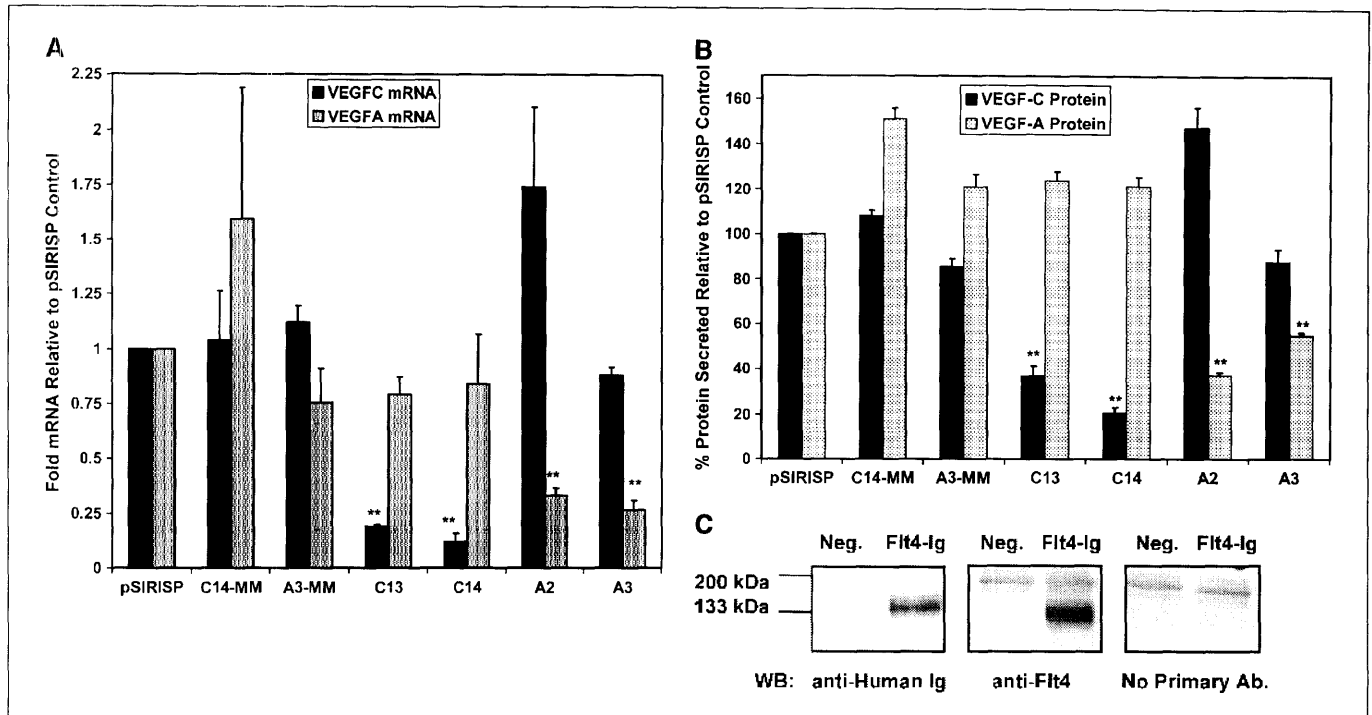


Figure 2. PC3-#82 cell expression and secretion of VEGF-C or VEGF-A can be reduced by siRNA. *A*, relative mRNA levels for VEGF-C (black) or VEGF-A (gray) were measured by quantitative PCR, and normalized to pSIRISP vector control. C13 and C14 cells express siRNAs against VEGF-C. A2 and A3 cells express siRNAs against VEGF-A. C14-MM and A3-MM (MM, mismatch) are siRNA specificity controls. siRNAs specifically down-regulated expression of the target gene and reduced accumulation of either VEGF-C or VEGF-A protein in conditioned medium, as assessed by ELISA (*B*). Control samples typically secreted ~2,000 pg VEGF-C/mL conditioned medium/24 hours, and ~200 pg VEGF-A/mL conditioned medium/24 hours. *C*, secretion of soluble VEGFR-3/Flt4-Ig fusion protein in PC3-#82 cells was confirmed by immunoprecipitating fusion protein from conditioned medium and Western blot (**, $P < 0.001$).

reflect the limited mRNA knock-down, and/or suggest that other angiogenic factors are sufficient for inducing tumor angiogenesis.

Ablation of prostate intratumoral lymphatics does not inhibit lymph node metastasis. PC-3 cells have been reported to metastasize infrequently from s.c. tumors (40). In contrast, prostate tumor cells introduced orthotopically metastasize in patterns similar to human prostate cancer, including invasion of lymph nodes, lung, and bone (34, 35). To model the early stages of metastasis, where cells must detach from the primary tumor before intravasating into vasculature, we used SOI to graft a single piece of solid tumor into the dorsolateral prostate lobes of CD-1 mice (Fig. 4A). Graft material was derived from s.c. tumors. As an advantage over other xenograft techniques, SOI minimizes the artificial dispersal of cells away from the site of implantation, as is often seen when tumor cells are injected as a suspension (41). As expected, the tumors introduced by SOI develop initially from a single focus in the interluminal spaces of the prostate (Fig. 6A, a). Between 2 and 3 months after implantation, ~50% of mice develop lymph node macrometastases. We find that hematogenous spread (circulating tumor cells in blood and lung metastasis) is strongly associated with lymphatic invasion (Supplementary Fig. S2), and primary tumors possess abundant blood and lymphatic vessels (data not shown; similar to Fig. 1).

To determine the metastatic effects of ablating lymphatic vessels in orthotopic prostate tumors, we used SOI to transplant PC3-#82 tumors expressing either VEGF-C siRNA (C14), Flt4-Ig, or controls. LVD was reduced by ~50% in both C14- and Flt4-Ig-expressing tumors (Fig. 4B). Although statistically significant ($P = 0.012$ for C14 versus control; $P = 0.0046$ for Flt4-Ig versus control), this reduction

was far less severe than was seen in s.c. tumors. Expression of either C14 siRNA or Flt4-Ig in orthotopic tumors did not affect the incidence of macroscopic lymph node metastasis (Fig. 4C), the average mass of macroscopically invaded lymph nodes (Fig. 4C; $P = 0.92$), or the average size of the primary tumors (data not shown). For lymph nodes without obvious macrometastases, histologic analysis identified micrometastases in virtually all samples analyzed, regardless of cell line (Supplementary Table S1).

To understand why inhibition of lymphangiogenesis was less effective in orthotopic versus s.c. tumors, we used ELISA to measure the human VEGF-C protein levels in s.c. and orthotopic tumors expressing C14 or siRNA control. The concentration of human VEGF-C protein in C14 orthotopic tumors was increased relative to C14 s.c. tumors and was correlated with LVD in both C14 and control tumors (Supplementary Fig. S3). Reduced siRNA-mediated inhibition of VEGF-C secretion over the duration of the experiment possibly accounted for less severe inhibition of tumor lymphangiogenesis. In the case of Flt4-Ig-expressing tumors, Western blot for VEGFR3/Flt4 indicated that, in some orthotopic tumors, expression of the fusion protein was also severely reduced (Supplementary Fig. S4).

To further ablate orthotopic intratumoral lymphatics, we generated a derivative of PC3-#82 that combined expression of VEGF-C siRNA and Flt4-Ig (Flt-C14), in addition to a cell line expressing both empty-vector controls (Ig-pSIRISP). Specific knock-down of VEGF-C mRNA and secretion of Flt4-Ig were again confirmed (Fig. 5A). As expected, Flt-C14 s.c. tumors possessed no lymphatic vessels, whereas Ig-pSIRISP control tumors had abundant LYVE-1 staining (Fig. 5B). When implanted orthotopically, Flt-C14 tumors ($n = 11$) exhibited a 92% reduction in LVD

versus controls ($n = 8$; $P < 0.001$). A single Flt4-C14 tumor possessed moderate LVD, and without this outlier, inhibition of LVD increases to 98% versus control. Interestingly, blood vessel density was also reduced ~35% in Flt-C14 tumors versus Ig-pSIRISP control.

Despite a >92% reduction in intratumoral lymphatics, the incidence of microscopic and macroscopic lymph node invasion, and the mass of macroscopically invaded lymph nodes were again largely unaffected in Flt-C14 tumors versus Ig-pSIRISP control (Fig. 5C; $P = 0.15$), or other controls used in this study (Figs. 4C and Fig. 5C). As before, nearly all local lymph nodes evaluated harbored micro- or macrometastatic tumor invasion (Supplementary Table S1). Also, we found no significant correlation between LVD and lymph node metastasis in individual orthotopic tumors whose lymphatics were ablated (Fig. 5D). Our data argue that intratumoral lymphangiogenesis is unnecessary for prostate cancer metastasis to lymph nodes.

Abundance of preexisting marginal lymphatics is unaffected in Flt-C14 orthotopic tumors. At least two possible explanations could account for how orthotopic prostate tumors metastasized efficiently to lymph nodes despite a >98% inhibition of intratumoral lymphangiogenesis in 10 of 11 Flt-C14 tumors. Formally, it is possible that a minority of lymphatic vessels (<2% of total) is

sufficient for metastasis. A more likely explanation is that marginal lymphatic vessels at the tumor-stromal margin—and not intratumoral lymphatics—are responsible for mediating lymph node metastasis.

Because orthotopic tumors were analyzed 2 to 3 months after implantation, the tumors tended to be large (~1 g; see Fig. 4A) and almost completely devoid of stromal tissue. To examine tumor interaction with preexisting marginal lymphatics, we transplanted Flt-C14 or control tumors using SOI and analyzed them 2 to 3 weeks after implantation. In most cases, tumors were not palpable and were found by sectioning through the dorsolateral prostate (Fig. 6A, a). As expected, primary tumors consistently arose from a single focus.

We stained microscopic Flt-C14 or control orthotopic tumors with LYVE-1 and found that both were in contact with lymphatics located at the tumor-stromal margin (Fig. 6A, b-d; data not shown for control tumors). In Flt-C14 tumors, all stages of lymphatic invasion were observed, including tumor growth up against individual lymphatic vessels without compression (Fig. 6A, b), intravasation of tumor cells into lymphatics (Fig. 6A, c), and crushing of vessels (Fig. 6A, d). Typically, these marginal lymphatics delineated the exact region of contact between the expanding tumor periphery and the surrounding prostatic stroma.

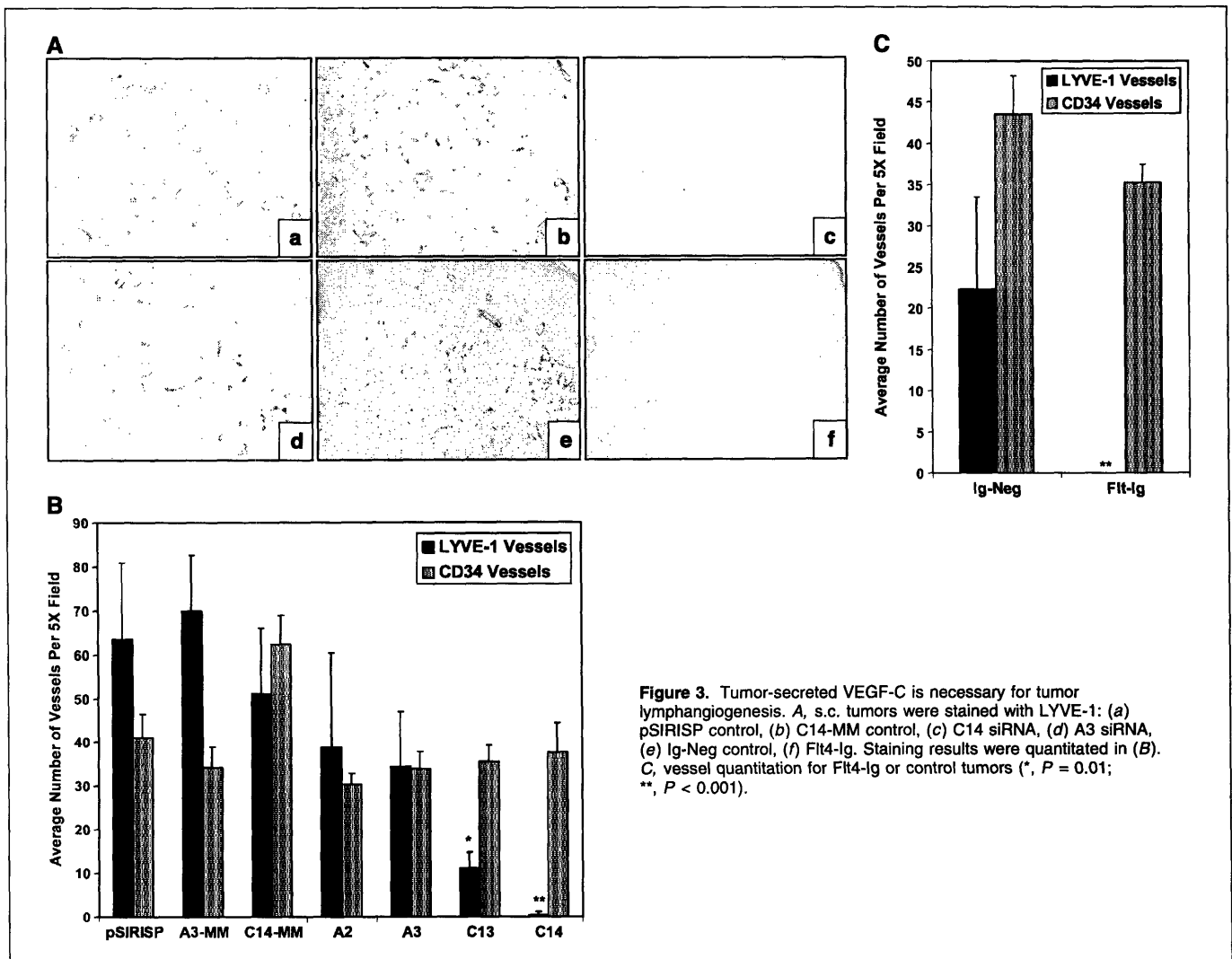


Figure 3. Tumor-secreted VEGF-C is necessary for tumor lymphangiogenesis. A, s.c. tumors were stained with LYVE-1: (a) pSIRISP control, (b) C14-MM control, (c) C14 siRNA, (d) A3 siRNA, (e) Ig-Neg control, (f) Flt4-Ig. Staining results were quantitated in (B). C, vessel quantitation for Flt4-Ig or control tumors (*, $P = 0.01$; **, $P < 0.001$).

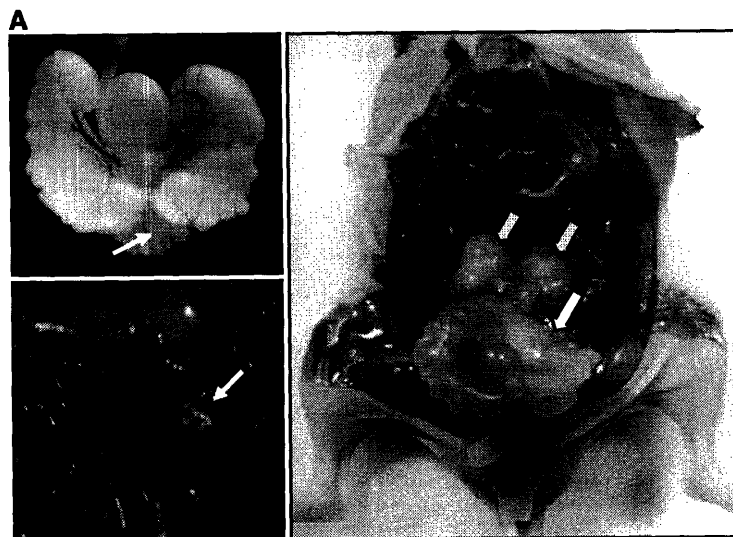
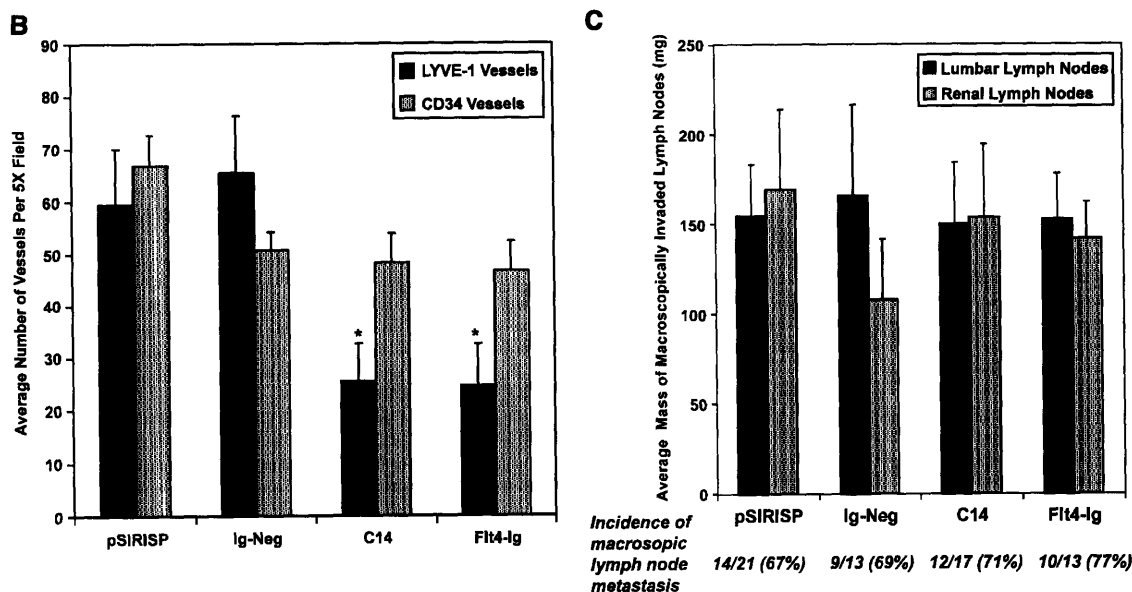


Figure 4. SOI of PC3-#82 cells yields primary tumors in the mouse prostate. Mouse urogenital system (*top left*), with the site of implantation indicated by an arrow (photograph courtesy Dr. Anne Donjacour, UC Davis). Graft material was labeled with CellTracker Green (*bottom left*), implanted into the dorsal prostate and immediately imaged under a fluorescence dissecting microscope. *Right*, a typical orthotopic primary tumor 2 to 3 months after implantation (*lower arrow*), along with paralumbar lymph node metastases (*upper arrows*). *B*, quantitation of lymphatic (black) and blood vessels (gray) from orthotopic tumors. *C*, metastasis to the draining (lumbar) and more distant (renal) lymph nodes were unaffected in all cases (for lumbar lymph node mass; $P = 0.92$ for C14 versus pSIRISP; $P = 0.81$ for Flt4-Ig versus Ig-Neg; and similarly not significant for renal lymph nodes; *, $P < 0.02$).



Quantitation of marginal lymphatics revealed little difference between Flt-C14 and control orthotopic tumors (Fig. 6B; $P = 0.55$). However, intratumoral lymphatics were present in control tumors but completely absent in Flt-C14 tumors (Fig. 6B). These results indicate that a combination of VEGF-C siRNA and Flt4-Ig fusion protein selectively inhibited intratumoral lymphangiogenesis without affecting marginal, possibly preexisting, lymphatics, and suggest that these vessels at the periphery are sufficient for mediating lymph node metastasis.

Spontaneous TRAMP tumors do not induce lymphangiogenesis. To extend our observations, we examined the lymphatics in spontaneous TRAMP tumors. TRAMP transgenic mice express the SV40 large T antigen driven by the prostate-specific rat probasin promoter (31). Prostatic intraepithelial neoplasia (PIN), a precursor of prostate cancer, appears as early as 10 weeks of age, and progresses to undifferentiated adenocarcinoma (42). TRAMP prostates are graded 1 to 6 (1 being normal prostate, and 6 being undifferentiated adenocarcinoma), based on

variables including cell differentiation and invasion through the basement membrane (37, 43). By 28 weeks, 100% of TRAMP mice were reported to harbor lymph node and/or lung metastases (44). Importantly, local and distant dissemination is predominantly seen only in mice with primary tumors of grade 4 or higher (37).

We examined the prostatic lymphatics in 8 normal C57BL/6 mice and 14 TRAMP mice at different ages and/or tumor stages. The lymphatics in normal prostates were located in the interluminal spaces outside individual ductal structures (Supplementary Fig. S5), and their abundance and location did not differ in mice between 15 and 35 weeks of age (data not shown). In TRAMP prostates, PIN develops from the initial expansion of luminal cells within ductal structures. As with wild-type prostates, lymphatics in TRAMP prostates were consistently located outside of ductal structures and did not infiltrate into tumorigenic areas (Fig. 6C). Tumorigenic prostates graded from 1 to 4 did not exhibit significant differences in LVD versus normal

prostates (Fig. 6D). In the most severe cases of prostate cancer (grades 5 and 6), the tumorigenic regions had overtaken the surrounding stroma, and lymphatic density in the prostate was reduced 7-fold versus either normal prostates or low-grade tumorigenic prostates (Fig. 6C and D; $P < 0.001$). Because metastasis to lymph nodes is predominantly seen only in high-grade TRAMP tumors (37), it is likely that these spontaneous tumors also use preexisting lymphatics located at the tumor-

stromal border prior to vessel compression and destruction. These results support our findings in the xenograft SOI model that intratumoral lymphangiogenesis is not required for lymph node metastasis.

Discussion

Lymph node status has traditionally been used as a prognostic indicator of prostate cancer aggressiveness, dissemination to

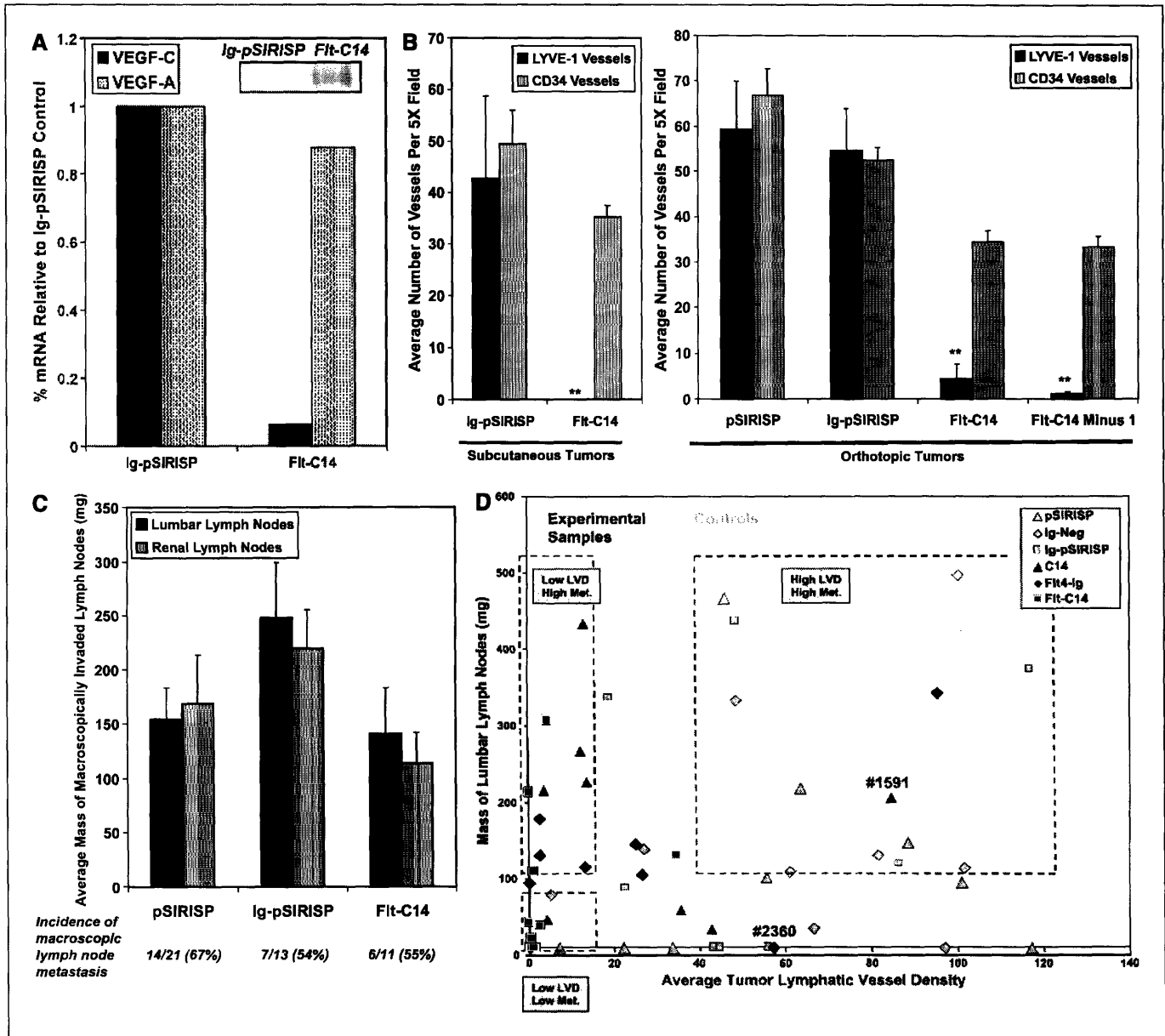


Figure 5. Combined expression of VEGF-C siRNA and Fit4-Ig in PC3-#82 cells effectively reduces orthotopic tumor LVD without markedly affecting lymph node metastasis. A, combined Fit-C14-expressing cells were validated for VEGF-C mRNA knock-down and secretion of fusion protein (inset). B, lymphatic and blood vessel densities were quantitated from s.c. (left) and orthotopic (right) primary tumors. Combination of Fit4-Ig with C14 siRNA inhibited average LVD 100% in s.c. tumors and >92% in orthotopic tumors (n = 11). In 10 of 11 Fit-C14 orthotopic tumors, average LVD was reduced >98% ("minus 1"), compared with Ig-pSIRISP control (n = 8). For reference, vessel density for pSIRISP vector control from Fig. 4B is also shown. C, metastasis to draining and more distant lymph nodes was not significantly affected in Fit-C14 tumors compared with Ig-pSIRISP control (P = 0.15 for lumbar lymph nodes) or pSIRISP control (P = 0.80; data reproduced from Fig. 4C). D, metastasis is not correlated with LVD in individual orthotopic tumors. Points, data from a single tumor/mouse. Control tumors (gray) and experimental tumors [black; refer to labels in (D) for cell line identification]. Top right box, tumors with heavy lymph node metastatic burdens (>100 mg mass, or ~10× the typical mass of uninvaded lymph nodes) and high LVD. Note that tumors in this zone consist predominantly of control samples (gray). Bottom left box, tumors with low lymph node metastatic burdens and low LVD. Note that tumors in this zone predominantly consist of samples where LVD was experimentally reduced (black). Top left box, tumors with heavy lymph node metastatic burdens despite low LVD. Note that all samples in this zone are experimentally manipulated (black). Tumor #1591 (C14) was subsequently found to have lost siRNA inhibition of VEGF-C (Supplementary Fig. S3), whereas tumor #2360 showed reduced Fit4-Ig protein levels (Supplementary Fig. S4; **, P < 0.001).

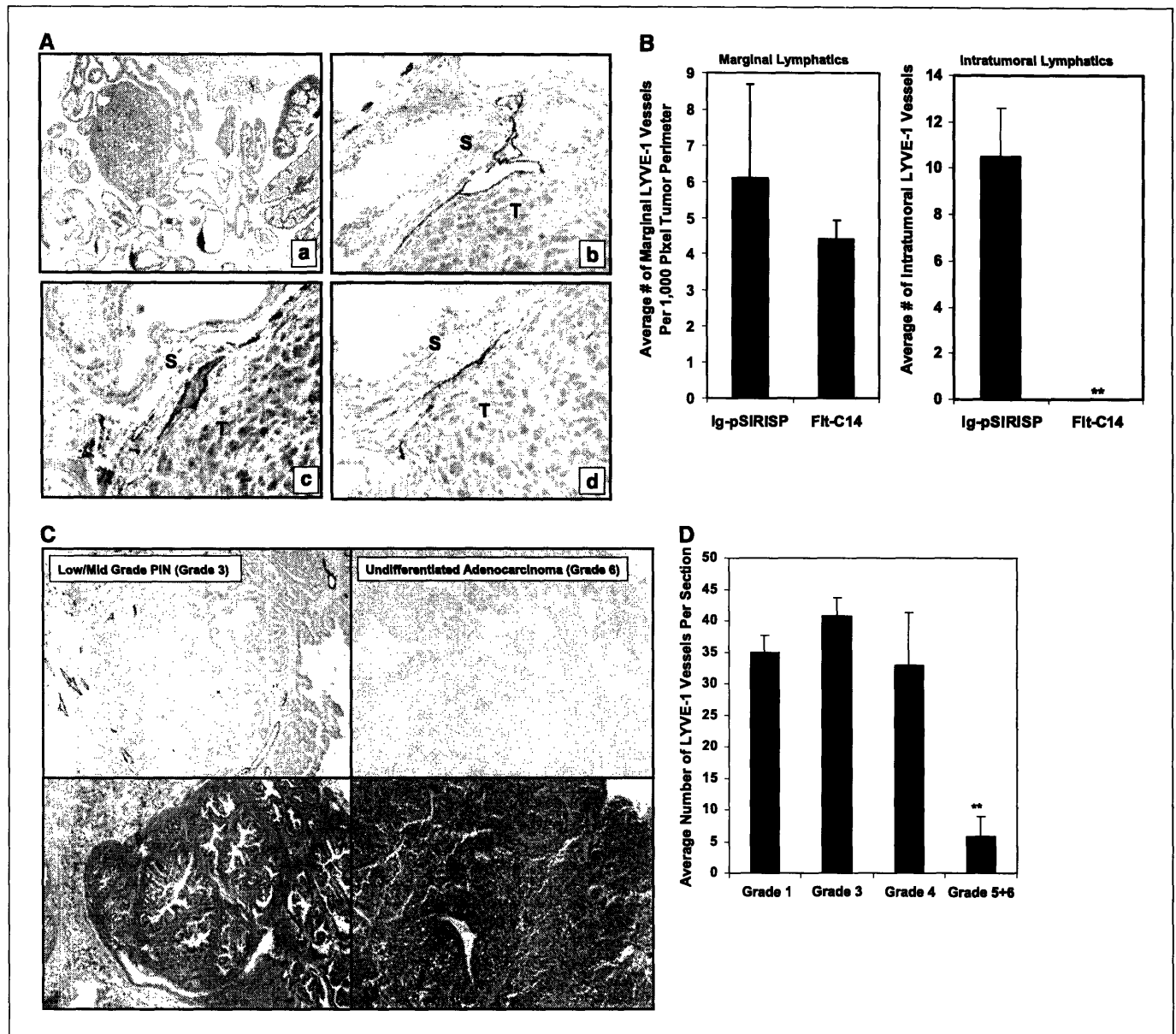


Figure 6. Marginal lymphatics are found at the tumor-stromal interface of Flt-C14 orthotopic tumors, and in the interluminal spaces outside regions of PIN in TRAMP prostates. *A*, H&E staining of the prostate 2 to 3 weeks after SOI reveals a single focal microscopic tumor (*star*) surrounded by prostatic ductal acinar structures (*a*). All stages of lymphatic invasion were seen in Flt-C14 orthotopic tumors stained with LYVE-1, including tumor growth against lymphatic vessels (*b*), intravasated vessels containing tumor cells (*c*), and compression of vessels (*d*). Note that, in all cases, marginal lymphatics delineated the tumor-stromal junction ("T," tumor region; "S," stromal region). *B*, quantitation of marginal lymphatics in Flt-C14 and control orthotopic tumors (*left*), and quantitation of intratumoral lymphatics (*right*). Flt-C14 tumors possessed marginal, but not intratumoral lymphatics. *C*, regions of grade 3 PIN (*left*), or grade 6 undifferentiated adenocarcinoma (*right*) from TRAMP prostates were stained with LYVE-1 (*upper*) or H&E (*bottom*). In samples with PIN, lymphatics were located in the stroma and excluded from tumorigenic regions. Lymphatics were mostly absent in regions of undifferentiated adenocarcinoma. *D*, quantitation of total lymphatics in normal and TRAMP prostate sections. Grades 5 to 6 TRAMP prostates possess significantly fewer lymphatic vessels than lower grade or normal (grade 1) prostates ($P < 0.001$).

distant sites and likelihood of recurrence after therapy (1–3, 45). Although recent clinical studies have examined the abundance of lymphatics and/or lymphatic growth factors in prostate cancer, the results have been difficult to interpret. In most cases, VEGFR-3/Flt4 was up-regulated in advanced or node-positive prostate cancer (9, 10, 46, 47). One study found augmented tyrosine phosphorylation of VEGFR-3/Flt4 in advanced versus early stage (node-negative) prostate cancer (46), whereas another found up-regulation of a truncated form of VEGFR3/Flt-4, but not full-length receptor (48). Furthermore, VEGF-C was up-regulated in some cases of metastatic prostate cancer (9, 10) but not in others

(46, 48). VEGF-D was also increased in node-positive versus node-negative prostate cancer in some studies (46, 48) but was unchanged in another (9).

Part of the complexity in analyzing these data arises from the difficulty of distinguishing whether VEGFR-3/Flt4 was up-regulated in tumor-associated lymphatics or in the tumor cells themselves (46–48). Indeed, *in vitro* studies have shown that prostate cancer cell lines can express the related receptors VEGFR-1/Flt1 (49, 50) and VEGFR-2/Flk1 (49–51). Furthermore, staining for VEGFR-3/Flt4 in one study of prostate cancer exclusively high-lighted tumor and epithelial cells, but not endothelial vessels (46).

In studies where VEGFR-3/Flt4 staining identified lymphatics associated with prostate cancer, the localization of these vessels was either reported to be peritumoral (10), or both peritumoral and intratumoral (9). However, VEGFR-3/Flt4 has also been found to be expressed in some tumor blood vessels (38). One clinical study of prostate cancer reported lymphatics primarily in the tumor periphery and nontumorigenic stromal regions (8). Because lymphatics were significantly reduced in tumors, the authors speculated that prostate cancer progression causes lymphatic destruction. LYVE-1-positive vessels were also correlated with increased Gleason score (8), but a detailed study comparing node-positive- with node-negative prostate cancer using LYVE-1 has not been done.

Up-regulated VEGFR-3/Flt4, VEGF-C, and VEGF-D have also been correlated with other variables of prostate cancer progression, including Gleason score (9, 10, 47) and PSA level (10, 47). Consequently, it is difficult to distinguish whether increased lymphatics actually facilitate nodal metastasis or are simply markers of more aggressive primary tumors. Similarly, in experimental mouse models, whether lymphangiogenesis is required for lymph node metastasis may depend on the innate aggressiveness of the tumor in question. It is possible that for tumors already adept at colonizing distant sites, preexisting lymphatics may be sufficient for lymph node metastasis, whereas less aggressive cancers may require additional vessels to disperse more cells and increase the probability of metastasis. This may explain why overexpression of insulin-like growth factor receptor I in pancreatic islet tumors by Hanahan's group yielded aggressive tumors that metastasized to lymph nodes without significant lymphangiogenesis [as reported by Alitalo et al. (ref. 52)].

Functional studies using assays for microlymphangiography and interstitial fluid pressure have suggested that intratumoral lymphatics may be nonfunctional (17, 22). Tumor compression of intratumoral lymphatic vessels may be responsible for the absence of function, although tumor-induced lymphatics may inherently be physiologically abnormal (23, 24). Although this apparent absence of function has been interpreted to suggest that intratumoral lymphatics are unimportant for metastasis, that hypothesis needs further testing.

In contrast with our results, work by others has shown that inhibiting tumor lymphatics with soluble VEGFR-3/Flt4-Ig fusion protein can reduce metastasis to lymph nodes both in xenograft models (25, 26, 28, 53, 54) and in Rip-Tag spontaneous tumors (27). In most studies, both peritumoral and intratumoral lymphatics were inhibited, although some have suggested that Flt4-Ig may have no effect on preexisting lymphatics (28, 30, 53, 54), or may inhibit peripheral, but not intratumoral, lymphatics (27). The varying effectiveness of Flt4-Ig may reflect how and when the inhibitor was administered, its concentration, diffusion to surrounding tissues, abundance of preexisting lymphatics, and local concentration of VEGF-C/D ligands. Several articles report that high-level, systemic expression of Flt4-Ig fusion protein can suppress metastasis (27, 53, 54). Recent work by Pytowski et al. has suggested that VEGF-C-mediated VEGFR-3 signaling might be unnecessary for the maintenance of preexisting lymphatics in the mouse tail (55). In any case, the relative importance of peritumoral versus intratumoral lymphatics in mediating lymph node spread has remained unclear. In addition, inhibiting lymphangiogenesis through the use of soluble receptor, VEGFR-3/Flt4 antibody (29) or VEGF-D antibody (18), has not distinguished between the ligands required for the process and/or the source of the ligands. VEGF-C/D may be secreted by tumors or from stromal sources including tumor-associated macrophages (56).

In this study, we have used the SOI model of human prostate cancer to show that intratumoral lymphangiogenesis can be

inhibited in tumors (Flt-C14) without significantly affecting lymph node metastasis. In early stage Flt-C14 tumors, we found that despite the absence of intratumoral lymphangiogenesis, the abundance of peritumoral lymphatics was not statistically different from controls, and in all cases, tumor-intravasated lymphatic vessels were observed. These data suggest that intratumoral lymphangiogenesis is unnecessary for lymph node metastasis in prostate cancer, and that marginal, possibly preexisting, lymphatics are sufficient. He et al. (53) reported that VEGF-C can promote dilation and sprouting in preexisting lymphatics and that this could be inhibited by high levels of systemic Flt4-Ig, although the tumor cells still coopted the preexisting lymphatics and lymph node metastases still occurred, albeit at reduced levels. Those results could be reconciled with ours if the high levels of Flt4-Ig partially inhibited the intravasation of tumor cells into preexisting lymphatics.

We have also obtained corroborative results using the TRAMP spontaneous model of prostate cancer. In TRAMP, metastasis to lymph nodes is primarily observed only in tumors of grade 4 or higher (37). In TRAMP prostates, we found that lymphatics were typically located outside the luminal acinar regions where PIN and adenocarcinoma develop. Peritumoral, but not intratumoral, lymphatics were seen and, as the tumors invaded through the basement membrane into surrounding stromal regions (grades 5 and 6), significantly fewer lymphatics were observed, suggesting the destruction of preexisting lymphatics and the absence of lymphangiogenesis. This is similar to human clinical prostate cancer (8), and also indicates that preexisting peritumoral lymphatics are sufficient for lymph node metastasis.

It remains to be determined whether lymph node metastasis is important for hematogenous dissemination. In our SOI model, we observed that hematogenous metastasis was strongly associated with lymph node invasion (Supplementary Fig. S2). These data may indicate that tumors enter the blood circulation indirectly via lymphatics, or that blood and lymphatic vessel intravasation occur simultaneously. Others have proposed that lymph nodes may act as bridgeheads where tumor cells with limited metastatic capability can proliferate and acquire additional mutations that allow further dissemination (57). Whether this hypothesis is accurate remains to be seen.

In summary, we have shown that, in prostate cancer, lymph node metastasis relies on peritumoral, and not intratumoral, lymphatics, suggesting that the peritumoral lymphatics that preexist before tumor development may be sufficient for disseminating tumor cells to local and more distal lymph nodes. Our results also suggest that inhibiting lymphangiogenesis may be easier than ablating preexisting lymphatics. As targeting lymphatic vasculature has recently been proposed as an antimetastatic approach for limiting the spread of primary tumors (13), this study shows that the need to target the surrounding marginal lymphatics is especially imperative.

Acknowledgments

Received 3/17/2005; revised 7/11/2005; accepted 8/30/2005.

Grant support: NIH grant RO1CA17007, Virginia and D.K. Ludwig Fund for Cancer Research, Prostate Cancer Foundation, and the Howard Hughes Medical Institute (R.O. Hynes), National Institute of General Medical Sciences Predoctoral Training Grant to the MIT Biology Department (S.Y. Wong).

The costs of publication of this article were defrayed in part by the payment of page charges. This article must therefore be hereby marked *advertisement* in accordance with 18 U.S.C. Section 1734 solely to indicate this fact.

We are very grateful to Kari Alitalo for the Flt4-Ig expression construct, Harvey Lodish for the ecotropic receptor construct, Bill Hahn for the pSIRISP retroviral vector, Erkki Ruoslahti for LYVE-1 antibody, Ailin Bai for TRAMP mice, Mark Rosenzweig for assistance with fluorescence tumor imaging; Drs. Anne Donjacour and Jose Galvez (UC Davis, Center for Comparative Medicine) for normal prostate pictures; and the MIT Division of Comparative Medicine for animal maintenance.

References

1. Flocks RH, Culp D, Porto R. Lymphatic spread from prostatic cancer. *J Urol* 1959;81:194-6.
2. Smith JA, Seaman JP, Gleidman JB, Middleton RG. Pelvic lymph node metastasis from prostatic cancer: influence of tumor grade and stage in 452 consecutive patients. *J Urol* 1982;130:290-2.
3. Bubendorf L, Schopfer A, Wagner U, et al. Metastatic patterns of prostate cancer: an autopsy study of 1,589 patients. *Hum Pathol* 2000;31:578-82.
4. Morton DL, Wen D, Wong JH, et al. Technical details of intraoperative lymphatic mapping for early stage melanoma. *Arch Surg* 1992;127:392-9.
5. Giuliano AE, Kirgan DM, Guenther JM, Morton DL. Lymphatic mapping and sentinel lymphadenectomy for breast cancer. *Ann Surg* 1994;220:391-401.
6. Nathanson SD. Insights into the mechanisms of lymph node metastasis. *Cancer* 2003;98:413-23.
7. Wittekind C. Diagnosis and staging of lymph node metastasis. *Recent Results Cancer Res* 2000;157:20-8.
8. Trojan L, Michel MS, Rensch F, Jackson DG, Alken P, Grobholz R. Lymph and blood vessel architecture in benign and malignant prostatic tissue: lack of lymphangiogenesis in prostate carcinoma assessed with novel lymphatic marker lymphatic vessel endothelial hyaluronan receptor (LYVE-1). *J Urol* 2004;172:103-7.
9. Zeng Y, Opeskin K, Baldwin ME, et al. Expression of vascular endothelial growth factor receptor-3 by lymphatic endothelial cells is associated with lymph node metastasis in prostate cancer. *Clin Cancer Res* 2004;10:5137-44.
10. Tsurusaki T, Kanda S, Sakai H, et al. Vascular endothelial growth factor-C expression in human prostatic carcinoma and its relationship to lymph node metastasis. *Br J Cancer* 1999;80:309-13.
11. Jain RK, Padera TP. Prevention and treatment of lymphatic metastasis by anti-lymphangiogenic therapy. *J Natl Cancer Inst* 2002;94:785-7.
12. He Y, Rajantie I, Ilmonen M, et al. Preexisting lymphatic endothelium but not endothelial progenitor cells are essential for tumor lymphangiogenesis and lymphatic metastasis. *Cancer Res* 2004;64:3737-40.
13. Achen MG, McColl BK, Stacker SA. Focus on lymphangiogenesis in tumor metastasis. *Cancer Cell* 2005;7:121-7.
14. Joutkov V, Pajusola K, Kaipainen A, et al. A novel vascular endothelial growth factor, VEGF-C, is a ligand for the Flt4 (VEGFR-3) and KDR (VEGFR-2) receptor tyrosine kinases. *EMBO J* 1996;15:290-8.
15. Skobe M, Hawighorst T, Jackson DG, et al. Induction of tumor lymphangiogenesis by VEGF-C promotes breast cancer metastasis. *Nat Med* 2001;7:192-8.
16. Mattila MM, Ruohola JK, Karpanen T, Jackson DG, Alitalo K, Harkonen PL. VEGF-C induced lymphangiogenesis is associated with lymph node metastasis in orthotopic MCF-7 tumors. *Int J Cancer* 2002;98:946-51.
17. Padera TP, Kadambi A, di Tomaso E, et al. Lymphatic metastasis in the absence of functional intratumor lymphatics. *Science* 2002;296:1883-6.
18. Stacker SA, Caesar C, Baldwin ME, et al. VEGF-D promotes the metastatic spread of tumor cells via the lymphatics. *Nat Med* 2001;7:186-91.
19. Cao R, Bjorn Dahl MA, Religa P, et al. PDGF-BB induces intratumoral lymphangiogenesis and promotes lymphatic metastasis. *Cancer Cell* 2004;6:333-45.
20. Mandriola SJ, Jussila L, Jeltsch M, et al. Vascular endothelial growth factor-C-mediated lymphangiogenesis promotes tumour metastasis. *EMBO J* 2001;20:672-82.
21. Pepper MS, Skobe M. Lymphatic endothelium: morphological, molecular and functional properties. *J Cell Biol* 2003;163:209-13.
22. Leu AJ, Berk DA, Lymboussaki A, Alitalo K, Jain R. Absence of functional lymphatics within a murine sarcoma: a molecular and functional evaluation. *Cancer Res* 2000;60:4324-7.
23. Padera TP, Stoll BR, Tooredman JB, Capen D, di Tomaso E, Jain RK. Pathology: cancer cells compress intratumour vessels. *Nature* 2004;427:695.
24. Isaka N, Padera TP, Hagedoorn J, Fukumura D, Jain RK. Peritumor lymphatics induced by vascular endothelial growth factor-C exhibit abnormal function. *Cancer Res* 2004;64:4400-4.
25. He Y, Kozaki K, Karpanen T, et al. Suppression of tumor lymphangiogenesis and lymph node metastasis by blocking vascular endothelial growth factor receptor-3 signaling. *J Natl Cancer Inst* 2002;94:819-25.
26. Krishnan J, Kirkin V, Steffen A, et al. Differential *in vivo* and *in vitro* expression of vascular endothelial growth factor (VEGF)-C and VEGF-D in tumors and its relationship to lymphatic metastasis in immunocompetent rats. *Cancer Res* 2003;63:713-22.
27. Crnic I, Strittmatter K, Cavallaro U, et al. Loss of neural cell adhesion molecule induces tumor metastasis by up-regulating lymphangiogenesis. *Cancer Res* 2004;64:8630-8.
28. Papoutsis M, Siemeister G, Weindel K, et al. Active interaction of human A375 melanoma cells with the lymphatics *in vivo*. *Histochem Cell Biol* 2000;114:373-85.
29. Shimizu K, Kubo H, Yamaguchi K, et al. Suppression of VEGFR-3 signaling inhibits lymph node metastasis in gastric cancer. *Cancer Sci* 2004;95:328-33.
30. He Y, Karpanen T, Alitalo K. Role of lymphangiogenic factors in tumor metastasis. *Biochim Biophys Acta* 2004;1654:3-12.
31. Greenberg NM, DeMayo F, Finegold MJ, et al. Prostate cancer in a transgenic mouse. *Proc Natl Acad Sci U S A* 1995;92:3439-43.
32. Karpanen T, Egeblad M, Karkkainen MJ, et al. Vascular endothelial growth factor C promotes tumor lymphangiogenesis and intralymphatic tumor growth. *Cancer Res* 2001;61:1786-90.
33. Masutomi K, Yu EY, Khurts S, et al. Telomerase maintains telomere structure in normal human cells. *Cell* 2003;114:241-53.
34. An Z, Wang X, Geller J, Moossa AR, Hoffman RM. Surgical orthotopic implantation allows high lung and lymph node metastatic expression of human prostate carcinoma cell line PC-3 in nude mice. *Prostate* 1998;34:169-74.
35. Chang XH, Fu YW, Na WL, Wang J, Sun H, Cai L. Improved metastatic animal model of human prostate carcinoma using surgical orthotopic implantation (SOI). *Anticancer Res* 1999;19:4199-202.
36. Laakkonen P, Porkka K, Hoffman JA, Ruoslahti E. A tumor-homing peptide with a targeting specificity related to lymphatic vessels. *Nat Med* 2002;8:751-5.
37. Hurwitz AA, Foster BA, Allison JP, Greenberg NM, Kwon ED. The TRAMP mouse as a model for prostate cancer. In: Coligan JE, Bierer BE, Margulies DH, Shevach EM, Strober W, editors. *Current Protocols in Immunology*. New York: John Wiley & Sons, Inc.; 2001. p. 20.5.1-20.5.23.
38. Valtola R, Salven P, Heikkilä P, et al. VEGFR-3 and its ligand VEGF-C are associated with angiogenesis in breast cancer. *Am J Pathol* 1999;154:1381-90.
39. Nagy JA, Vasile E, Feng D, et al. Vascular permeability factor/vascular endothelial growth factor induces lymphangiogenesis as well as angiogenesis. *J Exp Med* 2002;196:1497-506.
40. Glinskii AB, Smith BA, Jiang P, et al. Viable circulating metastatic cells produced in orthotopic but not ectopic prostate cancer models. *Cancer Res* 2003;63:4239-43.
41. Rubio N, Villacampa MM, El Hilali N, Blanco J. Metastatic burden in nude mice organs measured using prostate tumor PC-3 cells expressing the luciferase gene as a quantifiable tumor cell marker. *Prostate* 2000;44:133-43.
42. Gingrich JR, Barrios RJ, Kattan MW, Nahm HS, Finegold MJ, Greenberg NM. Androgen-independent prostate cancer progression in the TRAMP model. *Cancer Res* 1997;57:4687-91.
43. Gingrich JR, Barrios RJ, Foster BA, Greenberg NM. Pathologic progression of autochthonous prostate cancer in the TRAMP model. *Prostate Cancer Prostatic Dis* 1999;2:70-5.
44. Gingrich JR, Barrios RJ, Morton RA, et al. Metastatic prostate cancer in a transgenic mouse. *Cancer Res* 1996;56:4096-102.
45. Zincke H, Farrow GM, Myers RP, Benson RC, Furlow WL, Utz DC. Relationship between grade and stage of adenocarcinoma of the prostate and regional pelvic lymph node metastases. *J Urol* 1982;128:498-501.
46. Kaushal V, Mukunyadzi P, Dennis RA, Siegel ER, Johnson DE, Kohli M. Stage-specific characterization of the vascular endothelial growth factor axis in prostate cancer: expression of lymphangiogenic markers is associated with advanced-stage disease. *Clin Cancer Res* 2005;11:584-93.
47. Li R, Younes M, Wheeler TM, et al. Expression of the vascular endothelial growth factor receptor-3 (VEGFR-3) in human prostate. *Prostate* 2004;58:193-9.
48. Stearns ME, Wang M, Hu Y, Kim G, Garcia FU. Expression of a flt-4 (VEGFR3) splicing variant in primary human prostate tumors. VEGF D and flt-4 ($\Delta 773-1081$) overexpression is diagnostic for sentinel lymph node metastasis. *Lab Invest* 2004;84:785-95.
49. Chevalier S, Defoy I, Lacoste J, et al. Vascular endothelial growth factor and signaling in the prostate: more than angiogenesis. *Mol Cell Endocrinol* 2002;189:169-79.
50. Ferrer FA, Miller LJ, Lindquist R, et al. Expression of vascular endothelial growth factor receptors in human prostate cancer. *Urology* 1999;54:567-72.
51. De S, Chen J, Narizhneva NV, et al. Molecular pathway for cancer metastasis to bone. *J Biol Chem* 2003;278:39044-50.
52. Alitalo K, Mohla S, Ruoslahti E. Lymphangiogenesis and cancer: meeting report. *Cancer Res* 2004;64:9225-9.
53. He Y, Rajantie I, Pajusola K, et al. Vascular endothelial cell growth factor receptor 3-mediated activation of lymphatic endothelium is crucial for tumor cell entry and spread via lymphatic vessels. *Cancer Res* 2005;65:4739-46.
54. Lin J, Lalani AS, Harding TC, et al. Inhibition of lymphogenous metastasis using adeno-associated virus-mediated gene transfer of a soluble VEGFR-3 decoy receptor. *Cancer Res* 2005;65:6901-9.
55. Pytowski B, Goldman J, Persaud K, et al. Complete and specific inhibition of adult lymphatic regeneration by a novel VEGFR-3 neutralizing antibody. *J Natl Cancer Inst* 2005;97:14-21.
56. Schoppmann SF, Birner P, Stockl J, et al. Tumor-associated macrophages express lymphatic endothelial growth factors and are related to peritumoral lymphangiogenesis. *Am J Pathol* 2002;161:947-56.
57. Sleeman J. The lymph node as a bridgehead in the metastatic dissemination of tumors. *Recent Results Cancer Res* 2000;157:55-81.

Perspective

Lymphatic or Hematogenous Dissemination: How Does a Metastatic Tumor Cell Decide?

Sunny Y. Wong

Richard O. Hynes*

Howard Hughes Medical Institute; Center for Cancer Research and Department of Biology; Massachusetts Institute of Technology; Cambridge, Massachusetts USA

*Correspondence to: Richard O. Hynes; Howard Hughes Medical Institute; Center for Cancer Research and Department of Biology; Massachusetts Institute of Technology; 77 Massachusetts Avenue; Cambridge, Massachusetts 02139 USA; Tel.: 617.253.6422; Fax: 617.253.8357; Email: rohynes@mit.edu

Original manuscript submitted: 03/01/06

Manuscript accepted: 03/02/06

Previously published online as a *Cell Cycle* E-publication:

<http://www.landesbioscience.com/journals/cc/abstract.php?id=2646>

KEY WORDS

metastasis, intravasation, angiogenesis, lymphangiogenesis

ACKNOWLEDGEMENTS

The authors thank S. Astrof and L. Xu for critical reading of this manuscript, and acknowledge support from the NIH (RO1CA17007); the Virginia and D.K. Ludwig Fund for Cancer Research; the Prostate Cancer Foundation; and the Howard Hughes Medical Institute. S.Y. Wong was further supported by an NIGMS Predoctoral Training Grant to the MIT Biology Department and by a Koch Research Fellowship from the Center for Cancer Research.

ABSTRACT

The formation of distant metastases is the deadliest phase of cancer progression. Although numerous studies have identified genes and mechanisms that affect metastasis after tumors have reached secondary sites, our knowledge about how cancer cells initially gain access to systemic circulation is limited. Since tumors can enter the blood directly by intravasating into venous capillaries or indirectly via lymphatics, it is important to evaluate the relative contributions of both pathways as routes of egress from the primary site. Insights into tumor and stromal factors governing the intravasation process may help explain why certain tumors exhibit "preferred" pathways for metastatic dissemination, both clinically and in experimental animal models.

WHICH TUMORS METASTASIZE?

What makes a tumor cell metastatic? Certainly, proliferative ability at a distant site is essential for metastasis (Paget's "seed and soil" hypothesis), and difficulties in establishing secondary growth might explain why fewer than 0.01% of circulating tumor cells actually form metastases.¹⁻³ However, exactly what enables a cancer cell to complete the metastatic process is not entirely clear. While recent gene expression studies have suggested that distant metastases resemble their primary tumors of origin,^{4,5} other studies have indicated that the expression of specific genes is altered in metastatic cells.⁶⁻⁸ A model combining both these observations has speculated that cells derived from metastases and from their corresponding primary tumors share an overall gene expression signature that confers the ability to complete some, but not all, of the steps required for metastasis.^{7,9} On top of this, the altered expression of a limited number of additional genes may render a sub-population of cells fully competent for metastasis, without changing its overall similarity with the primary tumor.

Although metastasis is widely regarded as an inefficient process, most cancer patients die from metastases rather than from their primary tumors. Metastatic inefficiency is likely overcome by the sheer number of tumor cells that enter the systemic circulation daily, estimated in one study to be up to $\sim 4 \times 10^6$ tumor cells released per gram of primary tumor.¹⁰ Consequently, it is important that we gain a detailed understanding of how tumors complete the earliest steps of metastasis, including intravasation into vasculature.

In order to metastasize, cancer cells must first detach from the primary tumor and invade blood vessels or lymphatics. This may be a passive process where cells are simply sloughed off from the primary tumor or an active one involving directed migration.^{11,12} Almost certainly, a tumor's cell of origin and its accompanying differentiation program will affect its metastatic proclivity.¹³ Cells from connective tissue tumors such as fibrosarcomas and gliomas tend to migrate individually, for instance, whereas those from melanomas and carcinomas often migrate collectively.¹⁴ In addition, highly differentiated epithelial tumors may initially display collective migration, only to de-differentiate and exhibit single cell invasion, a process termed epithelial-to-mesenchymal-transition (EMT).¹⁵ Indeed, genes that promote EMT—including Twist,⁸ Slug and Snail transcription factors;¹⁶ and components of the TGF- β signaling pathway^{17,18}—have all been reported to enhance the earliest stages of metastasis. E-cadherin, which is often lost during EMT, is thought to suppress cell migration and tumor progression.¹⁹ Finally, stromal cells such as fibroblasts and macrophages have also been reported to affect metastasis by contributing growth factors (e.g., EGF, FGF-1), matrix metalloproteinases and chemotactic/pro-migratory factors (e.g., SF/HGF, chemokines).^{12,14}

BLOOD VESSEL OR LYMPHATIC DISSEMINATION?

Once a migratory cell(s) has detached from the primary tumor, it may intravasate into blood vessels or lymphatics. Either route of dissemination can lead to venous circulation, as lymphatics drain into blood, most commonly through the left lymphatic duct (thoracic duct) or the right lymphatic duct, and then subsequently into the subclavian veins. Along the way, lymphatic fluid is filtered by lymph nodes.

In the absence of overt metastases, hematogenous dissemination of tumors is assayed by detecting cancer cells in the peripheral blood of patients or from bone marrow aspirates.²⁰ The presence of circulating tumor cells and micrometastases can be determined by RT-PCR or immunohistochemistry (IHC), particularly for cytokeratins in the case of epithelial tumors. Lymphatic spread is also assayed by IHC and/or RT-PCR following surgical removal of regional lymph nodes. Tumors almost invariably invade lymph nodes in sequence, starting with the nearest (sentinel or draining) node, followed by increasingly distal ones.²¹ If the draining lymph node is uninvaded, other lymph nodes are also likely free of metastases.²²

Metastatic bias is illustrated by the fact that carcinomas and melanomas tend to develop lymph node metastases more frequently than sarcomas,¹⁴ although it is unclear whether this disparity is due to differences in intravasation and/or growth. Lymph nodes are often the first site of metastasis in a variety of cancers, and are critical for tumor staging and prognosis.²² In prostate cancer, for instance, 75% of patients bearing lymph node metastases at the time of diagnosis will possess bone metastases within 5 years, regardless of treatment.²³ The presence of tumor cells in the bone-marrow is also predictive of distant metastases in a variety of tumors, particularly carcinomas.²⁰ On the other hand, the prognostic value of circulating tumor cells in the blood is debated, as current techniques for detection suffer from problems such as low sensitivity and high rates of false positives.^{24,25} However, recent studies using an automated platform for detecting tumor cells in the blood, called CellSearch, have reported significant correlations between the presence of circulating tumor cells and poor clinical outcome for breast cancer patients.²⁶

The decision to intravasate into either blood or lymphatic vessels may rest largely on physical restrictions imposed on invasive tumors, although active mechanisms for attracting cells to specific types of vasculature have also recently been proposed (see below). Lymphatic capillaries lack the tight interendothelial junctions typically seen in blood vessels, as well as the surrounding layers of pericytes/smooth muscle cells and basement membranes.²⁷ This inevitably renders lymphatics “leaky” relative to blood vessels, thus lowering the barriers for tumor intravasation. In addition, tumor cell survival may benefit from the passive, low-shear system of fluid transport characteristic of lymphatics.

Accessibility of blood and lymphatic vasculature may also influence the pathway taken for metastasis. Induction of angiogenesis, the growth of blood vessels, has been shown to be necessary for tumors growing beyond 0.4 mm in diameter.^{28,29} Lymphangiogenesis, the growth of lymphatic vessels, has been inhibited by us³⁰ and others³¹⁻³⁷ in experimental mouse cancer models without affecting primary

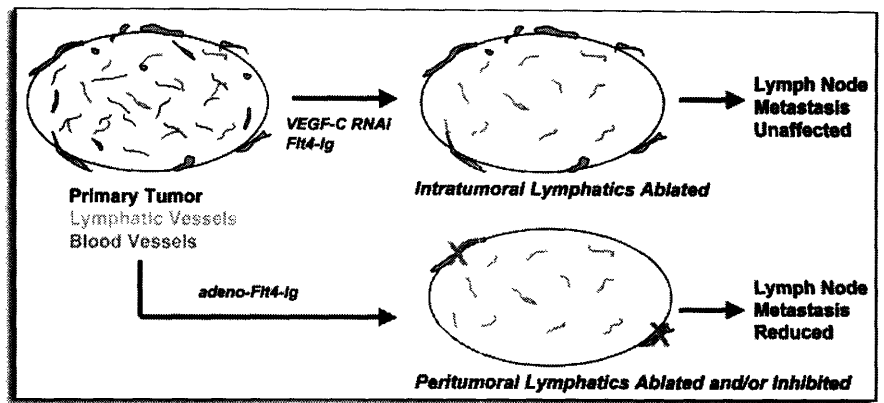


Figure 1. Tumors possess blood vessels (red) and, in some cases, lymphatics (green). Experimental ablation of intratumoral lymphatics does not inhibit lymph node metastasis (top).³⁰ Eliminating or inhibiting the activation of peritumoral lymphatics has been shown to reduce lymphatic spread (bottom).^{32,37,47} In addition, intratumoral lymphatics are absent in many tumors that nevertheless metastasize to lymph nodes.⁵¹ These observations imply that peritumoral lymphatics mediate the majority of tumor cell dissemination. (Flt4-Ig, soluble Flt4 receptor/VEGFR3; adeno, adenoviral delivery).

tumor growth. Because blood and lymphatic vessels share a common embryonic origin, and respond to many similar growth factors—VEGF-A, VEGF-C, VEGF-D, FGF2, PDGF-B, HGF and others³⁸—tumors might be expected to induce lymphangiogenesis concomitant with angiogenesis. But for reasons unclear, this is often not the case. While proliferating intratumoral lymphatics have been detected in human melanomas,³⁹ as well as in head and neck squamous cell carcinomas,⁴⁰ evidence for lymphangiogenesis in other cancers has been less well documented. The presence of anti-lymphangiogenic factors may be one reason why proliferating intratumoral lymphatics are not more commonly found in human clinical tumors,⁴¹ though the identity of these proposed factors is currently unknown.

Nonetheless, intratumoral lymphatics may provide a possible escape route from the primary tumor to draining lymph nodes, and indeed, several studies have reported that inhibition of lymphangiogenesis in xenograft tumor models can significantly reduce lymph node metastasis.^{31-33,36} However, other studies have suggested that intratumoral lymphatics are compressed and nonfunctional.⁴²⁻⁴⁵ This apparent absence of functional intratumoral lymphatics would imply that tumor cells intravasated into these vessels will encounter blockages and dead ends that actually impede metastasis. The fact that many tumors metastasize to local lymph nodes despite absence of lymphangiogenesis or functional intratumoral lymphatics, has led some to propose that it is the peripheral, peritumoral lymphatics that mediate tumor cell dissemination.^{37,46} We recently obtained results consistent with this hypothesis by selectively ablating intratumoral, but not peritumoral, lymphatics in a prostate cancer orthotopic model and showing that lymph node metastasis was not significantly altered.³⁰ Other studies that ablated peritumoral lymphatics or inhibited their “activation”—local vessel sprouting, dilation and permeability—were successful at reducing metastasis (Fig. 1).^{32,37,47} It is possible that the studies reporting metastatic inhibition associated with ablation of intratumoral lymphatics^{31-33,36} may actually reflect interference with tumor cell intravasation into peritumoral lymphatics. Recent clinical and spontaneous animal tumor studies have also reported that prostate,⁴⁸ breast^{49,50} and pancreatic tumors⁵¹ develop lymphatic metastases in the absence of intratumoral lymphangiogenesis.

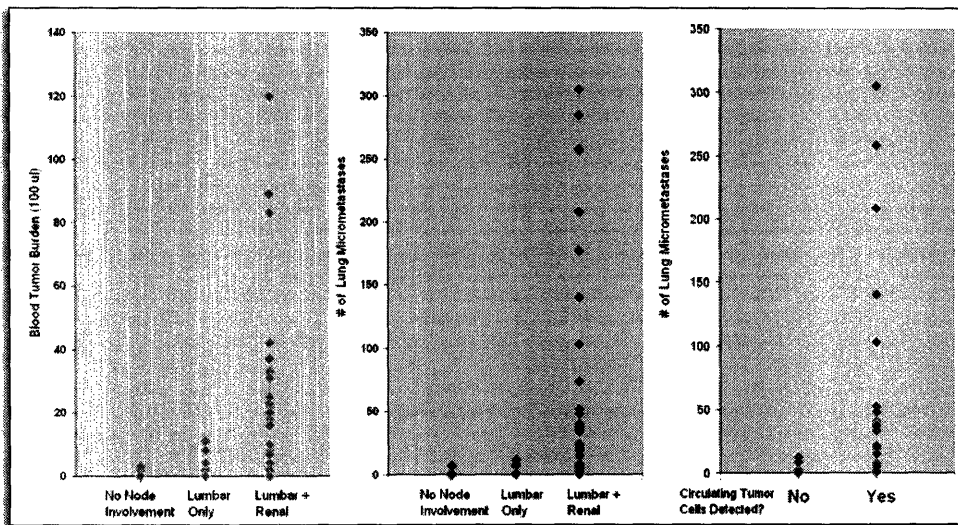


Figure 2. After surgical orthotopic implantation of human prostate PC-3 cells into nude mice, associations were observed among lymph node metastasis, circulating tumor cells and lung micrometastases. *Left*, significant numbers of circulating tumor cells in the blood were detected only in mice that bore macrometastases in both the lumbar and renal lymph nodes. *Middle*, similarly, most lung metastases were seen in mice with both lymph node sites invaded. *Right*, lung metastases were correlated with the presence of circulating tumor cells in the blood. (Reproduced with permission from ref. 30).

Perhaps the best approach for studying blood and lymphatic vessel intravasation is to observe the process in real time, using *in vivo* intravital microscopy. Wyckoff et al imaged rat mammary adenocarcinomas and discovered that metastatic cells were more likely to polarize towards blood vessels than were nonmetastatic cells.^{11,52} Interestingly, polarization of metastatic cells was explained by increased expression of EGF receptor, which made the cells chemotactic to EGF released by macrophages lining blood vessels. Furthermore, individual metastatic cells were seen intravasating into blood vessels using an amoeboid form of movement. Nonmetastatic cells, however, often fragmented upon crossing endothelial junctions. Consequently, the authors speculated that intravasation was a rate-limiting step for metastasis.

Although this work dealt with a limited number of established cell lines and did not examine lymphatics, it does raise several important considerations about the intravasation process. These considerations include the mode of cell migration utilized (individual amoeboid or fibroblastic movement, versus collective sheet/nest migration); the role of stromal cells in promoting polarized movement; and the effect of hemodynamic shear forces on cell viability—all of which may influence a tumor's preference for disseminating via blood vessels or lymphatics.

The type of cell movement undertaken is affected, in large part, by the surrounding extracellular matrix (ECM) and by the integrity of cell-cell junctions.¹⁴ Mesenchymal, or fibroblast-like, single cell migration tends to occur when mature, integrin-containing focal contacts develop in the presence of dense matrix networks. Amoeboid migration is favored under less adhesive conditions, as is often seen *in vivo* or in three-dimensional cultures, when focal contacts are lacking.⁵³ The speed of amoeboid migration is about 10–30 times faster than mesenchymal migration and is protease-independent.^{14,53} Given that lymphatic vessels lack basement membranes, and that ECM networks are likely less dense around peritumoral lymphatics than around intratumoral blood vessels, this would seem to favor rapid and efficient amoeboid-type intravasation

into lymphatic circulation. Lymphatic permeability may also allow passage of cell aggregates that have retained expression of homotypic cell-cell adhesion receptors such as cadherins.⁵⁴

In addition, active recruitment of tumor cells towards lymphatics may occur via EGF-EGFR-mediated chemotaxis, since macrophages have been found in proximity to lymphatic vessels.^{55,56} In one study, macrophages were even reported to transdifferentiate into lymphatics in response to inflammation in an eye cornea model,⁵⁷ though the generality of this finding remains to be determined. Lymphatic stromal cells have also been reported to be a source of EGF and IGF-I.⁵⁸ In addition, lymph node secretion of chemokines such as SCL/CCL21 and CCL1 may attract tumor cells that express the receptors CCR7 and CCR8, respectively.⁵⁹ Overexpression of CCR7 in B16 melanoma cells has been shown to increase lymph node metastasis,⁶⁰ and others have reported

that breast cancer cells or melanomas expressing CXCR4 may actively home to lymph nodes containing CXCL12/SDF-1 ligand.⁶¹ Activated cancer-associated fibroblasts may also secrete chemokines that enhance tumor growth and invasion.⁶²

Lastly, although intravasation into lymphatics may seem to be favored due to reduced shear stress inflicted upon the cell, increased hemodynamic flow rate may also help dislodge individual cells from the primary tumor. Disaggregation of cells under flow has been reported to be affected, at least in part, by levels of E-cadherin expression.⁵⁴

HOW DO TUMOR CELLS REACH SYSTEMIC CIRCULATION?

Viable tumor cells have been isolated in the blood of patients bearing nearly all types of cancer, including the most common forms of carcinomas.⁶³ Although the amount of time a tumor cell spends circulating throughout the body is believed to be short, the sheer number of cells potentially available for seeding distant metastases makes it imperative for us to understand how tumors gain initial access to systemic circulation.

In many clinical studies involving different human tumors, a positive association between lymphatic and hematogenous metastasis has generally been observed. For instance, Bubendorf et al reported that 84% of patients with node-positive prostate cancer bore evidence of hematogenous dissemination, as opposed to 16% of patients without local lymph node spread.⁶⁴ In breast cancer, lymph node metastasis has been linked with poor prognosis and distant metastasis,⁶⁵ and similar observations have also been noted in pancreatic cancer,⁶⁶ ovarian cancer,⁶⁷ and head and neck cancer,⁶⁸ among others.

Recently, we observed a strong correlation between lymphatic and hematogenous dissemination in a mouse orthotopic xenograft model of prostate cancer (Fig. 2).³⁰ As expected, the lymph nodes directly draining the prostate, the para-aortic/sub-lumbar lymph nodes, were invaded first by the tumors, followed by the more distant sub-renal lymph nodes. Mice that bore tumors which had not

formed macroscopic metastases in the lumbar lymph nodes (~50% of mice) also did not possess renal lymph node macro-metastases. Not surprisingly, the appearance of lung micrometastases was well-correlated with the detection of viable circulating tumor cells in the blood. Interestingly, however, significant numbers of lung metastases and circulating cells were found only in mice that possessed both renal and lumbar lymph node metastases, regardless of primary tumor size.

These clinical and experimental correlations can be interpreted in at least a couple of ways (Fig. 3). It is possible that some tumors may be unable to intravasate directly into blood vessels; thus they must establish satellite lymph node metastases first to disperse metastatic cells via the thoracic duct. Another possibility is that the primary tumors may be completely noninvasive until somehow triggered to metastasize via both lymphatics and blood vessels simultaneously. Either possibility would potentially yield an apparent correlation between lymphatic and hematogenous spread. But in the case of human patients, those with node-positive tumors at the time of diagnosis might be free of distal metastases in the first scenario but not in the second.

In support of the former possibility, Sleeman has noted that the physiology of lymph nodes may actually favor formation of local metastases that could serve as “bridgeheads” for further dissemination.⁶⁹ The low shear flow of lymphatic fluid coupled with the filtering of cells into a confined space—the subcapsular sinuses—may increase the local concentration of tumor cell aggregates in the node. This would be in contrast to the “scatter-shot” dispersal of individual tumor cells into large capillary beds such as the lung, where metastatic progression after seeding is known to be highly inefficient.¹ Indeed, increased cell aggregation has been previously found to enhance formation of experimental metastases.⁷⁰ Furthermore, according to Sleeman, tumor cells that have arrived in the subcapsular sinuses would not need to extravasate.⁶⁹

Others have proposed that lymph nodes may act as initial “selection” sites where tumor cells with partial metastatic competence could seed and expand, while selecting for increasingly malignant variants that could later spread to more distant sites.³² This would agree with hypotheses previously set forth that metastatic cells are similar to, but also different from, their primary tumors of origin.^{7,9}

If entrance into systemic circulation were dependent on lymphatics, experimental inhibition of lymph node metastasis should also inhibit hematogenous spread. But, while some have indeed reported such results,^{32,34,36} others found that inhibiting lymph node metastasis had no effect on lung metastasis.^{31,37,71} These findings are likely attributable to differences in the cell lines utilized and whether the cells were implanted orthotopically or ectopically. In another study, resection of MT-100-TC mammary carcinomas along with draining lymph nodes prevented metastatic recurrence, but removal of the primary tumors alone did not.⁷² This would suggest that MT-100-TC cells reached systemic circulation via lymphatics, a progression the authors termed “metachronous seeding.”

In contrast, the presence of hematogenous metastases in the absence of lymphatic spread would clearly indicate direct dispersal of tumor cells into blood vessels. This is a likely scenario for patients

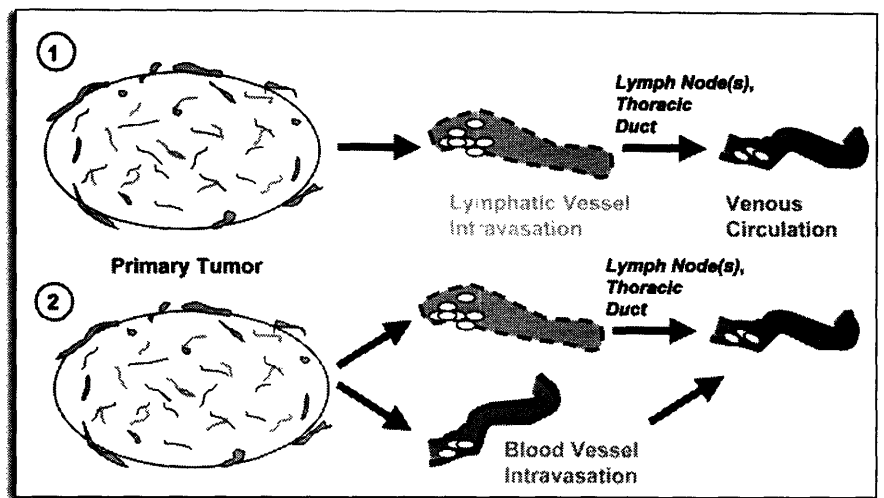


Figure 3. Two possible pathways for metastasis could explain why, in a mouse model of prostate cancer, hematogenous spread is observed only in the presence of significant lymphatic spread. (1) The tumors might be incapable of intravasating directly into blood vessels, so metastatic cells enter venous circulation indirectly via lymphatics (“metachronous seeding”). Or, the tumor is completely nonmetastatic until mobilized to metastasize via both lymphatic and hematogenous routes at the same time (2).

harboring bone marrow micrometastases in the absence of other detectable signs of spread, which has been reported to occur in 20–40% of carcinomas.⁷³ Interestingly, comparative genomic hybridization (CGH) analyses have suggested that malignant cells may disseminate through the blood very early in breast cancer.^{74,75} These cells were also found to be distinct from lymph node metastases by CGH, thus arguing against metachronous seeding.⁷⁴

Lastly, in patients harboring both lymphatic and hematogenous metastases, assessing the order of events remains difficult. One possible experimental approach to determine whether distant metastases arise directly from the primary tumor or indirectly from lymph nodes might be to construct a detailed time course tracking the relative temporal appearance of tumor cells in the blood and lymph nodes. If hematogenous spread occurs via lymphatics, for instance, malignant cells should appear in lymph nodes before blood. Such an approach could be coupled with methods such as CGH⁷⁴ or gene expression profiling⁷⁶ to track dispersed tumor cells. Detailed genomic analyses comparing primary tumors with micrometastases isolated from lymph nodes and/or distant sites should be able to distinguish the pathways undertaken for metastasis.

CONCLUSIONS

A confluence of factors likely influences whether primary tumors metastasize via blood vessel or lymphatic routes and, related to that, how tumor cells reach the systemic circulation. Differentiation programs innate to the cell of origin of each tumor may predetermine the metastatic phenotype, though additional genetic or epigenetic changes may also affect a cell’s ability to intravasate. Morphological differences between blood vessels and lymphatics will almost certainly affect the initial route of spread, and in this regard, peritumoral lymphatics might be considered a default pathway for tumors incapable of crossing blood endothelial boundaries. However, active mechanisms for attracting tumor cells towards one type of vasculature versus another cannot be discounted. In addition, the roles played by inflammatory⁷⁷ and host hematopoietic precursor cells⁷⁸ in affecting the process will need to be further examined.

At the same time, improved imaging techniques should allow simultaneous visualization of blood vessel and lymphatic intravasation within the same tumor, allowing direct measurements of the relative frequencies of each occurrence. In addition, genomic approaches combined with clustering algorithms should be able to elucidate molecular relationships between disseminated tumor cells and cells derived from the primary tumor and/or lymph node metastases. These studies will likely yield detailed information about how and when metastatic cells leave the primary tumor. Lastly, identification and validation of genes and proteins that affect the intravasation process and perhaps specify whether a tumor invades via blood vessel or lymphatic routes, as has been recently proposed,⁷⁹ will have valuable clinical implications for prognosis and treatment.

References

- Chambers AF, Groom AC, MacDonald IC. Dissemination and growth of cancer cells in metastatic sites. *Nat Rev Cancer* 2002; 2:563-72.
- Fidler IJ. The pathogenesis of cancer metastasis: The 'seed and soil' hypothesis revisited. *Nat Rev Cancer* 2003; 3:453-8.
- Luzzi KJ, MacDonald IC, Schmidt EE, Kerkvliet N, Morris VL, Chambers AF, Groom AC. Multistep nature of metastatic inefficiency. *Am J Pathol* 1998; 153:865-73.
- Ramaswamy S, Ross KN, Lander ES, Golub TR. A molecular signature of metastasis in primary solid tumors. *Nat Genet* 2003; 33:49-54.
- Veer LJ, Dai H, Vijver MJ, He YD, Hart AA, Mao M, Peterse HL, Kooy K, Marton MJ, Kiteveen AT, Schreiber GJ, Kerkhoven RM, Roberts C, Linsley PS, Bernards R, Friend SH. Gene expression profiling predicts clinical outcome of breast cancer. *Nature* 2002; 415:530-5.
- Clark EA, Golub TR, Lander ES, Hynes RO. Genomic analysis of metastasis reveals an essential role for RhoC. *Nature* 2000; 406:532-5.
- Kang Y, Siegel PM, Shu W, Drobnjak M, Kakonen SM, Cordon-Cardo C, Guise TA, Massague J. A multigenic program mediating breast cancer metastasis to bone. *Cancer Cell* 2003; 6:537-49.
- Yang J, Mani SA, Donaher JL, Ramaswamy S, Itzykson RA, Come C, Savagner P, Gitelman I, Richardson A, Weinberg RA. Twist, a master regulator of morphogenesis, plays an essential role in tumor metastasis. *Cell* 2004; 117:927-39.
- Hynes RO. Metastatic potential: Generic predisposition of the primary tumor or rare, metastatic variants-or both?. *Cell* 2003; 113:821-3.
- Butler TP, Gullino PM. Quantification of cell shedding into efferent blood of mammary adenocarcinoma. *Cancer Res* 1975; 35:3512-6.
- Wyckoff J, Wang W, Lin EY, Wang Y, Pixley F, Stanley ER, Graf T, Pollard JW, Segall J, Condeelis J. A paracrine loop between tumor cells and macrophages is required for tumor cell migration in mammary tumors. *Cancer Res* 2004; 64:7022-9.
- Condeelis J, Segall J. Intravital imaging of cell movement in tumours. *Nat Rev Cancer* 2003; 3:921-30.
- Gupta PB, Kuperwasser C, Brunet JP, Ramaswamy S, Kuo WL, Gray JW, Naber SP, Weinberg RA. The melanocyte differentiation program predisposes to metastasis after neoplastic transformation. *Nat Genet* 2005; 37:1047-54.
- Friedl P, Wolf K. Tumour-cell invasion and migration: Diversity and escape mechanisms. *Nat Rev Cancer* 2003; 3:362-74.
- Thiery J. Epithelial-mesenchymal transitions in tumor progression. *Nat Rev Cancer* 2002; 2:442-54.
- Kurrey NK, AK, Bapat SA. Snail and Slug are major determinants of ovarian cancer invasiveness at the transcription level. *Gynecol Oncol* 2005; 97:155-65.
- Ofi M, Akhurst RJ, Balmain A. Metastasis is driven by sequential elevation of H-ras and Smad2 levels. *Nat Cell Biol* 2002; 4:487-94.
- Siegel PM, Shu W, Cardiff RD, Muller WJ, Massague J. Transforming growth factor beta signaling impairs Neu-induced mammary tumorigenesis while promoting pulmonary metastasis. *Proc Natl Acad Sci USA* 2003; 100:8430-5.
- Perl AK, Wilgenbus P, Dahl U, Semb H, Christofori G. A causal role for E-cadherin in the transition from adenoma to carcinoma. *Nature* 1998; 392:190-3.
- Pantel K, Brakenhoff RH. Dissecting the metastatic cascade. *Nat Rev Cancer* 2004; 4:448-56.
- Nathanson SD. Insights into the mechanisms of lymph node metastasis. *Cancer* 2003; 98:413-23.
- Wittekind C. Diagnosis and staging of lymph node metastasis. *Recent Results Cancer Res: Lymphatic Metastasis and Sentinel Lymphonodectomy* 2000; 157:20-8.
- Smith JA, Seaman JP, Gleidman JB, Middleron RG. Pelvic lymph node metastasis from prostatic cancer: Influence of tumor grade and stage in 452 consecutive patients. *J Urol* 1982; 130:290-2.
- Smerage JB, Hayes DF. The measurement and therapeutic implications of circulating tumour cells in breast cancer. *Br J Cancer* 2005; 94:1-5.
- Su D, Yamaguchi K, Tanaka M. The characteristics of disseminated tumor cells in pancreatic cancer: A black box needs to be explored. *Pancreatol* 2005; 5:316-24.
- Cristofanilli M, Budd GT, Ellis MJ, Stopeck A, Matera J, Miller MC, Reuben JM, Doyle GV, Allard WJ, Terstappen LW, Haynes DF. Circulating tumor cells, disease progression, and survival in metastatic breast cancer. *N Engl J Med* 2004; 351:781-91.
- Alitalo K, Carmeliet P. Molecular mechanisms of lymphangiogenesis in health and disease. *Cancer Cell* 2002; 1:219-27.
- Gimbrone MA, Leapman SB, Cotran RS, Folkman J. Tumor dormancy in vivo by prevention of neovascularization. *J Exp Med* 1972; 136:261-76.
- Ferrara N. VEGF and the quest for tumor angiogenesis factors. *Nat Rev Cancer* 2002; 2:795-803.
- Wong SY, Haack H, Crowley D, Barry M, Bronson RT, Hynes RO. Tumor-secreted vascular endothelial growth factor-C is necessary for prostate cancer lymphangiogenesis, but lymphangiogenesis is unnecessary for lymph node metastasis. *Cancer Res* 2005; 65:9789-98.
- He Y, Kozaki K, Karpanen T, Koshikawa K, Yla-Herttuala S, Takahashi T, Alitalo K. Suppression of tumor lymphangiogenesis and lymph node metastasis by blocking vascular endothelial growth factor receptor-3 signaling. *J Natl Cancer Inst* 2002; 94:819-25.
- Krishnan J, Kirkin V, Steffen A, Hegen M, Weih D, Tomarev S, Wilting J, Sleeman JP. Differential in vivo and in vitro expression of vascular endothelial growth factor (VEGF)-C and VEGF-D in tumors and its relationship to lymphatic metastasis in immunocompetent rats. *Cancer Res* 2003; 63:713-22.
- Shimizu K, Kubo H, Yamaguchi K, Kawashima K, Ueda Y, Matsuo K, Awane K, Shimahara Y, Takabayashi A, Yamaoka Y, Satoh S. Suppression of VEGFR-3 signaling inhibits lymph node metastasis in gastric cancer. *Cancer Sci* 2004; 95:328-33.
- Chen Z, Varney ML, Backora MW, Cowan K, Solheim JC, Talmadge JE, Singh RK. Down-regulation of vascular endothelial cell growth factor-C expression using small interfering RNA vectors in mammary tumors inhibits tumor lymphangiogenesis and spontaneous metastasis and enhances survival. *Cancer Res* 2005; 65:9004-11.
- Karpanen T, Egeblad M, Karkkainen MJ, Kubo H, Yla-Herttuala S, Jaattela M, Alitalo K. Vascular endothelial growth factor C promotes tumor lymphangiogenesis and intralymphatic tumor growth. *Cancer Res* 2001; 61:1786-90.
- Lin J, Lalani AS, Harding TC, Gonzalez M, Wu WW, Luan B, Tu GH, Koprivnikar K, VanRoey MJ, He Y, Alitalo K, Jooss K. Inhibition of lymphogenous metastasis using adeno-associated virus-mediated gene transfer of a soluble VEGFR-3 decoy receptor. *Cancer Res* 2005; 65:6901-9.
- He Y, Rajantie I, Pajusola K, Jeltsch M, Holopainen T, Yla-Herttuala S, Harding T, Jooss K, Takahashi T, Alitalo K. Vascular endothelial cell growth factor receptor 3-mediated activation of lymphatic endothelium is crucial for tumor cell entry and spread via lymphatic vessels. *Cancer Res* 2005; 65:4739-46.
- Alitalo K, Tammele T, Petrova TV. Lymphangiogenesis in development and human disease. *Nature* 2005; 438:946-53.
- Dadras SS, Paul T, Bertoncini J, Brown LF, Muzikansky A, Jackson DG, Ellwanger U, Garbe C, Mihm MC, Detmar M. Tumor lymphangiogenesis: A novel prognostic indicator for cutaneous melanoma metastasis and survival. *Am J Pathol* 2003; 162:1951-60.
- Maula S, Luukkainen M, Grenman R, Jackson D, Jalkanen S, Ristamaki R. Intratumoral lymphatics are essential for the metastatic spread and prognosis in squamous cell carcinomas of the head and neck region. *Cancer Res* 2003; 63:1920-6.
- Alitalo K, Molla S, Ruoslahti E. Lymphangiogenesis and cancer: Meeting report. *Cancer Res* 2004; 64:9225-9.
- Padera TP, Kadambi A, di Tomaso E, Carreira CM, Brown EB, Boucher Y, Choi NC, Mathisen D, Wain J, Mark EJ, Munn LL, Jain RK. Lymphatic metastasis in the absence of functional intratumor lymphatics. *Science* 2002; 296:1883-6.
- Padera TP, Stoll BR, Tooredman JB, Capen D, di Tomaso E, Jain RK. Pathology: Cancer cells compress intratumour vessels. *Nature* 2004; 427:695.
- Isaka N, Padera TP, Hagendoorn J, Fukumura D, Jain RK. Peritumor lymphatics induced by vascular endothelial growth factor-C exhibit abnormal function. *Cancer Res* 2004; 64:4400-4.
- Leu AJ, Berk DA, Lybroussaki A, Alitalo K, Jain R. Absence of functional lymphatics within a murine sarcoma: A molecular and functional evaluation. *Cancer Res* 2000; 60:4324-7.
- Jain RK, Padera TP. Prevention and treatment of lymphatic metastasis by antilymphangiogenic therapy. *J Natl Cancer Inst* 2002; 94:785-7.
- Crnic I, Strittmatter K, Cavallaro U, Kopfstein L, Jussila L, Alitalo K, Christofori G. Loss of neural cell adhesion molecule induces tumor metastasis by upregulating lymphangiogenesis. *Cancer Res* 2004; 64:8630-8.
- Trojan I, Michel MS, Rensch F, Jackson DG, Alken P, Grobholz R. Lymph and blood vessel architecture in benign and malignant prostatic tissue: Lack of lymphangiogenesis in prostate carcinoma assessed with novel lymphatic marker lymphatic vessel endothelial hyaluronan receptor (LYVE-1). *J Urol* 2004; 172:103-7.
- Vleugel MM, Bos R, van der Groep P, Greijer AE, Shvarts A, Stel HV, van der Wall E, van Diest PJ. Lack of lymphangiogenesis during breast carcinogenesis. *J Clin Pathol* 2004; 57:746-51.
- Williams CS, Leek RD, Robson AM, Banerji S, Prevo R, Harris AL, Jackson DG. Absence of lymphangiogenesis and intratumoral lymph vessels in human metastatic breast cancer. *J Pathol* 2003; 200:195-206.
- Sipos B, Kojima M, Tiemann K, Klapper W, Kruse ML, Kalthoff H, Schniewind B, Tepel J, Weich H, Kerjaschki D, Kloppel G. Lymphatic spread of ductal pancreatic adenocarcinoma is independent of lymphangiogenesis. *J Pathol* 2005; 207:301-12.

52. Wyckoff JB, Jones JG, Condeelis JS, Segall JE. A critical step in metastasis: In vivo analysis of intravasation at the primary tumor. *Cancer Res* 2000; 60:2504-11.
53. Sahai F, Marshall CJ. Differing modes of tumour cell invasion have distinct requirements for *Rho/ROCK* signalling and extracellular proteolysis. *Nat Cell Biol* 2003; 5:711-8.
54. Byers SW, Sommers CL, Hoxter B, Mercurio AM, Tozeren A. Role of *E-cadherin* in the response of tumor cell aggregates to lymphatic, venous and arterial flow: Measurement of cell-cell adhesion strength. *J Cell Sci* 1995; 108:2053-64.
55. Schoppmann SF, Birner P, Stockl J, Kalt R, Ullrich R, Caucig C, Kriehuber E, Nagy K, Alitalo K, Kerjaschki D. Tumor-associated macrophages express lymphatic endothelial growth factors and are related to peritumoral lymphangiogenesis. *Am J Pathol* 2002; 161:947-56.
56. Skobe M, Hamberg LM, Hawighorst T, Schirner M, Wolf GL, Alitalo K, Detmar M. Concurrent induction of lymphangiogenesis, angiogenesis, and macrophage recruitment by vascular endothelial growth factor-C in melanoma. *Am J Pathol* 2001; 159:893-903.
57. Maruyama K, Li M, Cursiefen C, Jackson DG, Keino H, Tomita M, Rooijen NV, Takenaka H, D'Amore PA, Stein-Streilen J, Losordo DW, Streilein JW. Inflammation-induced lymphangiogenesis in the cornea arises from CD11b-positive macrophages. *J Clin Invest* 2005; 115:2363-72.
58. LeBedis C, Chen K, Fallavollita L, Boutros T, Brodt P. Peripheral lymph node stromal cells can promote growth and tumorigenicity of breast carcinoma cells through the release of *IGF-I* and *EGF*. *Int J Cancer* 2002; 100:2-8.
59. Homey B, Muller A, Zlotnik A. Chemokines: Agents for the immunotherapy of cancer?. *Nat Rev Immunol* 2002; 3:175-84.
60. Wiley HE, Gonzalez EB, Maki W, Wu M, Hwang ST. Expression of CC chemokine receptor-7 and regional lymph node metastasis of B16 murine melanoma. *J Natl Cancer Inst* 2001; 93:1638-43.
61. Muller A, Homey B, Soto H, Ge N, Catron D, Buchanan ME, McClanahan T, Murphy E, Yuan W, Wagner SN, Barrera JL, Mohar A, Verastegui E, Zlotnik A. Involvement of chemokine receptors in breast cancer metastasis. *Nature* 2001; 410:50-6.
62. Orimo A, Gupta PB, Sgroi DC, Arenzana-Seisdedos F, Delaunay T, Naeem R, Carey VJ, Richardson AL, Weinberg RA. Stromal fibroblasts present in invasive human breast carcinomas promote tumor growth and angiogenesis through elevated *SDF-1/CXCL12* secretion. *Cell* 2005; 121:335-48.
63. Allard WJ, Matera J, Miller MC, Repollet M, Connelly MC, Rao C, Tibbe AG, Uhr JW, Terstappen LW. Tumor cells circulate in the peripheral blood of all major carcinomas but not in healthy subjects or patients with nonmalignant diseases. *Clin Cancer Res* 2004; 10:6897-904.
64. Bubendorf L, Schopfer A, Wagner U, Sauter G, Moch H, Willi N, Gasser TC, Mihatsch MJ. Metastatic patterns of prostate cancer: An autopsy study of 1,589 patients. *Hum Pathol* 2000; 31:578-82.
65. Cianfrocca M, Goldstein LJ. Prognostic and predictive factors in early-stage breast cancer. *Oncologist* 2004; 9:606-16.
66. Yoshida T, Matsumoto T, Sasaki A, Shibata K, Aramaki M, Kitano S. Outcome of para-aortic node-positive pancreatic head and bile duct adenocarcinoma. *Am J Surg* 2004; 187:736-40.
67. Dvoretzky PM, Richards KA, Angel C, Rabinowitz L, Stoler MH, Beecham JB, Bonfiglio TA. Distribution of disease at autopsy in 100 women with ovarian cancer. *Hum Pathol* 1988; 19:57-63.
68. Leemans CR, Tiwari R, Nauta JJ, van der Waal I, Snow GB. Regional lymph node involvement and its significance in the development of distant metastases in head and neck carcinoma. *Cancer* 1993; 71:452-6.
69. Sleeman J. The lymph node as a bridgehead in the metastatic dissemination of tumors. *Recent Results Cancer Res* 2000; 157:55-81.
70. Glinsky VV, Glinsky GV, Glinsky OV, Huxley VH, Turk JR, Mossine VV, Deutscher SL, Pienta KJ, Quinn TP. Intravascular metastatic cancer cell homotypic aggregation at the sites of primary attachment to the endothelium. *Cancer Res* 2003; 63:3805-11.
71. He Y, Rajantie I, Ilmonen M, Makiinen T, Karkkainen MJ, Haiko P, Salven P, Alitalo K. Preexisting lymphatic endothelium but not endothelial progenitor cells are essential for tumor lymphangiogenesis and lymphatic metastasis. *Cancer Res* 2004; 64:3737-40.
72. Ward PM, Weiss L. Metachronous seeding of lymph node metastases in rats bearing the MT-100-TC mammary carcinoma: The effect of elective lymph node dissection. *Breast Cancer Res Treat* 1989; 14:315-20.
73. Pantel K, Cote RJ, Fodstad O. Detection and clinical importance of micrometastatic disease. *J Natl Cancer Inst* 1999; 91:1113-24.
74. Schmidt-Kittler O, Ragg T, Daskalakis A, Granzow M, Ahr A, Blankenstein TJ, Kaufmann M, Diebold J, Arnholdt H, Muller P, Bischoff J, Harich D, Schlimok G, Riethmuller G, Eils R, Klein CA. From latent disseminated cells to overt metastasis: Genetic analysis of systemic breast cancer progression. *Proc Natl Acad Sci USA* 2003; 100:7737-42.
75. Schardt JA, Meyer M, Hartmann CH, Schubert F, Schmidt-Kittler O, Fuhrmann C, Polzer B, Petronio M, Eils R, Klein CA. Genomic analysis of single cytokeratin-positive cells from bone marrow reveals early mutational events in breast cancer. *Cancer Cell* 2005; 8:227-39.
76. Smirnov DA, Zweitzig DR, Foulk BW, Miller MC, Doyle GV, Pienta KJ, Meropol NJ, Weiner LM, Cohen SJ, Moreno JG, Connelly MC, Terstappen LW, O'Hara SM. Global gene expression profiling of circulating tumor cells. *Cancer Res* 2005; 65:4993-7.
77. Schoppmann SF, Schindl M, Breiteneder-Geleff S, Soleiman A, Breitenecker G, Karner B, Birner P. Inflammatory stromal reaction correlates with lymphatic microvessel density in early-stage cervical cancer. *Anticancer Res* 2001; 21:3419-24.
78. Kaplan RN, Riba RD, Zacharoulis S, Bramley AH, Vincent L, Costa C, MacDonald DD, Jin DK, Shido K, Kerns SA, Zhu Z, Hicklin D, Wu Y, Port JL, Altorki N, Port ER, Ruggero D, Shmelkov SV, Jensen KK, Rafii S, Lyden D. VEGFR1-positive haematopoietic bone marrow progenitors initiate the premetastatic niche. *Nature* 2005; 438:820-7.
79. Woelfle U, Cloos J, Sauter G, Riethdorf L, Janicke F, van Diest P, Brakenhoff R, Pantel K. Molecular signature associated with bone marrow micrometastasis in human breast cancer. *Cancer Res* 2003; 63:5679-84.

PROSPECT

Tumor–Lymphatic Interactions in an Activated Stromal Microenvironment

Sunny Y. Wong¹ and Richard O. Hynes^{2*}

¹Howard^{Q3}Hughes Medical Institute

²Center^{Q4}for Cancer Research and Department of Biology, Massachusetts Institute of Technology, 77 Massachusetts Avenue, Cambridge, Massachusetts 02139

Abstract Metastasis to lymph nodes is a common feature of many human tumors and may facilitate dissemination to other parts of the body. Peritumoral lymphatics, which are located at the periphery of a primary tumor, appear to be anything but peripheral for metastasis, as recent studies have highlighted their critical role in disseminating tumor cells to local lymph nodes. The metastatic process, including lymphangiogenesis, is likely governed by a complex series of interactions among tumor cells, endothelial cells, and non-endothelial stromal components. Therefore, a detailed understanding of the biology of the tumor microenvironment, particularly as it pertains to peritumoral lymphatics near the tumor–stromal junction, may someday translate into clinical approaches that target metastasis at the invasive front. *J. Cell. Biochem.* 9999: 1–11, 2006. © 2006 Wiley-Liss, Inc.

Key words: metastasis; lymphangiogenesis; angiogenesis; microenvironment; stroma

There are numerous ways in which a tumor cell could succeed at metastasis but also many ways in which it could fail. In order to metastasize, a tumor cell must possess or acquire the ability to surmount a variety of obstacles—challenges that include de-adhesion from the primary tumor, intravasation into blood or lymphatic vessels, survival in circulation, extravasation, and growth at a secondary site. With so many barriers that need to be overcome, it is almost a wonder that tumors ever succeed at metastasis. One theme that has emerged is that tumors probably do not perform the feat alone but instead, receive significant input from the surrounding microenvironment. Another theme, as will become evident, is that

different tumors solve the metastatic problem in different ways.

Lymph nodes are the most common sites of metastasis for many cancers, including carcinomas [Sleeman, 2000]. There are likely to be several reasons for this. Tumors reach the draining lymph nodes via lymphatic vessels, which themselves appear to be ideal conduits for metastasis. Unlike blood vessels, lymphatics lack a basement membrane and are not surrounded by pericytes, thus making them relatively permeable to invading tumors. The low-pressure flow of lymphatic fluid also likely favors the survival of circulating tumor cells. And, upon reaching the node, metastatic cells are filtered into a confined space—the subcapsular sinuses—which may encourage the formation of aggregates that could protect against cell death [Sleeman, 2000].

These considerations offer a mechanistic, albeit incomplete, view of lymphatic metastasis, especially in light of recent studies that have identified other factors, particularly those extrinsic to the tumor cell that could affect the metastatic switch in profound ways. In order to examine the metastatic process thoroughly, one must also consider the contextual cues provided by a tumor's microenvironment. This microenvironment, or stroma, is comprised of a complex

Grant sponsor: NIH; Grant number: RO1CA17007; Grant sponsor: Virginia and D. K. Ludwig Fund for Cancer Research; Grant sponsor: Prostate Cancer Foundation; Grant sponsor: Howard Hughes Medical Institute; Grant sponsor: NIGMS Predoctoral Training Grant; Grant sponsor: Center for Cancer Research.

*Correspondence to: Richard O. Hynes, 40^{Q5}Ames Street, Cambridge, MA 02142-1308. E-mail: rohynes@mit.edu

Received XXXXX^{Q1}; Accepted XXXXX

DOI 10.1002/jcb.21146

Published online 00 Month 2006 in Wiley InterScience (www.interscience.wiley.com).

© 2006 Wiley-Liss, Inc.

mixture of fibroblasts, immune cells, endothelial cells, and endothelial-associated cells. Each cell type could potentially communicate with others, or with tumor cells, through secretion of a variety of signals, including growth factors, matrix molecules, chemokines, and proteinases. Indeed, the perception of metastasis as a solitary journey embarked upon by a single rogue cell can be regarded as overly simplistic and, these days, even antiquated. In this article, we will consider how different pair-wise cellular interactions might potentially affect a tumor's ability to metastasize to lymph nodes.

TUMOR-TO-LYMPHATIC ENDOTHELIAL CELL SIGNALING

Recent studies have suggested several possible scenarios by which tumors could directly affect the physiology of nearby lymphatics in ways that would favor metastasis. These possibilities include tumor-induced lymphangiogenesis, lymphatic activation, and pre-conditioning of lymph nodes prior to metastatic colonization.

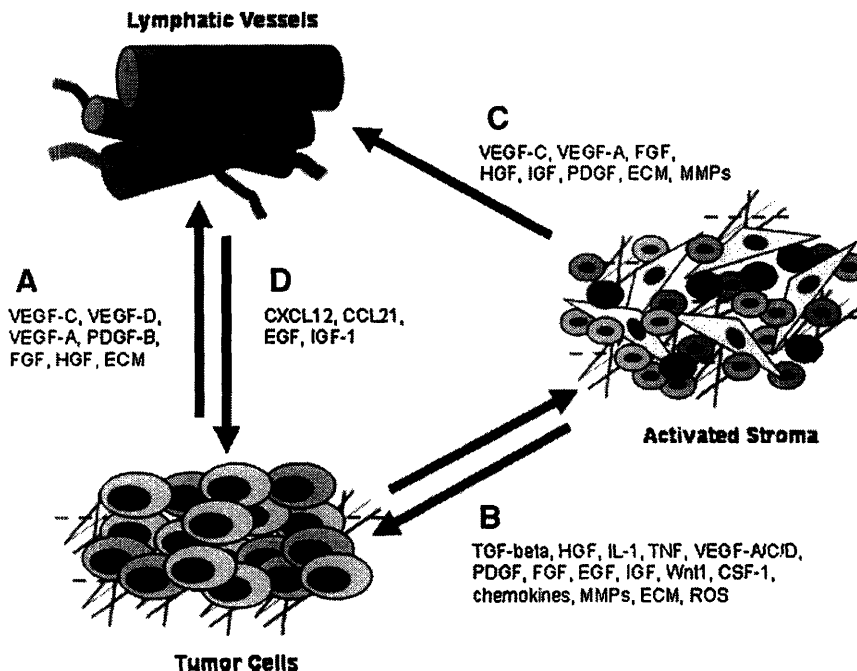


Fig. 1. Signals and interactions within the tumor microenvironment could potentially affect lymph node metastasis. **A:** Tumor-secreted factors have been reported to induce lymphangiogenesis, lymphatic activation, and pre-conditioning of lymph nodes for metastasis. **B:** Tumor cells can activate their surrounding stroma, while an activated stroma (fibroblasts, immune cells, etc.) can also induce increased tumorigenicity and metastasis in neoplastic cells. **C:** The stromal microenviron-

ment, particularly immune cells such as macrophages, can induce lymphangiogenesis through a variety of signals. **D:** The lymphatic endothelium and/or the lymph node can, in turn, release factors that recruit tumor cells. MMPs, matrix metalloproteinases; ECM, extracellular matrix; ROS, reactive oxygen species. [Color figure can be viewed in the online issue, which is available at www.interscience.wiley.com.]

ment, particularly immune cells such as macrophages, can induce lymphangiogenesis through a variety of signals. Although experimental results have lent support to each of these scenarios, it is important to note that direct signaling between tumor cells and lymphatic endothelial cells has not been demonstrated conclusively in vivo. As will be discussed later, immune cells such as macrophages might serve as important intermediaries for tumor-induced lymphangiogenesis. Overexpression studies using cancer xenograft models have been instrumental in identifying factors that can induce tumor lymphangiogenesis and, oftentimes, enhance lymph node metastasis (Fig. 1A). The first demonstration of this involved tumor overexpression of vascular endothelial growth factor-C (VEGF-C) and -D (VEGF-D), both of which increased lymphatic metastasis [Skobe et al., 2001; Stacker et al., 2001]. The predominant lymphatic receptor for these cytokines is VEGF receptor-3/Flt4, though proteolytic processing of VEGF-C/D by plasmin or by proprotein convertases can allow efficient binding to VEGF receptor-2/Flk1 [McColl et al., 2003; Siegfried et al., 2003]. Subsequent studies have also

identified additional lymphangiogenic factors, including VEGF-A, FGF2, PDGF-B, HGF, and others (reviewed in Alitalo et al., 2005). Because lymphatics and blood vessels share a common embryonic origin [Karkkainen et al., 2004], it is not surprising that these factors have previously been found to possess angiogenic activity.

Transgenic Rip-Tag mice overexpressing VEGF-C in the pancreas displayed de novo generation of lymphatics near β -cell islets and increased metastasis to the regional mesenteric lymph nodes [Mandriota et al., 2001]. Similarly, loss of the cell adhesion molecule N-CAM was associated with upregulated VEGF-C in pancreatic tumors, again yielding increased lymph node metastasis [Crnic et al., 2004]. The opposite result—reduced lymphangiogenesis—was commonly found when Flt4-mediated signaling was blocked. This has been accomplished by injecting antibodies against VEGF-D into tumor-bearing mice [Stacker et al., 2001], by adenoviral delivery of a truncated soluble receptor for Flt4 [He et al., 2002], or by expressing in tumor cells RNAi against VEGF-C [Chen et al., 2005; Wong et al., 2005]. In many cases, lymphatic spread was also concomitantly inhibited.

Although the degree of tumor lymphangiogenesis has been positively correlated with lymph node metastasis in many experimental models, others have observed that tumor-associated lymphatics are physiologically abnormal and non-functional for fluid drainage [Padera et al., 2002]. An important distinction needs to be made in that, in some cases, xenografted tumors have been found to induce both lymphatics within the tumor itself (intratumoral lymphatics) and lymphatics at the periphery (peritumoral lymphatics). We recently showed in an orthotopic model of prostate cancer that intratumoral lymphatics were unnecessary for efficient metastasis to draining lymph nodes [Wong et al., 2005]. This result is consistent with the view that peritumoral, and likely pre-existing, lymphatics at the invasive margin are the predominant routes of egress from the primary tumor [Padera et al., 2002]. This view is also supported by clinical data showing that the abundance of peritumoral, but not intratumoral, lymphatics correlated with metastasis in breast and prostate cancer; and that lymphangiogenesis does not occur in many tumors that nevertheless metastasize to lymph nodes,

including those of the breast, prostate and pancreas (reviewed in Wong and Hynes, 2006). In contrast, several clinical studies have correlated intratumoral lymphatic vessel density (LVD) with metastasis (reviewed by Stacker et al., 2002 and Achen et al., 2005). Consequently, the importance of tumor lymphangiogenesis in regard to metastasis is debatable, and may depend on the organ and/or experimental model in question. However, increased LVD might also merely be a marker of aggressive tumors that secrete high levels of lymphangiogenic cytokines and are poised to metastasize regardless of lymphangiogenesis.

Aside from increasing the abundance of lymphatic vessels in proximity to the tumor, activation of local lymphatic vessels has also been proposed as a way to enhance tumor cell intravasation and lymph node metastasis. He et al., recently noted that peritumoral lymphatics proximal to subcutaneous LNM35 lung tumors often displayed an “activated” phenotype—that is, increased vessel sprouting, dilation, and permeability [He et al., 2005]. Others have speculated that activated lymphatics might upregulate secretion of chemokines that could attract tumor cells [Alitalo et al., 2004]. This activated phenotype can apparently be reversed by adenoviral delivery of soluble Flt4 [He et al., 2005], an effect that is reminiscent of tumor blood vessel normalization, which is seen upon interference with VEGF-A- or Flk1-mediated signaling [Tong et al., 2004].

In addition to affecting lymphatics in their immediate vicinity, tumors have been reported to pre-condition future sites of metastasis in the lymph node. As observed by Hirakawa et al. [2005], carcinogen-induced squamous cell carcinomas in transgenic mice overexpressing VEGF-A in the skin displayed increased angiogenesis and lymphangiogenesis, as well as enhanced lymphatic and systemic metastasis. Surprisingly, increased lymphangiogenesis was also seen within draining lymph nodes prior to, and after, metastatic colonization. This suggests that tumors might somehow prepare the lymph node for metastasis. Although the exact mechanism underlying this phenomenon remains unclear, lymph-node lymphangiogenesis could perhaps be mediated directly by binding of VEGF-A to Flk1 on the surface of lymphatic endothelial cells. Or, VEGF-A might increase the permeability of local blood vessels, and the consequent extravasation of fluid might

serve as a lymphangiogenic signal. Interestingly, lymphangiogenesis within lymph node metastases was also proposed as a possible way for tumors to disseminate further throughout the lymphatic system and, subsequently, to systemic sites. At present, however, the exact implications and generalities of these novel findings remain to be seen.

BI-DIRECTIONAL SIGNALING BETWEEN TUMOR AND NON-ENDOTHELIAL STROMAL CELLS

Tumor cell communication with the surrounding non-endothelial stroma can likely tip the balance towards the metastatic phenotype. Not only can malignant cells provoke changes within their microenvironment, but abnormal stroma has also been found to enhance epithelial cell transformation and invasiveness. A consequence of these interactions might be induction of lymphangiogenic growth factors, in addition to an increased propensity by tumors to invade local lymphatics. Mobilization of inflammatory cells to the primary tumor is also likely to be an important component of both lymphangiogenesis and angiogenesis.

Based on clinical observations, as well as experimental studies in mice, it has long been known that tumor-associated stroma is frequently abnormal in appearance [Bhowmick and Moses, 2005]. In many cases, the usual boundary separating the epithelium from the stroma—the basement membrane—has been disrupted, with a corresponding loss of normal tissue architecture, altered extracellular matrix (ECM) deposition, increased inflammation, and neovasculogenesis. Cancer-associated fibroblasts (CAFs) often take on the appearance of an activated, or myofibroblastic, phenotype marked by the expression of α -smooth muscle actin. When cultured in vitro, CAFs have been reported to exhibit altered migratory properties as well as abnormal expression of growth factors and ECM [Cunha et al., 2003].

Importantly, transplantation/co-injection experiments have demonstrated that CAFs appear to be stably activated and can induce de novo tumorigenic growth in non-tumorigenic prostate epithelial cells [Olumi et al., 1999], or increased tumorigenicity in human MCF-7 breast cancer cells [Orimo et al., 2005]. Although the mechanism by which tumors activate their surrounding stroma is, at present, not entirely clear, the process likely involves a

complicated exchange of paracrine signals (Fig. 1B). One example of this complex dialog is illustrated in studies where several carcinoma cell lines, through secretion of IL-1, bFGF, and/or PDGF, induced co-cultured human skin fibroblasts to secrete HGF. HGF, in turn, bound its receptor, c-Met, on the surface of the tumor cells, which increased their growth, scattering and invasiveness [Nakamura et al., 1997]. In another example, human HaCaT keratinocytes, which are immortalized but non-tumorigenic, were reported to signal to fibroblasts in vitro through secretion of PDGF. In response, the fibroblasts upregulated FGF-7, which induced HaCaT cell proliferation and tumorigenicity [Brauchle et al., 1994].

While epithelial cell transformation has long been regarded as an initiating event for stromal activation, several recent studies have also shown that abnormal stroma may precede, and even induce, a malignant epithelial phenotype. For instance, irradiated fibroblasts can enhance tumorigenicity and/or invasiveness of lung, mammary, or pancreatic epithelial cells when co-injected in vivo, and similar effects have been reported when senescent fibroblasts were utilized (reviewed in Bhowmick et al., 2004b). In addition, human prostate BPH-1 cells can be made tumorigenic in mice when combined with hormone-activated urogenital mesenchyme [Cunha et al., 2003]. In many cases, the HGF-c-Met signaling axis appears to be crucial. Other stromally derived, paracrine signals involved with malignancy have been reported to include TGF- β , HGF, EGF, FGF, IGF, and Wnt1 [Bhowmick et al., 2004b]. In the case of TGF- β , its upregulation in fibroblasts has been shown to induce mammary carcinomas [Kuperwasser et al., 2004]. However, genetic deletion of TGF- β type II receptor specifically in fibroblasts was associated with upregulated HGF and resulted in induction of spontaneous prostate and forestomach carcinomas in mice [Bhowmick et al., 2004a]. Transgenic expression of constitutively active TGF- β type I receptor in the mammary gland has also been reported to increase tumor metastasis [Siegel et al., 2003]. The dual effects seen with TGF- β signaling—both as a positive and negative regulator of tumorigenesis—may largely be context- and cell-type dependent.

A similar dual effect on tumor progression has been observed in the case of matrix metalloproteinases (MMPs), which are secreted by both

tumor and stromal cells. MMPs function to degrade the surrounding ECM and can activate latent cytokines as well as other MMPs. Furthermore, MMPs can release matrix-bound growth factors (e.g., VEGF-A and FGF) that can induce angiogenesis and/or lymphangiogenesis, though cryptic collagen IV fragments released by MMP-9 can also possess potent anti-angiogenic activity [Hamano et al., 2003]. Experimentally, spontaneous mouse mammary tumor formation was enhanced by fibroblasts that overexpressed MMP-1 and MMP-7, but was inhibited when fibroblasts had lost MMP-11 (reviewed in Lynch and Matrisian, 2002). Transgenic expression of MMP-3 in mammary tumors has also been reported to promote epithelial-to-mesenchymal transition, a marker of enhanced cancer aggressiveness, through disruption of E-cadherin– β -catenin interactions [Sternlicht et al., 1999]. In addition, intravasation of human breast, prostate, and fibrosarcoma tumor cells into blood vessels has been shown to require the activity of MMP-9 and urokinase plasminogen activator in a chicken chorioallantoic membrane assay [Kim et al., 1998].

Another important component of the stromal microenvironment, the inflammatory cells of the innate immune system, is now regarded as a critical, if not indispensable, mediator of tumor progression [Coussens and Werb, 2002]. Immune cells are major sources of growth factors and cytokines that can induce tumor progression, invasiveness, angiogenesis, and lymphangiogenesis. Tumor and/or stromal fibroblastic secretion of chemokines and other cytokines such as VEGF-A and monocyte colony stimulating factor (M-CSF) are key to recruiting specific leukocyte populations. Macrophages, in particular, are chemotactic to VEGF-A, M-CSF, and monocyte chemotactic protein chemokines, and may be critical for lymphangiogenesis, as discussed below [Cursiefen et al., 2004]. Interestingly, a subset of tumor-associated macrophages (TAMs) has been found to express Flt4, and these may be recruited to tumors secreting VEGF-C/D [Schoppmann et al., 2002]. In addition to macrophages, neutrophils are also chemotactic to chemokines such as CXCL1/MIP-2 and are important for angiogenesis [Scapini et al., 2004]. Finally, natural killer cells have also been found to aid progression of pre-neoplastic mammary lesions through secretion of MMPs [Bissell and Radisky, 2001].

The importance of bi-directional signaling for inducing tumor cell invasion has been evidenced both in vivo and in vitro, in studies examining interactions between mammary carcinomas and macrophages. Tumor-secreted colony-stimulating factor 1 (CSF-1) was shown to be a chemotactic signal for macrophages expressing the CSF-1 receptor [Wang et al., 2005]. These TAMs reciprocated by secreting epidermal growth factor (EGF), which bound surface receptors on the tumor cells and induced a migratory gene expression program. The consequences of this—increased tumor invasiveness—have been observed by intravital microscopy, particularly at the periphery of mammary tumors, where macrophages were abundant. Furthermore, in CSF-1 knock-out mice, which display severe reductions of macrophages in most tissues, the growth of spontaneous mammary tumors was not affected relative to wild-type mice, but progression to invasion and metastasis was impaired [Lin et al., 2001].

In colorectal cancer, peak VEGF-C/-D expression was observed in tumor cells closest to the invasive margins [Onogawa et al., 2004]. It is, therefore, conceivable that soluble factors secreted by activated stromal cells located at the tumor–stromal interface may act on malignant cells to upregulate expression of lymphangiogenic factors, thus aiding indirectly in the metastatic process. Expression of VEGF-C is known to be regulated by cytokines, and, indeed, can be induced in a PI3-kinase-dependent manner by IGF, EGF, and PDGF in tumor cells [Tang et al., 2003]. Similarly, VEGF-C was upregulated by heregulin in breast cancer [Tsai et al., 2003] and by the inflammatory cytokines IL-1 β /IL-1 α and TNF- α [Ristimaki et al., 1998]. In many cases, activation of canonical signaling pathways known to be important for epithelial cell transformation, such as those mediated by Ras and Akt, has been implicated in upregulating expression of VEGF-A [Tan et al., 2004]. Hypoxic conditions or the presence of reactive oxygen species generated during the inflammatory response may also induce VEGF-A, which may then either stimulate lymphangiogenesis directly, or perhaps indirectly, as one study has suggested, by inducing squamous cell carcinomas to upregulate VEGF-C [Hirakawa et al., 2005].

These studies have been critical for delineating functionally important lines of communication

between tumor cells and stroma, and it is likely that other examples of bi-directional signaling remain to be uncovered. Some of the latter studies have also brought to center stage the importance of TAMs for mediating not only tumor progression to metastasis, but also likely, as will be discussed in the next section, the actual induction of angiogenesis and lymphangiogenesis.

NON-ENDOTHELIAL STROMAL-TO-LYMPHATIC ENDOTHELIAL CELL SIGNALING

The stromal fibroblasts and immune cells that surround tumors can exert direct effects on lymphatics by secreting growth factors, remodeling the ECM, and maybe even by incorporating into nascent lymphatic vessels (Fig. 1C). Stromal contributions to neovascularization are well documented and perhaps best observed in transgenic mice made to express GFP under control of the human VEGF-A promoter [Fukumura et al., 1998]. When these mice were crossed with the PyMT spontaneous mammary tumor model, the fibroblasts surrounding the neoplasm, but not the tumor cells themselves, were GFP-positive, suggesting that the main source of VEGF-A was stromally derived. Although it is tempting to speculate that many principles applying to tumor angiogenesis also apply to lymphangiogenesis—and many have indeed been shown to be relevant for both processes—it is important to remember that angiogenic tumors do not necessarily induce lymphangiogenesis. Furthermore, lymphangiogenesis has not often been seen in human clinical tumors, even in those that metastasize to lymph nodes. The reasons for this are unclear but almost certainly rest in the molecular differences between the two vessel types, as exemplified by the specificity of thrombospondin-1 for inhibiting CD36-expressing blood vessels but not lymphatics [Hawighorst et al., 2002].

In addition to VEGF-A, activated fibroblasts have been known to secrete many potential lymphangiogenic factors, including VEGF-C, FGF, HGF, IGF, and PDGF [Cunha et al., 2003]. In vitro stimulation of normal human skin fibroblasts with TGF- β and EGF induced secretion of both VEGF-C and VEGF-D, and this effect may, in part, underlie the activated fibroblastic phenotype [Trompezinski

et al., 2004]. CAFs in breast cancer were also found to enhance angiogenesis and tumor growth by secreting the chemokine SDF-1/CXCL12 [Orimo et al., 2005]. This mobilized and recruited endothelial precursor cells which were derived from the bone marrow and expressed the receptor CXCR4. SDF-1 has also recently been found to be important for retaining pro-angiogenic bone marrow-derived circulating cells that associated near blood vessels [Grunewald et al., 2006]. Whether these phenomena occur in other tumors, and whether similar mechanisms are important for inducing lymphangiogenesis, is still highly controversial.

Since stromal fibroblasts secrete abundant matrix proteins, their influence on the composition and ordering of the ECM microenvironment likely serves as another signal for blood vessels and lymphatics. During angiogenesis, endothelial cell matrix receptors such as integrins are upregulated and serve several important capacities such as enhancing VEGF-mediated signaling through direct association with Flk1 [Soldi et al., 1999]. In the case of lymphatics, cell proliferation in vitro seems dependent on the matrix molecule fibronectin, which may be supplied in vivo by tumor cells, fibroblasts, and/or endothelial cells [Zhang et al., 2005]. Lymphatic endothelial cell binding to fibronectin leads to direct association between the integrin β 1 subunit and Flt4, which may enhance VEGF-C/D signaling pathways [Wang et al., 2001]. The integrin heterodimer α 9 β 1 has also been implicated in the development of lymphatics and may act to bind ECM components like fibronectin and/or, as recently reported, VEGF-C and -D [Vlahakis et al., 2005]. Lastly, fibroblast-mediated contraction of the ECM, particularly of collagen networks, is increased when those cells are activated, and likely contributes to high tumor interstitial fluid pressure (IFP) [Heldin et al., 2004]. While high IFP is thought to signal the growth of new lymphatics, overwhelming IFP, as is often seen within tumors, can collapse intratumoral lymphatic vessels [Padera et al., 2002]. Thus, fibroblasts can potentially regulate not just the growth of new lymphatics, but also their function.

As mentioned previously, the role of immune cells in mediating angiogenesis and lymphangiogenesis has recently received great attention, leading to some valuable insights. Once

recruited to tumors, leukocytes release an abundant cache of cytokines and MMPs that can directly affect lymphatics. In support of this idea, the degree of inflammation in two studies of human cervical cancer positively correlated with both lymphatic vessel density and the number of VEGF-C-expressing peritumoral cells [Schoppmann et al., 2001, 2002]. Many of these cells were CD68+ macrophages that also expressed VEGF-C/D and Flt4. Increased inflammatory response, however, was negatively correlated with lymph node metastasis [Schoppmann et al., 2001]. These findings illustrate the complexities that shape the metastatic tendencies of a tumor—how, for instance, the stromal inflammatory reaction might wield a double-edged sword, acting both as a way to promote lymphangiogenesis and as an anti-tumor response.

But what exactly is the mechanism for inflammation-induced lymphangiogenesis? Novel findings have been obtained from experiments utilizing traditional xenograft models, as well as *de novo* lymphangiogenesis models involving either the murine cornea or Matrigel plugs implanted into mice. Many of these studies have confirmed the important role of macrophages, which have been found to secrete many potential lymphatic growth factors, including VEGF-C, VEGF-D, VEGF-A, and FGF [Cursiefen et al., 2004; Jin et al., 2006]. Expression of these factors seems to be induced in these cells by chemotactic factors such as M-CSF [Eubank et al., 2003] and possibly by an autocrine loop in a subpopulation that expresses Flt4 [Schoppmann et al., 2002; Eubank et al., 2003]. In addition, macrophage secretion of proteinases such as MMP-9 could remodel the ECM, thereby releasing additional cytokines while providing a hospitable environment for lymphatic proliferation [Carmeliet and Collen, 1998].

In the cornea, which is normally avascular, inflammation can induce local formation of blood and lymphatic vessels. Interestingly, CD11b+/LYVE-1+ macrophages have been reported to integrate into inflammation-induced lymphatics *in vivo* and could also form lymphatic-like tubes when cultured *in vitro* [Maruyama et al., 2005]. These findings were recently supported by studies in human renal transplants that had exhibited immune rejection, chronic inflammation and lymphatic proliferation [Kerjaschki et al., 2006]. Circula-

ting lymphatic progenitors derived either from a minor CD133+VEGFR-3+CD34+ subpopulation or from a major CD14+VEGFR-3+CD31+VEGFR-2- monocyte population incorporated into lymphatics. However, this was contrasted by findings in the same study where circulating progenitor cells did not incorporate into lymphatics associated with two cases of human carcinomas, an observation that had been similarly noted in tumor xenograft models utilizing B16 melanoma or Lewis lung carcinoma cells [He et al., 2004]. Therefore, at present, these data seem to suggest that proliferation of pre-existing lymphatics accounts for tumor lymphangiogenesis, though increased inflammation might coax macrophages to transdifferentiate into lymphatics. Obviously, the generality of these recent findings, while exciting, remains to be further validated in different systems.

Other as-yet-unknown factors affecting lymphatic growth will almost certainly be elucidated in future studies. For instance, CXCL-ERL+ chemokines can induce angiogenesis by binding the receptors CXCR2/CXCR1 on blood endothelial cells—do chemokines have any direct or indirect effects on lymphatics, which express SDF-1 and specifically express the atypical, and perhaps non-signaling, chemokine receptor D6 [Nibbs et al., 2001]? It is also known that blood vessels are molecularly heterogeneous, exhibiting tissue- and tumor-specific patterns of gene expression [St. Croix et al., 2000]. Most notably, sprouting angiogenic vessels upregulate the integrins $\alpha v \beta 3$ and $\alpha v \beta 5$, thereby possibly implicating specific matrix molecules such as vitronectin in angiogenesis [Carmeliet and Collen, 1998]. Since peritumoral lymphatics often appear physiologically distinct from normal lymphatics, these nascent lymphatics will almost certainly possess an altered gene expression program, and consequently, a unique reliance on different growth factors and matrix molecules.

LYMPHATIC-TO-TUMOR CELL SIGNALING

It is likely that some of the signals involved with homing circulating lymphocytes to lymph nodes might also be directing tumor cells to lymphatics. Among other components, there is evidence that chemokine receptors, selectins, integrins, as well as their respective ligands, are critically important for both processes.

However, circulating lymphocytes are recruited from the blood and initially roll along the luminal walls of the lymph node high endothelial venules (HEVs) before extravasation. This is dependent upon the binding of lymphocyte L-selectin primarily to peripheral node addressins on the HEVs. While malignant cells circulating in the blood might also reach distal lymph nodes by extravasating through HEVs, in most cases, human clinical tumors have been observed to invade lymph nodes in a step-wise fashion [Sleeman, 2000]. The nearest draining lymph node, or the sentinel node, is invaded first, followed by more distal nodes. Therefore, rather than reaching lymph nodes via HEVs, most tumor cells likely arrive at the node directly via afferent lymphatics.

Nevertheless, L-selectin has been shown to enhance tumor dissemination to both local and distal lymph nodes. Spontaneous RipTag pancreatic tumors overexpressing L-selectin metastasized to the draining mesenteric lymph nodes as well as to peripheral nodes, while tumors without L-selectin did not metastasize [Qian et al., 2001]. Addressins are not expressed on lymphatics but another L-selectin ligand, mannose receptor, is expressed and has been reported to be important for tumor cell binding to the lymphatic endothelium in lymph nodes [Irijala et al., 2003]. Normally, L-selectin interaction with mannose receptor regulates exit of lymphocytes from lymph nodes via efferent lymphatics [Irijala et al., 2001]; at present, it is unclear whether a similar mechanism is involved with tumor spread away from the node.

The finding that chemokines can home tumor cells to specific organs, including lymph nodes, suggests that a certain logic may underlie the pattern of metastasis exhibited by a particular tumor, and that this pattern can be deciphered, at least in part, by analyzing the distribution of specific chemokine receptor–ligand pairs (Fig. 1D). The first and most notable demonstration of this was performed by Muller et al. [2001], who showed that CXCL12/SDF-1 was preferentially expressed in the lymph nodes, lung, liver, and bone marrow. These are all common sites of metastasis for breast cancers, which express the SDF-1 receptor CXCR4. Inhibiting the interaction between this receptor–ligand pair *in vivo* reduced the ability of MDA-MB-231 breast cancer cells to metastasize to both lung and lymph nodes. Furthermore, the chemokine CCL21 was also found to be highly

expressed in lymph nodes, and its receptor, CCR7, is often present on the surface of breast cancer and melanoma cells. Indeed, work by others has shown that overexpressing CCR7 in B16 melanoma cells can augment lymph node metastasis [Wiley et al., 2001]. Finally, activated lymphatic endothelial cells may secrete increased levels of CCL1, which could possibly be a chemotactic signal for CCR8-expressing tumor cells [Alitalo et al., 2004].

Release of EGF and IGF-1 by lymphatic stromal cells might serve as additional factors that recruit tumor cells and/or enhance their proliferation in lymph nodes [LeBedis et al., 2002]. Also, tumors have recently been reported to induce the formation of pre-metastatic niches at future sites of metastasis [Kaplan et al., 2005]. These niches were composed of VEGFR1+ bone marrow-derived cells and matrix secreted by fibroblast-like stromal cells, and were important for metastatic colonization of different organs. It will be important to learn how signals originating from these niches, in turn, attract tumor cells to them, and whether conditioning of the lymph node might also precede lymphatic metastasis. In many ways, these findings have uncovered more questions than answers. Clearly, a great deal remains to be understood.

CONCLUSIONS

Lymph node metastasis is commonly seen for a variety of tumors and often guides the therapeutic course of action. While the presence of lymphatic metastasis may serve as an early warning sign for an aggressive primary tumor, perhaps more importantly, it might also be indicative of a cancer that has already spread to more distant sites in the body. Since lymphatics eventually connect with venous blood, lymph nodes might actually serve as the primary gateways for disseminating tumor cells into hematogenous circulation. Inhibit lymph node metastasis, so the reasoning goes, and distant metastasis would also be stopped, or at least severely hampered. Based on this view, it is critical that we better understand the molecular mechanisms that affect each of the steps involved.

The findings discussed here have helped us move away from the perception of metastasis as a black box relying on chance events, in many ways once thought to be unintelligible. They

have also revealed the intricacies of a process orchestrated by a multitude of players. Inflammatory cells, fibroblasts, endothelial cells, the cancer cells themselves—untangling the web of reciprocal and non-reciprocal signals that contribute to tumor dissemination will be especially important. So too will be the need to better understand the fundamental biology of the lymphatic endothelium and the processes relevant to metastasis, including lymphangiogenesis and other tumor-induced lymphatic abnormalities. Despite the complexity of the tumor microenvironment, there is good reason to believe that the myriad of cellular interactions that take place can be teased apart, broken down, understood. Knowledge gained from these and future studies will affect how we treat metastatic disease, and perhaps someday, allow us to prevent it altogether.

ACKNOWLEDGMENTS

This study was supported by NIH (RO1CA-17007); the Virginia and D.K. Ludwig Fund for Cancer Research; the Prostate Cancer Foundation; and the Howard Hughes Medical Institute. S.Y. Wong was further supported by an NIGMS Predoctoral Training Grant to the MIT Biology Department and by a Koch Research Fellowship from the Center for Cancer Research.

REFERENCES

- Achen MG, McColl BK, Stacker SA. 2005. Focus on lymphangiogenesis in tumor metastasis. *Cancer Cell* 7: 121–127.
- Alitalo K, Mohla S, Ruoslahti E. 2004. Lymphangiogenesis and cancer: Meeting report. *Cancer Res* 64:9225–9229.
- Alitalo K, Tammela T, Petrova TV. 2005. Lymphangiogenesis in development and human disease. *Nature* 438: 946–953.
- Bhowmick NA, Moses HL. 2005. Tumor-stroma interactions. *Curr Opin Genet Dev* 15:97–101.
- Bhowmick NA, Chytil A, Plieth D, Gorska AE, Dumont N, Shappell S, Washington MK, Neilson EG, Moses HL. 2004a. TGF-beta signaling in fibroblasts modulates the oncogenic potential of adjacent epithelia. *Science* 303: 848–851.
- Bhowmick NA, Neilson EG, Moses HL. 2004b. Stromal fibroblasts in cancer initiation and progression. *Nature* 432:332–337.
- Bissell MJ, Radisky D. 2001. Putting tumours in context. *Nat Rev Cancer* 1:46–54.
- Brauchle M, Angermeyer K, Hubner G, Werner S. 1994. Large induction of keratinocyte growth factor expression by serum growth factors and pro-inflammatory cytokines in cultured fibroblasts. *Oncogene* 9:3199–3204.
- Carmeliet P, Collen D. 1998. Vascular development and disorders: Molecular analysis and pathogenic insights. *Kidney Int* 53:1519–1549.
- Chen Z, Varney ML, Backora MW, Cowan K, Solheim JC, Talmadge JE, Singh RK. 2005. Down-regulation of vascular endothelial cell growth factor-C expression using small interfering RNA vectors in mammary tumors inhibits tumor lymphangiogenesis and spontaneous metastasis and enhances survival. *Cancer Res* 65: 9004–9011.
- Coussens LM, Werb Z. 2002. Inflammation and Cancer. *Nature* 420:860–867.
- Crnici I, Strittmatter K, Cavallaro U, Kopfstein L, Jussila L, Alitalo K, Christofori G. 2004. Loss of neural cell adhesion molecule induces tumor metastasis by up-regulating lymphangiogenesis. *Cancer Res* 64:8630–8638.
- Cunha GR, Hayward SW, Wang YZ, Ricke WA. 2003. Role of the stromal microenvironment in carcinogenesis of the prostate. *Int J Cancer* 107:1–10.
- Cursiefen C, Chen L, Borges LP, Jackson D, Cao J, Radziejewski C, D'Amore PA, Dana MR, Wiegand SJ, Streilein JW. 2004. VEGF-A stimulates lymphangiogenesis and hemangiogenesis in inflammatory neovascularization via macrophage recruitment. *J Clin Invest* 113: 1040–1050.
- Eubank TD, Galloway M, Montague CM, Waldman WJ, Marsh CB. 2003. M-CSF induces vascular endothelial growth factor production and angiogenic activity from human monocytes. *J Immunol* 171:2637–2643.
- Fukumura D, Xavier R, Sugiura T, Chen Y, Park EC, Lu N, Selig M, Nielsen G, Taksir T, Jain RK, Seed B. 1998. Tumor induction of VEGF promoter activity in stromal cells. *Cell* 94:715–725.
- Grunewald M, Avraham I, Dor Y, Bachar-Lustig E, Itin A, Yung S, Chimenti S, Landsman L, Abramovitch R, Keshet E. 2006. VEGF-induced adult neovascularization: Recruitment, retention, and role of accessory cells. *Cell* 124:175–189.
- Hamano Y, Zeisberg M, Sugimoto H, Lively JC, Maeshima Y, Yang C, Hynes RO, Werb Z, Sudhakar A, Kalluri R. 2003. Physiological levels of tumstatin, a fragment of collagen IV alpha3 chain, are generated by MMP-9 proteolysis and suppress angiogenesis via alphaV beta3 integrin. *Cancer Cell* 3:589–601.
- Hawthorst T, Oura H, Streit M, Janes L, Nguyen L, Brown LF, Oliver G, Jackson DG, Detmar M. 2002. Thrombospondin-1 selectively inhibits early-stage carcinogenesis and angiogenesis but not tumor lymphangiogenesis and lymphatic metastasis in transgenic mice. *Oncogene* 21: 7945–7956.
- He Y, Kozaki K, Karpanen T, Koshikawa K, Yla-Herttuala S, Takahashi T, Alitalo K. 2002. Suppression of tumor lymphangiogenesis and lymph node metastasis by blocking vascular endothelial growth factor receptor-3 signaling. *J Natl Cancer Inst* 94:819–825.
- He Y, Rajantie I, Ilmonen M, Makinen T, Karkkainen MJ, Haiko P, Salven P, Alitalo K. 2004. Preexisting lymphatic endothelium but not endothelial progenitor cells are essential for tumor lymphangiogenesis and lymphatic metastasis. *Cancer Res* 64:3737–3740.
- He Y, Rajantie I, Pajusola K, Jeltsch M, Holopainen T, Yla-Herttuala S, Harding T, Jooss K, Takahashi T, Alitalo K. 2005. Vascular endothelial cell growth factor receptor

- 3-mediated activation of lymphatic endothelium is crucial for tumor cell entry and spread via lymphatic vessels. *Cancer Res* 65:4739–4746.
- Heldin CH, Rubin K, Pietras K, Ostman A. 2004. High interstitial fluid pressure—An obstacle in cancer therapy. *Nat Rev Cancer* 4:806–813.
- Hirakawa S, Kodama S, Kunstfeld R, Kajiya K, Brown LF, Detmar M. 2005. VEGF-A induces tumor and sentinel lymph node lymphangiogenesis and promotes lymphatic metastasis. *J Exp Med* 201:1089–1099.
- Irjala H, Johansson EL, Grenman R, Alanen K, Salmi M, Jalkanen S. 2001. Mannose receptor is a novel ligand for L-selectin and mediates lymphocyte binding to lymphatic endothelium. *J Exp Med* 194:1033–1042.
- Irjala H, Alanen K, Grenman R, Heikkila P, Joensuu H, Jalkanen S. 2003. Mannose receptor (MR) and common lymphatic endothelial and vascular endothelial receptor (CLEVER)-1 direct the binding of cancer cells to the lymph vessel endothelium. *Cancer Res* 63:4671–4676.
- Jin H, Su J, Garmy-Susini B, Kleeman J, Varner J. 2006. Integrin alpha4-beta1 promotes monocyte trafficking and angiogenesis in tumors. *Cancer Res* 66:2146–2152.
- Kaplan RN, Riba RD, Zacharoulis S, Bramley AH, Vincent L, Costa C, MacDonald DD, Jin DK, Shido K, Kerns SA, Zhu Z, Hicklin D, Wu Y, Port JL, Altorki N, Port ER, Ruggero D, Shmelkov SV, Jensen KK, Rafii S, Lyden D. 2005. VEGFR1-positive haematopoietic bone marrow progenitors initiate the pre-metastatic niche. *Nature* 438:820–827.
- Karckainen MJ, Haiko P, Sainio K, Partanen J, Taipale J, Petrova TV, Jeltsch M, Jackson DG, Talikka M, Rauvala H, Betsholtz C, Alitalo K. 2004. Vascular endothelial growth factor C is required for sprouting of the first lymphatic vessels from embryonic veins. *Nat Immunol* 5:74–80.
- Kerjaschki D, Huttary N, Raab I, Regele H, Bojarski-Nagy K, Bartel G, Krober SM, Greinix H, Rosenmaier A, Karlhofer F, Wick N, Mazal PR. 2006. Lymphatic endothelial progenitor cells contribute to de novo lymphangiogenesis in human renal transplants. *Nat Med* 12:230–234.
- Kim J, Yu W, Kovalski K, Ossowski L. 1998. Requirement for specific proteases in cancer cell intravasation as revealed by a novel semiquantitative PCR-based assay. *Cell* 94:353–362.
- Kuperwasser C, Chavarría T, Wu M, Magrane G, Gray JW, Carey L, Richardson A, Weinberg RA. 2004. Reconstruction of functionally normal and malignant human breast tissues in mice. *Proc Natl Acad Sci* 101:4966–4971.
- LeBedis C, Chen K, Fallavollita L, Boutros T, Brodt P. 2002. Peripheral lymph node stromal cells can promote growth and tumorigenicity of breast carcinoma cells through the release of IGF-I and EGF. *Int J Cancer* 100:2–8.
- Lin EY, Nguyen AV, Russell RG, Pollard JW. 2001. Colony-stimulating factor 1 promotes progression of mammary tumors to malignancy. *J Exp Med* 193:727–739.
- Lynch CC, Matrisian LM. 2002. Matrix metalloproteinases in tumor-host cell communication. *Differentiation* 70:561–573.
- Mandriota SJ, Jussila L, Jeltsch M, Compagni A, Baetens D, Prevo R, Banerji S, Huarte J, Montesano R, Jackson DG, Orci L, Alitalo K, Christofori G, Pepper MS. 2001. Vascular endothelial growth factor-C-mediated lymphangiogenesis promotes tumour metastasis. *EMBO J* 20:672–682.
- Maruyama K, Ii M, Cursiefen C, Jackson DG, Keino H, Tomita M, Rooijen NV, Takenaka H, D'Amore PA, Stein-Streilen J, Losordo DW, Streilein JW. 2005. Inflammation-induced lymphangiogenesis in the cornea arises from CD11b-positive macrophages. *J Clin Invest* 115:2363–2372.
- McCull BK, Baldwin ME, Roufail S, Freeman C, Moritz RL, Simpson RJ, Alitalo K, Stacker SA, Achen MG. 2003. Plasmin activates the lymphangiogenic growth factors VEGF-C and VEGF-D. *J Exp Med* 198:863–868.
- Muller A, Homey B, Soto H, Ge N, Catron D, Buchanan ME, McClanahan T, Murphy E, Yuan W, Wagner SN, Barrera JL, Mohar A, Verastegui E, Zlotnik A. 2001. Involvement of chemokine receptors in breast cancer metastasis. *Nature* 410:50–56.
- Nakamura T, Matsumoto K, Kiritoshi A, Tano Y, Nakamura T. 1997. Induction of hepatocyte growth factor in fibroblasts by tumor-derived factors affects invasive growth of tumor cells: In vitro analysis of tumor-stromal interactions. *Cancer Res* 57:3305–3313.
- Nibbs RJ, Kriehuber E, Ponath PD, Parent D, Qin S, Campbell JD, Henderson A, Kerjaschki D, Maurer D, Graham GJ, Rot A. 2001. The beta-chemokine receptor D6 is expressed by lymphatic endothelium and a subset of vascular tumors. *Am J Pathol* 158:867–877.
- Olumi AF, Grossfeld GD, Hayward SW, Carroll PR, Tlsty TD, Cunha GR. 1999. Carcinoma-associated fibroblasts direct tumor progression of initiated human prostatic epithelium. *Cancer Res* 59:5002–5011.
- Onogawa S, Kitadai Y, Tanaka S, Kuwai T, Kimura S, Chayama K. 2004. Expression of VEGF-C and VEGF-D at the invasive edge correlates with lymph node metastasis and prognosis of patients with colorectal carcinoma. *Cancer Sci* 95:32–39.
- Orimo A, Gupta PB, Sgroi DC, Arenzana-Seisdedos F, Delaunay T, Naeem R, Carey VJ, Richardson AL, Weinberg RA. 2005. Stromal fibroblasts present in invasive human breast carcinomas promote tumor growth and angiogenesis through elevated SDF-1/CXCL12 secretion. *Cell* 121:335–348.
- Padera TP, Kadambi A, Tomaso Ed, Carreira CM, Brown EB, Boucher Y, Choi NC, Mathisen D, Wain J, Mark EJ, Munn LL, Jain RK. 2002. Lymphatic metastasis in the absence of functional intratumor lymphatics. *Science* 296:1883–1886.
- Qian F, Hanahan D, Weissman IL. 2001. L-selectin can facilitate metastasis to lymph nodes in a transgenic mouse model of carcinogenesis. *Proc Natl Acad Sci* 98:3976–3981.
- Ristimaki A, Narko K, Enholm B, Joukov V, Alitalo K. 1998. Proinflammatory cytokines regulate expression of the lymphatic endothelial mitogen vascular endothelial growth factor-C. *J Biol Chem* 273:8413–8418.
- Scapini P, Morini M, Tecchio C, Minghelli S, Carlo ED, Tanghetti E, Albini A, Lowell C, Berton G, Noonan DM, Cassatella MA. 2004. CXCL1/macrophage inflammatory protein-2-induced angiogenesis in vivo is mediated by neutrophil-derived vascular endothelial growth factor-A. *J Immunol* 172:5034–5040.
- Schoppmann SF, Schindl M, Breiteneder-Geleff S, Soleiman A, Breiteneker G, Karner B, Birner P. 2001.

- Inflammatory stromal reaction correlates with lymphatic microvessel density in early-stage cervical cancer. *Anticancer Res* 21:3419–3424.
- Schoppmann SF, Birner P, Stockl J, Kalt R, Ullrich R, Caucig C, Kriehuber E, Nagy K, Alitalo K, Kerjaschki D. 2002. Tumor-associated macrophages express lymphatic endothelial growth factors and are related to peritumoral lymphangiogenesis. *Am J Pathol* 161:947–956.
- Siegel PM, Shu W, Cardiff RD, Muller WJ, Massague J. 2003. Transforming growth factor beta signaling impairs Neu-induced mammary tumorigenesis while promoting pulmonary metastasis. *Proc Natl Acad Sci* 100:8430–8435.
- Siegfried G, Basak A, Cromlish JA, Benjannet S, Marcinkiewicz J, Chretien M, Seidah NG, Khatib AM. 2003. The secretory proprotein convertases furin, PC5, and PC7 activate VEGF-C to induce tumorigenesis. *J Clin Invest* 111:1723–1732.
- Skobe M, Hawighorst T, Jackson DG, Prevo R, Janes L, Velasco P, Riccardi L, Alitalo K, Claffey K, Detmar M. 2001. Induction of tumor lymphangiogenesis by VEGF-C promotes breast cancer metastasis. *Nat Med* 7:192–198.
- Sleeman J. 2000. The lymph node as a bridgehead in the metastatic dissemination of tumors. *Recent Results Cancer Res* 157:55–81.
- Soldi R, Mitola S, Strasly M, Defilippi P, Tarone G, Bussolino F. 1999. Role of alphavbeta3 integrin in the activation of vascular endothelial growth factor receptor-2. *EMBO J* 18:882–892.
- St. Croix B, Rago C, Velculescu V, Traverso G, Romans KE, Montgomery E, Lal A, Riggins GJ, Lengauer C, Vogelstein B, Kinzler KW. 2000. Genes expressed in human tumor endothelium. *Science* 289:1197–1202.
- Stacker SA, Caesar C, Baldwin ME, Thornton GE, Williams RA, Prevo R, Jackson DG, Nishikawa S, Kubo H, Achen MG. 2001. VEGF-D promotes the metastatic spread of tumor cells via the lymphatics. *Nat Med* 7:186–191.
- Stacker SA, Achen MG, Jussila L, Baldwin ME, Alitalo K. 2002. Lymphangiogenesis and cancer metastasis. *Nat Rev Cancer* 2:573–583.
- Sternlicht MD, Lochter A, Sympson CJ, Huey B, Rougier JP, Gray JW, Pinkel D, Bissell MJ, Werb Z. 1999. The stromal proteinase MMP3/stromelysin-1 promotes mammary carcinogenesis. *Cell* 98:137–146.
- Tan C, Cruet-Hennequart S, Troussard A, Fazli L, Costello P, Sutton K, Wheeler J, Gleave M, Sanghera J, Dedhar S. 2004. Regulation of tumor angiogenesis by integrin-linked kinase (ILK). *Cancer Cell* 5:79–90.
- Tang Y, Zhang D, Fallavollita L, Brodt P. 2003. Vascular endothelial growth factor C expression and lymph node metastasis are regulated by the type I insulin-like growth factor receptor. *Cancer Res* 63:1166–1171.
- Tong RT, Boucher Y, Kozin SV, Winkler F, Hicklin DJ, Jain RK. 2004. Vascular normalization by vascular endothelial growth factor receptor 2 blockade induces a pressure gradient across the vasculature and improves drug penetration in tumors. *Cancer Res* 64:3731–3736.
- Trompezinski S, Berthier-Vergnes O, Denis A, Schmitt D, Viac J. 2004. Comparative expression of vascular endothelial growth factor family members, VEGF-B, -C and -D, by normal human keratinocytes and fibroblasts. *Exp Dermatol* 13:98–105.
- Tsai PW, Shiah SG, Lin MT, Wu CW, Kuo ML. 2003. Up-regulation of vascular endothelial growth factor C in breast cancer cells by heregulin-beta 1. A critical role of p38/nuclear factor-kappa B signaling pathway. *J Biol Chem* 278:5750–5759.
- Vlahakis NE, Young BA, Atakilit A, Sheppard D. 2005. The lymphangiogenic vascular endothelial growth factors VEGF-C and -D are ligands for the integrin alpha9beta1. *J Biol Chem* 280:4544–4552.
- Wang JF, Zhang XF, Groopman JE. 2001. Stimulation of beta 1 integrin induces tyrosine phosphorylation of vascular endothelial growth factor receptor-3 and modulates cell migration. *J Biol Chem* 276:41950–41957.
- Wang W, Goswami S, Sahai E, Wyckoff JB, Segall JE, Condeelis JS. 2005. Tumor cells caught in the act of invading: Their strategy for enhanced cell motility. *Trends Cell Biol* 15:138–145.
- Wiley HE, Gonzalez EB, Maki W, Wu M, Hwang ST. 2001. Expression of CC chemokine receptor-7 and regional lymph node metastasis of B16 murine melanoma. *J Natl Cancer Inst* 93:1638–1643.
- Wong SY, Hynes RO. 2006. Lymphatic or hematogenous dissemination: How does a metastatic tumor cell decide? *Cell Cycle* 5:812–817.
- Wong SY, Haack H, Crowley D, Barry M, Bronson RT, Hynes RO. 2005. Tumor-secreted vascular endothelial growth factor-C is necessary for prostate cancer lymphangiogenesis, but lymphangiogenesis is unnecessary for lymph node metastasis. *Cancer Res* 65:9789–9798.
- Zhang X, Groopman JE, Wang JF. 2005. Extracellular matrix regulates endothelial functions through interaction of VEGFR-3 and integrin alpha5beta1. *J Cell Physiol* 202:205–214.

- Q1:** Please provide the history dates.
- Q2:** Please check the suitability of the suggested short title.
- Q3:** Please provide the complete location of the first affiliation, and check the second affiliation. Is it ok?
- Q4:** Please check and provide the links for the affiliations.
- Q5:** Please provide the degrees of the corresponding author.

ACKNOWLEDGEMENTS

I can honestly say that obtaining this Ph.D. was the most difficult challenge I have ever faced. Especially during those early years, when I was uncertain of what to do, when experiment after experiment seemed to fail or yield nebulous results, when even the most basic logic of this thesis hadn't yet been formed—I can say that my thesis advisor, **Richard Hynes**, saw me through it all and patiently allowed me to develop as a scientist. I will always appreciate and admire his scientific acumen, his wisdom, and the respect and fairness by which he treats every member of his lab. I will also always be grateful of the independence he gave me to pursue my scientific interests, trusting that, eventually, I might someday do more good experiments than bad.

This lab has been a wonderful and stimulating work environment, and for that, I thank all the current members of the Hynes lab: **Adam, Arjan, Denise, Hamid, Hui, Jane, Kaan, Mariette, Lei, Olga, Patrick, Shahin, Sophie, Steve** and **Yueyi**. The lab alumni have also been fantastic people to work with over the years, and these wonderful individuals have included **Aaron, Charlie, Chris, Daniela, Heather, Herbert, Jen, Joe, Marc, Sarah** and **Stephanie**. In particular, I will forever be in debt to **Herbert, Chris** and **Kaan**, who took me under their wings early on and got me started. I will miss each and every one of you.

I would also like to thank my professional collaborators and the support staff who have made so many of my experiments possible, especially **Denise**, of the histology facility; **Rod Bronson**, for his help with pathology; and the **MIT Division of Comparative Medicine**.

Of course, I have appreciated the support of the **MIT Department of Biology** ever since I arrived in Cambridge in the fall of 2000, and have benefited from the guidance of my thesis committee members, **Robert Weinberg** and **Monty Krieger**, who have prodded me along since my second year here. I would also like to thank the additional members of my thesis defense committee, **Mike Hemann** and **Rakesh Jain**, for their help, as well as **Jeremy Reiter**, at UCSF, for paving the way for my future post-doctoral studies in his lab.

I would be remiss if I didn't acknowledge the support of some of the people who first helped me realize my interest in experimental biology. For that, I am especially grateful to **Hugh Mason**, of the Boyce Thompson Institute, who took me into his lab when I was still a freshman, and also to **Lizabeth Richter**, who mentored me all through the years and taught me how to use my first micro-pipette. I also appreciate the help of **Charlie Arntzen**, also at BTI, who provided me with my first opportunity to publish a scientific piece of writing.

My time here in Cambridge/Boston has been a memorable experience, due greatly to my many wonderful roommates and neighbors at 69/71 Elm Street over the years: **Mark, Nate, Bill, Steve, Alex, Duc, Sarah, Kevin** and **Brian**. I will also miss my other classmates and friends when I'm out in San Francisco: **Stephanie, Derek, Mandy, Dave, Leslie, Shirley** and **Holly**. You have all been loyal friends and close confidants. In addition, I am thankful to the creative writing professors I've had at MIT, the former members of my writers' group, as well as the entire company of my theatrical play, who have all made life interesting around here.

Lastly, I would like to thank my brother, **Edmund**, and my **Parents**, who have pushed me relentlessly ever since I was a fetus to be the very best person I can possibly be.